

RAPID PYROLYSIS AND HYDROLYSIS OF COAL

by

Eric M. Suuberg

S.B., Chemical Engineering  
Massachusetts Institute of Technology (1974)

S.M., Chemical Engineering Practice  
Massachusetts Institute of Technology (1974)

S.B., Management  
Massachusetts Institute of Technology (1974)

S.M., Management  
Massachusetts Institute of Technology (1976)

Submitted in Partial Fulfillment  
of the Requirements for the  
Degree of Doctor of Science

at the

MASSACHUSETTS INSTITUTE OF TECHNOLOGY

August, 1977

*(i.e. February, 1978)*

Signature of Author

\_\_\_\_\_  
Department of Chemical Engineering,  
September, 1977

Certified by

\_\_\_\_\_  
Jack B. Howard, Thesis Supervisor

Accepted by

\_\_\_\_\_  
Glenn C. Williams, Chairman  
Departmental Committee on Graduate Theses

ARCHIVES  
MASSACHUSETTS INSTITUTE  
OF TECHNOLOGY

SEP 29 1978

LIBRARIES

# Rapid Pyrolysis and Hydropyrolysis of Coal

by  
Eric M. Suuberg

Submitted to the Department of Chemical Engineering in August, 1977 in partial fulfillment of the requirements for the degree of Doctor of Science from the Massachusetts Institute of Technology.

## ABSTRACT

Data were obtained on the composition and kinetics of formation of key compounds or classes of compounds resulting from the pyrolysis and hydropyrolysis of two coals (a Pittsburgh Seam Bituminous and a Montana Lignite) in a captive sample apparatus.

Thin layers of coal were heated in strips of stainless steel wire mesh at heating rates between 100 and 15,000°C/sec to peak temperatures between 150 and 1100°C. Samples were held at these peak temperatures for times ranging from 0 to 30 seconds. Pressures studied ranged from vacuum to 100 atm of either hydrogen or helium. Gaseous and light liquid products were analyzed by vapor phase chromatography; heavy liquids and solids were characterized by elemental analysis.

Pyrolysis results suggest that certain products ( $\text{CO}_2, \text{H}_2\text{O}$ ) are linked to particular structures within the coal (carboxyls, hydroxyls). These and other products of pyrolysis can be modelled as arising from one to many distinct first order reactions, a procedure which gives activation energies typical of pyrolysis of many simpler organic compounds. A free radical chain mechanism is supported.

The behavior of the non-softening Montana Lignite is markedly different from that of the highly caking Pittsburgh Seam Bituminous Coal. A hypothesis concerning the important role of hydroxyl groups during pyrolysis receives tentative support.

The effect of hydrogen during hydropyrolysis manifests itself principally during what would be the major hydrocarbon formation phases of ordinary pyrolysis. The yield enhancement observed during pyrolysis in gaseous hydrogen is reflected mainly in increased yields of methane.

Various previously proposed models and mechanisms of pyrolysis and hydropyrolysis are evaluated in light of the new data, and several new approaches and interpretations offered.

Thesis Supervisor: Jack B. Howard, Professor of Chemical Engineering

Department of Chemical Engineering  
Massachusetts Institute of Technology  
Cambridge, Massachusetts  
August, 1977

Professor Irving Kaplan  
Secretary of the Faculty  
Massachusetts Institute of Technology

Dear Professor Kaplan:

In accordance with the regulations of the faculty, I submit here-  
with a thesis entitled "Rapid Pyrolysis and Hydrolysis of Coal", in  
partial fulfillment of the requirements for the degree of Doctor of Science  
in Chemical Engineering at the Massachusetts Institute of Technology.

Respectfully submitted,

Eric M. Suuberg

ACKNOWLEDGEMENTS

First and foremost, I would like to thank my advisor, Professor Jack B. Howard for the years of guidance and inspiration he has provided. He has throughout the course of this work always given generously of his time; the very humble thanks I offer here cannot nearly express the depth of my gratitude.

Thanks also to the members of my thesis committee, Professors A.F. Sarofim, G.C. Williams, H.C. Hottel, H.P. Meissner, and R.A. Hites for a great deal of valuable advice.

Next to my advisor, my two closest colleagues throughout the course of this work have been Ted W. Bush and Dr. William A. Peters; my thanks to them for all of the assistance and advice they have provided.

I would like to thank Dr. Donald B. Anthony and Professors P. S. Virk and C.N. Satterfield for valuable discussions.

Many student colleagues have made valuable contributions to this work. Phil Lewellen introduced me to the use of the captive sample apparatus; Richard Caron has contributed many very valuable hours of experimental work; Kevin Bennett addressed the difficult question of the catalytic effect of the stainless steel screens; Scott Free has assisted with both experimental work and the analysis of results; Karen Hladik assisted with the development of the chromatographic techniques. My thanks also to Edmund Lau, Dr. Hunter Ficke, Jim Bittner, Dr. John Pohl, Dr. Hisashi Kobayashi, Toby Reitzen, Koon Neoh, Candy Clampitt, and Professor Albert Sacco for various discussions, assistance, and general moral support.

Technical assistance from Stan Mitchell, Charles Foshey, Art Clifford, and the Chemical Engineering Department Shop is gratefully acknowledged. Thanks for the typing of this manuscript are due Pat Coakley.



The author gratefully acknowledges personal support from the National Science Foundation Energy Traineeship Program, and equipment and supply support via the National Science Foundation-RANN contract AER 75-13673 and the United States Energy Research and Development Administration contract EX-76-A-01-2295.

EMALE,

ISALE,

VANAMALE

TABLE OF CONTENTS

	<u>Page</u>
LIST OF FIGURES . . . . .	9
LIST OF TABLES . . . . .	15
1.0 SUMMARY . . . . .	
1.1 Introduction . . . . .	17
1.2 Background Literature . . . . .	17
- Pyrolysis . . . . .	17
- Hydropyrolysis . . . . .	26
1.3 Apparatus and Procedure . . . . .	26
1.4 Results . . . . .	
- Pyrolysis of a Montana Lignite . . . . .	32
- Pyrolysis of a Pittsburgh Seam Bituminous Coal . . . . .	40
- Hydropyrolysis of a Montana Lignite . . . . .	53
- Hydropyrolysis of a Pittsburgh Seam Bituminous Coal . . . . .	61
1.5 Modelling and Discussion . . . . .	
- Pyrolysis . . . . .	69
- Hydropyrolysis . . . . .	79
1.6 Conclusions . . . . .	82
1.7 References for Summary Section . . . . .	83
2.0 INTRODUCTION	85
3.0 BACKGROUND	
3.1.0 The Importance of Coal Type in Determining Pyrolysis Behavior . . . . .	89
3.1.1 Mineral Matter in Coal . . . . .	92
3.1.2 Petrographic Analysis and its Relation to Pyrolysis Behavior . . . . .	99
3.1.3 The Chemical Structure of Coal . . . . .	104
- The Carbon-Hydrogen Structure . . . . .	106
- Oxygen Containing Functional Groups. . . . .	128
- Sulfur and Nitrogen . . . . .	133
- Summary and Application of Structural Data to Montana Lignite and Pittsburgh Seam Bituminous Coal . . . . .	135

TABLE OF CONTENTS (continued)

	<u>Page</u>
- A Synthesis of Data - An Evaluation of Various Coal Models . . . . .	135
- The Physical Structure of Coal . . . . .	151
3.2 Previous Work on Pyrolysis and Hydrolysis . . . . .	157
- Evaluation of Experimental Systems . . . . .	158
3.2.1 Mechanistic Implications from Studies of Pyrolysis of Coal and Model Compounds . . . . .	169
- Pyrolysis of Model Compounds . . . . .	173
- Mechanistic Implications of Structural Changes in Coals Undergoing Pyrolysis . . . . .	189
- Effect of Coal Type and Pyrolysis Conditions on Pyrolysis Behavior . . . . .	199
- Effect of Coal Type . . . . .	199
- Effect of Temperature . . . . .	203
- Effect of Heating Rate . . . . .	208
- Effect of Particle Diameter . . . . .	218
- Effect of Pressure . . . . .	222
3.2.2 Modelling of Pyrolysis Phenomena . . . . .	224
- Modelling of Mass Transport - Secondary Reaction Effects . . . . .	245
3.2.3 Hydrolysis . . . . .	251
- Effect of Coal Type . . . . .	255
- Effect of Temperature . . . . .	258
- Effect of Pressure . . . . .	260
- Effect of Heating Rate . . . . .	260
- Effect of Particle Diameter . . . . .	263
3.2.4 Mechanisms and Modelling of Hydrolysis . . . . .	263
4.0 APPARATUS AND PROCEDURE . . . . .	
4.1 Selection of Apparatus . . . . .	272
4.2 Apparatus Description . . . . .	273
4.3 Run Procedure . . . . .	282
4.4 Experimental Error Analysis . . . . .	283
5.0 RESULTS AND DISCUSSION . . . . .	
5.1 Pyrolysis of a Montana Lignite . . . . .	286
- Base Data . . . . .	286
- Effect of Temperature-Time History . . . . .	294
- Effect of Pressure . . . . .	294

TABLE OF CONTENTS (continued)

	<u>Page</u>
5.2 Pyrolysis of a Pittsburgh Seam Bituminous Coal . . . . .	
- Base Data . . . . .	300
- Effect of Temperature-Time History . . . . .	314
- Effect of Pressure . . . . .	315
- Effect of Particle Diameter . . . . .	318
5.3 Hydropyrolysis of a Montana Lignite . . . . .	319
5.4 Hydropyrolysis of a Pittsburgh Seam Bituminous Coal . . . . .	332
5.5 Discussion and Modelling of Pyrolysis Results . . . . .	340
- The Behavior of Functional Groups During Pyrolysis.	357
- Thermodynamic Aspects of Pyrolysis . . . . .	361
- Secondary Reactions and Mass Transport Limitations . . . . .	366
5.6 Discussion and Modelling of Hydropyrolysis Results . . . . .	371
6.0 CONCLUSIONS AND RECOMMENDATIONS . . . . .	377
- Recommendations for Future Work . . . . .	379
7.0 LITERATURE CITED . . . . .	382
A-1 LOCATION OF ORIGINAL DATA . . . . .	397
A-2 SUMMARY OF CHROMATOGRAPHIC RESPONSE FACTORS . . . . .	409
A-3 LISTING OF COMPUTER PROGRAMS USED TO ANALYZE DATA . . . . .	410
A-4 THE NEED FOR MORE COAL CONVERSION RESEARCH . . . . .	421

## LIST OF FIGURES

<u>Figure No.</u>		<u>Page</u>
1-1	Estimate of Coal Structural Parameters . . . . .	20
1-2	Model Structure for a Bituminous Coal Molecule . . . . .	21
1-3	Overall Mechanistic Scheme for Pyrolysis of Coal-Model Compounds . . . . .	23
1-4	Rates of Gas Evolution from Pyrolyzing Subbituminous Coal. . . . .	25
1-5	Captive Sample Apparatus and Heating System . . . . .	27
1-6	Sample Holding and Heating Assembly . . . . .	28
1-7	Pyrolysis Product Distributions from Lignite Heated to Different Peak Temperatures . . . . .	33
1-8	Yields of Methane, Ethylene, and Hydrogen from Lignite Pyrolysis to Different Peak Temperatures . . . . .	35
1-9	Yields of Water, Carbon Monoxide, and Carbon Dioxide from Lignite Pyrolysis to Different Peak Temperatures . . . . .	36
1-10	Elemental Compositions of Chars from Lignite Pyrolysis to Different Peak Temperatures . . . . .	38
1-11	Effect of Pressure on Product Yields from Lignite Pyrolyzed to Different Peak Temperatures . . . . .	41
1-12	Pyrolysis Product Distribution from Bituminous Coal Heated to Different Peak Temperatures . . . . .	42
1-13	Yields of Tar and Water from Bituminous Coal Pyrolysis . . . . .	44
1-14	Yields of Methane and Hydrogen from Bituminous Coal Pyrolysis . . . . .	45
1-15	Yields of Carbon Monoxide and Carbon Dioxide from Bituminous Coal Pyrolysis . . . . .	46
1-16	Yields of Various Hydrocarbon Gases from Bituminous Coal Pyrolysis . . . . .	47
1-17	Elemental Compositions of Chars from Bituminous Coal Pyrolysis . . . . .	48
1-18	Effect of Pressure and Particle Diameter on Product Yields from Bituminous Coal Pyrolyzed at Approximately 1000°C . . . . .	52

## LIST OF FIGURES

<u>Figure No.</u>		<u>Page</u>
1-19	Comparison of Weight Loss from Pyrolysis and Hydropyrolysis of Lignite to Different Peak Temperatures . . . . .	54
1-20	Yield of Methane from Pyrolysis and Hydropyrolysis of Lignite to Different Peak Temperatures . . . . .	55
1-21	Ethylene Yields from Lignite Pyrolysis and Hydropyrolysis. . . . .	58
1-22	Comparison of Char Compositions for Lignite Pyrolysis and Hydropyrolysis . . . . .	59
1-23	Effect of Temperature and Pressure on Incremental Yields from Hydropyrolysis of Lignite . . . . .	60
1-24	Comparison of Weight Loss from Pyrolysis and Hydropyrolysis of Bituminous Coal . . . . .	62
1-25	Comparison of Tar Yields from Pyrolysis and Hydropyrolysis of Bituminous Coal . . . . .	63
1-26	Comparison of Methane Yields from Pyrolysis and Hydropyrolysis of Bituminous Coal . . . . .	65
1-27	Effect of Particle Diameter on Total Yields from Pyrolysis and Hydropyrolysis of Bituminous Coal . . . . .	68
1-28	Comparison of Data on Overall Conversion of Lignite to Volatiles with Predictions from Single-Step First Order Pyrolysis Model . . . . .	72
1-29	Distributions of Activation Energies of Pyrolysis Reactions . . . . .	75
3.1-1	Comparison of C/H Ratios of Macerals . . . . .	100
3.1-2	Comparison of Pyrolysis Behavior of Macerals . . . . .	101
3.1-3	Adamantane Model Structure for Coal . . . . .	108
3.1-4	Variation of Aromaticity with Rank . . . . .	111
3.1-5	Average Number of Rings per Aromatic Cluster . . . . .	115
3.1-6	Aromaticity and Average Number of Rings per Aromatic Cluster for Various Macerals . . . . .	117
3.1-7	Variation of the Ring Condensation Index with Rank . . . . .	117
3.1-8	Variation of "Hydroaromatic" Hydrogen Content with Rank . . . . .	119

## LIST OF FIGURES (continued)

<u>Figure No.</u>		<u>Page</u>
3.1-9	Variation of Total, Aliphatic and Phenolic Hydrogen Content with Rank . . . . .	121
3.1-10	Variation of Methylene Hydrogen Content with Rank . . . . .	124
3.1-11	Variation of Methyl Hydrogen Content with Rank . . . . .	124
3.1-12	Variation of Hydroxyl Oxygen Content with Rank. . . . .	130
3.1-13	Variation of Carboxyl Oxygen Content with Rank . . . . .	130
3.1-14	Variation of Total Oxygen Content with Rank . . . . .	134
3.1-15 thru 3.1-21	Various Model Structures for Coal . . . . .	137-8, 142 144-6, 148
3.1-22	Coal Model Generation Flowsheet . . . . .	149
3.1-23	Microscopic Origin of Porosity . . . . .	152
3.1-24	Structural Parameters from X-ray Scattering Analysis of Coal . . . . .	153
3.1-25	Variation of Total Porosity with Rank . . . . .	155
3.1-26	Variation of Micro- and Transitional Porosity with Rank . . . . .	156
3.2-1	Effect of Bed Depth and Heating Rate on the Results of an ASTM-type Analysis . . . . .	167
3.2-2	Comparison of Natural Coalification and Pyrolysis on an Elemental Basis . . . . .	171
3.2-3	Variation of Weight Loss, Plasticity, and Dilation with Pyrolysis Temperature . . . . .	171
3.2-4	Overall Model for the Pyrolysis of Coal Model Compounds .	178
3.2-5	Relationship Between Plasticity, Weight Loss, and Chloroform Extractable Materials . . . . .	180
3.2-6	Pyrolysis Behavior of Some Coal Model Substances . . . . .	187
3.2-7	Changes in Physical Microstructure of Coal During Pyrolysis . . . . .	191
3.2-8	Changes in Chemical and Physical Structure of Coal During Pyrolysis . . . . .	195



## LIST OF FIGURES (continued)

<u>Figure No.</u>		<u>Page</u>
3.2-9	Comparison of Yields of Pyrolytic Water and Carbon Dioxide with Amounts of Hydroxyl and Carboxyl Groups in Coal . . . . .	204
3.2-10	Evolution of Gases During the Pyrolysis of a Subbituminous Coal . . . . .	206
3.2-11	Evolution of Gases During the Pyrolysis of Bituminous Coals. . . . .	207
3.2-12	The Effect of Temperature and Time on Total Volatiles Yield from Pyrolysis . . . . .	209
3.2-13	The Effect of Heating Rate on Total Volatiles Yield from Pyrolysis of a Lignite . . . . .	213
3.2-14	The Effect of Heating Rate on Ethane Evolution During Pyrolysis of a Bituminous Coal . . . . .	214
3.2-15	The Variation of the H/C and O/C Ratios of Coal During Pyrolysis . . . . .	215
3.2-16	Effect of Particle Diameter on Pyrolysis Weight Loss . . . . .	220
3.2-17	The Effect of External Pressure on Weight Loss During Pyrolysis . . . . .	221
3.2-18	Comparison of Distributions of Activation Energies from Modelling of Coal Pyrolysis . . . . .	237
3.2-19 thru 3.2-21	Effect of Time and Hydrogen Pressure on Weight Loss During the Pyrolysis and Hydropyrolysis of Coal	253-4, 256
3.2-22	Effect of Temperature on Weight Loss during Pyrolysis and Hydropyrolysis of Coal . . . . .	259
3.2-23	Effect of Hydrogen Pressure and Temperature on Methane-plus-Ethane Yield during Hydropyrolysis . . . . .	261
3.2-24	Effect of Hydrogen and Helium Pressure on Weight Loss during Pyrolysis and Hydropyrolysis . . . . .	262
3.2-25	Effect of Particle Diameter on Weight Loss During Pyrolysis and Hydropyrolysis . . . . .	264
3.2-26	Relationship Between Methane-plus-Ethane Yield and Coal Hydrogen Evolution during Hydropyrolysis . . . . .	268
3.2-27	Comparison of Distributions of Activation Energies of Hydropyrolysis Reactions . . . . .	271

## LIST OF FIGURES (continued)

<u>Figure No.</u>		<u>Page</u>
4-1	Schematic of Captive Sample Apparatus . . . . .	274
4-2	Detail of Captive Sample Apparatus Internals . . . . .	275
4-3	Circuit Used for the Control of Time-Temperature Histories . . . . .	277
4-4	Typical Time-Temperature Histories . . . . .	279
5.1-1	Pyrolysis Product Distributions from Lignite Heated to Different Peak Temperatures . . . . .	287
5.1-2	Yields of Methane, Ethylene, and Hydrogen from Lignite Pyrolysis to Different Peak Temperatures . . . . .	289
5.1-3	Yields of Water, Carbon Monoxide and Carbon Dioxide from Lignite Pyrolysis to Different Peak Temperatures . . . . .	290
5.1-4	Elemental Compositions of Chars from Lignite Pyrolysis to Different Peak Temperatures . . . . .	292
5.1-5	Effect of Pressure on Product Yields from Lignite Pyrolyzed to Different Peak Temperatures . . . . .	296
5.1-6	Effect of Pressure on the Yield of Methane from Lignite Pyrolyzed to Different Peak Temperatures . . . . .	297
5.2-1	Pyrolysis Product Distribution from Bituminous Coal Heated to Different Peak Temperatures . . . . .	301
5.2-2	Yields of Tar and Water from Bituminous Coal Pyrolysis. .	303
5.2-3	Yields of Methane and Hydrogen from Bituminous Coal Pyrolysis . . . . .	305
5.2-4	Yields of Carbon Monoxide and Carbon Dioxide from Bituminous Coal Pyrolysis . . . . .	306
5.2-5	Yields of Various Hydrocarbon Gases from Bituminous Coal Pyrolysis . . . . .	307
5.2-6	Elemental Compositions of Chars from Bituminous Coal Pyrolysis . . . . .	309
5.2-7	Effect of Pressure and Particle Diameter on Product Yields from Bituminous Coal Pyrolyzed at 1000°C . . . . .	316
5.2-8	Effect of Pressure on Yield of Tar from Bituminous Coal Pyrolysis . . . . .	317

## LIST OF FIGURES (continued)

<u>Figure No.</u>		<u>Page</u>
5.3-1	Comparison of Weight Loss from Pyrolysis and Hydropyrolysis of Lignite to Different Peak Temperatures . . . . .	320
5.3-2	Yield of Methane from Pyrolysis and Hydropyrolysis of Lignite to Different Peak Temperatures . . . . .	323
5.3-3	Yield of Ethylene from Pyrolysis and Hydropyrolysis of Lignite to Different Peak Temperatures . . . . .	324
5.3-4	Yields of Hydrocarbon Gases (other than Methane and Ethylene) from Pyrolysis and Hydropyrolysis of Lignite to Different Peak Temperatures. . . . .	326
5.3-5	Yields of Water, Carbon Monoxide, and Carbon Dioxide from Pyrolysis and Hydropyrolysis of Lignite to Different Peak Temperatures . . . . .	327
5.3-6	Comparison of Char Compositions from Pyrolysis and Hydropyrolysis of Lignite . . . . .	329
5.3-7	Effect of Temperature and Hydrogen Pressure on Increasing Yields Relative to Pyrolysis . . . . .	330
5.4-1	Comparison of Weight Loss from Pyrolysis and Hydropyrolysis of Bituminous Coal. . . . .	333
5.4-2	Comparison of Tar Yields from Pyrolysis and Hydropyrolysis of Bituminous Coal . . . . .	334
5.4-3	Comparison of Methane Yields from Pyrolysis and Hydropyrolysis of Bituminous Coal . . . . .	336
5.4-4	Effect of Particle Diameter on Total Yields from Pyrolysis and Hydropyrolysis of Bituminous Coal . . . . .	339
5.5-1	Comparison of Data on Overall Conversion of Lignite to Volatiles with Predictions from Single-Step First Order Pyrolysis Model . . . . .	344
5.5-2	Distribution of Activation Energies of Lignite Pyrolysis Reactions . . . . .	348
5.5-3	Comparison of H/C vs. O/C Trajectories for Pyrolysis of Different Samples of Bituminous Coal and Lignite . . . .	360
5.5-4	Variation of Product and Total Heating Values for Lignite Pyrolyzed to Different Peak Temperatures . . . . .	362
5.5-5	Comparison of Gas Composition Data with Calculated Equilibrium Values for Lignite Pyrolyzed to Different Peak Temperatures . . . . .	364

## LIST OF TABLES

<u>Table No.</u>		<u>Page</u>
1-1	Characteristics of the Coals Examined in this Study . . . . .	18
1-2	Carbon, Hydrogen, Oxygen, and Total Mass Balances for Lignite Pyrolysis . . . . .	39
1-3	Effect of Time-Temperature Histories on Yields from Pyrolysis of Bituminous Coal . . . . .	50
1-4	Comparison of Total Yields from Lignite Pyrolysis and Hydropyrolysis . . . . .	56
1-5	Comparison of Total Yields from Pyrolysis and Hydropyrolysis of Bituminous Coal . . . . .	66
1-6	Kinetic Parameters for Pyrolysis of Various Organic Materials . . . . .	71
1-7	Kinetic Parameters for Lignite Pyrolysis . . . . .	74
3.1-1	Characteristics of the Coals Examined in this Study . . . . .	90
3.1-2	Principal Reactions that Contribute to Mineral Matter Weight Loss . . . . .	94
3.1-3	Summary of Estimated Structural Parameters for Pittsburgh Seam No. 8 Bituminous Coal and Montana Lignite . . . . .	136
3.2-1	Experimental Techniques and Conditions . . . . .	159
3.2-2	Comparison of Experimental Yields with Proximate Volatile Matter . . . . .	165
3.2-3	Kinetic Parameters for Pyrolysis of Various Organic Materials . . . . .	174
3.2-4	Stability of Some Oxygenous Substances . . . . .	182
3.2-5	Comparison of Ultimate Yields of Pyrolysis Products from Coals of Various Rank . . . . .	200
3.2-6	Kinetic Parameters for Evolution of Some Non-Hydrocarbon Gases from Coal . . . . .	241
3.2-7	Kinetic Parameters for the Evolution of Hydrocarbon Gases from Coal . . . . .	242
3.2-8	Kinetic Parameters for Evolution of Hydrogen, Carbon Oxides and Some Hydrocarbons from a Subbituminous Coal. . . . .	244

## LIST OF TABLES

<u>Table No.</u>		<u>Page</u>
5.1-1	Carbon, Hydrogen, Oxygen, and Total Mass Balances for Lignite Pyrolysis . . . . .	293
5.1-2	Comparison of Yields from Atmospheric and High Pressure Pyrolysis of Lignite . . . . .	298
5.2-1	Effect of Time-Temperature Histories on Yields from Pyrolysis of Bituminous Coal . . . . .	311
5.2-2	Carbon, Hydrogen, Oxygen, and Total Mass Balances for Bituminous Coal Pyrolysis . . . . .	313
5.3-1	Comparison of Total Yields from Lignite Pyrolysis and Hydropyrolysis . . . . .	321
5.4-1	Comparison of Total Yields from Pyrolysis and Hydropyrolysis of Bituminous Coal . . . . .	337
5.5-1	A Summary of Pyrolysis Results . . . . .	341
5.5-2	Kinetic Parameters for Lignite Pyrolysis . . . . .	347

## 1.0 Summary

### 1.1 Introduction

Previous research at M.I.T. on coal pyrolysis in inert gas and in hydrogen (hydropyrolysis) was based on the measurement of coal weight loss, referred to as volatiles yield (Anthony, 1974; Anthony and Howard, 1976; Anthony et al., 1974, 1975, 1976). Although these previous studies made good progress towards explaining pyrolysis and hydropyrolysis phenomena, it was apparent that a fuller understanding of the phenomena could only be achieved via more detailed chemical analyses of the processes. To this end, this investigation has focussed upon product compositions (liquid, gaseous, and solid) and the kinetics of pyrolysis and hydropyrolysis.

Two coals were chosen for this study, a Pittsburgh Seam (No. 8) Bituminous Coal and a partially dried Montana Lignite. These coals are considered to be representative of the large reserves of Eastern U.S. caking coals and Western U.S. lignites, respectively. The analyses of these coals are presented in Table 1-1.

### 1.2 Background Literature

#### Pyrolysis

Unfortunately in studying coal pyrolysis the characterization of the reactant is as difficult, if not more difficult than, the characterization of the products of the process. Because coal is a somewhat heterogeneous insoluble solid with a large number of distinct moieties, many of the traditional chemical and spectroscopic techniques for organic structure determination cannot be applied easily or unambiguously. A brief review of current thinking on the structure of coal is presented in section 3.1 of this thesis. Some general structural characteristics can be inferred from

Table 1-1 Characteristics of the Coals Examined

Proximate Analysis, <u>Wt.% (as-received)</u>			Ultimate Analysis, <u>Wt.% (as-received)</u>			Petrographic Analysis, <u>Wt.% (mineral-matter-free)</u>		
	<u>Lignite</u> <sup>†</sup>	<u>Bituminous</u> <sup>††</sup>		<u>Lignite</u>	<u>Bituminous</u>		<u>Lignite</u>	<u>Bituminous</u>
Moisture	6.8	1.4	Carbon	59.3	67.8	Vitrinites	69.7	84.5
V.M.	36.9	38.9	Hydrogen	3.8	4.8	Semi-Fusinite	15.2	4.5
F.C.	46.4	48.4	Nitrogen	0.9	1.3	Fusinite	7.9	3.3
Ash	9.9	11.3	Sulfur	1.1	5.3	Micrinite	5.2	4.4
			Oxygen*	18.2	8.1	Exinite + Resinite	2.0	3.3
			Moisture	6.8	1.4			
			Ash	9.9	11.3			
<b>TOTAL</b>	<b>100.0</b>	<b>100.0</b>	<b>TOTAL</b>	<b>100.0</b>	<b>100.0</b>	<b>TOTAL</b>	<b>100.0</b>	<b>100.0</b>

\* By difference.

† The Lignite is a partially dried Montana Lignite from the Savage Mine of the Knife River Coal Mining Company.

†† The Pittsburgh Seam (No. 8) Bituminous coal is from the Ireland Mine of the Consolidation Coal Company.

a knowledge of the more traditional classification parameters, those from the proximate, ultimate, and petrographic analyses of the coal.

Fig. 1-1 summarizes some of the more important structural characteristics of the carbon-hydrogen skeletal structure of coal. The aromaticity (fa) is the fraction of carbon in coal which is present in aromatic structures. Fig. 1-1 presents various estimates of aromaticity as a function of coal rank (represented by the weight percent carbon in the coal, on a dry, mineral matter free basis). For reference, the Montana lignite (74.7% C, d.m.m.f.) is estimated to have an aromaticity of about 0.7, and the Pittsburgh Seam bituminous (80.7% C, d.m.m.f.) around 0.8.

While the carbon in both coals is predominantly located in aromatic structures, other evidence suggests that these aromatic structures are not the large fused ring aromatic clusters once thought to be the backbone of coal structure. Instead, as the data in the lower half of Fig. 1-1 suggest, the average size of the average aromatic ring clusters is only 1 or 2 rings in the case of lignite, and 3-4 rings in the case of the bituminous coal. Based on these data (and many other structural details described in section 3.1) Given (1960) proposed his now classic model of a coal molecule shown in Fig. 1-2. The essential feature of the model is that coal is a polymer-like material composed of repeating 9-10 dihydroanthracene units. The fact that hydroaromatic hydrogen can be thought of as evenly distributed throughout the structure has important ramifications with regard to the chemistry of pyrolysis. Also important to the chemistry of pyrolysis is the distribution of oxygen functional groups.

Based on work with model compounds Van Krevelen (in collaboration with Wolfs and Waterman, 1960) advanced a general theory of coal pyrolysis. These model substances were polycondensation products of various polycyclic aromatics with formaldehyde and had the general structure (possibly



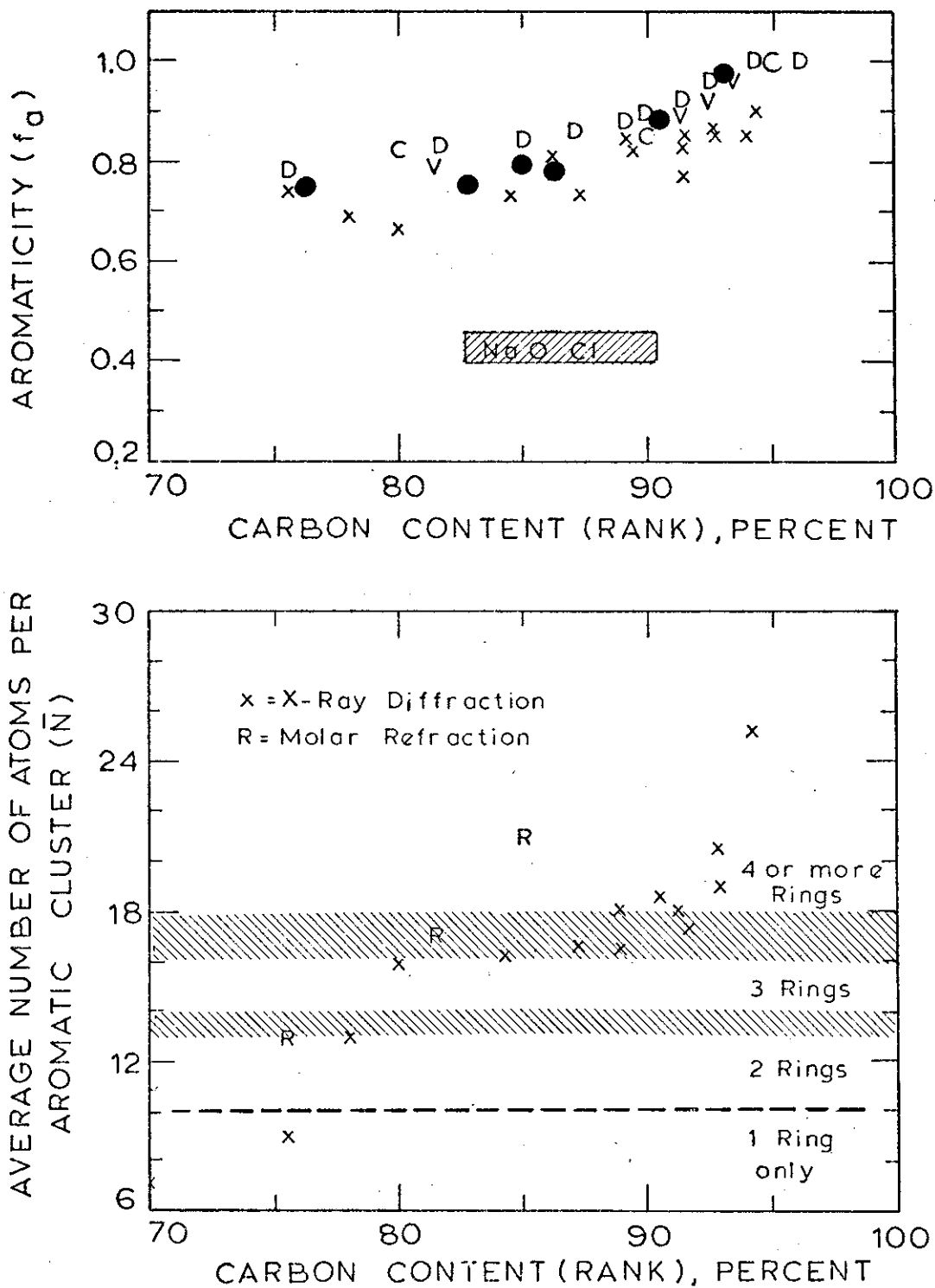


Figure 1-1. Estimates of Coal Structural Parameters (X points, Cartz and Hirsch, 1960; C, D, V, R points, Van Krevelen, 1961; • points, VanderHart and Retcofsky, 1976; 'NaOCl', Chakrabartty and Kretschmer, 1974).

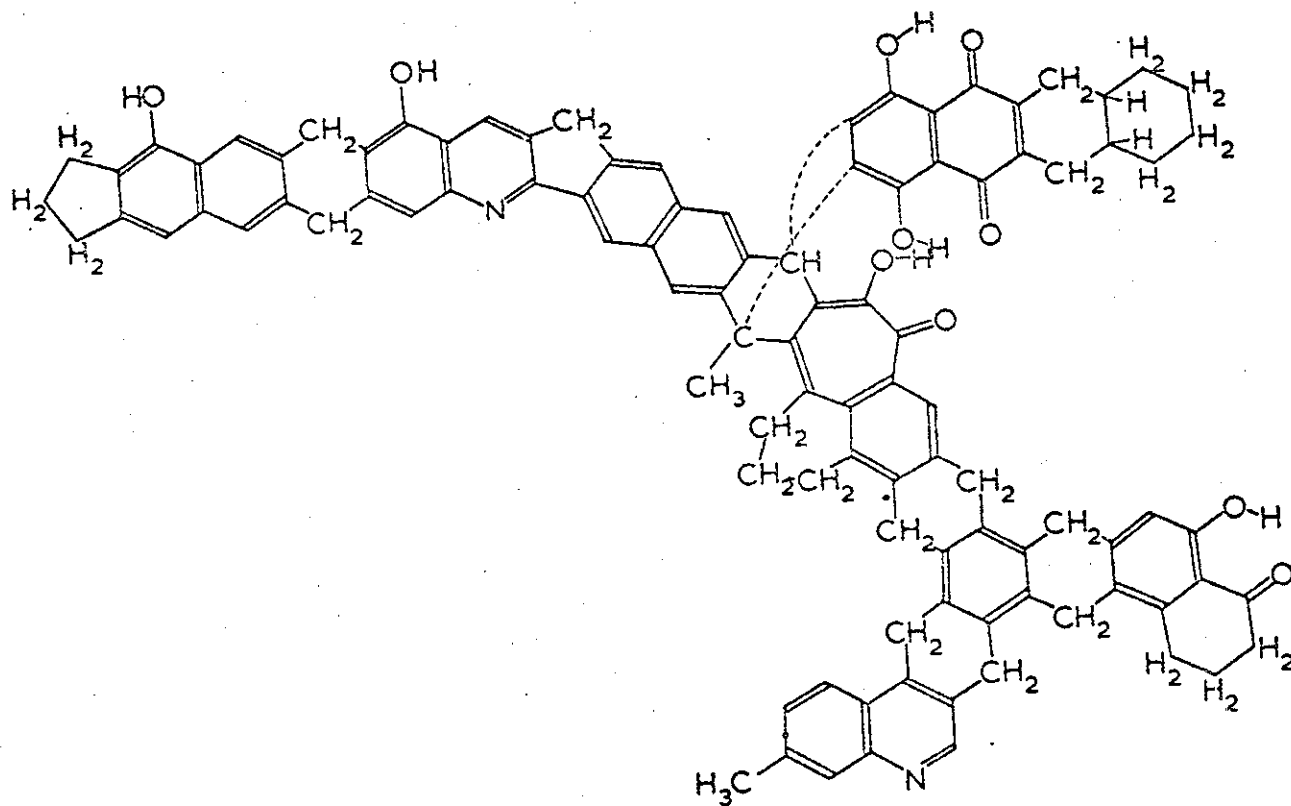
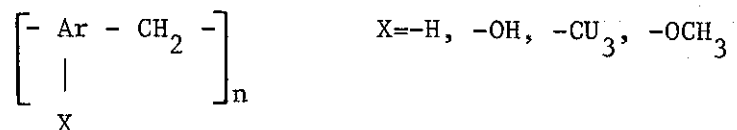


FIGURE 1-2. MODEL STRUCTURE FOR A BITUMINOUS COAL MOLECULE, GIVEN (1960)

branched):



The theory is summarized in Fig. 1-3 and the essential elements of the theory include:

- "Depolymerization" occurs in a completely random manner and is followed by hydrogen disproportionation. The hydrogen in the aliphatic bridging structures or on alkyl substituents is that which stabilizes free radicals. Radicals which cannot be stabilized by hydrogen repolymerize and form the coke residue; stabilized light molecular weight materials are volatile.
- After primary carbonization is complete and the remaining solid is heavily cross-linked and aromatic in nature, the remaining aliphatic hydrogens and the bulk of the aromatic hydrogens are lost.
- The addition of hydroxyl functional groups (X=OH) onto the substance significantly decreases the yield of tar compared to the analogous substance with no -OH group. This is explained in terms of a competition for reactive aliphatic hydrogen between water and hydrocarbon forming reactions.

The concept of hydrogen donor structures within the coal is supported by existence of chloroform extractable (hydrogen-rich) material in the coal. Removal of this material prior to pyrolysis destroys the softening properties of otherwise caking coal (Brown and Waters, 1966). The softening phenomenon is clear indication for the existence of lower molecular weight species in the coal - it is not a physical melting phenomenon.

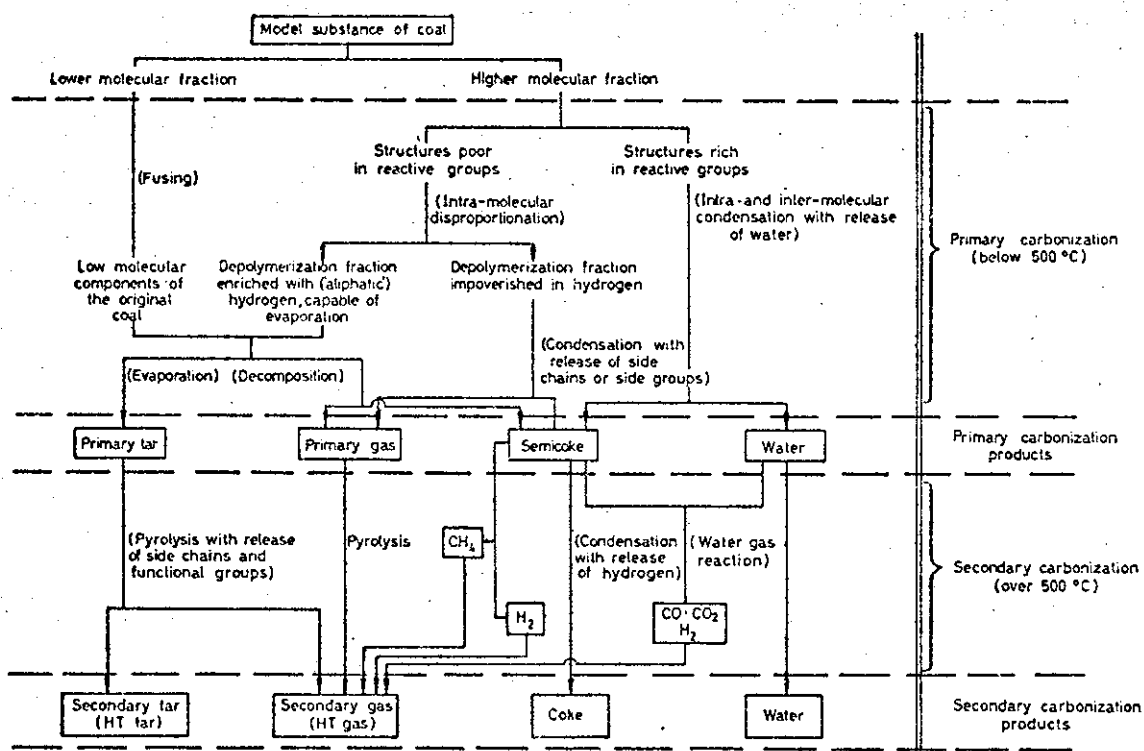


FIGURE 1-3. OVERALL MECHANISTIC SCHEME FOR PYROLYSIS OF COAL-MODEL COMPOUNDS. (WOLFS ET AL., 1960)

Because of the large number of distinct chemical moieties which characterize coal, it is not surprising that more success has not been attained by correlation of the weight loss with simple overall rate laws:

$$\frac{dV}{dt} = k(V^* - V)^n$$

where  $k = k_0 \exp(-E/RT)$ , the Arrhenius rate constant

$V$  = volatile yield at time  $t$

$V^*$  = volatile yield at time  $t \rightarrow \infty$

$n$  = reaction order

Recognizing this fact, Anthony et al. (1975) proposed to model the pyrolysis of coal as being composed of a large number of distinct reactions  $i$ :

$$\frac{dV_i}{dt} = k_i(V_i^* - V_i)$$

For mathematical convenience, it was decided that the reactions  $i$  should be distributed according to activation energy by the Gaussian form (mean activation energy  $E_0$ , standard deviation  $\sigma$ )

$$f(E) = \left[ \sigma(2\pi)^{1/2} \right]^{-1} \exp \left[ -(E - E_0)^2 / 2\sigma^2 \right]$$

Anthony et al. enjoyed good success fitting data on pyrolysis of the same two coals as examined in the present study.

Further verification for the concept of a wide distribution of activation energies for pyrolysis is provided by some recent data on gas evolution during pyrolysis (Campbell and Stephens, 1976, Fig. 1-4). For a more detailed discussion of pyrolysis models, the reader is referred to a recent review of the pyrolysis literature by Anthony and Howard (1976).

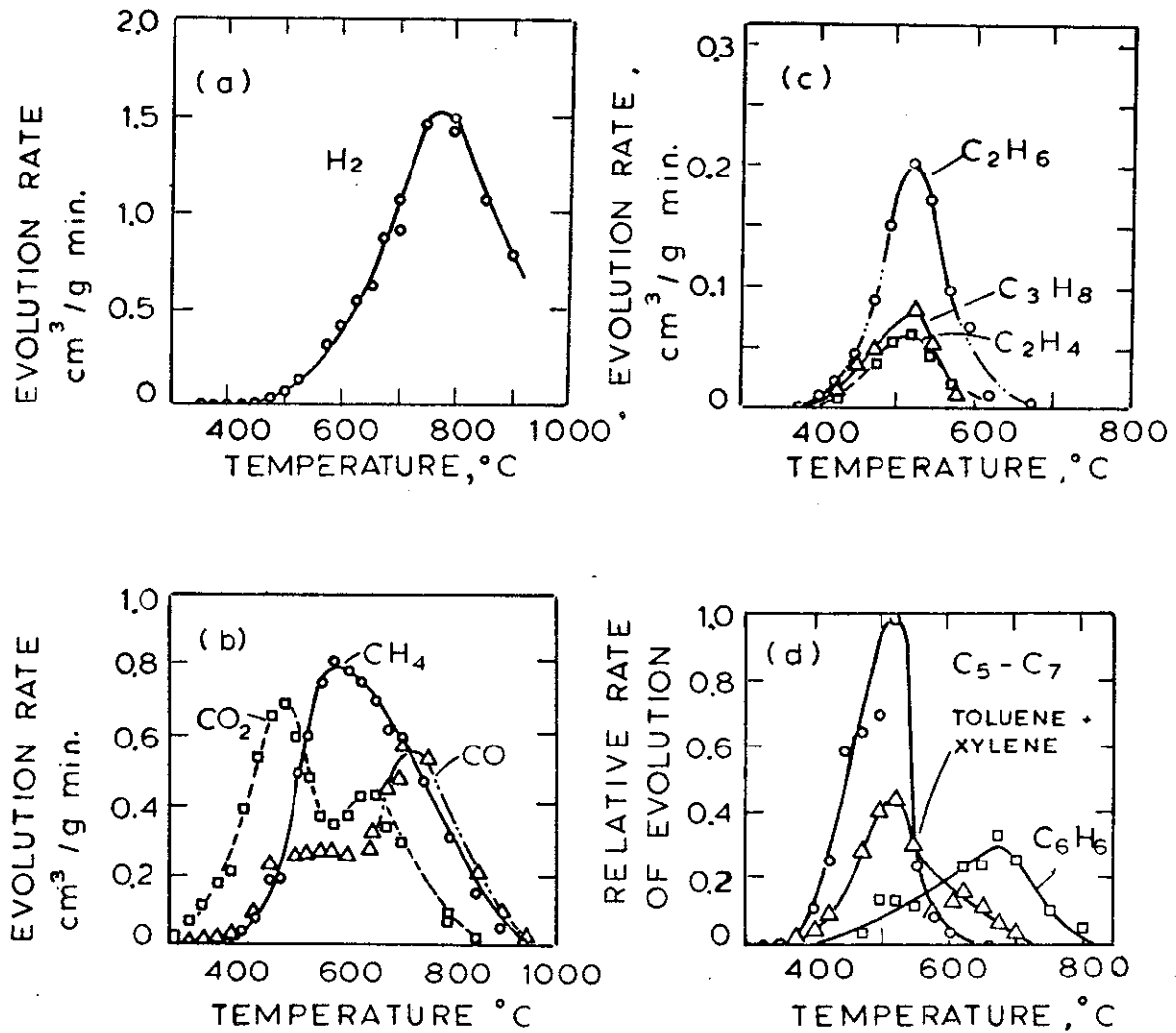
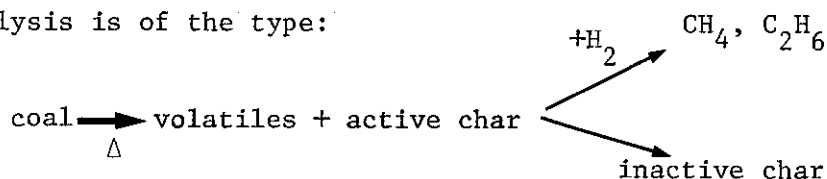


Figure 1-4. Evolution of Gases During the Pyrolysis of a Subbituminous Coal (Campbell and Stevens, 1976; (a), (b), (c) in terms of S.T.P. cm<sup>3</sup>/g coal-min; (d) relative to peak of C<sub>5</sub> - C<sub>7</sub> curve).

## Hydropyrolysis

The study of Hydropyrolysis is still in its infancy compared to the study of pyrolysis (the early interest in the latter primarily due to an interest in coke-making). Hydropyrolysis is a phenomenon distinct from slow hydrogasification ( $C + 2H_2 = CH_4$ ). It is characterized by a rate of the same order as pyrolysis and several orders of magnitude faster than slow hydrogasification.

It is felt that the general scheme relating pyrolysis and hydro-pyrolysis is of the type:



The modelling of hydropyrolysis has focussed principally on the competition between hydrogenation and "deactivation" of active sites within the char.

### 1.3 Apparatus and Procedure

The apparatus (Fig. 1-5) consists of five components: the reactor, designed to contain a coal sample in a gaseous environment of known pressure and composition; the electrical system, used to expose the sample to a controlled time-temperature history; the time-temperature monitoring system; the product collection system; and the product analysis system.

The reactor designed for atmospheric-pressure and vacuum pyrolysis work, consists of a 6-inch (15.24 cm) long, 3-inch (7.62 cm) diameter pyrex glass pipe, blind-flanged at both ends by stainless steel plates having electrical feedthroughs and gas inlet and outlet ports. The coal sample is held and heated in the vessel by a folded strip of 325 mesh stainless

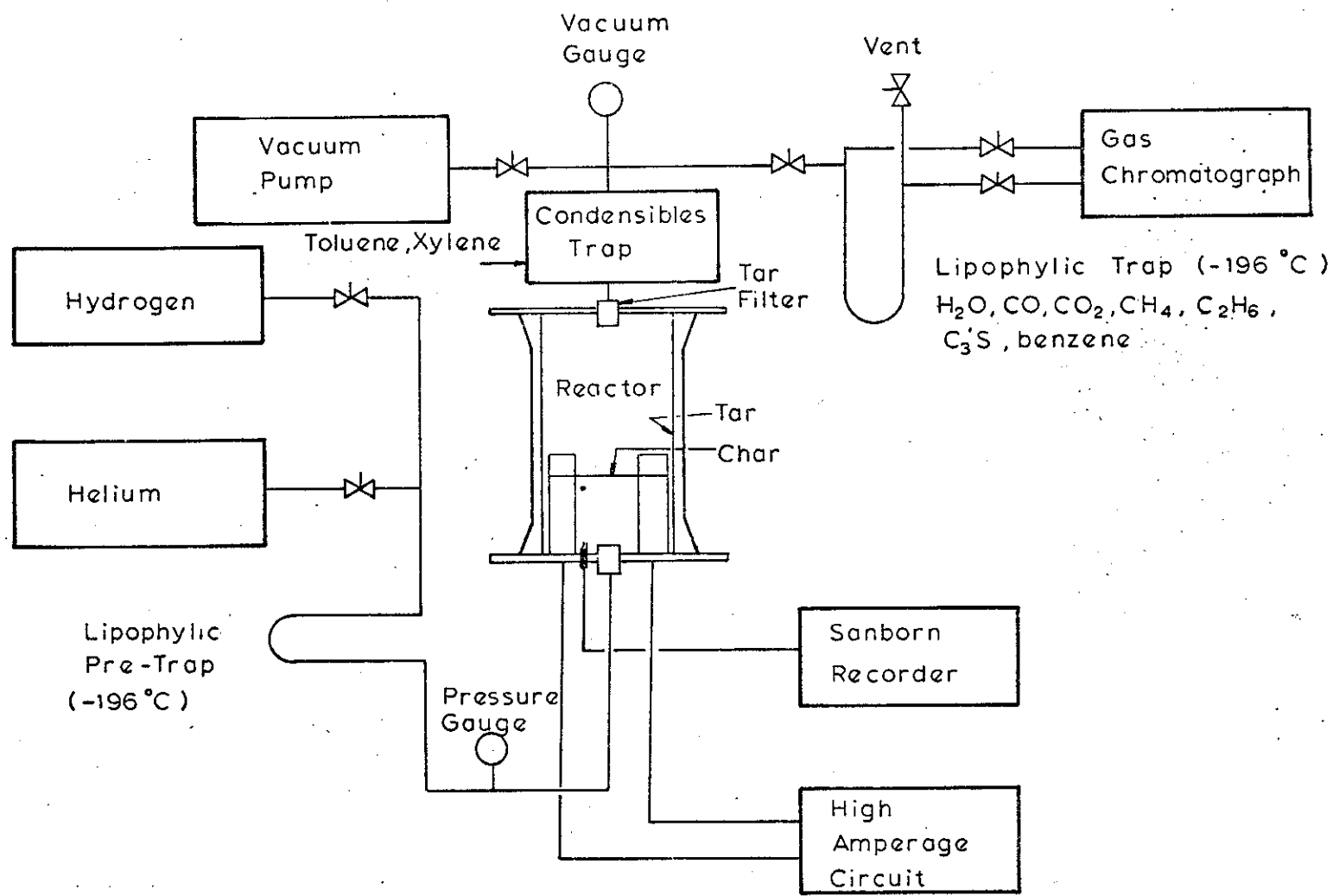


FIGURE 1-5. CAPTIVE SAMPLE APPARATUS AND HEATING SYSTEM.



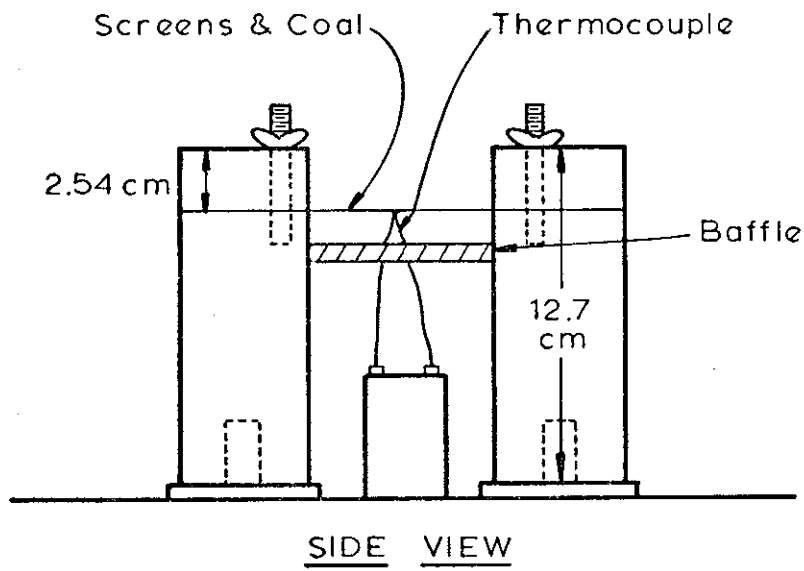
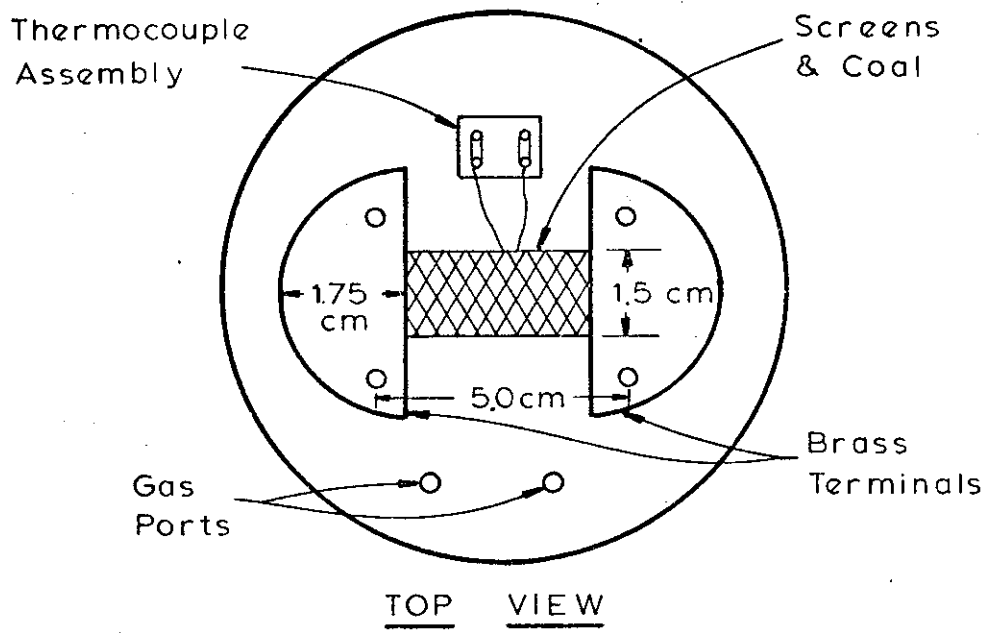


FIGURE 1-6. SAMPLE HOLDING AND HEATING ASSEMBLY

steel screen positioned between two relatively massive brass electrodes as shown in Fig. 1-6. The reactor used for high pressure hydrogenation work is similar, except of course that the shell is stainless steel rather than glass.

The electrical system consists of two automobile storage batteries connected in series to the reactor electrodes through a time-controlled relay switch which cuts in either of two variable resistors at a predetermined time. This circuitry permits independent control of heating rate ( $10^2 - 10^4$  °C/s) and final sample holding time and temperature (150-1100 °C for up to 30 s). The temperature-time history of coal is recorded by a chromel-alumel thermocouple (24  $\mu$ m wire diam., 75  $\mu$ m bead diameter) placed within the sample and connected to a Sanborn fast-response recorder.

Approximately 10-15 mg of powdered coal is spread in a layer one to two particles deep on a preweighed screen which is reweighed and inserted between the brass electrodes. The reactor is evacuated and flushed three to five times with helium and then set at the desired experimental pressure. The sample temperature is raised at a desired rate to a desired holding value which is then maintained until the circuit is broken. Sample cooling by convection and radiation then occurs rapidly since the electrodes, the vessel and its gaseous contents remain cold during the experiment, but not so rapidly as to avoid the occurrence of significant weight loss during cooling.

The yield of char, which remains on the screen, is determined gravimetrically. Products that condense at room temperature (tars and oils, hereafter defined as tars) are collected primarily on foil liners within the reactor and on a paper filter at the exit of the reactor. Any condensation on non-lined reactor surfaces is collected by washing with

methylene chloride soaked filter paper. The tar from all three collections is measured gravimetrically.

Products in the vapor phase at room temperature are collected at the conclusion of a run by purging the reactor vapors through two lipophilic traps. The first trap consists of a 3 inch (7.62 cm) long, 1/4 inch (0.635 cm) diameter tube containing 50/80 mesh Porapak Q chromatographic packing. The trap is operated at room temperature, and collects intermediate weight oils such as benzene, toluene, and xylene. The second trap is a 15 inch to 5 foot long, 1/4 inch diameter tube (38.1 cm x 0.625 cm) also packed with Porapak Q but operated at  $-196^{\circ}\text{C}$  in a dewar of liquid nitrogen. This trap collects all fixed gases produced by pyrolysis, with the exception of hydrogen which is determined by direct vapor phase sampling with a precision syringe.

Products are released for gas chromatographic analysis by warming the first trap to  $240^{\circ}\text{C}$  and the second to  $100^{\circ}\text{C}$ . The intermediate weight oils from the first trap are analyzed on either a 50/80 mesh, 3% OV-17 Porapak Q column, 6 ft x 1/8 in (183 cm x 0.318 cm) 50/80 mesh Porapak Q column, temperature programmed from  $-70$  to  $240^{\circ}\text{C}$  at a rate of  $16^{\circ}\text{C}/\text{min}$ . The hydrogen is analyzed on a 10 ft x 1/8 in (305 cm x 0.318 cm) 80/100 mesh Spherocarb column at  $0^{\circ}\text{C}$ . A Perkin-Elmer Model 3920 B chromatograph with dual thermal conductivity/flame ionization detectors and a Perkin-Elmer Model 1 integrator are used for all the analyses.

Elemental analyses of the raw coal and char samples were performed by Galbraith Laboratories, Inc. of Knoxville, Tennessee.

The weight of the coal and screen was determined to within  $\pm 0.01$  mg; hence, the uncertainty of the total weight loss measurement is about 0.1% by weight of the coal. The products quantitated chromatographically

(except H<sub>2</sub>O) are subject to calibration uncertainties of 1 to 3% of the mass of the species measured. The water measurements were somewhat more troublesome because of (1) moisture loss from the coal during the short time lapse between weighing the sample and performing the run and (2) moisture gain by the experimental system during assembly under high humidity conditions. The net uncertainty in the measured water yields caused by these opposing effects is about 2% by weight of the coal. The tar measurement has its largest uncertainty in the washing procedure. The maximum error for atmospheric pressure runs is about 1% by weight of the coal. The inherent uncertainty of the thermocouple measurements is about  $\pm 8^{\circ}\text{C}$  over the present range of temperatures. The ability of the selected thermocouple effectively to track the temperature of the sample at the highest heating rates was confirmed by experiments with thermocouples of different bead diameters.

Some discoloration of the screen used to hold the sample caused concern that the screen may be a source of error, for example through catalysis of primary pyrolysis or secondary cracking reactions. Experimental assessment of the role of the screen included passivation of the surface with a vacuum deposited layer of gold on some screens and copper on others, and variation of the number of layers of untreated screen through which the volatiles had to escape. Both gold and copper are less catalytic to cracking reactions than is stainless steel, and diffusion of these metals in stainless steel is too slow to destroy the integrity of the surface layer in even the longest residence times of this study. None of these cases lead to significant differences in the total yield of volatiles or in the composition of gaseous products included in the present study. Therefore, any error caused by the screen appears to be negligible for present purposes.

This result is not surprising in view of the high escape velocity of volatiles from the sample and hence the low residence time of volatiles near hot screens. Nevertheless, untreated stainless steel screens in a similar apparatus are reported (P. Solomon, United Technologies, personal communication, 1976) to react significantly with hydrogen sulfide.

This species is not of present concern.

#### 1.4 Results

##### Pyrolysis of a Montana Lignite

All results in this section are reported for the partially dried (as-received) Montana lignite in the particle size range 53-88 $\mu$  (74 $\mu$  average diameter).

With the exception of the data points carrying a double symbol (see below), the volatile product compositions shown in Fig. 1-7 were obtained when different samples of the lignite under 1 atm (101.3 kPa) of helium were heated at approximately 1000°C/s to various peak temperatures indicated on the abscissa. The samples were cooled at roughly 200°C/s beginning immediately when the peak temperature was attained. The total yield of any product or group of products is given on the ordinate as a weight percent of the partially dried lignite.

The lowest curve represents the yield of tar as defined above, which increases with increasing temperature to an asymptotic maxima of about 5.4% by weight of the lignite at temperatures above 750 to 800°C. This material has an empirical formula of  $\text{CH}_{1.5}^{\text{O}}_{0.1}\text{N}_{0.01}$ .

The distance between the tar curve and the next one above it represents hydrogen and all hydrocarbons lighter than tar. The maximum yield of these species occurs at the higher temperatures and is only about 3.3% by weight.

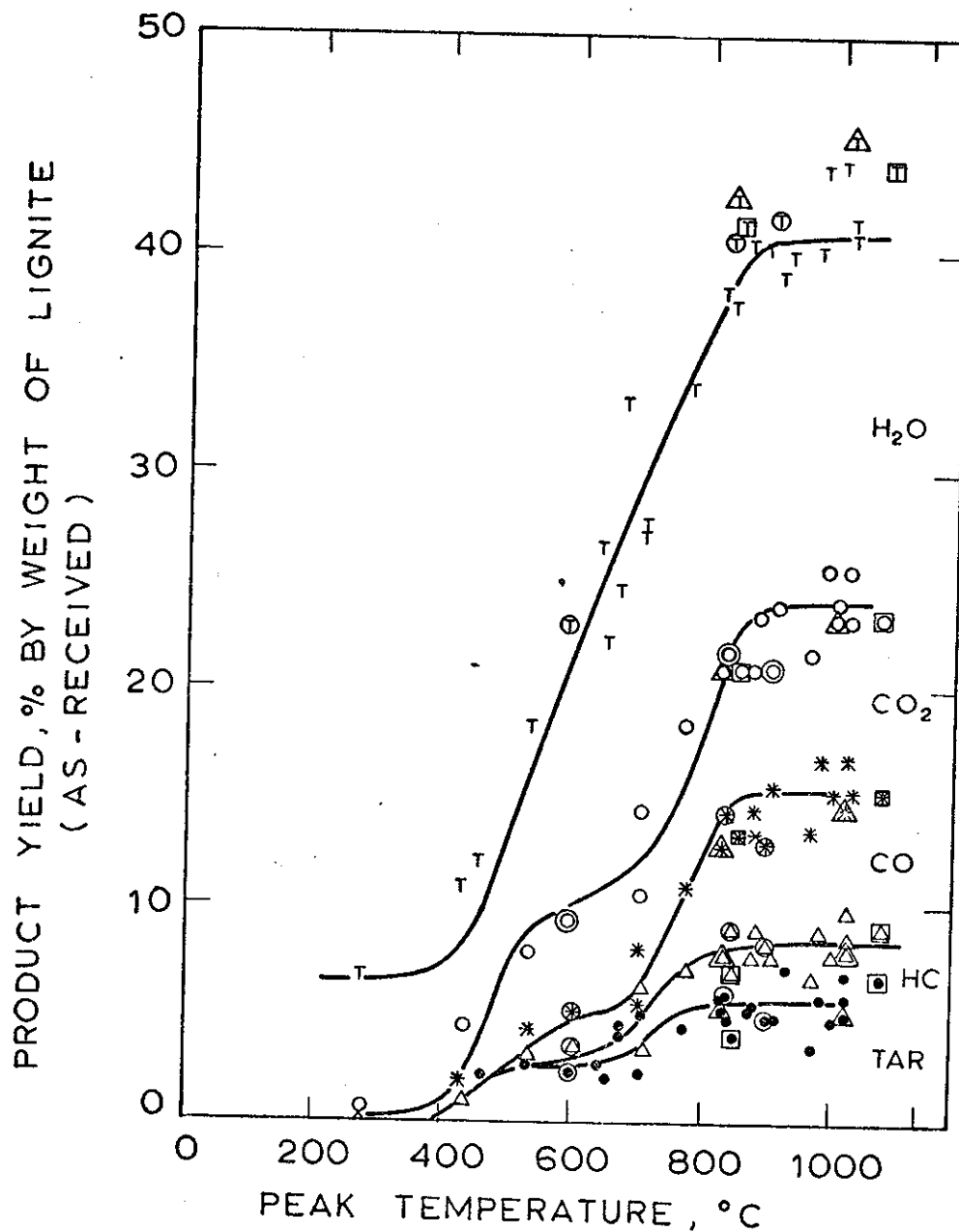


Figure 1-7. Pyrolysis Product Distributions from Lignite Heated to Different Peak Temperatures ((●)tar; (Δ)tar and other hydrocarbons(HC); (\*)tar,HC, and CO; (o)tar,HC,CO, and CO<sub>2</sub>; (T) total, i.e., tar HC,CO,CO<sub>2</sub>, and H<sub>2</sub>O. Pressure=1 atm (He). Heating Rates: basic, 1000°C/s;(pts inside o) 7100 to 10,000°C/s;(pts inside Δ) 270 to 470°C/s;(pts inside □)2-step heating.)

of the lignite. The main components are methane (1.4%), ethylene (0.6%), and hydrogen (0.5%), with identified ethane, propylene, propane, and benzene and unidentified trace hydrocarbons making up the balance. The effect of temperature on yields of methane, hydrogen and ethylene is shown in Fig. 1-8. When the peak temperature is increased above 500°C the methane and ethylene yields increase rapidly to small asymptotic values in the range 600 - 700°C. Further increase in temperature beyond 700°C effects a dramatic increase in the yield of both species, and a second asymptote is reached at about 850°C for ethylene and about 900°C for methane. The yield of tar also exhibits a similar two-step behavior but hydrogen production, on the other hand, appears to occur in one step at relatively high temperatures.

The top curve in Fig. 1-7 represents the total yield of volatiles while, proceeding downward, the first, second and third regions between adjacent curves represent the yields of water, carbon dioxide, and carbon monoxide, respectively. The yields of these principal oxygenated species are shown in more detail in Fig. 1-9 where all three appear to approach high-temperature asymptotic yields of 16.5% for water, 8.4% for carbon dioxide, and 7.1% for carbon monoxide. The carbon oxides each exhibit also a lower-temperature asymptote.

Although most of the pyrolysis is complete for peak temperatures above about 900 to 1000°C, there is in fact yet a third step in the curves for the carbon oxides which occurs at about 1100°C and therefore does not appear in Fig. 1-9. Since this temperature is the upper limit of the apparatus, investigation of this third step was accomplished by use of a longer residence time technique. The coal was heated at 1000°C/s to 1000°C and there held for 5 to 10 s rather than being immediately cooled as before.

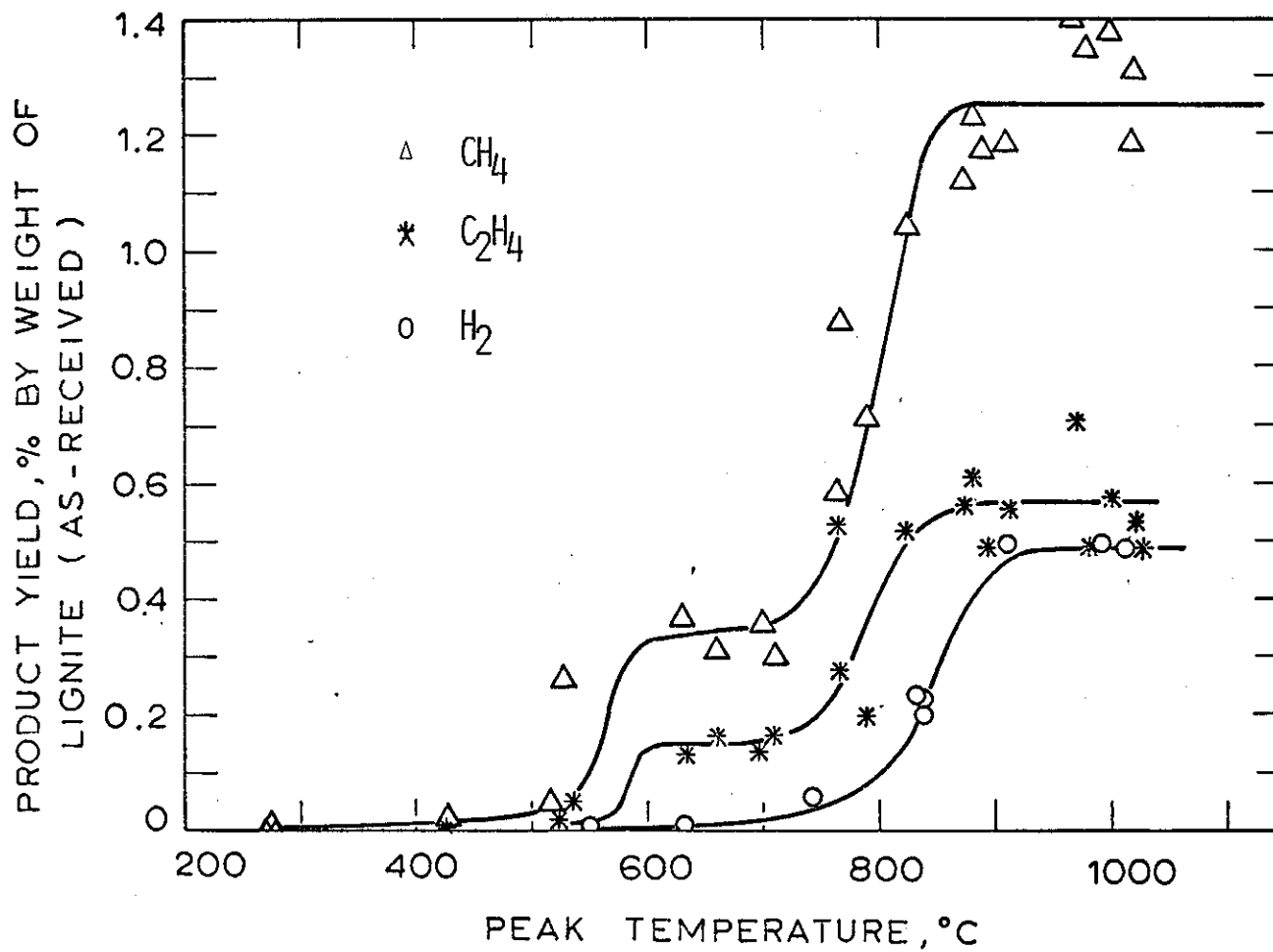


Figure 1-8. Yields of Methane, Ethylene, and Hydrogen from Lignite Pyrolysis to Different Peak Temperatures. (Pressure=1 atm He. Heating Rate=1000°C/s)



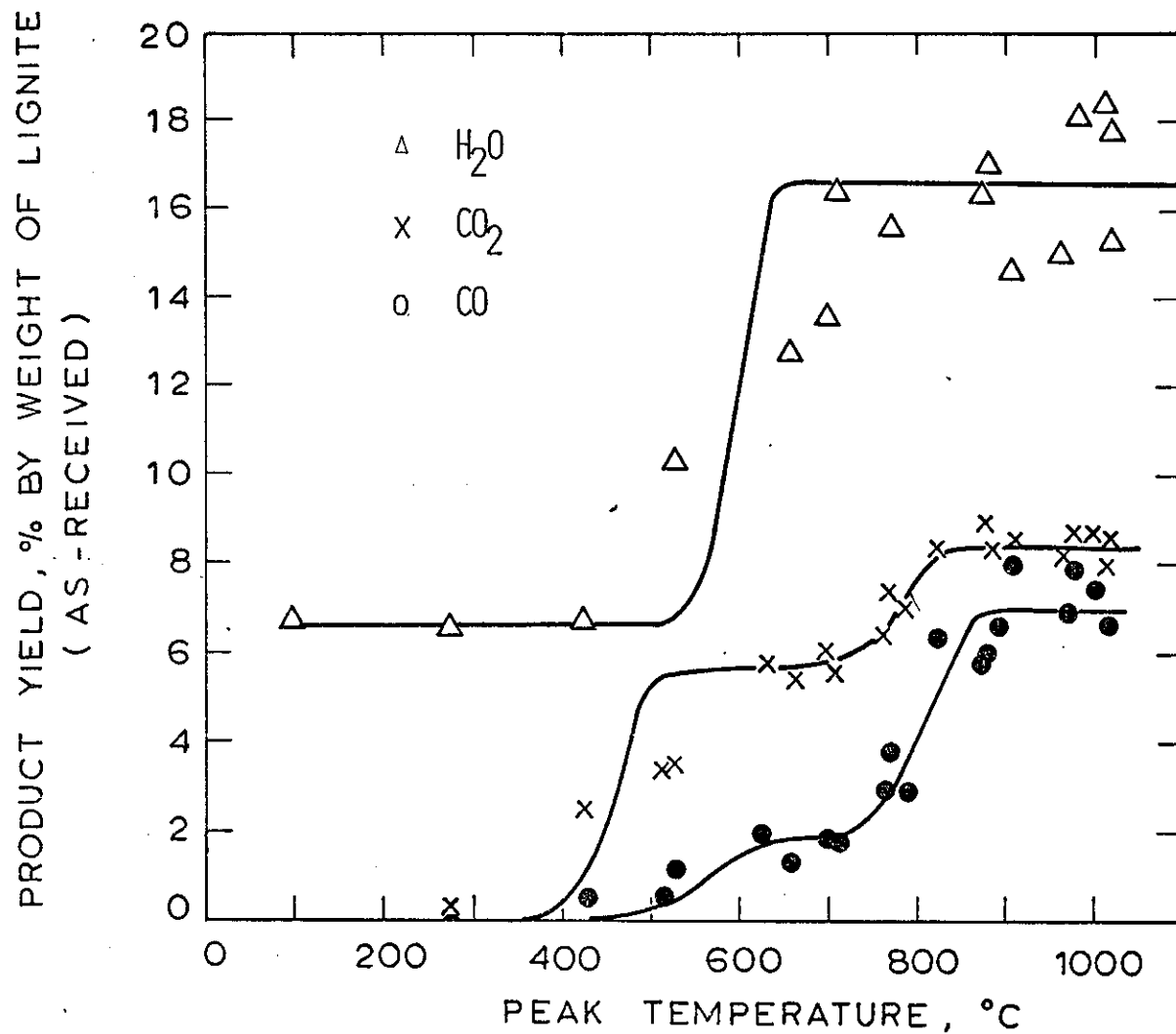


FIGURE I-9. YIELDS OF WATER, CARBON MONOXIDE, AND CARBON DIOXIDE FROM LIGNITE PYROLYSIS TO DIFFERENT PEAK TEMPERATURES (PRESSURE= 1ATM HE, HEATING RATE= 1000°C/s)

The resulting carbon monoxide yield exhibits a final asymptote of 9.4% while that of carbon dioxide is 9.5%. The yields of the other species were not changed by the additional residence time. Thus prolonged heating at 1000°C gave a total volatiles yield of 44.0% by weight of the lignite which is close to the ASTM volatile matter plus moisture (43.7%).

Elemental analyses of selected char samples are shown in Fig. 1-10. Although over 40% by weight of the lignite is volatilized at the higher temperatures, only 22% of the carbon is volatilized. Most of the volatile material comes from hydrogen and oxygen, which is consistent with the observed predominance of water among the volatile products. Pyrolysis at the higher temperatures removes about 70% of the sulfur from the solid material, but the nitrogen is reduced by only about 25%. Consequently, the sulfur content (percent by weight) in the char is lower than that of the lignite, but the reverse is true for nitrogen.

Elemental balances were calculated for runs in which both volatile products and char were analyzed. For estimation purposes, trace hydrocarbons (total less than 1% by weight of the lignite) were assumed to be 90% carbon and 10% hydrogen by weight. Typical results for four runs to different peak temperatures are presented in Table 1-2 along with total mass balances. Whereas the mass balances are excellent and the carbon and hydrogen balances are satisfactory, the oxygen balances are marginal. Since oxygen in char is determined by difference, uncertainties inherent in the other measurements are absorbed in the oxygen values.

Data points inside squares in Fig. 1-7 were obtained with the base conditions given above but modified as follows. The lignite was first heated to an intermediate temperature and then cooled to room temperature as before. The resulting char was then heated to a higher temperature and

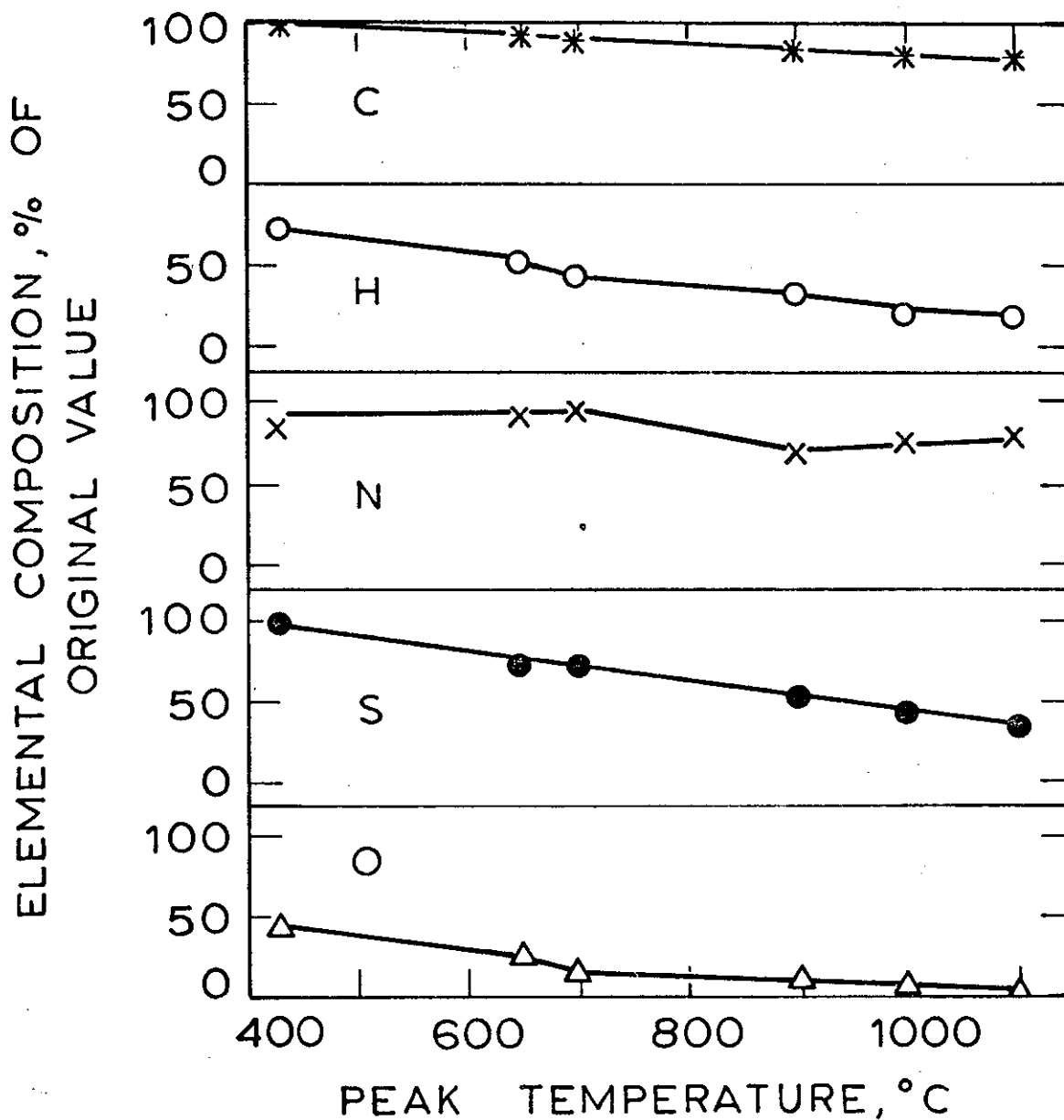


Figure 1-10. Elemental Compositions of Chars from Lignite Pyrolysis to Different Peak Temperatures [(\*) C; (o) H; (\*) N; (●) S; (Δ) O. Pressure = 1 atm (helium). Heating rate = 1000°C/s].

Table 1-2 Carbon, Hydrogen, Oxygen and Total Mass Balances for Lignite Pyrolysis

Product	Yield, weight % of Lignite (as-received) <sup>+</sup> , in Four Runs to Different Peak Temperatures															
	Peak Temperature 430°C				Peak Temperature 710°C				Peak Temperature 910°C				Peak Temperature 1000°C			
	Total	C	H	O	Total	C	H	O	Total	C	H	O	Total	C	H	O
CO <sub>2</sub>	2.5	0.68	-	1.8	5.5	1.5	-	4.0	8.6	2.3	-	6.3	8.7	2.4	-	6.3
CO	0.46	0.20	-	0.26	1.8	0.77	-	1.0	8.0	3.4	-	4.6	7.5	3.2	-	4.3
HC*	0.02	0.02	0.0	-	0.95	0.79	0.17	-	2.6	2.1	0.49	-	3.0	2.4	0.58	-
Tar	1.5	1.3	0.15	-	2.3	2.1	0.23	-	4.9	4.4	0.49	-	4.7	4.3	0.47	-
H <sub>2</sub> O	6.6	-	0.73	5.9	16	-	1.8	14	15	-	1.7	13	19	-	2.1	17
H <sub>2</sub>	0.0	-	0.0	-	0.01	-	0.01	-	0.50	-	0.50	-	0.50	-	0.50	-
Char	89.0	64.0	2.8	11.0	73.0	53.6	1.5	3.1	60.9	47.5	1.2	2.6	55.8	44.2	0.55	1.1
Total	100	66.2	3.68	19.0	99.9	58.8	3.71	22.1	101	59.7	4.38	26.5	99.2	56.5	4.20	28.7
Closure	100%	112%	81%	79%	100%	99%	82%	91%	101%	101%	97%	110%	99%	95%	93%	119%

\* Hydrocarbons other than tar

<sup>+</sup> Lignite (as-received) is 59.3%C, 4.53% H and 24.2%O, including H and O in lignite moisture.

again cooled. The figure shows cumulative product yields for both cycles. The intermediate temperatures for the points at 855°C and 1070°C are 480°C and 670°C, respectively. The yields of all products in both cases are not significantly different from those obtained when the lignite is heated directly to the final peak temperature. Such behavior is indicative of multiple parallel independent reactions as opposed to competitive reactions.

The encircled data points in Fig. 1-7 were obtained at heating rates of 7,100 to 10,000°C/s which is approximately ten-times higher than that of the base data. The points in triangles represent data taken at 270 to 470°C/s. No clear effect of heating rate is observed over the range here used. It is shown below that this behavior is expected for independent parallel, rather than competitive reactions.

A small effect of external pressure (vacuum to 69 atm. of helium) was observed on the results of lignite pyrolysis (Fig. 1-11). Since the effect of pressure is much larger in the case of bituminous coal, discussion of the effect will be reserved until the next section.

It should be noted that under no conditions did the lignite show any evidence of softening, swelling, or agglomerating. There was, however, some evidence of decrepitation of the lignite particles, as some small flecks of coal appeared to be mixed with the tar.

#### Pyrolysis of a Pittsburgh Seam Bituminous Coal

As in the previous section, all results in this section are for particles in the size range 53-88 $\mu$  (74 $\mu$  average) unless otherwise noted.

Figure 1-12 presents an overview of volatile product evolution during bituminous coal pyrolysis. The time-temperature histories implied by the peak temperature are the same as described in the lignite section.

PRODUCT YIELD, WEIGHT % OF LIGNITE (AS RECEIVED)

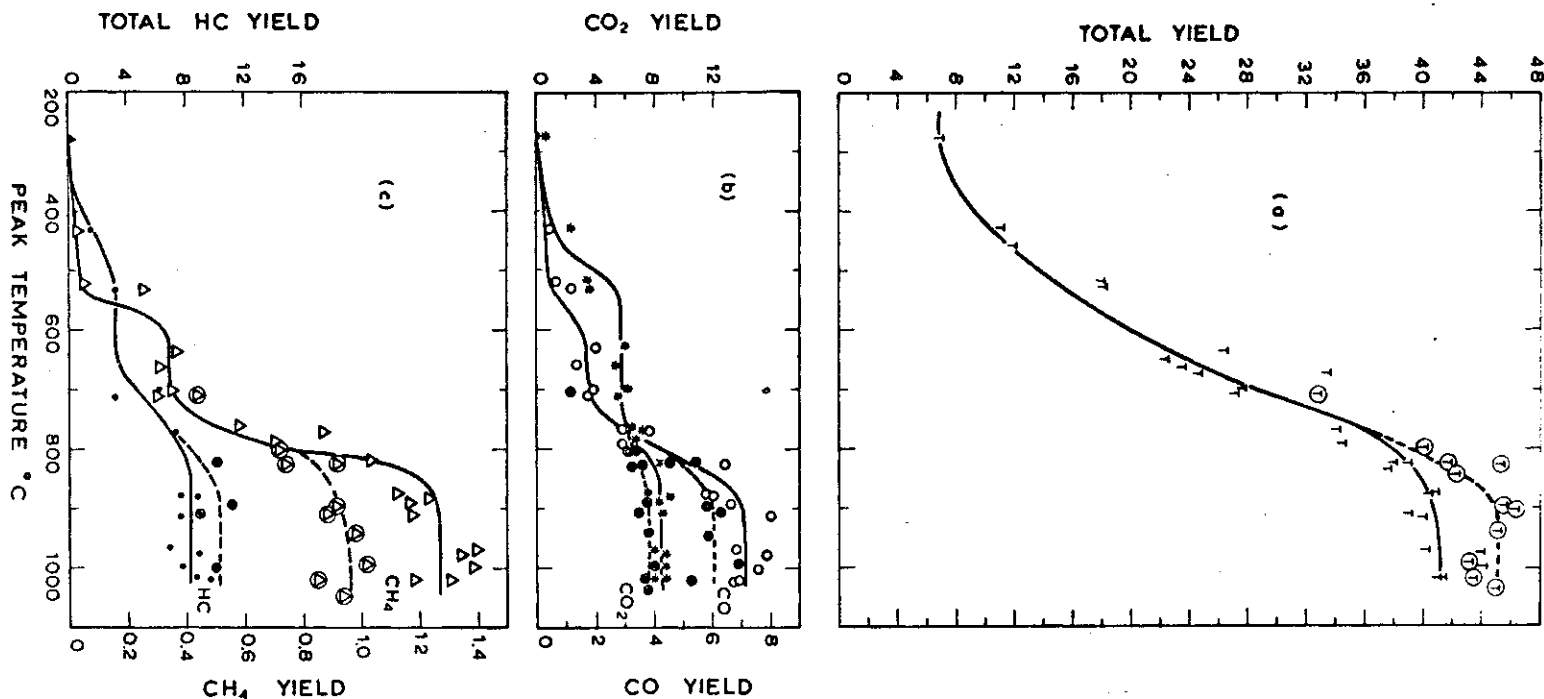


Figure 1-11. Effect of Pressure on Product Yields from Lignite Pyrolyzed to Different Peak Temperatures [Pressure: (single points and solid curves) 1 atm; (points inside 0 and dashed curves)  $6.6 \times 10^{-5}$  atm. Heating rate =  $1000^\circ\text{C/s}$ . (T) total, i.e., tar, all other hydrocarbons,  $\text{H}_2\text{O}$ ,  $\text{CO}_2$  and  $\text{CO}$ ; (o)  $\text{CO}$ ; (\*)  $\text{CO}_2$ ; ( $\Delta$ )  $\text{CH}_4$ ; (●) total hydrocarbons including tar].

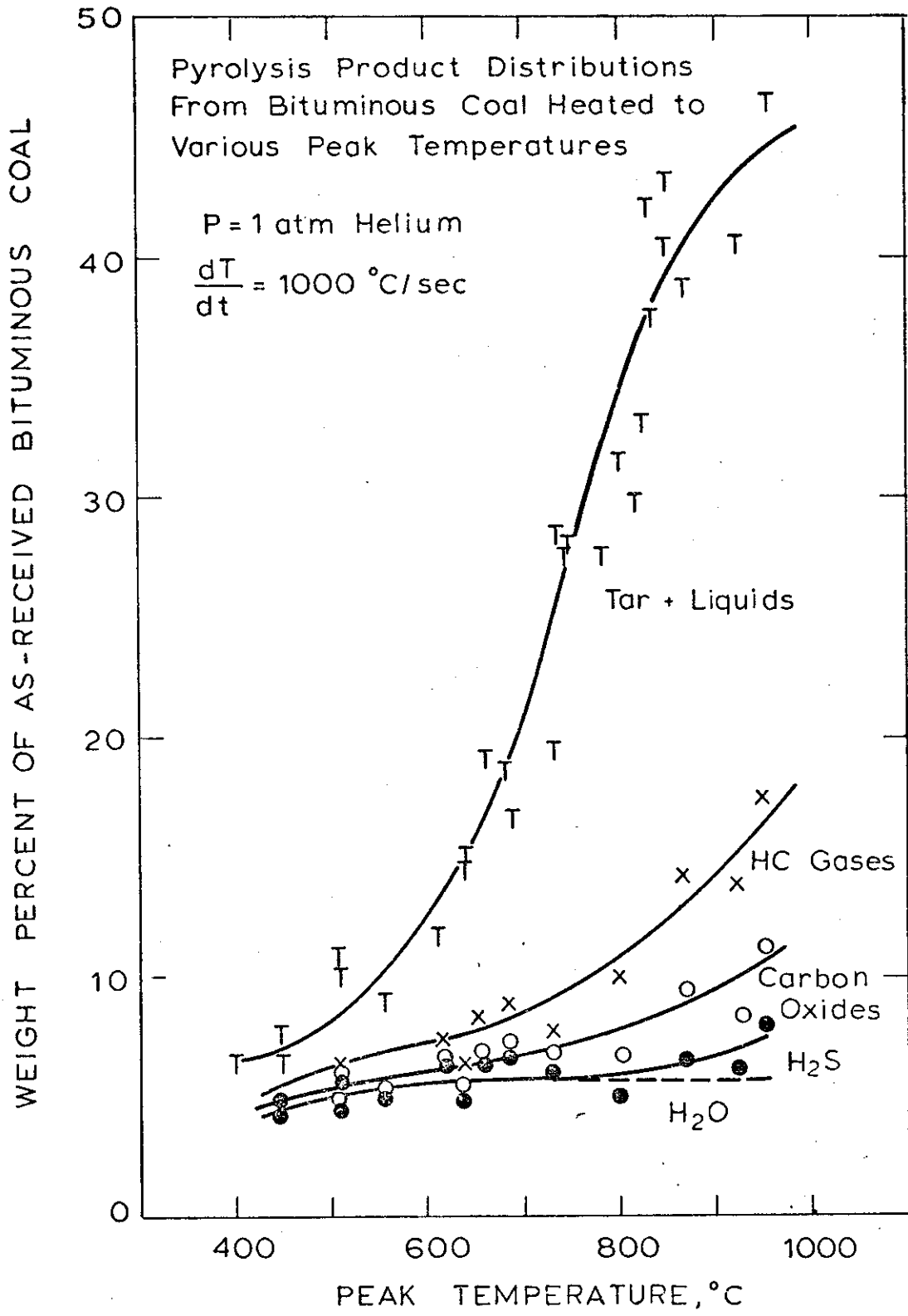


FIGURE 1-12. PYROLYSIS PRODUCT DISTRIBUTION FROM BITUMINOUS COAL HEATED TO DIFFERENT PEAK TEMPERATURES.

Comparison of Figs. 1-12 and 1-7 points up a major difference between lignite pyrolysis and bituminous coal pyrolysis; while in the former case, the products are dominated by light oxygenated species, in the latter case heavy tars (Empirical formula  $\text{CH}_{1.1}\text{O}_{0.08}\text{N}_{0.01}$ ) predominate. The two coals also exhibit markedly different physical behavior during pyrolysis. While the lignite is completely non softening, the bituminous coal exhibits a very fluid behavior upon heating to over  $700^{\circ}\text{C}$  (the onset of softening can begin at peak temperatures as low as  $400^{\circ}\text{C}$ ). At temperatures over  $700^{\circ}\text{C}$ , the concept of a particle diameter no longer makes sense; rather, fluid coal forms a uniform layer on the screen.

Fig. 1-13 displays the behavior of the tar and water products separately. The results in the left hand portion of the figure are for the previously described completely non-isothermal time temperature history. The right hand portion of the figure shows data obtained in a set of runs wherein the peak temperature is isothermally held for a few seconds before the quench is initiated. Such runs are useful for establishing the existence of high temperature asymptotes. Fig. 1-13 shows that most water is produced at rather low peak temperatures ( $<400^{\circ}\text{C}$ ). Tar production begins at a peak temperature of about  $400^{\circ}\text{C}$  and continues through  $900^{\circ}\text{C}$ .

Fig. 1-14 through 1-16 show the behavior of various other volatile components, plotted in the same manner as Fig. 1-13. The evolution curves for bituminous pyrolysis are distinctly different from those for lignite pyrolysis as in no case is a two step behavior observed.

Fig. 1-17 gives the results of analyses of the bituminous char. During pyrolysis at  $1000^{\circ}\text{C}$ , roughly half of the carbon originally present in the coal is volatilized while almost 90% of the hydrogen is volatilized. The extent of carbon volatilization is about twice as high as that observed for the lignite. As in the case of lignite, almost  $2/3$  of the nitrogen is



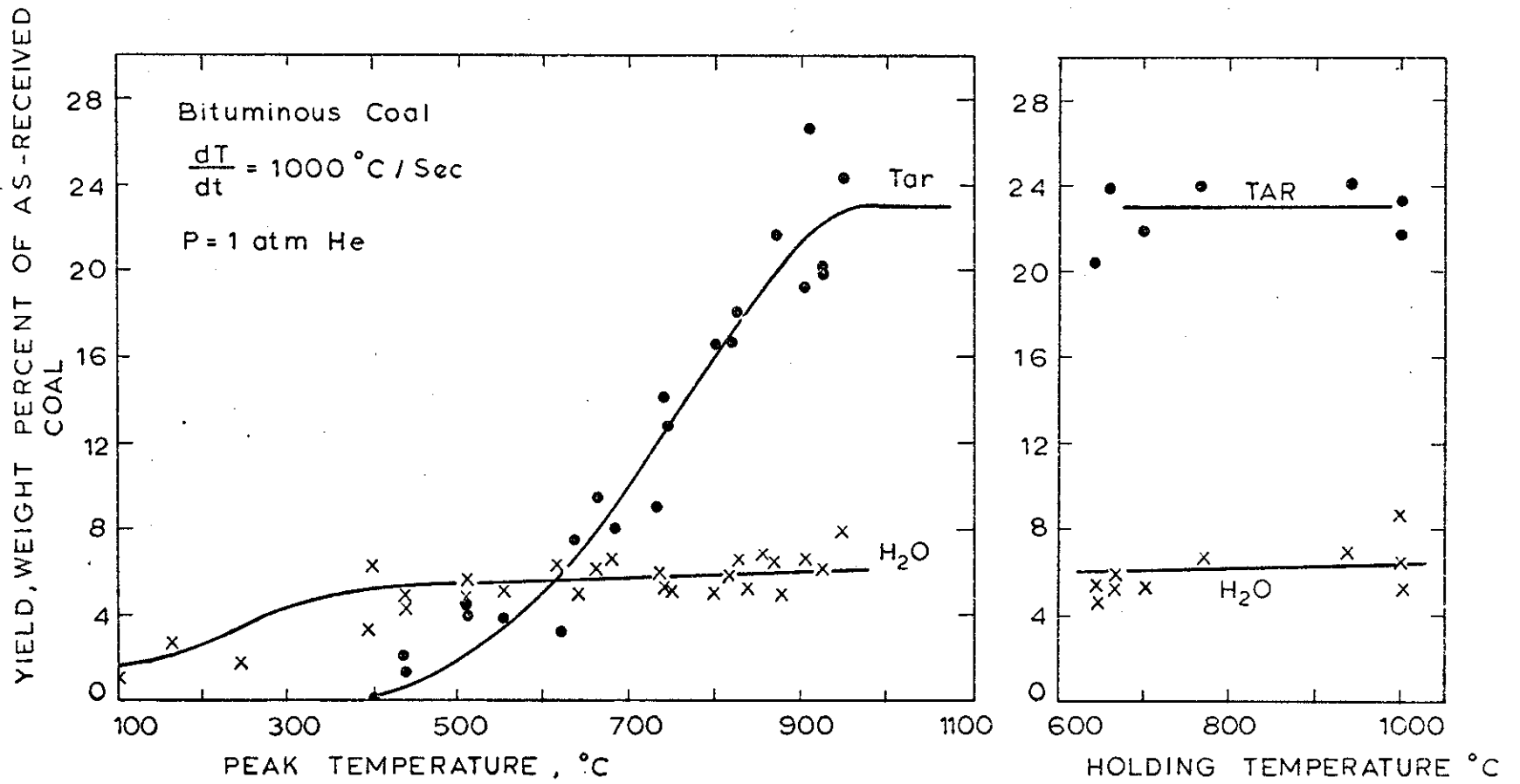


FIGURE 1-13. YIELDS OF TAR AND WATER FROM BITUMINOUS COAL PYROLYSIS.

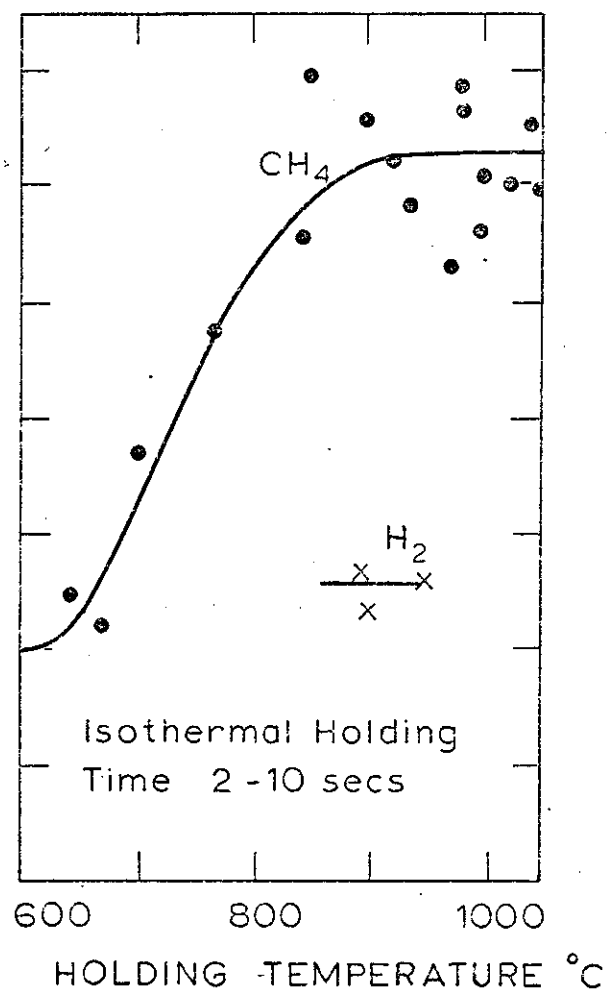
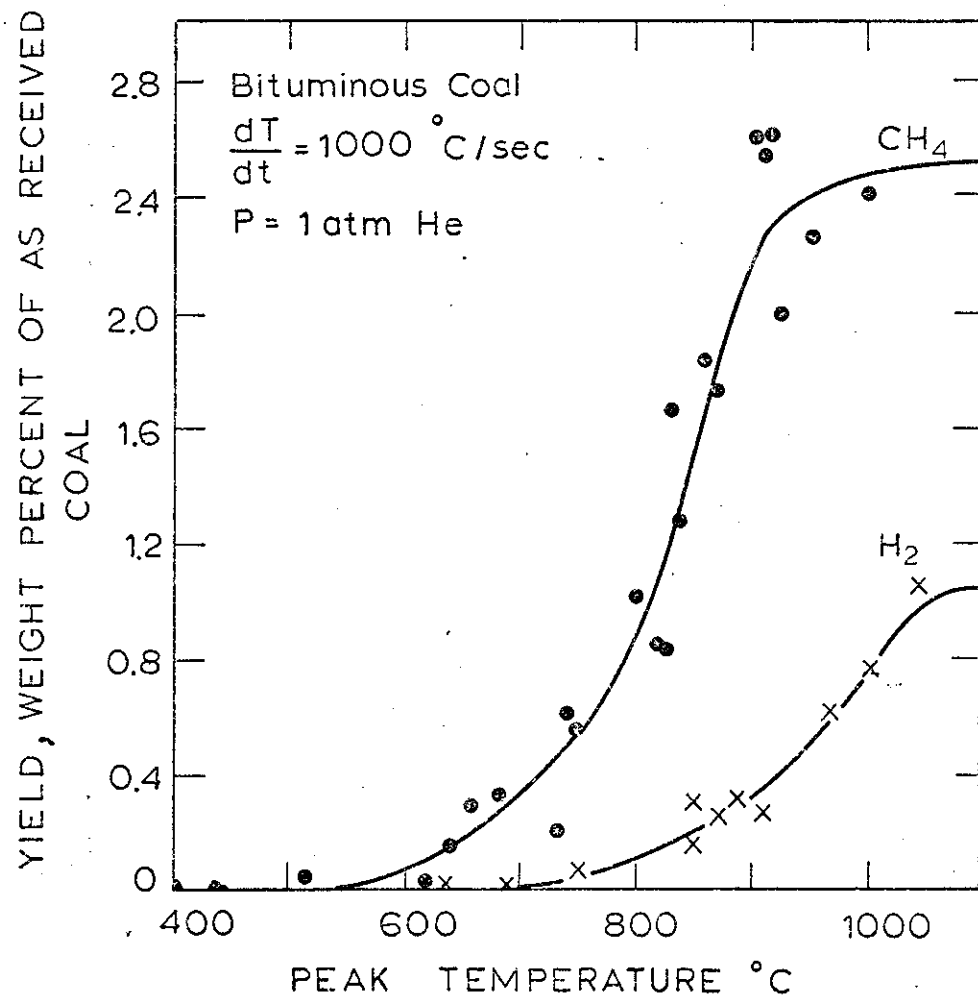


FIGURE 1-14. YIELDS OF METHANE AND HYDROGEN FROM BITUMINOUS COAL PYROLYSIS.

YIELD, WEIGHT PERCENT OF AS RECEIVED  
COAL

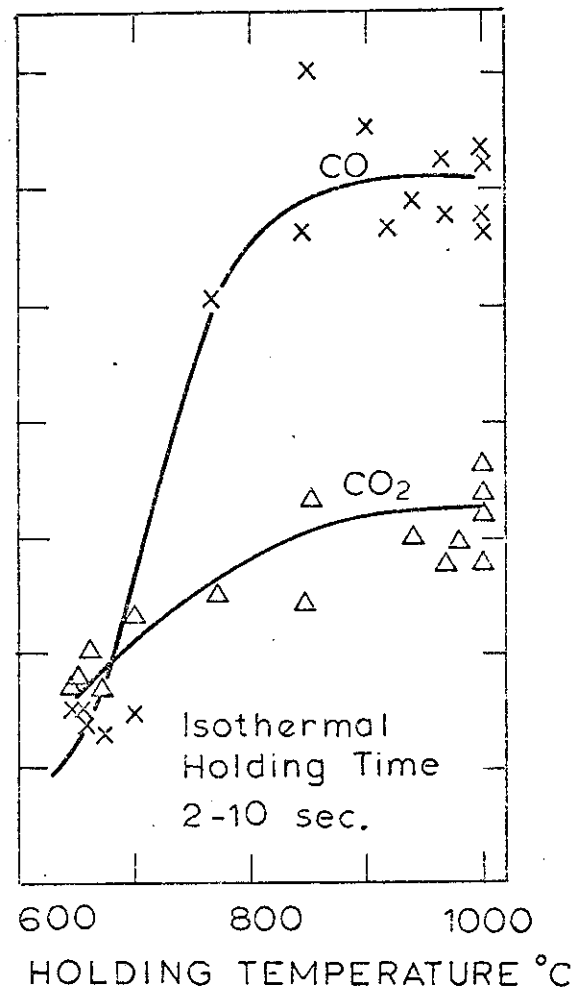
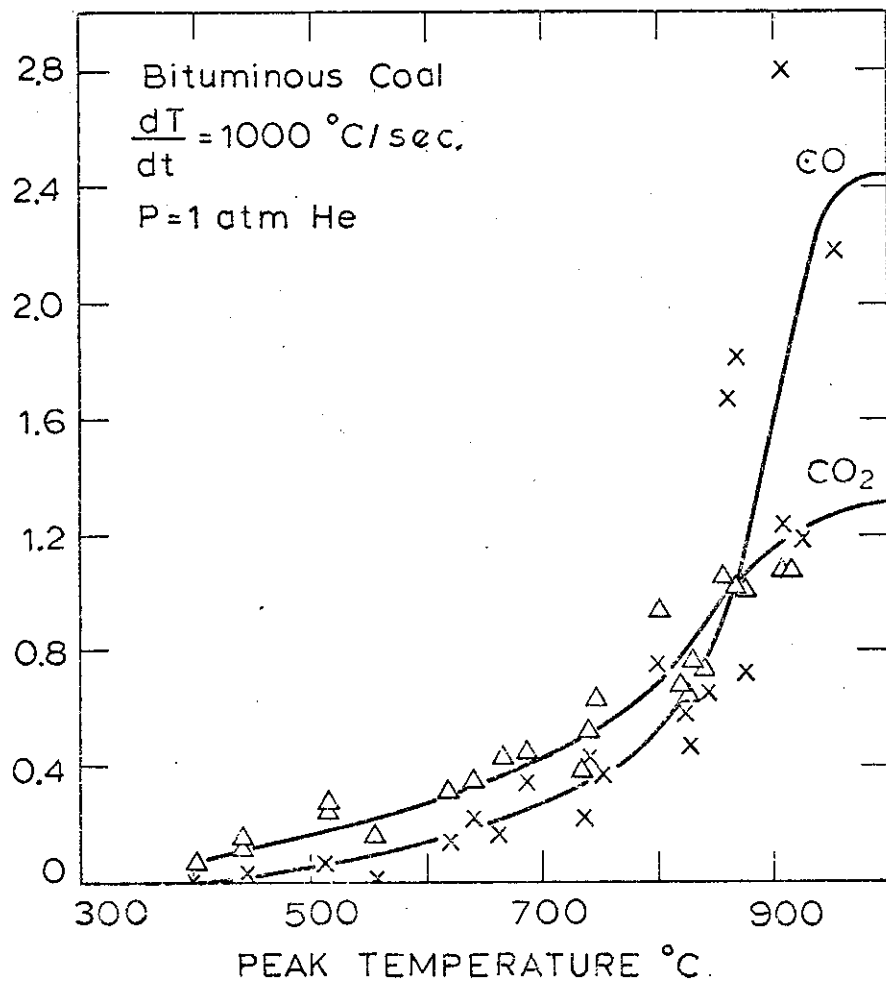


FIGURE 1-15. YIELDS OF CARBON MONOXIDE AND CARBON DIOXIDE FROM BITUMINOUS COAL PYROLYSIS

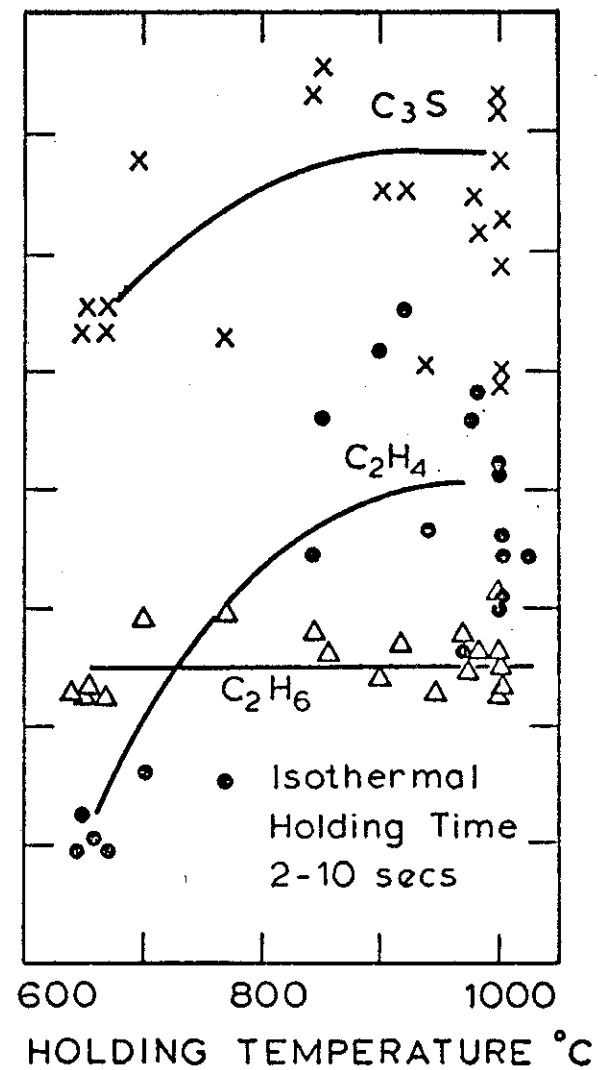
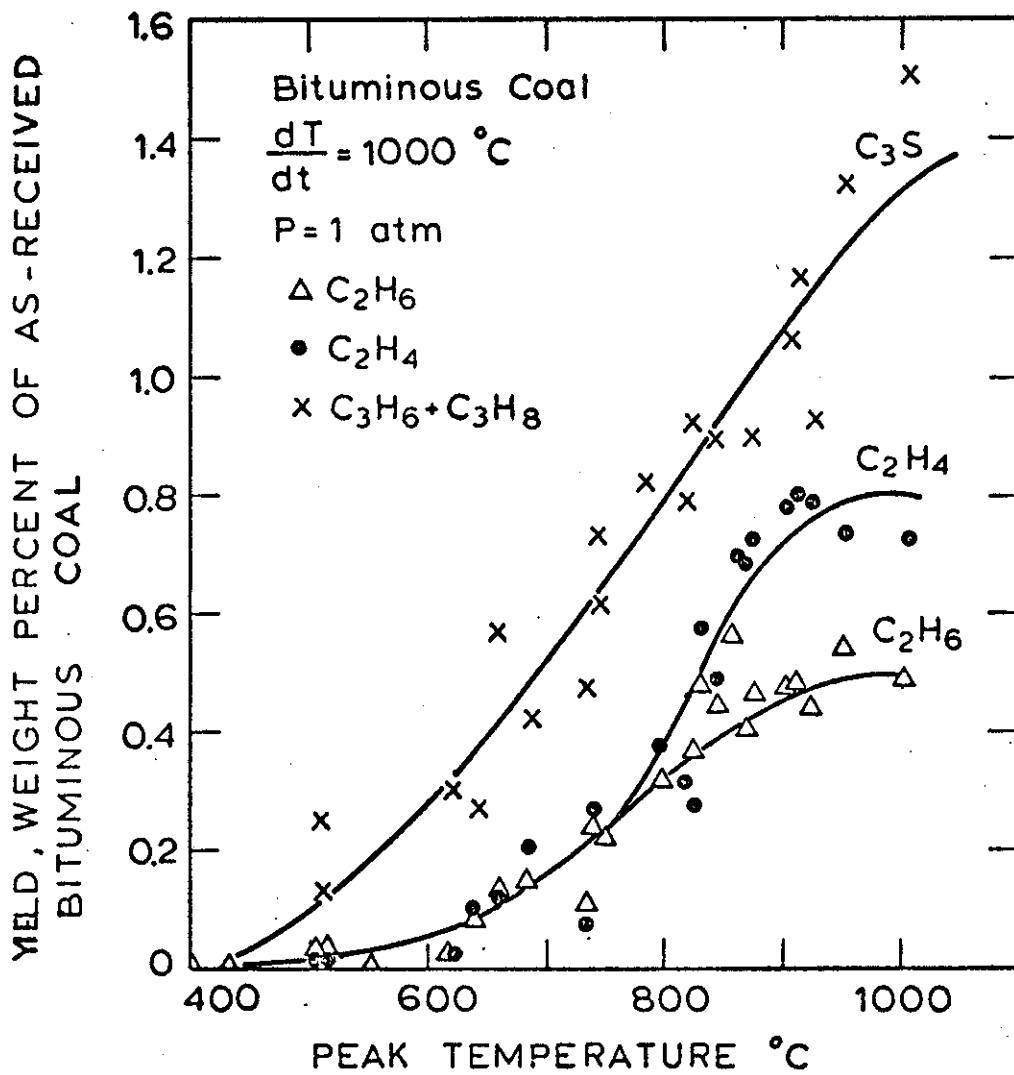


FIGURE 1-16. YIELDS OF VARIOUS HYDROCARBON GASES FROM BITUMINOUS COAL PYROLYSIS.

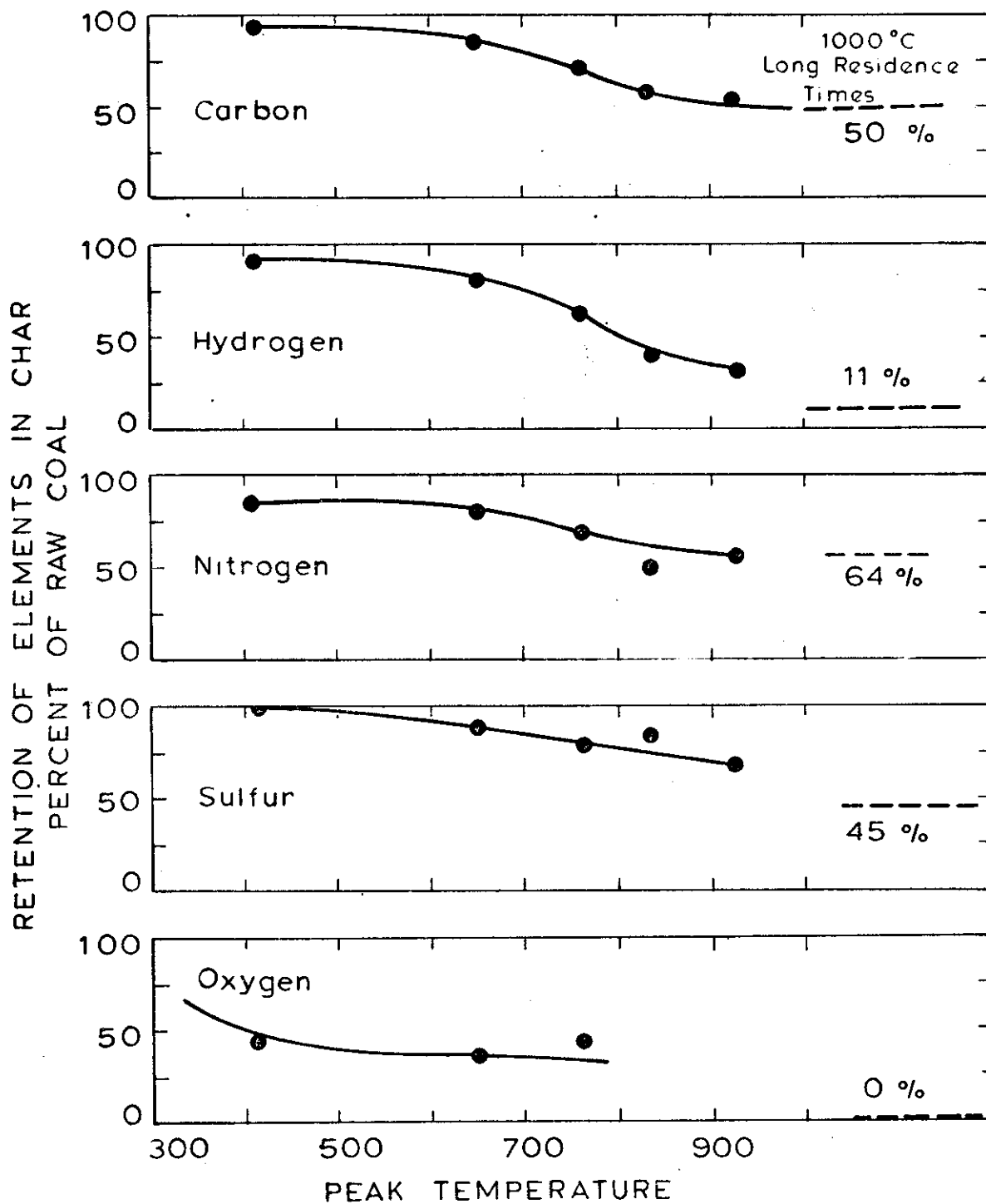


Figure 1-17. Elemental Compositions of Chars from Bituminous Coal Pyrolysis

left behind in the char, even at 1000°C. The sulfur is evolved rapidly between a peak temperature of 925°C and the isothermal 1000°C asymptote. The oxygen shows essentially two step behavior. There is an initial loss at a peak temperature below 400°C, certainly corresponding to the evolution of pyrolytic water. The next sharp drop presumably corresponds to the period of major CO evolution, between 800 and 900°C.

The total yields of all products are summarized in the first column of Table 1-3. It can be seen that the total measured weight loss (47%) exceeds ASTM moisture plus volatiles yield (40.3%) by 17%. Such behavior is common during rapid pyrolysis in a dispersed phase. It is felt that this reflects the fact that repolymerization of tar into the sample may occur in the fixed bed environment of an ASTM test crucible. Table 1-17 also shows that the overall mass balance closure is fair (about 94%). Element balances (not shown) fall in the range  $100 \pm 10\%$ . It is felt that most of the loss is associated with failure to collect 100% of the tar product.

The results shown in Table 1-3 also suggest but a slight effect of variation of heating rate on total yield. A bit more significant is the slight reduction in yield in the case in which the coal was heated in two stages (with intermediate cooling) to the final temperature. These results suggest that within the range of heating rates studied here, the reactions at high temperature occur independently of those which occur at lower temperatures.

Fig. 1-18 shows that mass transport limitations play an important role in determining the composition of volatiles obtained from pyrolysis of bituminous coal. Increasing external pressure from 0.05 mm to 69 atm of helium reduces total product yields by almost 14%. Over the same range

Table 1-3. Effect of Time-Temperature Histories on Yields from Pyrolysis of Bituminous Coal

Products	Heating Rate 1000°C/sec		350-450°C/sec	13000-15000°C/sec	2-Step <sup>a</sup>
	wt.% of coal	mole % of dry gas	wt.%	wt.%	wt.%
CO	2.4	9.9	2.4	2.3	2.1
CO <sub>2</sub>	1.2	3.1	1.6	1.1	1.6
H <sub>2</sub> O	7.8	-	7.6	7.7	7.7
CH <sub>4</sub>	2.5	18.0	2.2	2.4	2.5
C <sub>2</sub> H <sub>4</sub>	0.8	3.3	0.4	0.7	0.3
C <sub>2</sub> H <sub>6</sub>	0.5	1.9	0.6	0.6	0.6
C <sub>3</sub> H <sub>6</sub> +C <sub>3</sub> H <sub>8</sub>	1.3	3.5	1.1	1.2	1.3
H <sub>2</sub>	1.0	57.7	NM <sup>d</sup>	NM <sup>d</sup>	NM <sup>d</sup>
other HC gas <sup>b</sup>	1.3	2.6	1.1	1.5	0.9
HC liquids <sup>c</sup>	2.4	-	2.3	2.7	2.4
Tar	<u>23.0</u>	-	<u>22.4</u>	<u>23.0</u>	<u>22.0</u>
Total	44.3 <sup>e</sup>		41.7	43.7	41.4
Measured Total	47.0		46.0	47.0	44.7
Unaccounted For	2.7		3.3	3.3	3.3
ASTM volatiles & Moisture	40.3		40.3	40.3	40.3

(con't)

50

Effect of Time-Temperature Histories on Yields from Pyrolysis of Bituminous Coal (continued)

All results on as-received wt. basis. Isothermal runs 850-1000°C with holding time 2-10 seconds.

P = 1 atm. He

Notes

<sup>a</sup>Sum of two step process; coal heated first at about 650°C for 3 seconds and cooled. Reheated to about 1000°C for about 3 seconds

<sup>b</sup>All other hydrocarbon gases not listed separately

<sup>c</sup>Hydrocarbon products from condensable trap

<sup>d</sup>NM = not Measured

<sup>e</sup>Columns may not add because of round off

<sup>f</sup>H<sub>2</sub>O includes H<sub>2</sub>S yield, roughly 1% by wt of coal at these temperatures



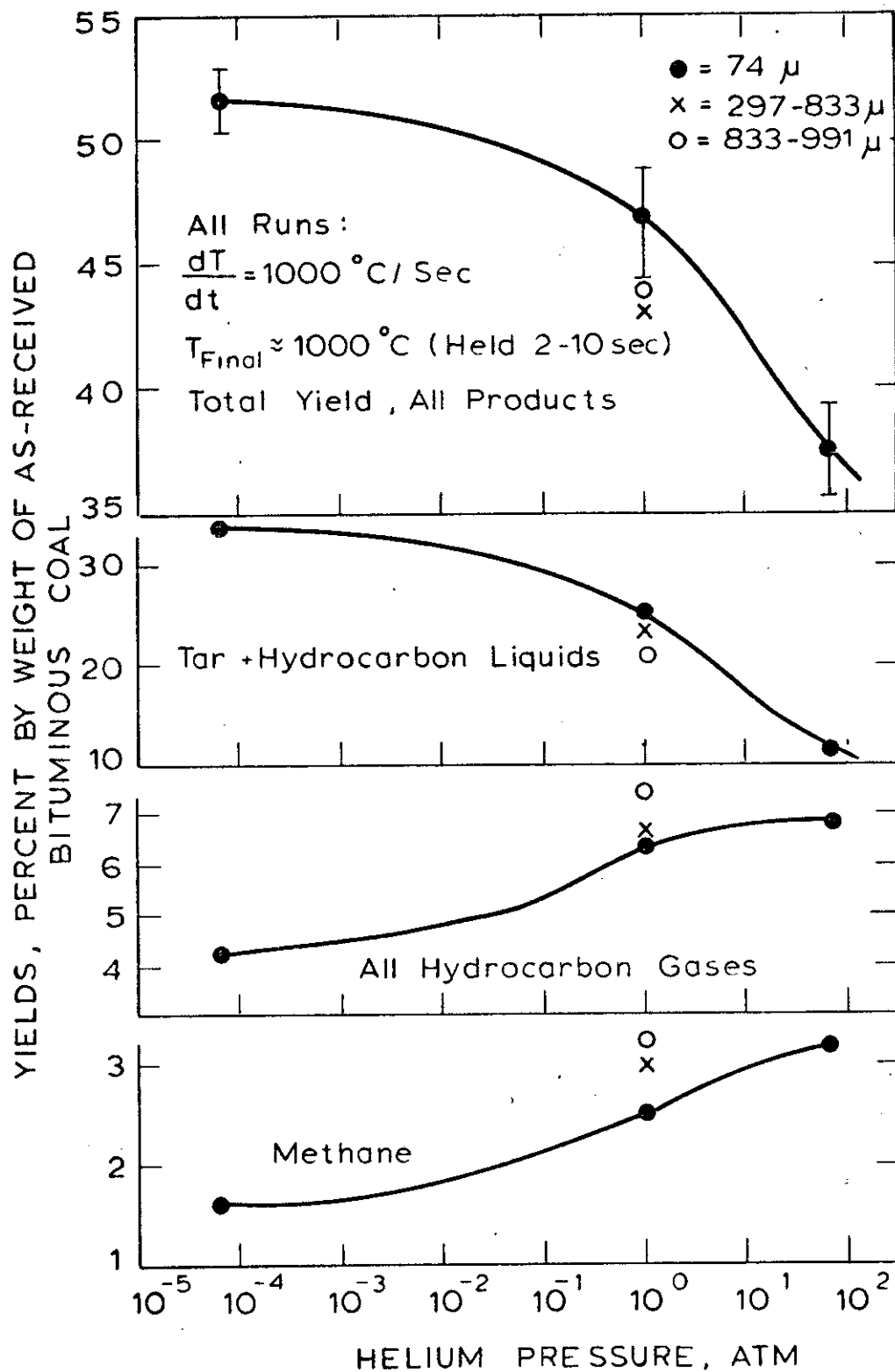


Figure 1-18. Effect of Pressure and Particle Diameter on Product Yields from Bituminous Coal Pyrolyzed at 1000°C.

of pressure, the tar yield decreases by about 20%. This is offset, partly, by an increase in the yield of hydrocarbon gases (presumably tar cracking products). The trend exhibited by variation of particle diameter is consistent with that observed for variation of external pressure.

#### Hydropyrolysis of a Montana Lignite

Again, all results are for particles in the size range  $53 - 88\mu$  unless otherwise noted. The convention of reporting all results on a percent by weight of as-received lignite is retained here, although mass balance closure by a simple summation of product yields is of course no longer possible.

The data in Fig. 1-19 seem to imply that there is a temperature below which the presence of hydrogen has no effect on weight loss (roughly in the range  $700-800^{\circ}\text{C}$ ). Perhaps not coincidentally, this is the same range of temperatures over which variations in inert gas pressure begin to have an effect on lignite pyrolysis yields (Fig. 1-11). Of course, increasing the pressure of inert gas always serves to reduce total yields, while increasing the pressure of hydrogen gas (above 1 to 10 atmospheres) serves to increase total yields. Table 1-4 compares the total yields of various products obtained at "long" residence times from ordinary 1 atm. He pyrolysis, high pressure (69 atm. He) pyrolysis, and high pressure (69 atm.  $\text{H}_2$ ) hydropyrolysis. It is immediately apparent that the incremental yield due to hydropyrolysis is due largely to an increase in methane and other hydrocarbon species. The reduced yields of carbon oxides are not surprising since reverse water gas shift and other water forming reactions are thermodynamically favored.

Since methane is obviously the key component in the enhanced yield observed during hydropyrolysis, Fig. 1-20 tracks its behavior alone.

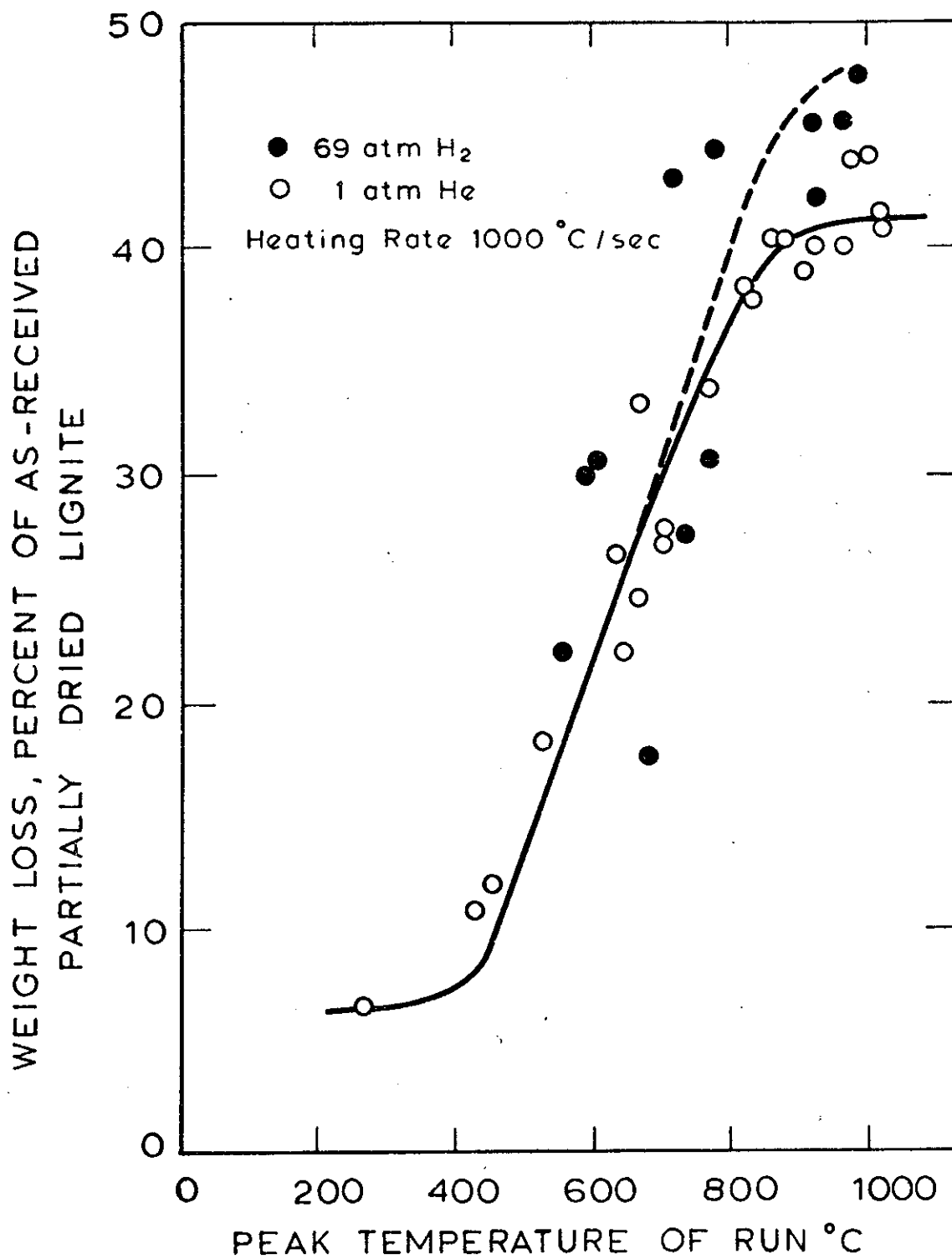


Figure 1-19. Comparison of Total Weight Loss from Pyrolysis and Hydropyrolysis of Lignite to Different Peak Temperatures.

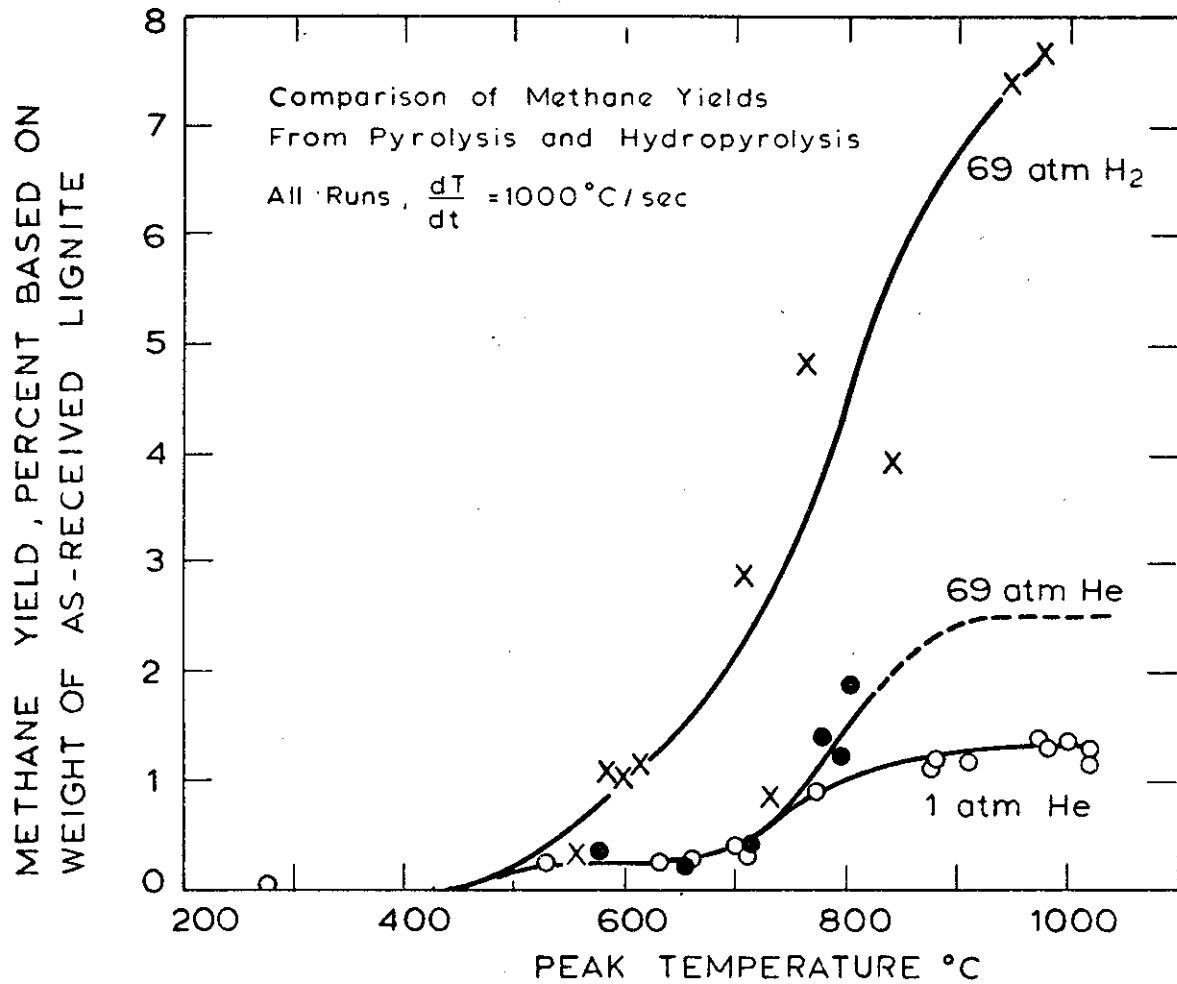


Figure 1-20. Yields of Methane from Pyrolysis and Hydropyrolysis of Lignite to Different Peak Temperatures.

Table 1-4. Comparison of Total Yields from Lignite Pyrolysis and Hydropyrolysis

	<u>Pyrolysis</u> <u>1 atm. He</u>	<u>Hydropyrolysis</u> <u>69 atm. H<sub>2</sub></u>	<u>Pyrolysis</u> <u>69 atm He</u>
CO <sub>2</sub>	9.5	8.5	10.6
CO	9.4	7.1	9.0
CH <sub>4</sub>	1.3	9.5	2.5
C <sub>2</sub> H <sub>4</sub>	0.6	6.2	0.6
C <sub>2</sub> H <sub>6</sub>	0.2	1.4	0.2
OTHER HC	0.8	4.1	1.7
H <sub>2</sub> O	16.5	16.0	12.9
H <sub>2</sub>	0.5	N.M.	N.M.
tar	5.4	~ 8	~ 3
Measured Total Weight Loss	44.0	51.5	40.2

Samples held approximately 10 seconds at 850-1000°C

Contrary to the picture presented by the total weight loss behavior in Fig. 1-19, methane yields show an effect of hydrogen at temperatures as low as 600°C. Comparison of the three sets of data suggest that the enhanced methane yield observed during 600°C hydrolysis is due to interaction of coal and external hydrogen, rather than being an effect induced only by the high external pressure (the so-called "autohydrogenation" effect).

It is also interesting to note the behavior of ethylene during hydrolysis (Fig. 1-21). Whereas the external inert gas pressure has virtually no effect on ethylene yields, the presence of hydrogen completely inhibits the high temperature stage of ethylene formation.

Among the other products of hydrolysis, the hydrocarbon gases (other than methane and ethylene) show behavior similar to that of methane. The oxygenated products seem rather unaffected except for the very high temperature stage of carbon oxide formation, which appears to be inhibited. It is difficult to say much concerning the tar yield because of a considerable amount of scatter. It appears as though the maximum total yield of tar plus hydrocarbon liquids is about 10% wt.

The results of the ultimate analyses of lignite chars produced by pyrolysis are shown in Fig. 1-22. Both carbon and nitrogen conversions are enhanced by hydrolysis, but the conversions of oxygen, hydrogen and sulfur appear largely unaffected.

As has already been demonstrated, a large portion of the yield during hydrolysis is the result of ordinary pyrolytic processes. Therefore, in examining the effect of pressure on yields, Fig. 1-23 expresses total yield and methane yield as increments over yields from atmospheric pressure pyrolysis. This data imply no clear functionality of

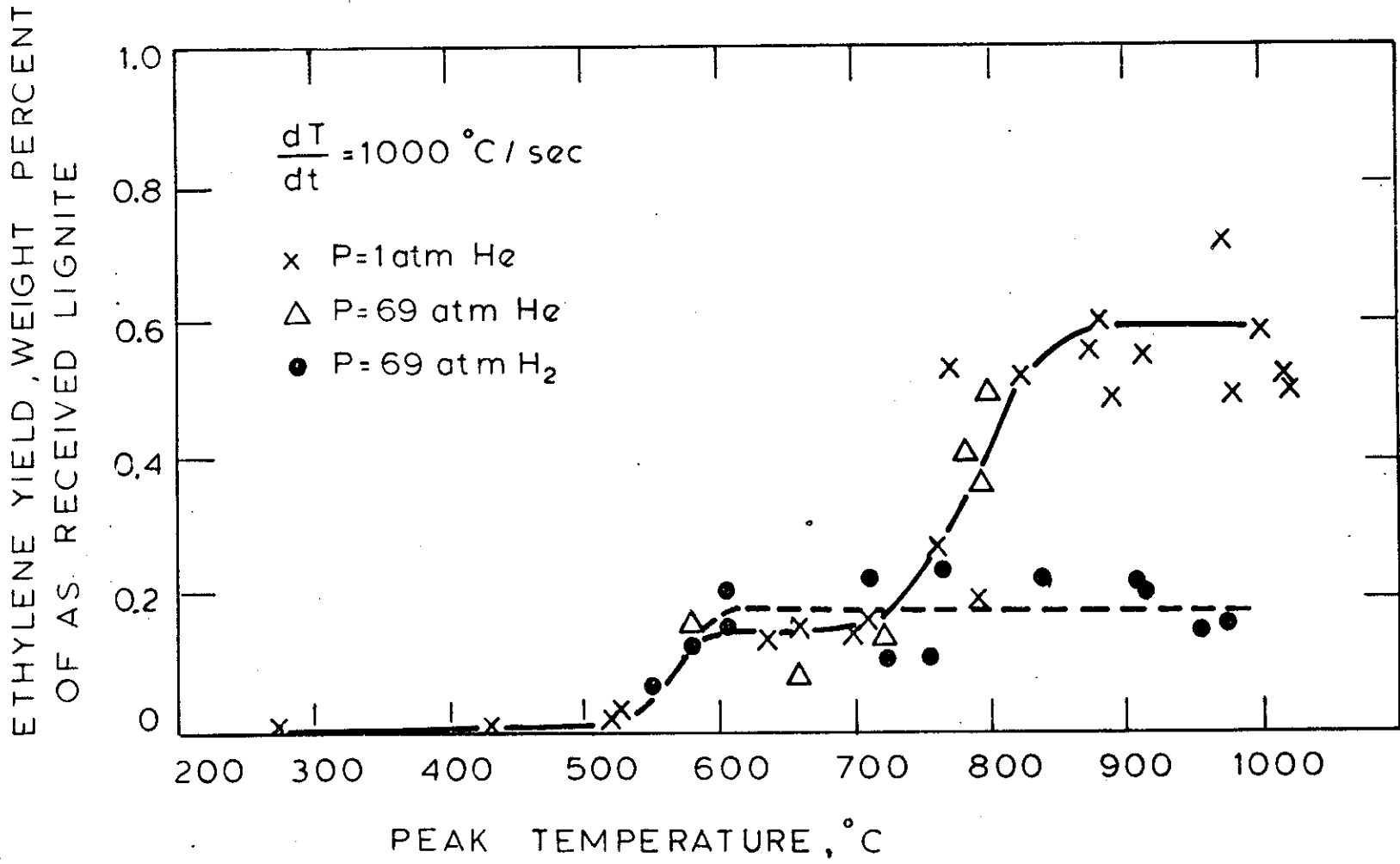


Figure 1-21. Yields of Ethylene from Pyrolysis and Hydrolysis of Lignite to Different Peak Temperatures.

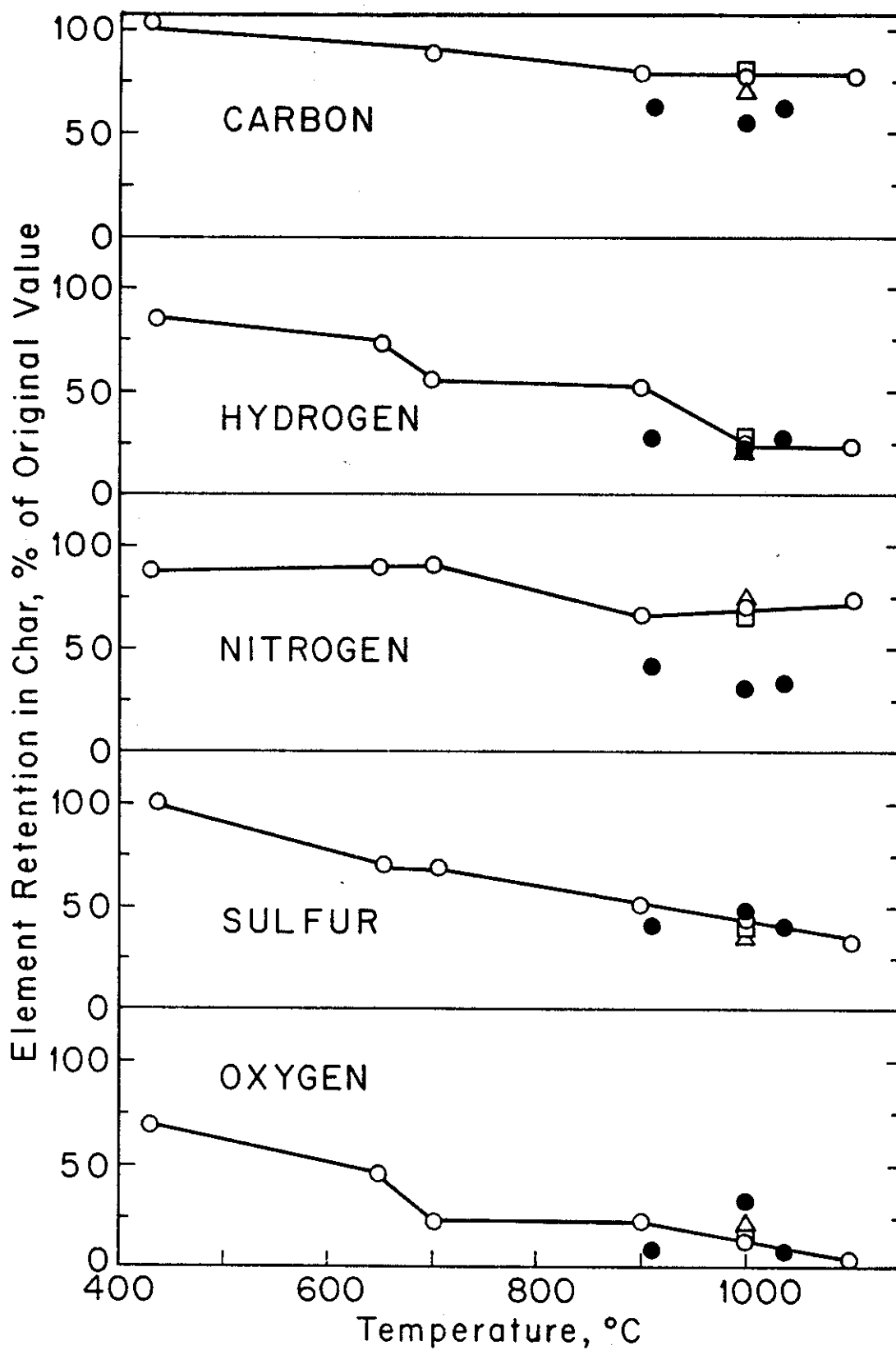


Figure 1-22. Comparison of Char Compositions from Pyrolysis and Hydro-pyrolysis of Lignite (o), 1 atm He, zero residence time at peak temperature; (Δ) 1 atm He, 5-20 sec. residence time; (□) 69 atm He, 5-10 sec. residence time; (●) 69 atm H<sub>2</sub>, residence time 2-30 sec.



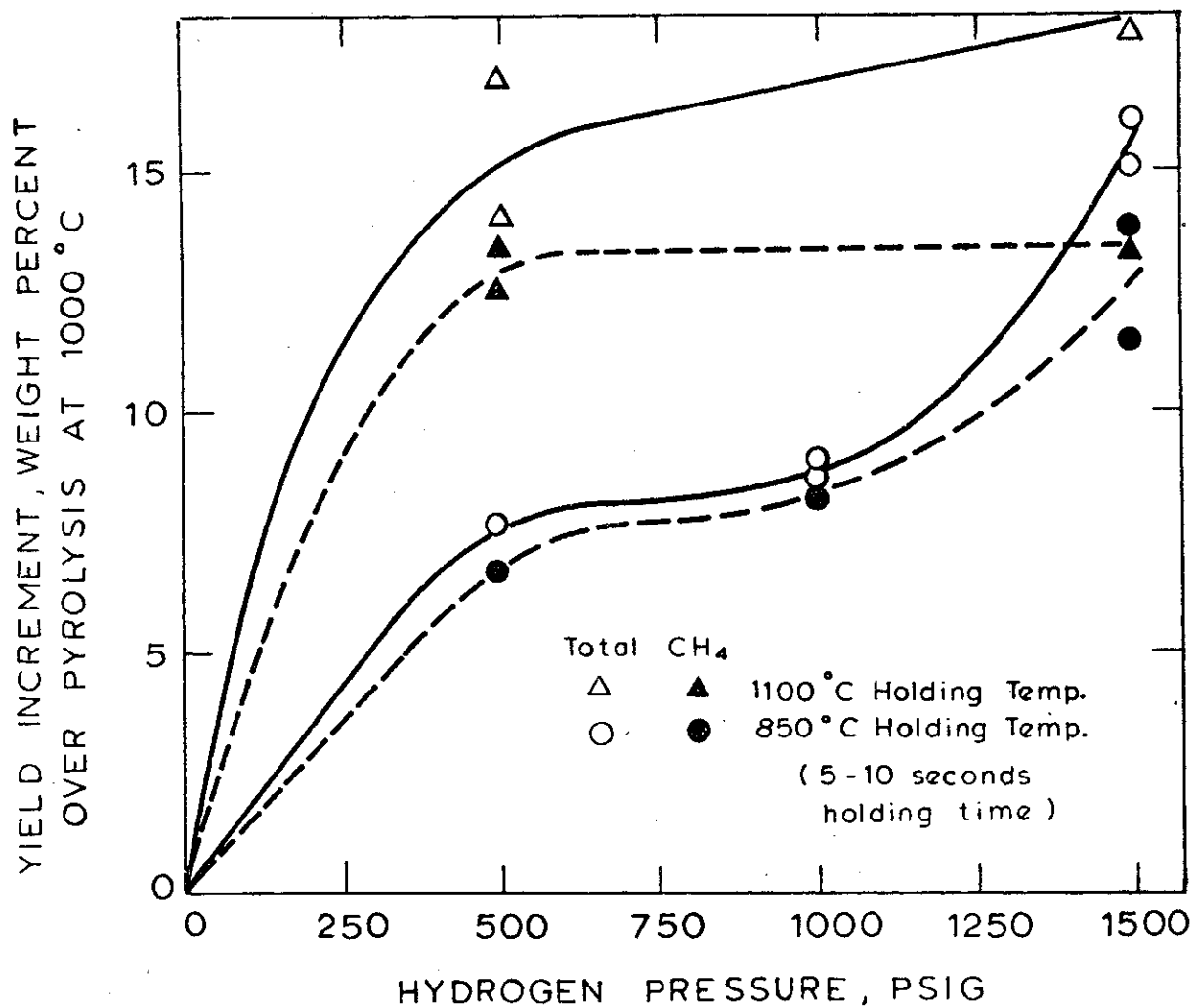


Figure 1-23. Effect of Temperature and Hydrogen Pressure on Increasing Yields Relative to Pyrolysis (Basis 44% weight loss, 1.3% CH<sub>4</sub> during 1 atm He pyrolysis at either 850° or 1100°C).

of pressure for either total yield or methane yield. These results also point out that an increase in temperature may be as effective in promoting higher yields as in an increase in pressure (compare the points at 1100°C and 500 psig H<sub>2</sub> and 850°C and 1500 psig H<sub>2</sub>). In all cases, methane is principally responsible for the bulk of the incremental yield.

The effect of particle diameter was quickly examined (with particles in the 295 - 990μ range) and judged to be insignificant.

#### Hydropyrolysis of a Pittsburgh Seam No. 8 Bituminous Coal

As for the lignite, the base case for bituminous hydropyrolysis involves particles in the size range 53 - 88μ and a hydrogen pressure of 1000 psig (69 atm. absolute).

Fig. 1-24 shows a comparison of total yields obtained during pyrolysis at 1 atm. and at 69 atm. of helium pressure, and from hydropyrolysis at 69 atm. of hydrogen pressure. A comparison of the pyrolysis results obtained at 1 atm. and 69 atm. of helium pressure illustrate again the previously discussed effect of pressure on pyrolysis. Since the helium is of course chemically inert, its effect is purely physical. The fact that the total yields from 69 atm. hydropyrolysis are comparable to the yields from 1 atm. pyrolysis implies that the hydrogen must interact with the coal chemically in a manner which boosts yields. This interaction, according to these data, begins at temperatures in the range 700 to 800°C. Anthony et al. (1976) have advanced a theory which postulates that the hydrogen serves to "stabilize" volatiles which may otherwise be lost to cracking reactions. The data in Fig. 1-24 may be supportive of this picture, but the data in Fig. 1-25 shed further light upon the nature of the process.

In Fig. 1-25, the yield of tar, the principal product of bituminous

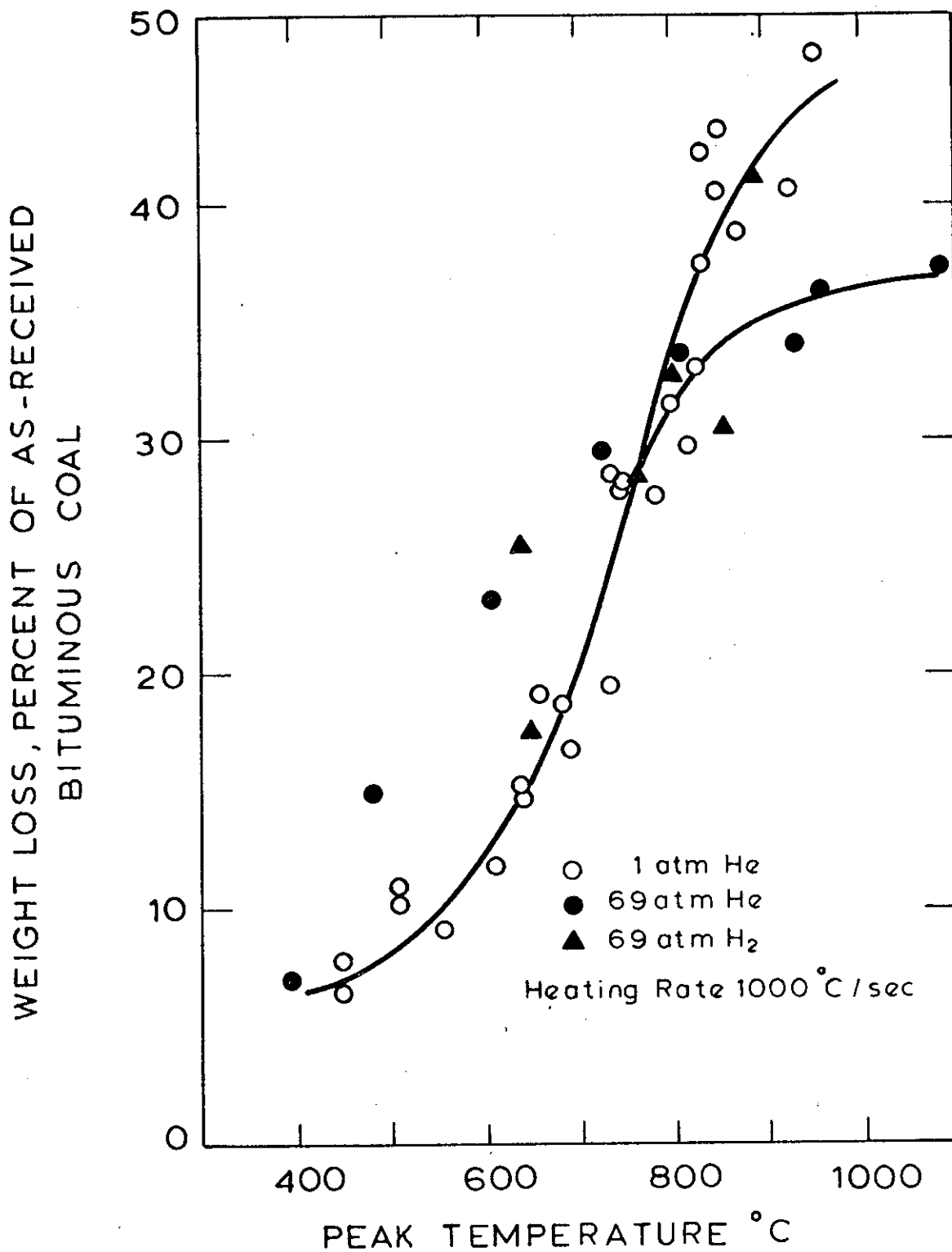


Figure 1-24. Comparison of Total Weight Loss from Pyrolysis and Hydrolysis of Bituminous Coal.

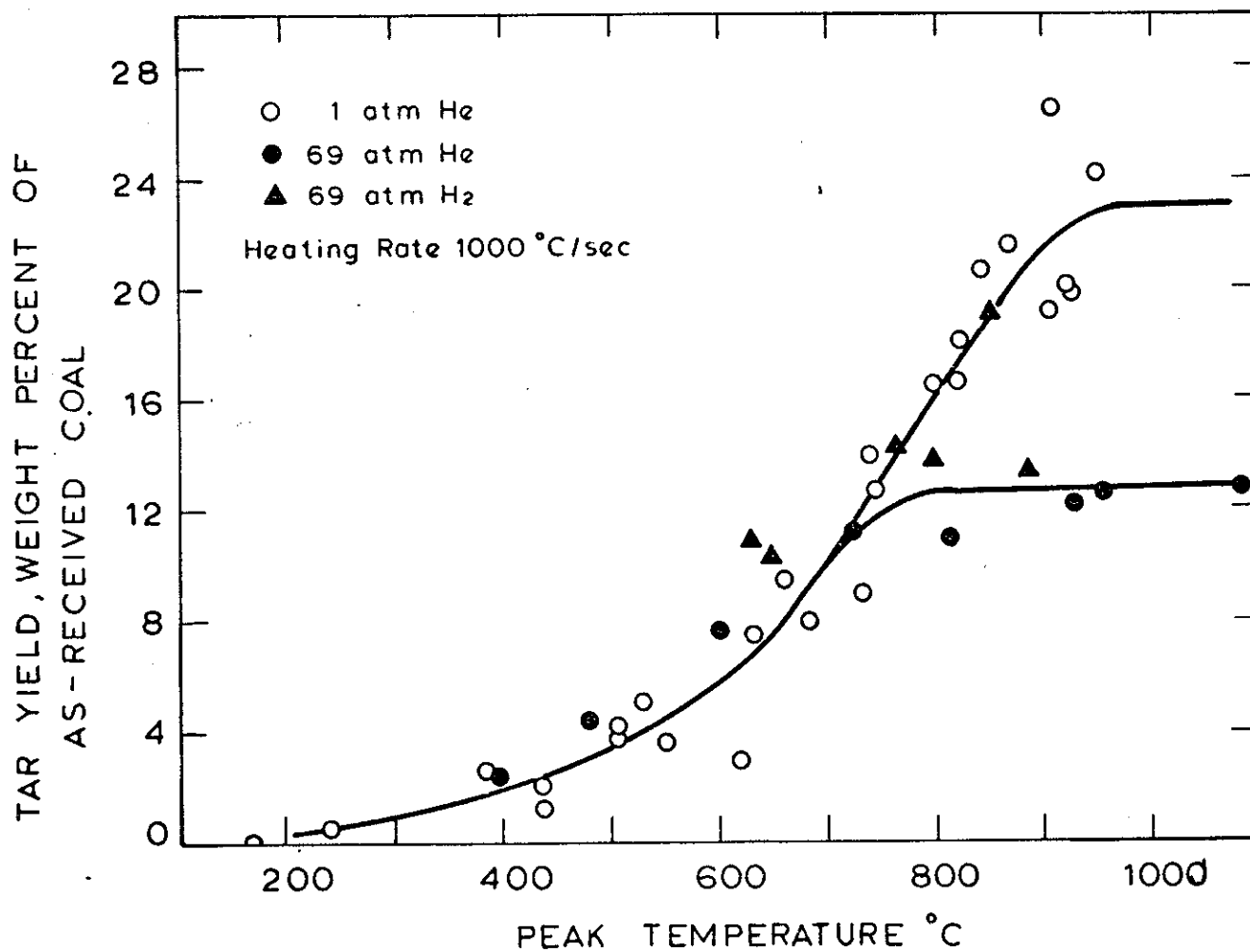


Figure 1-25. Comparison of Tar Yields from Pyrolysis and Hydropyrolysis of Bituminous Coal (note 69 atm H<sub>2</sub> asymptote drawn coincident with 69 atm He asymptote based on results of non-zero holding time runs not shown here).

1 atm. pyrolysis, is plotted for the 1 and 69 atm. He pyrolysis and 69 atm. H<sub>2</sub> hydrolysis cases. The results are striking in that they show that hydrogen does not act to stabilize the tar as such; the yields of tar from 69 atm. pyrolysis and 69 atm. hydrolysis are comparable. The indicated asymptote for tar yield from hydrolysis (at 12.5%) is obtained from runs in which the coal is held at temperatures between 850 and 1050°C for up to 20 seconds.

The fact that the tar itself is not being stabilized suggests several possibilities for the yield enhancing effect of hydrogen. The first is that the hydrogen interferes with the tar forming reactions and stabilizes tar "precursors". Another possibility is that the hydrogen serves to stabilize tar cracking (or hydrocracking) products. A third possibility is that the hydrogen physically interferes with the escape of tar and promotes its cracking in a manner precisely analogous to that of the helium; the yield enhancement is the result of an unrelated (or indirectly related) chemical process.

Fig. 1-26 compares the yields of methane from pyrolysis and hydrolysis. These data suggest that the chemical interaction of hydrogen with the coal actually begins at rather low peak temperatures (<600°C).

Table 1-5 summarizes the results for 69 atm hydrolysis and compares them with atmospheric pressure pyrolysis results. The hydrolysis results were all obtained at temperatures above 900°C, held for between 12 and 20 seconds. It is apparent from comparison of the results in Figs. 1-24, 1-26 and Table 1-5 that methane is the principal product formed during the isothermal period. During the non-isothermal period, Table 1-5 shows an additional weight loss of roughly 20% while the yield of methane has increased by roughly 15%.

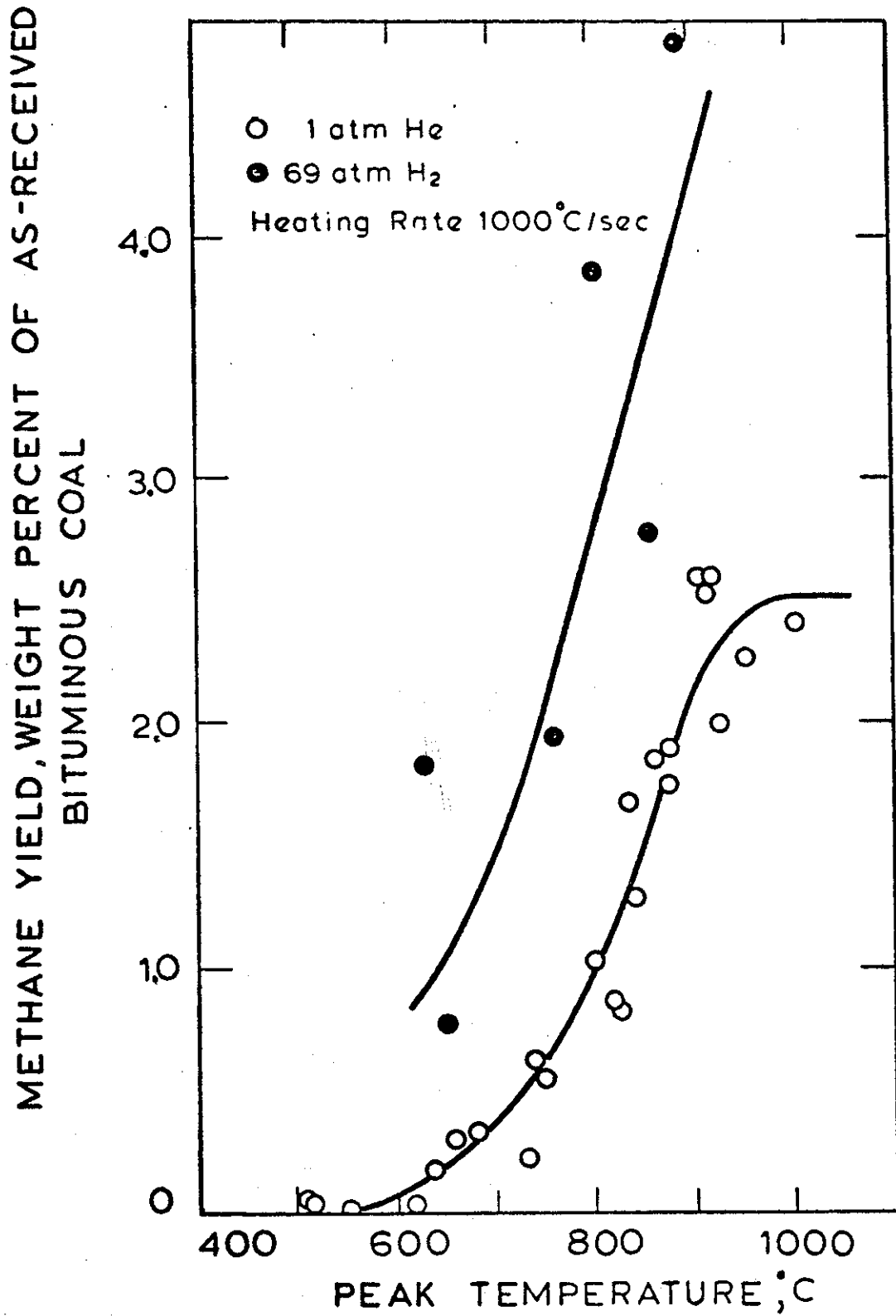


Figure 1-26. Comparison of Methane Yields from Pyrolysis and Hydrolysis of Bituminous Coal.

Table 1-5. Comparison of Yields from Atmospheric Pressure Pyrolysis and 69 atm. Hydrolysis of Bituminous Coal.

	<u>1 atm. He</u>	<u>69 atm. H<sub>2</sub></u>
Total weight loss (as.rcvd.)	47.0%	61.8%
Tar	23.	12.
CO	2.4	- <sup>†</sup>
CO <sub>2</sub>	1.2	1.3
H <sub>2</sub> O	6.8	- <sup>†</sup>
H <sub>2</sub>	1.0	-
CH <sub>4</sub>	2.5	23.2
C <sub>2</sub> H <sub>4</sub>	0.8	0.4
C <sub>2</sub> H <sub>6</sub>	0.5	2.3
C <sub>3</sub> H <sub>6</sub> + C <sub>3</sub> H <sub>8</sub>	1.3	0.7
C <sub>6</sub> H <sub>6</sub>	trace*	2.2
other HC gases	1.3	2.0
light HC liquids	2.4	3.1

All hydrolysis runs involve heating the coal to temperature 900°C and holding isothermally for 12 to 20 seconds.

\*The trace amount of benzene found during pyrolysis is usually included in the "other HC gases" or "light HC liquids".

<sup>†</sup>Measurements unreliable, not reported.

There are several parallels between lignite hydrolysis and bituminous coal hydrolysis. The role of methane as the predominant product is the most obvious. Others include the decreased yield of ethylene and increased yield of ethane, relative to the pyrolysis base case.

The figures in Table 1-5 are naturally averages over several runs. Not included in the average was a run done at roughly 1080°C (14 seconds) in which the total yield was over 70% (representing a d.a.f. conversion of about 80%) and the yield of methane was nearly 40% (representing a carbon conversion to methane of about 44%).

As observed by Anthony et al. (1976), increasing particle diameter has a rather deleterious effect on total yields obtained from hydrolysis. Fig. 1-27 presents data from this investigation. The trends are similar to those observed by Anthony et al., although there are some small quantitative differences. The data for hydrolysis are somewhat more sensitive to the temperature of the isothermal holding period than are the data for pyrolysis (demonstrated in Fig. 1-23). Therefore, while the pyrolysis data in Fig. 1-27 include results of experiments run for any more than 2 seconds at temperatures over 850°C, the hydrolysis data chosen for presentation were only those from temperatures between 900 and 1050°C and with isothermal holding times greater than 10 (but all less than 20) seconds.

The following table shows the principal differences in product compositions:

<u>Product</u>	<u>74</u>	<u>570</u>	<u>910</u>
Tar	12	13	12
CH <sub>4</sub>	23	19	20
C <sub>2</sub> H <sub>6</sub>	2.3	1.7	1.6
other HC gases	3.1	1.4	1.2
light HC liquids	5.3	3.6	5.2
CO <sub>2</sub>	1.3	1.0	1.4



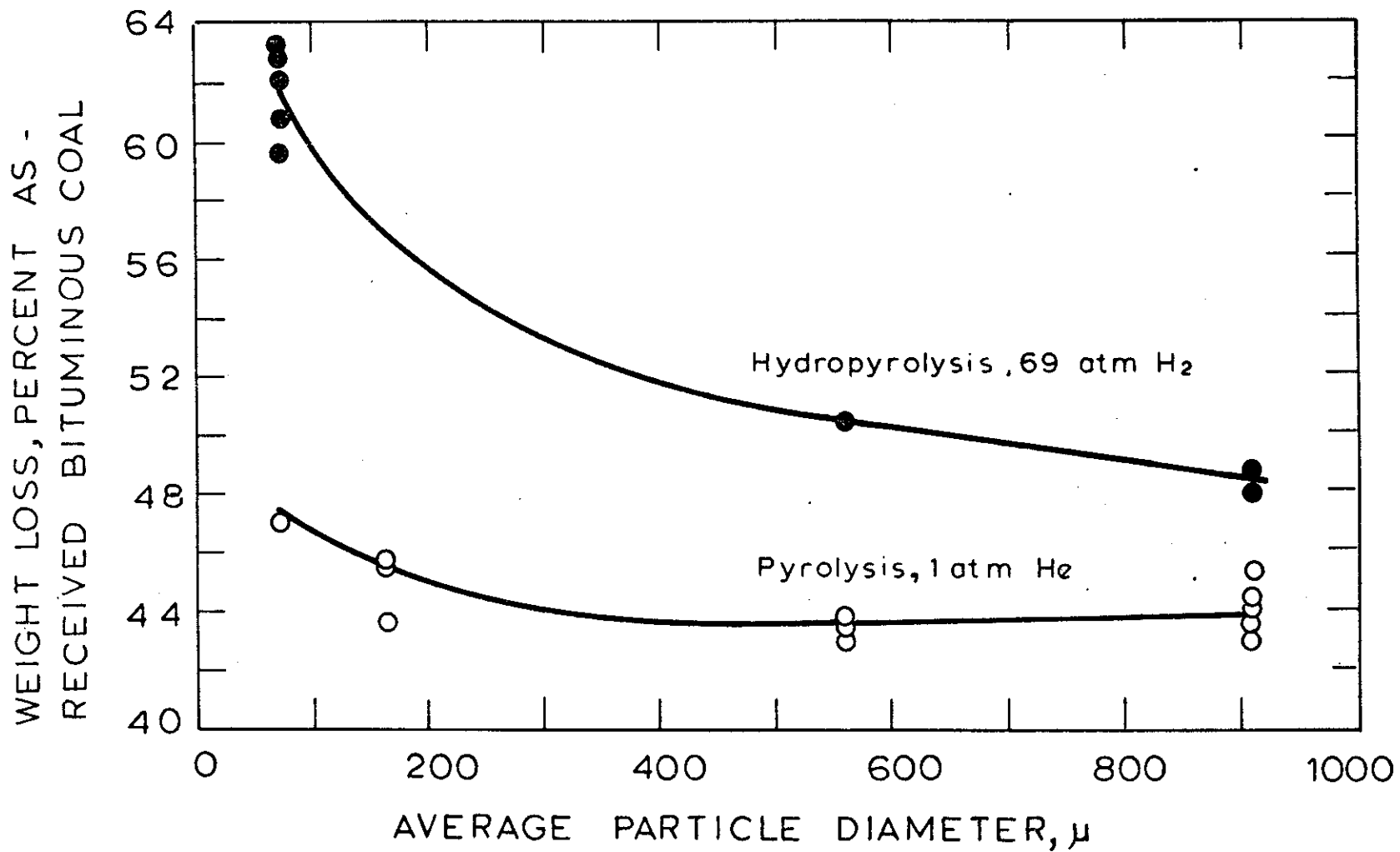


Figure 1-27. Effect of Particle Diameter on Total Yields from Pyrolysis and Hydropyrolysis of Bituminous Coal.

Since carbon monoxide, water, and sulfur compound measurements are not available for all cases, total mass balances are not possible.

## 1.5 Modelling and Discussion

### Pyrolysis

With the products in the present study dominated by a few individual species and classes of species, e.g. tar, there is interest in determining whether pyrolysis can be effectively modelled as only a few reactions representing the production of these key products.

As a first test of this approach, the appearance of product  $i$  is modelled as a reaction first-order in the amount of  $i$  yet to be produced. Thus for the reaction



the assumed first-order rate is

$$dV_i/dt = k_i(V_i^* - V_i) \quad (2)$$

and the rate constant is assumed to be

$$k_i = k_{i0} \exp(-E_i/RT) \quad (3)$$

where  $k_{i0}$  is the pre-exponential factor,  $E_i$  is the activation energy of reaction  $i$ ,  $V_i$  is the amount of product  $i$  produced up to time  $t$ ,  $V_i^*$  is the amount of product  $i$  which could potentially be produced, (i.e., at  $t = \infty$ ),  $T$  is the absolute temperature, and  $R$  is the gas constant.

Assuming that temperature increases linearly with time, as it does in these experiments, with the constant rate  $dT/dt = m$ , solution of the above equations gives

$$\int_0^{V_i} dV_i / (V_i^* - V_i) = \int_0^T (k_{i0}/m) \exp(-E_i/RT) dT \quad (4)$$

Since  $R_i/RT \gg 1$  is a good approximation for coal decomposition reactions, the solution becomes

$$(V_i^* - V_i)/V_i^* = \exp[-(k_{i0}RT^2/mE_i)\exp(-E_i/RT)] \quad (5)$$

This equation is plotted in Fig. 1-28 for activation energies typical of organic decomposition reactions (see Table 1-6) and a typical pre-exponential factor of  $k_{i0} = 1.67 \times 10^{13} \text{ s}^{-1}$ . The inadequacy of the single-reaction model in fitting the data on total yield of volatiles is evident from this figure; nevertheless, this approach has been taken by many workers for correlating pyrolysis data.

It can be seen from the wide range of materials listed in Table 1-6 that organic decomposition reactions encompass a wide range of activation energies and pre-exponentials. It is not surprising that coal, the chemical structure of which is far more complex than that of the materials in Table 1-6 decomposes thermally to produce numerous products and that these products exhibit different activation energies. When a single first-order reaction is used to model coal pyrolysis, the activation energy and pre-exponential factor are forced to be very low in order to fit the overall temperature dependence that actually results from the occurrence of different reactions in different temperature intervals. The results are sometimes interpreted as reflecting transport limitations because the parameters are too low for organic decompositions. This point is further discussed elsewhere (Anthony and Howard, 1976).

Many of the products of lignite and bituminous coal are obviously not characterized by single first order processes. In the case of lignite, the rather distinct stepwise behavior of some species suggests use

Table 1-6. Kinetic Parameters for Pyrolysis of Various Organic Materials

Material Pyrolyzed	Product <sup>a</sup>	Experimental Temp., °C	Activation Energy, kcal/mole	Pre-Exponential Factor, s <sup>-1</sup>	Reference
Ferulic Acid (C <sub>10</sub> H <sub>10</sub> O <sub>4</sub> )	CO <sub>2</sub>	150-250	27.7	6.0x10 <sup>9</sup>	Jüntgen and Van Heek, 1968; 1970
Perylene Tetracarboxylic Acid Anhydride (C <sub>24</sub> H <sub>8</sub> O <sub>6</sub> )	CO <sub>2</sub>	400-600	71.5	5.2x10 <sup>17</sup>	Jüntgen and Van Heek, 1968; 1970
	CO <sub>2</sub>	400-600	64.9	5.0x10 <sup>16</sup>	Jüntgen and Van Heek, 1968; 1970
Protocatechuic Acid (C <sub>7</sub> H <sub>6</sub> O <sub>4</sub> )	(H <sub>2</sub> O) <sub>1</sub>	50-300	18.8	2.7x10 <sup>8</sup>	Jüntgen and Van Heek, 1968; 1970
	(H <sub>2</sub> O) <sub>2</sub>	50-300	42.4	2.3x10 <sup>5</sup>	Jüntgen and Van Heek, 1968; 1970
	CO <sub>2</sub>	50-300	40.4	1.6x10 <sup>15</sup>	Jüntgen and Van Heek, 1968; 1970
Naphthalene Tetracarboxylic Acid (C <sub>14</sub> H <sub>8</sub> O <sub>8</sub> )	H <sub>2</sub> O	100-250	33.5	1.2x10 <sup>13</sup>	Jüntgen and Van Heek, 1968; 1970
Mellitic Acid (C <sub>12</sub> H <sub>6</sub> O <sub>12</sub> )	H <sub>2</sub> O	230 <sup>b</sup>	16.6	2.3x10 <sup>5</sup>	Jüntgen and Van Heek, 1970
Tartaric Acid (C <sub>4</sub> H <sub>6</sub> O <sub>6</sub> )	H <sub>2</sub> O	195 <sup>b</sup>	42.9	6.7x10 <sup>17</sup>	Jüntgen and Van Heek, 1970
Polystyrene (C <sub>8</sub> H <sub>8</sub> ) <sub>n</sub>	overall	394 <sup>b</sup>	77	8.3x10 <sup>22</sup>	Fuoss <i>et al.</i> , 1964
	overall	335-355 <sup>b</sup>	58	9.0x10 <sup>15</sup>	Madorsky, 1952
Teflon (C <sub>2</sub> F <sub>4</sub> ) <sub>n</sub>	overall	575 <sup>b</sup>	67-69	4.3x10 <sup>14</sup>	Fuoss <i>et al.</i> , 1964
Polyethylene (C <sub>2</sub> H <sub>4</sub> ) <sub>n</sub> "Phase 1"	overall	385-405	48	5.2x10 <sup>11</sup>	Madorsky, 1952
	overall	385-405	71	8.7x10 <sup>18</sup>	Madorsky, 1952
Hydrogenated Polystyrene (C <sub>8</sub> H <sub>14</sub> ) <sub>n</sub>	overall	335-350	52	1.4x10 <sup>14</sup>	Madorsky, 1953
Polymeta-methylstyrene (C <sub>9</sub> H <sub>10</sub> ) <sub>n</sub>	overall	333-353	59	7.2x10 <sup>16</sup>	Madorsky, 1953
Polyalpha-methylstyrene (C <sub>9</sub> H <sub>10</sub> ) <sub>n</sub>	overall	273-288	58	8.3x10 <sup>18</sup>	Madorsky, 1953
Polymethyl-methacrylate (C <sub>5</sub> H <sub>8</sub> O <sub>2</sub> ) <sub>n</sub>	overall	240-270	33	3.6x10 <sup>9</sup>	Madorsky, 1953
	overall	310-325	55	1.8x10 <sup>16</sup>	Madorsky, 1953
Polymethylacrylate (C <sub>4</sub> H <sub>6</sub> O <sub>2</sub> ) <sub>n</sub>	overall	285-300	37	1.4x10 <sup>10</sup>	Madorsky, 1953
Cellulose (C <sub>5</sub> H <sub>10</sub> O <sub>5</sub> ) <sub>n</sub>	overall	250-1000	33.4	6.8x10 <sup>9</sup>	Lewellen <i>et al.</i> , in press
	overall	250-350	35	3.3x10 <sup>11</sup>	Jüntgen and Van Heek, 1970; Van Krevelen <i>et al.</i> , 1951

a. Denotes species whose evolution is described by the parameters given. Two different stages of water evolution are denoted by (H<sub>2</sub>O)<sub>1</sub> and (H<sub>2</sub>O)<sub>2</sub>. Overall refers to all products combined.

b. Temperature of maximum pyrolysis rate.

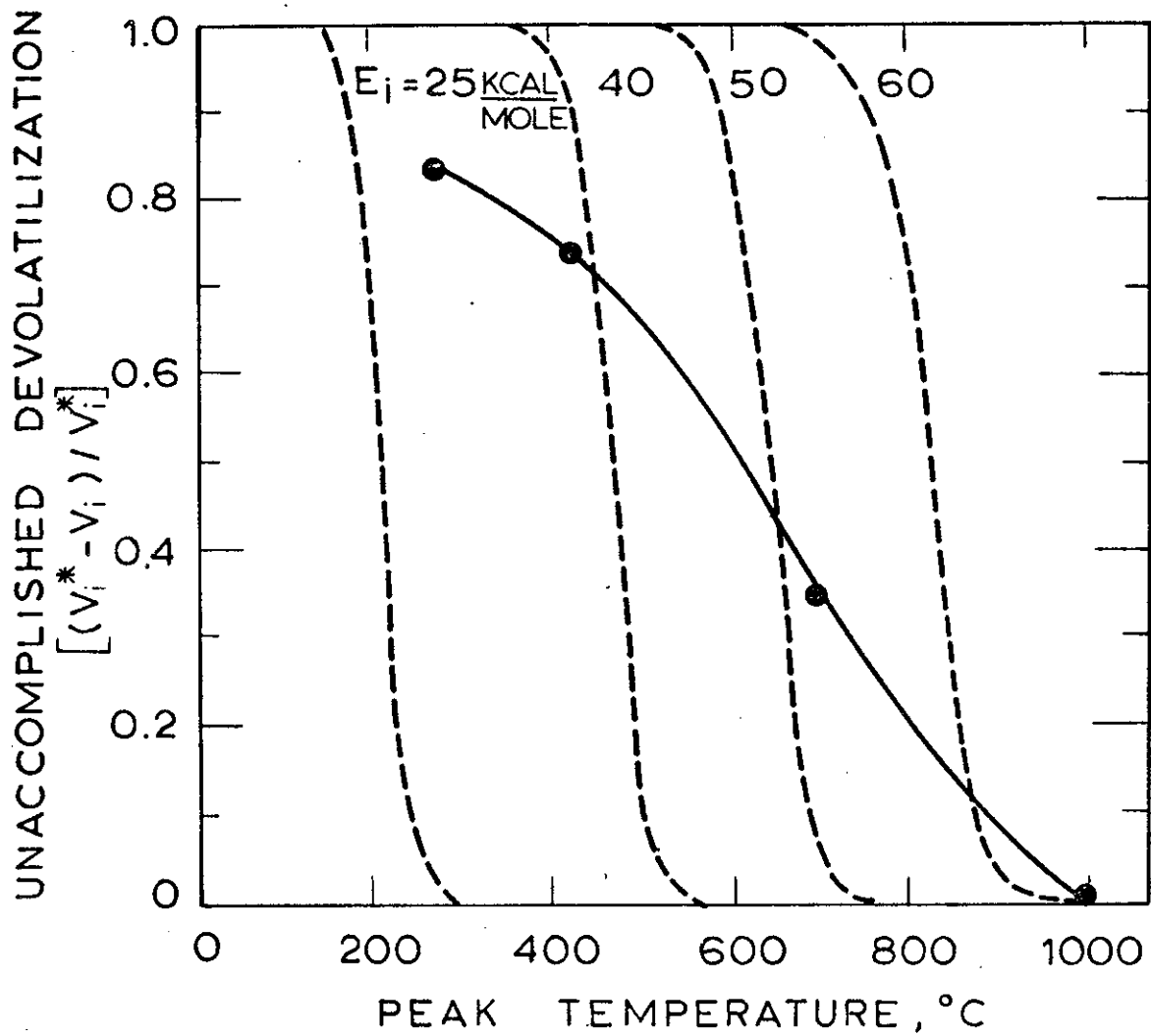


Figure 1-28. Comparison of Data on Overall Conversion of Lignite to Volatiles with Predictions from Single-Step First-Order Pyrolysis Model [(•) data; (dashed curves) predictions from model].

of two (or three) first order steps. Application of such an approach to the lignite data resulted in the kinetic parameters shown in Table 1-7. Comparison with the values in Table 1-6 indicates that the values so obtained are reasonable. The curves shown in Figs. 1-7, 1-8, and 1-9 were calculated using these parameters and the model, for a standardized experiment in which coal is heated at 1000°C/s to peak temperature, and then cooled at 200°C/s back to room temperature. The curves fit the data well for most species, and modelling with only one or two reactions appears sufficient in all cases except the carbon oxides which require a third reaction for data above about 1000°C (not shown here). Figure 1-7 shows how the various individual reactions cooperate to give a smooth total weight loss curve. Again, this figure emphasizes that a large fraction of the total weight loss is due to the oxygenated species.

In order to compare the present kinetic parameters with those obtained before for the same type of coal using the previously described distributed activation energy model (Anthony, 1974; Anthony et al., 1975), the frequency distribution of the present activation energies is derived from Table 1-7 as follows.

Data points in Fig. 1-29 represent the cumulative ultimate yields of all volatile components having activation energies less than or equal to those of the indicated points. Each point is labelled with the component whose ultimate yield is added to those of all other components shown of all other components shown on points to the left to give the indicated cumulative yield; e.g., the vertical distance between two adjacent points represents the ultimate yield of the component specified on the higher point. The slope of the smooth curve drawn through the data gives the frequency distribution curve  $dV_{cum}^*/V_{tot}^* dE$ , which is here normalized so that the area under a segment of the curve between two values of

Table 1-7. Kinetic Parameters for Lignite Pyrolysis

Product	Stage	$E_i$ , kcal/mole	$\log (k_{10}/s^{-1})$	$V_i^*$ , Wt.% of lignite (as-received)
CO <sub>2</sub>	1	36.2	11.33	5.70
	2	64.3	13.71	2.70
	3	42.0	6.74	1.09
CO	1	44.4	12.26	1.77
	2	59.5	12.42	5.35
	3	58.4	9.77	2.26
CH <sub>4</sub>	1	51.6	14.21	0.34
	2	69.4	14.67	0.92
C <sub>2</sub> H <sub>4</sub>	1	74.8	20.25	0.15
	2	60.4	12.85	0.41
HC <sup>a</sup>		70.1	16.23	0.95
Tar	1	37.4	11.88	2.45
	2	75.3	17.30	2.93
H <sub>2</sub> O		51.4	13.90	16.5
H <sub>2</sub>		88.8	18.20	0.50
Total				44.0

<sup>a</sup>Hydrocarbons other than CH<sub>4</sub>, C<sub>2</sub>H<sub>4</sub> and Tar

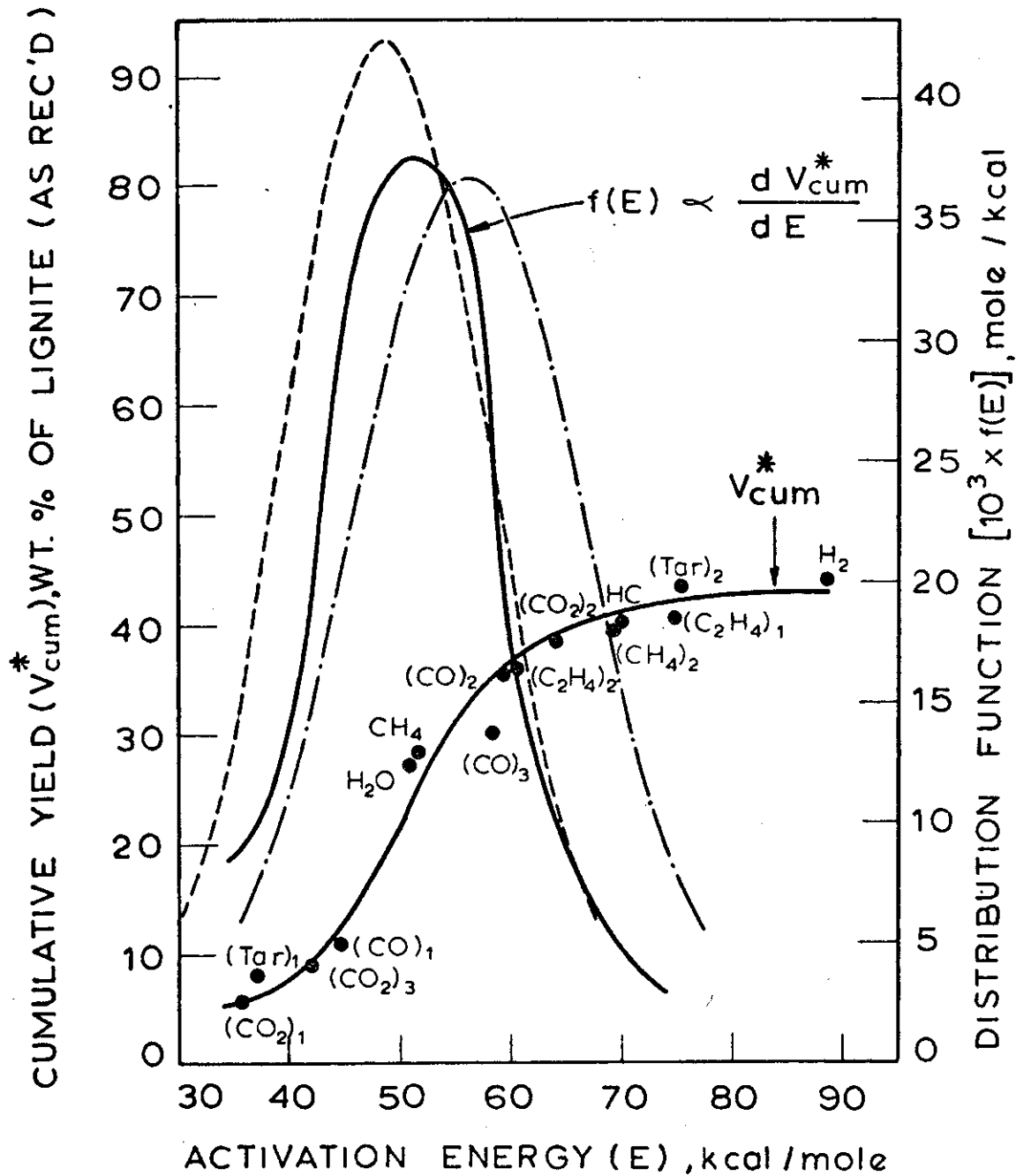


Figure 1-29. Distributions of Activation Energies of Pyrolysis Reactions [(●) cumulative yields, from present base data, of components indicated to left of and including a given point; (solid curves) present results based on volatiles yields; (broken curves) previous results (Anthony and Howard, 1976; Anthony, 1974) based on weight loss data and two different sets of kinetic parameters].



activation energy is the percentage of the total ultimate volatile yield that is associated with activation energies in the specified interval.

For comparison, Fig. 1-29 presents the Gaussian distributions derived by Anthony et al. (broken curves). The left distribution was derived by allowing the pre-exponential to be an adjustable parameter, and the right hand distribution was derived from a case in which the pre-exponential was set to  $1.67 \times 10^{13} \text{ sec}^{-1}$ . The similarity of the three distributions provides support for the use of a distributed activation energies model in the absence of detailed product analysis data.

The application of the first order model to bituminous coal pyrolysis is considerably more difficult. The model was first tried in a single first-order reaction form for each product. Assuming that each product arises from only one particular type of reaction or reactive structure leads to activation energies which are rather low (10-40 kcal/mole). The interpretation of such values is difficult inasmuch as they are generally too low to represent simple radical chain processes (see section 5.5 of the thesis), and they are too high to be reflecting a mass transport limitation. The preferred interpretation is that the process is chemically controlled by several processes acting in concert to give the observed broad temperature dependence.

Application of a two-first-order-step model, which was successful for many of the lignite results, gave a fair fit of the data in some (e.g. CO, CH<sub>4</sub>) cases. The parameter values so derived were close to those obtained for the lignite case, very likely reflecting the similarity of the processes leading to these products in both coals. However, several products (e.g. tar) appeared to be produced by many more than two reactions, given their rather broad, smooth temperature dependence. This suggested the use of a distributed activation energies model for each product, an approach used previously for the modelling of hydrocarbon gas evolution from pyrolyzing coal (Hanbaba et al., 1968).

The differences observed in the modelling of the lignite and bituminous coal pyrolysis phenomena reaffirm that the processes are **chemically quite** different. As examination of Figs. 1-7 through 1-9 reveals, there are apparently five distinct phases during lignite pyrolysis. The first occurs at very low temperatures ( $\sim 100^{\circ}\text{C}$ ) and is associated with moisture evolution. The second phase at  $1000^{\circ}\text{C/s}$  heating rate begins at about  $450^{\circ}\text{C}$  and is associated with a large initial evolution of carbon dioxide, probably from low-activation energy decarboxylations. The loss of carboxyl groups as carbon dioxide at relatively low temperatures has been reported for lignites (H.C. Howard, 1963). A small amount of hydrocarbon products is also evolved at this stage. The third phase involves evolution of water chemically formed in the range  $600\text{--}700^{\circ}\text{C}$ . The fourth phase involves a final rapid evolution of carbon containing species. Carbon oxides, tar, hydrogen, and hydrocarbon gases are all rapidly evolved in the temperature range  $700\text{--}900^{\circ}\text{C}$ , where little water is produced. The fifth phase is the previously discussed high temperature formation of carbon oxides. To be compared with the foregoing, the pyrolysis of bituminous coal occurs in four somewhat less distinct phases. Again, surface moisture is driven off at low ( $<100^{\circ}\text{C}$ ) temperatures followed by the liberation of pyrolytically formed water at peak temperatures just below  $400^{\circ}\text{C}$ . Between  $400$  and  $900^{\circ}\text{C}$ , the coal softens and the bulk of the hydrocarbons are evolved. Above  $900^{\circ}\text{C}$ ,  $\text{CO}$  and  $\text{H}_2$  are the principal products evolved.

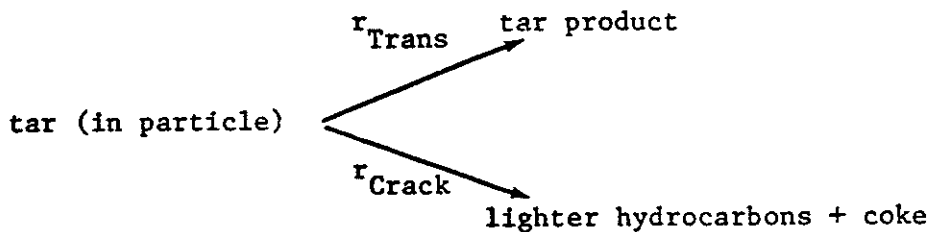
It appears, as Wolfs et al. (1960) hypothesized, that hydroxyl functional groups may be playing a key role in determining pyrolysis behavior. In the case of lignite pyrolysis, hydrocarbon formation is observed at temperatures between  $500$  and  $600^{\circ}\text{C}$  and between  $700$  and  $900^{\circ}\text{C}$ , but not between  $600$  and  $700^{\circ}\text{C}$  (evident in Fig. 1-8). This "plateau"

coincides with the principal water formation step. During pyrolysis of bituminous coal, water formation occurs prior to the hydrocarbon formation phase, and no plateau is observed. It is possible that the hydroxyl groups consume hydrogen which could otherwise serve to stabilize hydrocarbon radicals; in the absence of hydrogen, these radicals repolymerize to form a solid cross-linked residue. The bituminous coal has a higher initial hydrogen to carbon ratio; when the removal of hydrogen in the form of pyrolytically formed water is allowed for, the bituminous coal has a much higher effective hydrogen to carbon ratio than the lignite.

#### Secondary Reactions and Mass Transport Limitations

This section will focus principally on the behavior of the bituminous coal; the lignite showed only small effects of external pressure variation. Fig. 1-24 and 1-25 show that the principal effects of increased pressure during pyrolysis are observed only above peak temperatures of 700 to 750°C. At these temperatures, the coal has already completely softened and forms a uniform layer on the screens. The thickness of this layer does show some dependence on the diameter of the original coal particles.

From an analysis of compositional changes occurring with increased mass transport resistance, it is apparent that the principal reactions involved are of the tar cracking variety (Fig. 1-18). Thus transport of the tar appears to be in competition with secondary cracking reactions:



where  $r_{\text{Trans}}$  and  $r_{\text{Crack}}$  represent the rates of transport and cracking, respectively. Under pseudo steady conditions, the ratio of actually

observed tar (X) to the maximum possible yield( $X^*$ ) is given by

$$\frac{X}{X^*} = \frac{r_{\text{Trans}}}{r_{\text{Trans}} + r_{\text{Crack}}} = \frac{1}{1 + (r_{\text{Crack}}/r_{\text{Trans}})}$$

Anthony et al. (1975) proposed  $r_{\text{Trans}} = k_T/P_{\text{Ext}}$ , by analogy with a diffusion coefficient ( $k_T$  is a constant and  $P_{\text{Ext}}$  is the pressure within the reactor). An equation of this form was quite successful in modelling weight loss data of the type shown in Fig. 1-18.

Although the escape of the bulk of the volatiles is certainly not characteristic of diffusion (the volatiles are seen to emerge as jets from the surface of the coal), an equation with a  $1/P$  pressure dependence fits the very strong pressure dependence of tar yield in the range from high vacuum to atmospheric, while simple models of pressure driven flow cannot. The implication is that while the transport of gaseous products out of the coal is governed by hydrodynamic flow, the transport of tar away from the coal may be an evaporative process. Estimates of the vapor pressure of tar support this view.

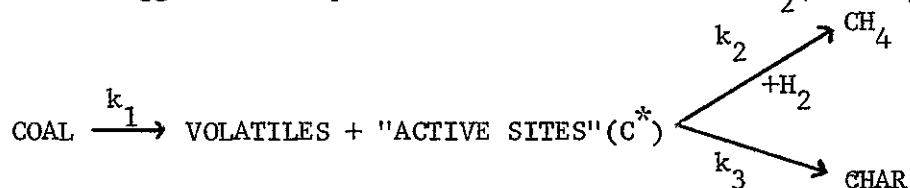
It is also possible to estimate the activation energy of the cracking reactions by noting that they always begin to manifest themselves in the range of peak temperatures between 700 and 800° C. Since the typical experiment involves a heating rate of 1000° C/sec and a cooling rate of 200° C/sec, then it can be shown from the previously derived equation for non-isothermal kinetics that the cracking reactions have a minimum activation energy close to 60 kcal/mole (assuming an Arrhenius pre-exponential of around  $10^{13} \text{ sec}^{-1}$ ).

### 1.5.2 Hydropyrolysis

It appears that the interaction of pyrolyzing coal and externally provided gaseous hydrogen begins at temperatures marking the principal hydrocarbon formation steps of ordinary pyrolysis. All of the products observed during ordinary

pyrolysis are also observed during hydrolysis; the product chiefly responsible for the increased yields observed during hydrolysis is methane. It is likely that the hydrogen acts to stabilize radicals formed during cleavage of hydrocarbon linkages within the coal.

In the case of lignite hydrolysis, in which the variation of particle diameter indicated a regime of primarily chemical control, the pressure dependence of product yields is apparently complicated, but a model of the form indicated below is suggested for pressures less than 69 atm  $H_2$  (=1000 psig, see Fig. 1-23).



It can be shown by assuming a 'quasi steady-state' for the concentration of active sites that the ultimate yield of methane predicted by the above competitive model is

$$(CH_4) = \frac{\frac{k_2 C_o^*}{k_3} P_{H_2}}{\frac{k_2 C_o^*}{k_3} P_{H_2} + 1}$$

(assuming that the methane forming reaction is first order in hydrogen pressure and that the initial concentration of active sites is  $C_o^*$ ). Zahradnik and Glenn (1971) and Johnson (1977) have used such an empirical form with some success. The data at pressures greater than 1000 psig in Fig. 1-23 obviously cannot be explained by such a simple form.

Anthony et al. (1976) suggested that the principal mechanism of interaction of externally provided hydrogen gas with pyrolyzing coal is via stabilization of reactive volatiles. Although the data in Fig. 1-25 clearly show that the tar itself is not stabilized during hydrolysis (yields from 69 atm hydrolysis are as low as those from 69 atm pyrolysis), other products of tar hydrocracking are evident.

Lignite pyrolysis produces rather low yields of tar, even under vacuum conditions. The lignite does however show substantially enhanced yields during hydro-pyrolysis. The principal product responsible for the enhanced yields is methane; the other major products of lignite pyrolysis remain largely unaffected by the presence of hydrogen. This may be construed as evidence for a heterogeneous process.

Since the data in Figures 1-19 and 1-24 suggest that hydrogen begins to have a measurable effect on weight loss at peak temperatures between 700 and 800°C, then the reaction  $k_1$  may be characterized by the same type of distribution of activation energies as the secondary reactions; i.e. with a large fraction of the reactions having activation energies over 60 kcal/mole.

## 1.6 Conclusions

The following are the major conclusions of this investigation:

1. Coal rank and pyrolysis temperature are the most significant determinants of product composition.
2. There is very little effect of heating rate on the composition of volatiles or the kinetics of their formation (conclusion drawn for high rates of heating primarily).
3. Variation of particle diameter and external pressure can substantially affect the character of products produced during pyrolysis. This effect is most pronounced in a coal normally characterized by high yields of tar and is minimal in a lignite which produces little tar. It is felt that secondary tar cracking reactions may be the reason for the frequent discrepancy between the results of the standard proximate volatile matter test and rapid pyrolysis yields.
4. There is good correlation between certain products of pyrolysis (e.g.  $\text{CO}_2$ ,  $\text{H}_2\text{O}$ ) and structural features of the raw coal (e.g. carboxyl groups, hydroxyl groups). The rather important role ascribed to hydroxyl groups by Wolfs et al. (1960) has received support from these data.
5. The pyrolysis process occurs in several distinct stages, each characterized by a particular set of products. A pyrolysis model describing weight loss behavior with a distribution of activation energies has received support from individual product kinetic data.
6. A small effect of hydrogen gas can be seen rather 'early' in the pyrolysis process, but the full effects of hydrolysis are not observed until a substantial portion of the ordinary pyrolysis process has run its course. In the case of bituminous coal hydrolysis, hydrogen has no apparent effect on a portion of the tar which is formed at low temperatures. Hydrogen does not stabilize high temperature tar, but may stabilize small tar fragments.

### 1.7 References for this Section

- Anthony, D.B., "Rapid Devolatilization and Hydrogasification of Pulverized Coal," Sc.D. thesis, Massachusetts Institute of Technology, Cambridge, Mass., 1974.
- Anthony, D.B., J.B. Howard, H.P. Meissner, and H.C. Hottel, "Apparatus for Determining High Pressure Coal-Hydrogen Reaction Kinetics under Rapid Heating Conditions," Rev. Sci. Instrum. 45, 992 (1974).
- Anthony, D.B., J.B. Howard, H.C. Hottel, and H.P. Meissner, "Rapid Devolatilization of Pulverized Coal," Fifteen Symposium (International) on Combustion, p. 1303, The Combustion Institute, Pittsburgh, Pa. (1975).
- Anthony, D.B., J.B. Howard, H.C. Hottel, and H.P. Meissner, "Rapid Devolatilization and Hydrogasification of Bituminous Coal," Fuel 55, 121 (1976).
- Anthony, D.B., and J.B. Howard, "Coal Devolatilization and Hydrogasification," A.I.Ch.E. J. 22, 625 (1976).
- Brown, H.R. and P.L. Waters, "The Function of Solvent Extraction Products in the Coking Process - I", Fuel, 45, 17 (1966).
- Campbell, J.H. and D.R. Stephens, "Kinetic Studies of Gas Evolution during Pyrolysis of Subbituminous Coal", Am. Chem. Soc., Div. Fuel Chem. Preprints, 21, No. 7, 94 (1976).
- Cartz, L. and P.B. Hirsch, "A Contribution to the Structure of Coals from X-Ray Diffraction Studies", Phil. Trans. Roy. Soc. London, 252 A, No. 1019, 557 (1960).
- Chakrabartty, S.R. and N. Berkowitz, "Studies on the Structure of Coals - 3", Fuel, 53, 240, (1974).
- Fuoss, R.M., I.O. Salzer and H.S. Wilson, "Evaluation of Rate Constants from Thermogravimetric Data", J. Polymer Sci., A-2, 3147 (1964).
- Given, P.H., "The Distribution of Hydrogen in Coals and Its Relation to Coal Structure", Fuel, 39, 147 (1960).
- Hanbaba, P., H. Juntgen, and W. Peters, "Nicht-isotherme Reaktionskinetik der Kohlenpyrolyse, Teil II: Erweiterung der Theorie der Gasabspaltung und experimentelle Bestätigung an Steinkohlen," Brennstoff-Chem. 49, 368 (1968).
- Howard, H.C., "Pyrolytic Reactions of Coal," in Chemistry of Coal Utilization, pp. 340-394, Supplementary Volume, H.H. Lowry, ed., Wiley, New York (1963).
- Johnson, J.L., "Kinetics of Initial Coal Hydrogasification Stages", Am. Chem. Soc., Div. Fuel Chem. Preprints, 22, No.1, 17 (1977).



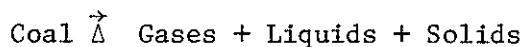
- Jüntgen, H. and K.H. Van Heek, "Gas Release from Coal as a Function of the Rate of Heating," Fuel 47, 103 (1968).
- Jüntgen, H. and K.H. Van Heek, "Reaktionsabläufe unter nichtisothermen Bedingungen," in Fortschritte der chemischen Forschung, vol. 13, pp. 601-699, Springer-Verlag, Berlin (1970).
- Lewellen, P.C., W.A. Peters, and J.B. Howard, "Cellulose Pyrolysis Kinetics and Char Formation Mechanism" Sixteenth Symposium (International) on Combustion, The Combustion Institute, Pittsburgh, Pa. (in press).
- Madorsky, S.L., "Rates of Thermal Degradation of Polystyrene and Polyethylene in a Vacuum," J. Polymer Science IX (2), 133 (1952).
- Madorsky, S.L., "Rates and Activation Energies of Thermal Degradation of Styrene and Acrylate Polymers in a Vacuum," J. Polymer Science XI (5), 491 (1953).
- Vander Hart, D.L. and H.L. Retcofsky, "Analysis of the Aromatic Content of Whole Coals by High-Power Proton Decoupled C-13 NMR", Stanford Res. Inst. Coal Chemistry Workshop, Paper No. 15 (1976).
- Van Krevelen, D.W., Coal, Elsevier Publishing Co., Amsterdam (1961).
- Van Krevelen, D.W., C. Van Heerden, and F.J. Huntjens, "Physiochemical Aspects of the Pyrolysis of Coal and Related Organic Compounds," Fuel 30, 253 (1951). [Numerical results modified by Jüntgen and Van Heek (1970).]
- Wolfs, P.M.J., D.W. Van Krevelen and H.I. Waterman, "Chemical Structure and Properties of Coal - XXV", Fuel 39, 25 (1960).
- Zahradnik, R.L. and R.A. Glenn, "Direct Methanation of Coal," Fuel 50, 77, (1971).

## 2.0 Introduction

There is very likely no need to present here a lengthy discussion on the importance of coal conversion research; the U.S. appears committed, in the foreseeable future, to a heavy dependence on fossil fuels, of which coal is the most abundant. It is not surprising then that both the popular press and professional engineering literature abound with the results of ongoing coal research, and calls for yet further research. Nor is this interest in coal conversion only a recent phenomenon. Included in the appendix to this thesis is an editorial appearing in Industrial and Engineering Chemistry in 1942, calling for more research in the area. This exhortation from 33 years ago may be even more timely today.

The conversion of coal to usable energy can be either direct, via combustion, or indirect via synthetic fuels produced from coal (e.g. synthetic natural gas, coal oil, solvent refined solids). Much of the chemistry of interest in coal conversion work occurs at temperatures above which the raw coal itself begins spontaneously to decompose (generally above 350°C). This thermally induced degradation is termed pyrolysis and synonyms include carbonization or devolatilization.

The pyrolysis reaction yields three classes of products, as shown below:



The nature and relative amounts of these products depend on a number of factors:

1. The chemical and physical characteristics of the raw coal
2. The time-temperature history to which the coal is exposed (including heating rate).
3. The preparation of the coal (e.g. particle diameter).

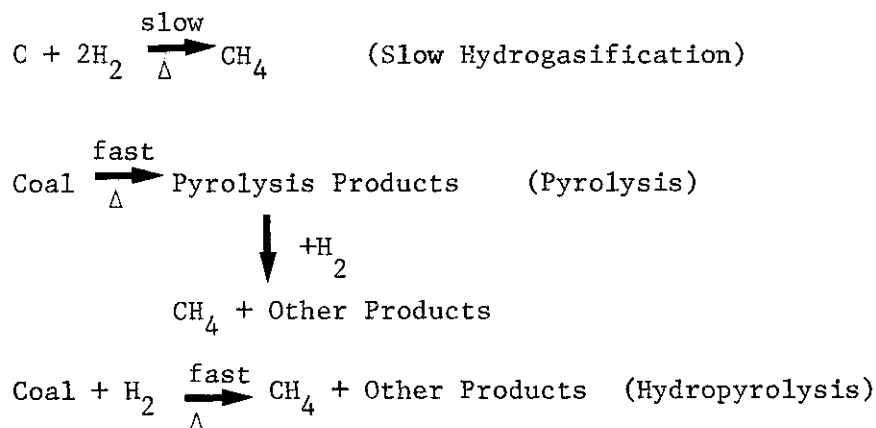
4. The nature of the reactor in which the coal is pyrolyzed (including total operating pressure, presence of any reactive gases, product residence time, catalytic surfaces, etc.)

These variables can all play major roles in determining the nature of a pyrolysis process, and will be examined in detail on this thesis.

Pyrolysis itself (that is, thermal degradation of coal in an inert gaseous environment) can serve as a coal conversion process. The processes used to produce metallurgical coke and coal tar chemicals are simple pyrolysis processes. Recently, there has been increasing interest in using processes based only upon pyrolysis to produce crude synthetic fuels.

In other types of conversion processes, pyrolysis is either a precursor to the chemistry of interest, or else occurs concurrently with it. Examples include hydrogasification and combustion of coal. In the latter case, the inflammability of pulverized coal is strongly tied to the pyrolysis behavior of the coal (see Essenhigh and Howard, 1971).

Hydrogasification of coal to synthetic natural gas ( $\text{CH}_4$ ) also involves a partially pyrolytic mechanism:



Hydropyrolysis simply implies pyrolysis in a gaseous hydrogen environment. The hydropyrolysis (synonyms hydrocarbonization, flash hydrogenation) reaction is many times faster than the slow hydrogasification reaction.

Because of the high rates of conversion and reportedly high yields which can be obtained via hydrolysis, a fair amount of interest has recently been focussed upon this reaction. This thesis will explore how hydrolysis is related to ordinary pyrolysis.

To summarize, the pyrolysis phenomenon is common to all thermally induced coal conversion processes. To gain a fuller understanding of coal pyrolysis phenomena will have two benefits. In the short term, there is interest in pyrolysis itself as a coal conversion process; while the work herein described is not concerned with the development of any particular process, the results obtained can help guide design of such processes. In the longer term, an understanding of the pyrolysis phenomena will help provide insight into many other types of reactions involving coal.

The objectives of this investigation are, broadly speaking, to provide a comprehensive picture of the chemical and physical processes occurring during pyrolysis, and to explain them in terms of the effect of significant variables. The specific objectives of this thesis were:

- Characterization of the products of pyrolysis and hydrolysis as a function of the previously listed variables.
- Determination of the chemical kinetics of pyrolysis and hydrolysis.
- Examination of the interrelationship between pyrolysis and hydrolysis.
- Development of models to explain observed phenomena.

It is apparent that some of the above objectives are much more firmly in hand than others. The nature of the work has been primarily exploratory, mandated to a great extent by the large number of variables considered. The results presented here can provide direction for many future studies.

### Introduction to Nomenclature and Conventions

This section defines a few terms and conventions used throughout this thesis. All coal analyses are reported on an as-received basis except where otherwise noted. The decision to use the as-received basis (that is, uncorrected for the moisture and ash content of the coal) was based on a desire to provide results which convey the truest picture of overall coal behavior. In all cases, sufficient information is provided to correct the results to one of the other standard bases:

1. dry (= moisture free, MF) - All mass ratios calculated relative to the mass of coal after drying according to A.S.T.M. procedure.

$$\text{Percent dry} = \frac{\text{percent as-received} \times 100}{100 - \text{percent moisture}}$$

2. Moisture and ash free (MAF = Dry Ash Free, DAF) - All mass ratios calculated relative to the mass of coal corrected for moisture and ash content, as determined by the A.S.T.M. procedure.

$$\text{percent maf} = \frac{\text{percent as-received} \times 100}{100 - \text{percent moisture} - \text{percent ash}}$$

3. Dry mineral matter free (DMMF) - calculated as dry, ash free except substituting mineral matter content for ash (not equivalent). The significance of the difference between a dmmf basis and a daf basis will be explored in a later section.

### 3.0 Background

#### 3.1 The Importance of Coal Type in Determining Pyrolysis Behavior

The chemical and physical nature of a raw coal or lignite has a profound effect upon its behavior during pyrolysis. It has long been recognized that coals of different ranks give markedly different products upon pyrolysis. Lignites give fairly high yields of volatiles, but not much tar, and the chars do not agglomerate strongly. Bituminous coals can also give a high yield of volatiles, but a large fraction can be in the form of tar. Bituminous chars also are frequently swollen and/or strongly agglomerated. Anthracites give low volatile yields and do not "cake". Even within the single rank classification of "bituminous coals", the differences in pyrolysis behavior are large, as is evidenced by the fact that some bituminous coals are highly valued for their coke-making characteristics, while others are not suitable for coke-making.

In this section, the important chemical and physical characteristics of coal are briefly reviewed, as is some of the evidence for how these factors influence the pyrolysis behavior of coals. Coal is, in general, comprised of an inorganic part and an organic part. The first subsection is concerned with the constitution of the inorganic part, the second subsection with the organic fraction viewed on a macroscopic scale, and the third subsection with the organic fraction viewed on a molecular level.

In this work, two coals were chosen as being representative of two important classes of U.S. coals. The first was a partially dried Montana Lignite from the Savage Mine of the Knife River Coal Mining Company. This lignite was chosen as a representative of the large reserves of low-rank Western coals. Table 3.1-1 gives the usual analyses for the lignite and for the second coal studied, a Pittsburgh Seam

Table 3.1-1 Characteristics of the Coals Examined

<u>Proximate Analysis,</u> <u>Wt.% (as-received)</u>			<u>Ultimate Analysis,</u> <u>Wt.% (as-received)</u>			<u>Petrographic Analysis,</u> <u>Wt.% (mineral-matter-free)</u>		
	<u>Lignite</u> <sup>†</sup>	<u>Bituminous</u> <sup>††</sup>		<u>Lignite</u>	<u>Bituminous</u>		<u>Lignite</u>	<u>Bituminous</u>
Moisture	6.8	1.4	Carbon	59.3	67.8	Vitrinites	69.7	84.5
V.M.	36.9	38.9	Hydrogen	3.8	4.8	Semi-Fusinite	15.2	4.5
F.C.	46.4	48.4	Nitrogen	0.9	1.3	Fusinite	7.9	3.3
Ash	9.9	11.3	Sulfur	1.1	5.3	Micrinite	5.2	4.4
			Oxygen*	18.2	8.1	Exinite + Resinite	2.0	3.3
			Moisture	6.8	1.4			
			Ash	9.9	11.3			
TOTAL	100.0	100.0	TOTAL	100.0	100.0	TOTAL	100.0	100.0

\* By difference.

† The Lignite is a partially dried Montana Lignite from the Savage Mine of the Knife River Coal Mining Company.

†† The Pittsburgh Seam (No. 8) Bituminous coal is from the Ireland Mine of the Consolidation Coal Company.

96

(No. 8) Bituminous from the Ireland Mine of the Consolidation Coal Company. The bituminous coal is considered representative of Eastern U.S. high-sulfur caking coals.

It is noted that the lignite is "partially dried". The decision to use a lignite in this form rather than "as-mined" was primarily dictated by an interest in product analysis. Since the lignite is an as-mined state contained about 30% moisture by weight, the water product would have acted as a diluent in product streams, making analysis of the more interesting hydrocarbon fractions more difficult.

Referring to Table 3.1-1, the volatile matter (V.M.) test for coal is in itself a pyrolysis experiment, i.e. pyrolysis for 7 minutes at 950°C. Typically, the values of the volatile matter plus moisture (determined by drying at 107°C) from standard ASTM procedures are less than total yields available from rapid pyrolysis, implying that "fixed carbon" (F.C.) is not necessarily such for all pyrolysis processes. (The fixed carbon is calculated by difference from the weight of the coal less volatile matter, less moisture, and less ash as determined by complete combustion of the sample). Reasons for the difference between volatile matter as determined by the ASTM vs. rapid pyrolysis will be discussed in various section of this thesis.

The significance of the behavior of coal mineral matter on the otherwise straightforward ultimate analysis will be discussed in the next subsection, and the influences of the petrographic composition on pyrolysis work in the subsection following that.



### 3.1.1 Mineral Matter in Coal

A good review of the literature on mineral matter in coal is provided by Ode (in Lowry, 1963). A large amount of data has also been gathered on the behavior of ash and mineral matter in coals similar to those examined in this work (Padia, 1976).

There is often a minor problem in interpretation of literature data on coal compositions caused by a failure to distinguish between the ash and mineral matter contents of a coal. Since a determination of the ash "content" is a much more straightforward and standard measurement than a direct mineral matter determination, the value of the former is often used where, strictly speaking, only the value of the latter is correct. This is especially important in determination of the oxygen content of the coal, since this quantity is typically calculated by difference after all else (i.e. C,H,N,S,ash,moisture) in the coal has been accounted for. Some of the factors which account for the difference between the weight of ash and mineral matter are water of hydration and CO<sub>2</sub> being driven off from clay minerals and carbonates, and pyrites burning to iron oxides, liberating sulfur oxides which may or may not be captured by other coal mineral components (such as cations in low-rank coals). It has been determined empirically that a fair estimate of mineral matter content is available from ash values and a knowledge of the tar sulfur content of the coal by use of the Parr formula (ASTM Standard Specifications for Classification of Coals by Rank D388-38):

$$\text{Mineral Matter (wt\%)} = 1.08 \times \text{Ash(wt\%)} + 0.55 \times \text{Sulfur(wt\%)}$$

Given (1975) suggests an improvement upon the Parr formula, based on mineral matter determinations by acid demineralization:

$$\text{Mineral Matter} = 1.13 \times \text{Ash} + 0.47 \text{ S pyritic} + 0.5 \text{ Cl}$$

According to this formula, the coals used in this study have the following mineral matter contents:

	<u>Ash</u>	<u>Mineral Matter</u>
Montana Lignite	9.9	11.3
Pittsburgh Seam Bituminous	11.3	14.1

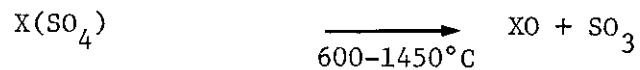
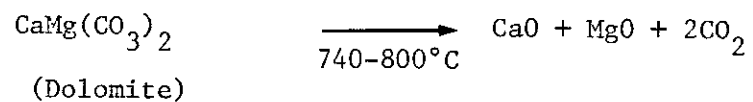
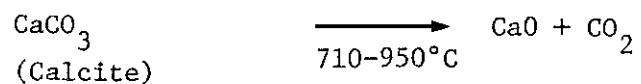
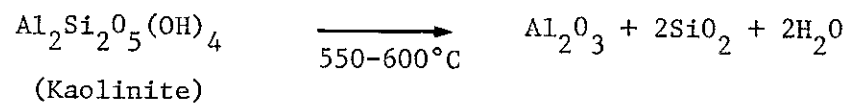
A better estimate of the mineral matter is available from a detailed study of the mineral matter in coals obtained from the same mines (Padia, 1976). Padia derived the following stoichiometrically based relationship between mineral matter and ash composition (see Table 3.1-2 for reactions considered):

$$\begin{aligned} \text{Mineral Matter} = & \text{Ash} + 0.625 \text{ S pyr. coal} + 0.833 \left[ \begin{array}{l} \text{S}_{\text{sulfate}} \text{ coal}^{-\text{S}} \\ \text{sulfate} \text{ coal} \end{array} \times \frac{\text{Ash}}{100} \right] \\ & + \frac{\text{Ash}}{100} \left[ 0.162(\text{SiO}_2 + \text{Al}_2\text{O}_3)_{\text{Ash}} + 0.79(\text{CaO})_{\text{Ash}} \right. \\ & \left. + 1.1(\text{MgO})_{\text{Ash}} \right] \end{aligned}$$

(where all quantities are weight percents)

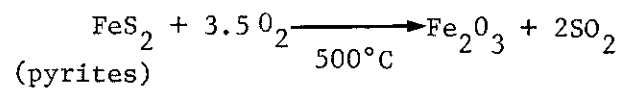
This correlation gives good agreement with low temperature ashing (LTA) results. Low temperature ashing involves oxidizing the organic material in coal with an oxygen plasma at a temperature no higher than 180°C, presumably leaving the mineral matter intact. Given et al. (1975) feel that low temperature ashing may still lead to errors in mineral

Table 3.1-2 Principal Reactions that Contribute to Mineral Matter Weight Loss (after Padia, 1976)



X = Ca, Mg, "Fe<sub>2/3</sub>"

During oxidation only:



matter determination because oxidized organic sulfur may react with and be retained in the mineral matter. They suggest that the acid leaching technique of Bishop and Ward (1958) is the only reliable technique for mineral matter determination.

A straightforward improvement, based on simple stoichiometry, can be made to the formula suggested by Padia. Since  $\text{SiO}_2$  in coal ash can arise from either Kaolinite dehydration (as assumed in deriving the formula) or from inert Quartz, it would be more appropriate to base the term for Kaolinite dehydration on  $\text{Al}_2\text{O}_3$  alone, rather than the sum of  $\text{Al}_2\text{O}_3 + \text{SiO}_2$ . The revision leads to the following:

$$\begin{aligned} \text{Mineral Matter} = & \text{Ash} + 0.625(\text{S pyritic}) + 0.833 \left[ \text{S}_{\text{coal}}^{\text{sulfate}} - \text{S}_{\text{ash}}^{\text{sulfate}} \times \frac{\text{Ash}}{100} \right] \\ & + \frac{\text{Ash}}{100} \left[ 0.354(\text{Al}_2\text{O}_3)_{\text{Ash}} + 0.79(\text{CaO})_{\text{Ash}} + 1.1(\text{MgO})_{\text{Ash}} \right] \end{aligned}$$

where, again "Ash" represents the weight percent of ash residence based on raw coal, and all other quantities represent weight percents of the ash itself, except for the term for sulfate content of the coal.

By assuming that the ash compositions found by Padia hold for the samples under study here, the following ash compositions can be used for determining mineral matter:

<u>Percent by weight of raw coal</u>	<u>Montana Lignite</u>	<u>Pittsburgh Bituminous</u>
Total Ash	9.95	11.33
$Al_2O_3 \times \frac{Ash}{100}$	1.62	2.17
$CaO \times \frac{Ash}{100}$	3.18	0.61
$MgO \times \frac{Ash}{100}$	0.96	0.08
$S_{\text{sulfate ash}} \times \frac{Ash}{100}$	0.537	0.186
$S_{\text{sulfate coal}}$	0.0791	0.751
$S_{\text{pyr coal}}$	0.220	2.74
$S_{\text{org coal}}$	0.82	1.77
Mineral Matter (by revised Padia formula)	13.9	14.8
Organic Oxygen (by diff., as-rcvd., corrected for inorganic C, H, S)	15.6	8.48

Although final results were not available at the time of this writing, preliminary indications are that agreement between the formula and the method of Bishop and Ward is acceptable.

Since in deriving the mineral matter formula, it is assumed that all  $Al_2O_3$  came from kaolinite dehydration, that all  $CO_2$  came from calcite ( $CaCO_3$ ), or dolomite ( $CaCO_3 \cdot MgCO_3$ ) decomposition, and that sulfur oxides could come from sulfate decompositions, then it should be possible to back-calculate the inorganic oxygen loss (which, when it appears as  $H_2O$  and  $CO_2$  product is indistinguishable from organic oxygen). Again, the relevant reactions are given in Table 3.1-2.

$$\text{Oxygen in } H_2O \text{ from Kaolinite} = \left(\frac{16}{18}\right) (.354) (Al_2O_3 \times \frac{Ash}{100})$$

$$\text{Oxygen in CO}_2 \text{ from Calcite} = \left(\frac{32}{44}\right) (0.79) \left(\text{CaO} \times \frac{\text{Ash}}{100}\right)$$

$$\text{Oxygen in CO}_2 \text{ from Dolomite} = \left(\frac{32}{44}\right) (1.1) \left(\text{MgO} \times \frac{\text{Ash}}{100}\right)$$

$$\text{Oxygen in SO}_3 \text{ from Sulfates} = \left(\frac{48}{80}\right) \left( S_{\text{sulfate coal}} - S_{\text{sulfate ash}} \times \frac{\text{Ash}}{100} \right)$$

This summation yields for the two coals:

	<u>Lignite</u>	<u>Bituminous</u>
Inorganic oxygen as H <sub>2</sub> O	0.5	.68
as CO <sub>2</sub>	<u>2.6</u>	<u>.76</u> (and SO <sub>x</sub> )
Total Inorganic O	3.1	1.44
Organic O	<u>15.6</u>	<u>8.48</u>
Total O	18.7	9.92

The total oxygen is the appropriate value for computing oxygen mass balances, while the organic oxygen is the correct value for structural considerations. Note that in the case of the lignite, the actual total oxygen is within 5% of the oxygen computed by difference, assuming the ash measurement to represent mineral matter, while in the case of bituminous coal, the by difference-ash value is more than 20% different.

The other important role which the mineral matter can play in coal is that of catalyst for organic reactions. Unfortunately opinion is somewhat divided on the effect of various components. Alkali metals have long been thought to have catalytic effect on the reaction of coals and chars with hydrogen. Various oxides, carbonates and chloride salts have been impregnated into coals and chars by various techniques to enhance conversion rates. For example, the Batelle Treated Coal (BTC) Process involves impregnation of a Pittsburgh Seam #8 coal with CaO by treatment of the coal in an aqueous solution of CaO and NaOH (the coal

studied is very similar to that studied in this thesis). The reactivity of the coal to hydrogen, as measured by weight loss, is substantially increased, and it appears that the rate of initial devolatilization may also be increased (Chauhan et al., 1977). However, the treatment of coal with strong alkali (such as NaOH) may have other important structural effects, such as turning phenolic hydroxyls into phenoxy salts. As will be discussed in the section on pyrolytic mechanisms, this may hinder certain condensation reactions within the coal structure, and have an effect on yield only on that basis, rather than a catalytic basis.

From some work on hydrogasification of a (non-coal derived) char mixed with various minerals, Tomita et al. (1977) conclude that many calcium containing minerals inhibit the hydrogasification process while iron-containing species catalyze it.

Lignites contain many carboxylic groups, most of which are in salt form (this will be discussed in the section on coal structure). It has been suggested that the cations associated with the carboxylates can have catalytic effect. A study in which an acid ion-exchanged lignite is pyrolyzed or hydrolypyrolyzed may shed light on the catalytic significance of these structures. Johnson (1975a) found a marked effect of cationic calcium and sodium species during slow hydrogasification and steam gasification of lignite. It is not certain whether this effect can manifest itself during rapid pyrolysis or hydrolypyrolysis.

A careful study comparing the rapid pyrolysis and hydrolypyrolysis behavior of raw and acid demineralized coals could shed a great deal of light on the auto-catalysis question.

### 3.1.2 Petrographic Analysis and its Relation to Pyrolysis Behavior

An important chemical characteristic of coal is the heterogeneity of its organic material. Coal petrography is concerned with the characterization of coal as an "organic rock" composed of varying amounts of real minerals (e.g.  $\text{SiO}_2$ ) and "organic minerals", known as macerals. Maceral fractions are observable by microscopic examination of thin sections of coal with transmitted light (in which the different maceral types show up as various shades of reds, yellows, browns, blacks) or by examination of polished samples under reflected light (in which the macerals show up as black, white, or various shades of gray). Some of the maceral fractions show distinctly their fossil origins (e.g. woody tissue, plant spores, charred woody tissue).

Although there are many more readily identifiable maceral components, for ease of discussion, they are categorized into three principal maceral groups:

- Vitrinites
- Exinites
- Inertinites

Unfortunately, a particular maceral can vary considerably, both compositionally and chemical behavior-wise, from coal to coal. Some details of chemical structure are given in the next section, here only broad trends are noted. The differences between macerals decrease with increasing "rank" (age or extent of coalification—higher rank coals have higher carbon contents). This is illustrated in Fig. 3.1-1 in which the atomic C/H ratio is plotted as a function of rank for the three principal maceral groups (Kessler, 1973).

From the standpoint of physical and chemical properties, exinites



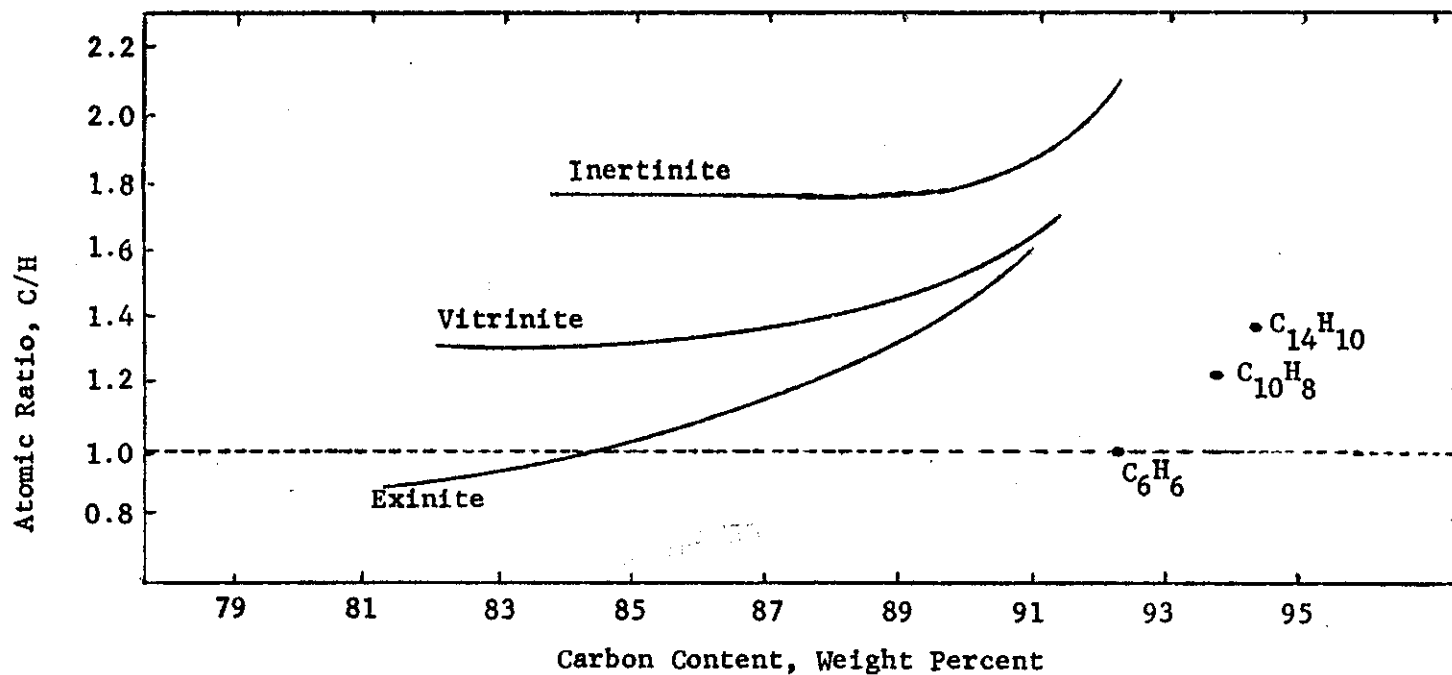


Figure 3.1-1. Comparison of C/H Ratios of Macerals of Different Rank (Kessler, 1973; also indicated for reference, values for benzene (C<sub>6</sub>H<sub>6</sub>), naphthalene (C<sub>10</sub>H<sub>8</sub>), and anthracene (C<sub>14</sub>H<sub>10</sub>)).

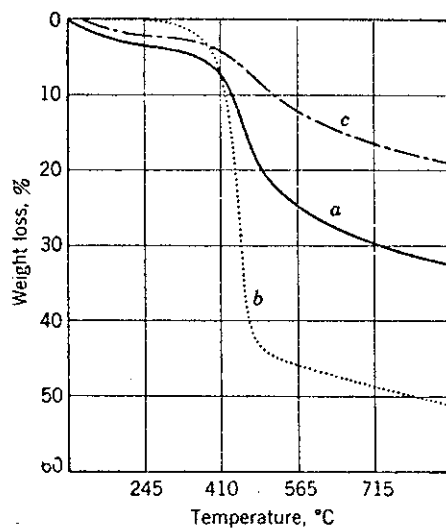


Figure 3.1-2. Comparison of Pyrolysis Behavior of Macerals (Kroger and Pohl, in Howard, 1963).

are characterized by the highest hydrogen content, volatile matter content and heating value of all the macerals of a particular rank. Inertinites have the highest density and greatest degree of aromaticity at any particular rank. Vitrinite, which is by far the most abundant of the three maceral groups, usually exhibits chemical and physical properties between the extremes of exinite and inertinite (Dryden, 1963).

The rank and overall chemical composition of a coal are alone not sufficient, in general terms, to predict the pyrolysis behavior of that coal. As has already been noted, exinites give higher yields of volatiles than do vitrinites, which in turn give higher yields than do inertinites (represented by micrinite in Fig. 3.1-2). It appears that in addition to differences in total yields, there are compositional differences among the products from the three maceral groups. For example, exinites produce significantly more tar and more straight char paraffins and olefins than vitrinites, whose products tend to be more "phenolic" in nature (Howard, 1963 and Boyer et al., 1961).

There have, naturally, been many attempts to relate petrographic composition to coking behavior. In general, only coals of bituminous rank are able to "coke" (soften, partially decompose, and resolidify to a hard, carbon-rich solid). Vitrinite is the maceral which is primarily responsible for this coking behavior. Exinites become more fluid during pyrolysis, but volatilize to such a great extent that they cannot form a coke. Inertinites, as their name implies, do not participate in the coking reactions to any great extent, but their presence in small quantities contributes to the mechanical strength of cokes. (Given, 1976). The liquefaction behavior of macerals mirrors their pyrolysis behavior--vitrinites and exinites are much more easily converted to liquid products

than is inertinite (Davis, 1976).

The coals chosen for the present study are characterized by high vitrinite contents (see Table 3.1-1). It is this component which is expected to determine principally the pyrolysis behavior of these coals. The lignite has a fairly high inertinite content (fusinite + semi-fusinite + micrinite = 28.3 vol.%, mineral matter free basis). This material may be expected to act almost as a "diluent" in the same sense as mineral matter. In neither coal is the exinite (exinite + resinite) present in large enough quantities to be a major actor, but it is sure to contribute a large fraction of its weight to volatile product, which, because of richer hydrogen content, may be a rather more desirable product than those from vitrinite.

It may reasonably be asked, then, given the rather striking differences between maceral fractions, would it not make sense to study them separately? The answer would almost certainly be yes but for two important factors. The first is that good maceral separation is difficult (especially exinite), and the second is that individual maceral work alone can provide only a partial answer to the question of how real coals behave during pyrolysis or hydrolysis (there may well be important interaction effects). The decision was made, in this rather exploratory work, to first get data on the composite material, that is, on the whole coal.

One final note of caution concerning the difference in maceral fractions; each of the different petrographic components has a different resistance to mechanical breakage (Parks, 1963); consequently the grinding and sifting operations involved in preparing experimental particles

run the risk of enriching a sample in certain fractions relative to others. Thus a systematic study of the effect of particle diameter on yields may be measuring this effect in addition to a mass transfer effect. This effect was briefly studied during the course of this thesis, and it is tentatively concluded, at least with bituminous coal, that maceral enrichment was not a major factor in particle diameter effects (see section on discussion of experimental results). Such a conclusion is not universal, however, inasmuch as it is claimed that more reactive components are preferentially reduced to smaller sizes, and this is the principle behind the Burstlein and Sovaco processes of coke blending (Biemann et al., 1963).

### 3.1.3. The Chemical Structure of Coal

The pyrolysis of relatively simple hydrocarbon compounds is complex and/or poorly understood. Therefore, it comes as little surprise that the chemical mechanisms of coal pyrolysis are poorly understood.

The characterization of the products of coal pyrolysis is a sizable task - as already noted, the products are usually present in all the three states of matter, gaseous, liquid, and solid. The number of distinct chemical species is large, and to facilitate data analysis one must usually resort to judiciously grouping the products into a few key classes of compounds. The analysis of the pyrolysis products is of course, the subject of another section of this thesis.

Unfortunately in studying coal pyrolysis the characterization of the reactant is as difficult, if not more difficult than, the characterization of the products of the process. Because coal is a somewhat heterogenous insoluble solid with a large number of distinct properties, many of the

traditional chemical and spectroscopic techniques for organic structure determination cannot be applied easily or unambiguously. Therefore there is still a fair amount of debate over what constitutes a representative structure for a "coal molecule" (and even over whether such a concept even makes sense).

No attempts have been made during the course of the work described in this thesis to determine directly the chemical structure of the principal coals studied. These structural characteristics must therefore be inferred from a knowledge of the more traditional classification parameters, those from the proximate, ultimate, and petrographic analyses of the coal.

This section is intended to serve as a brief review of current thinking on the structure of coals. There are a number of more extensive reviews available on the subject. Some of the older work in the field can be found in various reviews in Lowry (1945). More recent reviews are those in Francis (1961), in Van Krevelen (1961), and those by Dryden, and Tschamler and de Ruiter (both in Lowry, 1963) Speight (spectroscopic techniques, primarily, 1971), Tingey and Morrey (1973), and those each year by Pennsylvania State University during its Short Course on Coal (e.g. Given, 1976).

Most studies of coal structure have focussed upon the vitrinite maceral, in some studies by design, but in others on whole coals, merely because vitrinite is the most plentiful of the macerals and hence dominates the behavior of the coal. It should therefore be kept in mind that the results given below, except where they are given for individual maceral components, represent averages over all the macerals contained

within a particular coal.

The literature on coal structure determination also contains a fair amount of information derived from work on "coal extracts" and other solvated coal fractions. An attempt has been made to stay away from these results to as great an extent as possible. The reason for this reluctance to include data from solvation type work (which renders a liquid product that is amenable to more powerful analysis techniques) hinges upon the word "fraction"; coal is never 100% soluble under conditions which are likely to preserve its basic structure. Since the fraction that is soluble cannot be simply related to any particular maceral components, the information derived on "coal liquids" represents information on an ill-defined fraction of the coal, and is therefore difficult to apply. The recently developed technique of coal "depolymerization" with phenol-BF<sub>3</sub> permits conversion to soluble fragments under relatively mild conditions (presumably with a fair amount of structure preservation). Because in some low rank coals almost total depolymerization and solution of vitrinite and exinite fractions were possible, this technique holds promise for structural determination work (Herédy and co-workers, 1962, 1963, 1964, 1965, 1966).

#### The Carbon-Hydrogen Structure

It is generally accepted that an important structural characteristic of coal is its aromaticity, defined as the fraction of carbon in the coal (or maceral) which is aromatic in nature. Thus much of the work involved in characterization of the carbon skeleton has involved determining both the aromaticity and the average number of rings in condensed polycyclic aromatic "clusters", as a function of coal rank

(or carbon content). A large number of approaches have been employed, some principally in the "chemical" domain, and others in the "physical" domain.

In the chemical domain, one finds techniques such as polarography (controlled potential electrolysis), lithium reduction, catalytic hydrogenolysis, controlled oxidation. These techniques, and their shortcomings are succinctly described by Dryden (Lowry, 1963). A rather recent attempt at controlled oxidation involved the treatment of coals and model compounds with sodium hypochlorite (Chakrabartty and coworkers, 1972, 1974, 1974a). The interpretation of these results was that aromaticities derived by the various physical techniques (described below) were substantially overestimated, and that coal was really characterized by a polyamantane type skeletal structure (Fig. 3-1.3). Since the publication of these theories, a number of workers have suggested that the hypochlorite oxidation is not specific enough, and that the products of coal liquefaction do not support the existence of adamantane-like structures in coal (Mayo, 1975, 1976, Ghosh et al., 1975, Aczel et al., 1975, 1976, Landolt, 1975). Recently, the reaction of fluorine gas with coal has provided further substantiation for aromaticities derived by various physical techniques, and also cast doubt upon the hypochlorite work (Huston, et al., 1976).

The estimates of aromaticity obtained by physical means seem to be still more reliable than those by the older chemical techniques. The following table, adapted from Tschamler and de Ruiter, (Lowry, 1963) shows the various physical techniques that have been employed in studying the structure of coal and the type of structural information derived from each.



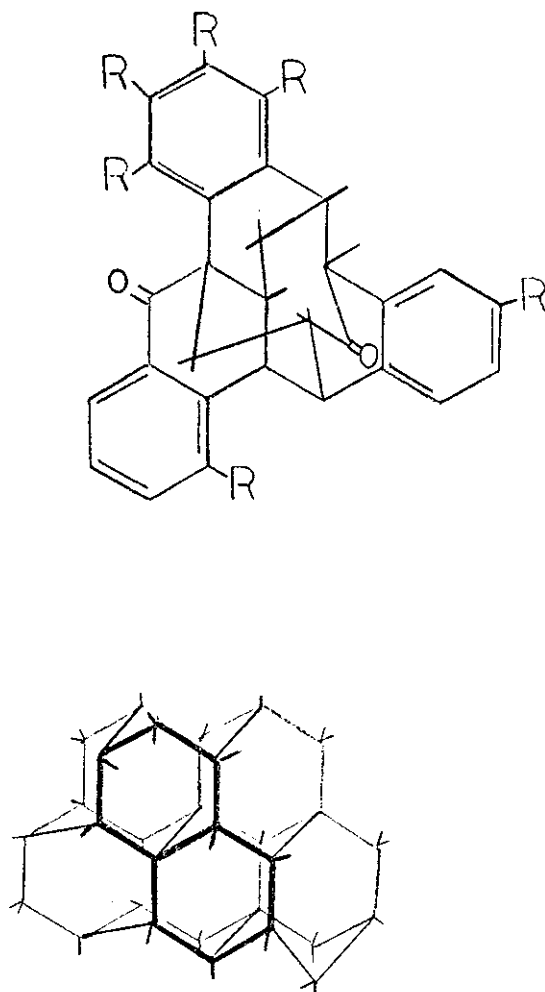


Figure 3.1-3. Polyamantane Structures for Coal Proposed by Chakrabartty and Berkowitz (1974).

<u>Measurement Technique</u>	<u>Type of Informatin Obtained</u>
X-ray diffraction	<ul style="list-style-type: none"> <li>- Single distribution of aromatic ring systems</li> <li>- Average diameter of aromatic lamellae</li> <li>- Mean Bond Length</li> <li>- Average thickness of the packets of lamellae</li> <li>- Aromaticity</li> </ul>
Ultraviolet and visible absorption	<ul style="list-style-type: none"> <li>- Aromaticity (mostly applied to coal extracts)</li> <li>- Average aromatic ring size</li> </ul>
Reflectance, Refractive index (molecular refraction)	<ul style="list-style-type: none"> <li>- Aromatic "surface area"</li> <li>- Optical anisotropy</li> </ul>
Infrared absorption	<ul style="list-style-type: none"> <li>- Ratio of aromatic to aliphatic hydrogen</li> <li>- Presence of particular structures (e.g. -OH, CHar, CHal, (C=C)ar, C=O)</li> <li>- Aromaticity (?)</li> </ul>
Electronic spin resonance	<ul style="list-style-type: none"> <li>- Presence of free radicals</li> </ul>
<sup>1</sup> H(P roton) Nuclear magnetic resonance	<ul style="list-style-type: none"> <li>- Ratio of aromatic to aliphatic hydrogen</li> </ul>
Carbon-13 Nuclear magnetic resonance	<ul style="list-style-type: none"> <li>- Aromaticity</li> <li>- Structural Features</li> </ul>
Electrical Conductivity	<ul style="list-style-type: none"> <li>- Changes in size of aromatic ring systems</li> </ul>
Diamagnetic susceptability	<ul style="list-style-type: none"> <li>- Average number of aromatic rings</li> </ul>
Dielectric constant	<ul style="list-style-type: none"> <li>- Dipole moment</li> </ul>
Sound velocity	<ul style="list-style-type: none"> <li>- Aromaticity</li> </ul>
Density (molar volume)	<ul style="list-style-type: none"> <li>- Aromaticity</li> <li>- Ring condensation index</li> </ul>

It is beyond the scope of this brief review to present details of all these techniques and their results; again, the reader is referred to the previously cited reviews on the subject.

As is apparent from the table, there have been many techniques applied to the study of aromaticity. The results of several of these are shown in Fig. 3-1.4. Included in the figure are three sets of data from Van Krevelen (1961), which were obtained via "physical constitution analyses", a set of data from the x-ray scattering work of Cartz and Hirsch (1960), and some rather recent carbon-13 nuclear magnetic resonance work by VanderHart and Retcofsky (1976).

By doing empirical studies on many hydrocarbons Van Krevelen and several coworkers developed several ingenious correlations between measurable physical properties and some much more difficult to measure structural parameters. The C's in Fig. 3.1-4 refer to data on vitrinites for which heats of combustion and elemental composition were the measured quantities and the aromaticity ( $f_a$  = ratio of aromatic carbon to total carbon) and ring condensation index ( $2[R-1]/C$ , where R = number of saturated plus unsaturated rings per coal "unit" and C = number of carbon atoms per coal "unit") are calculated. The D's refer to the case in which elemental composition and vitrinite density were the measured properties, and the V's to the case in which elemental composition and the velocity of sound waves in vitrinites were measured.

The x-ray work of Hirsch (together with Cartz and Diamond) provided much additional valuable data on the skeletal structure of coal (see one of the reviews for references to other x-ray studies of coal). The work involved comparing the x-ray spectrum of coal (at large and medium

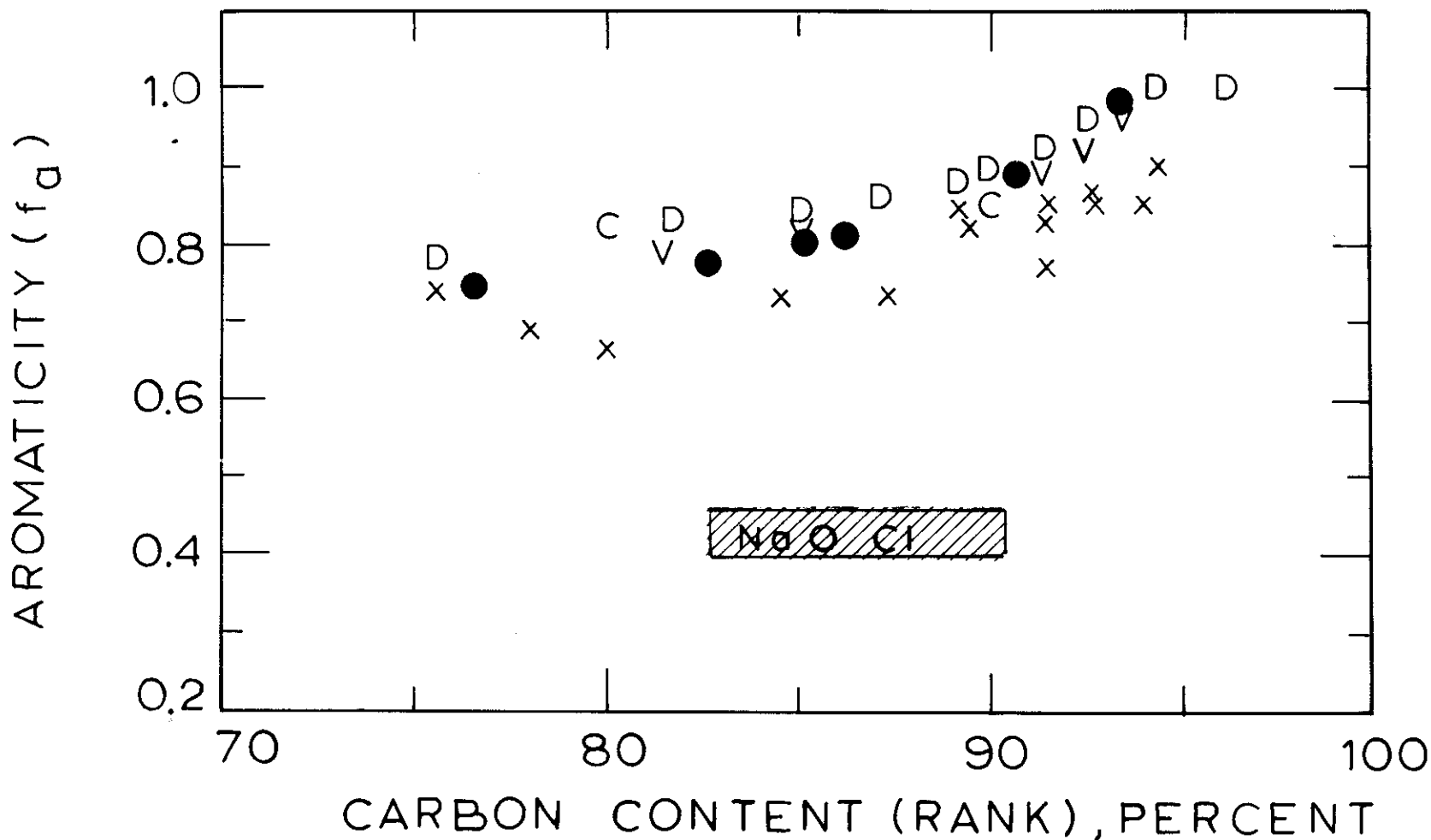


Figure 3.1-4 Variation of Aromaticity with Rank (X = X-ray Diffraction Data, Cartz and Hirsch, 1960; C = Heat of Combustion Data, D = Molar Density Data, V = Velocity of Sound Data, Van Krevelen, 1961; Na O Cl = Sodium Hypochlorite Oxidation Data, Chakrabartty and Kretschmer, 1974; ● = C-13 NMR Data, Vander Hart and Retcofsky, 1976).

///

scattering angles) to model spectra for small aromatic crystallites, and from that comparison developing histograms of the fraction of carbon present in each size of crystallite. From these and other data and assumptions, Hirsch was able to determine the size distribution of aromatic ring systems, their mean bond length, the average thickness of the packets of lamellae (or "layers"), and the aromaticity of several vitrains and maceral enriched components.

Hirsch's data on aromaticity fall consistently below Van Krevelen's, but it is not surprising that agreement is not better because of the large number of assumptions embodied in all these analyses. Unfortunately a subsequent test of Hirsch's method of analyzing the x-ray spectra cast serious doubt upon the reliability of his data (Brooks and Stephens, 1965; many of the cited reviews unfortunately were published before this evidence came to light).

The application of carbon-13 NMR to solid coal structure determinations was made possible by relatively recent development of  $^{13}\text{C} - ^1\text{H}$  cross polarization technique (Pines et al., 1977). It appears that the cross polarization technique may be made even more powerful when combined with "magic angle" spinning; Bartuska et al, (1976) were able to obtain well resolved spectra of lignites and anthracites, materials with which VanderHart and Retcofsky had difficulties.

The carbon-13 Nuclear Magnetic Resonance ( $^{13}\text{C}$ -NMR) data of VanderHart and Retcofsky (1976) appear to support the trends evident in both Van Krevelen's and Cartz and Hirsch's data, but agree much more closely with Van Krevelen's estimates. Not shown on the figure are some  $^{13}\text{C}$ -NMR data recently presented by Farcasiu et al. (1976, data attributed to Pines).

These data, for bituminous and subbituminous coals suggest aromaticities up to 50% lower than those obtained on comparable rank coals by VanderHart and Retcofsky. But because of the apparently large uncertainty (12-19% absolute) in these data, combined with a lack of details concerning the measurement, they were not included here (for comparison, VanderHart and Retcofsky claimed 4% accuracy in their work, but curiously their spectra did not appear to be better resolved than those presented by Farcasiu).

Although uncertainties still remain, the agreement between the data from three (or five, if one counts each physical constitution technique separately) widely varying methods is sufficiently good, so that some predictive power may already be available. In general, the degree of aromaticity increases continuously with rank, rising sharply above 90% carbon content. In no case have any of the "physical" methods provided any support for Chakrabartty's sodium hypochlorite oxidation results (shown on Fig. 3.1-4 as "NaOCl").

Noting on Fig. 3.1-4 the carbon contents of the Montana lignite (74.7%C) and Pittsburgh seam bituminous coal (80.7%C) used in this study, it can be seen that the aromaticity of the lignite might be expected to be in the range 0.65 to 0.7, while that of the bituminous is in the range 0.75 to 0.8. It should also certainly be noted that using the total carbon content for the coals masks potentially significant differences between the different maceral fractions in the coals. This will be discussed below.

Of course aromaticity alone does not completely characterize the carbon skeletal structure. Information on the distribution of aromatic

and non-aromatic carbon is necessary as well, and is presented in Fig. 3.1-5. Again, utilizing data from Van Krevelen (1961) and Cartz and Hirsch (1960), the average number of atoms per aromatic "cluster" is plotted as a function of rank (carbon content). Van Krevelen's data are, again, from physical constitution analysis, this time from measurements of refractive indices and independent estimates of aromaticity. Hirsch's data are from direct measurements of x-ray scattering from crystallites, but again open to question of reliability. These data appear to indicate that in low rank vitrinites, although over 60% of the carbon is aromatic in nature, most of it exists in single or double ring structures, presumably linked by some non-aromatic carbons. Looking at averages alone may be misleading, but the distribution data from Cartz and Hirsch may be debatable. Recognizing this uncertainty, Cartz and Hirsch claim lignites possess very few aromatic structures larger than one benzene ring in size, and that bituminous coals may be characterized by aromatic structures one to three rings in size. These aromatic structures are linked by non-aromatic carbon or heteroatom linkages.

According to both sets of data, the average size of condensed aromatic systems rises sharply as one approaches anthracite rank. Van Krevelen has measured the properties of anthracites as semiconductors and has concluded that the following average cluster sizes may be reasonable:

<u>Percent Carbon</u>	<u>Average Number of Atoms per Cluster</u>
91.7	40
93.7	45
94.2	50
95.0	55
96.0	>60

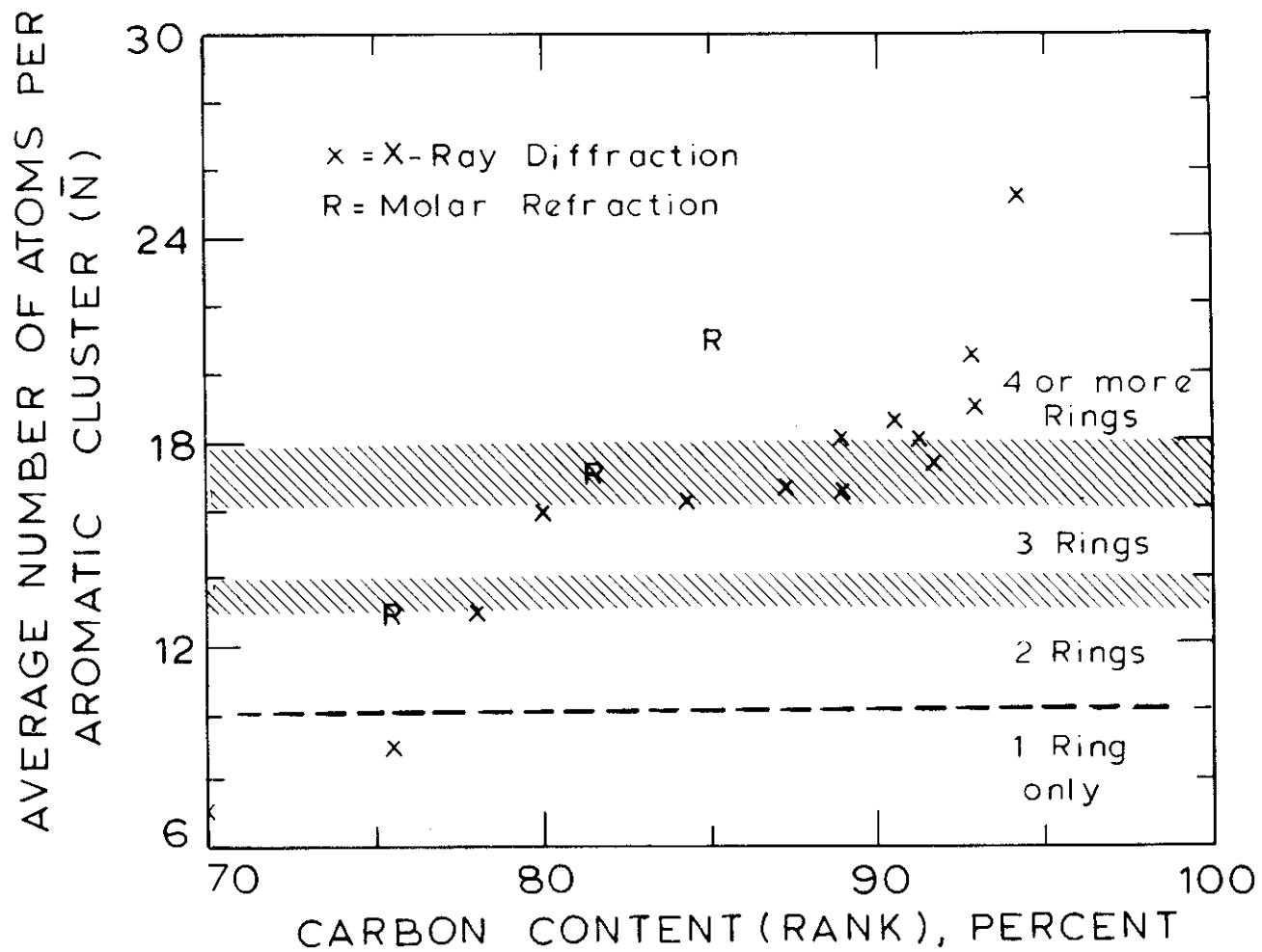


Figure 3.1-5 Average Number of Rings per Aromatic Cluster (X = Xray Diffraction Data, Cartz and Hirsch, 1960; R = Molar Refraction Data, Van Krevelen, 1961).



There have been other attempts made to measure indirectly average ring sizes in coal by measuring ring sizes in coal extracts, but these techniques suffer from the obvious shortcoming that since coal is not 100% soluble, one is examining a sample that is not necessarily representative of whole coal.

It was stated above that for a particular carbon content, different maceral fractions may have quite different characteristics. Figure 3.1-6 shows aromaticity and cluster data for various macerals, again taken from Van Krevelen's density and refraction estimates (curves, data omitted), Cartz & Hirsch's x-ray data (points), and Tschamler and de Ruiter's x-ray measurements (points in boxes, 1966). The inertinites are seen to be most highly aromatic, with the largest ring clusters, and the exinites least aromatic, with the smallest ring clusters. For the relatively low rank coals employed in this study, the differences in average ring size seem to be small between the macerals, but to say much about relative aromaticities would require a dangerous extrapolation.

The concept of a ring condensation index was introduced earlier, and is shown plotted as a function of vitrinite rank in Fig. 3.1-7 (data again from Van Krevelen density estimates, 1961). Again,  $R$  is the average number of rings per structural unit, both aromatic and non-aromatic, and  $C$  is the average number of carbon atoms per structural unit. As was also reflected in the previous figure, the exinites have the smallest ring groupings, while the inertinites have the largest. More easily visualized than the ring condensation index is  $R$  itself, the number of rings per mean structural unit. Van Krevelen chose to represent the coal as a "polymer", made up of monomers containing one "average" condensed

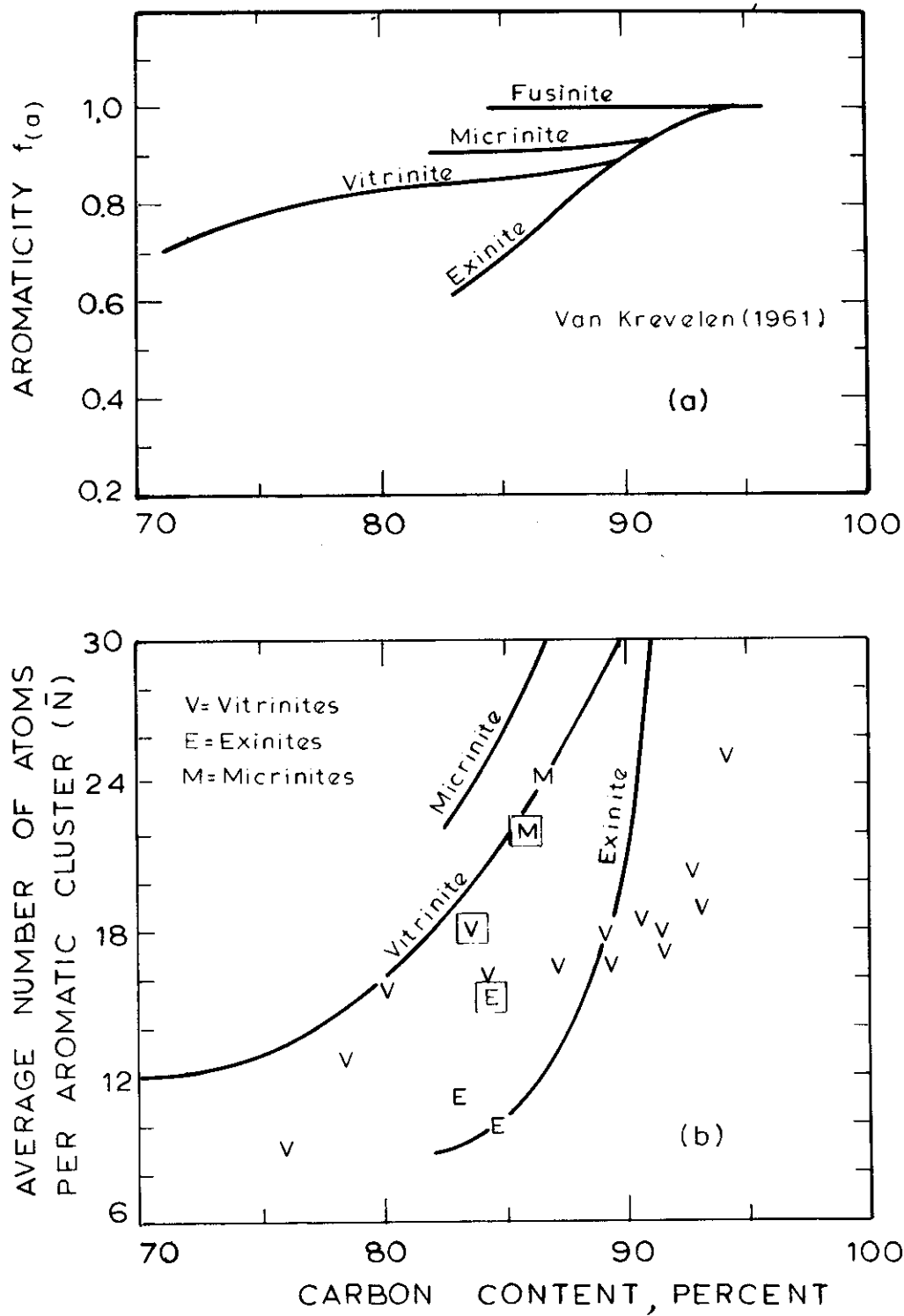


Figure 3.1-6 Aromaticity and Average Number of Rings Per Aromatic Cluster for Various Macerals (in (b); curves, Van Krevelen, 1961; Single Points, Cartz and Hirsch, 1960; Points with Double Symbol, Tschamler and deRuiter, 1966).

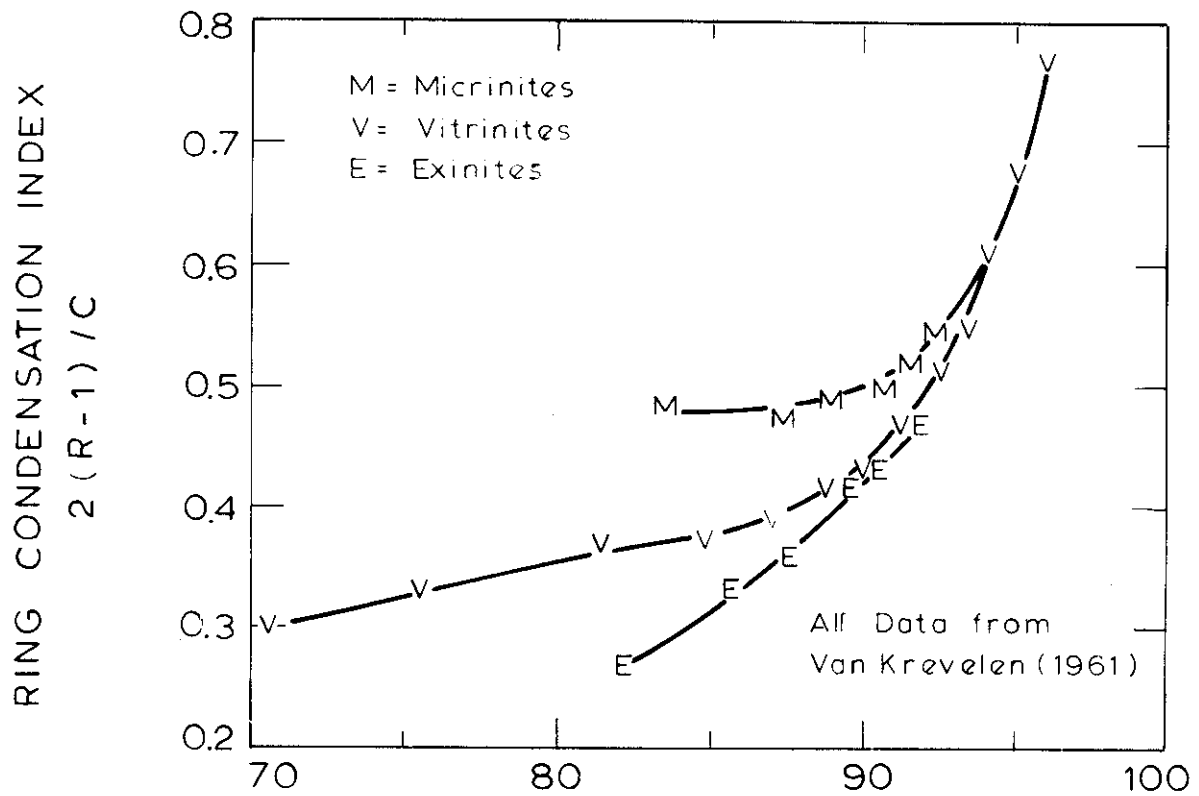


Figure 3.1-7 Variation of the Ring Condensation Index with Rank.

aromatic structure. Since we have an estimate for the average number of aromatic carbons per cluster ( $\bar{N}$ ) and the aromaticity ( $f_a$ ), then C and R are directly calculable:

$$C = \bar{N}/f_a$$

$$R = \left(\frac{C}{2}\right) (\text{Ring condensation index}) + 1$$

Recognizing previously cited dangers inherent in such a calculation, if we assume reasonable values for  $\bar{N}$  and  $f_a$  for the Montana lignite and Pittsburgh seam bituminous studied here, one obtains the "average" values shown below:

	$f_a$	$\bar{N}$	$\frac{2(R-1)}{C}$	$C$	$R$
Montana lignite	.7	10	.32	14	3.2
Pitts- burgh seam bituminous	.8	14	.35	18	4.2

The conclusion from these admittedly very rough figures is that both coals must have some non-aromatic ring content (since  $\bar{N} = 10$  and 14 implies 2 and 3 ring aromatic structures). This may naturally suggest hydroaromatic structures for which there is now substantial experimental verification.

Mazumdar et al. (1962) employed sulfur and Reggel et al. (1968) developed a technique for catalytically dehydrogenating hydroaromatic structures in coal and the latter group presented the data shown in Fig. 3.1-8 (for bituminous, and subbituminous vitrains and for anthracites). Reggel et al. conclude from their data that low rank bituminous coals show the greatest amount of hydroaromatic behavior because higher rank involves more aromatic character, while lower rank coals (i.e. subbituminous and lignite vitrains) have not yet fully developed hydroaromatic character. The Montana lignite would fall in the range of .25 hydrocarbons liberated per carbon (or 3-4 per "average structural

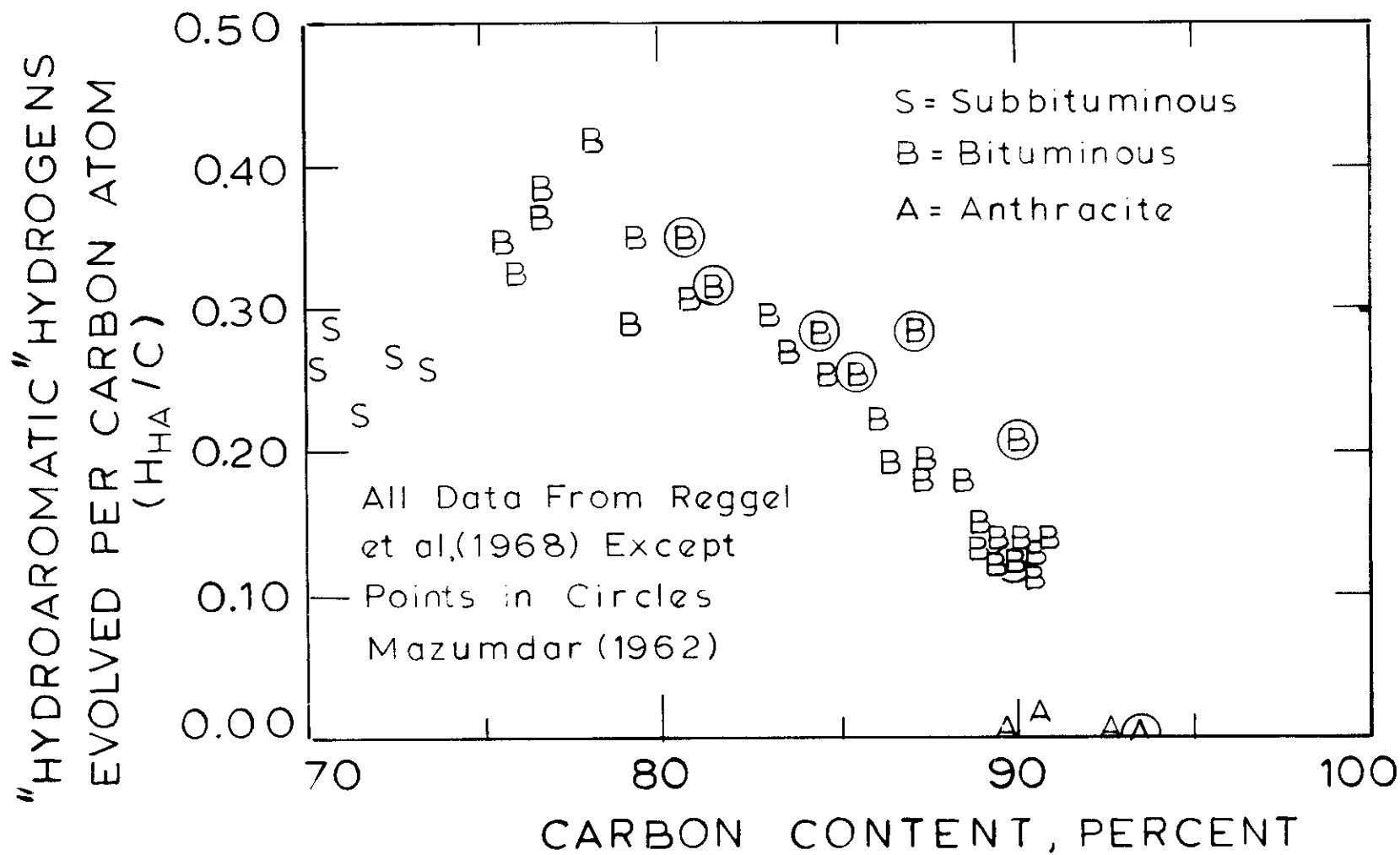


Figure 3.1-8 Variation of "Hydroaromatic" Hydrogen Content with Rank.

unit") and the Pittsburgh bituminous in the .3 to .4 range (or 5-8 per average structural unit). Within the rather large uncertainty of such calculations, both these values could be consistent with the previously derived aromatic cluster sizes and ring condensation indices. For whole coals, these hydroaromatic hydrogen values may be a bit high; Reggel et al. (1971) in later work showed that the hydroaromatic content of whole coals was consistently lower than that of vitrains by about .01 to .05 ( $\frac{H_{Ha}}{C}$ ), for bituminous coals).

Unfortunately data on total hydrogen distribution is not plentiful and its reliability is frequently questioned. Chemical techniques have provided some of the necessary data (such as that for hydroaromatic hydrogen and phenolic hydrogen), while spectroscopic techniques ( $^1H$ -NMR and infrared (IR)) have provided others.

Figure 3.1-9 gives data for total hydrogen distribution in various coals and maceral fractions. The upper band represents a compilation of data for coals from all over the world (after Mazumdar, 1972, as an atomic H/C ratio) as a function of rank (expressed as carbon weight percent, dmmf). Above approximately 75% carbon, deviations from the band are rare whereas at about 70% carbon, deviations of up to .05 outside the band may occur.

Data on aliphatic hydrogen content was obtained by both chemical means (Mazumdar et al., 1962, Van Krevelen, 1961) and by infrared spectroscopy, sometimes combined with NMR (Brown and Hirsch, 1955, Ladner and Stacey, 1963, Tschamler and deRuiter, 1962 and 1966, Oelert, 1968 and references within these papers). Although the data again shows a fair spread and is somewhat sparse for low ranked coals, the trend is clear; with increasing rank (and therefore aromaticity), the amount of aliphatic hydrogen decreases.

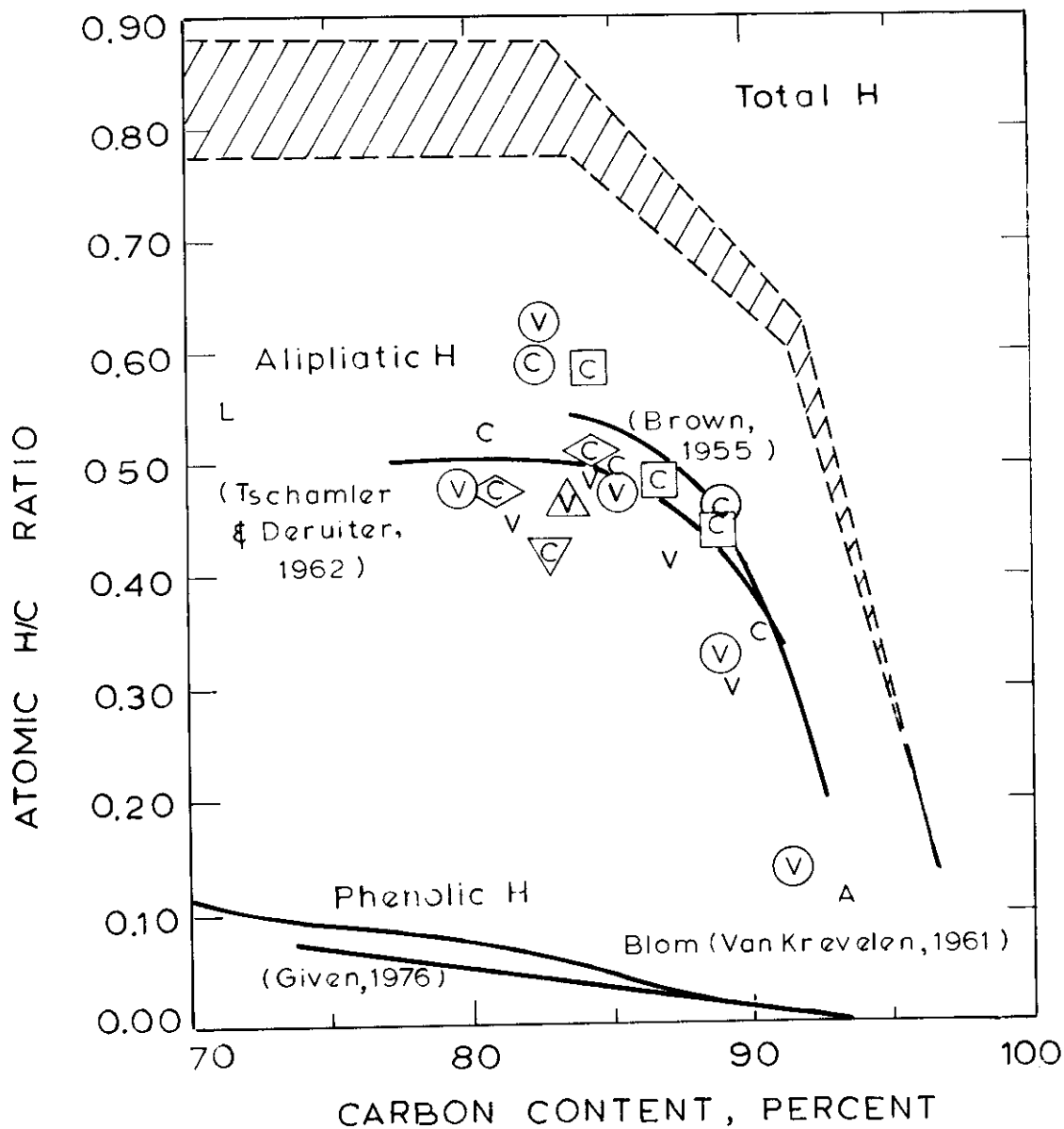
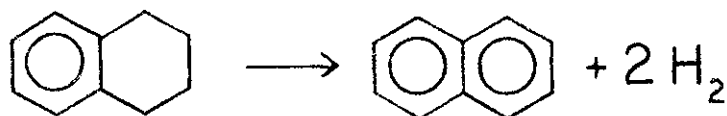


Figure 3.1-9 Variation of Total, Aliphatic, and Phenolic Hydrogen Content with Rank (Total H curve after Mazumdar, 1972; other curves as marked; Single Points, Mazumdar et al., 1962; Pts. in ( $\square$ ), Oelert, 1968; Pts. in ( $\circ$ ), Ladner and Stacey, 1963; Pt. in ( $\Delta$ ) Tschamler and de Ruiter, 1966; Pt. in ( $\nabla$ ), Van Krevelen, 1963; Pts. in ( $\diamond$ ), Mazumdar, 1964; (C) = Whole Coal; (V) = Vitrinite; (L) = Lignite; (A) = Anthracite).

There is a great deal of overlap between the principal IR bands of coal hydroxyl groups (a  $3300\text{ cm}^{-1}$  stretch) and aromatic hydrogens (a  $3030\text{ cm}^{-1}$  stretch). To therefore measure phenolic hydrogens separately from aromatic hydrogens is difficult. As a result, chemical techniques are often used to determine phenolic hydroxyl hydrogen, and aromatic hydrogen contents are determined by difference ( $H_{\text{total}} = H_{\text{aromatic}} + H_{\text{aliphatic}} + H_{\text{OH}}$ ). Figure 3.1-9 shows some hydroxyl hydrogen values as functions of rank from studies by Blom (described in Van Krevelen, 1961) and by Given (1976). In low rank coals, some carboxylate groups are also present; if these carboxylic groups were in acidic form, these would contribute to the  $H_{\text{OH}}$  value as well, but Given (1976) reports that treatment of lignites with mineral acid causes a change in the IR spectrum which suggests that these groups in nature are mostly in the metal cationic salt form. Oxygen functional groups will be discussed in the next section.

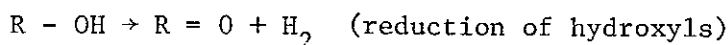
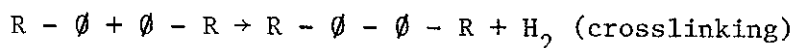
It may be implied by comparison of Figs. 3.1-8 and 3.1-9 that all hydroaromatic rings cannot be unsubstituted. If one considers as a model the dehydrogenation of tetralin to naphthalene,



clearly there are twice as many hydroaromatic hydrogens (displaying aliphatic characteristics in an IR analysis) as there are hydrogen atoms liberated. If one extrapolates this behavior to a coal of about 80% carbon content, then it might be guessed that the coal has at least .6 to .7 aliphatic hydrogens per carbon atom. The data in Fig. 3.1-9



suggest that this would be on the high side, and that direct interpretation of the data in Fig. 3.1-8 as one half of all hydroaromatic hydrogen would be incorrect (the other half assumed aromatized during catalytic dehydrogenation). Two factors could help to explain the discrepancy, one structural and one experimental. Experimentally, a number of possible side reactions could occur during dehydrogenation:



The decreased solubility of dehydrogenated coal could be ascribed to the first reaction. Reggel et al. (1968) however feel this is only a minor contributor in the hydrogen evolution process.

Structurally, some hydroaromatic hydrogen may be present in tertiary  $\begin{array}{c} | \\ -\text{C}-\text{H} \\ | \end{array}$  rather than secondary  $\begin{array}{c} | \\ \text{H}-\text{C}-\text{H} \\ | \end{array}$  structures. Clearly the interpretation of catalytically liberated hydrogen as one half of all hydroaromatic hydrogen is not correct in this case.

Thus the data on the distribution of aliphatic hydrogen between methyl ( $-\text{CH}_3$ ), methylene ( $-\text{CH}_2-$ ) and methin ( $-\text{C}-\text{H}$ ) groups is also of interest. Reliable data on the distribution of hydrogen among these three types of aliphatic carbon is difficult to obtain for whole coals or macerals. Broad-line NMR estimates of the fraction of methylene hydrogen were obtained by Ladner and Stacey (1961, 1964) and their results are shown plotted in Fig. 3.1-10. Also shown are values measured and calculated from the literature by Tschamler and DeRuiter (assuming peri- $\text{CH}_3$  groups contribute negligibly, (1962, 1966)). The amount of hydrogen present as part of  $\text{CH}_3$  in various coals is shown in Fig. 3.1-11. The curves were obtained by chemical means (Mazumdar et al., 1966, and references therein). The upper curve was determined by low temperature pyrolysis of the sample,

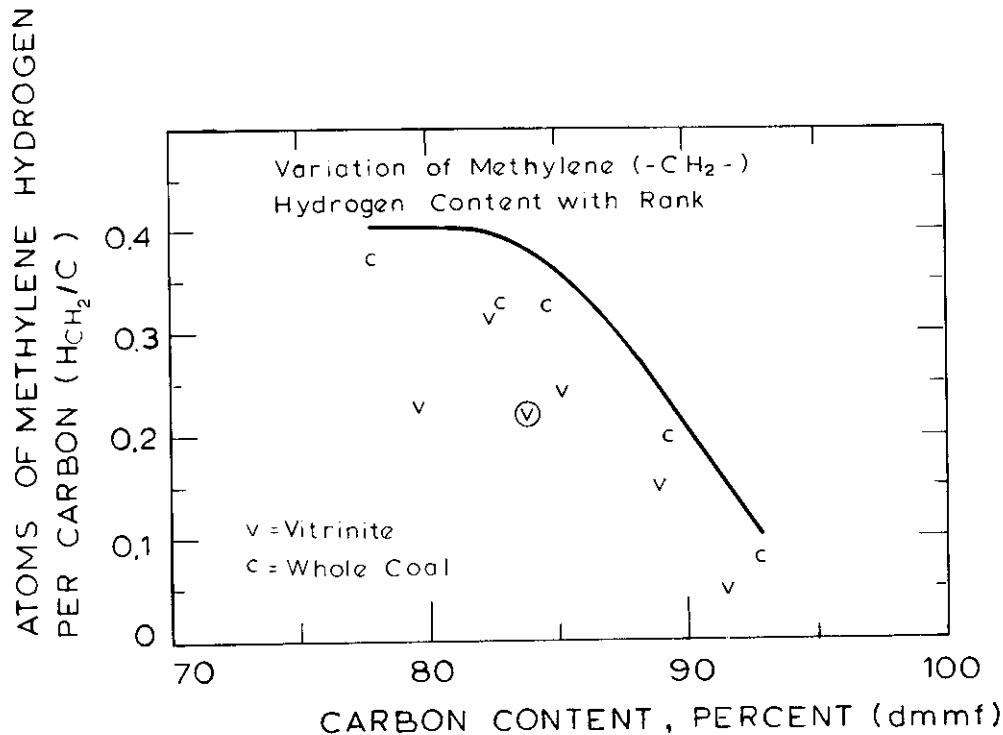


Figure 3.1-10 Variation of Methylene Hydrogen Content with Rank (Curve, Tschamler and deRuiter, 1962; Single Points Ladner and Stacey, 1963, 1964; Pt. in (o) Tschamler and deRuiter, 1966).

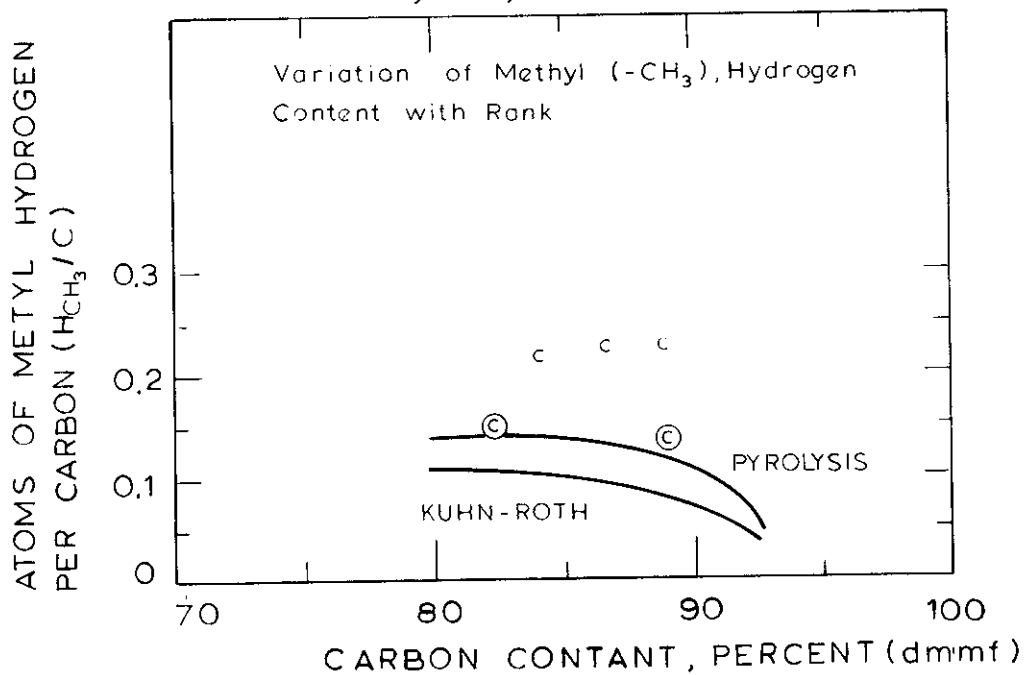


Figure 3.1-11 Variation of Methyl Hydrogen Content with Rank (curves, Mazumdar et al., 1966; Single Points, Oelert, 1968; Pts. in (o) Bent et al., 1964).

wherein it was assumed that all methane product originated from methyl structures in coal. The lower curve represents an estimate of the methyl content obtained by the Kuhn-Roth method (involving oxidation of the methyl groups to acetic acid, steam distilling and titrating). Also shown are data from Bent et al. (1964) from a combined chemical method - IR study. The data of Oelert (1968) are considerably higher and probably not as reliable, since he assumed that no tertiary aliphatic CH bonds are present in coal, in order to arrive at his estimates from IR absorption measurements. As will be discussed in the pyrolysis mechanism section, estimates of methyl content by pyrolysis are somewhat risky.

Unfortunately hydrogen distribution data are rather sparse for coal in the low rank range of interest in this study, and extrapolation to very low rank is always dangerous. Very approximate estimates of the hydrogen character of these coals are derived as follows, and presented as part of Table 3.1-3. The measured total hydrogen to carbon ratios  $H_{TOT}/C$  are obtained from ultimate analysis of the coal. The approximate aliphatic ( $H_{al}/C$ ) and phenolic ( $H_{OH}/C$ ) hydrogen contents are estimated from the data in Fig. 3.1-9. It is then possible to calculate the aromatic hydrogen content as:

$$\frac{H_{ar}}{C} = \frac{H_{TOT}}{C} - \frac{H_{al}}{C} - \frac{H_{OH}}{C}$$

The portion of aliphatic hydrogen in methylene ( $H_{CH_2}/C$ ) groups is estimated (by extrapolation in the case of lignite) from Fig. 3.1-10. Similarly the content of methyl ( $H_{CH_3}/C$ ) hydrogen is estimated from 3.1-11. The content of methin ( $H_{CH}/C$ ) hydrogen is then calculated by difference:

$$\frac{H_{CH}}{C} = \frac{H_{al}}{C} - \frac{H_{CH_2}}{C} - \frac{H_{CH_3}}{C}$$

Finally, the maximum amount of hydrogen which can be liberated by catalytic

dehydrogenation from hydroaromatic structures is estimated (note that this probably does not equal total hydroaromatic hydrogen content, because some methylene hydrogens will be left behind as part of the aromatic structures formed during the process). The maximum amount is calculated as:

$$\left(\frac{H_{HA}}{C}\right) = \frac{1}{2}\left(\frac{H_{CH_2}}{C}\right) + \left(\frac{H_{CH}}{C}\right)$$

It may be noted that given these values for the aliphatic hydrogen distribution, the values for hydroaromatic hydrogen in Fig. 3.1-8 do appear on the high side (since methyl groups cannot be hydroaromatic). But again caution must be exercised in coming to such a conclusion, because petrographic composition effects can play a role. In Fig. 3.1-10 it is clear that vitrinites have a consistently lower methylene content than whole coals. This is probably due to the contribution of exinites in the whole coals. A number of studies have compared the hydrogen distributions of various macerals. The results of some work in this area are shown below (the macerals in any column are all from the same coal):

	<u>%C</u>	<u><math>\frac{H_{TOT}}{C}</math></u>	<u><math>\frac{H_{al}}{C}</math></u>	<u>%C</u>	<u><math>\frac{H_{TOT}}{C}</math></u>	<u><math>\frac{H_{al}}{C}</math></u>	<u>%C</u>	<u><math>\frac{H_{TOT}}{C}</math></u>	<u><math>\frac{H_{al}}{C}</math></u>
Exinite	84.1	.99	.76	81.0	1.03	.96	82.6	1.08	.97
Vitrinite	83.9	.78	.47	79.6	.74	.23	82.3	.80	.32
Inertinite	85.7	.54	.24	90.3	.37	.15	91.6	.47	.14

Tschamler and deRuiter  
(1966)

Ladner and Stacey  
(1963)

The differences are obviously very large, and the presence of a significant amount of low rank exinite will change the aliphatic hydrogen content quite substantially.

Before leaving the subject of hydrogen distribution in coals, two other points are worth noting. The first involves the existence of methylene bridges. Brown et al. (1960) concluded from NMR studies of coal distillates, that no " $\alpha$ " methylene "bridges" (i.e. methylene as a single methylene group attached to two different aromatic structures e.g.

$\emptyset - \text{CH}_2 - \emptyset$ ), exist in coal. This view has been questioned by Heredy et al., (1965) based on NMR studies of "depolymerized" coal. The latter group claims that vacuum pyrolysis of coal is likely to rupture the coal structure right at methylene bridge sites, converting methylene to methyl groups, thus destroying them, while depolymerization in phenol- $\text{BF}_3$  severs the bond, but protects the methylene group by an "aromatic interchange" with phenol. Thus, according to Heredy et al., methylene bridge groups exist and can be expected to be very active during pyrolysis processes. This argument seems like a plausible explanation for the findings of Brown et al.

Another important facet of the carbon hydrogen skeletal structure, which has not been addressed, is the degree of ring substitution and the related issue of the distribution of lengths of paraffin substituents. There has not been any spectroscopic evidence presented to date to suggest any unsubstituted olefinic structures in coals, so these are not considered (see Brown et al., 1960).

Mazumdar et al. (1962) suggest that the sum of the percentages of aromatic and hydroaromatic carbon are relatively constant at about  $88 \pm 3\%$ . While this figure is not precisely supported by the evidence presented thus far, it seems to be a fair approximation. Since the methyl groups contribute apparently a constant 4 to 5% of

of the weight of carbon, this leaves a maximum of perhaps 10% of the carbon available for paraffinic chains. Mazumdar feels that these chains are probably no longer than ethyl groups. This view is supported by the relatively low yields of long chain paraffins during carbonization of coal, and during extraction (Franz, 1975). This view again must be tempered by consideration of the differences between macerals; exinites are much more aliphatic in nature than the other macerals, sometimes exhibiting alicyclic terpene character. Also, there is recent evidence for very long chain paraffins in coal liquefaction products (Oblad, 1977).

A structural parameter which is frequently calculated is the aromatic substitution index, defined as:

$$S_{ar} = \frac{C_{\text{aromatic substituted}} + C_{\text{aromatic condensed}}}{C_{\text{aromatic total}}} = 1 - \left( \frac{H_{ar}}{C} \times \frac{1}{f_a} \right)$$

It can be seen that both low and medium rank coals will be characterized by substitution indices in the range 0.6 to 0.8, that is, 60 to 80% of all aromatic carbons are not attached to hydrogen. Thus even though coal carbon is primarily concentrated into an aromatic structure, the bulk of its hydrogen is concentrated in non-aromatic structures.

#### Oxygen Containing Functional Groups

Oxygen plays a prominent role in determining the chemical nature of coal. Although it is not present in as large quantities as are carbon or hydrogen (on an atomic basis), it has nevertheless been ascribed an important role in determining the course of pyrolysis processes.

The presence of hydroxyl groups has already been discussed with respect to hydroxyl hydrogen. Dryden (1963) presents a good summary of the many techniques used to determine coal hydroxyl content. Coal contains few measurable alcoholic hydroxyl groups, and as has already been discussed, carboxylic hydroxyls are typically in salt form (when they are present at all). Hence, phenolic hydroxyl is the only hydroxyl group of any concern. Figure 3.1-12 presents the results of Blom (Van Krevelen, 1961) and Given et al. (1976). In the latter work, a straight line was fitted to the data of 37 coals in the range of about 74 to 91% C (dmmf). The resulting relation was

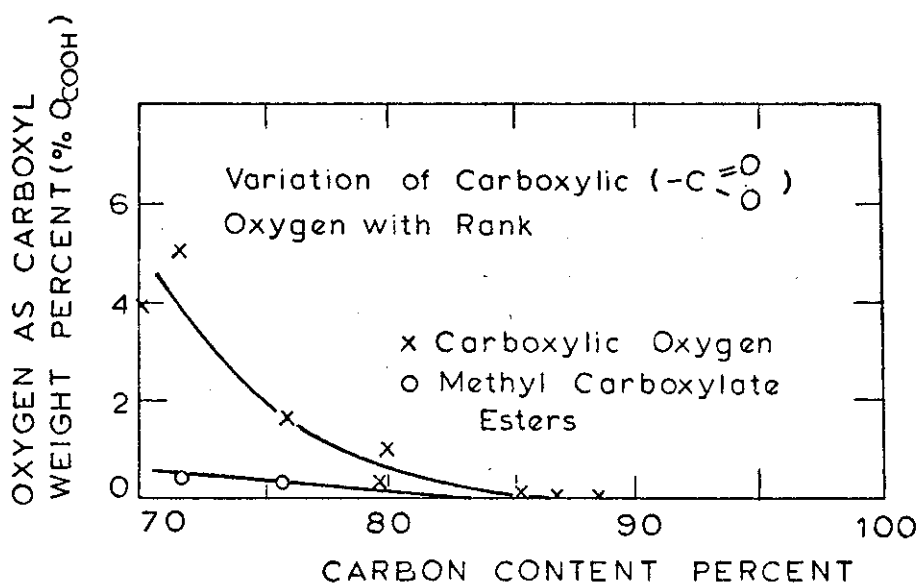
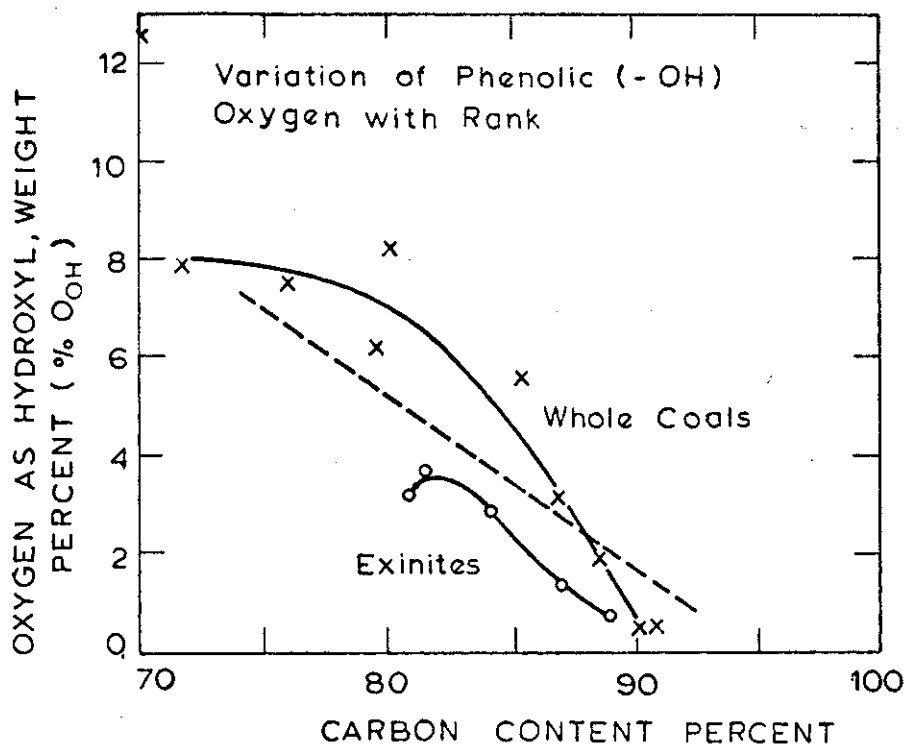
$$O_{OH} (\%, \text{dmmf}) = 33.2 - .35 (\% C)$$

$$\text{or } \left( \frac{O_{OH}}{C} \right)_{\text{atomic}} = \frac{24.9}{C(\%, \text{dmmf})} - .263$$

The agreement of this correlation with the earlier results of Blom is fair. Fig. 3.1-12 compares the results of the two studies, and also shows data for the exinite maceral, clearly indicating the latter has lower hydroxyl content. In general, vitrinites have the highest hydroxyl content of the principal maceral types.

Van Krevelen (1961) and Dryden (1963) both give several other sets of data for hydroxyl contents of coals; the decision to draw the curve as shown through Blom's data was based upon a knowledge of some of these additional studies.

Fig. 3.1-13 gives some data on oxygen content in the carboxylic acid (salt) form and carboxylate methyl ester form. It can clearly be seen that these structures are important in low rank coals and lignites,



TOP: Figure 3.1-12 Hydroxyl Content of Coals of Various Rank ((x) Blom, in Van Krevelen, 1961; (---) Given, 1976; (o) Given et al., 1960).

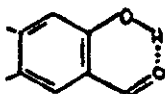
BOTTOM: Figure 3.1-13 Carboxylic Oxygen Content of Coals of Various Rank (all data from Blom).



but have almost entirely disappeared by the time rank increases to bituminous levels. More recent work by Maher and Schafer (1976) provides support for the trend of these data, but suggests slightly higher values, especially for lower ranks of lignite.

The balance of the oxygen is in either ether or carbonyl form. Unfortunately, distinguishing between these types is difficult because as yet, no satisfactory tests specific to either have been developed. Van Krevelen (1961) and Dryden (1963) outline the many chemical approaches which have been employed. Typically, it is thought, on the basis of chemical tests, that at least half of the non-phenolic, non-carboxylic oxygen is in carbonyl form, most likely as quinone-like structures. However, the infrared spectra have been very confusing with respect to oxygen functional group determination.

Carbonyl groups typically absorb at  $1700\text{ cm}^{-1}$  in the infrared. In coals, unless they are of the low rank variety (in which carboxyl groups are known to be present via chemical techniques), there is no absorption at this wavenumber. Rather, there is an absorption at about  $1600\text{ cm}^{-1}$  which can be attributed to either an aromatic C-C absorption, carboxylate anion absorption, or a strongly chelated carbonyl absorption (a chelated compound is one in which an internal hydrogen bond exists, as in:



Objections have been raised to the latter interpretation because there would be no logical reason why all carbonyl groups should have to be strongly chelated quinones. (Given, 1976). On the other hand, Friedel (1966) points out that the amount of carbonyl present in such structures would

not have to be large to produce a significant absorption. To further complicate interpretation of this band, it has also been noted that the K Br - H<sub>2</sub>O complex can also contribute absorption in that region (solid coal is pressed into K Br pellets in IR sample preparation). At present, the weight of evidence supports the view that the 1600 cm<sup>-1</sup> band is at least in part due to carbonyl structures (Speight, 1971).

Ether oxygen (C-O) typically absorbs in the 1000 to 1300 cm<sup>-1</sup> range. Unfortunately, this band also contains phenol (C-O) stretching, alcoholic (C-O) stretching, and various H-C-C bending vibrations (Tschamler and deRuiter, 1963). Thus IR spectra in the region where ether information can be found, are very broad and indistinct.

Except for the previously cited data on methoxy content, chemically derived data on ether oxygen in coal is also rare. One instance is the work of Bhaumik et al. (1963), which appears to involve a modification of the Zeisel method used in methoxy determination. These workers arrive at a figure of approximately 2% by weight of bituminous coal as ether oxygen (and increasing with decreasing rank from 88 to 79% C).

For a coal of 80% C content, the following estimates can be made:

Hydroxyl oxygen	-	6%	(Figure 3.1-12)
Carboxyl oxygen	-	1%	(Figure 3.1-13)
Ether oxygen	-	2%	(see above)
Carbonyl (quinone) oxygen	-	2%	(Assuming ether: carbonyl = 1:1)
total oxygen		11%	


This value is reasonable for a coal of this rank, and in fair agreement with the results of this study. It appears that

some fraction of the discrepancy may be due to hydroxyl oxygen content (as revealed by pyrolysis). This will be discussed in a later section. The lignite worked with in this study has a total oxygen content of about 18.7% as received (22.4% daf) and an estimated organic O content of 19.7% dmf. The sum of hydroxyl, methoxy, and carboxyl oxygen is 13%, which implies 6-7% as ether and carboxyl. For, comparison, the data obtained by Blom are plotted in a cumulative fashion in Fig. 3.1-14. (Van Krevelen (1961), in reporting Blom's results, recognized the uncertainty in the carboxyl results by marking them with a question mark.)

There is, as has already been discussed, a fair amount of oxygen associated with the mineral matter in coal. It is important to keep this contribution in mind in constructing an oxygen balance about the pyrolysis system.

#### Sulfur and Nitrogen

Data on the forms of organic nitrogen and sulfur in coal are scarce. Van Krevelen (1961) cites data which suggest that nitrogen is primarily in aromatic ring form. In a review of the information on the role of nitrogen in the structures of fossil fuels, Pohl (1976) concludes that most of the nitrogen is present in pyridine-like aromatic structures.

Not a great deal more is known about the role of sulfur in coal structure. Van Krevelen (1961) in a review of the literature finds evidence of both thioethers and thiophenic structures. Thioethers (R-S-R) are favored in low rank coals, while thiophenic structures  predominate in high rank coals. Some more recent reviews concerning the nature of sulfur compounds in coal are those by Given et al. (1963) and

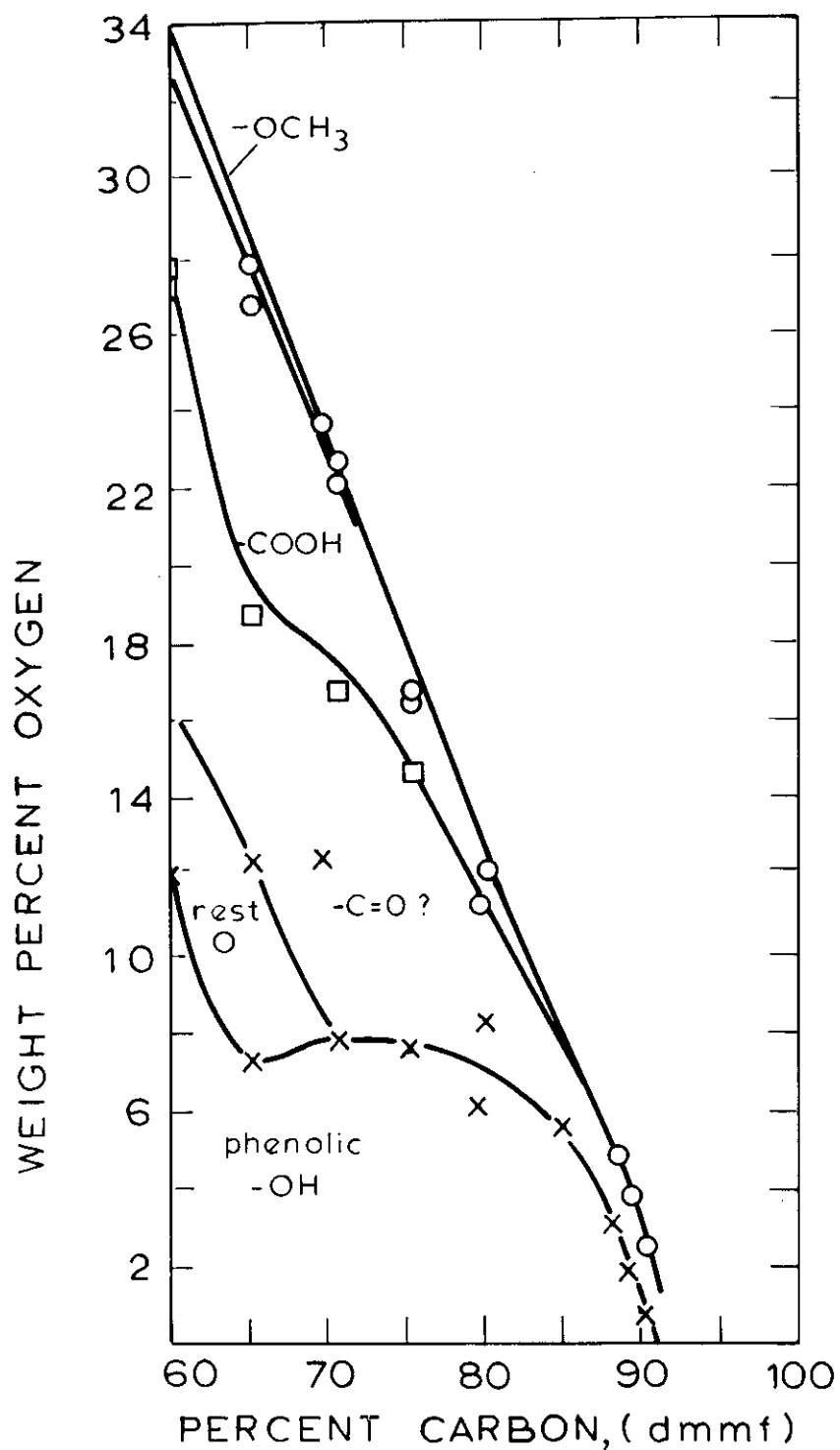


Figure 3.1-14 Variation of Total Oxygen Content with Rank (Blom, as given in Van Krevelen, 1961).

Attar and Corcoran (1977). The latter group estimates that the organic sulfur in bituminous coal is present as thiophenic, as aromatic (Ar-S-), and aliphatic (R-S-) sulfides in the ratio 50:30:20%. Some other recent evidence for the heteroaromatic forms of sulfur and nitrogen in coals is provided by an oxidative technique described by Winans et al. (1976).

Although nitrogen and sulfur compounds in coal are currently of great interest because they produce environmentally harmful oxides upon combustion, this thesis does not focus heavily upon them.

#### Summary and Application of Structural Data to Montana Lignite and Pittsburgh Seam Bituminous

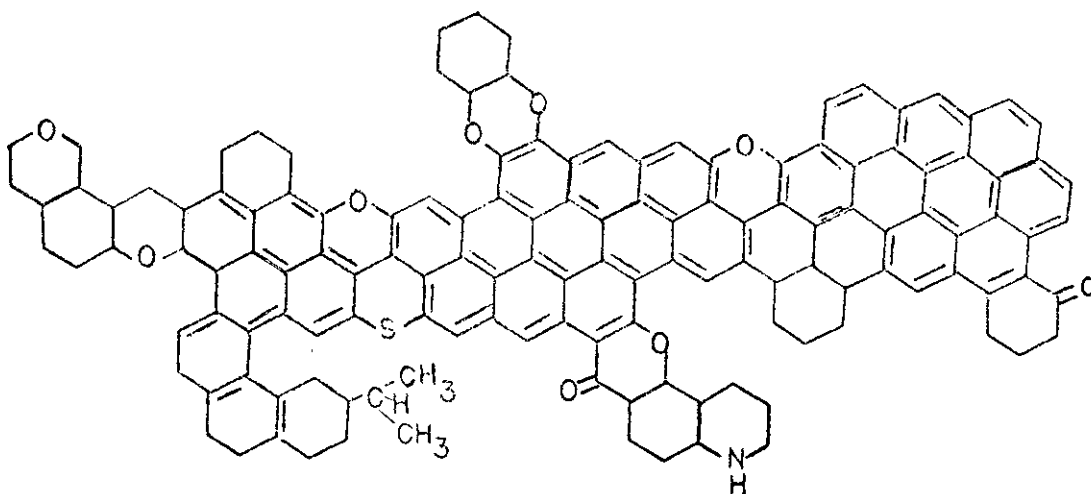
It should once again be emphasized that any inferences concerning the structures of the coals studied in this thesis are drawn from data on elemental compositions and maceral compositions alone. To advance the understanding of pyrolysis beyond that which is achieved in this thesis demands that more attention be focussed on tracking changes in the bulk phase more closely. For now, the best guesses concerning structure are summarized in Table 3.1-13.

#### A Synthesis of Data - An Evaluation of Various Coal Models

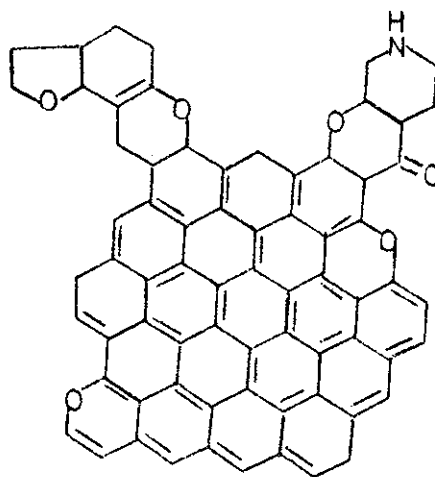
It is logical to proceed from the gathering of average structural data to the construction of a model for the average structural unit of coal. But it must be kept in mind that average structural units are statistical in nature and that the model that, on paper, fits all presently available structural data, may actually exist nowhere within the coal. This is especially true if one uses average structural data from whole coals, which can have several structurally very different maceral fractions.

Table 3.1-3 Summary of Estimated Structural Parameters for Pittsburgh Seam No. 8 Bituminous and Montana Lignite

	<u>Montana</u> <u>Lignite</u>	<u>Pittsburgh Seam</u> <u>No. 8</u>
Ultimate Analysis (dmmf)		
C	73.5	80.5
H	4.7	5.6
N	1.1	1.5
S	1.0	2.1
O	19.7	10.1
H/C	0.77	0.83
O/C	0.21	0.09
Aromaticity, fa	0.7	0.8
Aromatic carbons per cluster, $\bar{N}$	10	14
Carbon Atoms per average structural unit, C	14	18
Total rings per average structural unit, R	3-4	4-5
Aromatic rings per average structural unit	1-2	3-4
Aliphatic hydrogen content, $H_{al}/C$	0.55	0.50
Methylene Hydrogen Content, $H_{CH_2}/C$	0.38	0.35
Methyl Hydrogen Content, $H_{CH_3}/C$	0.10	0.10
Methin Hydrogen Content, $H_{CH}/C$	0.07	0.05
"Hydroaromatic" Hydrogen Content Removable by Catalytic Dehydrogenation, (Maximum)	0.26	0.23
Phenolic Hydrogen Content, $H_{OH}/C$	0.10	0.06
Aromatic Hydrogen Content, $H_{ar}/C$ (by Difference)	0.12	0.27
Hydroxyl Oxygen, % dmmf	8	5.5
Carboxyl Oxygen, % dmmf	4	0.5
Carbonyl Oxygen, % dmmf	4	2.0
Ether Oxygen, % dmmf	4	2.0
	(by Difference)	



$C_{135} H_{97} O_9 NS$   
 (47.0 x 22.5 x 9.0 Å)



$C_{70} H_{41} O_6 N$   
 (16.5 x 19.5 x 6.0 Å)

Figure 3.1-15. Model Structures for Coal (Fuchs and Sandhoff, 1942).

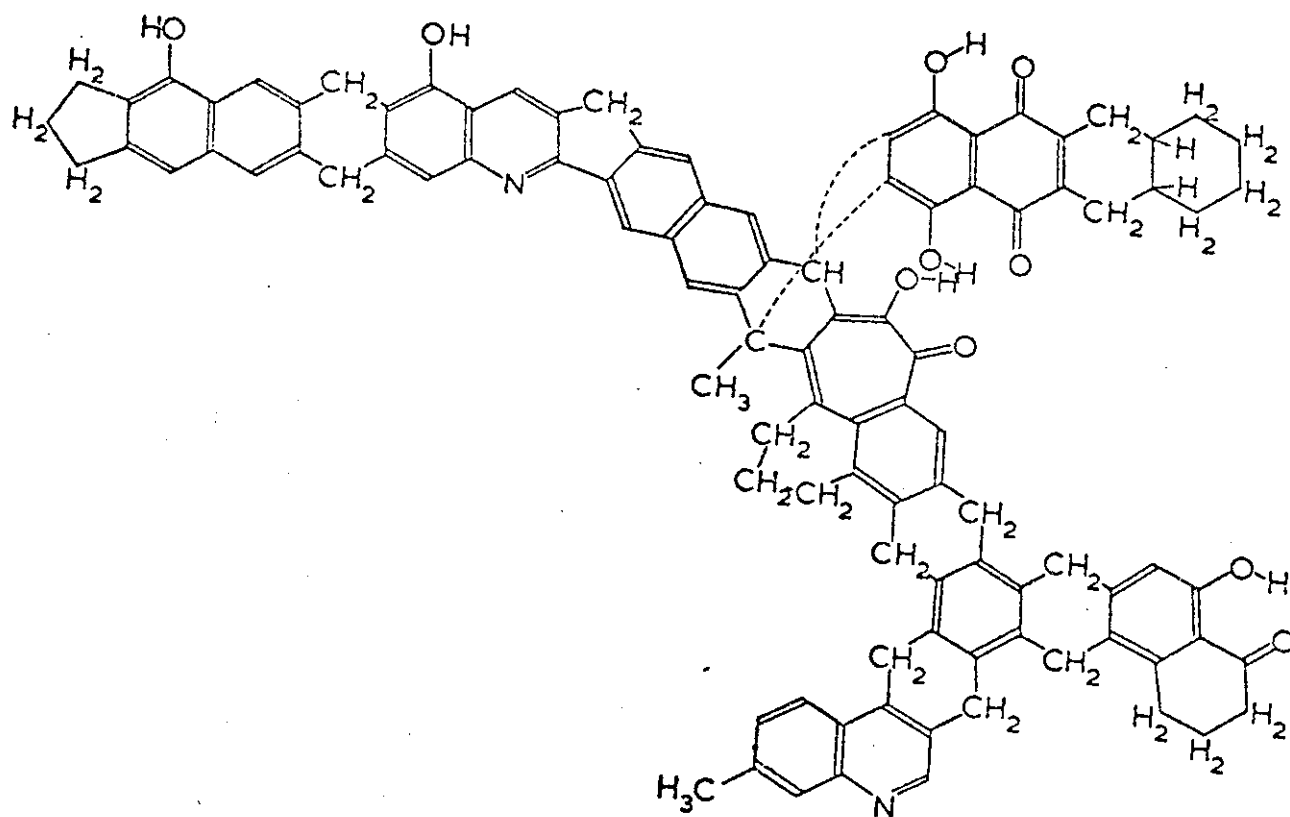


Figure 3.1-16. Proposed Model Structure for Coal (Given, 1960; empirical formula  $C_{102}H_{78}O_{10}N_2$ ).



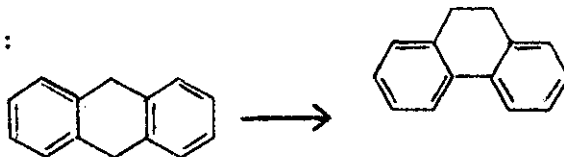
If one keeps these possible pitfalls in mind, then a model structure can be an effective aid in visualizing the reactions possible in a coal of a particular rank. The literature has an abundance candidate models; unfortunately some based on outdated structural information are still cited in discussions of coal chemistry. The rather recent model of Chakrabartty et al. (1974) has already been discussed and ruled out; its basic carbon skeletal structure (admantane-like, see Fig. 3.1-3) is inconsistent with the bulk of data on carbon aromaticity in coal.

Fig. 3.1-15 shows the classic models of Fuchs and Sandhoff (1942). The "chicken-wire" structure of coal suggested by these models is inappropriate, based upon the average cluster sizes shown for coals of the given rank; the models have far too many condensed rings.

The model structure proposed by Given (1960) is among the most frequently cited of structural models (Fig. 3.1-16). Instead of presenting a single average structural unit, Given presented an average coal "molecule" which was built up of many repeating 9,10 dihydroanthracene units. The model as originally postulated did not take into account a few observed properties of coal; its resistance to methylation with diazomethane and the absence of any change in the  $1600\text{ cm}^{-1}$  IR band upon acetylation ( $-\text{OH} + \text{CH}_3\text{-X} \rightarrow -\text{OCH}_3 + \text{HX}$ ), due to the destruction of the strongly chelated hydroxy-quinonoid structures (Given, 1960). Speight (1971) cites later evidence which does, however, lend support to the chelated structure theory.

In a later revision of his model, Given (1962) reviewed the NMR data of Brown et al. (1960) obtained on vacuum "distillates" of shock-carbonized coal and concluded that the inclusion of methylene bridges in

the model was inappropriate. Instead, he proposed making a minor change from his original 9,10 dihydroanthracene structure to a dihydrophenanthrene structure:



Some other optical properties suggested that this might be a favorable change to make as well. However the recent "depolymerization" work of Herédy et al. (1965) suggests that methylene bridges do indeed exist, and that the only reason they might not be observed in vacuum distillates is because they are so thermally labile.

In light of the above evidence, and in noting that the dihydrophenanthrene is a more strained ring system than that of dihydroanthracene, it would seem that the carbon-hydrogen structure as originally proposed may be the more acceptable. The question of oxygen functionalities remains unanswered, though in his revision, Given suggests that fewer of the chelated quinonoid carbonyls should be present, and more ketonic structures should be included. In light of current thinking, perhaps some carbonyls should be eliminated altogether, in favor of ether linkages.

The model contained no sulfur and the author has later pointed out (Given, 1976) that based on the molecular weight of the model (data from coal extract work suggests the 1000-4000 range) and the low sulfur content of the particular coal studied, fewer than one sulfur atom should have been included.

An important aspect of coal models is their stereochemistry because it is thought the the irregular, buckled shape gives rise to the large amount of microporous ( $D_{\text{pore}} \approx 10 \text{ \AA}$ ) volume formed in coals. Given

introduced a fair amount of stereochemical complexity into his model with the small group that is attached to the center of his model molecule. Cartz and Hirsch (1960) proposed a model based on their x-ray work which also took stereochemistry heavily into account. Their model was based on much the same structural data as Given's and it is not surprising to see some similarity, although the Cartz and Hirsch models is drawn for a higher rank of coal. This model appears to be reasonably sound as well, but Given seems to have paid more attention to detail and can therefore account for more phenomena (e.g. the  $1600\text{ cm}^{-1}$  IR band).

Hill and Lyon (1962) suggested the structure shown in Fig. 3.1-17. It is somewhat more difficult to analyze this model in terms of the average structural parameters presented earlier because the definition of an average structure is not clear in this case. It appears that the proposed structure has some features which are not consistent with the current thinking on structure. There seems to be too little in the way of hydroaromatic hydrogen, and too much in the way of long chain aliphatics (though evidence from Utah coals is frequently said to favor this view). The carbonyls appear in quinonoid structures with no chelating. The carboxylate groups may be inappropriate in coals with such large condensed ring aromatic structures (inconsistency in rank implied) and they should probably not appear as acids but as acid salts. The alcoholic functionalities are also not present in higher rank coals. There are undoubtedly many other details which could be picked out as shortcomings; as far as explaining the physical properties and reactions of coal there appear to be several better models.

Mazumdar et al. (1962) suggested a series of models which traced the

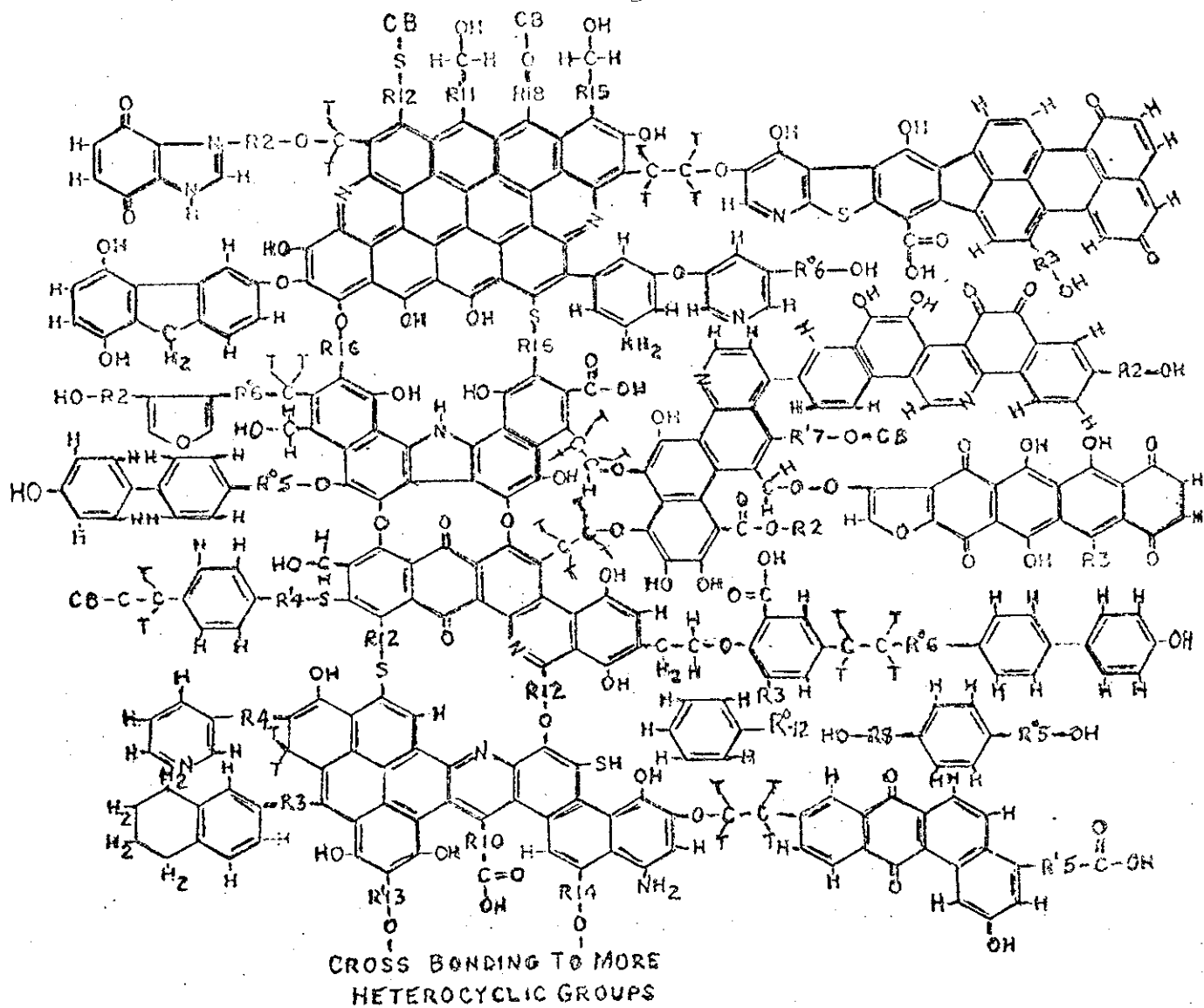


Figure 3.1-17. Model Structure for Coal (Hill and Lyon, 1962).

process of natural coalification from a lignite to an anthracite (Fig. 3.1-18). They propose that coals are really mixtures of materials at various stages of coalification, and that a bituminous coal will have elements of structures I, II, and IIIA all present at the same time, with relative amounts depending upon rank. However, they postulate that the transition from bituminous coal to anthracite must be much more severe, involving the much more substantial change depicted in going from structure IIIB to IV (although the reasons for needing to hypothesize a severe change in conditions are not clear).

These structures I-IV clearly represent only single average structural units which must be built into "molecules" by linkage to other similar structures. There are again some details which can be used to question the models; the average number of condensed aromatic rings in the lignite (I) appears high, and the carboxylates should be in salt form.

Van Krevelen (1963) takes a similar approach in hypothesizing a mechanism of coalification by examination of average structural units (Fig. 3.1-19). These models appear less concerned with the details of structure as with mechanisms of coalification.

Wender (1975) proposed structures for the four ranks of coal shown in Fig. 3.1-20. Although he emphasizes that these are not coal models, they are convenient ways of representing these coals in order to understand the types of reactions they can undergo. Most interesting in this regard is the structure he proposes for the lignite, which is quite markedly different from the traditional "chicken wire". Wender rightfully points up the need for more complete structural characterization of low rank coals.

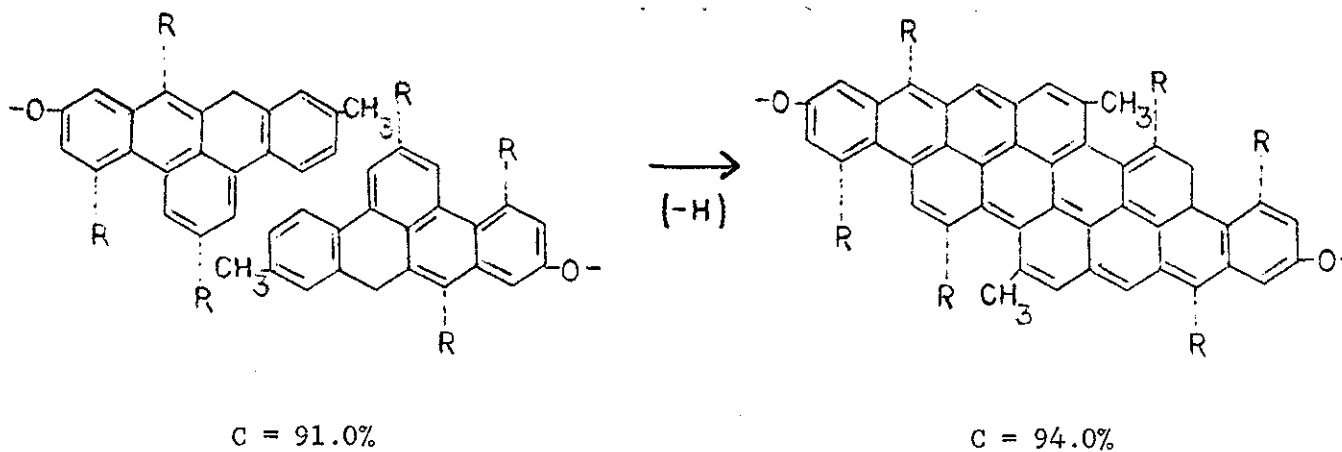
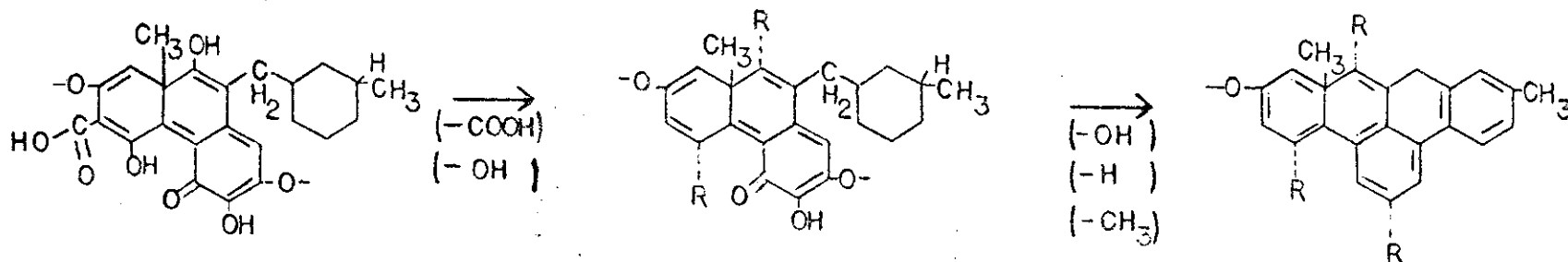


Figure 3.1-18. Model Structures for Coals of Various Rank Showing Coalification Process (Mazumdar, 1962).

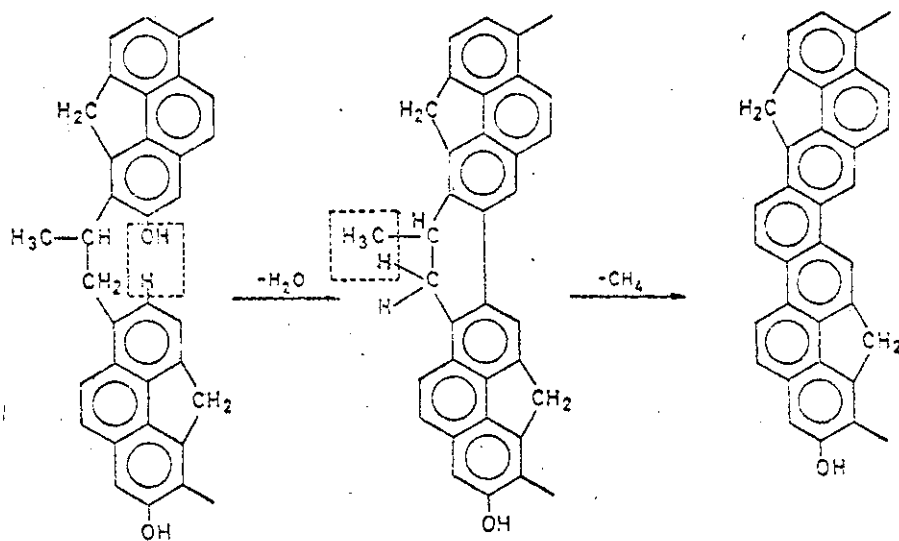
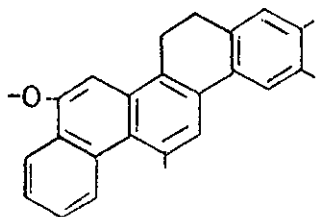
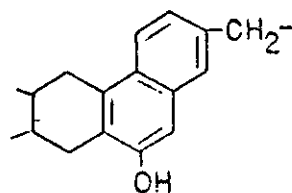


Figure 3.1-19. Various Model Structures for Coals and Examples of the coalification Process (Van Krevelen, 1963).



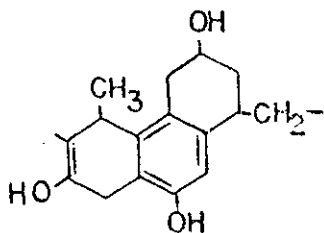
Pocahontas No. 3 Bed, W.Va. (LVB)

	<u>% MAF</u>
C	90.7
H	4.6
O	2.8
N	1.3
S	0.6
VM	18.7



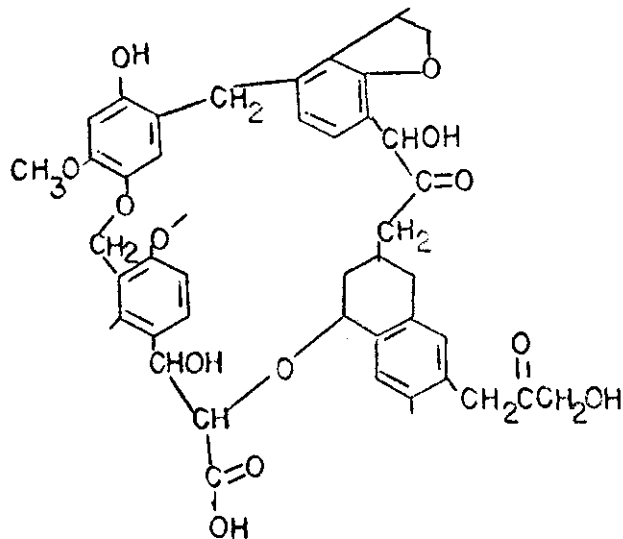
Pittsburgh Bed (HVAB)

	<u>% MAF</u>
C	84.2
H	5.6
O	6.9
N	1.6
S	1.7
VM	39.9



Mammoth Bed, Wyo. (Subbituminous A)

	<u>% MAF</u>
C	76.7
H	5.6
O	15.5
N	1.3
S	0.9
VM	43.6



Beulah Zap Bed, N.D. (Lignite)

	<u>% MAF</u>
C	72.6
H	4.9
O	20.2
N	1.1
S	1.2
VM	45.9

Figure 3.1-20. Examples of Possible Structures for Coals of Various Ranks (Wender, 1975).



An interesting model (Fig. 3.1-21) is proposed by Wiser (presented in Wolk et al., 1975). Again, the author (Wiser, 1977) emphasized that this is not a model of coal, but rather an attempt to show what kind of structures may be present in bituminous coal. It is interesting in its attempt to show the forms which sulfur, nitrogen, and ether oxygen may assume in a coal structure.

Gavalas and co-workers (Cheong et al, 1975 ; Oka et al., 1977; Cheong, 1977) have recently taken an interesting approach to modelling coal pyrolysis, based upon a statistical model of coal structure statistically degrading. Fig. 3.1-22 shows a flow sheet for model generation. It relies on a number of measured quantities,  $H_{\alpha}/H_{\beta}$  (ratio of alpha hydrogens, those on a carbon attached to an aromatic ring, to beta position - hydrogens, those on a carbon one or more atoms removed from an aromatic ring),  $H_{ar}/H_{al}$  (the ratio of aromatic to aliphatic hydrogens),  $(H/C)$  corrected (the hydrogen to carbon ratio of the coal, removing carbons in carboxyl and carbonyl groups), and  $\rho_{eff}$  (the measured solid density correcting for heteroatoms, micropore volume, and carboxyl and carbonyl structures). Gavalas et al. chose to obtain  $H_{\alpha}/H_{\beta}$  and  $H_{ar}/H_{al}$  by proton NMR of coal extracts or pyrolysis tars, which of course is risky. Further, the values for the carboxyl and carbonyl contents of the coal are calculated from yields of  $CO_2$  and CO during pyrolysis, also rather risky.

The structure determination program also requires initial values for the  $C_{ar}$  (the number of aromatic carbons per "cluster").  $H_{ar}$  (the number of peripheral sites per cluster), and the amounts of methylene, ethylene and longer chain alkyl bridges per unit. These values are all assumed. Because of the large number of assumptions involved in deriving

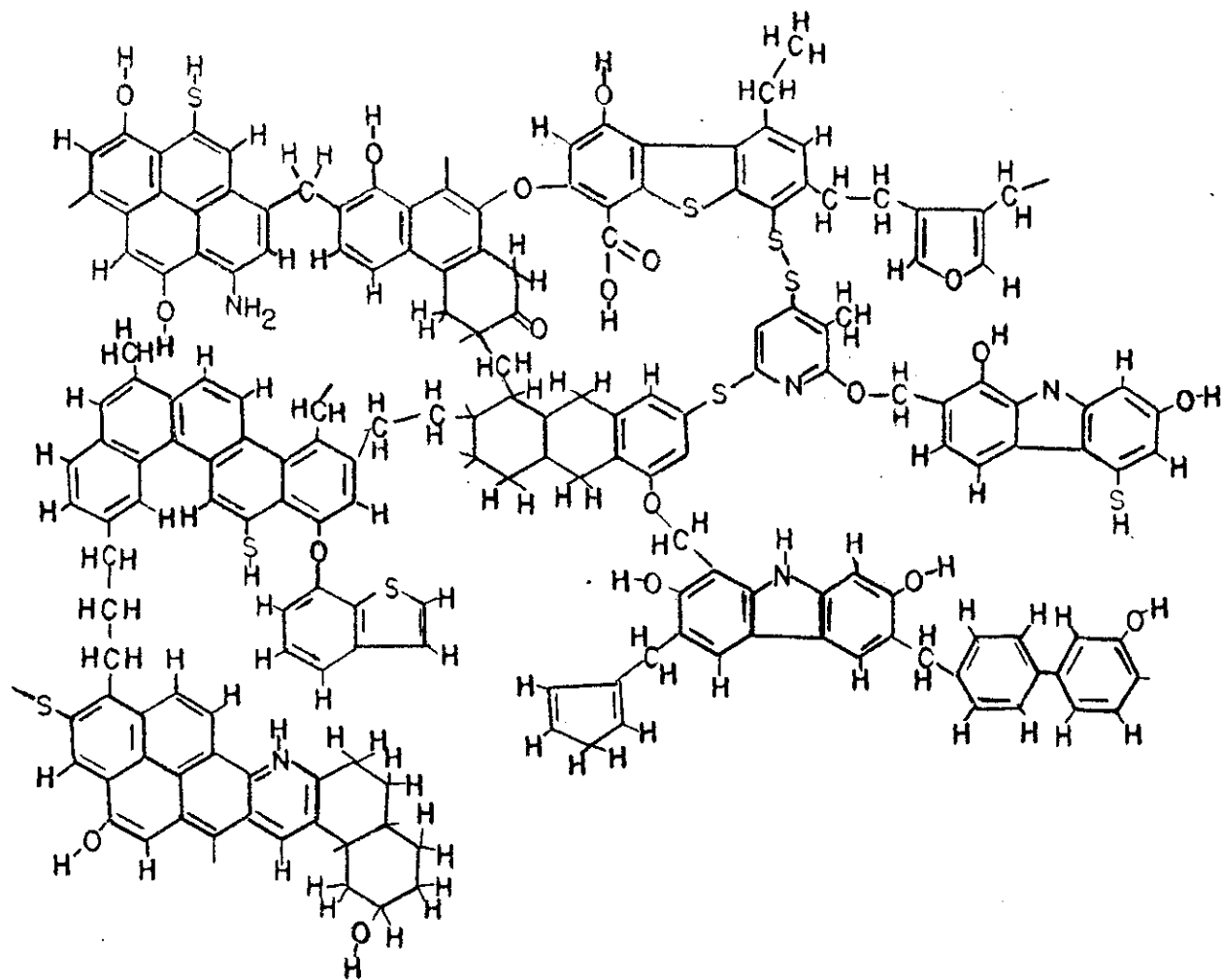
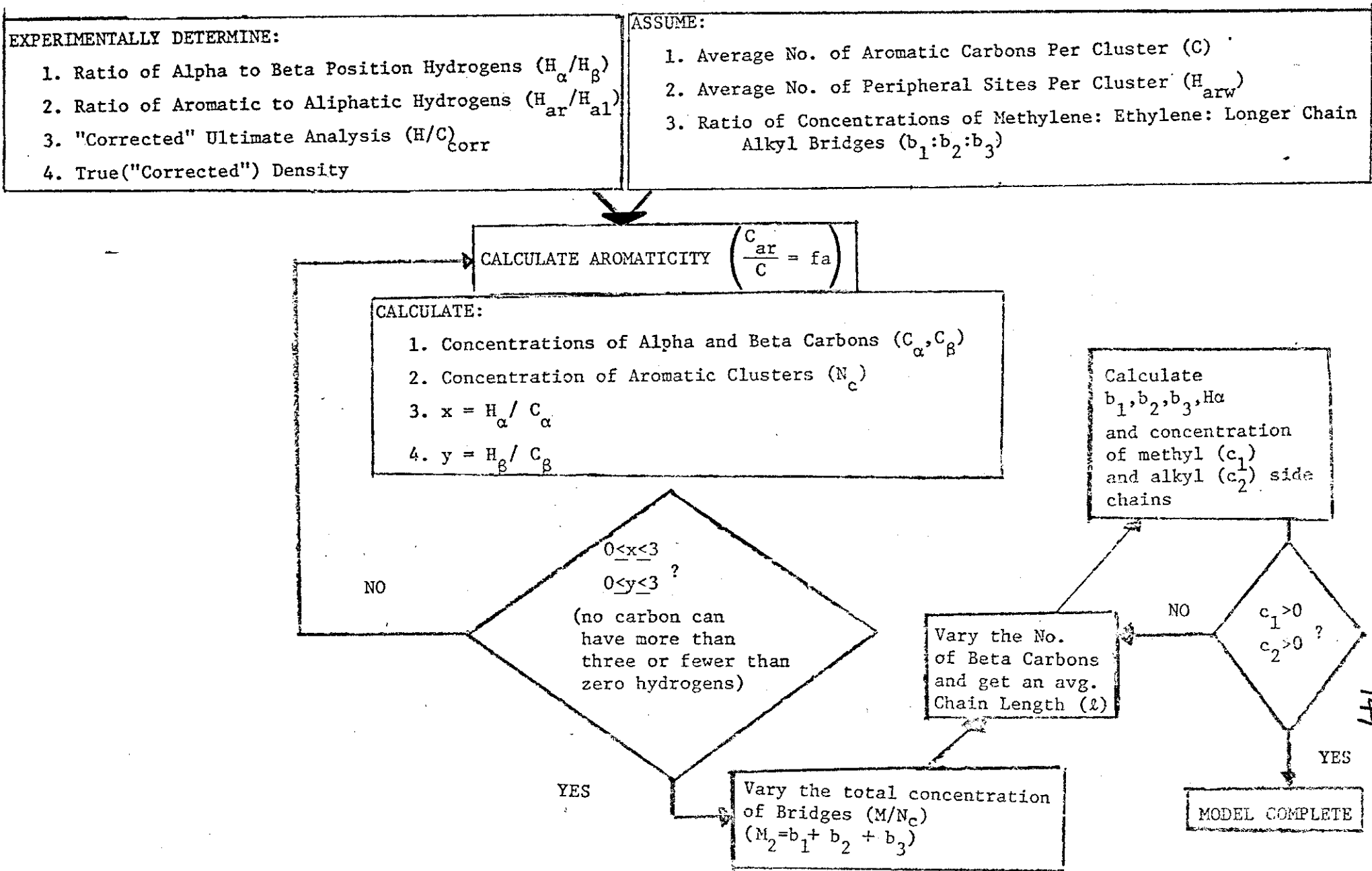


Figure 3.1-21. Examples of Structures Which can be Found in Coals  
(Wiser, in Wolk et al., 1975).

Figure 3.1-22. Flow Sheet for Synthesis of Coal Model Structures (Cheong, 1977).



the model, a rather thorough sensitivity analysis seems warranted; this especially in light of the apparent sensitivity of the pyrolysis model (discussed in the pyrolysis modelling section) to the concentrations of the various aliphatic bridges. Also in its earlier versions, the model did not account for the potentially significant structural role of oxygen (aside from tying up carbon atoms), a situation which is apparently the subject of much current attention (Gavalas, 1977).

One final aspect of the problem of screening coal structures is that of thermodynamics. As is well established, the heat of combustion of coal can be fairly accurately estimated by summation of the contributions of its constituent elements. Since this implies (in low oxygen coals) that the heat of formation of the coal substance itself must be near zero, this can be used as a screening factor for higher rank coal structures (Anthony, 1974). Unfortunately, as Anthony found by applying a group contribution estimation technique to some coal models, the heats of formation of both the Given model ( $\Delta H^{\circ}f = 55 \text{ Btu/lb} = 30 \text{ kcal/mole}$ ) and the Fuchs and Sandhoff model (b) ( $\Delta H^{\circ}f = 92 \text{ Btu/lb} = 76 \text{ kcal/mole}$ ) are both reasonable in this regard. Hence, Anthony concludes (and the evidence in this section reinforces that conclusion) that thermodynamics alone is not sufficient basis to distinguish between "good" models and "poor" models. Nor does this evaluation criterion seem at all promising for lignites, which have substantial oxygen contents, and non-zero heats of formation.

### The Physical Structure of Coal

The study of the chemistry of coal pyrolysis and hydrolysis may unfortunately be very much clouded by mass transport effects. The modelling of intra-particle mass transport phenomena is unfortunately very difficult. Each coal particle may be viewed as a tiny chemical reactor, which at the beginning of the process contains many distinct solid phases (e.g. mineral, vitrinite, exinite, fusinite, etc.) any of which can participate in the chemical processes via reaction or as a catalyst. These solid phases are crisscrossed by a network of pores ranging in size from a few Angstroms to a few microns. On a microscopic level, the currently widely accepted view of pore structure is that due to Hirsch and co-workers (1954, 1960), shown in Fig. 3.1-23. Recalling the stereochemistry of the coal model proposed by Given or that by Cartz and Hirsch, it is clear that these structures have some relatively planar aromatic structures and some very non-planar tetrahedral carbon "buckling". When many of these molecules are placed in close proximity to one another, as in a coal molecule, a large amount of entanglement is bound to occur. Where two or more planar aromatic regions are in close proximity to one another, "layered stack" formation occurs. In the limit of coalification, where the carbon is 100% aromatic, one can obtain the neatly layered structure of pure graphite. Where layer formation cannot occur and steric hindrance prevents close approach of molecules, micropores of molecular dimensions can occur. Intermediate angle x-ray scattering gave the results shown in Fig. 3.1-24, showing the average number of (aromatic) layers per "stack" and the average interlayer spacing as a function of rank (Cartz and Hirsch, 1960). These

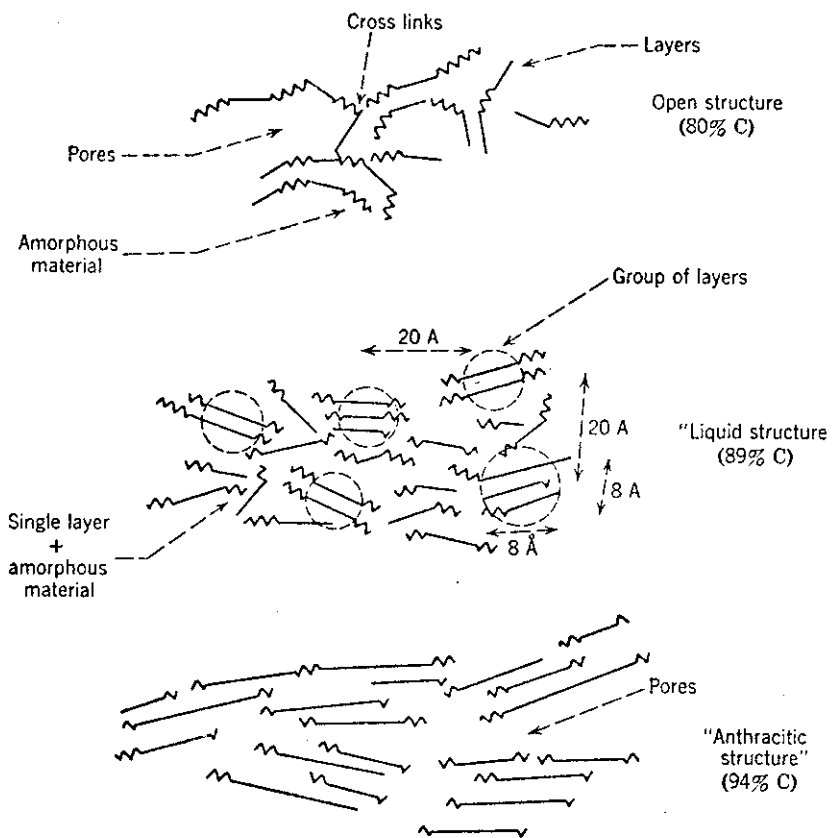


Figure 3. 1-23. Microscopic Origin of Porosity (Hirsch, in Dryden, 1963).

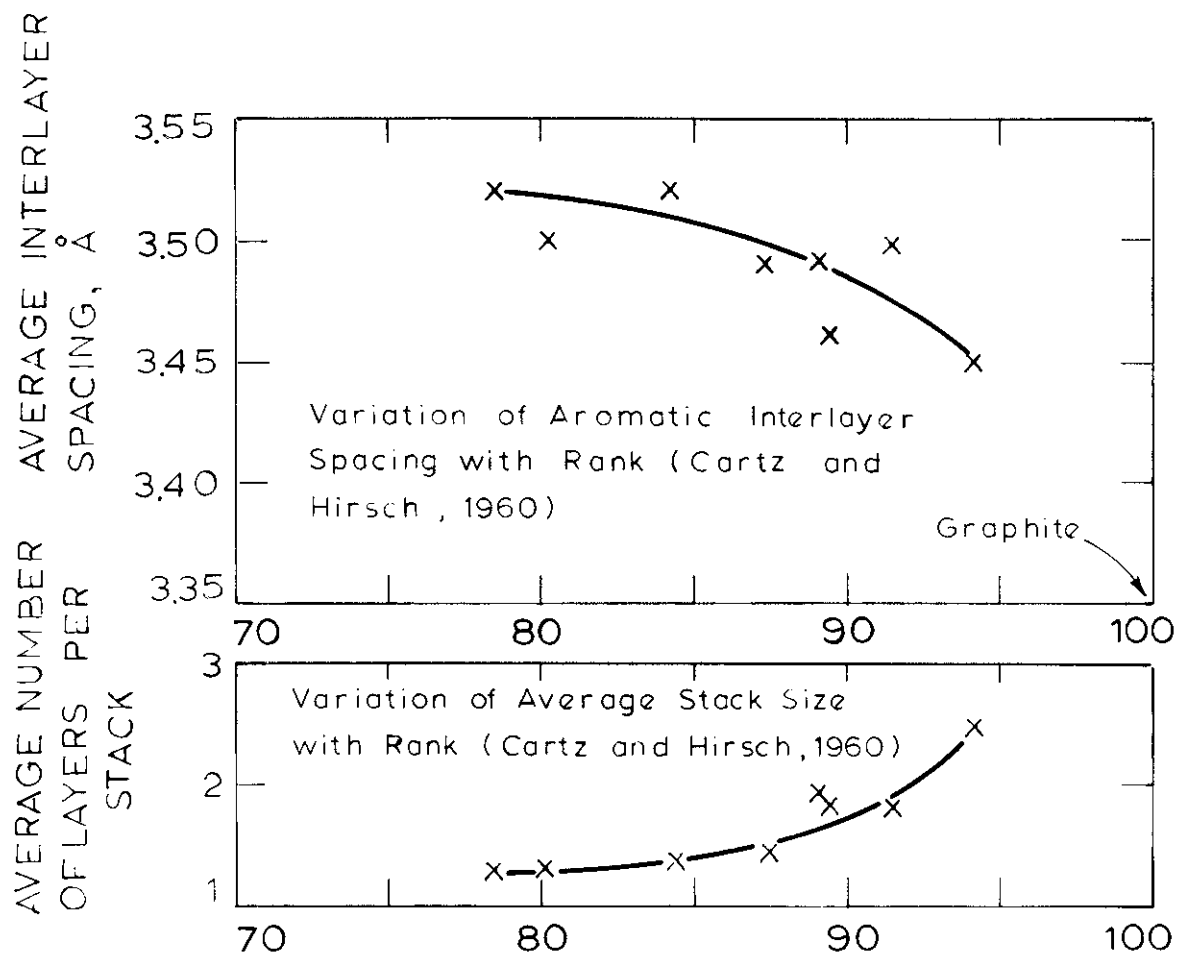


Figure 3.1-24 Structural Parameters from X-ray Scattering Studies of Coal.

interlayer voids are too small to be penetrated by helium, and will not be corrected for in helium density measurements. Pores of diameter greater than about  $4 \text{ \AA}$  can be penetrated by helium, provided there are no constrictions of less than  $4 \text{ \AA}$  preventing entry.

Fig. 3.1-25 shows the variation of total porosity with rank. As one might expect, the general trend is decreasing porosity with increasing rank. Fig. 3.1-26 shows that this porosity is principally due to micropores (with diameters between  $4$  and  $12 \text{ \AA}$ ) in the high rank coals, while in the low rank coals porosity is principally due to macropores, those with diameters greater than  $300 \text{ \AA}$  ( $.03\mu$ ). Such large pores cannot be viewed as gaps between two molecules; macropores must represent gaps in the macrostructure of coal. In low rank bituminous coals, the so-called "transitional pores" (diameters between  $12$  and  $300 \text{ \AA}$ ) contribute a large fraction of the pore volume.

Thus the lignite used in this study would be characterized primarily by a macroporous structure characterized by pores of greater than  $.03\mu$ , but containing a non-negligible volume of micropores of less than  $12 \text{ \AA}$  in size.

Although the bituminous coal examined in this study can be characterized in terms of micro-, macro- and transitional pores as well, far more important in determining the mass transport out of bituminous coal may be its softening behavior; rather than flowing out of the pores of a pyrolyzing bituminous coal particle, volatiles actually "bubble" out. This behavior will be discussed further in a later section.



TOTAL POROSITY ( $\text{cm}^3/\text{gm}$ )

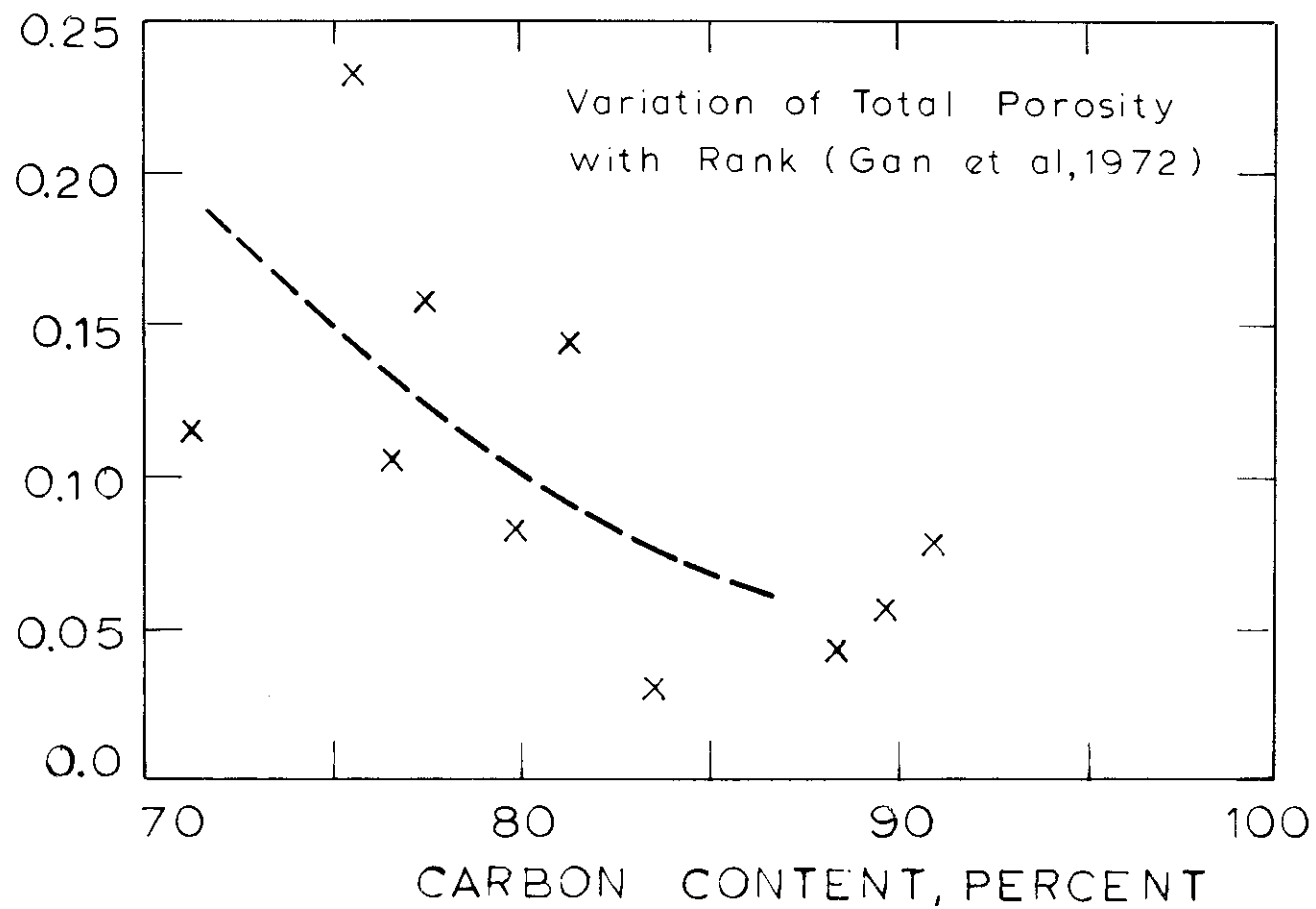


Figure 3.1-25 Variation of Total Porosity with Rank.

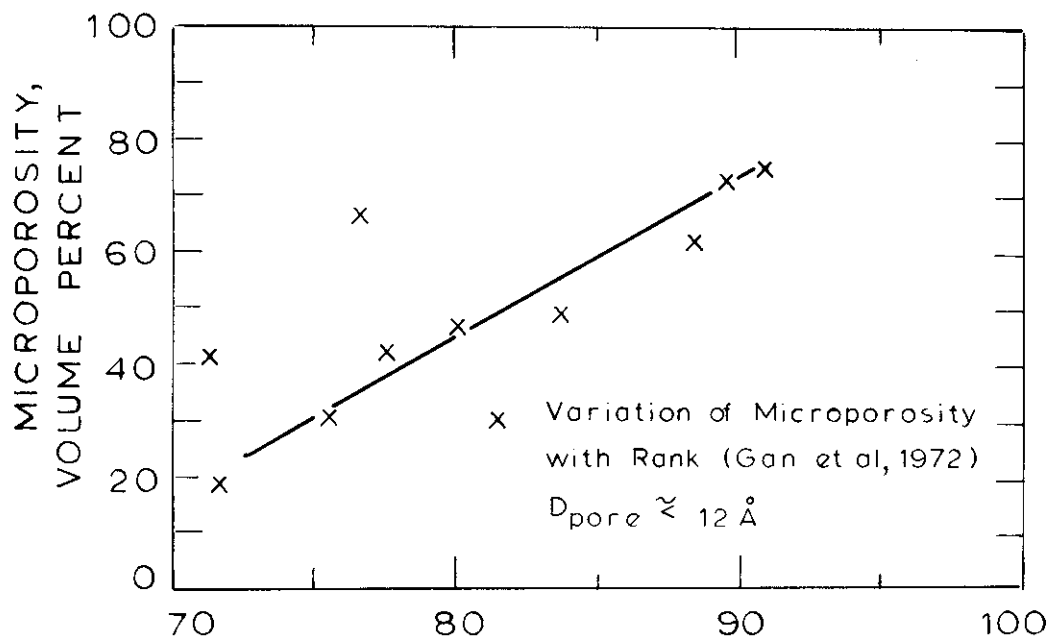
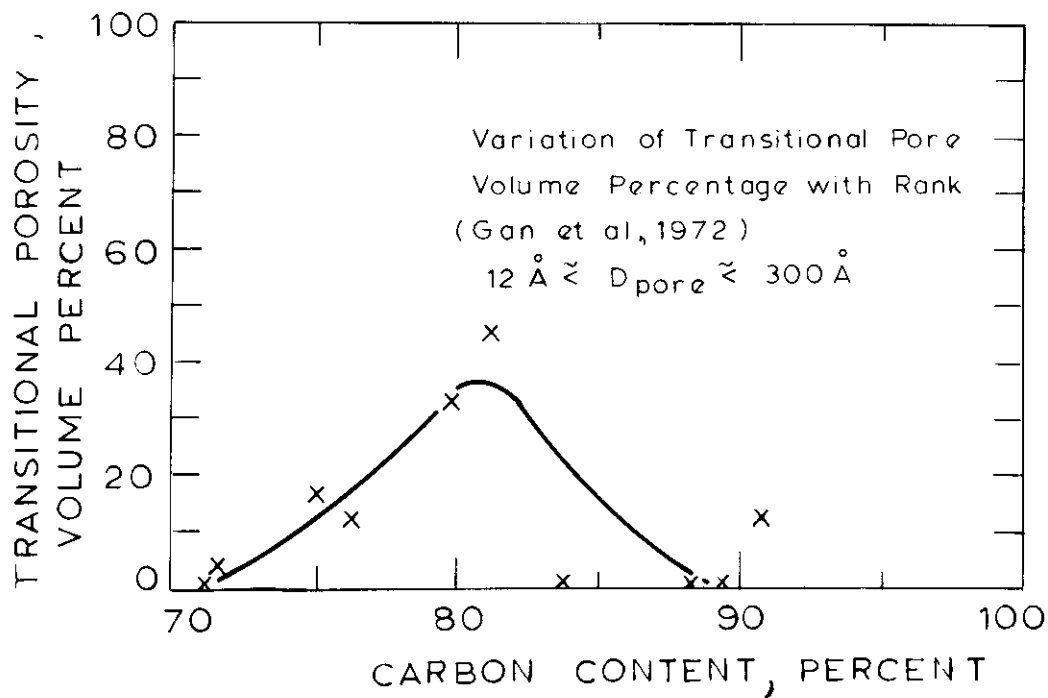


Figure 3.1-26 Variation of Micro- and Transitional-Porosity with Rank.



### 3.2 Previous Work on Pyrolysis and Hydropyrolysis

There exists an extensive body of literature on coal pyrolysis. Over the last several years, a number of good reviews have been published, including those by J.B. Howard and Anthony (1976) and H.C. Howard (in Lowry (1963)). The former also reviews the hydropyrolysis literature; this interrelation of pyrolytic and hydropyrolytic processes will be examined throughout this thesis. Currently, J.B. Howard (1977) is preparing a new in-depth review of significant recent research in the area of pyrolytic reactions of coal. Other shorter reviews of the pyrolysis literature include those by Van Krevelen (Chapter XIV, 1961), Jones (1964), Yellow (1965); Badzioch (1961 and 1967), and Essenhig and J.B. Howard (1971).

In addition to the review noted in the previous paragraph, other recent reviews that deal with hydropyrolytic phenomena include those by Von Fredersdorff and Elliot (1963) and Pycioch et al. (1972).

Since there are several good, recent reviews of the literature, an exhaustive literature review will not be attempted here. Instead, examples are chosen somewhat selectively, with preference being given to recent work, and any work which sheds light on fundamental mechanisms. As has already been discussed, in the study of pyrolysis and hydropyrolysis of coal, six classes of variables play an important role in determining total yields and compositions of products. These are again:

1. The Chemical and Physical Characteristics of the Raw Coal
2. The Time-Temperature History to which the Coal is exposed.
3. The Partial Pressure of Hydrogen within the reactor used to hydropyrolyze the coal.
4. The Total Pressure within the reactor used to pyrolyze the coal

5. The initial physical characteristics of the coal as controlled by the experimenter (e.g. particle size, extent of drying, "aging").
6. The reactor, product residence times, catalytic surfaces, etc.

The first of these variables has already received some attention in the preceding sections; in this section the chemical characteristics will be related to pyrolysis behavior.

#### Evaluation of Experimental Systems

All too often, in studies involving any or all of the first five classes of variables, the sixth may be relegated a relatively unimportant role. This is not good practice in any experimental work. In the case of coal, however, where the phenomena being studied are very complex to start with, it may be easy to lose sight of the influence of uncontrolled system variables.

Anthony and Howard (1976) and Howard (1977) recognize the important role that experimental design can play in the interpretability of experimental data. Table 3.2-1 is taken from Howard (1977), and gives an indication of the wide range of techniques used to study pyrolysis and hydrolysis. It should be noted that the Table does not include some of the more advanced or exotic techniques which have been applied, such as shock tubes, plasma jets, flash tubes and lasers (see Anthony and Howard for references). In general, these very fast, high energy input techniques have been exploratory, and not concerned with the mechanisms of pyrolysis at conditions of commercial interest. In high temperature plasmas, acetylene is the major hydrocarbon product if the processes is conducted in hydrogen or inert gas, while running in nitrogen can lead to

Table 3.2-1 Experimental Techniques and Conditions  
(Howard, 1977)

<u>Investigator</u>	<u>Technique</u>	<u>Residence Time, s</u>	<u>Temp., °C</u>	<u>Heating Rate, °C/s</u>	<u>Press., atm</u>	<u>Ambient Gas</u>	<u>Particle Size, μm</u>
<u>CAPTIVE SAMPLE TECHNIQUES</u>							
Standard Proximate Analysis (ASTM,1974)	Crucible	420	950	15-20	1.0	Air (lid on)	≤ 250
Wiser <u>et al.</u> (1967)	Crucible	300- 72,000	400-500	15-20	1.0	N <sub>2</sub>	250-420
Portal and Tan (1974)	Crucible and basket	15-1,200	550-1,150	0.5-250	1.0	N <sub>2</sub>	≤ 45-88
Gray <u>et al.</u> (1974)	Crucible	420	950-1,200	0.3-20	1.0	N <sub>2</sub>	≤ 200
Kobayashi (1976)	Crucible	1,800-3,600	270-1,830	0.5-5	1.0	Ar	27-90
Campbell (1976); Campbell and Stephens (1976)	Basket	Up to 18,000	110-1,000	0.056	1.0	Ar,N <sub>2</sub> ,H <sub>2</sub> ,CO	1,700-3,600
Hiteshue <u>et al.</u> (1962a,b;1964)	Fixed bed, gas swept	20-900	480-1,200	10	18-400	H <sub>2</sub>	250-600
Feldkirchner and Linden(1963); Feldkirchner and Huebler(1965)	Fixed bed, gas swept	10-480	700-930	100-300 (seems high)	34-168	H <sub>2</sub> ,H <sub>2</sub> O	840-1,000
Jüntgen and Van Heek(1968, 1977); Van Heek <u>et al.</u> (1973).	Fixed bed, gas swept	1,000- 1,000,000	400-1,100	0.0001 -0.5	1-70	He,H <sub>2</sub> ,H <sub>2</sub> O	≤2,000
Vestal <u>et al.</u> (1969); Yergey <u>et al.</u> (1974)	Fixed bed, gas swept	600- 60,000	≤1,000	0.02-2	≤5	H <sub>2</sub> ,He	37-74
Moseley and Paterson(1965a)	Railway heater	15-165	815-950	25	18-95	H <sub>2</sub>	150-300
Feldkirchner and Johnson (1968); Johnson(1971)	Thermo- balance	Several to 7,200	≤925	≤100	≤100	H <sub>2</sub> ,N <sub>2</sub> , H <sub>2</sub> O,etc.	420-850

Table 3.2-1 Experimental Techniques and Conditions (continued)  
(Howard, 1977)

<u>Investigator</u>	<u>Technique</u>	<u>Residence Time</u>	<u>Temp., °C</u>	<u>Heating Rate, °C/s</u>	<u>Press., atm.</u>	<u>Ambient Gas</u>	<u>Particle Size, μm</u>
Gardner <u>et al.</u> (1974)	Thermo-balance	25-3,000	850-950	-	35-69	H <sub>2</sub>	500-1,000
Loison and Chauvin (1964)	Elec.grid	0.7	<1,050	1,500	Vacuum	-	50-80
Rau and Robertson (1966)	Elec.grid	1-1.5	900-1,200	600	1.0	-	250-420
Juntgen and Van Heek (1968)	Elec.grid	0.7	<1,000	<several 1,000	Vacuum	-	50-60
Koch <u>et al.</u> (1969)	Elec.grid	7	<1,500	167	Vacuum	-	75-630
Mentser <u>et al.</u> (1970, 1974)	Elec.grid	0.05-0.15	400-1,200	8,250	Vacuum	-	44-53
Cheong <u>et al.</u> (1975)	Elec.grid	<1-1,800	300-1,000	<1,000	Vac.-3.4	-	90-360
Solomon (1977)	Elec.grid	5-80	<1,000	600	Vacuum	-	44-370
Anthony <u>et al.</u> (1974, 1975, 1976); this study	Elec.grid	0.1-30	400-1,100	100-12,000	0.001-100	H <sub>2</sub> , He, N <sub>2</sub>	53-1,000
Blair <u>et al.</u> (1977)	Elec. ribbon	0.02-20	350-1,700	200-20,000	1.0	He	510-620
Squires <u>et al.</u> (1975); Graff <u>et al.</u> (1976); Dobner <u>et al.</u> (1976)	Ring of coal, gas swept	1-6 (gas), 10-30 (solid)	600-1,000	650	100	H <sub>2</sub>	<44
<u>COAL-FLOW TECHNIQUES</u>							
Stone <u>et al.</u> (1954)	Fluidized bed	10-2,500	400-700	-	1.0	N <sub>2</sub>	200-600
Peters (1960); Peters and Bertling (1965)	Mechanically stirred bed	<0.5-10	600-1,100	50-200	1.0	N <sub>2</sub>	1,000-1,500
Pitt (1962)	Fluidized bed	10-6,000	400-700	-	1.0	-	200-600

Table 3.2-1 Experimental Techniques and Conditions (continued)  
(Howard, 1977)

<u>Investigator</u>	<u>Technique</u>	<u>Residence Time</u>	<u>Temp., °C</u>	<u>Heating Rate, °C/s</u>	<u>Press., atm.</u>	<u>Ambient Gas</u>	<u>Particle Size, μm</u>
Jones <u>et al.</u> (1964)	Fluidized bed	~2,400	425-1,095	1,000+	1.0	N <sub>2</sub> ,H <sub>2</sub> O	<1,000
Smith and Wailes(1975)	Fluidized bed	-	-	-	1.0	N <sub>2</sub>	-
Friedman(1975)	Fluidized bed	1,800-3,600	300-650	-	1.0	H <sub>2</sub> O	250-710
Birch <u>et al.</u> (1960,1969)	Fluidized bed	500-9,500	500-950	-	21-42	H <sub>2</sub> ,etc.	150-710
Hamrin <u>et al.</u> (1973); Maa <u>et al.</u> (1975)	Fluidized bed	3,600-26,600	600-870	0.06-0.25	1.0	H <sub>2</sub> ,H <sub>2</sub> S,N <sub>2</sub>	100-600
Eddinger <u>et al.</u> (1966)	Entrained flow	0.008-0.04	625-1,000	2,500+	1.0	He	6,150
Friedman <u>et al.</u> (1968)	Entrained flow	0.004-2	400-1,000	650-4,300	1.0	He,N <sub>2</sub> ,H <sub>2</sub> O	<150,74, and 5
Howard and Essenhigh(1967)	P.f.flame	0-0.8	200-1,550	<22,000	1.0	Air	80% ≤ 74
Sass (1972)	Entrained flow	A few	540-650	10,000	1.0	-	25-80
Smith and Wailes(1975)	Entrained flow	0.5	400-700	-	1.0	N <sub>2</sub>	-
Badzioch(1967); Badzioch and Hawksley(1970)	Entrained flow	0.03-0.11	400-1,000	25,000-50,000	1.0	N <sub>2</sub>	11-73
Kimber and Gray(1967a,b)	Entrained flow	0.012-0.11	780-2,000	100,000-400,000	1.0	Ar	23-76

Table 3.2-1 Experimental Techniques and Conditions (continued)  
(Howard, 1977)

<u>Investigator</u>	<u>Technique</u>	<u>Residence Time, s</u>	<u>Temp. °C</u>	<u>Heating Rate, °C/s</u>	<u>Press., atm</u>	<u>Ambient Gas</u>	<u>Particle Size, μm</u>
Kobayashi(1976); Kobayashi <u>et al.</u> (1977)	Entrained flow	0.001-0.22	700-1,800	10,000-200,000	1.0	Ar	38-45
Nsakala <u>et al.</u> (1977)	Entrained flow	0.3	810	8,000	1.0	N <sub>2</sub>	50-180
Ubhayaker <u>et al.</u> (1977)	Entrained flow	0.007-0.07	1,500-2,000	≤130,000	1.0	CO <sub>2</sub> , H <sub>2</sub> O, N <sub>2</sub>	70%≤74
Belt <u>et al.</u> (1971,1972)	Entrained flow	≤1	815-1,040	-	1-28	H <sub>2</sub> , N <sub>2</sub>	70%≤74
Coates <u>et al.</u> (1974)	Entrained flow	0.012-0.34	650-1,370	-	1.0	H <sub>2</sub> , H <sub>2</sub> O, etc.	≤74
Moseley and Paterson(1965b)	Entrained flow	0.17-2.5	790-1,000	1,000+	50-520	H <sub>2</sub>	100-150
Glenn <u>et al.</u> (1967)	Entrained flow	2.4-10.4	920-970	-	70-84	H <sub>2</sub> , CO etc.	≤44
Johnson(1975)	Entrained flow	5-14	480-845	28(or very fast)	18-52	H <sub>2</sub> , He	75-90
Fallon and Steinberg(1977)	Entrained flow	12-20	450-820	-	100-140	H <sub>2</sub>	≤150
Shapatina <u>et al.</u> (1960)	Free fall	0.45-14,400	≤550	-	45-490	N <sub>2</sub>	150-200
Moseley and Paterson(1967)	Free fall	A few	840-1,000	-	45-490	H <sub>2</sub>	100-150
Feldmann <u>et al.</u> (1970)	Free fall	A few	650-900	-	35-205	H <sub>2</sub>	150-300
Kobayashi(1976)	Free fall	~1	760-1560	-	1.0	Ar	38-45



large yields of hydrogen cyanide (Bond et al., 1966; Krukonis et al., 1973). Such products suggest a rather dramatic decomposition of the basic hydrocarbon structure of coal, which is undesirable if one wishes to maximize the yield of liquid products from coal. The high energy inputs required by plasma pyrolysis systems make them rather uninteresting for most coal conversion work, with the possible exception of acetylene production.

Traditionally, work aimed at producing data relevant to coal conversion to synthetic fuels has focussed on temperatures below 1100-1200°C, while work aimed at producing pyrolysis data for combustion systems has gone to higher temperatures, 1500-2000°C. It is important to recognize the important effect that temperature can have on ultimate yields; the higher the temperature, the more processes become possible as more stable structures become "activated". Thus it is usually unfair to compare total yields of products from coal pyrolyzed at 550°C to those from pyrolysis at 1500°C. Comparison of data from non-isothermal pyrolysis of coal at two different heating rates also frequently causes confusion. A statement such as "chemical phenomenon A is observed when coal is heated to temperature T" is almost meaningless, unless one knows over what time temperature T is reached, e.g. in a microsecond or a million years. This point will be discussed further in the section on modelling.

In addition to the importance of the ultimate temperature, heating rate, and solids residence time in determining the outcome of a process, there are much more subtle factors which may cloud the interpretation of data. These generally fall into the heat and mass transfer categories.

One example of this is that the amount of time that volatile products

from coal pyrolysis or hydrolysis spend in a reactive environment can have a large influence on their chemical nature. In the ASTM standard test for volatile matter (which is a pyrolysis experiment at 950°C for 7 minutes) coal is pyrolyzed in a covered crucible. The volatile matter can escape from the crucible, but only after an indeterminately long residence time in close proximity to hot char, with which it (or strictly speaking, its tar components) can repolymerize or on which it can crack and coke. It is frequently observed that the total yields (V\*) from various rapid heating experiments are substantially higher than those from ASTM determinations of proximate volatile matter (prox. VM in Table 3.2-2, Howard, 1977). While such an effect is frequently credited to the higher heating rates (upwards of 500°C/sec compared to about 15-20°C/sec for an ASTM analysis) influencing the direction of a set of competitive reactions in a favorable fashion, another explanation may also exist. It has been demonstrated (Gray et al., 1974; Portal and Tan, 1972) that the size of the sample in the ASTM crucible has an influence on volatiles yield; the smaller the sample, the higher the yield (see Fig. 3.2-1). Since Portal and Tan did their tests under a nitrogen purge, an oxidation effect can be ruled out. The implication for these results is that the shorter the time needed for volatile matter to escape the very reactive environment of the coal sample, the less likely it is to crack and coke therein, thereby reducing yields. Since in most rapid heating work, the samples are better dispersed for reasons of heat transfer, it is logical that they should also be subject to fewer secondary reactions. In the electrical grid system used in this study and by several other workers (see Table 3.2-1), if the containment vessel is large enough, and filled

Table 3.2-2 Comparison of Experimental Yields with Proximate Volatile Matter

<u>Investigators, Coals, and Conditions</u>	<u>Prox. VM</u>	<u>Exp'l<sup>a</sup> Y*</u>	<u>V*/VM</u>
Loison and Chauvin(1964)			
Maigre Oignies	8.4	8.4	1.00
Bergmannsgluck (MF <sup>d</sup> basis;	18.1	23.6	1.30
Emma heated to	20.4	24.5	1.25
Lens-Lieven 1000°C at	24.4	26.7	1.09
Flenus de Bruay 1500°C/s	31.0	39.6	1.18
Wendell III	33.9	34.5	1.02
Faulquemont	36.4	36.7	1.01
Rau and Robertson(1966)			
Colver (MVB <sup>b</sup> )	25.3	19	0.75
Kopperston #3 (HVAB <sup>c</sup> ) (MF <sup>d</sup> basis;	31.6	36	1.14
Federal (Pitts.HVAB <sup>c</sup> ) heated to	37.7	49	1.30
Elkol (Wyo.Subbit.) 950°C at	40.7	48	1.17
Orient #3 (HVB <sup>b</sup> ) 600°C/s)	44.0	41	0.93
Kimber and Gray(1967a,b)			
NCB 902 30μ (MAF basis;	38.3	71	1.85
(particle median 30μ <sup>e</sup> heated to	38.3	72	1.88
diameter shown) 53μ 1900°C at	40.0	69	1.73
			10 <sup>5</sup> to 10 <sup>6</sup> °C/s)
Badzioch and Hawksley(1970)			
NCB 203 (K)	17.7	17.7	1.00
NCB 301a(J)	22.7	20.6	0.91
NCB 301b(H) (MAF <sup>f</sup> basis;	25.2	26.0	1.03
NCB 602 (E) heated to	34.3	44.2	1.29
NCB 401 (G) 950°C at	34.4	35.1	1.02
NCB 601 (F) 25,000-	35.3	45.1	1.28
NCB 802 (D) 50,000°C/s)	36.1	47.0	1.30
NCB 902 (B)	36.4	40.0	1.10
NCB 802 (C)	37.8	42.8	1.13
NCB 902 (A)	37.9	42.9	1.13
Mentser et al.(1974)			
Pocohontas #3	16.8	18.5	1.10
Lower Kittanning (MF <sup>d</sup> basis;	25.3	30.8	1.22
Pittsburgh heated to	35.1	47.9	1.36
Rock Springs 1200°C at	37.7	42.4	1.12
Colchester 8000°C/s)	48.0	55.8	1.16
Anthony et al.(1975)			
Pittsburgh #8 (MAF <sup>f</sup> basis;	46.2	53.7 <sup>g</sup>	1.16
Montana heated to	46.2	41.1	0.89
			1000°C at
			650-10,000°C/s)

Table 3.2-2 Comparison of Experimental Yields with Proximate Volatile Matter

<u>Investigators, Coals, and Conditions</u>	<u>Prox. VM</u>	<u>Exp'l<sup>a</sup> V*</u>	<u>V*/VM</u>
Kobayashi <u>et al.</u> (1977)	46.8	63	1.35
Pittsburgh #8 (MAF <sup>f</sup> basis; Montana Lignite heated to 1800°C at 2 x 10 <sup>5</sup> °C/s)	46.1	62	1.34
Ubhayakar <u>et al.</u> (1977)			
Pittsburgh Seam (MAF <sup>f</sup> basis; heated to 2000°C at 1.3 x 10 <sup>5</sup> °C/s)	42.5	65	1.53
This study (MAF <sup>f</sup> basis; Pitts- burgh #8 heated to 1000°C at 1000°C/s)	44.6	52.2	1.17
Montana Lignite	44.3	44.8	1.01
Montana Lignite <sup>h</sup>	46.1	50.0	1.08

a. Peak weight loss corresponding to V\* was achieved at the final (highest) temperature in all cases except Mentser et al. where the peak occurs at intermediate temperatures; b. Medium volatile bituminous; c. High volatile A bituminous; d. Moisture-free; f. Moisture- and ash-free; e. Previous sample recycled; g. A range up to 56.2 given previously (Anthony and Howard, 1976) is not used here since the higher value reflects behavior at reduced pressure; h. Samples of coal examined by Kobayashi et al. (1977) run in captive sample apparatus.

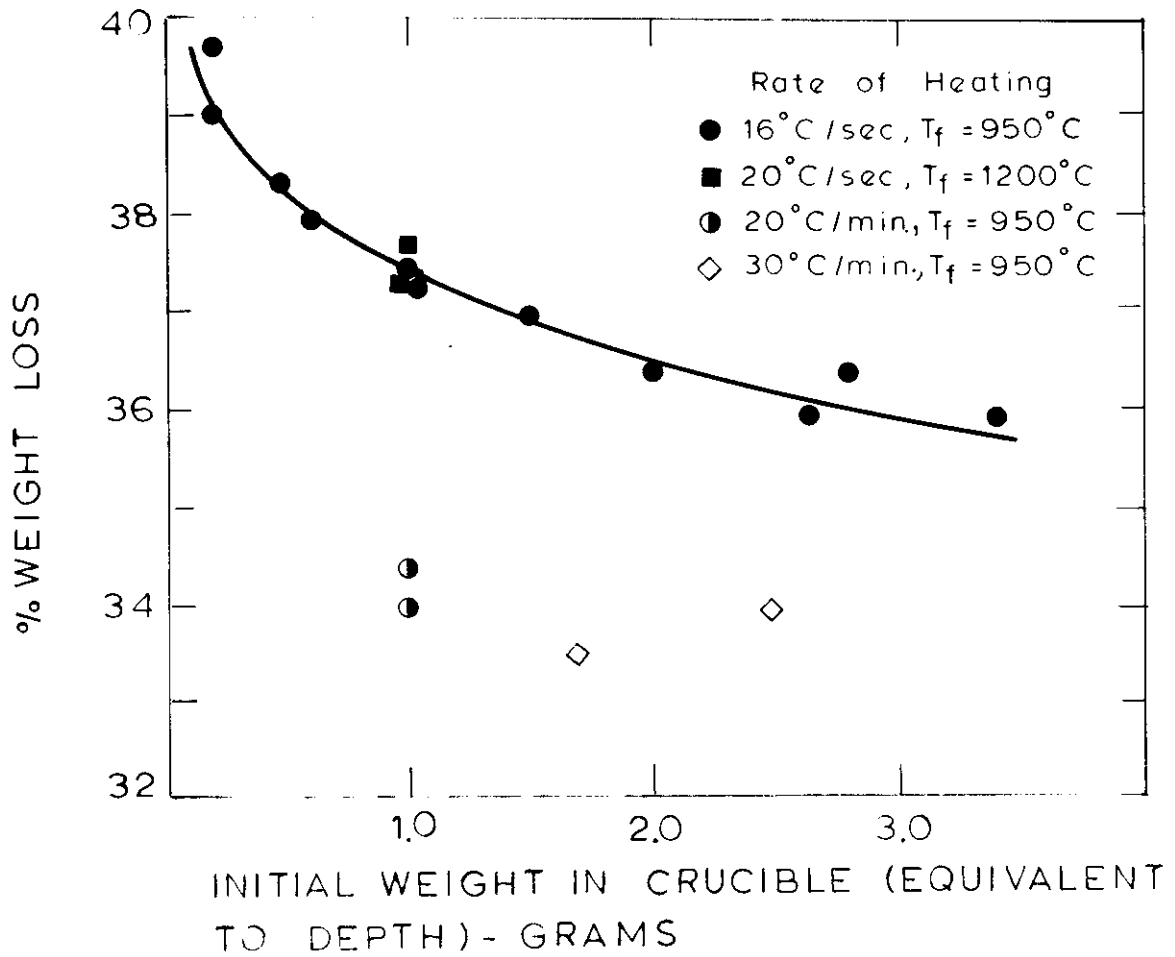


Figure 3.2-1 Effect of Bed Depth and Heating Rate on the Results of an ASTM-Type Analysis (Gray et al., 1973).

with "cold gas", the volatiles escape velocity is sufficiently high so that they have almost zero residence time at temperatures at which they can crack. Naturally the difference between rapid heating technique results and the ASTM analysis should decrease with decreasing yield of "crackable" (tar) product. This is shown to be the case with the data from several studies listed in Table 3.2-2.

Also with regard to Table 3.2-2, the data of Kimber and Gray (1967a,b), Kobayashi (1977) and Ubhayaker et al. (1977) should be treated separately because of the very high temperatures involved in those studies.

Techniques involving crucibles and fixed beds have the common feature of rather low heating rates (see Table 3.2-1), and sometimes rather ill-defined temperature profiles. The latter can lead to serious difficulties in modelling kinetics. Electrical element heating of small samples of coal can overcome both of these difficulties, but introduced the problem of fast response temperature measurement.

Coal flow techniques can also be used to rapidly heat coal, and usually approximate real process conditions more closely than captive sample techniques. Unfortunately direct particle temperature measurement is usually impossible. In entrained flow experiments, the particle and vapor residence times are coupled, which can lead to the problem that if the coal residence time is sufficient for it to react to a given extent, then the vapor phase residence time may be sufficient for primary volatiles to undergo secondary reactions (Kobayashi, 1977; Sass, 1972; Lau, 1977).

In coal "free fall" experiments, wherein the coal particles are dropped under the influence of gravity through a hot medium, the coal particle residence times are somewhat difficult to estimate, because as they

devolatilize, the particles can swell, shrink, bubble, break, and emit jets of volatiles. This is not a problem where optical techniques can be applied to determining residence times, but in high pressure systems this is frequently not possible, or at least very difficult.

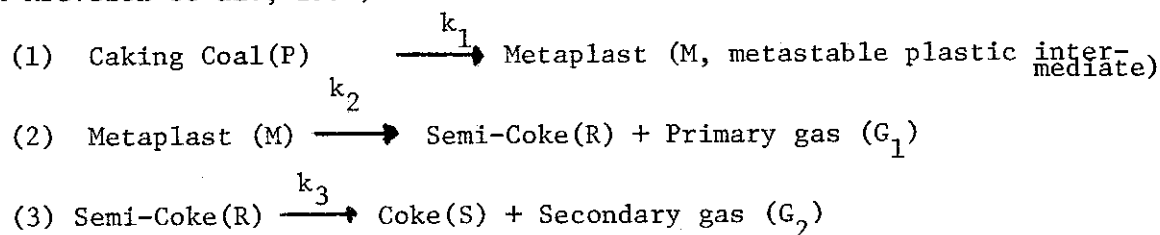
Fluidized beds are sometimes difficult to operate with coal because of agglomeration problems. Analysis of experimental data is difficult because of the complicated mixing phenomena involved.

If in any experimental system, a differential approach to product analysis is employed, i.e. real time product analysis, then sampling lags due to long times of transit between sample and analyzer (or large "dead volumes") can cause serious difficulties in interpretation of data (e.g. Blair, 1977). On the other hand, the integral approach is much more tedious, and requires careful accounting of all aspects of time-temperature history; heatup of the sample, any isothermal period, and cooldown of the sample.

### 3.2.1 Mechanistic Implications from Studies of Pyrolysis of Coal and Model Compounds

The "modern age" of coal pyrolysis research began in the 1950's with workers in several countries making important contributions to the understanding of pyrolysis phenomena. Van Krevelen et al (1951) observed the now familiar behavior of carbonizing coal on an atomic H/C vs O/C plot and noted that regardless of where in the so-called "coal band" (the spread of allowable H/C vs O/C ratios found in nature) one began, the H/C vs O/C trajectory during pyrolysis would almost always be outside the coal band and terminate at a common "pole" the so called "carbonization pole" at an H/C ratio of about .28 (see Fig. 3.2-2). This

evidence confirmed that pyrolysis was not merely a faster form of natural coalification. In most of the early work on pyrolysis, emphasis was placed upon gaining an understanding of the phenomena associated with coking of coal. During this process, the coal swells and softens to a viscoelastic (plastic) state. Only bituminous coals show this behavior, lignites and anthracites do not. This work led to a class model of decomposition of caking coals (Van Krevelen et al., 1956):



In developing this picture of pyrolysis, the following observed sequence of phenomena (observed at low heating rates, e.g. 3°C/min) was accounted for:

1. A softening of the coal
2. A swelling of the plastic mass with volatiles evolution
3. A resolidification of the mass

Mechanistically, this theory was somewhat vague and accounted for the three reaction steps in the following general terms (Van Krevelen, 1961) Reaction (1) - A depolymerization reaction in which an unstable intermediate is formed. This intermediate is responsible for fluidity. It was not established whether this implied that the entire coal mass was fluid, or if the intermediate merely acted as a "solvent" or "lubricant" for insoluble portions of the coal. Based on the results of Dryden and Pankhurst (1955), the latter seems plausible. They concluded that a small amount of chloroform soluble material formed just prior to softening



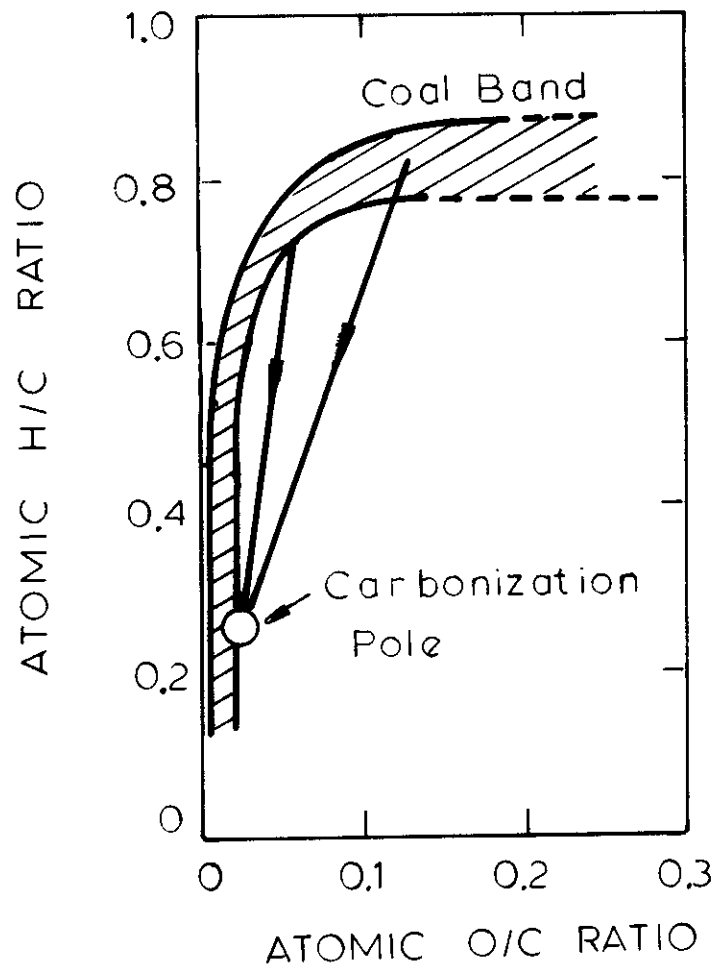


Figure 3.2-2 Comparison of Natural Coalification and Pyrolysis on an Elemental Basis (Van Krevelen et al., 1951).

RATE OF WEIGHT LOSS  
WT % / °C

PLASTICITY  
ARBITRARY  
UNITS

DILATION  
%

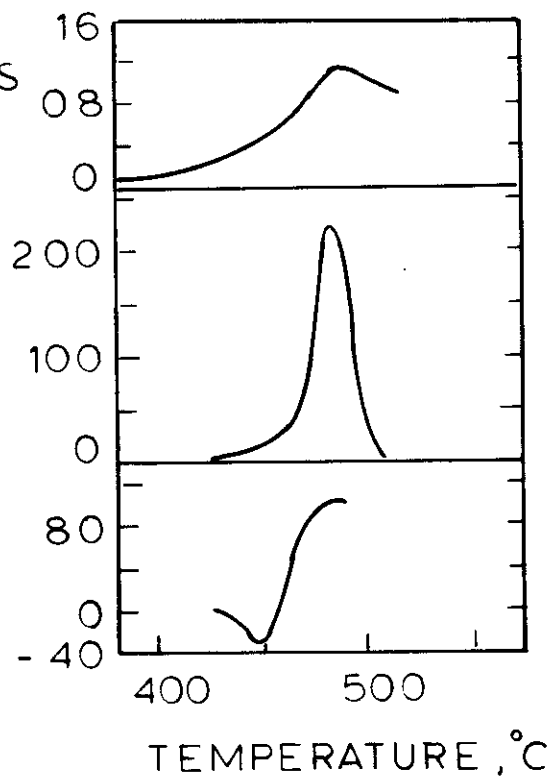


Figure 3.2-3 Variation of Weight Loss, Plasticity and Dilation with Pyrolysis Temperature (Van Krevelen et al., 1956).

was a principal agent in softening. Removal of this material (of order 5-10% by weight) by chloroform extraction from coal preheated to about 300-400°C rendered the coal non-softening and non-agglomerating. Amazingly, if the extract was mixed with non-coking coal, the latter acquired softening and swelling characteristics. Later work by Brown and Waters (1966) suggests that the chloroform extractable material is largely present as such before pyrolysis, but inaccessible through micropores. Its effect is seen during the initial stages of pyrolysis because it is an effective hydrogen donor material. This point will be discussed in more detail later.

Reaction (2) - A cracking reaction in which tar is vaporized and nonaromatic side groups are split off. The coal begins to resolidify primarily because of condensation reactions leading to heavy molecular weight semi-coke, but may also lose plasticity because a "solvent" or "lubricant" phase reacted or volatilized away.

Reaction (3) - A secondary degassing reaction in which semi-coke units are welded together by methane and hydrogen elimination reactions, to leave behind a true coke. Figure 3.2-3 shows some typical data used by Van Krevelen to formulate his model. The data show how the weight loss, plasticity and dilation (swelling) properties all seem to have roughly the same temperature dependence. The plasticity of plastic coals is measured with a Geisler rotating viscosimeter; the minimum viscosity of good coking coals is generally in the range of  $10^4$  to  $10^5$  poise. By assuming first order models for each of the reaction steps, and by examining the variation of the maximum in the devolatilization curve with increasing heating rate, Van Krevelen (1961) concluded that the process was characterized by an activation energy in the range of 50-60 kcal/mole.

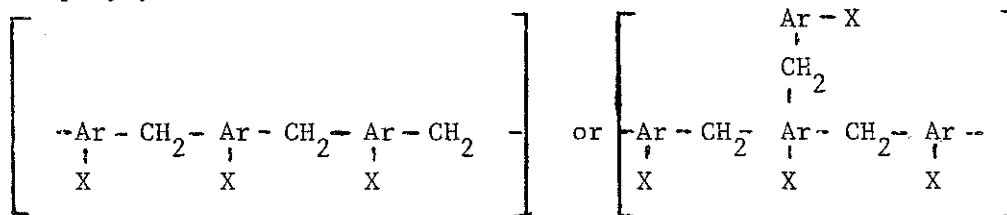
For comparison, Table 3.2-3 (Suuberg et al. 1977) lists the activation energies of decomposition of various polymers and "coal-model compounds" whose thermal degradations were studied by various workers using various techniques. Although there is a considerable spread in the values, it can be seen that the activation energies found by Van Krevelen compare favorably.

It should also be noted that at the same time as Van Krevelen was developing his model, Fitzgerald (1955, 1956, 1956a) was working along similar lines.

#### Pyrolysis of Model Compounds

Because of the rather difficult problem of understanding the mechanism of pyrolysis of compounds whose structures are essentially unknown, there have been several attempts to synthesize coal-like substances and study them, or to rely upon analogies offered by ordinary commercial type polymer degradations.

Van Krevelen (in collaboration with Wolfs and Waterman 1959, 1960) also did extensive work with "model substances" i.e. substances of well defined chemical structure and whose pyrolytic behavior was in some way similar to that of coal. This work involves studies of various polycyclic aromatics as well as polycondensation products (with formaldehyde) of polycyclic aromatics (Ar). These had structures of the following type:



where X could be hydrogen or a functional substitute (e.g.  $-\text{CH}_3$ ,  $-\text{OH}$ ,  $-\text{OCH}_3$ )

Table 3.2-3. Kinetic Parameters for Pyrolysis of Various Organic Materials

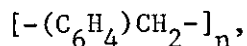
Material Pyrolyzed	Product <sup>a</sup>	Experi- mental Temp., °C	Activation Energy, kcal/mole	Pre- Exponen- tial Factor, s <sup>-1</sup>	Reference
Ferulic Acid (C <sub>10</sub> H <sub>10</sub> O <sub>4</sub> )	CO <sub>2</sub>	150-250	27.7	6.0x10 <sup>9</sup>	Jüntgen and Van Heek, 1968; 1970
Perylene Tetracarboxylic Acid Anhydride (C <sub>24</sub> H <sub>8</sub> O <sub>6</sub> )	CO <sub>2</sub>	400-600	71.5	5.2x10 <sup>17</sup>	Jüntgen and Van Heek, 1968; 1970
	CO <sup>2</sup>	400-600	64.9	5.0x10 <sup>16</sup>	Jüntgen and Van Heek, 1968; 1970
Protocatechuic Acid (C <sub>7</sub> H <sub>6</sub> O <sub>4</sub> )	(H <sub>2</sub> O) <sub>1</sub>	50-300	18.8	2.7x10 <sup>8</sup>	Jüntgen and Van Heek, 1968; 1970
	(H <sub>2</sub> O) <sub>2</sub>	50-300	42.4	2.3x10 <sup>5</sup>	Jüntgen and Van Heek, 1968; 1970
	CO <sub>2</sub>	50-300	40.4	1.6x10 <sup>15</sup>	Jüntgen and Van Heek, 1968; 1970
Naphthalene Tetracarboxylic Acid (C <sub>14</sub> H <sub>8</sub> O <sub>8</sub> )	H <sub>2</sub> O	100-250	33.5	1.2x10 <sup>13</sup>	Jüntgen and Van Heek, 1968; 1970
Mellitic Acid (C <sub>12</sub> H <sub>6</sub> O <sub>12</sub> )	H <sub>2</sub> O	230 <sup>b</sup>	16.6	2.3x10 <sup>5</sup>	Jüntgen and Van Heek, 1970
Tartaric Acid (C <sub>4</sub> H <sub>6</sub> O <sub>6</sub> )	H <sub>2</sub> O	195 <sup>b</sup>	42.9	6.7x10 <sup>17</sup>	Jüntgen and Van Heek, 1970
Polystyrene (C <sub>8</sub> H <sub>8</sub> ) <sub>n</sub>	overall	394 <sup>b</sup>	77	8.3x10 <sup>22</sup>	Fuoss <i>et al.</i> , 1964
	overall	335-355 <sup>b</sup>	58	9.0x10 <sup>15</sup>	Madorsky, 1952
Teflon (C <sub>2</sub> F <sub>4</sub> ) <sub>n</sub>	overall	575 <sup>b</sup>	67-69	4.3x10 <sup>14</sup>	Fuoss <i>et al.</i> , 1964
Polyethylene (C <sub>2</sub> H <sub>4</sub> ) <sub>n</sub> "Phase 1" "Phase 2"	overall	385-405	48	5.2x10 <sup>11</sup>	Madorsky, 1952
	overall	385-405	71	8.7x10 <sup>18</sup>	Madorsky, 1952
Hydrogenated Polystyrene (C <sub>8</sub> H <sub>14</sub> ) <sub>n</sub>	overall	335-350	52	1.4x10 <sup>14</sup>	Madorsky, 1953
Polymeta-methylstyrene (C <sub>9</sub> H <sub>10</sub> ) <sub>n</sub>	overall	333-353	59	7.2x10 <sup>16</sup>	Madorsky, 1953
Polyalpha-methylstyrene (C <sub>9</sub> H <sub>10</sub> ) <sub>n</sub>	overall	273-298	58	8.3x10 <sup>18</sup>	Madorsky, 1953
Polymethyl-methacrylate (C <sub>5</sub> H <sub>8</sub> O <sub>2</sub> ) <sub>n</sub> Avg. Molecular Wt. 150,000 Avg. Molecular Wt. 5,100,000	overall	240-270	33	3.6x10 <sup>9</sup>	Madorsky, 1953
	overall	310-325	55	1.8x10 <sup>16</sup>	Madorsky, 1953
Polymethylacrylate (C <sub>4</sub> H <sub>6</sub> O <sub>2</sub> ) <sub>n</sub>	overall	285-300	37	1.4x10 <sup>10</sup>	Madorsky, 1953
Cellulose (C <sub>6</sub> H <sub>10</sub> O <sub>5</sub> ) <sub>n</sub>	overall	250-1000	33.4	6.8x10 <sup>9</sup>	Lewellen <i>et al.</i> , in press
		250-350	35	3.3x10 <sup>11</sup>	Jüntgen and Van Heek, 1970; Van Krevelen <i>et al.</i> , 1951

a. Denotes species whose evolution is described by the parameters given. Two different stages of water evolution are denoted by (H<sub>2</sub>O)<sub>1</sub> and (H<sub>2</sub>O)<sub>2</sub>. Overall refers to all products combined.

b. Temperature of maximum pyrolysis rate.

The following conclusions were drawn from studies with no additional functional groups added (i.e. X = H) :

- At the low (3°C/min) heating rates studied, some reaction could occur at a temperature below the boiling point of the products formed, hence evaporation governed part of the observed behavior.
- "Depolymerization" of the aromatic polycondensate (by rupture of methylene bridges) occurred in a completely random manner, and hydrogen disproportionation led to formation of methyl groups.
- At the above stated heating rate, tar formation essentially ceases at about 500°C, a temperature which roughly corresponds to the end of the plastic stage of coal at the same heating rate (see Fig. 3.2-3).
- The hydrogen in the residue at the end of primary carbonization (reaction (2)) is approximately equal to the theoretical, aromatic hydrogen content of the residue, were it completely composed of monomer aromatic units. For example, starting with a polycondensate of benzene (prepared by condensation of benzyl chloride) the starting material is characterized by the form:



then the residue ("semicoke") has a final hydrogen content of 4 atoms per "unit". The concept of a monomer unit remaining in the residue is rather ill-defined; what is really meant is that for every seven carbons remaining in the char, there are about four hydrogens remaining (and the volatiles have been hydrogen "rich" relative to the starting material).

- After primary carbonization is complete, the secondary degassing reactions occur, yielding only gaseous, and not tar product. At the completion of this

process, the residue is almost pure carbon.

In summary the author conclude that there is no difference in the original material between future tar or coke units, and that the course of primary carbonization is determined only by "aliphatic" hydrogen, and that of secondary carbonization only by "aromatic" hydrogen. Further, based on radioactive carbon tracer work, they conclude that the liberation of hydrocarbon gas during secondary degassing is not due to complete decomposition of "monomer" units, but evenly divided among all units. Presumably this implies that some of the remaining vestiges of aliphatic carbon are being eliminated while the aromatic carbons remain in the char.

Since real coal contains various functional groups, the effect of including these types of structures in the polycondensation model substances was also investigated.

The addition of hydroxyl ( $X = OH$ ) groups onto the polycondensates (e.g. phenol-formaldehyde resin) has a number of significant effects

- The yield of tar is much smaller than from the analogous substance with no  $-OH$  group.
- The plasticity during carbonization is reduced or eliminated.
- The decomposition is a more complicated function of temperature
- There is a large effect of heating rate on all characteristics, including yield.

These observations are explained by a competing reaction mechanism. During primary decomposition, the depolymerization reaction competes with a direct condensation mechanism involving the hydroxyl groups. The hydroxyl groups react with some of the available reactive hydrogen, leaving a site which can participate in a condensation reaction. It

appears that the re-condensation reaction has a lower activation energy than the depolymerization reaction because it is favored at lower heating rates. (The competing reaction phenomenon will be discussed in the section modelling work).

Methyl substituents ( $X = -CH_3$ ) served to increase the evolution of gas (mostly methane) during primary carbonization. It is postulated, however, that the methane does not all originate from stripping of methyl groups (again, based on  $^{14}C$  tracer data). The methyl groups rather seem to be acting as sources of additional hydrogen during primary carbonization.

Ethoxy substituents ( $X = -OCH_3$ ) have a much less dramatic effect on depolymerization reactions when compared to hydroxyl substituents. All of the hydrogen from the ethoxy group is lost during carbonization, as any other aliphatic hydrogen would be. However, the yield of tar is lower than that from the base case (unsubstituted), and the authors attribute this to side reactions with oxygen, such as water formation, removing some of the otherwise available hydrogen.

In a compound with both hydroxyl and methyl substituents (a p-cresol-formaldehyde resin), the behavior is much like that of an unsubstituted compound, with the exception of higher gas yields; apparently the extra hydrogen from the methyl groups satisfies the "extra need" for hydrogen imposed by the presence of the hydroxyl group.

The overall course of pyrolysis of all these model compounds is represented by Fig. 3.2-4 (Wolfs et al., 1960).

It is noteworthy that the important role that this model ascribes to hydrogen donating groups seems to be very much in line with the previously described chloroform extraction work. Brown and Waters (1966) showed that

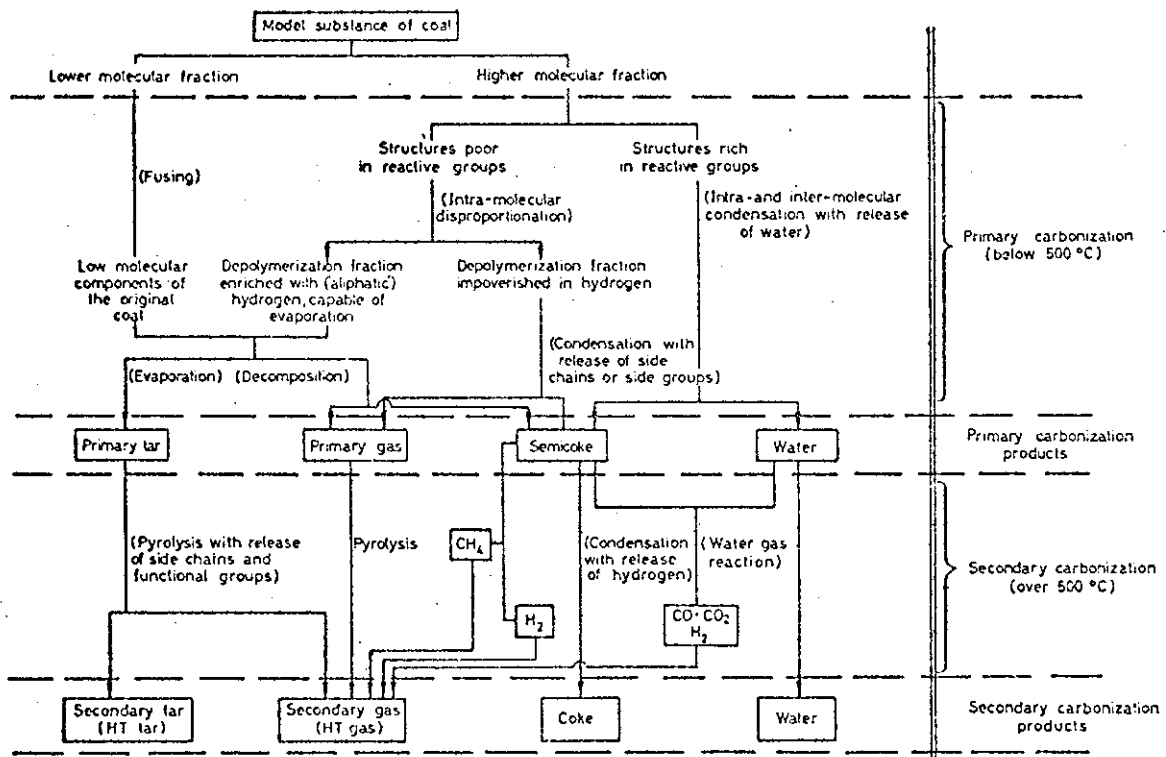


Figure 3.2-4. Overall Model for the Pyrolysis of Coal-Model Compounds.



the chloroform extractable material which plays such a prominent role in determining plasticity, is always hydrogen rich, relative to the raw coal. The fact that it is mostly extractable only after preheating to temperatures just below the plastic state (see Fig. 3.2-5) could imply that the material is becoming "mobile" at these temperatures, and thus can participate in this hydrogen donation mechanism throughout the coal. The two-step behavior of the extractables, shown in Fig. 3.2-5, is typical.

Wiser (1968) and Neavel (1975) draw parallels between the above internal coal "solvation" process, and coal liquefaction in the presence of an external hydrogen donor solvent (e.g. tetralin). Neavel proposes the following sequence of events during pyrolysis:

1. The mobility of micelles (packets of molecules) begins around 350-400°C (slow heating) as Van der Waals forces and hydrogen bonds are weakened (physical melting). The bitumen (the chloroform extractables) serves as a solvating vehicle and hydrogen donor during this phase.
2. The viscosity decreases as bond rupture leads to reduction of molecular size, but only as long as the free radicals formed are stabilized by donor hydrogen.
3. As donor-hydrogen is depleted, the radicals formed will stabilize by condensation or repolymerization, and viscosity will again increase. Light molecular weight materials will continue to volatilize, or will be incorporated into the residue via radical reactions.
4. The metaplast sets up as a semi-coke.

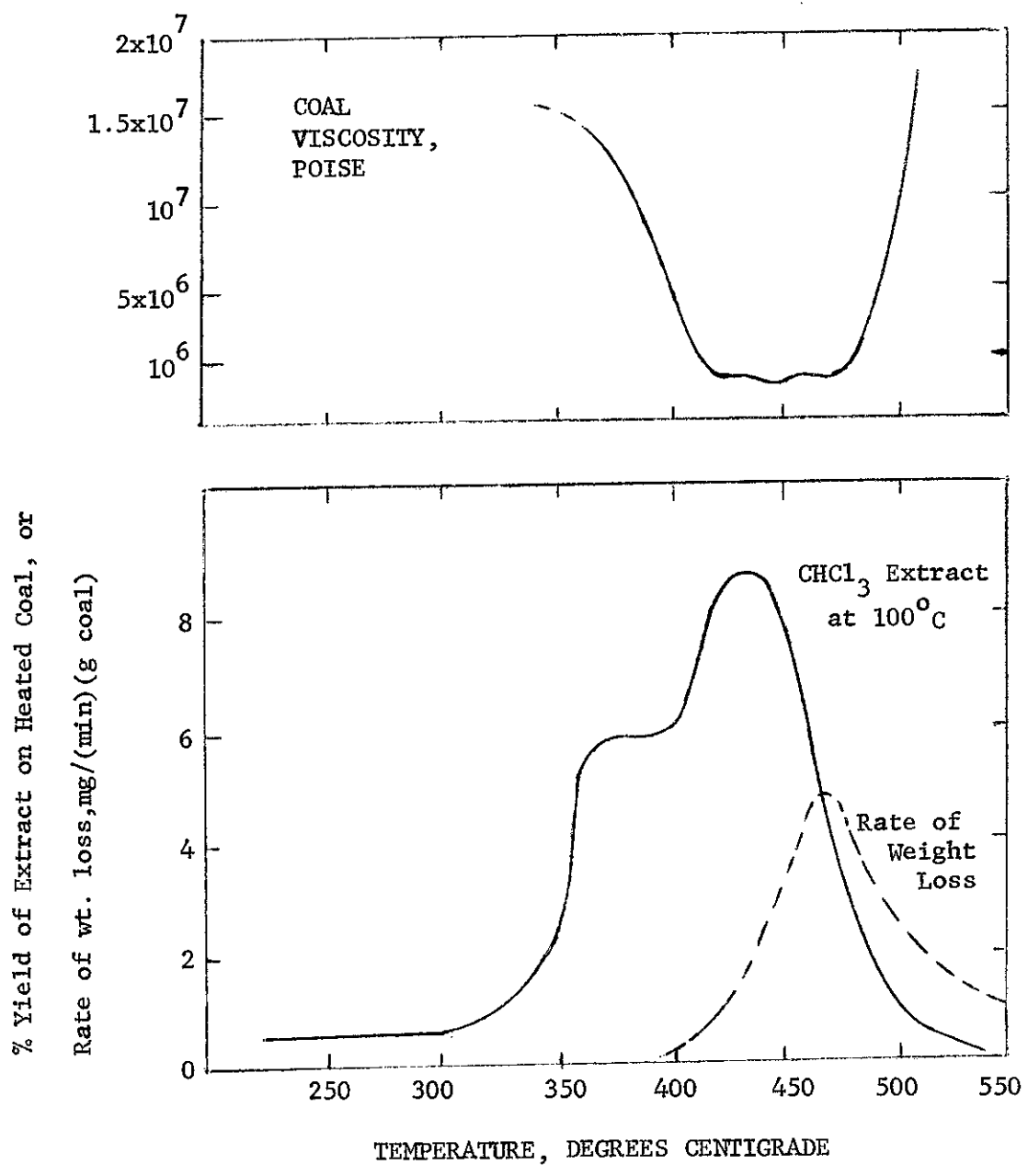


Figure 3.2-5. Relationship Between Plasticity, Weight Loss, and Chloroform Extractable Materials (Brown and Waters, 1966, from Squires, 1975).

From this analysis, four characteristics are necessary and sufficient for plastic development

- Lamellae-bridging structures that can be thermally broken.  
(lamellae are layers of molecules in more or less parallel alignment - graphite is an example of a completely lamellar substance).
- An indigenous supply of hydroaromatic hydrogen (Van Krevelen's work suggests only aliphatic hydrogen is necessary, but Neavel points out that hydroaromatic may be most easily abstracted).  
It can also be noted that some normally non-plastic coals can be made to behave plastically if pyrolyzed in the presence of high pressure (1000 psi) hydrogen gas.
- An intrinsic capability of micelles and lamellae to become mobile, "melt", independently of bond rupture.
- A coal of high enough rank (not previously unoxidized) so that relatively weak oxygen bonds cannot consume the available hydrogen and crosslink the char before plasticity can set in.

As regards the relative strength or weakness of various oxygen bonds, Van Krevelen (1961) presents data on the stabilities of various types of functional groups (Table 3.2-4). It can be seen that oxygens attached to aromatic structures are quite stable, relative to those attached to aliphatic carbons. But it should also be borne in mind that phenolic hydroxyls can decompose at temperatures which are still below the decomposition temperatures of carbon-carbon bands.

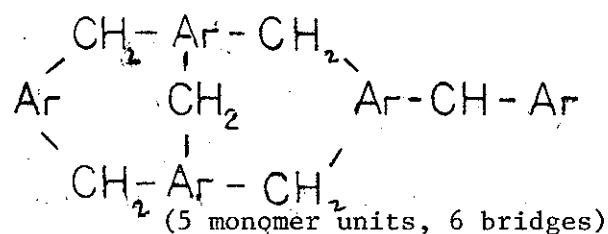
One final facet of Van Krevelen's work with model compounds is the

Table 3.2-4 Stability of Some Oxygenous Substances, from Van Krevelen (1961)

Oxygen function	Substance considered	Decomposes at °C
$\begin{array}{c}   &   \\ \text{R}-\text{O}-\text{C}-\text{O}-\text{C}-\text{O}-\text{R} \\   &   \end{array}$	Polyformaldehyde, cane sugar polyoxymethylene bridge between two aromatic units	200-250
$\begin{array}{c}   &   \\ \text{R}-\text{ar}-\text{C}-\text{O}-\text{C}-\text{ar}-\text{R} \\   &   \end{array}$	Dibenzylethers	200-250
$\begin{array}{c}   &   &   \\ \text{R}-\text{C}-\text{O}-\text{C}-\text{O}-\text{C}-\text{R} \\   &   &   \end{array}$	Cellulose	325-350
$\begin{array}{c}   \\ \text{R}-\text{C}-\text{O}-\text{ar}-\text{R} \\   \end{array}$	Lignin, phenetole-formaldehyde resin	380-430
$\begin{array}{c}   \\ \text{R}-\text{ar}-\text{C}-\text{ar}-\text{OH} \\   \end{array}$	Phenol and p-cresolformaldehyde resin	380-430
$\text{R}-\text{ar}-\text{O}-\text{ar}-\text{r}$	p-Polyphenylether, phenyl-2- naphthylether, the polyconden- sation product of this sub- stance with formaldehyde	400-500
$\begin{array}{c} & / & \\ =\text{C} & & \\ & \backslash & \\ & & \text{C}=\text{O} \\ & / & \\ =\text{C} & & \end{array}$	dibenzanthrone	490

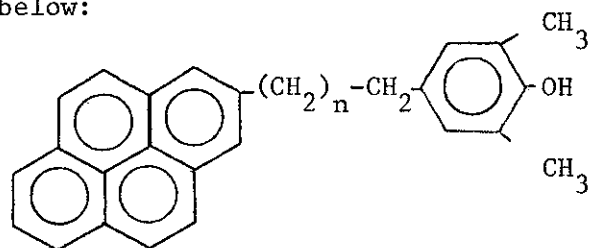
dependence of softening behavior upon the degree of polymerization, i.e. the number of methylene bridges per aromatic cluster monomer. If there is, on the average, fewer than one bridge per monomer as in this sample structure  $\text{Ar}-\text{CH}_2-\text{Ar}-\text{CH}_2-\text{Ar}-\text{CH}_2-\text{Ar}-\text{CH}_2-\text{Ar}$  (5 monomers, 4 bridges), then physical softening or melting may be a possibility.

If there are, however, more than one bridge per monomer, as below, then it is suggested that depolymerization is a prerequisite for softening:



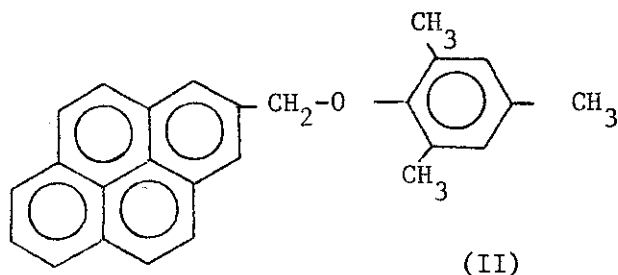
In concluding this section on Van Krevelen's considerable contributions to the understanding of pyrolytic phenomena, it would be fair to say that his work provides significant insights into the processes occurring during pyrolysis, and begins to provide predictive power.

Another set of classic coal model substance studies are those of Depp, Neuworth and coworkers (1956,1957). These workers examined a class of compounds prepared by condensation of pyrene alkanolic acid with 2,6 - xylenol and another class by condensation of pyrenyl chloride with 2,4,6 methylphenol or 3,5xylenol. Examples of the resulting structure are shown below:



$n = 0,1,3$

(I)



These structures contain no carbonyls, because the authors felt that the evidence supporting their existence was not strong. The compounds were pyrolyzed at temperatures of 425°C attained at an average of 3-4°C/min. Detailed product analyses were conducted. In all cases, the yields of tar from the model compounds was far in excess of that which was obtained from Pittsburgh seam bituminous coal, but this is not surprising because the model molecules were undoubtedly much smaller than the average "coal molecule".

The results from pyrolysis of compounds of Type (I) seems to support some of the conclusions reached by Van Krevelen, namely:

- As would be predicted, the aliphatic linkages rupture first, producing free radicals that abstract hydrogen from other aliphatic linkages.
- Formation of rather stable structures resulted from hydrogen abstraction, and these would eventually become part of the coke.

Study of the model substance containing the ether linkage (II) yielded the expected result; the labile bond is the ether-alkyl bond which upon free radical rupture is stabilized by hydrogen capture.

Czuchajowski (1961) applied infrared spectroscopic methods to the study of pyrolysis of model compounds. Among the substances examined was the same class of polycondensed aromatics as Wolfs, Van Krevelen and Waterman studied. It was found that the 1600  $\text{cm}^{-1}$  band (see section on coal structure) was indeed present in non-oxygenated polycondensed

aromatics, but curiously its intensity decreased with the increasing size of the polycondensed aromatic nuclei (it is strongest in the polyphenyl resin, and weak in phenanthrene, pyrene, and chrysene resins). Upon carbonization, model substances and coals with carbonyls present (presumably quinonoid) showed markedly different changes from the above compounds in  $1600\text{ cm}^{-1}$  absorption with temperature. Polycondensates and polyphenyls show a consistent trend towards lower  $1600\text{ cm}^{-1}$  absorptions with temperature, consistent with a view that condensation is occurring. The decrease in the  $1600\text{ cm}^{-1}$  band is much more dramatic in substances where chelated carbonyls are thought to exist. The fact that the decrease in the absorptions at both  $1600\text{ cm}^{-1}$  and  $3300\text{ cm}^{-1}$  parallel each other during the initial phases of carbonization of compounds suspected of containing chelated carbonyls is encouraging. Although chelated hydroxyl does not absorb at  $3300\text{ cm}^{-1}$ , it might be expected to behave in a similar manner to unchelated hydroxyl. Then the fact that hydroxyl groups are being eliminated at the same rate that the presumed chelated quinones are disappearing seems to be strong evidence for their existence. Although not discussed by the author, the disappearance of the  $1600\text{ cm}^{-1}$  band should occur with an increase of a band closer to  $1700\text{ cm}^{-1}$ , unless the carbonyl structures are destroyed at relatively low temperatures (which should not be the case, based on Van Krevelen's data).

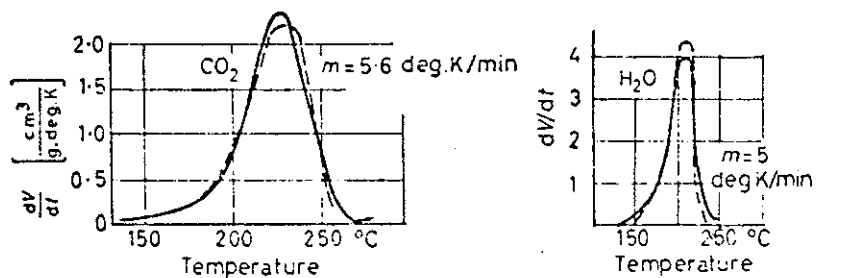
Also observed by Czuchajowski was the fact that the temperature dependence of the disappearance of hydrogen bonded hydroxyl is dependent on the degree of structural condensation. In raising the degree of condensation of humic acids (alkali soluble products of plant lignin decomposition), the temperature of disappearance of the  $3300\text{ cm}^{-1}$  band can be raised from  $380^{\circ}\text{C}$  to  $500^{\circ}\text{C}$ .

Sweeting and Wilshire (1962) studied the pyrolysis of several  $\omega$ -diphenylalkanes ( $C_6H_5(CH_2)_n C_6H_5$ ,  $n = 1,2,3,4,6$ ). Their evidence appears to reconfirm the mechanistic picture developed by the other studies described in this section.

Jüntgen and Van Heek (1968) studied the decomposition of various aromatic systems substituted with oxygen functional groups. Their data, taken at about 3.5 to 5.8°C min heating rates are summarized in Fig. 3.2-6 and included in Table 3.2-3. The authors feel that the low value for the activation energy for the first step of water release from protocatechic acid indicates physical rather than chemical control (the 100+°C temperature supports this view). In addition to the substances given in Fig. 3.2-6, Jüntgen and Van Heek (1970) also studied the release of water during various other anhydride and ester forming reactions, and correct the analysis of data on cellulose degradation experiments run by Van Krevelen et al. (1951, see Table 3.2-3). It is not clear how much can be concluded mechanistically from these data, since no data are given concerning other products or the behavior of the solid phase. Some of the activation energies look reasonable, in terms of absolute reaction rate theory applied to solids (see section 3.2.5). It is rather unlikely, however, that any of the structures studied can be found in coal, at least in significant quantities.

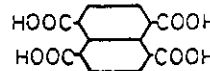
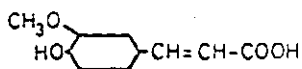
Another entirely different approach to model substances involves attempts to "create" coal from various plant materials or lignites by hydrothermal treatment. Khemchandani et al. (1974,1976) recently described their attempts with sawdust, cork, and lignite. Such work is principally aimed at determining the mechanism of coalification. The model coal substances so derived are inappropriate for detailed mechanistic studies





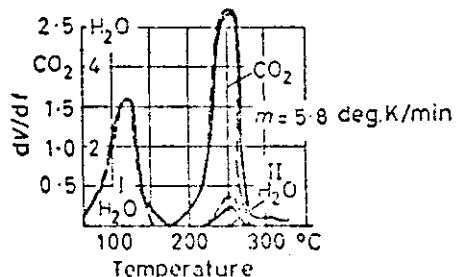
1 Decarboxylation of ferulic acid

3 Anhydride formation from naphthalene tetracarboxylic acid

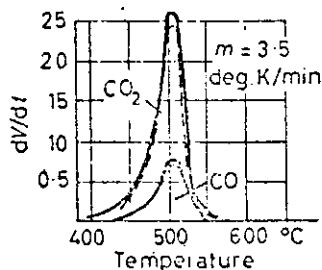
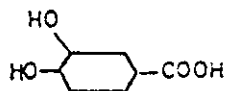


Calculated values:

Reaction	E, kcal/mol	K <sub>0</sub> , min <sup>-1</sup>
1	27.7	3.6 × 10 <sup>11</sup>
2	H <sub>2</sub> O	18.8
	CO <sub>2</sub>	40.4
3	33.5	7.0 × 10 <sup>14</sup>
4	CO	64.9
	CO <sub>2</sub>	71.5



2 Release of water from and decarboxylation of protocatechuic acid



4 Decomposition of perylene tetracarboxylic acid anhydride

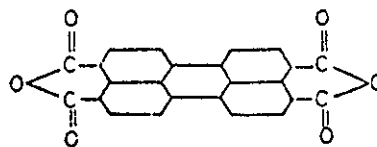


Figure 3.2-6. The Pyrolysis Behavior of Some Coal-Model Substances (Jüntgen and Van Heek, 1968).

of coal carbonization, since their chemical structure is in general, as ill-defined as coal's itself.

The degradation of naturally occurring polymers (e.g. cellulose) and a whole range of man-made polymers (e.g. polystyrene, polymethyl acrylate, polyvinyl alcohol) has quite naturally attracted a good deal of interest among coal researchers. To try to review the literature on thermal degradation of polymers is far beyond the scope of this review. General references on the topic are the books by Grassie (1956) and Madorsky (1964), and a brief discussion, naturally enough, by Van Krevelen (1976).

As has already been indicated, Table 3.2-3 gives a variety of activation energies and pre-exponentials for various polymer decomposition reactions. The fact that so many depolymerization reactions have activation energies comparable to coal "depolymerization" is hardly surprising if one considers them to both proceed principally by radical processes. However it is difficult to apply such tidy polymer concepts as the "ceiling temperature" (the temperature above which the rate of depolymerization becomes faster than that of (re)polymerization; see Dainton and Ivin, 1948). Nor is the elucidation of mechanisms of degradation of even "simple" polymers always straightforward. Except for perhaps being able to shed new light on the behavior of particular functional groups (which can in itself be very valuable), the literature on the thermal degradation of polymers (the small subset reviewed by this author) does not alter the basic mechanistic picture derived from substances closer in structure to coal.

An interesting facet of the study of thermal degradation of cellulose is that it has shown something of a dependence on heating rate (Martin, 1964; Lewellen et al. 1976). Again, it is not clear whether enhanced

transport of volatiles is principally responsible, or whether the primary decomposition is a competitive reaction process.

In concluding this section on model compounds, it can be seen that the results are, in general, what a sound knowledge of organic chemistry might lead one to expect. The work has usually been qualitative in nature, rationalization of observed behavior with still only tentative efforts at developing quantitative understanding (predictive power). The implication in terms of coals, with far less completely characterized structures than these model compounds, is that detailed predictive capability may be a long way off. This may be especially true in terms of systems where mass and heat transport characteristics are very different from those studied (recall most model work has been done at slow rates of heating).

With regard to new directions in model compound work, the efforts of Gavalas (discussed in the section on coal structure) will be watched with considerable interest. Although constructing his "model compounds" and reaction pathways by computer rather than by experiment, it will be interesting to see how these "model compounds" compare to real coal behavior. The success (or failure) of these efforts may go a long way towards explaining how simple or complex model substances must be to effectively simulate coal pyrolysis behavior.

#### Mechanistic Implications of Structural Changes in Coals Undergoing Pyrolysis

Brown (1955a) examined the infrared spectra of coals pyrolyzed to 800°C at a rate of 1.25°C/min, and held for one hour and found rather little change in the spectra of a caking and a coking coal up to 300 or 400°C. At 460°C, however, very marked changes become apparent. Whereas the coal started with a ratio of ( $H_{\text{aromatic}}/H_{\text{aliphatic}}$ ) of about 0.5, by 460°C

the ratio is about 2. Hydrogen bonded phenolic OH groups are removed primarily between 460 and 550°C and C-C crosslinks between aromatic systems are formed. By 550°C little of the aliphatic structure is left, and aromatic hydrogen is being removed. Brown concludes that his data support Van Krevelen's metaplast model.

An interesting conclusion of Brown's work also concerns the difference between caking and coking coals. He concludes that a good coking coal is characterized by a lower hydroxyl content than a caking coal and feels that the presence of -OH in the temperature range 400-460°C may be an important factor in determining coking quality.

Diamond (1960) conducted x-ray studies of vitrains pyrolyzed at temperatures up to 1000°C. The x-ray techniques involved were the same as those employed by Cartz and Hirsch (1960) in their studies of structural characteristics of vitrains. Diamond did not carefully control heating rate; samples were permitted to rise to temperature exponentially in 3 hours, and then maintained at temperature for 3 hours. In examining Diamond's data (Fig. 3.2-7) we must bear in mind the objections to the x-ray analysis technique raised by Brooks and Stephens (1965); this has its greatest impact on the uncertainty in layer diameter (of planar aromatic regions).

It is immediately striking in examining Fig. 3.2-7 to see how some structural property changes seem well correlated with others and totally uncorrelated with yet others. For purposes of this discussion, the behavior of 84% C caking bituminous coal will be focused upon. Up until about 300°C relatively little has apparently happened. Weight loss is about 6%, and the mean layer diameter, intralayer carbon-carbon band distance and mean interlayer spacing are all roughly the same as for the

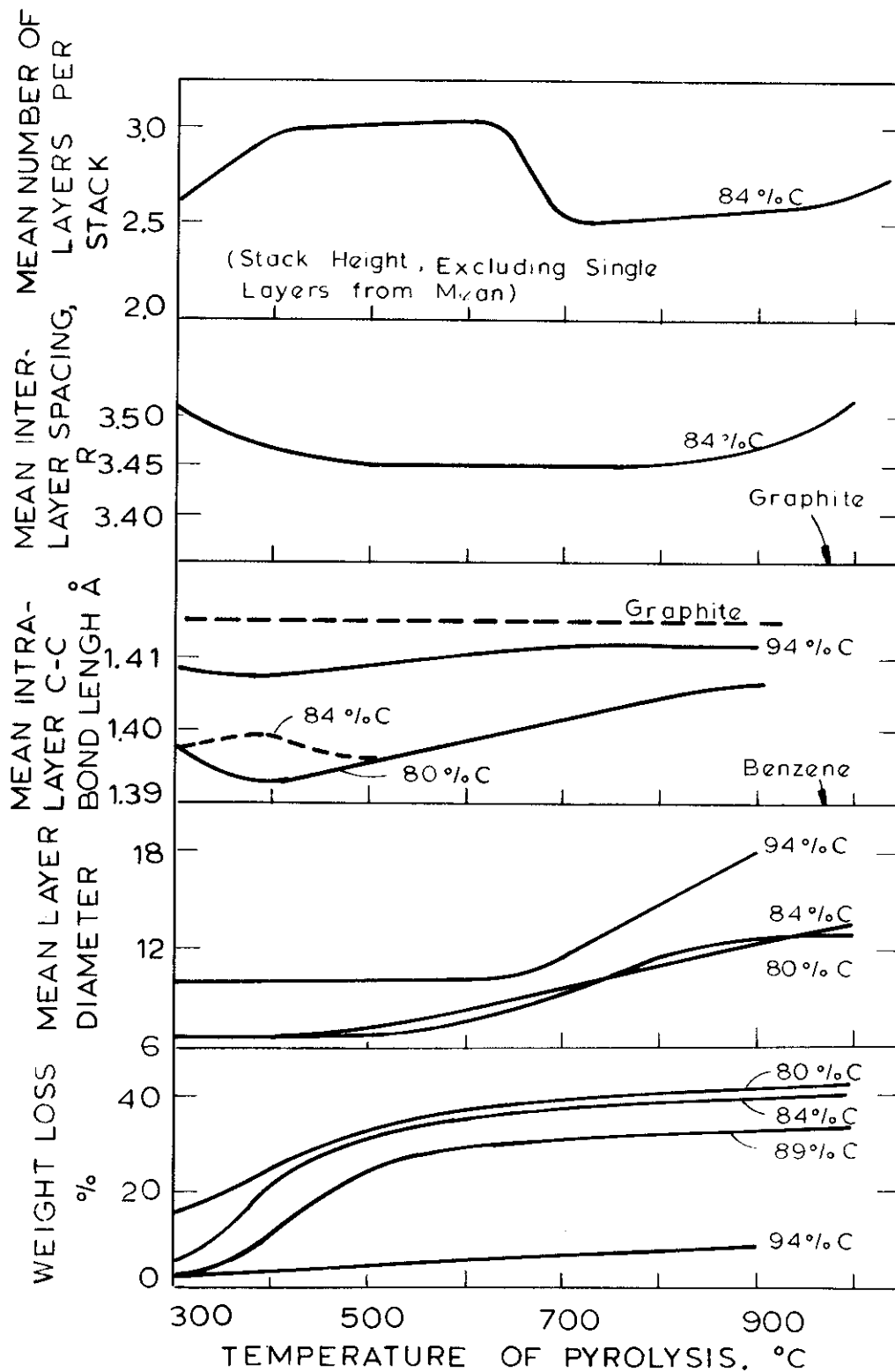


Figure 3.2-7 Changes in Physical Microstructure of Coal During Pyrolysis (Diamond, 1960).

raw coal, as reported by Cartz and Hirsch (1960).

Weight loss increases sharply between 300 and 400°C, over this range some hydroxyl groups are probably being eliminated, and some tar formation may begin. Little additional aromatization is in evidence, but the mean interlayer distance falls, perhaps indicating the physical melting of micelles. In the range 400-500°C, the remaining hydroxyl oxygen is eliminated, condensation reactions (leading to larger layer diameters) commence, the average interlayer spacing is at a minimum, and the mean C-C bond distance is at a minimum. The maximum in the average number of layers per stack (or stack height) was also observed in earlier x-ray work with softening coals by Blayden et al. (1943).

In the range of 400-500°C, the average length of carbon-carbon bonds exhibits a minimum. This decrease in bond distance can be rationalized in part by the existence of free radicals which increase bond order and thereby decrease bond lengths. However, Diamond feels that this explanation may be subsidiary to one in which aliphatic side chains (C-C bond length 1.54 Å) are removed, thus decreasing the average intralayer bond length slightly.

Finally, as temperatures above 600°C, are attained, the rate of weight loss falls off and the secondary degasification phase begins, wherein a large amount of aromatization occurs, as evidenced by the increase in average layer diameter and the approach of the C-C bond length toward the graphite limit. Curiously, the mean number of layers per stack drops, but Diamond attributes this to the spreading out of lamellar layers by mergers of smaller layers. It can be seen that the mean interlayer spacing does not approach that of graphite. This observation is reasonable in that many coals cannot be graphitized by heating. Diamond implies that this

may be due to stereochemical hindrances such as the existence of non-planar small layers or amorphous carbon.

In comparing the behavior of various bituminous coals and an anthracite, Diamond notes that among bituminous coals, the carbonization temperature plays a larger role in determining structure than does original rank. The anthracite, however, appears to be much more "ordered" to start with and approaches graphitization much more closely than bituminous coals. The work of Blayden et al. showed that a low rank coal (a Polish Brown coal of 68.2% C, daf) behaved in somewhat the same manner as bituminous coals with respect to the increase in mean layer diameter with temperature. Although the brown coal and anthracites studied by Blayden did not show maxima in the stack height as did bituminous coals in the range 400-500°C, they did nevertheless show the same type of minima between 700° and 1000°C.

The aforementioned maximum in stack height, in the range 400-600°C is then a property of softening coals. Blayden discovered that height of the maximum could be increased and sharpened by decreasing the heating rate from 5°C/min to 2°C/min. Furthermore, pyridine extraction of the components responsible for fluidity also eliminated the maximum. These data provide firm support for the theories on coal plasticity already presented. Namely, the first step in the pyrolysis of a softening coal involves the softening of micelles, which allows greater ordering of stacks, and that the extractible portion acts as a solvating agent and/or hydrogen donor during this process. The chloroform extractable portion of the coal, discussed previously, is probably the more "active" fraction of the pyridine extract studied by these workers. These observations also lend support to some other theories advanced previously. The evolution of tar and elimination of hydroxyl groups does not immediately

lead to much of an increase in the average size of the aromatic nuclei. Thus the material evolving probably has the same type of aromatic character as that left behind (in terms of the size range of polycyclic nuclei evolved vs those in the residue). The difference in products at the early stages of pyrolysis probably is one of the degree of hydrogenation vs degree of crosslinking. Large increases in aromatization begin only when the rate of weight loss has already fallen to very low levels.

Marsh and Stadler (1967) discuss the relationship between the x-ray studies of changes upon pyrolysis, and compare them to the changes observed by polarized light and electron diffraction. The 400-500°C growth of "anisotropic spheres" of 10-100 $\mu$  has been observed by polarized light microscopy of softened coals. These spheres are regions of macroscopic order which are detected by optical methods involving relatively long wavelengths. X-ray studies of structure, because of the much shorter wavelength of radiation involved, do not detect this long-range order (presumably due to stacking of macromolecules), but only detect the short range order due to overlap of small "pieces" of the macromolecules

Oelert (1968) used infrared spectroscopy to obtain quite detailed information on the chemical changes occurring during slow (0.05°C/min) pyrolysis at low temperatures (3 hours at 500°C, maximum). Fig. 3.2-8 presents a few of the results obtained. The values for CH<sub>3</sub> and CH<sub>aromatic</sub> were taken directly from spectral bands at 1380 cm<sup>-1</sup> and 910-650 cm<sup>-1</sup> respectively. Phenolic groups were estimated by acetylation followed by monitoring of the 1750 cm<sup>-1</sup> band. CH<sub>2</sub> was calculated by difference from a knowledge of the ultimate analysis. (This group may then also contain some tertiary CH hydrogen.) Aromatic carbon not bound to hydrogen or oxygen was also calculated by difference (and so must contain some



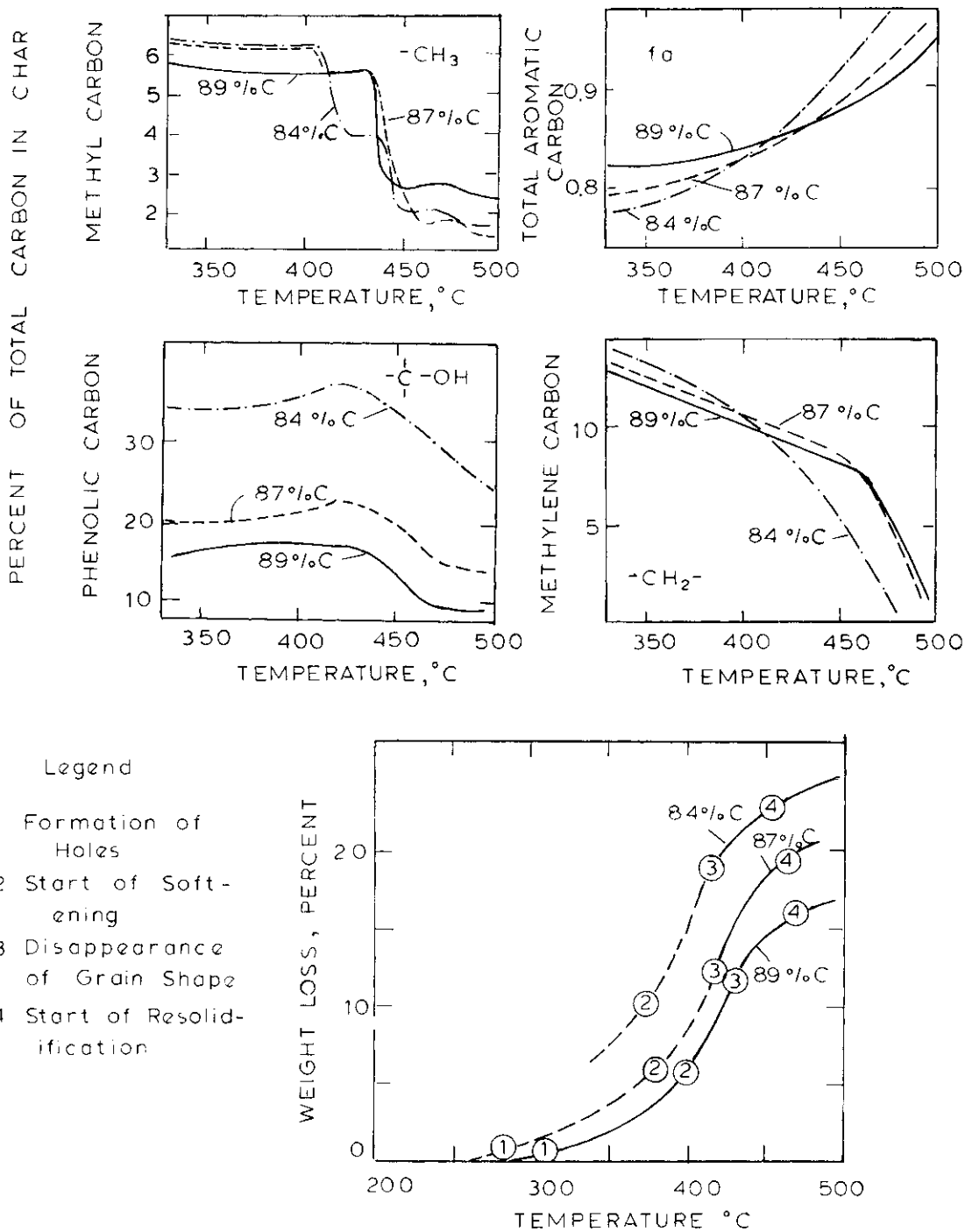


Figure 3.2-8 Changes in the Chemical and Physical Structures of Coal During Pyrolysis (Oelert, 1968; Heating Rate  $0.85^{\circ}\text{C}/\text{min.}$ )

tertiary CH carbons). The assignment of the 1640-1540  $\text{cm}^{-1}$  band to quinonic carbonyl groups is also questionable. Thus in a few respects these results must be considered approximations. The fact that the calculated aromaticities of the raw coals are reasonable lends support to the approximations employed.

Oelert observes that in all cases, there is a loss of methyl carbon (to the extent of 20-30%, not shown in Fig. 3.2-8) prior to softening of the coal. In the case where such measurements were available, this initial loss of methyl coincides with a gain in methylene-carbon. It may be inferred from this behavior that at least part of this initial loss of methyl carbon is due to the type of hydrogen donation mechanism postulated by Van Krevelen, rather than a simple loss of methyl as methane. The data in this regard are somewhat sketchy, though, and do not include volatile product analyses, which might help settle the issue.

Within the range of temperatures associated with plasticity, the contents of both methyl and methylene carbons decrease, while the content of aromatic carbon begins to increase. The more dramatic increases in aromaticity begin after a fairly substantial portion of the weight loss has occurred, but prior to resolidication of the plastic coal. The behavior of the phenolic groups was rather peculiar, in that their content went through a slight maximum (see Fig. 3.2-8). The author attributed this phenomenon to light oxidation during handling of samples. The temperature of decomposition of phenolic groups is upwards of 450°C, which compares reasonably favorably with the temperatures observed by Czuchajowski (1961) in his work with low-rank coals.

Unfortunately, the use of the band containing the much disputed 1600  $\text{cm}^{-1}$  band to quantify quinonic oxygen leads to some uneasiness about the reported

behavior of those groups. The decomposition temperatures reported by Oelert are in the range 430-500°C.

Oelert compares the yield of methane from thermovolumetric experiments with that calculated from the methyl content, were all methyl ultimately to become methane. The results are given below (all for 500°C):

<u>Coal (V.M.%)</u>	<u>CH<sub>4</sub> from Experiment</u>	<u>CH<sub>4</sub> calculated from IR data</u>
13	80.0	80.7
17	80.5	88.7
20	88.0	100.3
22	88.8	107.1
27	89.0	111.2
35	84.0	98.9
37	81.3	86.9
39	81.6	90.4

The calculated values are always too high, by as much as 25%. The author's interpretation is that methyl groups play a dominant role in methane formation. It is not clear from these data alone whether the "hydrogen donor" role ascribed to them by Wolfs et al. (1960) is also supported.

Broad-line NMR measurements of coals and chars have been made by Ladner and Stacey (1965). The rather modest decrease in the second moment below 400°C (at a heating rate of 1 1/4°C min) is consistent with Oelert's picture that methylene (plus "hindered" methyl, if present) do not decrease by much below this temperature. Above 400°C, there is a marked decrease in both.

It can be concluded, based on the results presented in this section, that the theory of coal pyrolysis originally postulated by Van Krevelen and Fitzgerald and their co-workers has gained considerable experimental backing. There remain a great many areas, however, which could very profitably be explored further (e.g. the very important role of hydroxyl groups, the determination of the precise nature of "hydrogen-donor" - hydrogen recipient interactions).

The mechanistic studies of date have mostly been involved with pyrolysis at relatively slow rates of heating; it would be of considerable

interest to compare the behavior at slow rates of heating to that at high rates of heating. The range of temperatures studied has occasionally been low as well, but at least in the case of infrared studies this has partly been dictated by the nature of the experiment (coal pyrolyzed slowly to temperatures much above 500°C becomes opaque in the infrared). In general, no one technique will be able to yield all of the information of interest. In the past, interest has also been heavily oriented towards coals that show softening upon heating; with current interest in utilization of low-rank (generally non-softening) coals, it becomes necessary to focus more upon the differences in the mechanisms of pyrolysis of high and low rank coals.

This study, for reasons of time and resources, has not been able to employ the techniques described above for elucidation of the mechanism of pyrolysis. Instead of approaching the problem by direct measurement of physical and chemical processes occurring in the reactant (coal/char), the approach has been from the other direction, namely, examination of products. The identity of the products and the time-temperature history used to produce them are used to infer what may actually be going on in the coal/char. Such an approach is necessarily fraught with empiricism, as there is no way to establish that a particular product (that itself may not be particularly well characterized) results from the reaction of some particular structure(s). The exception to this generalization is perhaps in clever experimentation, whereby one chemically changes the original structure in a known way and monitors the change in products (typical examples being the use of deuterated and radioactively labelled species). The difficulty with coal is that the reactant is so ill-understood that it is difficult to change any particular feature in a known manner and yet leave the coal structure otherwise unchanged.

In recent years, the continued development of more sophisticated analysis tools for the study of heavy liquid and solid organics bodes well for the study of coal and its reactions.

### Effect of Coal Type and Pyrolysis Conditions on Pyrolysis Behavior

This section explores briefly the evidence for the effect or lack of effect of the variables listed in section 3.0. For a more thorough treatment, the reader is referred to Anthony and Howard (1976) or Howard (1977).

#### Effect of Coal Type

Table 3.2-5 lists the results of various workers on various coals. There are a large number of final temperatures and heating rates involved, so caution must be exercised in making direct intercomparisons. The results from this study and those of Loison and Chauvin (1964) were both obtained at heating rates of about 1000°C/sec and final temperatures of about 1000°C, so they constitute a relatively consistent set. The data of Campbell and Stephens (1976), Fitzgerald and Van Krevelen (1959), and Jüntgen and Van Heek (1977, also Hanbaba et al., 1968) were all obtained at low heating rates. It is not clear whether the lower  $V^*/VM$  values obtained by Fitzgerald and Van Krevelen are due to an effect of heating rate, volatiles cracking, or merely because lower temperatures were involved than in the work of Loison and Chauvin and this study. The next section will discuss the importance of temperature in more detail.

In general, the data suggest

- Methane and Ethane yields rise, and then fall again with rank. The scatter in these data partly masks this behavior, but the same phenomenon has been reported by Hanbaba et al. (1968).

Table 3.2-5 Comparison of Ultimate Yields of Pyrolysis Products from Coals of Various Rank, Part I

<u>% by Weight</u>	(1)	(2)	(1)	(3)	(4)	(5)	(3)	(3)	(3)	(4)	(3)
C (daf)	71.2	73.5	77.9	80.0	80.2	83.6	85.0	85.8	86.7	86.8	87.3
H (daf)	4.6	5.8	5.5	5.1	4.9	5.1	5.2	5.1	4.9	5.3	4.7
N (daf)	1.1	1.2	1.4	-	1.2	1.6	-	-	-	2.0	-
O (daf)	21.8	18.7	9.3	12.7	13.4	7.6	8.2	6.3	6.3	4.7	5.3
VM (daf)	44.3	-	44.6	38.6	41.9	39.5	36.7	32.9	29.2	30.6	22.6
ash(dry)	10.6	9.1	11.5	5.7	2.0	4.0	7.7	5.8	16.4	4.8	9.7
T°C	1000	1000	1000	1050	730	To ~ 1000°	1050	1050	1050	730	1050
$\frac{dT}{dt}$ °C/sec	1000	0.06	1000	1500	0.03	$4 \times 10^{-5}$ to .03	1500	1500	1500	0.03	1500
<u>daf Yield of Gases, % by Wt.</u>											
CO	11.3	5.8	2.8	6.0	6.4	3.2	2.5	4.0	2.5	1.9	1.5
CO <sub>2</sub>	11.4	11.3	1.4	2.8	1.6	0.81	0.93	1.6	1.5	0.41	0.63
H <sub>2</sub> O	11.6	-	6.2	5.5	7.0	2.4	4.4	4.7	3.1	4.0	2.7
H <sub>2</sub>	0.60	1.1	1.2	1.0	1.4	3.1	0.93	0.99	1.2	1.9	1.1
N <sub>2</sub>	-	-	-	-	-	0.95	-	-	-	-	-
CH <sub>4</sub>	1.6	4.7	2.9	2.2	2.9	4.1	3.1	2.5	3.1	4.1	2.9
C <sub>2</sub> H <sub>4</sub>	0.67	0.23	0.95	-	0.16	0.17	-	-	-	0.20	-
C <sub>2</sub> H <sub>6</sub>	<u>0.28</u>	<u>0.87</u>	<u>0.58</u>	<u>-</u>	<u>(0.40)</u>	<u>0.74</u>	<u>-</u>	<u>-</u>	<u>-</u>	<u>0.82</u>	<u>-</u>
Sum of Above	37.5	-	16.0	17.5	19.9	15.5	11.9	13.8	11.4	13.3	8.8
Tar (daf)	6.5	-	26.3	20.0	-	-	24.3	2.67	20.5	-	17.6
V* /VM	1.01	-	1.17	1.01	0.88	-	1.02	1.18	1.09	0.98	1.25

(1) This study

(2) Campbell and Stevens (1976)

(3) Loison and Chauvin (1964)

(4) Campbell and Stevens (1976)

(5) Campbell and Stevens (1976)

200

Table 3.2-5 Comparison of Ultimate Yields of Pyrolysis Products from Coals of Various Rank, Part II

<u>% by Weight</u>	(5)	(3)	(4)	(5)	(3)	(5)	(4)	(4)
C (daf)	87.5	87.9	88.6	89.3	90.1	91.0	91.7	93.7
H (daf)	4.6	4.5	5.0	4.3	3.7	4.0	4.1	3.5
N (daf)	1.7	-	2.3	1.6	-	1.6	1.9	1.4
O (daf)	5.3	5.0	3.7	3.0	4.3	2.1	1.9	1.0
VM (daf)	28.9	19.4	23.3	19.1	10.0	10.0	13.7	8.2
Ash(dry)	7.4	6.8	3.7	6.5	16.3	6.6	0.8	1.7
T°C	To ~ 1000°	1050	730	To ~ 1000°	1050	To ~ 600°	730	730
$\frac{dT}{dt}$ °C sec	$4 \times 10^{-5}$ to .03	1500	0.03	$4 \times 10^{-5}$ to .03	1500	low	0.03	0.03
<u>daf Yield of Gases, % by Wt.</u>								
CO	1.9	1.2	1.6	1.7	2.3	1.6	1.3	1.1
CO <sub>2</sub>	0.75	0.61	0.26	0.71	0.79	0.63	0.08	0.0
H <sub>2</sub> O	1.3	3.2	3.1	1.1	1.8	0.72	0.96	0.0
H <sub>2</sub>	3.4	1.2	2.2	3.5	1.1	3.8	2.3	2.3
N <sub>2</sub>	0.66	-	-	0.42	-	0.35	-	-
CH <sub>4</sub>	4.7	3.0	4.4	4.4	1.1	2.8	3.5	2.4
C <sub>2</sub> H <sub>4</sub>	0.15	-	0.21	0.13	-	0.04	0.13	0.06
C <sub>2</sub> H <sub>6</sub>	<u>0.74</u>	<u>-</u>	<u>0.67</u>	<u>0.51</u>	<u>-</u>	<u>0.12</u>	<u>0.27</u>	<u>0.07</u>
Sum of Above	13.6	9.2	12.4	12.5	7.1	10.1	8.5	5.9
Tar (daf)	-	15.7	-	-	2.1	-	-	-
V* /VM	-	1.30	0.90	-	1.00	-	0.80	0.73

(1) This study

(2) Campbell and Stevens (1976)

(3) Loison and Chauvin (1964)

(4) Fitzgerald and Van Krevelen (1959)

(5) Hanbaba et al. (1968) Jlantgen and Van Heek (1977)

201

- Ethylene yield increases with decreasing rank.
- Oxygenated species all increase with decreasing rank.
- Tar (in this case, generally room temperature condensable molecular weight >120) yields show a distinct maximum in the low rank bituminous range. Lignites and very high rank coals do not produce much.

The production of hydrogen gas is particularly sensitive to the amount of secondary reaction possible in the system and also to the length of time a coke is held at temperature (driving off the remaining aromatic hydrogen). The hydrogen values obtained by Jüntgen and coworkers appear high when compared to the results of all other workers. The amount of hydrogen in H<sub>2</sub> and CH<sub>4</sub> alone often accounts for more than is present in the coal to begin with. Even leaving out these questionable values, no clear trend is evident.

Jüntgen and coworkers were, however, able to measure the yield of molecular nitrogen. The values obtained represent significant percentages of the nitrogen in the raw coals.

These data suggest that some predictive power may already be available. Fig. 3.2-9 shows a comparison of phenolic oxygen content with pyrolytically formed water (not moisture) oxygen content. The agreement with the curve suggested by Given (previously discussed) is outstanding, with the exception of the water from the lignite used in this study and the data from Jüntgen and Van Heek (1977), which appear to be consistently low.

Agreement between carboxylic oxygen and oxygen in the CO<sub>2</sub> product is not as good, but is nevertheless acceptable at high ranks. The discrepancy at low ranks is again more sizable. There is evidence in the literature that the loss of carboxyl groups from low rank coals is



among the lowest temperature pyrolysis phenomena. The appearance of a large amount of  $\text{CO}_2$  as the first major (chemically evolved) species during pyrolysis of the lignite in this study is suggestive of this behavior; the yield from the low temperature phase of pyrolysis of this lignite and Campbell and Stephen's subbituminous coal are shown as circles in Fig. 3.2-9. This staged behavior during pyrolysis will be discussed at length later. The agreement with the carboxyl content is then fairly good. Assuming the carboxyl content estimates are accurate, then it must be the case that  $\text{CO}_2$  arises from other sources as well, especially in low rank coals. A small amount may be due to the carbonate mineral decomposition, but at least in the case of the lignite in this study, this can account for but 1/3 of the additional  $\text{CO}_2$ . Thus some  $\text{CO}_2$  must be formed from non-carboxyl structures during pyrolysis. The remaining coal oxygen is evolved as part of the tars, or as  $\text{CO}$ .

The mechanistic origins of the various hydrocarbons is much less well determined. As discussed in the previous section, IR evidence suggests that methane yields are consistently lower than that which would be expected from methyl carbon.

#### Effect of Temperature

In studying the thermal decomposition of a pure substance A, if one postulates that the reaction is first order and governed by an Arrhenius rate law, then the extent of reaction is simply derived from an appropriate integration of

$$\frac{d(A)}{dt} = -k_0 e^{-E/RT} (A)$$

If  $k_0$  is a typical  $10^{13} \text{ sec}^{-1}$  and E a typical 55 kcal/mole, then a reaction which at low temperature carbonization temperatures  $500^\circ\text{C}$  takes over 4 minutes, can occur in .2 milliseconds at  $1000^\circ\text{C}$ .

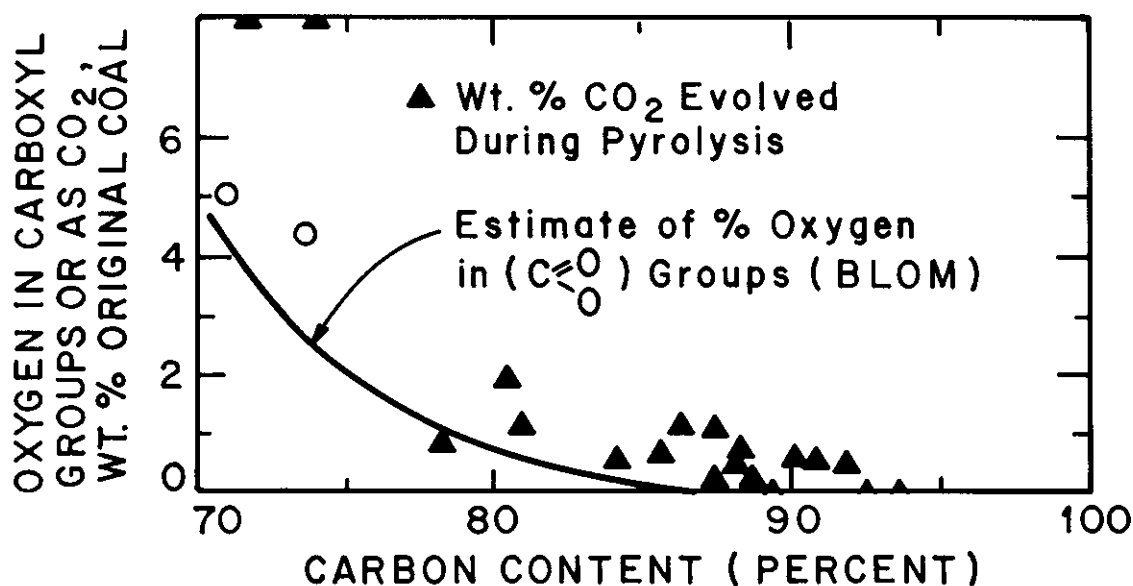
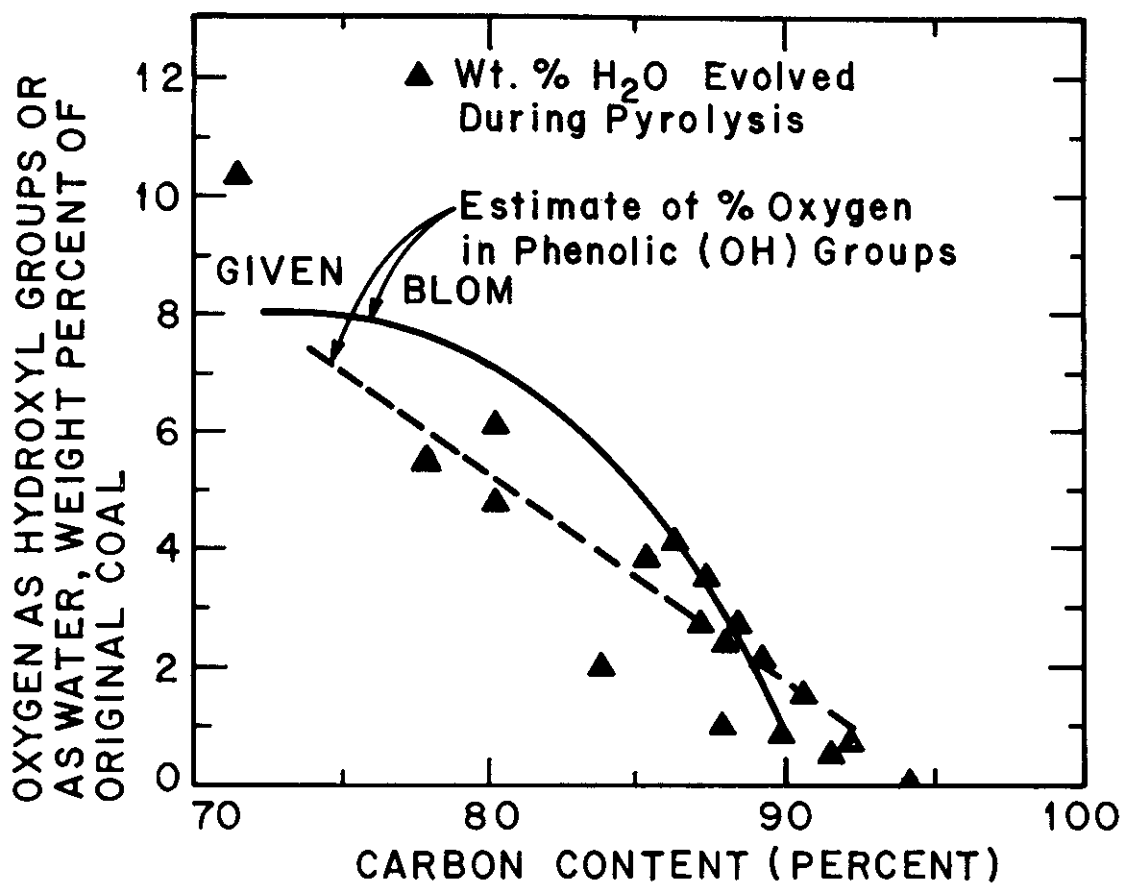


Figure 3.2-9 Comparison of Yields of Pyrolytic Water and Carbon Dioxide with Amounts of Hydroxyl and Carboxyl Groups in Coal.

Since coal is a heterogeneous material with many types of reactive sites (any site can be reactive if the temperature is sufficiently high), it is natural to expect that its pyrolysis will involve many different types of reaction pathways, each with its own characteristic activation energy. The overall behavior of the coal will be determined by a set of reactions some perhaps parallel and independent, others consecutive, others perhaps competitive.

It is in this respect also that the A.S.T.M. proximate volatile matter test is arbitrary—heating for seven minutes at 950°C does not ensure "complete" reaction of the coal. It ensures that some, but not necessarily all, reactions have gone to completion.

It is also for this reason that the data of Kimber and Gray (1967a,b), Kobayashi (1977), and Ubhayakar et al. (1977) (Table 3.2-2) and Blair et al. (1977) are not directly comparable to the other data; because of the exceedingly high temperatures involved in these studies (1800–2000°C), a completely different set of decomposition reactions with very high activation energies could be involved.

Many pyrolysis studies have focussed upon obtaining time-temperature resolved rates of production of various gaseous species from coal. From these data, kinetic constants can be determined, and an overall model of coal pyrolysis formulated. Two of the more recent studies of this kind have been those of Jüntgen and Van Heek (1971, 1977) and of Campbell and Stephens (1976). Fig. 3.2-10 and 3.2-11 present some of their data. Both sets of data appeared in integrated form in Table 3.2-5 as yields obtained up to 1000°C (by heating at slow rates, 1 – 3.5°C/min).

Both sets of data show how some products are formed in 2 or more distinct stages ( $\text{CO}_2$ ,  $\text{CO}$ ), while other products are characterized by a single, rather broad peak. The data in both cases were obtained by

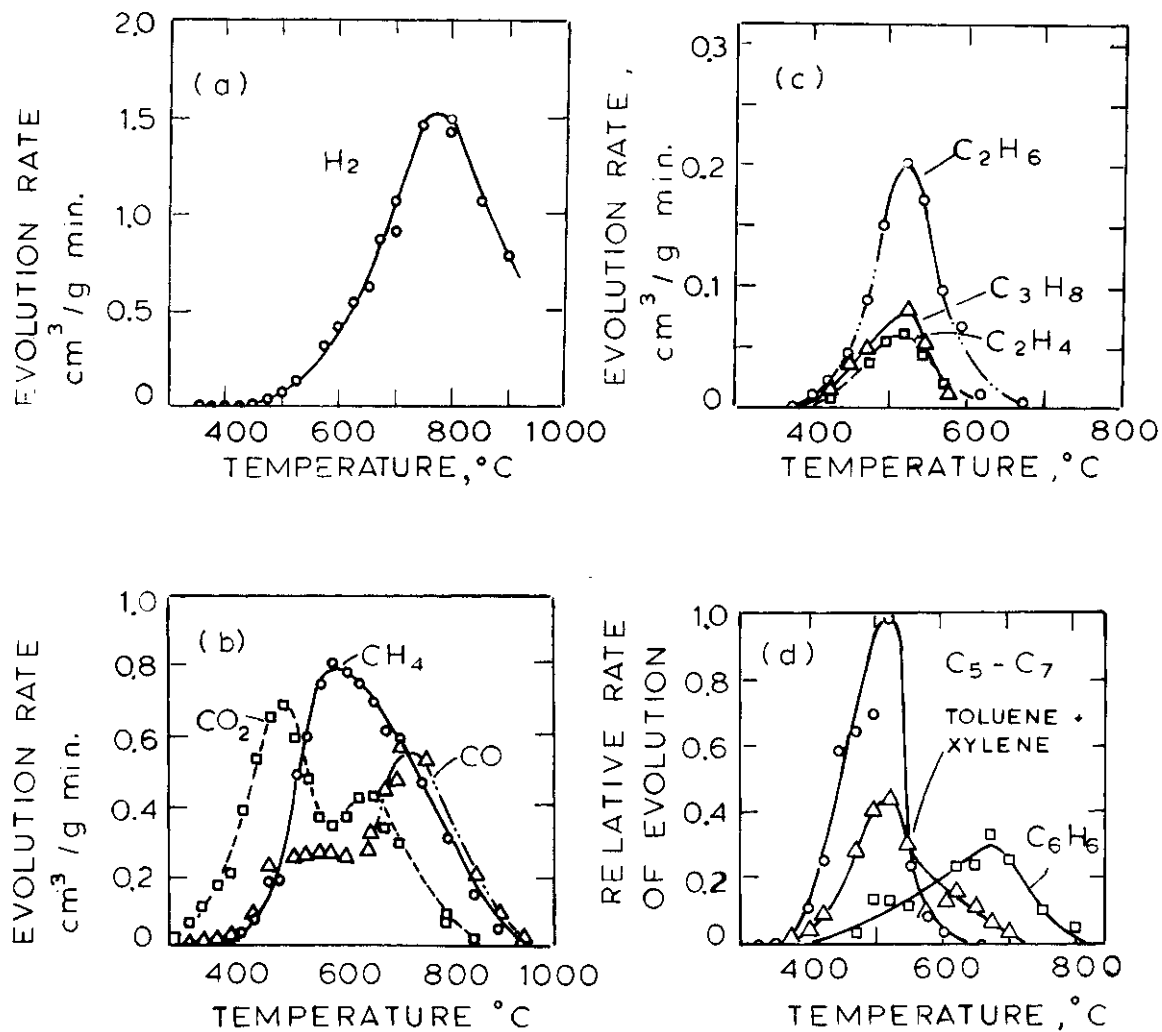


Figure 3.2-10 Evolution of Gases During the Pyrolysis of a Subbituminous Coal (Campbell and Stevens, 1976; (a), (b), (c) in terms of S.T.P. cm<sup>3</sup>/g coal-min; (d) relative to peak of C<sub>5</sub> - C<sub>7</sub> curve).

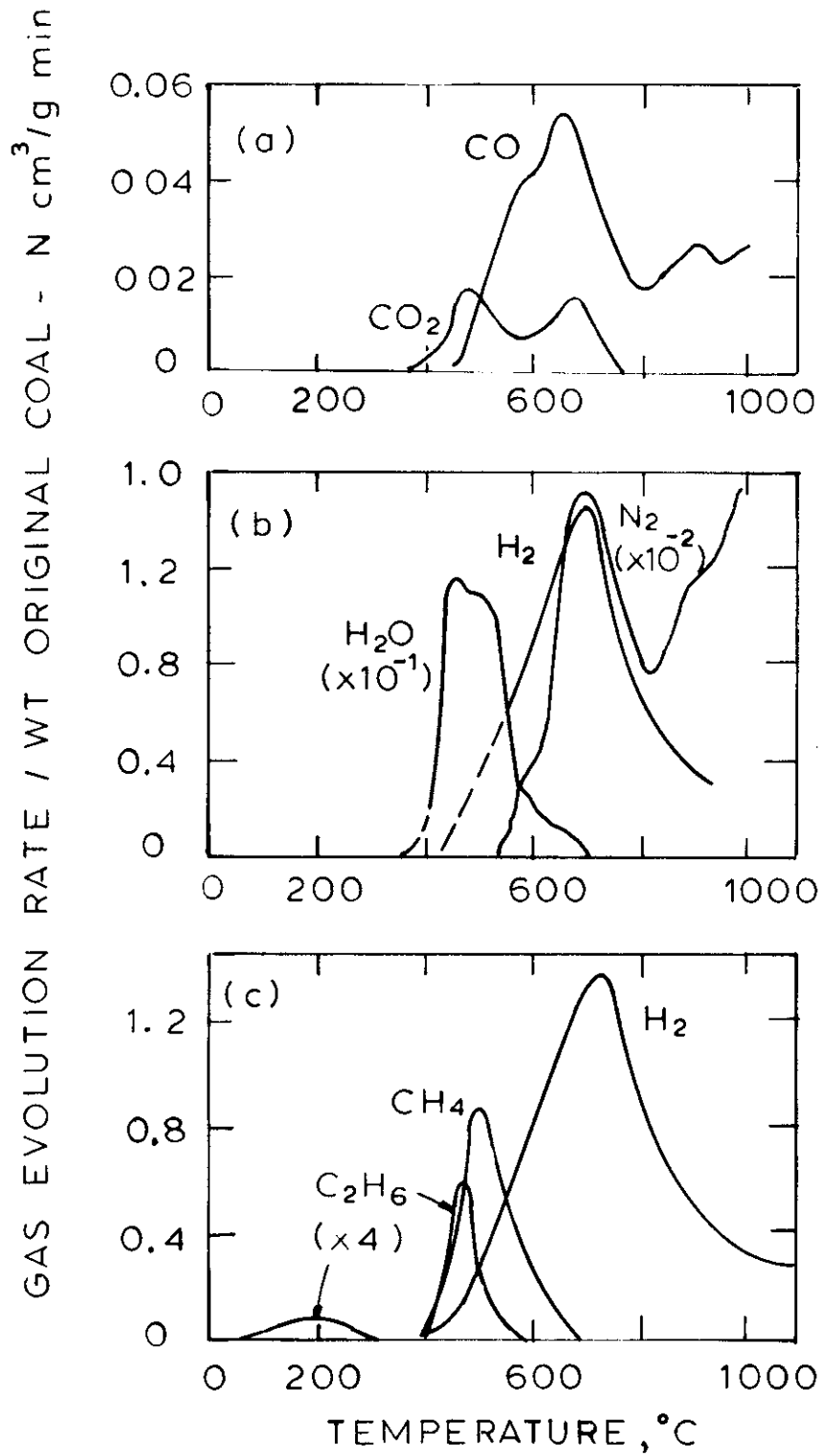


Figure 3.2-11 Evolution of Gases During the Pyrolysis of Bituminous Coals (Jüntgen and Van Heek, 1977; Non-Hydrocarbon Gases (a), (b) measured at a heating rate of  $1^{\circ}\text{C}/\text{min}$ , Hydrocarbons (c) at a heating rate of  $2^{\circ}\text{C}/\text{min}$ ).

on-line mass spectroscopy, but in neither case was mention made concerning possible sampling lags. Presumably the low heating rates involved help to avoid the troublesome measurement lags observed by Blair et al. (1977) at higher heating rates. A comparison between the data obtained by these workers and the results of this study will be discussed in a later section.

In summing up the contributions of all individual products, a smoothed overall weight loss curve usually results. Fig. 3.2-12 shows a family of such overall weight loss curves as functions of the residence time at a particular temperature (Howard, 1977). The data shown were collected by various techniques and on various coals. The apparent asymptote at 1000°C may not be a true asymptote, in light of the higher weight losses obtained at higher temperatures.

#### Effect of Heating Rate

The effect of heating rate on mechanism and yield is one of the most discussed topics in coal pyrolysis research. In the early 1950's several Russian workers studied the differences between products of pyrolysis formed in slow decomposition in a retort and those from rapid pyrolysis in superheated steam. This work has been reviewed by Badzioch (1961). The conclusion reached was that rapid pyrolysis led to a substantially different mix of products than slow pyrolysis. From analyses of this data, Chukhanov (1956) postulated five sets of parallel first order reactions. The first was very rapid and resulted in the production of CO<sub>2</sub> and water. The other sets included slower tar and hydrocarbon forming reactions, and very slow (order of hours at 500°C) degassing reactions.

Peters (1960) and Peters and Bertling (1965) have compared the pyrolysis of coal in a standard Fischer assay retort (heating rate

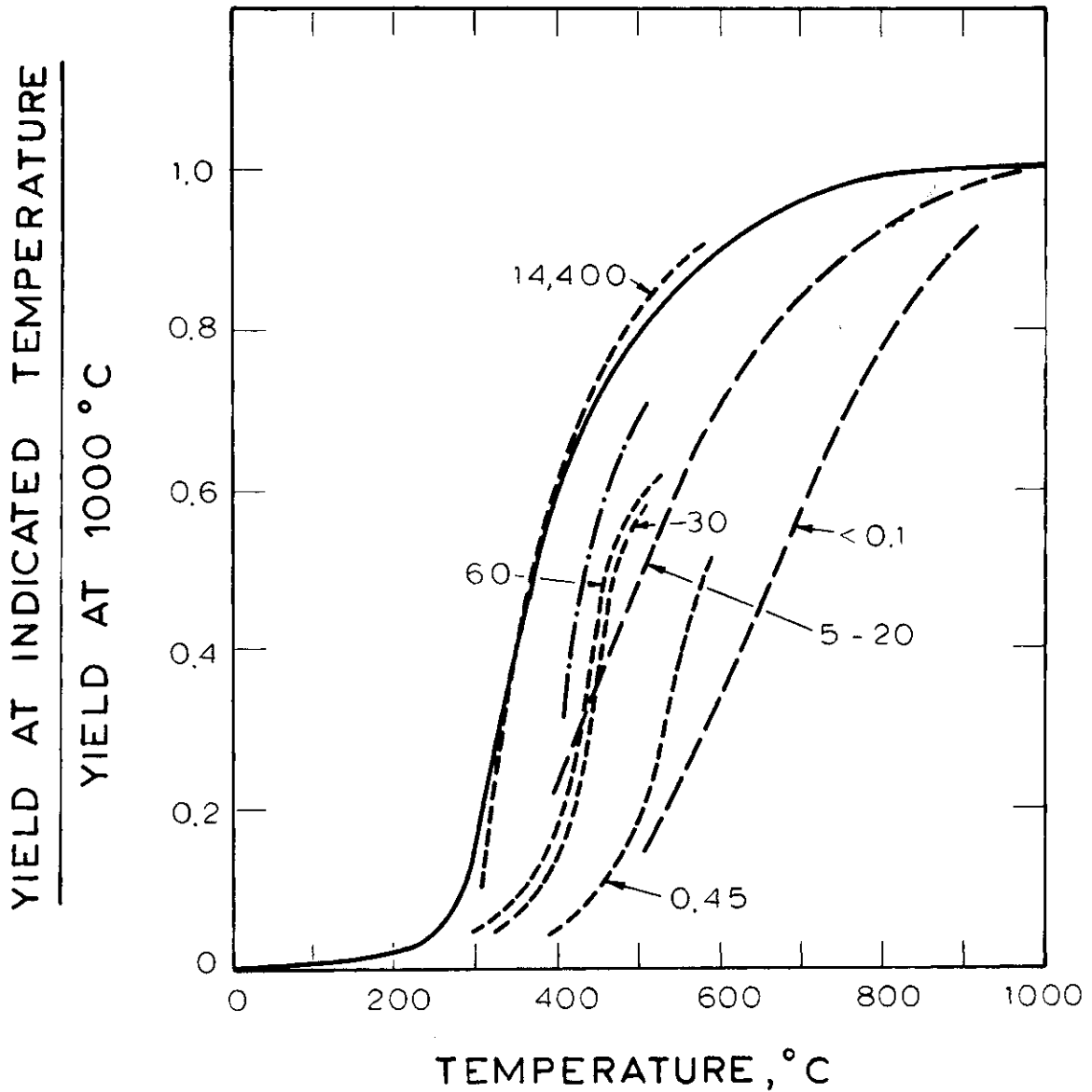


Figure 3.2-12 The Effect of Temperature and Time on Total Volatiles Yield from Pyrolysis (compiled by Howard, 1977); times on curves (sec); curves solid, Dryden (1957); short dashes, Shapatina et al. (1960); long dashes, Anthony et al. (1975); alternating long and short dashes, Wiser et al. (1967)].

about 12°C/min to 600°C) and in a mechanically fluidized bed, wherein heating rates of 100 to 1000 times higher than in the Fischer retort were possible.

Although the yield of gas varied by only a few percent between the two cases, the gas from the retort was significantly higher in hydrogen content. This, combined with the fact that the tar yield is lower from the retort, leads to the conclusion that either tar is initially formed in the same quantities in both systems but subsequently is coked in the retort, or that the fluid bed yield of tar is higher because of a chemical effect induced by the higher heating rate. Unfortunately because the processing environments being compared are very different (in this work as well as the earlier Russian work) no firm conclusions could be reached on the importance of heating rate alone. Anthony and Howard (1976) suggest that the difference in experimental environment (and its effect on transport of potentially reactive volatiles away from the reaction zone) may play an important role in causing the pseudo-effect of heating rate to be observed. Rapid heating experiments are generally dispersed phase experiments, hence volatiles have less opportunity to contact coal and be "repolymerized" and coked. This is not intended to imply, however, that heating rate cannot have an effect on total yields (due to competition between process with different activation energies). Van Krevelen (1961, see section on Model Compounds) found a large effect of heating rate on total yield of volatiles from pyrolysis of a hydroxyl substituted polycondensed aromatic system, but no effect on the unsubstituted polycondensate. He theorized that in the case of the substituted polycondensate, a competitive reaction mechanism was responsible for the effect, and that it must involve



some kind of repolymerization via hydroxyl groups.

An effect of heating rate need not only be a manifestation of competing chemical processes, it could also arise because of competition between a physical and chemical process. Corrales and Van Krevelen (1960) demonstrated a sorption effect of organics on coal. In low heating rate processes, it is possible that the temperature at which a substance is formed within the coal is sufficiently low so that it cannot immediately vaporize, whereas at higher heating rates, its temperature of formation is sufficiently high so that it essentially vaporizes immediately and cannot react. If this is the true sequence of events it implies a rather strong temperature dependence of the rate of vaporization, relative to the activation energies of the formation and cracking reactions. There is no evidence to suggest whether this is realistic. It has also been suggested (Van Krevelen et al., 1956; Loison and Chauvin, 1964; Badzuich, 1967) that another mechanism responsible for enhancement of yield of tar is physical carrying away of "metaplast" or even small pieces of coal. During rapid heating, reaction temperatures can be reached in fractions of a second, resulting in a very rapid, violent evolution of gas. It has been observed during the course of this study that some decrepitation of the lignite occurs, and that small flecks of the parent coal are thrown off, to be included with the tar. It is likely that the mist of "tar" evolved from the pyrolyzing bituminous coal may also be partially "non-volatile" material, though no distinct pieces of particle are observed. The loss of this material can contribute to the higher weight loss from high heating rate experiments, but again it is only a pseudo-effect, because the non volatile material physically

carried away would not be as likely to be observed as product if the high heating rates were somehow attained in a large fixed bed.

A legitimate concern in the analysis of data from rapid heating rate experiments is one of heat transfer limitations, both external and internal to the particle.

Badzioch (1967) has shown by calculation that the center of a 100 $\mu$  particle heated at a rate of 10<sup>4</sup>°C/sec can lag the surface by 50°C, but that this was acceptable for most kinetic analyses, since the extent of reaction during this phase was extremely small (chemical rate control). Koch et al.(1960) determined various values of "critical diameter" as a function of heating rate. This critical diameter reflects the particle size above which the pyrolysis at a given rate of heating (of the surface) shifts from chemical control to heat transfer control.

Below some sample results

Heating Rate °C/sec	100	1000	10,000
Critical diameter $\mu$	2000	500	200

Anthony and Howard also cite some unpublished MIT data that show that the transition occurs at 100 to 1000  $\mu$  for a heating rate of 600°C/sec. Mills et al. (1975) have also concluded that particles of 74 $\mu$  diameter (as used in this study) show chemical, rather than heat transfer, control.

A number of recent experimental studies have helped shed more light on the question of effect of heating rate. Anthony (1974, Anthony and Howard, 1976) studied the effect of heating rate in the range 180 to 10,000°C/sec and found no effect on the ultimate weight loss from a Montana lignite. The same set of kinetic parameters was found to hold over the entire range as well. Data are shown in Fig. 3.2-13. The results for bituminous coal similarly showed no major effect between 1000 and 10,000°C/sec.

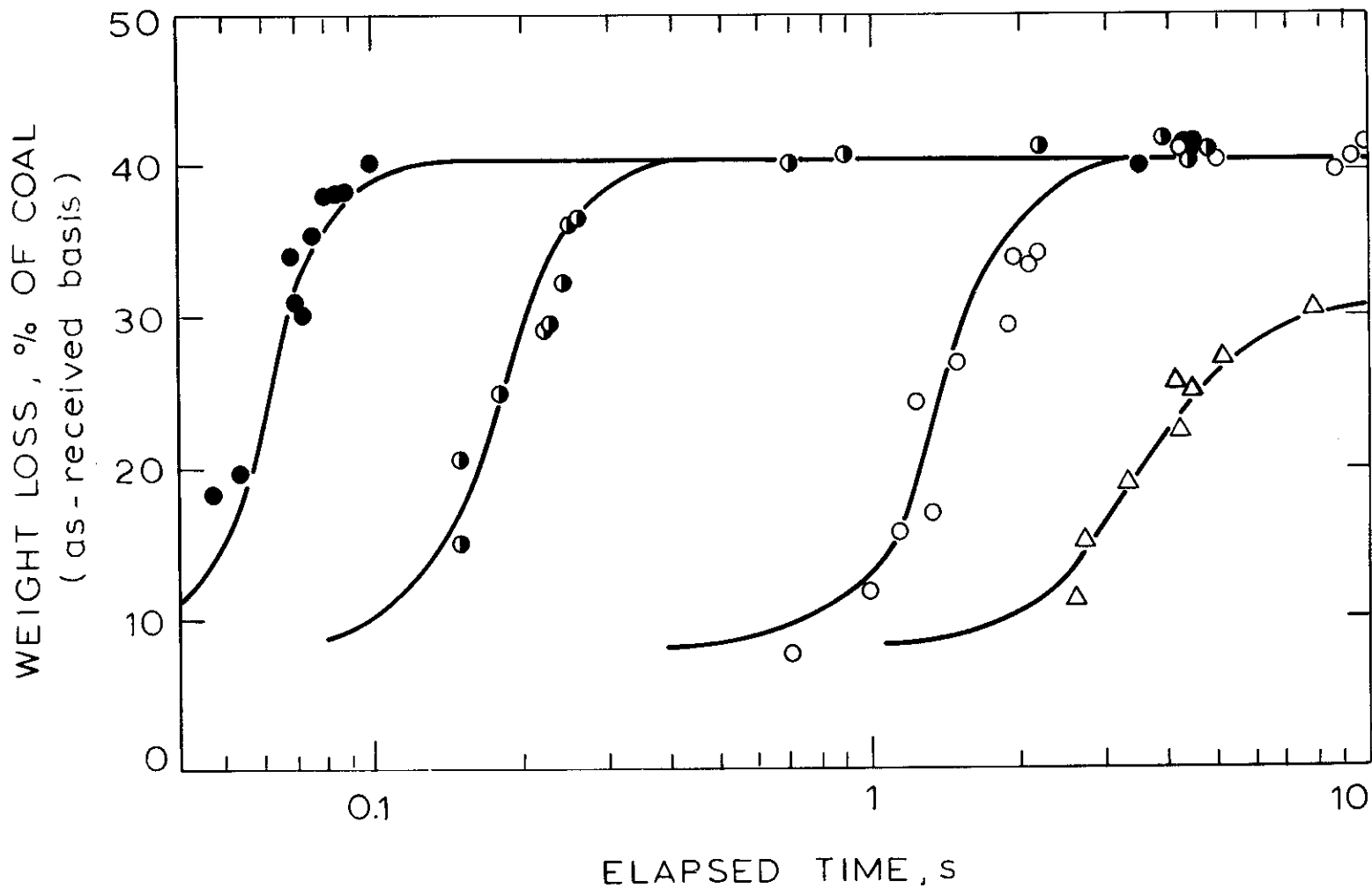


Figure 3.2-13 The Effect of Heating Rate on Total Volatiles Yield from Pyrolysis of a Lignite (Anthony (1974); Savage Mine lignite;  $t = 0$  at initiation of heating; pressure, 1.0 atm helium; mean particle diameter,  $70\mu\text{m}$ ; final temperature (if attained)- $1,000^\circ\text{C}$  ( $\bullet$ ,  $\circ$ ,  $\circ$ ),  $700^\circ\text{C}$  ( $\Delta$ ); nominal heating rate ( $^\circ\text{C/s}$ )-10,000 ( $\bullet$ ), 3000 ( $\circ$ ), 650 ( $\circ$ ), 180 ( $\Delta$ )).

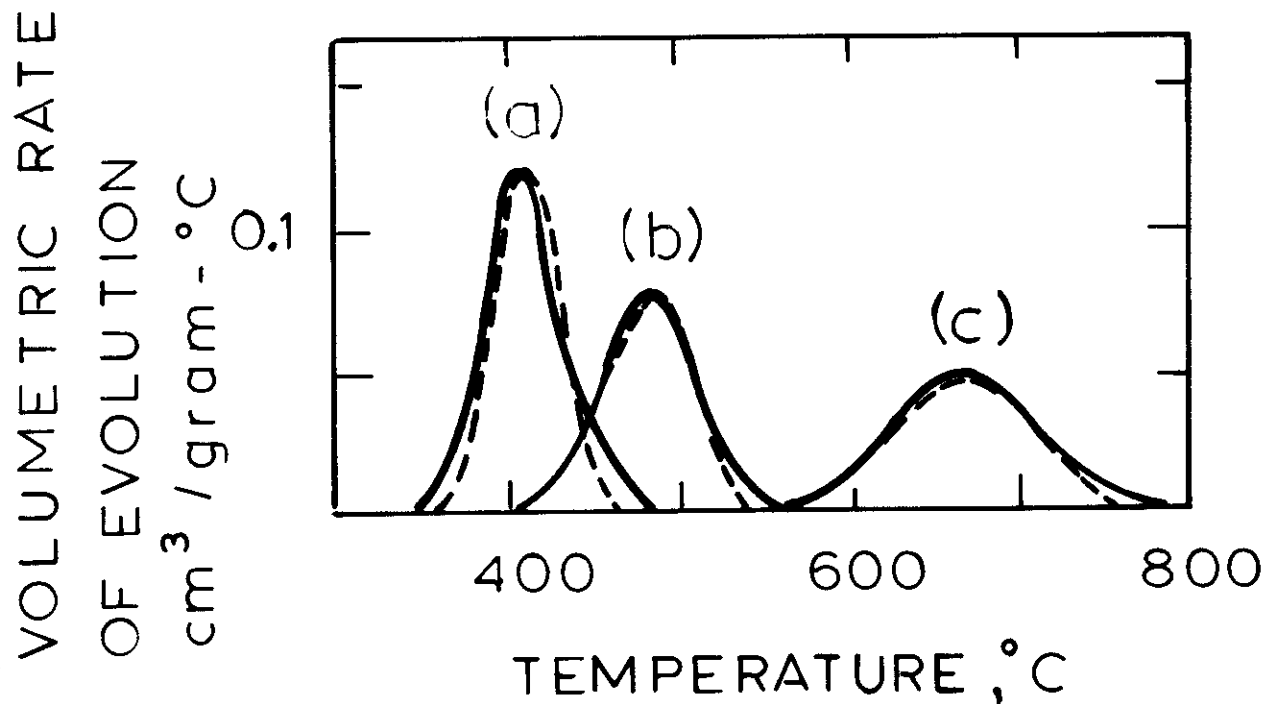


Figure 3.2-14 The Effect of Heating Rate on Ethane Evolution During Pyrolysis of a Bituminous Coal During Pyrolysis of a Bituminous Coal (Jüntgen and Van Heek, 1968; heating rates (a) 0.02°C/min; (b) 2°C/min; (c) 10<sup>4</sup>°C/min. Dashed curves, calculated with activation energy = 40.9 to 42.7 kcal/mole in all cases).

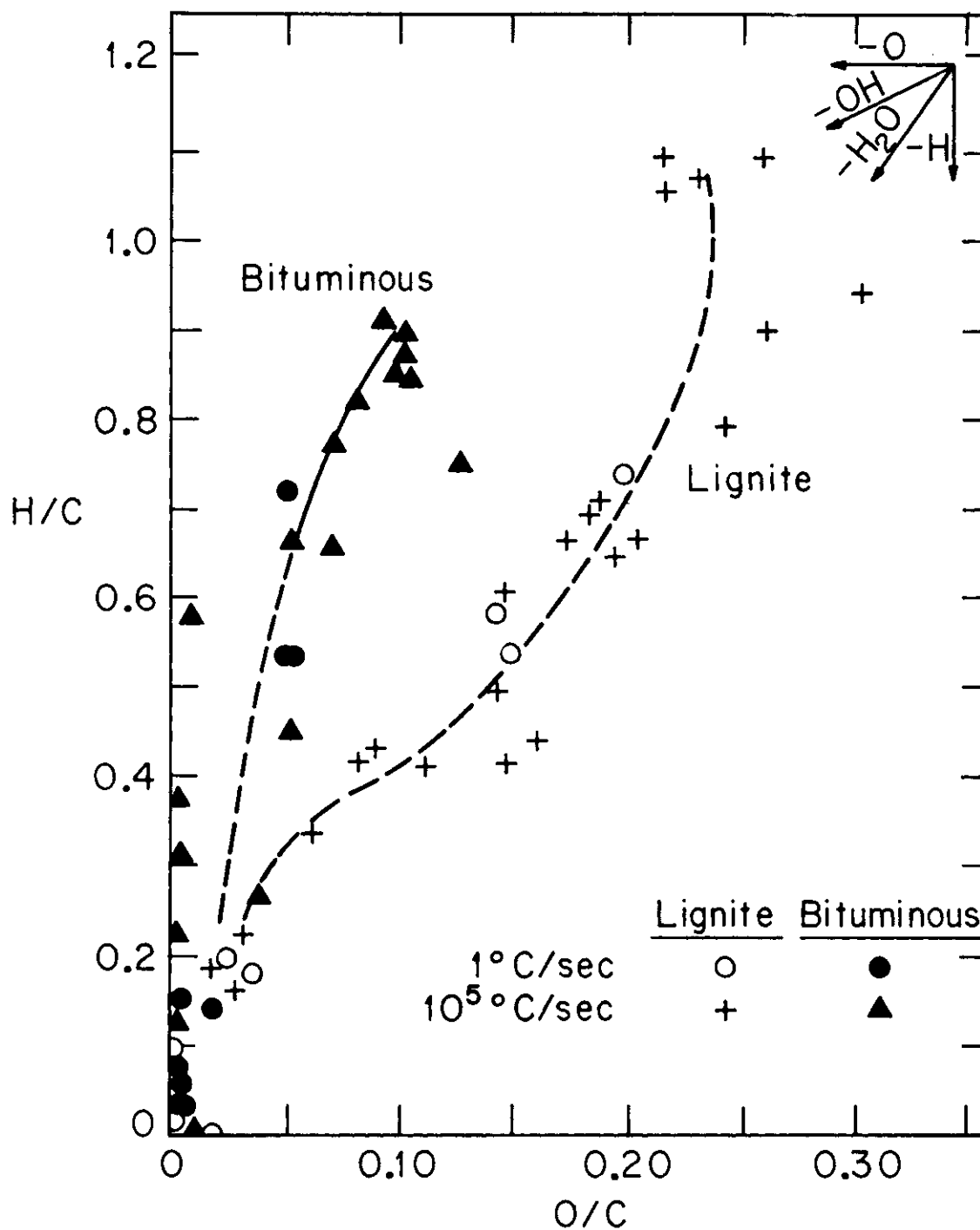


Figure 3.2-15. The Variation of the Atomic H/C and O/C Ratios During Pyrolysis (Kobayashi, 1976).

Another set of data which suggest a relatively unimportant role for heating rate are those from Jüntgen and Van Heek (1968). Fig. 3.2-14 shows data obtained by these workers ranging from  $10^{-2}$ °C/min up to  $10^4$ °C/min. In order to study the effect, two types of apparatus were employed, the low heating rates in a fixed bed in a furnace, the high heating rates on an electrically heated grid. The calculated curves were drawn using the "best-fit" parameters shown above the curves. The model to which these parameters were fit was a first order model (in ethane product). The derivation of the model will be described in the subsequent section on modelling. The activation energies show a great insensitivity towards heating rate, but the results also point up how large an effect heating rate can have upon the temperature at which a process occurs. The maximum rate of evolution of ethane occurs at about 400°C at a heating rate of  $10^{-2}$ °C/min, and at a temperature of 675°C at a rate of  $10^4$ °C/min.

Unfortunately, from these data alone it is possible to conclude only that the primary mechanism of ethane formation does not change with heating rate. To conclude that no other changes have occurred requires an integration of the curve to get total yield (not provided). From other data provided by this group (Hanbaba et al., 1968), the total yield of ethane does go up slightly as heating rate is increased from  $2.5 \times 10^{-3}$ °C/min to .88°C/min.

A bit of indirect evidence for lack of effect of heating rate is provided by the data of Kobayashi (1977). Fig. 3.2-15 shows the variation of H/C ratio vs O/C ratio for a Pittsburgh Seam Bituminous coal and a Montana lignite upon pyrolysis. The coals were pyrolyzed in two ways. One involved use of a small ceramic crucible, which attained

temperatures of about 2000°C at heating rates on the order of 0.5 - 5°C/sec. The other data were obtained from an entrained flow reactor in which the heating rates were calculated to be 10,000-200,000 °C/sec. The fact that both sets of data fall along the same curve seems to imply that the mechanism of pyrolysis at high and low heating rates is the same because the same elements are being eliminated in the same ratios. The fact that the ultimate weight loss from the crucible experiments were about 20% lower than those from the laminar flow furnace could be explained in a number of ways:

- Incomplete material collection in the entrained flow system. (Although weight losses were checked with as as a tracer).
- Secondary reactions within the crucible which result in coke formation from volatiles.
- The fact that heating rate does not show an effect on this H/C vs O/C plot might imply that the difference begins to manifest itself only at a very low value of O/C.

In heating up to 1800°C rapidly, the initial course of pyrolysis may be the same as that observed at lower rates and temperatures. The last phase of slow, low temperature pyrolysis is the "degassing" phase wherein hydrogen is lost. Perhaps the fact that this phase is reached very quickly and is carried out at much higher temperatures than normal permits more efficient utilization of this residual hydrogen. The data of Blair et al.(1977) show no significant effect of heating rate in the range 500°C/sec to 20,000°C/sec in pyrolysis work at 1400°C, yet attains weight losses of the same order as Kobayashi. Blair did however see a rather large percentage increase in volatiles yield between 1000°C and 1400°C, suggesting that pyrolysis at high temperatures and high

heating rates gives a yield enhancement attributable more to the former than to the latter.

#### Effect of Particle Diameter

In addition to the previously described studies which defined the maximum particle diameters acceptable for use in particular pyrolysis experiments, there have been other studies which have sought to develop correlations between weight loss and particle diameter. These studies have naturally focussed upon a range of particle diameters much greater than those involved in this study.

Peters (1960) postulated an empirical model of the form:

$$\text{Rate of wt loss} = 0.03(T_a - 330)/D^{0.26} \quad (3.2-1)$$

$T_a$  = ambient temperature ( $^{\circ}\text{C}$ )

$D$  = particle diameter (mm)

The form was interpreted as describing a propagation of an evaporation front ( $T \approx 330^{\circ}\text{C}$ ) through the coal matrix. The particles studied were in the range 250 to 2000 $\mu$ .

Essenhigh (1963) modeled the devolatilization of coal particles as an "evaporative" phenomenon. The rate of the process is controlled by the transport of volatiles through a porous solid matrix. These volatiles are produced at the surface of a shrinking, spherical liquid core. The time required for devolatilization is given by:

$$t_v = K_v D^2 \quad (3.2-2)$$

$K_v$  is a constant inversely proportional to the char permeability and directly proportional to the volatile matter content of the coal.

The correlation was derived for particles of diameter 295 to 4760 $\mu$ .

Howard and Anthony (1976) point out the contradiction between the above two models, but attribute it to the possible temperature dependence



of  $K_v$ . They also point out that since the form of Equation 3.2-2 is that of the Fourier group ( $\alpha t/D^2$ ), then the nature of the model is determined by the interpretation of  $K_v$ . Experimental verification of the form of the equation does not distinguish between a mass transport limitation, as postulated, or a heat transport limitation whereby  $K_v$  is interpreted as a thermal diffusivity.

Howard and Essenhigh (1967) demonstrated that extrapolation of Equation 3.2-2 to particle diameters much less than about  $150\mu$  is inappropriate. Based on this and the evidence in the previous subsection, the choice of a particle diameter less than  $100\mu$  assures chemical control.

Anthony (1974; Anthony and Howard, 1976) studied the effect of particle diameter in the range  $53-1000\mu$ . The samples were held at  $1000^\circ\text{C}$  for 5-20 seconds in an electrical grid system. This residence time was sufficient to assure complete reaction of even the largest particles. The results (Fig. 3.2-16) show only a slight effect of diameter on total weight loss; about a 3% total decrease from the largest particle to the smallest.

Such an effect is consistent with the picture that has already been advanced; anything that is done to keep volatiles in contact with a hot reactive environment will lead to cracking and loss of yield. In the present case, the reactive environment is the coal particle itself, and the larger the coal particle, the longer the average transport time out of the particle.

Unfortunately, unlike most other types of systems where mass transport effects can be directly assessed by variation of the characteristic dimension of the system (i.e. particle diameter), in the case of coal, this approach involves the risk of potentially changing the nature of the chemical reactant as well. This point has already been discussed

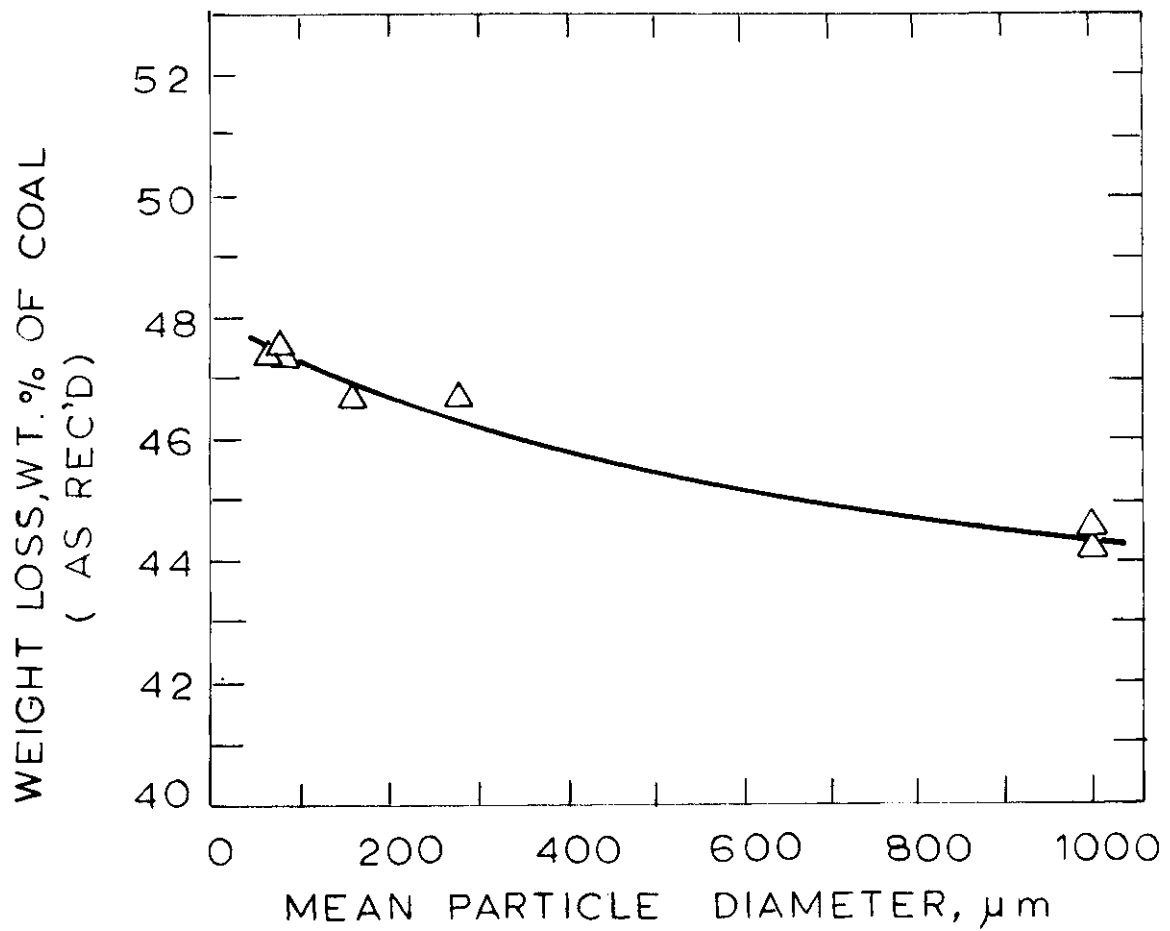


Figure 3.2-16 Effect of Particle Diameter on Pyrolysis Weight Loss (Anthony et al. 1976; 1000°C final temperature; Pittsburgh Seam Bituminous coal; 1 atm Helium Pressure).

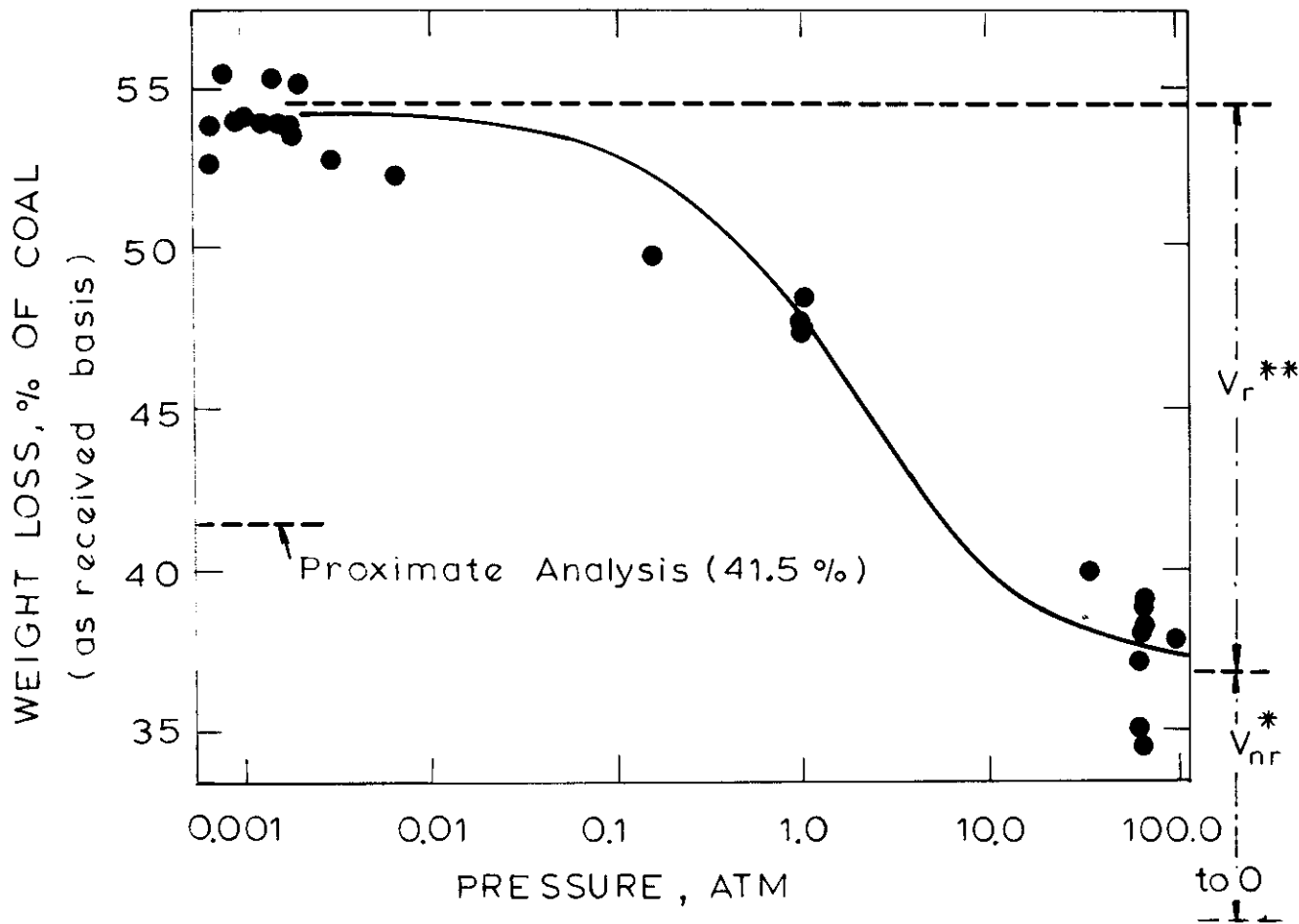


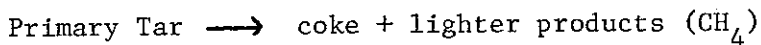
Figure 3.2-17 The Effect of External Pressure on Weight Loss During Pyrolysis (Anthony et al., 1975; Data for 1000°C pyrolysis in Helium; see Eq. 3.2-50 for explanation of symbols on right hand axis).

in the section on petrography.

Variation of external pressure as a means of varying mass transfer resistance offers clear advantages over variation of particle diameter in several respects. It avoids the problem of maceral enrichment, and it also permits in the present apparatus the variation of mass transfer resistance almost independently of heat transfer resistance. Data from pyrolyses run at non-atmospheric pressures are presented in the next section.

Effect of Pressure

Variation of the pressure of inert gas present during pyrolysis appears to have its largest effect in the yield of tar (H.C. Howard, 1963). There are no models which satisfactorily account for all the observed behavior, but it is believed that the general class of reactions responsible can be described by



In building a model for secondary reactions in coal, it is important to recognize that the reactions that lead to a loss of product on a weight basis can easily lead to a gain on a molar basis. In general, the weight ratio of gas to tar products increases with increasing pyrolysis pressure, as does the number of moles of gas produced per unit weight of coal.

In work on a Pittsburgh seam bituminous coal, Anthony et al. (1975) found a rather large effect of helium pressure in the range .001 to 100 atmospheres (see Fig. 3.2-17). Using the same rapid grid heating technique, they found virtually no effect on a Montana lignite. These data support the view that volatiles fraction which is most effected by variations in the external pressure during pyrolysis, is the tar fraction. This view is also supported by the data of Loison and Chauvin (1964) who

have observed increased yields of rather non-volatile tar from vacuum pyrolysis.

A well established pyrolysis phenomenon is the so-called autohydrogenation phenomenon, which involves an increase in the yield of  $\text{CH}_4$  with increasing inert gas pressure, while the yield of molecular hydrogen decreases. Recent evidence for this phenomenon is provided by Rennhack (1964). In this work, Rennhack first partially carbonized a high volatile bituminous coal at  $580^\circ\text{C}$ . This char was then pyrolyzed at higher temperatures ( $850^\circ\text{C}$  attained at  $5^\circ\text{C}/\text{min}$ ) and the rates of formation of hydrogen and methane were recorded as functions of temperature under both 1 and 20 atmospheres of nitrogen. It was noted that the rates of formation were such that for a given temperature, although the ratio of  $\text{H}_2$  to  $\text{CH}_4$  varied, the sum

$$\Sigma \text{H} = 2 \text{H}_2 + \text{CH}_4$$

was independent of pressure. It was hypothesized by the author that molecular hydrogen and methane represent the products of two competing reaction pathways involving hydrogen radicals. Since the overall rate of hydrogen loss from the char was independent of pressure, the formation of hydrogen radical intermediates must be rate controlling. Because these experiments were run with char rather than raw coal, it was possible that the reactions responsible for the behavior were largely of the so-called "slow degassing" variety, leading to increasing aromatization of the coke.

Recently, Banerjee et al. (1973) studied the pyrolysis of several coals in vacuum and various gases. An anthracitic coal (92.9% C, 14.4 VM, daf) displayed relatively little difference between pyrolysis in vacuum and under nitrogen and argon (unfortunately, the actual pressure was not specified, but presumably is atmospheric). A lignite (73.5% C, 55.8% VM) showed somewhat more effect, and the largest effect was shown

by a "tertiary" coal (80.7% C, 43.7% VM). Pyrolysis in vacuum dramatically decreased the yield of ethylene from pyrolysis of the latter coal.

The effect of external pressure has been modelled by a few workers; these models will be described in the following section. This thesis includes additional data on the effect of pressure on product composition and pyrolysis kinetics.

### 3.2.2 Modelling of Pyrolysis Phenomena

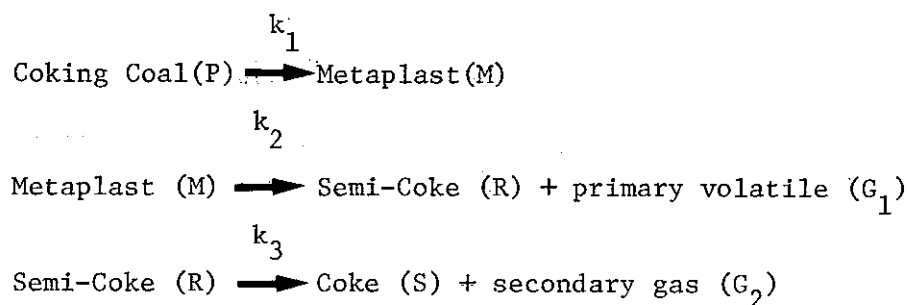
This section described first, the models derived to explain pyrolysis rate phenomena on a purely chemical basis and then, the models developed to account for the finite rate of mass transport out of the particle and the competitive reaction phenomena involved.

It should be emphasized at the outset that there is at present no one model which is suitable for describing all pyrolysis phenomena. A truly general model would have to account for the wide range of behavior observed in going from non-softening lignites, through softening bituminous and back to a non-softening process in anthracite. It must account for the entire spectrum of products observed and the effects of various operating parameters (e.g. pressure, particle size) on this spectrum.

A few physically based (e.g. heat mass transfer limited) models have already been presented in the preceding sections. It is assumed in presenting the "basic models" that such transport limitations do not exist. This view is modified somewhat in the subsection on "transport models".

#### Basic Models

The classic Van Krevelen-Fitzgerald model for pyrolysis of a coking coal has already been presented:



The first stage of the process, characterized by rate constant  $k_1$ , results in the formation of a meta-stable plastic intermediate (the metaplast, M). The second stage, characterized by rate constant  $k_2$ , describes the resolidification of the intermediate material. The third step, whose rate is governed by  $k_3$ , involves the degassing of the resolidified mass.

These steps were described mathematically by Chermin and Van Krevelen (1957) and later again by Van Krevelen (1961). The rate expressions for the three steps are derived assuming first order kinetics:

$$-\frac{dP}{dt} = k_1 P \quad (3.2-3)$$

$$\frac{dM}{dt} = k_1 P - k_2 M \quad (3.2-4)$$

$$\frac{dG}{dt} = \frac{dG_1}{dt} + \frac{dG_2}{dt} = k_2 M + k_3 R \quad (3.2-5)$$

where  $t$  is time, the  $k$ 's are rate constants ( $\text{time}^{-1}$ ), and  $P, M, R, G$ , represent the weights of raw coal, metaplast, semi-coke and volatiles respectively. It is assumed that  $k_2 \approx k_3$ , based on the fact that the temperature of maximum rate of weight loss is very close to the temperature of maximum fluidity for coking coal. (see Fig. 3.2-3). It can, however, be noted that since plasticity is proportional to  $M$ , the model can predict essentially non-plastic behavior if  $k_2 \gg k_1$ . A further simplification is possible in that the secondary degasification reaction only becomes important after most weight loss has occurred.

Therefore, if interest is focussed on the early phases of pyrolysis

$$\frac{dG_2}{dt} \approx 0 \quad T < T \text{ maximum devolatilization rate}$$

Thus (3.2-5), (3.2-4), and (3.2-6), respectively, can be written as

$$\frac{dG}{dt} = k M \quad (3.2-6)$$

$$\frac{dM}{dt} = k (P - M) \quad (3.2-7)$$

and

$$\frac{dP}{dt} = k P \quad (3.2-8)$$

Solution of this set is straightforward in an isothermal system, but analytical solution is difficult in the usually encountered case of an approximately linear temperature rise ( $T = mt$ ). Chermin and Van Krevelen approximate the linear temperature rate with the function:

$$a t = \exp(-2T_i/T) \quad (3.2-9)$$

The parameters  $a$  and  $T_i$  are adjustable, and the function is approximately linear for  $0.8 \leq (T/T_i) \leq 1.3$ . In this range

$$a = \frac{2m}{e^{2T_i}} = \frac{m}{3.69 T_i} \quad (3.2-10)$$

Employing this function, the solutions of (3.2-6), (3.2-7), and (3.2-8) are given by:

$$P = P_0 \exp[-k't] \quad (3.2-11)$$

$$M = P_0 k't \exp[-k't] \quad (3.2-12)$$

$$G = P_0 \{1 - (k't + 1) \exp[-k't]\} \quad (3.2-13)$$



where  $P_0$  is the amount of coking coal present at time zero and  $k'$  is given in terms of the Arrhenius pre-exponential ( $k_0$ ) and activation energy ( $E$ ) as:

$$k' = \frac{k_0 \exp(-E/RT)}{\frac{E}{2RT_i} + 1} \quad (3.2-14)$$

Upon application of equation (3.2-12) to real weight loss data, Chermin and Van Krevelen obtained activation energies ranging from 52 to 59 kcal/mole for various samples of coal heated at rates between 0.6 and 6.6°C/min to 600°C. This result clearly does not include secondary degassing reactions.

In order to model the secondary degassing reactions by a first order process, Chermin and Van Krevelen resorted to a distributed activation energies model (though not by that name). Distributed activation energies models have frequently been successfully applied to describe various aspects of coal pyrolysis; other applications will be presented later in this section.

The form of the distribution function chosen in this case was:

$$E_3 = A + B\psi \quad (3.2-15)$$

where  $E_3$  is the activation energy for secondary degasification,  $A$  and  $B$  are constants, and  $\psi$  is the percentage of volatile matter yet to be evolved from the semi-coke. The overall of secondary degasification is given by:

$$\frac{dG_2}{dt} = k_3^0 \exp(-E_3/RT) \quad (3.2-16)$$

where  $k_3^0$  is the Arrhenius pre-exponential. In fitting these equations to data on pyrolysis, it was found that the following set of parameters

was satisfactory:

$$k_0 = k_3^0 = 8.33 \times 10^{13} \text{ sec}^{-1}$$

$$E = 50 \text{ kcal/mole}$$

$$E_3 = 100 - 3.29\psi \text{ kcal/mole } (\psi < 14\%)$$

It is again encouraging to note that the activation energy for primary decomposition is typical of those for other, simpler organic decomposition reactions (see Table 3.2-3). The choice of values for the pre-exponentials and  $E_3$  were presumably guided by other physical evidence. The activation energy of  $E_3$  was set according to the evidence on the nature of carbon-hydrogen bonds. The C-H bond has a bond energy of about 100 kcal/mole. Since secondary degassing involves aromatization with evolution of hydrogen or, as Rennhack (1964) later showed, compounds whose rate of evolution are determined by hydrogen radical formation, it is logical that a fairly high activation energy should apply.

There is a fair amount of debate in the literature, however, concerning activation energies for high temperature hydrogen evolution. Worrall and Walker (1959) claim zero order kinetics and an activation energy of 96 kcal/mole, interpreted as desorption of "chemisorbed" hydrogen. Berkowitz and den Hartog (1962) claim a first order process with an activation energy 8-15 kcal/mole, interpreted as a pseudo-activation energy for lamellar movements. More recently, Campbell and Stephens (1976), using a first order model, obtained a value of 22.3 kcal/mole, in fair apparent agreement with Berkowitz and den Hartog. Campbell and Stephens, however, correctly point out that these low values of the activation energy

may be artificial. If a distribution of activation energies, as assumed by Chermin and Van Krevelen, does exist, then a broad temperature dependence by hydrogen release is forced, and modelling with a single (not distributed) first order expression will require artificially low values of the activation energy and pre-exponential. The results of Rennhack (1964) support this conclusion and suggest a distribution of high activation energies.

The selection of a pre-exponential factor of approximate order  $10^{13}$   $\text{sec}^{-1}$  by Chermin and Van Krevelen also has basis in general chemical principles. The derivation of the principal equation of absolute reaction rate theory for solids (or any other reactant; see for instance, Krantz and Eyring, 1976) involves calculation of the average speed of a molecule crossing a transition state-product barrier:

$$\bar{v} = \left( \frac{k_B T}{2\pi m} \right)^{1/2} \quad (3.2-17)$$

where the expression is derived from one dimensional statistical mechanics for a molecule of mass  $M$  and temperature  $T$ .  $k_B$  is the Boltzmann constant. The "width" of the activation energy barrier is assumed to be  $\Delta$ . The rate of reaction is determined by  $(\bar{v}/\Delta)$  times the number of molecules in "position" (i.e. activated) to cross the barrier at any time. This number is calculable from the ratio of the partition functions of activated to non-activated states. By breaking one degree of vibrational freedom (in the direction of bond breakage) out of the activated state partition function and treating it as the translational motion of a particle of mass  $M$  in a one dimensional "box" of length  $\Delta$ , one obtains

$$Q_T = \frac{(2\pi M k_B T)^{1/2}}{h} \Delta \quad (3.2-18)$$

The product  $(Q_T) \left(\frac{\bar{V}}{\Delta}\right)$  leads to a term  $(k_B T/h)$ . The remaining terms in the ratio of partition functions give rise to a pseudo equilibrium constant of activation  $K = \exp(-\Delta G^\ddagger / RT)$ .

The overall rate constant is given by

$$k = \left(\frac{\bar{V}}{\Delta}\right) (Q_T^\ddagger K^\ddagger) = \left(\frac{k_B T}{h}\right) \exp\left[-\frac{\Delta G^\ddagger}{RT}\right] \quad (3.2-19)$$

Rewriting this in terms of other thermodynamic functions:

$$k = \left(\frac{k_B T}{h}\right) \exp\left[\frac{\Delta S^\ddagger}{R}\right] \exp\left[-\frac{\Delta H^\ddagger}{RT}\right] \quad (3.2-20)$$

Then by analogy with the standard Arrhenius result:

$$\left(\frac{\partial \ln k}{\partial T}\right)_{V \text{ or } P} = \frac{E}{RT^2} \quad (3.2-21)$$

In a condensed phase, (3.2-20) gives

$$\left(\frac{\partial \ln k}{\partial T}\right)_P = \frac{\Delta H^\ddagger + RT}{RT^2} \quad (3.2-22)$$

And thus,

$$E = \Delta H^\ddagger + RT \quad (3.2-23)$$

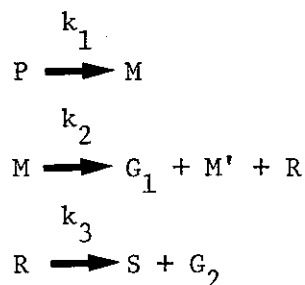
and

$$k_0 = \left(\frac{e k_B T}{h}\right) \exp\left[\frac{\Delta S^\ddagger}{R}\right] \quad (3.2-24)$$

Choosing a reasonable value for temperature (about 500°C in Chermin and Van Krevelen's work) leads to a theoretical value of  $k$  of about  $4.4 \times 10^{13} \text{ sec}^{-1}$ , if one assumes the entropy of activation is zero. Deviations of  $\Delta S^\ddagger$  from zero will lead to higher or lower pre-exponential factors. These deviations can physically arise from an activation process which proceeds via an activated complex which is "loose" or "tight" relative to a ground state molecule.

In an attempt to improve the robustness of the model, Chermin and Van Krevelen included a term to account for the physical loss of

metaplast as a tar mist carried away by rapidly evolving gas. This loss would be accounted for in the overall reaction scheme as a modification of the second reaction in the sequence, giving:



which leads to the rate expressions:

$$-\frac{dP}{dt} = k_1 P \quad (\text{as before, 3.2-3})$$

$$\frac{dM}{dt} = k_1 P - k_2 M(1 + k' M) \quad (3.2-25)$$

and

$$\frac{dG}{dt} = \frac{d(G_1 + M')}{dt} + \frac{dG_2}{dt} = k_2 M(1 + k' M) + k_3 R \quad (3.2-26)$$

In deriving the above equations, it was assumed that the amount of Metaplast (M') carried away at any time is proportional to both the amount of metaplast present (M) and the rate of devolatilization at that moment. This naturally leads to the pseudo second order form shown by (3.2-25). Chermin and Van Krevelen offer no solution to this set except to note that the maximum devolatilization rate must increase with heating rate. The properties of this kind of model will be explored further in a later section, with regard to the findings of this thesis.

Recent years have seen a number of simple models based upon weight loss data alone. Badzioch and Hawksley (1970) correlated the maximum obtainable weight loss with ASTM type volatile matter determinations. The expression for maximum weight loss is given by:

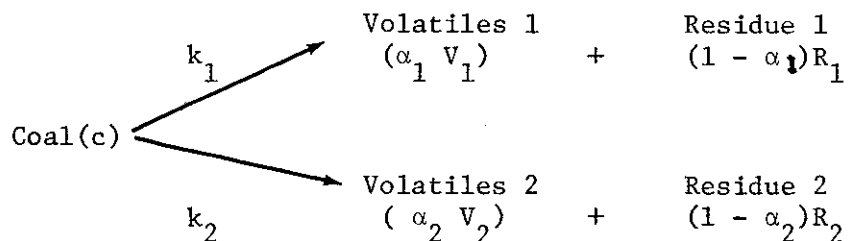
$$\Delta W_{\text{MAX}} = Q(\text{VM})(1 - C) \quad (3.2-27)$$

where VM is the original volatile matter in the coal, C is the fractional retention of volatile matter at  $t = \infty$ , and Q is a somewhat scattered function of rank. The value of activation energy derived from a simple first order model is low (about 18 kcal/mole) as one would expect from such a model.

Howard and Essenhigh (1967) used a two step first order model to describe pyrolysis occurring in a flame front. The calculated values of the activation energy were again low, 3.4 and 27.7 kcal/mole.

Wiser et al. (1967) examined various pyrolysis models and concluded that the order of reaction changed with extent of pyrolysis. Based on the rate of weight loss during the first 60 minutes (at temperatures between 409° and 497°C), Wiser et al. concluded that the process was second order with an activation energy of 36.6 kcal/mole. The next 100 minutes was first order with an activation energy of 5.36 kcal/mole, and is followed by a zero order reaction phase. This view was supported by the data of Skylar et al. (1969).

Kobayashi (1976) suggested a simple competitive model, consisting of two first order reactions:



with  $k_1$  and  $k_2$  the standard form Arrhenius rate constants for the following rate equations

$$\frac{dM_C}{dt} = -(k_1 + k_2) M_C \quad (3.2-28)$$

$$\frac{dM_{V1}}{dt} = -\alpha_1 M_C \quad (3.2-29)$$

$$\frac{dM_{V2}}{dt} = -\alpha_2 M_C \quad (3.2-30)$$

The model fits the data from rapid heating (calculated heating rates of  $10^4$  to  $10^5$  °C/sec, calculated maximum temperature about 1800°C) experiments well with activation energies of about 25 and 40 kcal/mole for the two steps, for both a lignite and bituminous coal (Kobayashi et al., 1977).

Unfortunately, the utility of these types of simple first order, nth order, and competitive reaction models (and there are several more, see Anthony and Howard, 1976) must be questioned if the results are to be applied outside the range of operating parameters for which they were derived. Whereas the metaplast model of Chermin and Van Krevelen is based upon mechanistic grounds and is backed by measurements of several different properties of coals and model substances, these simple weight loss models are generally only correlative tools. The very low activation energies obtained via these models is to be expected, since they sweep many different processes into a single rate constant. Similarly it is not clear, from a mechanistic viewpoint, what significance can be attached to reaction orders or competitive reaction steps in a process where a large number of distinct processes manifest themselves at different temperatures.

Several approaches to using weight loss data alone to develop a multiple reaction model have been cited. Chermin and Van Krevelen postulated the secondary degassing reactions were linearly distributed in activation energy (Equation 3.2-15). Howard and Essenhigh (1967) postulated two activation energies in the devolatilization of combusting pulverized coal. Pitt (1962) developed a model based upon a distribution of activation energies. Working with a fluidized bed of coal at temperatures from 300 to 650°C, Pitt measured the average volatile matter remaining in the coal after a given length of pyrolysis time (10 seconds to 100 minutes), and based upon a multiplicity of first order reactions of form

$$\frac{dn_i}{dt} = -k_i n_i \quad (3.2-31)$$

obtained the distribution function for  $n_i$  vs. activation energy shown in Fig. 3.2-18.

Anthony et al. (1975) used a similar approach, but were able to study the behavior of the distribution analytically by assuming it to be Gaussian in form. Studying the weight loss of a Pittsburgh Seam Bituminous and a Montana lignite heated rapidly (up to 10<sup>4</sup>°C/sec, temperatures up to 1000°C), Anthony first fit his data to a single first order model of the form:

$$\frac{dV}{dt} = k(V^* - V) \quad (3.2-32)$$

where

$V$  = fractional weight loss at time  $t$

$V^*$  = fractional weight loss at "long" times

$k$  = Arrhenius rate constant

The activation energies obtained by fitting this model to weight loss data were the usual low (7-13 kcal/mole) values obtained from first



order models. A much more mechanistically satisfying range of values was obtained from a distributed activation energies model.

Instead of the single first order model (3.2-32), a multitude of independent first order decomposition reactions exist, each of the form:

$$\frac{dV_i}{dt} = k_i (V_i^* - V_i) \quad (3.2-33)$$

$$\text{with } k_i = k_{i0} \exp(-E_i/RT) \quad (3.2-34)$$

where

$E_i$  = activation energy for reaction i

$k_{i0}$  = Arrhenius pre-exponential for reaction i

$V_i$  = fractional weight loss at time t due to reaction i

$V_i^*$  = fraction of weight loss at long times due to reaction i

Then, by integration over an arbitrary time temperature history

$$\frac{V_i^* - V_i}{V_i^*} = \exp \int_0^t -k_i dt \quad (3.2-35)$$

The activation energies are assumed distributed according to the function:

$$f(E_i) = \frac{1}{\sqrt{2\pi}\sigma} \exp[-(E_i - E_0)^2 / 2\sigma^2], \quad (3.2-36)$$

which is the Gaussian distribution, with mean activation energy  $E_0$  and standard deviation  $\sigma$  (units of kcal/mole). The contribution of each reaction i to total weight loss is then:

$$dV^* = V^* f(E) dE \quad (3.2-37)$$

(dropping the subscript i)

Since for the Gaussian distribution

$$\int_{-\infty}^{\infty} f(E) dE = 1 \quad (3.2-38)$$

the total fractional unaccomplished devolatilization is given by integration of (3.2-35)

$$\frac{V^* - V}{V^*} = \int_0^{\infty} \exp\left[-\int_0^t k dt\right] f(E) dE \quad (3.2-39)$$

Substitution of the definitions of the Arrhenius rate constant and Gaussian functions gives:

$$\frac{V^* - V}{V^*} = \frac{1}{\sigma\sqrt{2\pi}} \int_0^{\infty} \exp\left[-k_0 \int_0^t \exp(-E/RT) dt - \frac{(E-E_0)^2}{2\sigma^2}\right] dE \quad (3.2-40)$$

where it has been assumed that for simplicity all  $k_i = k_0$ .

Although this assumption robs the model of some generality, it is a property of the Arrhenius function that rather small uncertainties in fitting  $E$  leads to rather large uncertainties in  $k_0$ . Hence, the confidence in  $k_0$  values from the usually scattered coal data is low anyway.

In fitting his bituminous coal and lignite data to this model, Anthony obtained the following results

	Pittsburgh No. 8		Montana Lignite	
	$k_0$ fixed		$k_0$ "best fit"	$k_0$ fixed
$k_0$ (sec <sup>-1</sup> )	$1.67 \times 10^{13}$		$1.07 \times 10^{10}$	$1.67 \times 10^{13}$
$E_0$ (kcal/mole)	54.8		48.7	56.3
$\sigma$ (kcal/mole)	17.2		9.4	7.0

The results from the Montana lignite are compared to Pitt's distribution of activation energies in Fig. 3.2-18. Also shown is the distribution of activation energies for secondary degassing assumed by Chermin and Van Krevelen.

It can be seen from the data for lignite that fixing  $k_0$  at a value approximately suggested by absolute reaction rate theory gives slightly

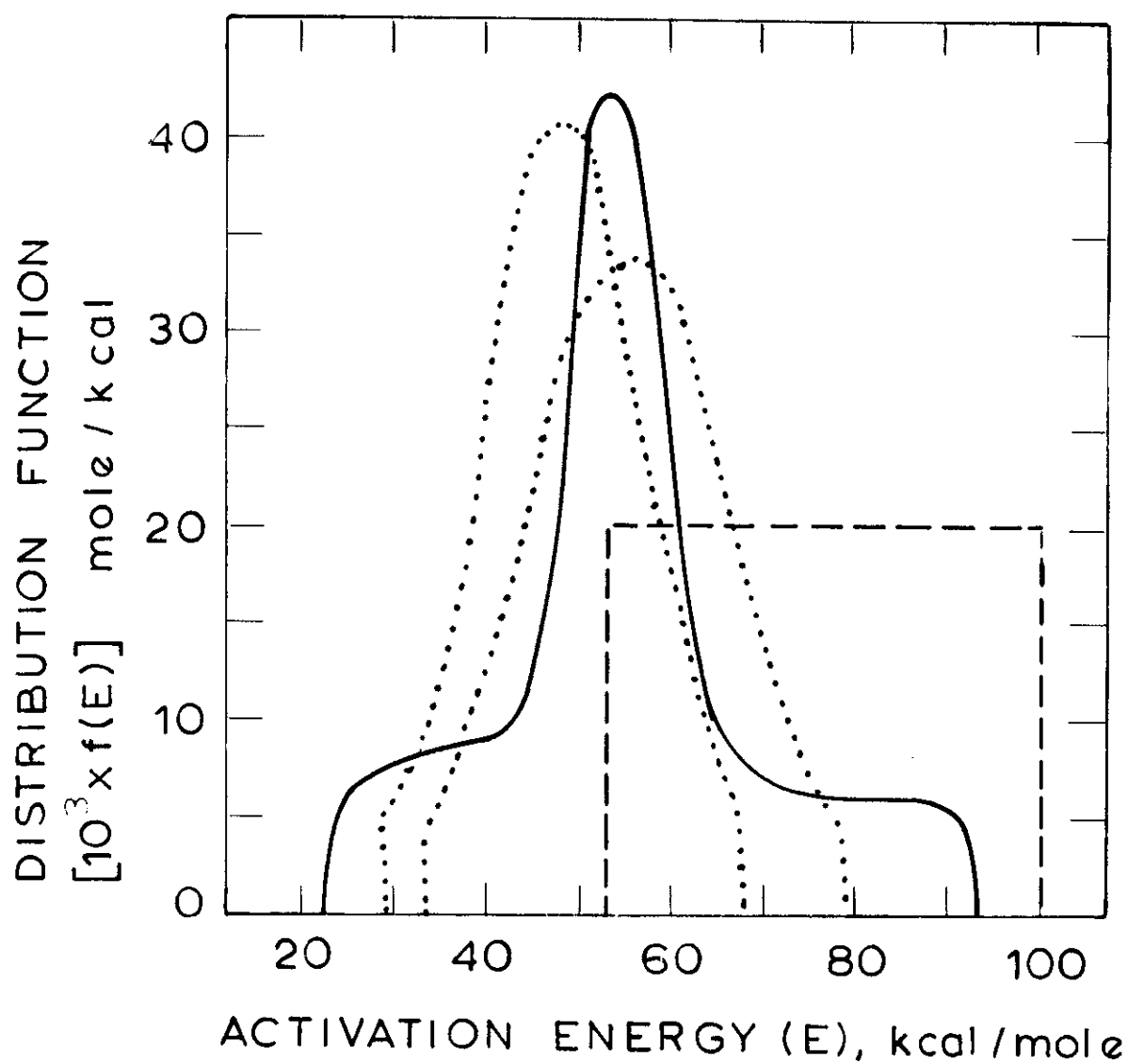
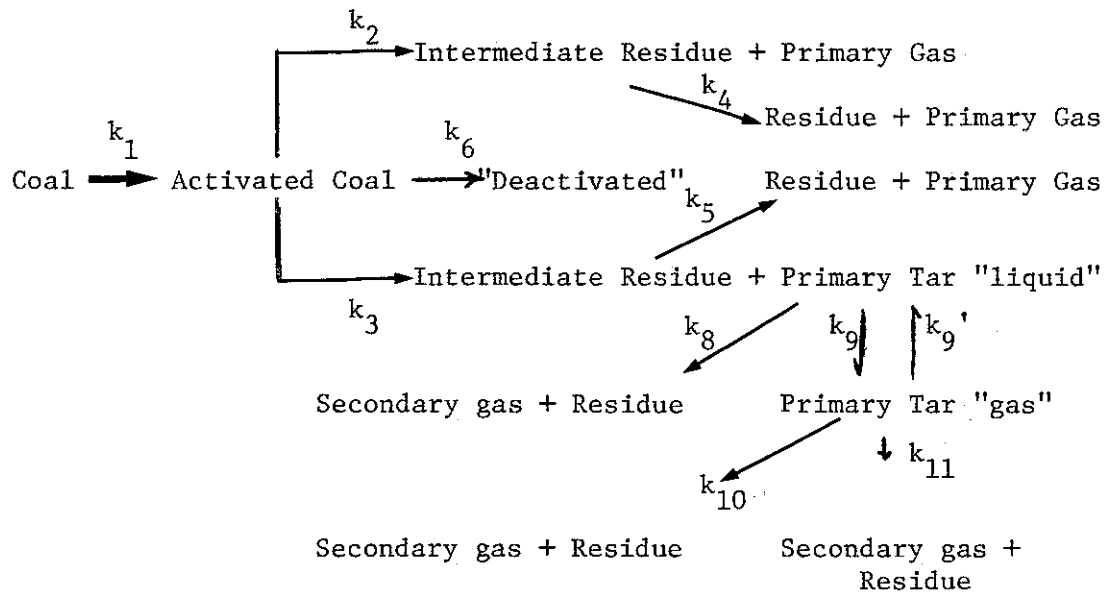


Figure 3.2-18 Comparison of Distributions of Activation Energies from Modelling of Coal Pyrolysis [curves; solid, Pitt (1962); dotted, Anthony et al. (1975), left- $k = 1.07 \times 10^{10} \text{s}^{-1}$ , right- $k_0 = 1.67 \times 10^{13} \text{s}^{-1}$  dashed, Chermin and Van Krevelen (1957)].

different results than those obtained by letting  $k_0$  be fit by a least squares fitting just as  $\sigma$  and  $E_0$ . However the values obtained by either technique are in good agreement with those of Table 3.2-3 and those obtained by Chermin and Van Krevelen for primary decomposition.

Another recently proposed model for pyrolysis is shown below (Reidelbach and Summerfield, 1975):



As is obvious by the complicated nature of the model, it accounts for many phenomena. However recent experimental results (calorimetric, Antal et al., 1977) have cast some doubt upon the very first step in the model, hypothesized to be second order with a high activation energy. This has led to a simplified model with six reaction steps, 1 reversible, and 19 adjustable parameters (Antal et al., 1977). A large number of adjustable parameters does not necessarily speak for or against a particular model. Certainly the modelling of coal pyrolysis phenomena can require many, many more than even 19 parameters if detailed predictive power is desired. But the key to success of multi-parameter models is in the tying of parameters to measurable, mechanistically

meaningful quantities.

The work of Jüntgen and Van Heek (1968, 1969, 1970, 1977) and Hanbaba, Jüntgen and Van Heek (1968) has focussed upon the evolution of pyrolytically formed gases at heating rates ranging from  $4 \times 10^{-5} \text{ }^\circ\text{C}/\text{sec}$  to over  $1000 \text{ }^\circ\text{C}/\text{sec}$ . It was pointed out by these workers that in experiments in which the coal was heated at a rate of  $0.01 \text{ }^\circ\text{C}/\text{min}$  the to  $700 \text{ }^\circ\text{C}$ , a single run lasts 47 days! Some of the results obtained by these workers have already been presented in Table 3.2-5 and Fig. 3.2-11.

In general, results were modelled by a series of independent first order models. The equation for a single reaction  $i$  is, again:

$$\frac{dV_i}{dt} = k_i (V_i^* - V_i) \quad (3.2-33)$$

If a linear heating rate is imposed on the system:

$$\frac{dT}{dt} = m, \quad (3.2-41)$$

then solution of the differential equation yields the following result for fractional unaccomplished devolatilization:

$$\frac{V_i^* - V_i}{V_i^*} = \exp\left[-\frac{k_{i0} RT^2}{m E_i} \exp\left(-\frac{E_i}{RT}\right)\right] \quad (3.2-42)$$

$$\text{for } E_i/RT \gg 1$$

The rate of weight loss at any particular temperature is given by:

$$\frac{dV_i}{dt} = V_i^* k_{i0} \exp\left[-\frac{E_i}{RT} - \frac{k_{i0} RT^2}{m E_i} \exp\left(-\frac{E_i}{RT}\right)\right] \quad (3.2-43)$$

It should be noted that these equations are only correct for the instant at which temperature  $T$  is reached. For instance, it is not appropriate to use (3.2-42) to predict total yield from a process in which the coal was heated to a peak temperature  $T$  and held there, or even cooled

from T at finite rate. For the case in which coal is heated to a temperature for a time  $\tau$ , (3.2-42) and (3.2-43) can be modified to:

$$\frac{V_i^* - V_i}{V_i^*} = \exp \left[ -k_{i0} \left( \frac{RT^2}{m E_i} + \tau \right) \exp \left( -\frac{E_i}{RT} \right) \right] \quad (3.2-44)$$

$$\frac{dV_i}{dt} = V_i^* k_{i0} \exp \left[ -\frac{E_i}{RT} - \left( \frac{k_{i0} RT^2}{m E_i} - k_{i0} \tau \right) \exp \left( -\frac{E_i}{RT} \right) \right] \quad (3.2-45)$$

A finite cooling rate can be accounted for by equations (3.2-42) and (3.2-43) if it is assumed that the cooling is linear at a rate  $m$  (not necessarily the same  $m$  as for heating) and if  $V_i^*$  is replaced by a "modified"  $V_i^*$  equal to the amount of volatile material left at the start of the cooling period.

Jüntgen and coworkers were primarily concerned with equations of the form of (3.2-43) for analysis of their data. Two different approaches were employed. The first involved the modelling of non-hydrocarbon gases by two separate first order processes. The kinetic parameters derived for this two step behavior (see Fig. 3.2-10) are shown in Table 3.2-6. Another set of data, for hydrocarbon gases, was analyzed in terms of reaction "complexes". Each reaction complex is characterized by a large number of independent, parallel first order reactions having a Gaussian distribution of activation energies (characterized by a mean  $E_0$  and standard deviation  $\sigma$ ) and a Gaussian distribution of pre-exponentials (characterized by a mean  $k_{00}$  and a standard deviation  $\Delta \log k_0$ ). The results are shown in Table 3.2-7, for some of the curves displayed in Fig. 3.2-11. The fit is good, but not surprisingly so in light of the large number of parameters involved.

Campbell and Stephens obtained data of the same kind on a subbituminous coal. They employed 1, 2, or 3 independent first order reactions to model

Table 3.2-6 Kinetic Parameters for the Evolution of Some Nonhydrocarbon Gases from Coals (Jüntgen and Van Heek, 1977)

Coal <sup>a</sup>	Peak 1		Peak 2		V* (both peaks), wt.% of coal
	E, kcal/mole	k <sub>o</sub> , s <sup>-1</sup>	E, kcal/mole	k, s <sup>-1</sup>	
<u>H<sub>2</sub>O</u>					
1	33.5	3.3 x 10 <sup>6</sup>	34.0	5.8 x 10 <sup>5</sup>	0.72
2	32.0	1.3 x 10 <sup>6</sup>	33.5	1.7 x 10 <sup>5</sup>	1.10
3	31.4	1.1 x 10 <sup>6</sup>	33.1	1.5 x 10 <sup>5</sup>	1.31
4	31.0	1.0 x 10 <sup>6</sup>	33.0	1.4 x 10 <sup>5</sup>	2.43
<u>CO<sub>2</sub></u>					
1	26.5	1.2 x 10 <sup>4</sup>	45.5	1.1 x 10 <sup>7</sup>	0.63
2	25.8	1.0 x 10 <sup>4</sup>	41.9	2.3 x 10 <sup>6</sup>	0.71
3	23.0	1.3 x 10 <sup>3</sup>	39.5	6.5 x 10 <sup>5</sup>	0.25
4	21.8	7.5 x 10 <sup>2</sup>	37.0	1.7 x 10 <sup>5</sup>	0.81
<u>CO</u>					
1	27.0	3.3 x 10 <sup>3</sup>	41.0	2.0 x 10 <sup>6</sup>	1.59
2	26.5	1.5 x 10 <sup>3</sup>	40.2	1.7 x 10 <sup>6</sup>	1.70
3	25.5	1.3 x 10 <sup>3</sup>	38.5	3.8 x 10 <sup>5</sup>	1.94
4	22.0	1.7 x 10 <sup>2</sup>	33.0	3.3 x 10 <sup>4</sup>	3.15
<u>N<sub>2</sub></u>					
1	50.4	4.2 x 10 <sup>7</sup>	72.5	1.3 x 10 <sup>7</sup>	0.35
2	46.0	7.5 x 10 <sup>6</sup>	67.0	8.3 x 10 <sup>6</sup>	0.42
3	42.6	1.5 x 10 <sup>6</sup>	64.5	2.5 x 10 <sup>6</sup>	0.66
4	39.0	3.3 x 10 <sup>5</sup>	59.5	1.0 x 10 <sup>6</sup>	0.95

<sup>a</sup>Coals: (1) Heinrich; (2) Dickebank; (3) Gustav; (4) Fürst Leopold

Table 3.2-7 Kinetic Parameters for the Evolution of Hydrocarbon Gases from Coal (Hanbaba, 1967; Hanbaba *et al.*, 1968; Jüntgen and Van Heek 1969 and 1970)

Gas	Coal <sup>a</sup>	$E_o$ , kcal/mole	$\sigma$ kcal/mole	$k_{oo}/1.67$ $s^{-1}$	$\Delta \log k_o$	$V^*$ wt.% of coal
CH <sub>4</sub>	1	53.5	6.0	10 <sup>12</sup>	0.6	2.11
	1	58.0	6.0	10 <sup>12</sup>	0.6	0.84
	1	62.0	6.0	10 <sup>12</sup>	0.6	0.81
	1	69.0	6.0	10 <sup>12</sup>	0.6	0.49
C <sub>2</sub> H <sub>6</sub>	1	59.7	4.0	10 <sup>15</sup>	0.4	0.31
	1	56.0	5.0	10 <sup>13</sup>	0.5	0.39
	1	62.0	5.0	10 <sup>13</sup>	0.5	0.01
C <sub>3</sub> H <sub>6</sub>	1	60.0	4.0	10 <sup>15</sup>	0.4	0.26
C <sub>3</sub> H <sub>8</sub>	1	56.5	3.5	10 <sup>14</sup>	0.35	0.29
	2	58.3	3.0	10 <sup>14</sup>	0.3	0.26
	3	59.5	2.5	10 <sup>14</sup>	0.25	0.12
	4	62.0	3.0	10 <sup>14</sup>	0.3	0.01
cis-2-C <sub>4</sub> H <sub>8</sub>	1	60.0	4.0	10 <sup>15</sup>	0.4	0.03
n-C <sub>4</sub> H <sub>10</sub>	1	59.3	3.5	10 <sup>15</sup>	0.35	0.13

<sup>a</sup>Coals (1) Fürst Leopold; (2) Gustav; (3) Dickebank; (4) Heinrich.



their data (see Fig. 3.2-10) and obtained the results shown in Table 3.2-8. Some of the values obtained by Jüntgen and coworkers and Campbell and Stephens are difficult to interpret because they are rather low. Both systems involved on line monitoring of products, but because of the slow heating rates involved (1-3.3°C/min for most of the data in the tables), it is difficult to attribute the low parameter ranges to sampling lags resulting in "dispersion" of sample. The activation energies seem typically too high to be related to diffusional processes, but too low for chemical processes. It has already been pointed out with regard to the low activation energy obtained by Campbell and Stephens for H<sub>2</sub> that this could be due to modelling of a distributed activation energy phenomenon with a single activation energy. This could explain also why Jüntgen and Van Heek's hydrocarbon gas parameters seem more "reasonable" than Campbell and Stephens values.

The model currently under development by Gavalas and coworkers (Cheong, 1977, Cheong et al., 1975) has already been discussed several times. The section on coal structures and model compounds have described the theoretical "construction" of coal model substances on the computer. Having constructed a model, the pyrolysis algorithm involves selection from a table of fifty-seven different types of reactions that structures in the coal could undergo. Literature values provide the basic kinetic parameters for the model. Cheong considers two important chemical phenomena to be considered in application of literature gas phase kinetic data to materials in a condensed phase. These are the so-called "cage" and "gel" effects. The cage effect manifests itself in bridge scission type reactions, e.g.,

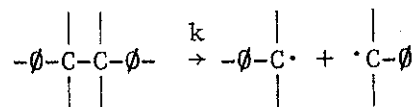


Table 3.2-8 Kinetic Parameters for Evolution of Hydrogen, Carbon Oxides and Some Hydrocarbons from a Subbituminous Coal [Campbell and Stephens, 1976. Roland Seam (Wyodak mine) coal]

Gas	Peak	E, kcal/mole	$k_o, s^{-1}$	V* wt.% of coal
H <sub>2</sub>		22.3	20	1.02
CH <sub>4</sub>	1	31.0	$1.7 \times 10^5$	1.42
	2	31.0	$2.8 \times 10^4$	1.56
	3	35.3	$3.0 \times 10^4$	1.42
	total			4.40
C <sub>2</sub> H <sub>4</sub>		33.4	$2.3 \times 10^6$	0.22
C <sub>2</sub> H <sub>6</sub>		33.4	$1.7 \times 10^6$	0.81
C <sub>3</sub> H <sub>8</sub>		35.0	$7.3 \times 10^6$	0.43
CO	1	18.0	55	1.58
	2	30.2	$2.5 \times 10^3$	3.68
	total			5.26
CO <sub>2</sub>	1	19.5	550	5.49
	2	23.0	230	4.75
	total			10.24
Total				22.38

Depending upon what else the aromatic structures are linked to, the dissociated species may not be truly free of one another. Steric hindrance may prevent the radicals from participating in any chemistry except recombination. Hence, the observed rate of bond scission  $k'$  may be somewhat lower than the true rate  $k$ , and the apparent  $k_0$  is below its theoretical value as derived from 3.2-24.

The "gel" effect again primarily affects functional groups on aromatic clusters. In this case, it serves to decrease the rate at which functional groups on strongly bridged aromatics can participate in hydrogen abstraction and radical recombination reactions.

Because of the large number of parameters involved in this model, a vigorous program of sensitivity testing would seem to be necessary. The first version of the program, when subjected to sensitivity tests (Cheong, 1977) singled out structural parameters related to the number and distribution of aliphatic bridges as being important in determining weight loss, whereas aromaticity and average ring size did not have profound effect in the ranges tested. Also identified as an important variable is the fraction of coal volume near to a "surface", whence volatiles could escape (Cheong, 1977).

Experimental verification of this model is likely to be difficult. Since the model accounts for so many different effects, it is not clear what would constitute a satisfactory test. It also may be difficult to discern a "failure" in the structure generation scheme from a failure in the reaction scheme, in the event that predicted products do not match real products.

#### Modelling of Mass Transport-Secondary Reaction Effects

A secondary reaction is generally defined as any reaction in which

already formed volatiles participate. This could include the reactions of volatiles that have already formed but not escaped the coal particle, or it could include the reactions between volatiles which have escaped a particle, but must yet escape the hot reactor environment. Examples of the latter could include reactions between char and volatiles in carbonizing retorts, coke ovens, and even the ASTM crucible, which reduce tar yield and increase gas yield. Eddinger et al. (1966) found clear evidence for the coking of coal tars in a transport reactor used to study coal pyrolysis. Small flecks of "vapor-cracked" carbon were visible both separately and as a coating on char particles.

Although the reactions of vapor phase volatiles will be vitally important in any applications involving pyrolysis, the modelling and prediction of these phenomena can draw upon an extensive body of literature. Unfortunately, the role of secondary reactions within coal particles are much less well understood.

Perhaps the first task in examining these phenomena would be to offer a working definition of the difference between primary and secondary reaction phenomena within a coal particle. It is tempting to say that any volatile species that is formed by scission of a bond from a non-volatile species is the product of a primary reaction. This definition would however exclude some material which is perhaps fluid on the surface of the coal, but could either 1) be carried away with the volatile matter by Chermin and Van Krevelen's "entrained" metaplast mechanism, or 2) only slowly vaporize as the particle is further heated. If we extend the definition of primary reactions to include those which form these pseudo-volatiles, then the definition for secondary reactions must become those reactions which 1) render primary species which would otherwise (by some mechanism

end up as "volatile matter", totally or partially in volatile and

2) reactions within the particle among gaseous species, or between vapor species and condensed materials, such as  $\text{CO}_2 + \text{C} \rightarrow 2\text{CO}$ ,  $\text{H}_2\text{O} + \text{C} \rightarrow \text{H}_2 + \text{CO}$ ,  $\text{H}_2\text{O} + \text{CO} \rightleftharpoons \text{H}_2 + \text{CO}_2$ ,  $2\text{H}_2 + \text{C} \rightleftharpoons \text{CH}_4$ .

From a total yield standpoint, the first set of reactions is the more important. Pyrolysis tars can have molecular weights in the hundreds or even thousands of grams per mole (Weiler, 1963). Though much of the data on coal tars has been obtained from coke oven products, the recent results obtained by Cheong et al. (1975) on tars produced in an electrical grid system indicate that a little less than 40% (by weight) are in the range 300-700 g/mole, about 40-50% in the range 700-1000 g/mole, and a little less than 20% are over 1000 g/mole in molecular weight (from a Hamilton C Bituminous coal, pyrolyzed at about 500°C). Thus the "loss" of a mole of tar to the residue could have a significant depressing effect on total yield, even if in subsequent cracking reactions several moles of light products (e.g.  $\text{CH}_4$ ,  $\text{H}_2$ ) were produced.

With the foregoing background, examination of the literature reveals rather few solid attempts to account for the competition between mass transport and secondary reactions within pyrolysis coal particles. It should be emphasized at the outset that the modes of transport will likely be somewhat different in softening and non-softening coals. The latter retain a well defined pore structure during pyrolysis, consisting of macro- ( $>300\text{\AA}$ ) micro- ( $<12\text{\AA}$ ) transitional pores ( $12-300\text{\AA}$ ). Naturally, the nature of this porosity does change upon carbonization, generally increasing with increasing temperature. However, the micropores gradually are closed off to even helium at sufficiently high temperatures (Franklin, 1949). This is attributed to micellar rearrangement during carbonization

and could reflect closer "packing" of molecules.

The modes of transport in a softening coal can be expected to be somewhat different from that in non-softening coals. It is a well known phenomenon that plastic coals rapidly bubble during pyrolysis, much as a boiling liquid. Occasionally, individual particles can be seen to blow up into balloon-like structures (cenospheres) many times their original size. Chermin and Van Krevelen in their model describe the possibility that rapidly evolving gas could burst through the surface and carry away droplets of metaplast.

Another model which focussed principally upon transport in softening coals is that of Lewellen (1975). The model is divided into four phases; bubble initiation, growth, coalescence, and escape. It is assumed that the secondary reactions of volatiles occur only within bubbles and that the bubbles act as well stirred reactors. The reactions are characterized as primarily repolymerizations at the walls of the bubble. Thus the competition between transport and secondary reactions depends upon the chemical rate of secondary reactions and the rate of escape of bubbles, which in turn depends on "fluid coal" parameters such as viscosity and, less importantly, surface tension. Although the trends of experimental data were often matched (e.g. viscosity vs. time, cenosphere formation vs. time, reduction in yield vs. particle diameter), the model is perhaps somewhat weak in one respect. The volatiles within the bubbles are assumed to be representative of the entire spectrum of products, and are treated in a completely time averaged, homogeneous fashion. While this may indeed lead to very reasonable results concerning the bubbling fluid behavior of coal, it is likely to weaken the robustness of the model in studying secondary reaction phenomena. Assuming, for instance, that the model

describes a coal that produces 30% by weight tar, and 15% gas, and these have molecular weights of 400 and 20 respectively, then on a molar basis, the tar is present in quantities an order of magnitude less than gaseous, non-crackable, species. Further, it is not clear what the partitioning of tar between vapor and condensed phase should be.

The vapor pressure of coal tar can be calculated from correlations suggested by Homann (1976) for aromatic and partially hydrogenated aromatics (with or without small aliphatic side chains), as may well characterize coal tar. The following was derived from these correlations:

$$\log P_{\text{TORR}} = -102.5 \frac{\text{MW}^{.654}}{T(^{\circ}\text{K})} + 7.97 \pm 0.35 \quad (3.2-46)$$

where MW is molecular weight .

Selected results are shown below:

T°C	Molecular weight	
	400	1000
800	0.04 atm	$2 \times 10^{-7}$ atm
1000	0.9	$5 \times 10^{-5}$
1300	13	$7 \times 10^{-3}$

These figures are not intended to be more than rough guides to the vapor pressure of these heavy species; several corrections can be suggested (non-idealities of fluid phase, Poynting correction, etc.). It appears though that at the primary temperatures of tar formation during rapid pyrolysis (500-800°C), most tar is relatively non-volatile. This suggests a number of possibilities:

- The tar is not subject to vapor phase transport but is removed as a mist, as per Chermin and Van Krevelen.
- The tar is transported in the vapor phase as lighter molecular weight species and reacts therein to give heavier species which

are carried along by the escaping vapor pyrolysis products.

- The tar is sufficiently volatile within the coal melt "solution" to vaporize (i.e. a very high liquid phase activity coefficient), although it has a low vapor pressure.

Somewhat more general than Lewellen's bubble model is the transport model proposed by Anthony et al. (1975). This model is based on weight loss data alone and is stated in broad terms as:

$$\dot{Q} - k_M C - k_1 C = dC/dt \quad (3.2-47)$$

where  $\dot{Q}$  is the rate of formation of volatiles subject to cracking reactions (gm/sec per gm of original coal),  $k_M$  is a mass transfer coefficient ( $\text{sec}^{-1}$ ),  $C$  is the reactive species concentration (gm/gm of original coal) and  $k_1$  the rate constant of secondary, repolymerization-type reactions ( $\text{sec}^{-1}$ ).

Pseudo steady state is assumed, because the vapor phase holdup is considered negligible, thus  $dC/dt \approx 0$ . It is also assumed that  $k_M = k_C/P$  by analogy with a diffusion coefficient. Further, it is clear that the rate of loss of "reactive" volatiles must be equal to their rate of transport,  $dV_R/dt = k_M C = k_C C/P$ . Thus:

$$\frac{dV_R}{dt} = \frac{\dot{Q}}{(1 + k_1 P/k_c)} \quad (3.2-48)$$

Integration with respect to time gives

$$V_R^* = V_R^{**}/(1 + k_1 P/k_c) \quad (3.2-49)$$

where  $\int_0^\infty \dot{Q} dt = V_R^{**}$ , the total amount of reactive volatile formed.

Considering a fraction of volatiles not subject to cracking reactions ( $V_{NR}^*$ ), one obtained for a total yield from a pyrolysis process:

$$V^* = V_{NR}^* + V_R^{**}/(1 + k_1 P/k_c) \quad (3.2-50)$$

With this form, Anthony obtained the curve shown through his data in



Fig. 3.2-17.

This model can be faulted for the manner in which it introduces the pressure effect. The escape of volatiles from a coal particle is obviously not a diffusion process, but a hydrodynamic flow phenomenon. It has been observed in this work that the escape velocities of volatiles may be of order 10 cm/sec. Nevertheless, the fit obtained with reasonable parameter values is intriguing and this type of model will be explored further in a later section of this thesis.

The pyrolysis models of Reidelbach and Summerfield (1975) and Cheong (1977) offer rather little new insight into the issue of transport models. The former only considers tar "vaporization" in a non-quantitative manner, while the latter considers simple diffusion external to the particle and Darcy's law within the particle. The physical significance of Darcy's law in a softened, bubbling coal particle is not clear, but its use for a non-softening coal may be acceptable. James and Mills (1976) have developed a pyrolysis model (similar to Chermin and Van Krevelen's) but including transport through a coal "melt", and which semi-quantitatively predicts the effect of pressure on pyrolysis.

### 3.2.3 Hydropyrolysis

The body of literature on hydropyrolysis is considerably smaller than that on ordinary pyrolysis. The reader is referred to Anthony and Howard (1976) for a more complete review than will be presented here. Hydropyrolysis is the term used to describe the initial very rapid phase of hydrogasification of coal (complete volatilization in gaseous hydrogen). Until relatively recently (Dent, 1944), this initial period of high reactivity was not considered to be much more than ordinary pyrolysis, occurring as a precursor to the much slower hydrogasification of char.

Assuming some rate parameters "typical" of pyrolysis,  $k_0 = 10^{13} \text{ sec}^{-1}$ ,  $E = 50 \text{ kcal/mole}$ , the rate constant for ordinary pyrolysis at  $927^\circ\text{C}$  is

easily calculated,  $k = 7816 \text{ sec}^{-1}$ . At this same temperature and a pressure of hydrogen of 100 atmospheres, the data of Feldkirchner and Linden (1963) suggest a rate constant of  $k = 8.3 \times 10^{-4} \text{ sec}^{-1}$  for the slow hydrogasification of char, a difference of almost seven orders of magnitude in rate.

Fig. 3.2-19 and 3.2-20 show two examples of the nature of hydropyrolytic reactions. The data of Johnson (1971), show a very rapid initial pyrolytic reaction (d). The total volatiles yield from ordinary pyrolysis is considerably augmented by the presence of hydrogen (b), and is apparently an increasing function of the pressure of hydrogen (a). The transition to a slow hydrogasification regime is clearly shown by the gentle rise in curves (a), (b), and (c) at times longer than about 60 seconds. Comparison of the slopes of curves (b) and (c) at long times suggests that they are roughly parallel, indicating that hydrogasification proceeds at the same slow rate regardless of the method of preparation of the char.

Because the thermobalance used by Johnson did not allow taking of data at very short ( $< 10$  seconds) residence times, that system could not accurately track the hydropyrolysis phenomenon. The electrical grid system of Anthony et al. (1975) gave data with much better short residence time resolution (Fig. 3.2-20). The lowest curves in both (A) and (B) are for ordinary pyrolysis in helium. These data show how dramatically hydrogen serves to increase volatiles yield in the short times associated with pyrolysis. Again, the effect is larger with increasing pressure.

The work of Hiteshue et al. (1962, 1962a, 1964) and of Moseley and Paterson (1965, 1965a, 1967) show the significance of the pressure effect. Hiteshue demonstrated that by pyrolyzing at very high hydrogen pressure (6000 psig = 409 atmospheres), the yield of volatiles from a Pittsburgh Seam

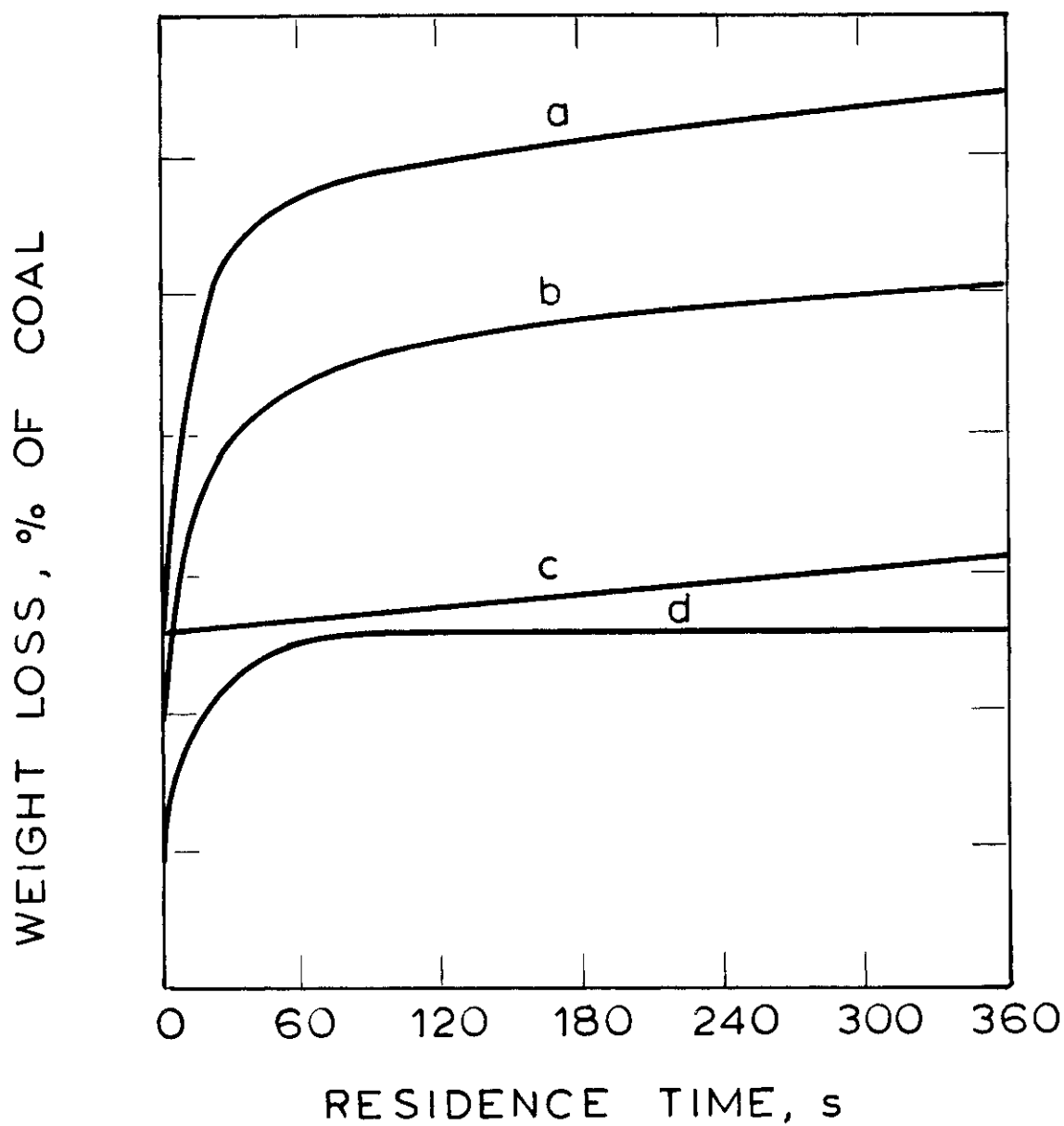


Figure 3.2-19 Effect of Time and Hydrogen Pressure on Weight Loss during Pyrolysis and Hydrolysis of Coal [Johnson (1971); Bituminous Coal, final temperature, 927°C. (a) coal, 69 atm H<sub>2</sub>; (b) coal, 35 atm H<sub>2</sub>; (c) N<sub>2</sub>-pretreated char, 35 atm H<sub>2</sub>; (d) coal, 35 atm N<sub>2</sub>].

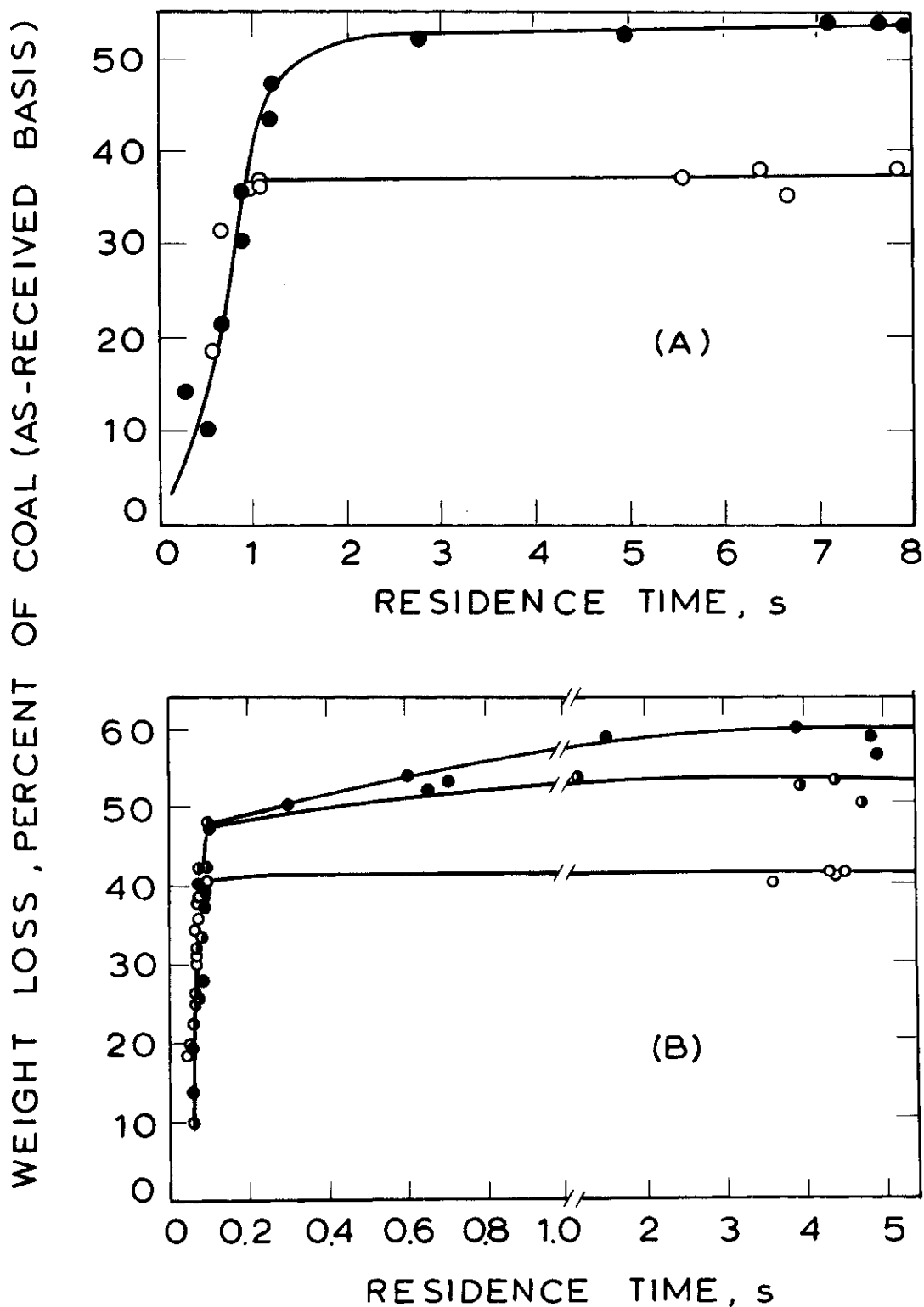


Figure 3.2-20 Effect of Time and Hydrogen Pressure on Weight Loss during Pyrolysis and Hydropyrolysis of Coal (Anthony and Howard, 1976; (A) Pittsburgh Seam bituminous coal; final temperature, 900°C, nominal heating rate, 750°C/s; pressure, 69 atm; (o) helium; (●) hydrogen. (B) Montana lignite (Savage Mine); final (holding) temperature, 1000°C; nominal heating rate, 10,000°C/s; (o) helium, 69 atm; (●) hydrogen, 69 atm; (●) hydrogen, 103 atm).

bituminous coal (37.5% VM, daf) could reach almost 75% in the time it took to heat to 800°C and cool back down again (on the order of a minute). Over 90% yield was obtained in about 15 minutes. Moseley and Paterson showed that over 95% yield could be obtained in 15-20 seconds from a non-caking bituminous coal (39.0% VM, daf) by heating to 850-950°C in 490 atmospheres of helium. Of course, commercial interest in such high pressure work is limited because of the expense and hazards of working with hydrogen at high temperatures and pressures (in systems as large as would be of interest for coal conversion). The safety aspect is sublimely underscored by a footnote to a data table of Hiteshue et al., which for an entry at 800°C and 6000 psig H<sub>2</sub> simply read - "reactor ruptured".

Anthony and Howard (1976) have drawn from the literature the results of several workers, and compared them as shown in Fig. 3.2-21. Most of the data are for work on Pittsburgh Seam bituminous coal, at temperatures between 800 and 950°C. The apparently anomolous variation in residence time with temperature actually reflects the effect of the different heating rates used to obtain the data shown, and the authors suggest that the curves shown in the insert are the idealized trends. As heating rate increases ( $a > b > c$ ), the time required to reach a particular conversion decreases. As the hydrogen partial pressure is increased ( $d > e$ ), so is the amount of conversion which is possible before reverting to the long time slow hydrogasification assymptote. This analysis suggests that there is no major effect of heating rate on the process. The following subsextions briefly sketch the effect of the major variables on the course of hydrolyrolysis.

#### Effect of Coal Type

The fact that different coals behave in markedly different ways during

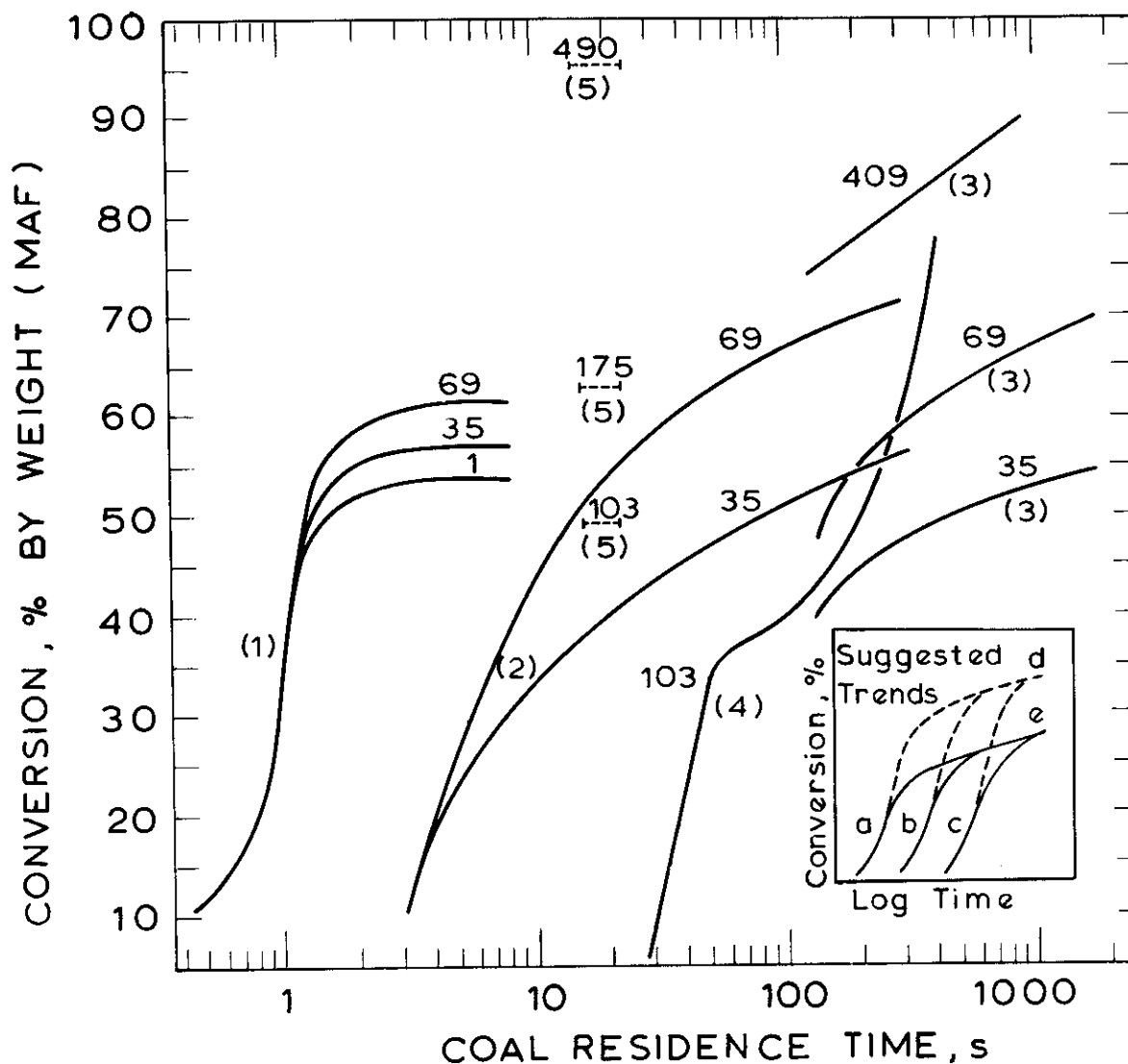


Figure 3.2-21 Effect of Hydrogen and Helium Pressure on Weight Loss during Pyrolysis and Hydropyrolysis of Coal (Overview prepared by Anthony and Howard, 1976; numbers in parentheses: (1) Anthony et al. (1976); (2) Johnson (1971); (3) Hiteshue et al. (1962b) 409 atm with 1% Mo catalyst, (1964) 35 and 69 atm; (4) Feldkirchner and Linden (1963); (5) Moseley and Paterson (1967). Hydrogen pressure, atm: numbers on curves. Final (holding) temperature (1) 900°C; (2) 927°C; (3) 800°C; (4) 927°C; (5) 850°-950°C. Curves-Pittsburgh Seam bituminous; dashed lines-Warwickshire bituminous. Insert: Idealized suggested trends].

pyrolysis would lead one to believe that such should also be the case during hydrolysis. This is confirmed by various pieces of data, though the picture is not nearly as complete as for pyrolysis. The coals which cake under pyrolytic conditions still cake under hydrolytic conditions, while the lignite used in this study seems to cake under no conditions. It has, however, been reported (Kawa et al., 1959) that a normally non-caking sub-bituminous coal showed caking tendency when hydrolyzed at 1000 psig of hydrogen pressure and a temperature of 500-600°C. The data of Anthony (1974) suggest that, as with pyrolysis, there are differences in the rates of hydrolysis of different coals. Anthony and Howard (1976) point out that the data on Fig. 3.2-21 show an effect of coal type as well. Whereas Anthony et al. (1976) could reach a level of conversion of over 60% (daf) in about 2 seconds by 69 atm (=1000 psi) hydrolysis, the yield obtained by Moseley and Paterson (1967) in 15-20 seconds at roughly the same temperature and a pressure approximately 2.5 times higher (175 atm) is comparable; the implication is that the coal used by Moseley and Paterson is more difficult to hydrolyze.

It is often difficult to judge the effect of hydrolysis alone on the yields of individual products. Sometimes the data are clouded by methane formed during slow-hydrogasification (in runs involving long solids residence times) or by vapor phase secondary reactions of volatiles, such as the water-gas shift or hydrocracking of tars. For this reason, the electrical grid system employed in this study offers a real advantage, in that it has a near-zero vapor phase residence time and a very short solid residence time.

Although there are important differences between coals, there also exist some similarities. Johnson (1977) studied hydrolysis with an

entrained flow, tubular reactor. Although observing differences between the behavior of several coals during initial pyrolytic degradation, he observed that in the next rapid hydroxyrolytic phase, methane and ethane were the principal products in all cases. Further, the yield of carbon evolved in ethane plus methane correlated in a straight line fashion with the evolution of coal hydrogen. Mechanistically, this shows a clear correlation between the path of pyrolysis and that of hydroxyrolysis, which before was only suggested by kinetic data. This correlation holds, regardless of the rank of the starting coal (lignite through bituminous). These results will be discussed further in the subsection on mechanisms and modelling.

#### Effect of Temperature

Fig. 3.2-22 presents the results of Anthony et al. (1976) on bituminous coal. Coals were heated to the indicated temperatures at heating rates of between 65 and 750°C and held for 5 to 20 seconds except for the points in which 2-step heating of the coal was carried out. In these cases, chars from low temperature runs were re-heated to the higher indicated temperatures.

These data support the view that hydroxyrolysis and pyrolysis are concurrent processes, and that the hydrogen acts, presumably, to stabilize hydrogen starved radicals formed during pyrolysis. The lack of effect of heating at an intermediate temperature in either pyrolysis or hydroxyrolysis would speak against a competitive reaction mechanism as the principal explanation of the temperature effect of yield. Instead, a picture in line with a heterogeneous solid with a wide distribution of activation energies is supported. The fact that pyrolysis and hydroxyrolysis curves diverge only above a particular temperature (about 600°C) suggests that at temperatures lower than this, the hydrogen may play no role in the



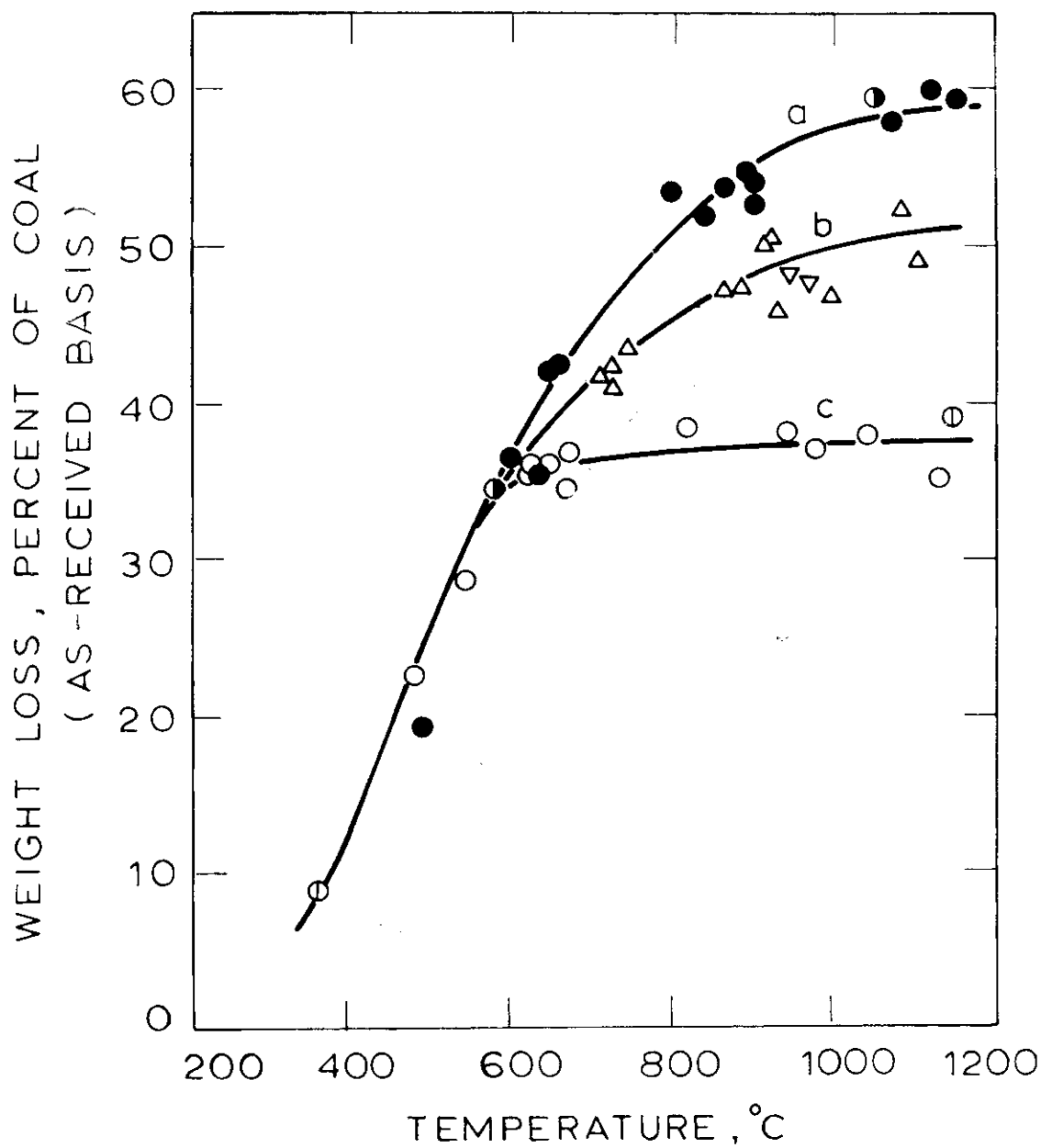


Figure 3.2-22 Effect of Temperature on Weight Loss during Pyrolysis and Hydrolysis of Bituminous Coal (Anthony et al., 1976; 5 to 20 sec. residence time; (●) 60 atm Hydrogen; (○) 69 atm Helium; (▽), (△), 1 atm Helium, Nitrogen).

pyrolysis reactions (though this picture must be supported by analysis of the solid phase before the conclusion can be considered firm).

#### Effect of Pressure

A number of figures already presented show data regarding the effect of pressure on hydrolysis yield. The data of Johnson (1977) (Fig. 3.2-23) shows the effect of various combinations of temperature and pressure on total methane plus ethane yield. The difference in yield between the hydrolysis case and the pyrolytic base case shows that no simple relationship exists between the incremental yield of product and pressure. The beneficial effect of hydrogen is higher, the higher in temperature one operates. This effect will be explored further in this thesis.

Also of interest in the data of Johnson is the fact that the yield from a case in which the total system pressure equalled the hydrogen pressure (18 atmospheres) is indistinguishable from a case in which the hydrogen partial pressure was 18 atm., but the total pressure was built to 36 atm. by the addition of helium. The data of Anthony (1974) show that this result is, in fact, not generalizable (see Fig. 3.2-24). These data suggest that the deleterious effect that increasing external pressure has on yield during ordinary pyrolysis is in competition with the beneficial effect that hydrogen exhibits. This theory is presented in a model developed by Anthony et al. (1976), presented in the subsection on mechanisms and modelling.

#### Effect of Heating Rate

Opinion on the effect of heating rate on hydrolysis is as divided as opinion on its effect on pyrolysis. The data of Anthony et al. (1976) suggest rather little effect in the range studied  $65-10^4$ °C/sec. Other workers (Pyrcioch et al., 1972) support this claim with respect to effect

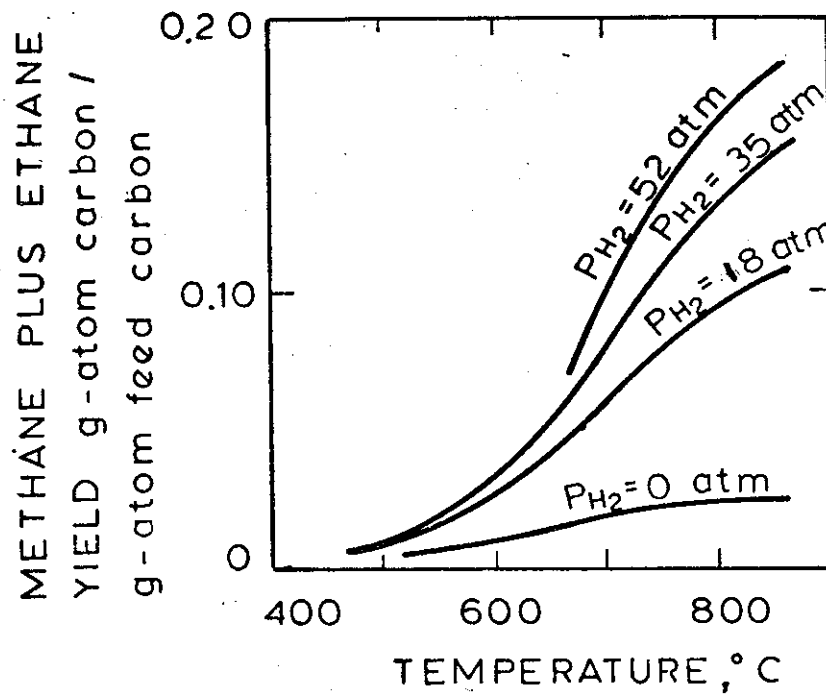


Figure 3.2-23. Effect of Temperature and Hydrogen Pressure on Total Methane-Plus-Ethane Yields During Hydropyrolysis of Montana Lignite (Johnson, 1977).

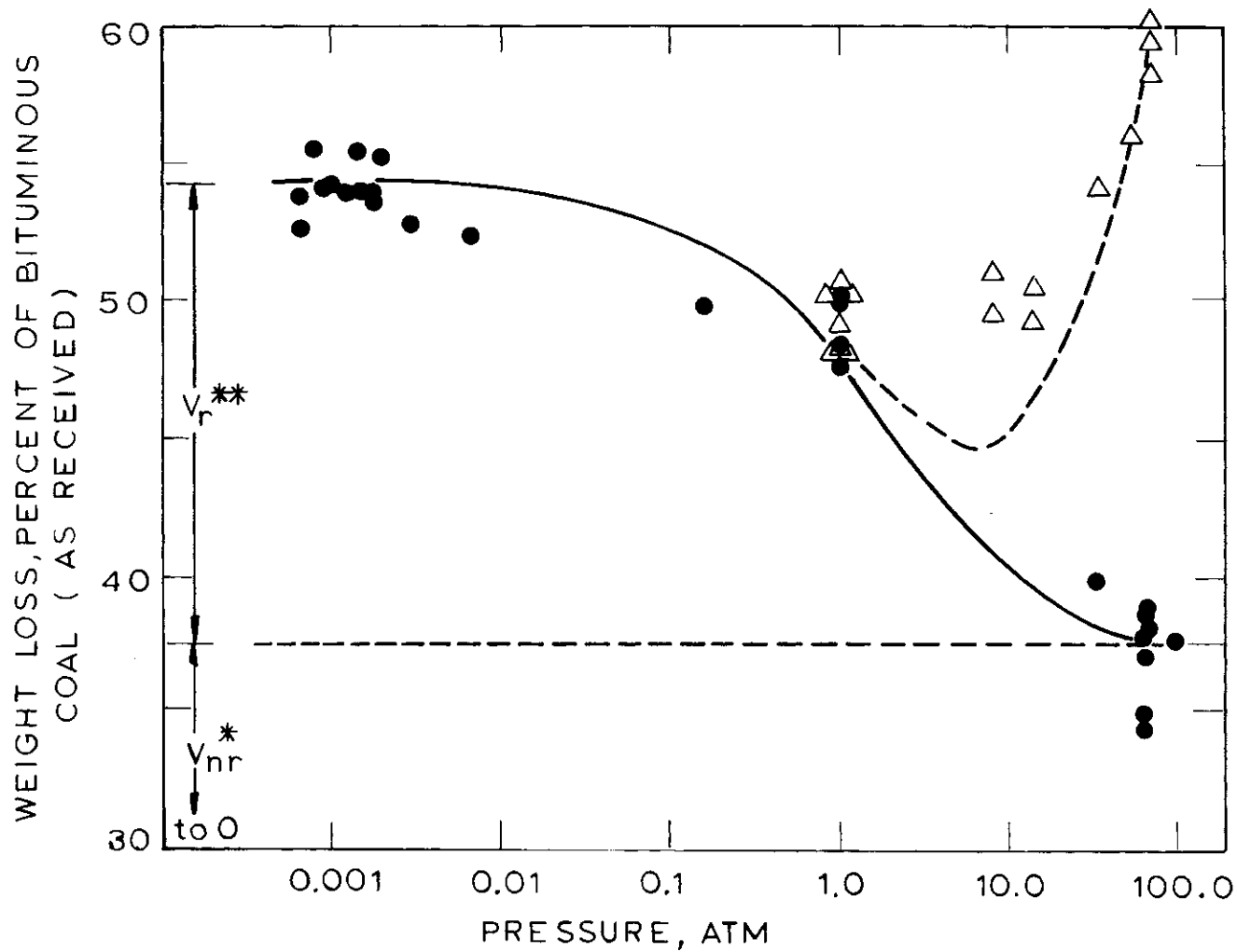


Figure 3.2-24 Effect of Hydrogen and Helium Pressure on Weight Loss during Pyrolysis and Hydrolysis (Anthony et al., 1976; final temperature 1000°C; ( $\Delta$ ) Hydrogen; (o) Helium; see eq. (3.2-60) for explanation of other symbols).

on hydrogasification yields, but others (Von Fredersdorff and Elliott, 1963) suggest that higher heating rates may retard hydrogasification.

#### Effect of Particle Diameter

The fact that hydropyrolysis, unlike pyrolysis, involves the contacting of two reactants in separate phases suggests that mass transport effects can play a key role. While the variation of particle diameter was found to play some role in determining the nature of pyrolysis products, the effect is modest compared to that observed during hydropyrolysis. Fig.3.2-25 compares the variation of pyrolysis volatile yields with the variation in hydropyrolysis yields, for a range of particle diameters  $50\mu$  to  $1000\mu$  in size (Anthony et al., 1976). This thesis explores the effect of particle diameter on hydropyrolysis product distributions as well as total yield.

The modelling of mass transport effects in hydropyrolysis must include all of the complexity of pyrolysis and then some, since the system involves a reactant that must be transported to the particle against an outward flow of volatiles.

#### 3.2.4 Mechanisms and Modelling of Hydropyrolysis

A pseudo-mechanistic term which has been coined in explaining the phenomenon of hydropyrolysis is that of "rapid-rate carbon". The use of this term conveys the impression that coal is composed of two distinctly different carbon fractions, one which can be gasified quickly with hydrogen (contributing to a higher yield of volatile matter than obtained by pyrolysis) and one which can only rather slowly be hydrogasified.

It is clear from much of the available data that pyrolysis proceeds at a rate similar to that of hydropyrolysis, and it may be construed that the pyrolysis is a precursor to hydropyrolysis. Some recent work by Virk et al. (1974) resulted in the conclusion that pyrolysis was indeed the

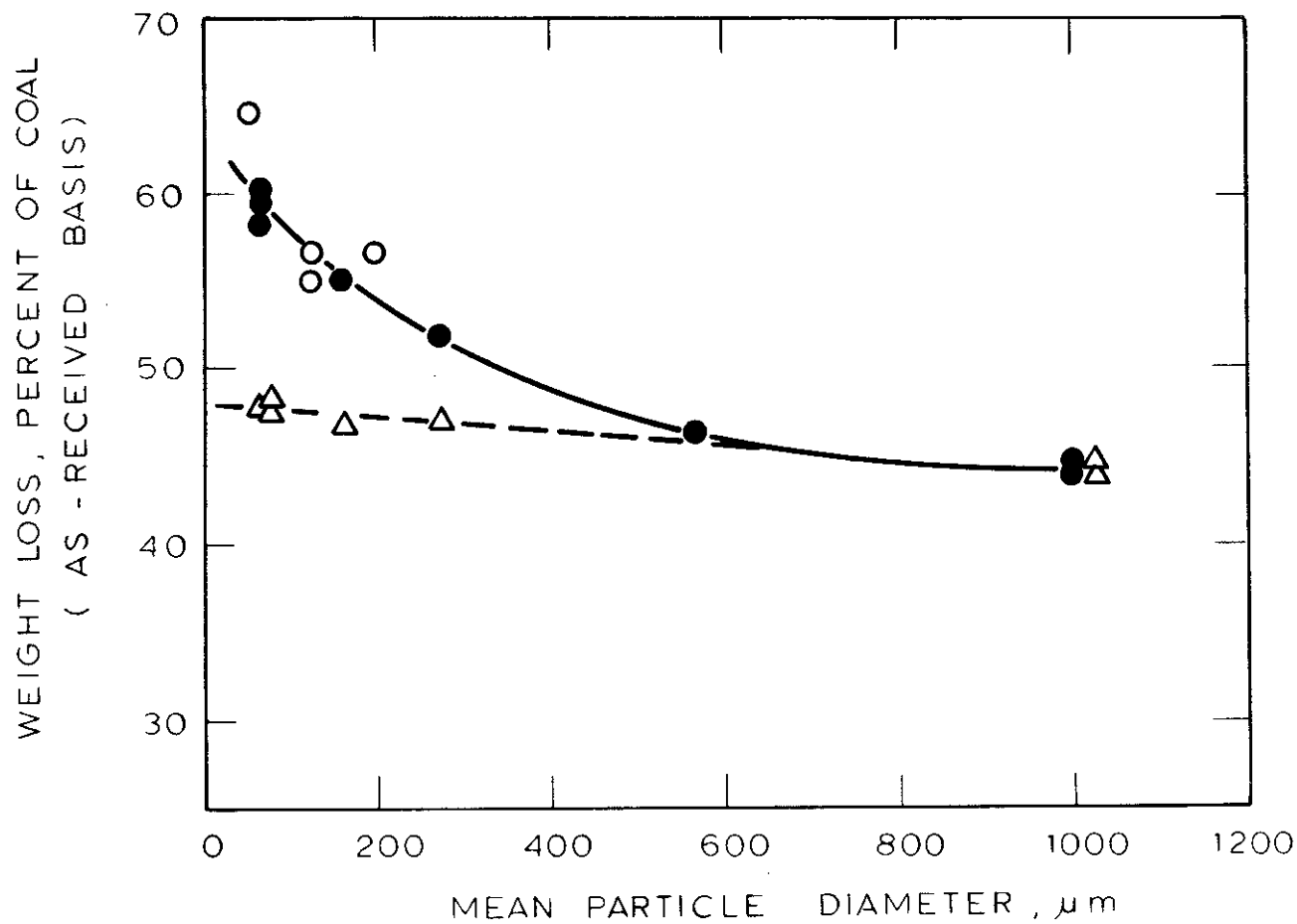


Figure 3.2-25 Effect of Particle Diameter on Weight Loss during Pyrolysis and Hydrolysis  
 (o) Moseley and Paterson (1967), Warwickshire coal, 175 atm  $\text{H}_2$ , 920°C final temperature,  
 (●) and ( $\Delta$ ) Anthony et al. (1976), Pittsburgh Seam coal, 1000°C final temperature, 69 atm  
 $\text{H}_2$  (●), 1 atm He ( $\Delta$ )].

264

rate determining step in the hydrolysis of various pure aromatic compounds.

It may be possible to view the role of externally provided hydrogen as being the same as the hydrogen donating aliphatic groups present in coal itself. The hydrogen serves to stabilize free radicals as they form within the coal. From the data of Anthony et al. (1976), Fig. 3.2-22 it can be seen that the hydrogen does not begin to have a very marked effect on weight loss prior to about 600°C. Since the char is held at this temperature for a sufficiently long time for rapid evolution of volatiles to have ceased, it appears that mass transport limitations in the form of "diffusion against a wind" should no longer be present. Thus chemical rate control is suggested; the bond rupture process which leads to the formation of "rapid rate" carbon has not yet commenced at 600°C.

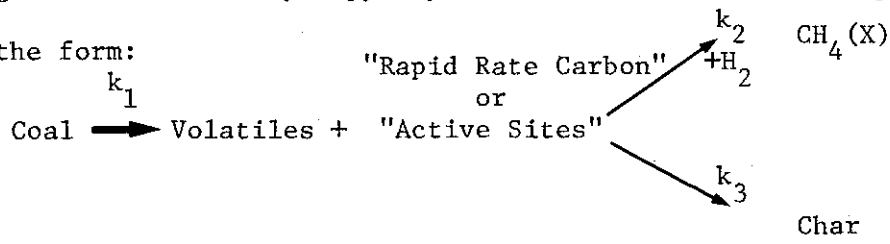
Thus a model of a form analogous to the single first order model for coal pyrolysis is mechanistically inadequate. Anthony and Howard (1976) review the use of this form of model:

$$dX/dt = k P_{H_2} (X^* - X) \tag{3.2-51}$$

- where X = measure of conversion
- X\* = measure of "rapid-rate" carbon
- P<sub>H<sub>2</sub></sub> = pressure of hydrogen

The activation energies reported are low, just as for the same form of model applied to pyrolysis.

Another general class of hydrolysis models involves the competitive reactions of the form:



Moseley and Paterson (1965) assumed in their formulation of the model that the methanation reaction did not consume active sites:

$$\frac{dX}{dt} = k_2 P_{H_2} C^* \quad (3.2-52)$$

Active sites were assumed to disappear by a separate first order cross-linking mechanism

$$\frac{dC^*}{dt} = -k_3 C^* \quad (3.2-53)$$

Solving (3.2-53) for the initial condition  $C^*(t=0) = C_0^*$ , substituting into (3.2-52) and solving:

$$X = \left( \frac{k_2 C_0^*}{k_3} \right) [1 - \exp(-k_3 t)] P_{H_2} \quad (3.2-54)$$

It can be seen that for "long" times, the predicted asymptotic yield of methane is proportional to the partial pressure of hydrogen, and to the relative rate of methanation to cross-linking. This form correlates well with the high pressure data of Moseley and Patterson, but not well with the lower pressure (<100 atm) data obtained by Zahradnik and Glenn (1971).

Therefore Zahradnik and Glenn modified the form of (3.2-52) to include loss of active sites (or rapid rate carbon) in methanation, and changed the form of (3.2-53) to

$$\frac{dC^*}{dt} = k_2 P_{H_2} C^* - k_3 C^* \quad (3.2-55)$$

The solution to (3.2-52) then becomes:

$$X = \frac{\left( \frac{k_2 C_0^*}{k_3} P_{H_2} \right)}{\left( 1 + \frac{k_2}{k_3} P_{H_2} \right)} [1 - \exp\{- (k_2 P_{H_2} + k_3) t\}] \quad (3.2-56)$$



The "long-time" total yield of methane is not a simple linear function of hydrogen pressure in this formulation. The calculation for the total amount of methane formed during hydrolysis was also corrected by adding a constant term for that produced during ordinary pyrolysis. Zahradnik and Glenn also point out that an expression identical to that obtained from (3.2-56) for  $X$  as  $t \rightarrow \infty$ , is obtained by assuming zero order kinetics throughout; they caution that successful correlation of data by an equation of the form of (3.2-56) does not constitute evidence for any particular mechanism. Nevertheless, their model appears more realistic than that of Moseley and Paterson.

Johnson (1977) proposed a model along similar lines, but extends it to correlate the disappearance of coal hydrogen with methane formation. The methane plus ethane yield  $Y$  (corrected for that evolved during pyrolysis and due to cracking of  $C_3$ 's) is given by:

$$Y = \frac{m(n_H - n_H^\circ)}{x - y + my} \quad (3.2-57)$$

where

$$m = \left( \frac{k_2/k_3}{1 + k_2/k_3} \right)$$

$n_H$  = total coal hydrogen gasified  $\left( \frac{\text{atoms}}{\text{atoms feed carbon}} \right)$

$n_H^\circ$  = total coal hydrogen gasified during primary devolatilization

$x$  = atomic ratio, hydrogen to carbon in char

$y$  = atomic ratio, hydrogen to carbon in rapid rate carbon plus char

The results are shown in Fig. 3.2-26. Because the slope of the lines is a function of hydrogen pressure, the ratio  $k_2/k_3$  must be a linear function of pressure. It should be noted that this result, substituted into (3.2-57), gives an equation of precisely the same empirical form

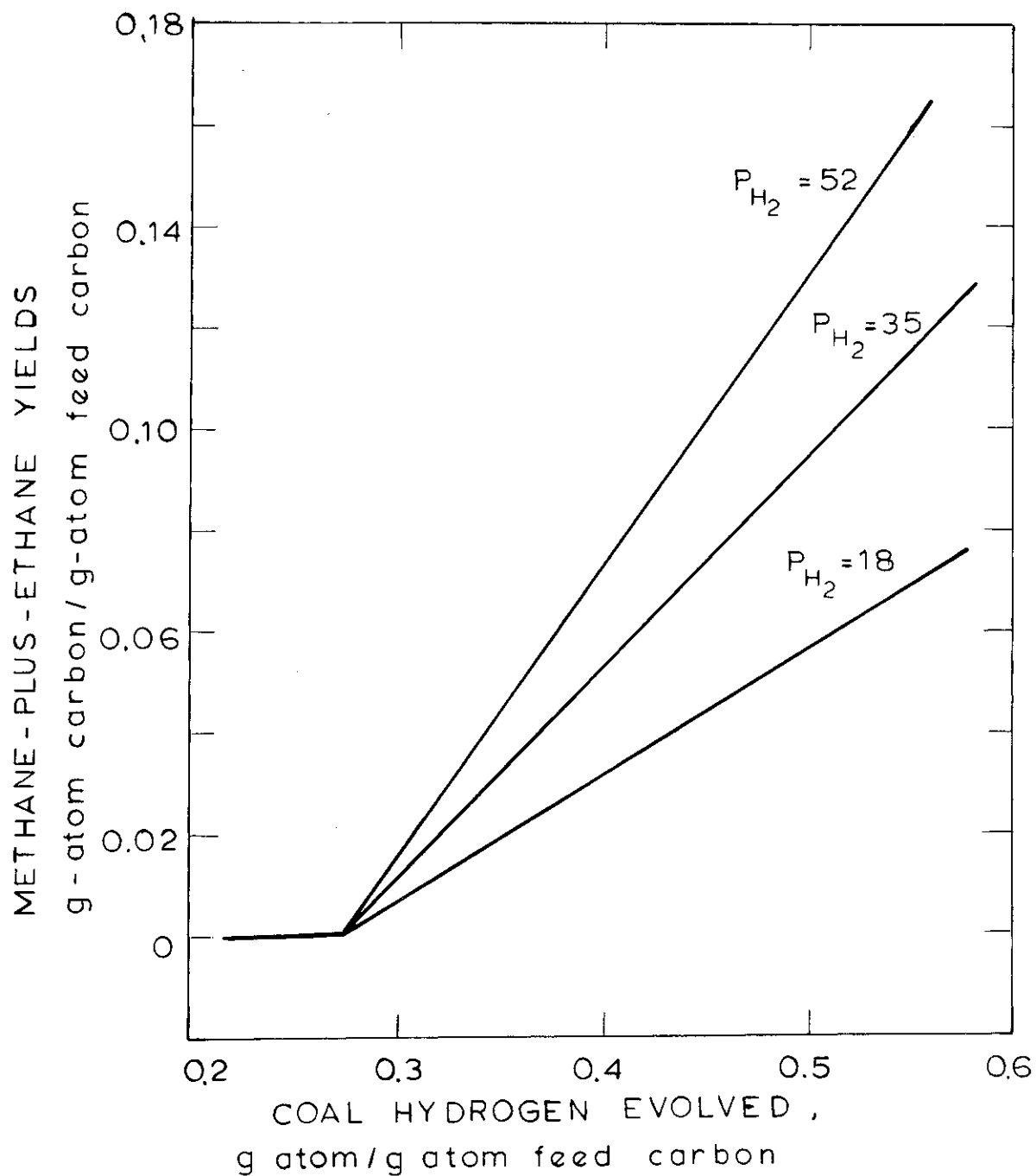


Figure 3.2-26 Relationship Between Methane-Plus-Ethane Yield and Coal Hydrogen Evolution during Hydrolysis (Johnson, 1977, Lignites, Subbituminous, and Bituminous Coals).

as Zahradnik and Glenn's, (3.2-56).

Johnson assumes further that the process of conversion of coal to rapid rate carbon (which he terms active intermediates) occurs by a first order process with a distribution of activation energies. He assumes a completely flat distribution, and derives the following kinetic parameters for the reaction  $\text{Coal} \xrightarrow{k_1} \text{"Active intermediates"}$

$$k_{01} = 1.97 \times 10^{10} \text{ sec}^{-1} \text{ (for all reactions)}$$

$$E_{\text{MINIMUM}} = 40.8 \text{ kcal/mole}$$

$$E_{\text{MAXIMUM}} = 62.9 \text{ kcal/mole}$$

A model with a somewhat different mechanistic basis is that proposed by Anthony et al. (1976). This model involved a modification of the previously derived model for the effect of mass transport and secondary reactions during pyrolysis (Equations 3.2-47 through 3.2-50). Again, beginning with a material balance on reactive volatiles within the particle (see 3.2-47)

$$\dot{Q} - K_M C - k_1 C - k_2 P_{H_2} C = \frac{dC}{dt} \tag{3.2-58}$$

The only new term added is  $k_2 P_{H_2} C$ , the rate of hydrogenation of "reactive" volatiles, which is included as a loss term because it is assumed that reactive volatiles, those which can be lost to cracking, can instead be stabilized by hydrogenation. The rate at which reactive volatiles leave the particle then becomes:

$$\frac{dV_R}{dt} = K_M C + k_2 P_{H_2} C \tag{3.2-59}$$

Solution, as before, yields:

$$V^* = V_{NR}^* + V_R^* [1 + k_1 / (k_c / P + k_2 P_{H_2})]^{-1} + k_3 P_{H_2} \tag{3.2-60}$$

where  $V^*$  = total observed yield  
 $V_{NR}^*$  = yield of non-reactive volatiles, not including those stabilized by hydrogenation  
 $P$  = total pressure  
 $P_{H_2}$  = hydrogen partial pressure  
 $k_1, k_2$  = rate constants for cracking, hydrogenation reactions  
 $k_c = K_M/P$ ,  $K_M$  = mass transfer coefficient

The last term,  $k_3 P_{H_2}$ , is a term included to account for direct hydrogenation of the solid phase. Its form is similar to the Moseley and Paterson model (3.2-54) at long times.

With this model, Anthony et al. (1976) were able to fit data for bituminous coal which showed that low hydrogen pressures can actually suppress yields relative to vacuum pyrolysis conditions (see Fig. 3.2-24).

Anthony et al. used their previously described Gaussian distribution of activation energies model to estimate kinetic parameters for the formation of reactive and non reactive volatiles. It was estimated that the overall pyrolysis process was characterized by a mean activation energy of about 55 kcal/mole, but that the reactive volatiles were characterized by the higher activation energy "tail" of the distribution, with activation energies of over 61 kcal/mole (see Fig. 3.2-27). It may be recalled that this was the upper limit of the activation energy distribution found by Johnson; that agreement is not better is not surprising. Whereas Johnson's model depicts the enhancement of hydrolysis yield as due primarily to heterogeneous reactions after a very rapid initial pyrolysis phase, Anthony et al. model the devolatilization as a continuation of pyrolysis and base enhanced yield upon stabilization of reactive volatiles.

These models will both be further evaluated in light of the data presented in this thesis.

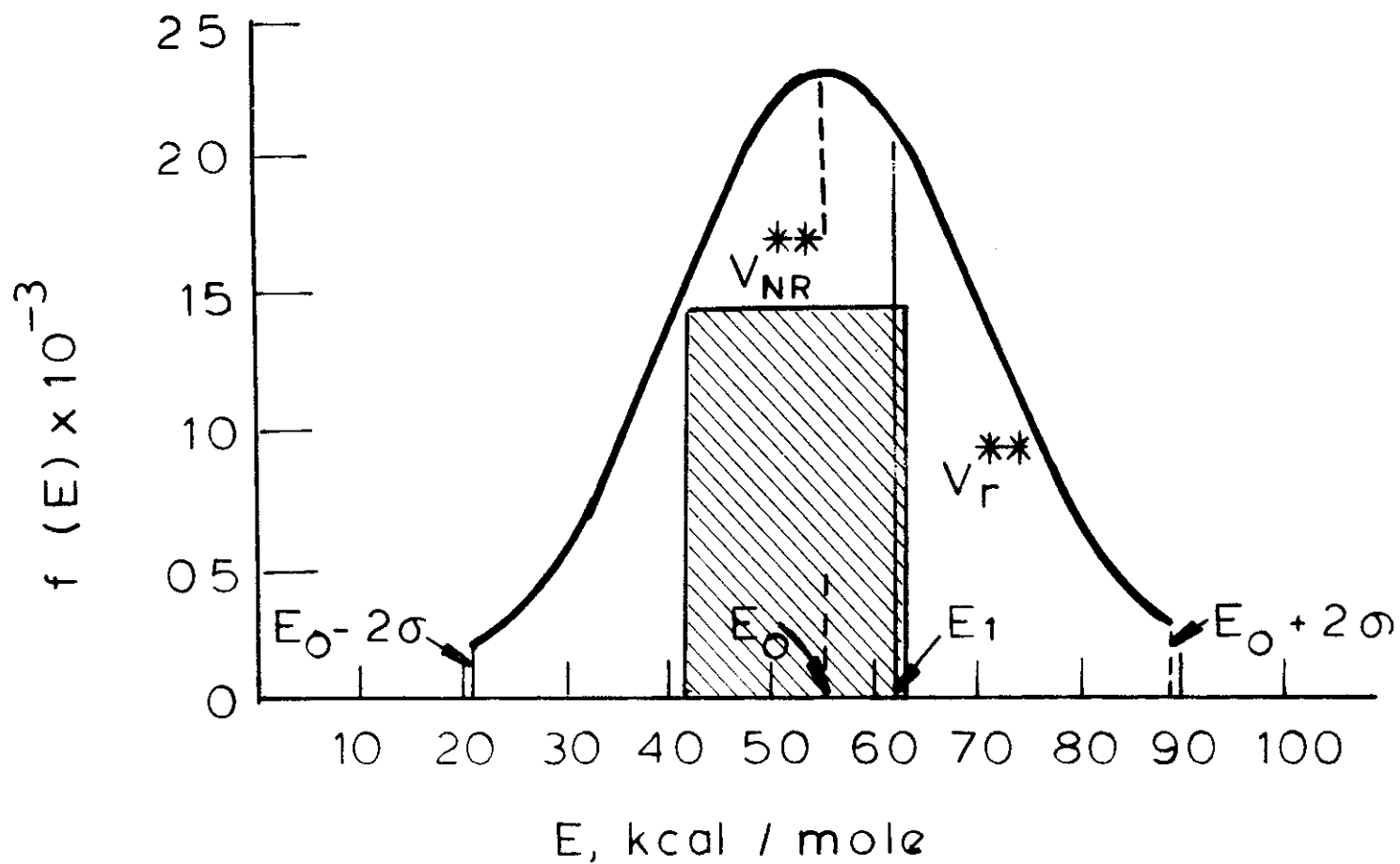


Figure 3.2-27 Comparison of Distributions of Activation Energies of Hydropyrolysis Reactions (Solid curve and dashed lines, Anthony et al., 1976 for a Pittsburgh Seam Bituminous Coal, symbols per equations (3.2-60) and 3.2-40), with  $E_1$  = minimum activation energy of volatiles-hydrogen interaction; Shaded Figure, Johnson, 1977, showing distribution of activation energies for formation of active sites).

#### 4. APPARATUS AND PROCEDURE

##### 4.1 Selection of Apparatus

A brief review of the various types of experimental systems employed to study pyrolysis and hydrolyrolysis was presented in section 3.2 , and also in Anthony and Howard (1976).

The interest of this thesis in obtaining kinetic data led to the selection of an electrical grid system as designed by Anthony (1974; et al., 1974). This system has a number of distinct advantages:

- Independent control of heating rate and final time and temperature.
- Good heat transfer characteristics
- Accuracy of measurement of time temperature history
- Near zero vapor phase residence time, independent of coal residence time.
- Rapid quenching of coal sample.
- Ability to work at a range of pressures, full vacuum to 100 atm.

A number of other workers besides Anthony have employed the electrical grid technique, they are listed in Table 3.2-1.

It is sometimes asked why a thermogravimetric system is not employed, which together with real time gas measurement, would enable one to obtain differential, rather than integral, data. If a system of this kind were readily available or easily constructed, it might indeed be a powerful device. Unfortunately, such systems generally have the drawback that they are not flexible enough to cover the wide range of conditions of interest in this thesis (e.g. ability to heat and track weight losses at a programming rate of up to 10,000°C/sec to 1100°C, amenable to full vacuum up to 100 atm of H<sub>2</sub>). As has also been mentioned, real time

sampling of gases evolving from rapidly heated coal requires great care, since sampling lags make analysis of kinetic data difficult.

The present system, though admittedly far from "perfect", has the desirable features that it is both simple (experimentally and analytically) and relatively inexpensive.

#### 4.2 Apparatus Description

An overview of the entire experimental apparatus is presented in Fig. 4-1. The apparatus consists of five components: the reactor, designed to contain a coal sample in a gaseous environment of known pressure and composition; the electrical system, used to expose the sample to a controlled time-temperature history; the time-temperature monitoring system; the product collection system; and the product analysis system. The reactor shown in Fig. 4-1 is actually either of two reactors: the reactor employed for atmospheric-pressure helium and vacuum pyrolysis work consists of a 6-inch (15.24 cm) long, 3-inch (7.62 cm) diameter pyrex glass pipe, blind-flanged at both ends by stainless steel plates having electrical feed-throughs and gas inlet and outlet ports. The coal sample is held and heated in the vessel by a folded strip of stainless steel screen positioned between two relatively massive brass electrodes as shown in Fig. 4.2. The small size of the sample holder, and hence coal samples, is dictated by the desire to have temperature uniformity across the entire sample. Workers with larger screens report difficulty in maintaining uniformity.

The reactor employed for high pressure work was that actually designed and built by Anthony, suitably modified to permit product collection. The vessel itself is fabricated from 316 SS, and designed for a 3000 psig working pressure. The internals shown in Fig. 4-2 are the same for both vessels.

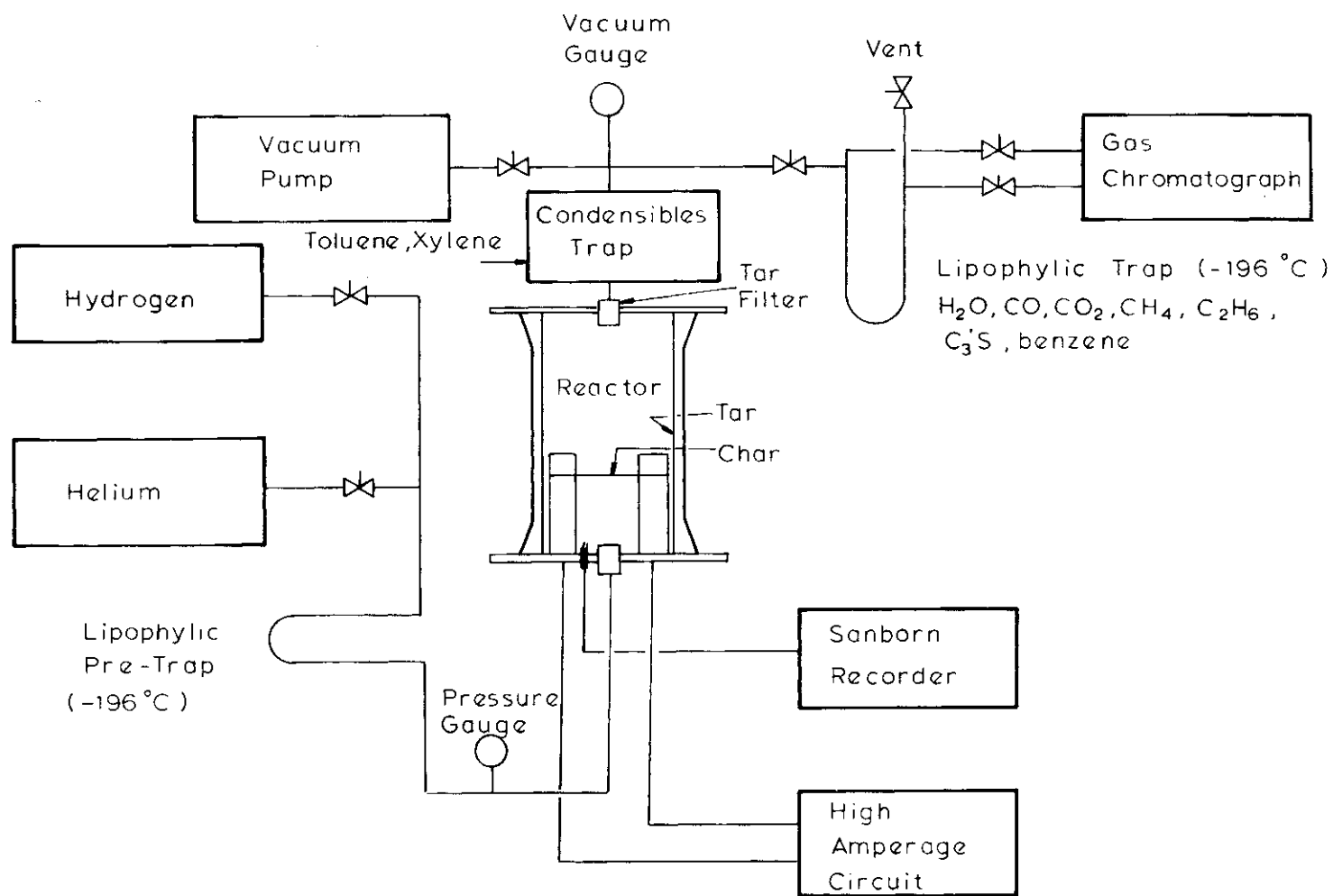


Figure 4-1 Schematic of Captive Sample Apparatus.



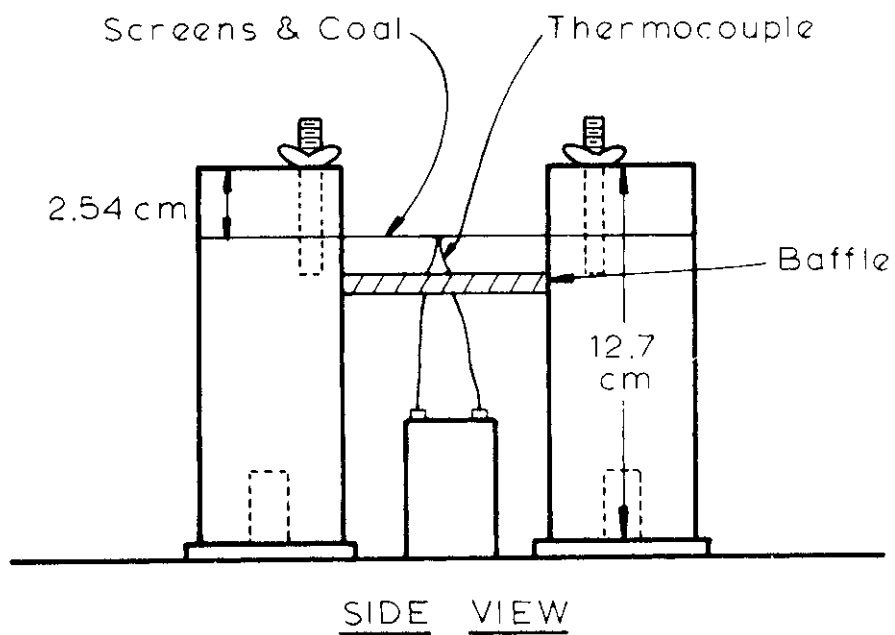
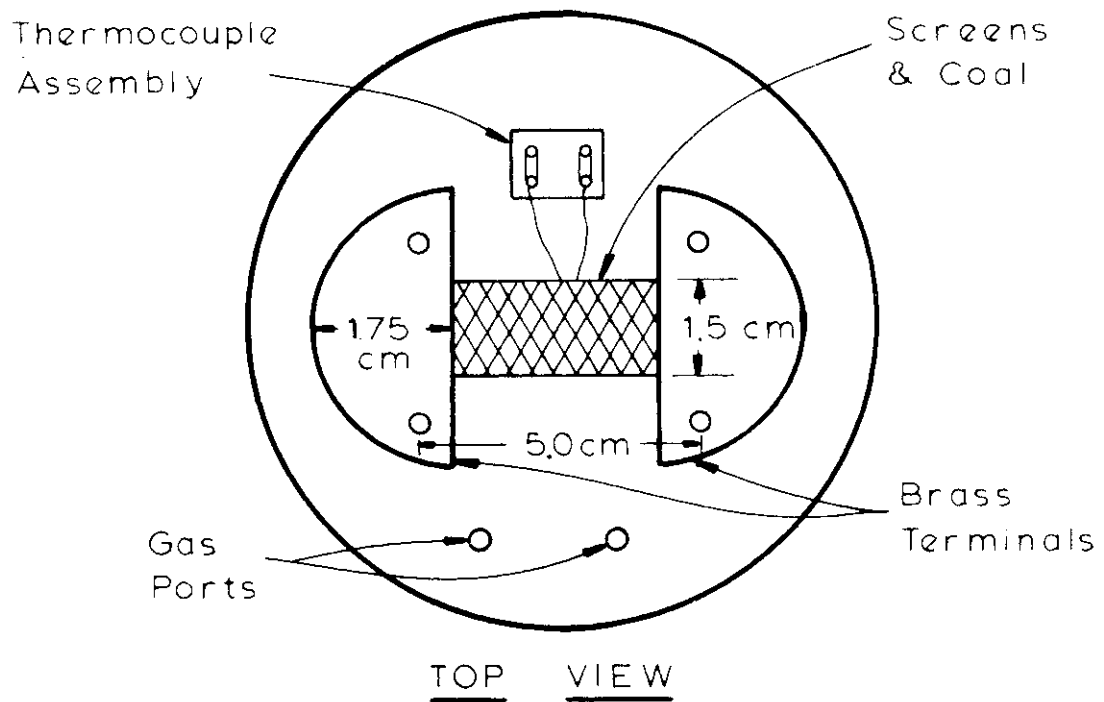


Figure 4-2. Detail of Captive Sample Apparatus Internals

All tubing, with the exception of vacuum lines, is standard wall 1/8" or 1/4" stainless steel with compression type tube fittings. The choice of stainless steel was dictated partly by safety considerations and partly by concern for chemical cleanliness of product carrying tubes. All piping was washed with solvent and dried prior to assembly.

Additional safety features, associated with use of the high pressure vessel but not shown on Fig. 4-1, include a rupture disc assembly (2900 psig burst) and a standard bomb blanket, draped over the high pressure vessel during runs. The control panel is sited remotely from the high pressure apparatus, being separated from the high pressure apparatus, by a free swinging 1 1/8" wood panel.

The stainless steel screen holder and heater is a piece of 325 mesh, type 304 stainless steel, cut to 4.5 x 5.0 cm. It is folded over onto itself twice (as a letter for insertion into an envelope) to form a "sandwich" of the dimensions shown in Fig. 4-2. Folding twice forms a pocket which prevents coal particle loss from the sides, while the electrodes clamp the ends firmly shut. Each run begins with a "fresh" screen. Screens are always prefired at over 1000°C in the experimental apparatus to ensure cleanliness. After such treatment, the screen never loses additional weight under experimental conditions.

The electrical system consists of two 12-volt automobile storage batteries connected in series to the reactor electrodes through a timer-controlled relay switch which connects either of two variable resistors at a predetermined time. This circuitry permits independent control of heating rate ( $10^2 - 10^4$  °C/s) and final sample holding time and temperature (150-1100°C for up to 30 s). The details of this circuitry are shown in Fig. 4-3. The temperature-time history of the coal is recorded by a

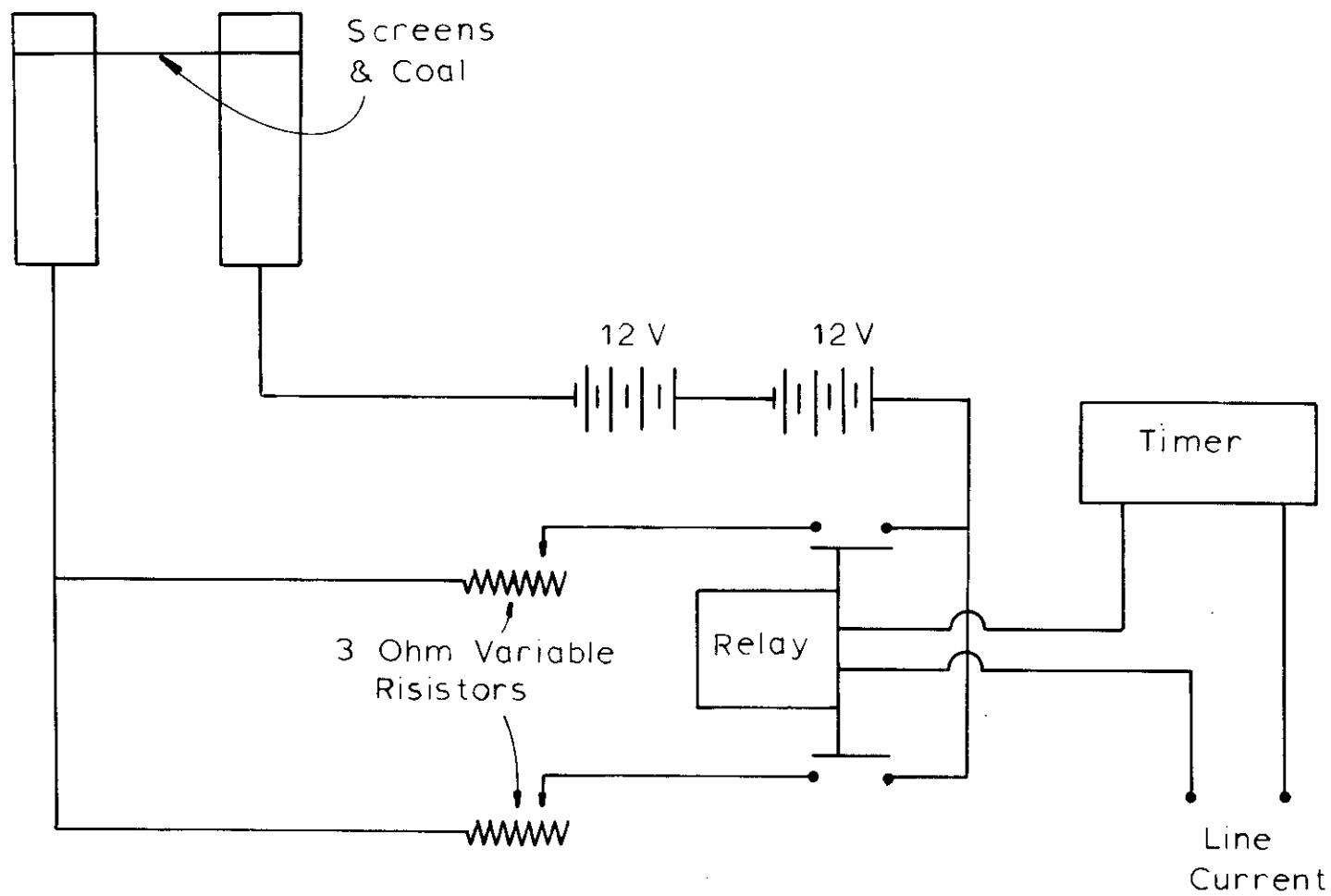


Figure 4-3 Circuit Used for the Control of Time-Temperature Histories

chromel-alumel thermocouple (24  $\mu\text{m}$  wire diam., 75  $\mu\text{m}$  bead diameter) placed within the sample and connected to a Sanborn fast-response recorder.

Fig. 4-4 shows some typical time-temperature histories obtained by use of this system. Since the quenching of the sample occurs by natural cooling (radiative, conductive, convective), there is a slight variation in the cooling behavior from run to run. This is especially true when comparing vacuum runs to runs done at high pressures. In the average, the cooling rate at 1 atmosphere of helium is of order 200°C/sec. This variation is of no concern, however, since the actual time-temperature is always recorded, and accounted for in the kinetic analysis.

The product collection system is made up of several elements arranged in a "train" fashion. Within the reactor, the char is completely retained on the screen. Tar is collected on various aluminum foil reactor liners, on a small paper filter, held firmly in a fitting at the exit to the reactor, and on various unlined surfaces within the reactor. This latter fraction is recovered by a solvent ( $\text{CH}_2\text{Cl}_2$ , reagent grade) wash of the reactor internals.

Downstream of the tar filter at the reactor exit is a condensable product trap, which in most applications consists of a two inch length of 3% OV-17 on 80/100 mesh (150-170 $\mu$ ) Anakron Q followed by about a two inch length of 50/80 mesh (177-297 $\mu$ ) Porapak Q or Chromasorb 102 (standard gas chromatographic packings) packed into 1/4" O.D. (0.635cm) stainless steel tubing. This trap serves to remove (at room temperature) from the gas purge those components too low boiling to be condensed within the reactor, but too high boiling to analyzed with the gaseous products. Aromatics falling roughly between benzene, and naphthalene in molecular weight have been observed in this trap. Water and benzene were generally not retained

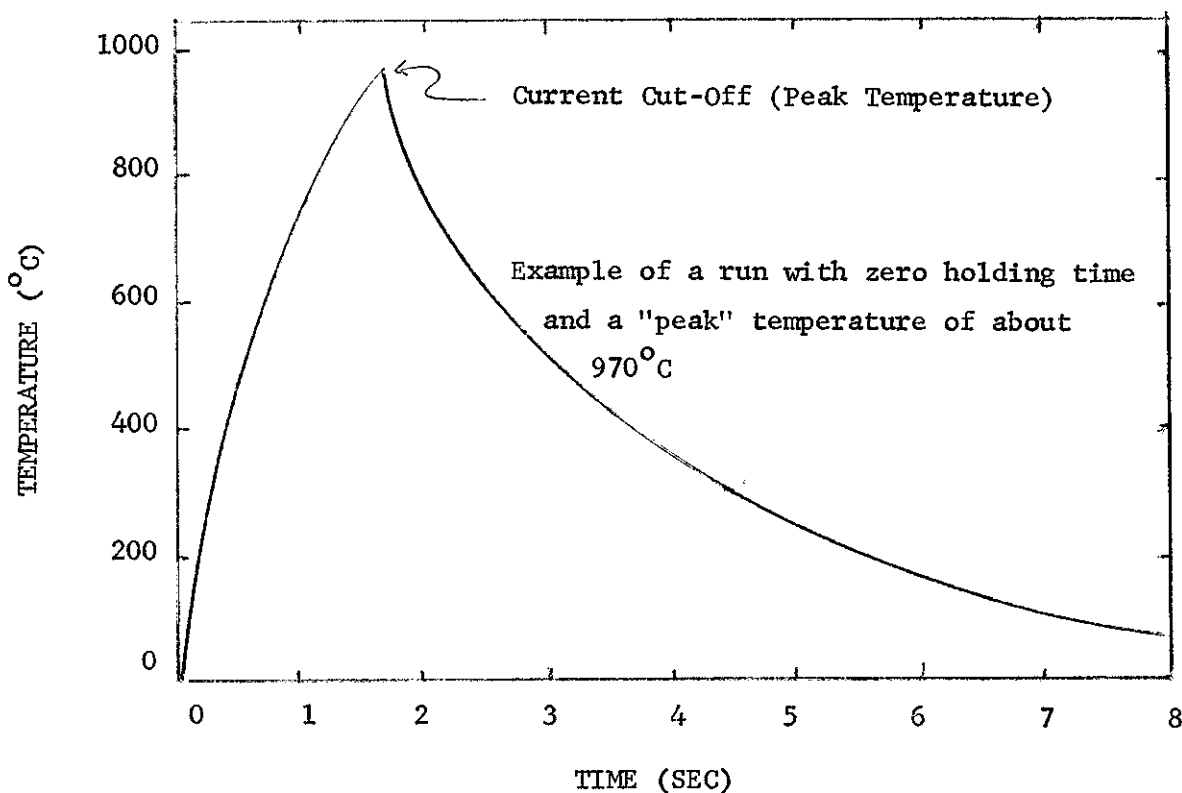
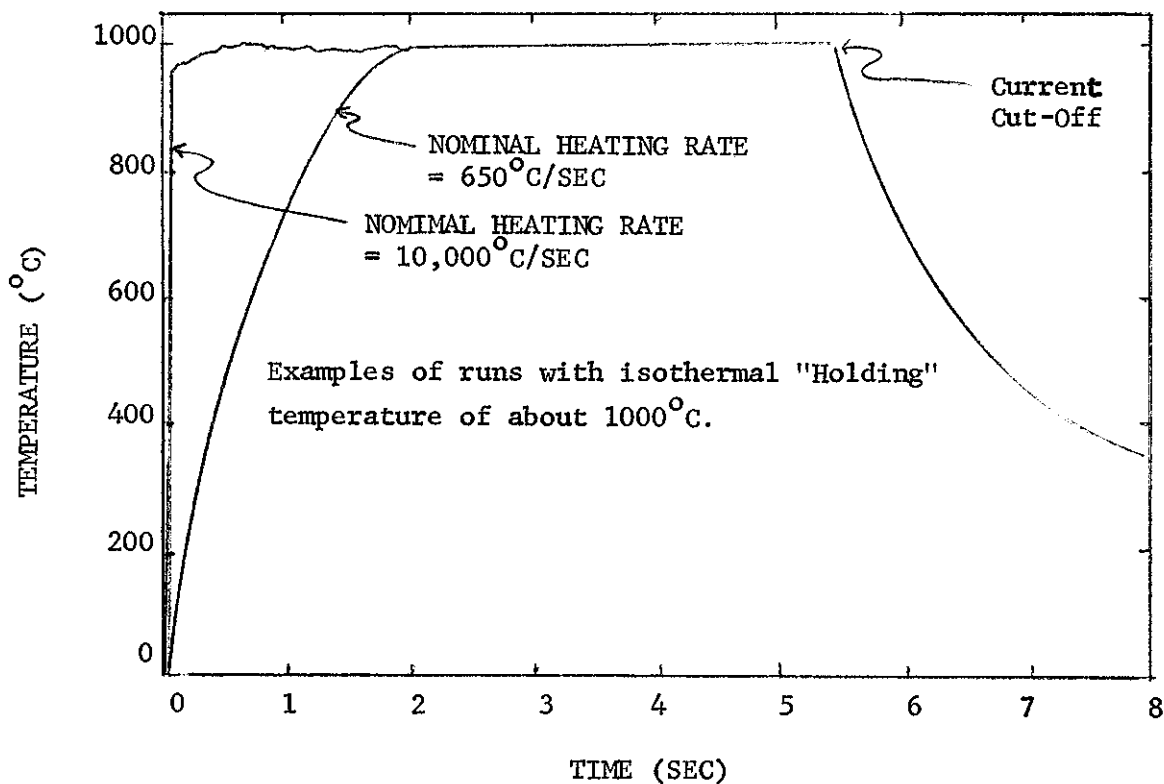


Figure 4-4. Examples of "Typical" Time-Temperature Histories (nominal heating rate is based on the time required to reach 85% of the final temperature, assuming a linear rise in temperature with time to that point).

in this trap. However since these compounds (especially the latter) tend to have some affinity for porous polymer-type packings such as Porapak Q or Chromasorb 102, it is generally advisable to check the performance of each individual trap with respect to retention of these compounds.

The other occasionally employed condensible product trap (in place of the above) consisted of a 6 inch length of 1/4 O.D. (15.2 cm x 0.635 cm) stainless steem tubing, packed with glass beads and cooled in an alcohol-dry ice bath. This trap was used only in conjunction with the low pressure apparatus, in an effort to knock out water from the product gas purge. Normal operation in the low pressure vessel involved use of the OV-17 porous polymer-packed trap which had the advantage of room temperature operation. Warming these traps to roughly 240°C releases the trapped products.

Downstream of the condensibles trap is a cryogenic adsorbent trap for retention of gaseous products (the so-called "Lipophylic Trap"). All gaseous pyrolysis products higher in molecular weight than hydrogen are retained in this trap. For operation of the low pressure vessel, this trap consists of a 15 inch long, 1/4" diameter (38.1 cm x 0.635 cm) tube also packed with Porapak Q, but operated at -196°C in a dewar of liquid nitrogen. In experiments with the high pressure system, the same type of trap was employed but the length was increased to roughly 5 ft (152 cm). This length was mandated by the significantly higher purge rates required in high pressure operation compared to low pressure operation. Warming of this trap to 100°C in a beaker of boiling water releases all trapped gases for analysis.

Hydrogen, as a product of pyrolysis, is determined by direct sampling

of the gases inside the vessel. The low pressure vessel is equipped with a small rubber septum for removal of gas samples with a precision syringe. Hydrogen product is not measured in high pressure pyrolysis runs.

All in-house product analysis involves vapor phase chromatography. A Perkin-Elmer Model 3920B chromatograph with dual thermal conductivity/flame ionization detectors and a Perkin-Elmer Model 1 integrator are used for all the analyses.

The intermediate weight oils, those from the room temperature OV-17/porous polymer trap, are analyzed on either a 50/80 mesh (177-297 $\mu$ ) 3% OV-17 or Porapak Q column, 6 ft x 1/8 inch (183 cm x 0.318 cm). Routine quantitation involves only total hydrocarbon measurement rather than individual species identification, because of the small quantities involved.

The gases from the liquid nitrogen trap are analyzed on a 12 ft x 1/4 inch, 50/80 mesh (366 cm x 0.635 cm, 177-297 $\mu$ ) Porapak Q column, temperature programmed from -70° to 240°C at a rate of 16°C/min. The hydrogen is analyzed on a 10 ft x 1/8 inch, 80/100 mesh (305 cm x 0.318 cm, 150-170 $\mu$ ) Spherocarb column at 30°C.

A few times, gas chromatographic analysis of tars was attempted using the OV-17 column described above, or a Dexsil 300 column of the same length, temperature programmed to roughly 350°C. Although a few clearly identifiable peaks were observed (e.g. pyrene) and a host of small near-baseline peaks were obtained, it was obvious that vapor phase chromatography of the tars was inappropriate because of the high molecular weights of the materials involved.

The whole system was frequently tested by conducting "blank" runs (runs in which no products should be present), and by injection of known

quantities of various sample product materials. The blank runs indicated the need to purify the incoming gases. Although the hydrogen and helium used were very high purity (~99.995%), the liquid nitrogen adsorbent very effectively concentrated any impurities from the feed gases. The addition of upstream adsorbent traps identical to those downstream eliminated this problem (shown in Fig. 4-1 as a "lipophylic pre-trap").

#### 4.3 Run Procedure

Approximately 10-15 mg of powdered coal is spread in a layer one to two particles deep on a preweighed screen which is reweighed and inserted between the brass electrodes. The reactor is evacuated and flushed three to five times with helium and then set at the desired experimental pressure. The sample temperature is raised at a desired rate to a desired holding value which is then maintained until the circuit is broken. Sample cooling by convection and radiation then occurs rapidly since the electrodes, the vessel and its gaseous contents remain cold during the experiment, but not so rapidly as to avoid the occurrence of significant weight loss during cooling.

The yield of char, which remains on the screen, is determined gravimetrically. Products that condense at room temperature (tars and oils, hereafter defined as tars) are collected primarily on foil liners within the reactor and on a paper filter at the exit of the reactor. Any condensation on non-lined reactor surfaces is collected by washing with methylene chloride soaked filter paper. The tar from all three collections is measured gravimetrically.



Products in the vapor phase at room temperature are collected at the conclusion of a run by purging the reactor contents through the room temperature and cryogenic lipophylic traps. These traps are then individually analyzed at the conclusion of the purge. Since the entire volume of gas produced during pyrolysis is trapped and analyzed, components present in quantities of .01 mg, representing about 0.1% of the original coal, could easily be quantitated. The chromatographic response factors used for calculation of gas yields, together with a sample calculation, are shown in the Appendix.

Elemental analysis of the raw coal, char, and tar samples were performed by Galbraith Laboratories, Inc. of Knoxville, Tennessee. Because of the very small experimental sample size involved, it was usually necessary to combine chars from several samples run under similar conditions to provide enough sample for analysis. The reproducibility of elemental analyses were frequently checked by requesting duplicate analyses. The dependence of reported results on the size of the sample provided (generally 30-60 mg of char was analyzed) was also checked by providing larger samples. The reproducibility of results on raw coals was uniformly good, while that on chars was acceptable (sulfur being the most troublesome component).

#### 4.4 Experimental Error Analysis

The weight of the coal and screen was determined to within  $\pm 0.01$  mg; hence, the uncertainty of the total weight loss measurement is about 0.1% by weight of the coal. The products quantitated chromatographically (except  $H_2O$ ) are subject to calibration uncertainties of 1 to 3% of the mass of the species measured. The water measurements were somewhat

more troublesome because of (1) moisture loss from the coal during the short time lapse between weighing the sample and performing the run and (2) moisture gain by the experimental system during assembly under high humidity conditions. The net uncertainty in the measured water yields caused by these opposing effects is about 2% by weight of the coal (except in the case of some hydrolysis runs, which will be discussed on an individual basis). The tar measurement has its largest uncertainty in the washing procedure. The maximum error for atmospheric pressure runs is about 1 % by weight of the coal. The inherent uncertainty of the thermocouple measurements is about  $\pm 8^{\circ}\text{C}$  over the present range of temperatures. The ability of the selected thermocouple to effectively track the temperature of the sample at the highest heating rates was confirmed by experiments with thermocouples of a different bead diameter.

Some discoloration of the screen used to hold the sample caused concern that the screen may be a source of error, for example through catalysis of primary pyrolysis or secondary cracking reactions. Experimental assessment of the role of the screen included passivation of the surface with a vacuum deposited layer of gold on some screens and copper on others, and variation of the number of layers of untreated screen through which the volatiles had to escape. Both gold and copper are less catalytic to cracking reactions than is stainless steel, and diffusion of these metals in stainless steel is too slow to destroy the integrity of the surface layer in even the longest residence times of this study. None of these cases lead to significant differences in the total yield of volatiles or in the composition of gaseous products included in the present study. Therefore, any error caused by the screen appears to be negligible for present purposes. This result is not surprising in

view of the high escape velocity of volatiles from the sample hence the low residence time of volatiles near hot screens. Nevertheless, untreated stainless steel screens in a similar apparatus are reported to react significantly with hydrogen sulfide (Solomon, 1976). This compounds was not determined in the present work, except in a few select cases.

## 5.0 RESULTS AND DISCUSSION

### 5.1 Pyrolysis of a Montana Lignite

All the results reported in this section are for the partially dried Montana lignite described in Table 3.1-1. The particle size range examined is 53-88 $\mu$ , with an average particle diameter of 74 $\mu$ . All mass yield results are here reported on an as-received basis.

#### Base Data

With the exception of the data points carrying a double symbol (see below), the volatile product compositions shown in Fig. 5.1-1 were obtained when different samples of the lignite under 1 atm of helium were heated at approximately 1000°C/s to various peak temperatures indicated on the abscissa. The samples were cooled at roughly 200°C/s beginning immediately when the peak temperature was attained. The total yield of any product or group of products is given on the ordinate as a weight percent of the partially dried lignite.

The lowest curve represents the yield of tar as defined above, which increases with increasing temperature to an asymptotic maximum of about 5.4% by weight of the lignite at temperatures above 750 to 800°C. The tar appears to have two primary components. One is a heavy, tawny brown liquid-like material which deposits as a film on surfaces. The other consists of dark brown objects which give the impression of being solid pieces of lignite that were presumably broken off the parent material and carried away with the volatiles. These "particles", some of which appear to be agglomerates, are for the most part smaller than 10  $\mu$ m across but sometimes as large as 25  $\mu$ m. About 75% of the tar, including most of the tawny liquid and a fraction of the particles, appears to dissolve in methylene chloride. Elemental analysis of the methylene chloride soluble material gives an approximate empirical formula  $\text{CH}_{1.5}\text{O}_{0.1}\text{N}_{0.01}$ . The indicated oxygen content may be too high due to some oxidation in the presence of air. Extensive analysis of any one tar sample is difficult because of the small yields.

The distance between the tar curve and the next one above it represents hydrogen and all hydrocarbons lighter than tar. The maximum yield of these species occurs at the higher temperatures and is only about 3.3% by weight of the lignite. The main components are methane

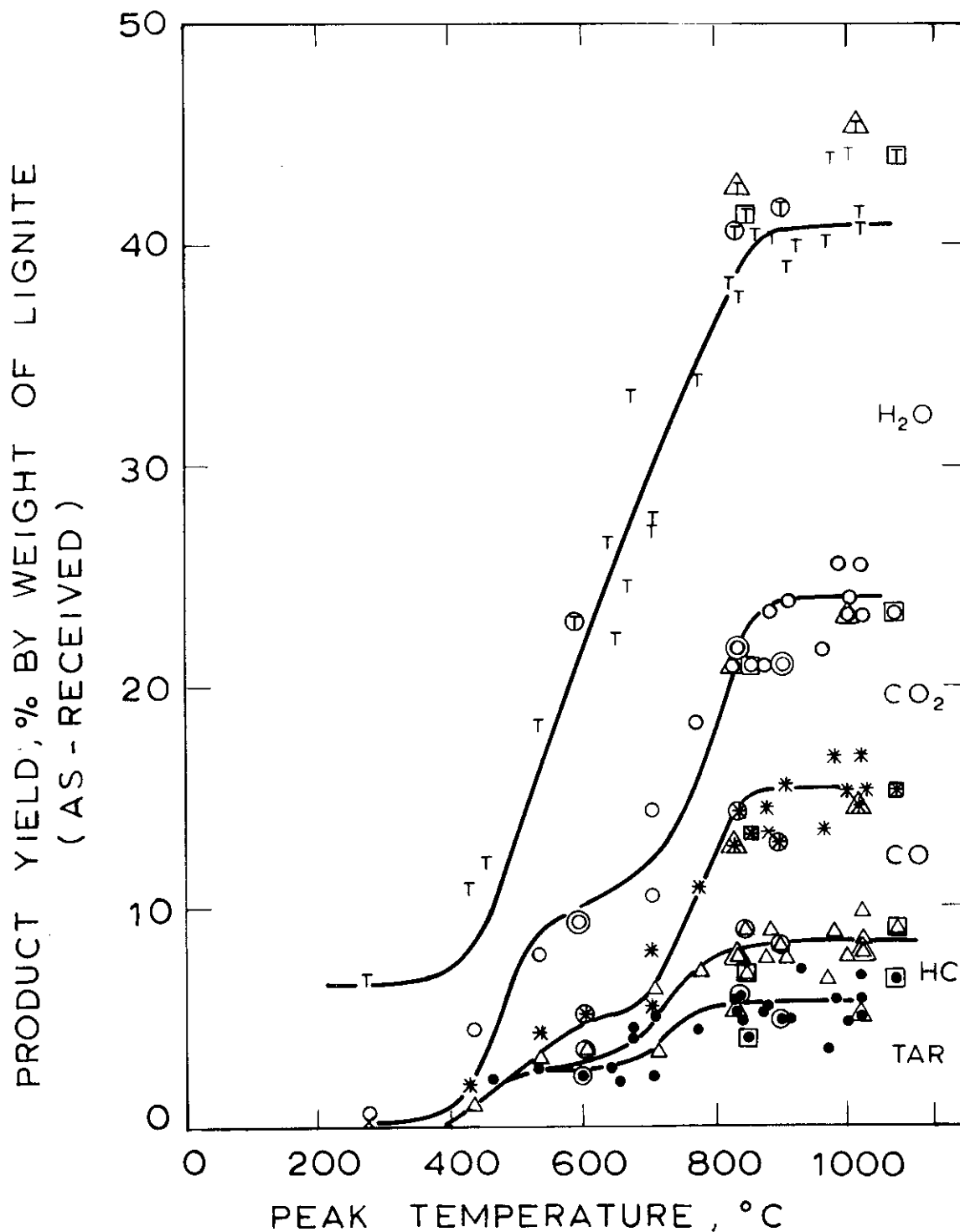


Figure 5.1-1 Pyrolysis Product Distributions from Lignite Heated to Different Peak Temperatures [(●) tar; (Δ) tar and other hydrocarbons (HC); (\*) tar, HC and CO; (o) tar, HC, CO, and CO<sub>2</sub>; (T) total, i.e., tar, HC, CO, CO<sub>2</sub>, and H<sub>2</sub>O. Pressure = 1 atm (helium); Heating rate: (single points) 1000°C/s; (points inside o) 7,100 to 10,000°C/s; (points inside Δ) 270 to 470°C/s; (points inside □) 1000°C/s, but two-step heating.]

(1.3%), ethylene\* (0.6%), and hydrogen (0.5%), with identified ethane, propylene, propane, and benzene and unidentified trace hydrocarbons making up the balance. The effect of temperature on the yields of methane, hydrogen and ethylene is shown in Fig. 5.1-2. When the peak temperature is increased above 500°C the methane and ethylene yields increase rapidly to small asymptotic values in the range 600-700°C. Further increase in temperature beyond 700°C effects a dramatic increase in the yield of both species, and a second asymptote is reached at about 850°C for ethylene and about 900°C for methane. The yield of tar also exhibits a similar two-step behavior but hydrogen production, on the other hand, appears to occur in one step at relatively high temperatures.

The top curve in Fig. 5.1-1 represents the total yield of volatiles while, proceeding downward, the first, second and third regions between adjacent curves represent the yields of water, carbon dioxide, and carbon monoxide, respectively. The yields of these principal oxygenated species are shown in more detail in Fig. 5.1-3 where all three appear to approach high-temperature asymptotic yields of 16.5% for water, 8.4% for carbon dioxide, and 7.1% for carbon monoxide. The carbon oxides each exhibit also a lower-temperature asymptote.

Although most of the pyrolysis is complete for peak temperatures above 900 to 1000°C, there is in fact yet a third step in the curves for the carbon oxides which occurs at about 1100°C and therefore does not appear in Fig. 5.1-3. Since this temperature is the upper limit of the apparatus, investigation of this third step was accomplished by use of a longer residence time technique.

The coal was heated at 1000°C/s to 1000°C and there held for 5 to 10 s rather than being immediately cooled as before. The resulting carbon monoxide yield exhibits a final asymptote of 9.4% while that of carbon dioxide is 9.5%. The yields of the other species were not changed by the additional residence time. Thus prolonged heating at 1000°C gave a total volatiles yield of 44.0% by weight of the lignite which is close to the ASTM volatile matter plus moisture (43.7%).

---

\*The analysis neglected any acetylene present, which would be eluted with ethylene.

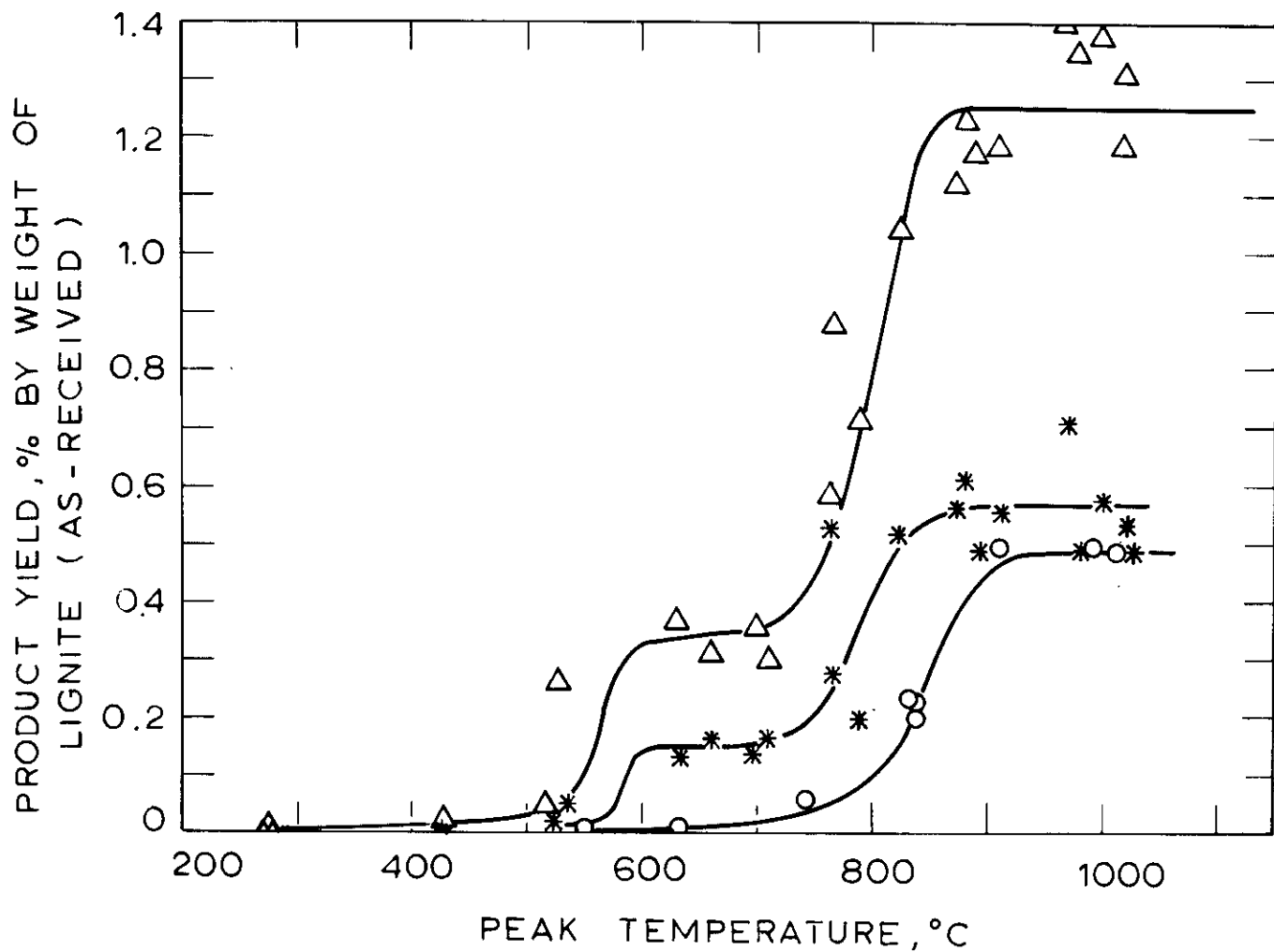


Figure 5.1-2 Yields of Methane, Ethylene and Hydrogen from Lignite Pyrolysis to Different Peak Temperatures [( $\Delta$ )  $\text{CH}_4$ ; (\*)  $\text{C}_2\text{H}_4$ ; (o)  $\text{H}_2$ . Pressure = 1 atm (helium). Heating rate =  $1000^\circ\text{C/s}$ ].

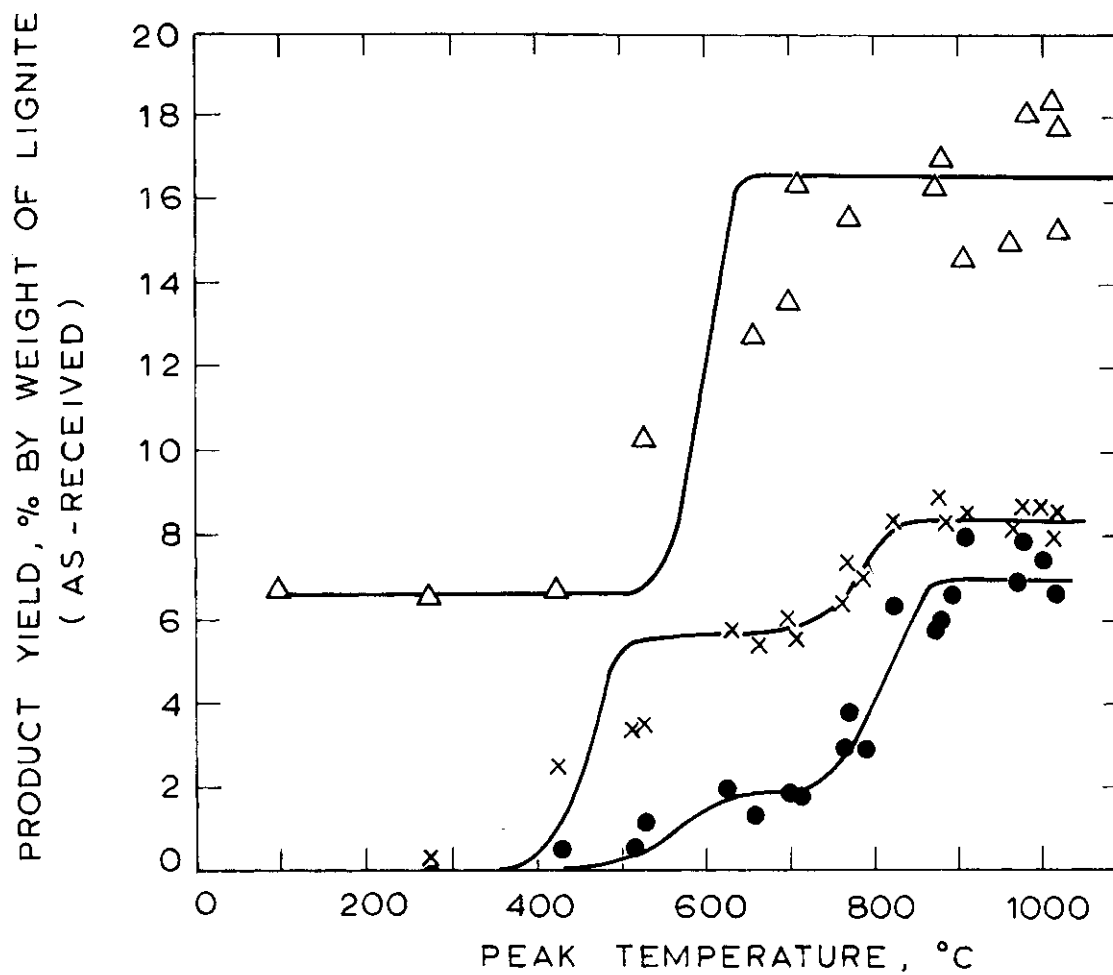


Figure 5.1-3 Yields of Water, Carbon Monoxide, and Carbon Dioxide from Lignite Pyrolysis to Different Peak Temperatures [( $\Delta$ )  $H_2O$ ; (x)  $CO_2$ ; ( $\bullet$ ) CO. Pressure = 1 atm (helium). Heating rate =  $1000^\circ C/s$ ].



Elemental analyses of selected char samples are shown in Fig. 5.1-4. Although over 40% by weight of the lignite is volatilized at the higher temperatures, only 22% of the carbon is volatilized. Most of the volatile material comes from hydrogen and oxygen, which is consistent with the observed predominance of water among the volatile products. Pyrolysis at the higher temperatures removes about 70% of the sulfur from the solid material, but the nitrogen is reduced by only about 25%. Consequently, the sulfur content (percent by weight) in the char is lower than that of the lignite, but the reverse is true for nitrogen. Similar data obtained in an entrained flow reactor show that the fractional evolutions of sulfur and nitrogen are increased to at least 85% and 65%, respectively, as the pyrolysis of Montana lignite is extended to 1800°C (Kobayashi et al., in press; Kobayashi, 1976). The weight of ASTM ash in the char from most of the present experiments is less than that in the raw lignite, which is qualitatively similar to a previous observation (Kobayashi et al., in press; Kobayashi, 1976).

Elemental balances were calculated for runs in which both volatile products and char were analyzed. For estimation purposes, trace hydrocarbons (total less than 1% by weight of the lignite) were assumed to be 90% carbon and 10% hydrogen by weight. The tar was assumed to have an empirical formula equivalent to that given above for the principal, methylene chloride soluble, fraction. Typical results for four runs to different peak temperatures are presented in Table 5.1-1 along with total mass balances. Whereas the mass balances are excellent and the carbon and hydrogen balances are satisfactory, the oxygen balances are marginal. Since, as has been discussed, oxygen in char is determined by difference, uncertainties inherent in the other measurements are absorbed in the oxygen values.

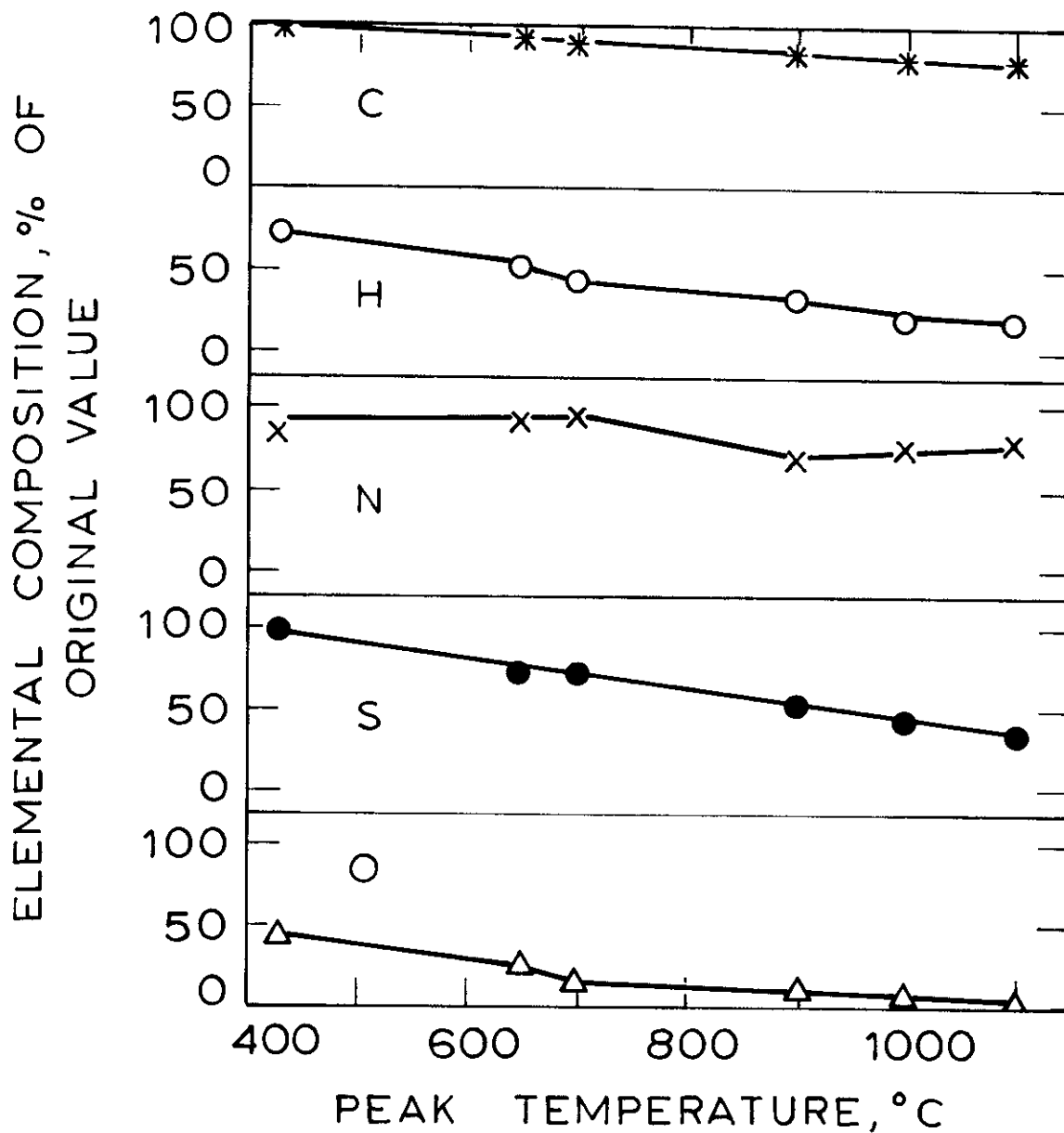


Figure 5.1-4 Elemental Compositions of Chars from Lignite Pyrolysis to Different Peak Temperatures [(\*) C; (o) H; (\*) N; (●) S; (Δ) O. Pressure = 1 atm (helium). Heating rate = 1000°C/s].

Table 5.1-1 Carbon, Hydrogen, Oxygen and Total Mass Balances for Lignite Pyrolysis

Product	Yield, weight % of Lignite (as-received) <sup>†</sup> , in Four Runs to Different Peak Temperatures															
	Peak Temperature 430°C				Peak Temperature 710°C				Peak Temperature 910°C				Peak Temperature 1000°C			
	<u>Total</u>	<u>C</u>	<u>H</u>	<u>O</u>	<u>Total</u>	<u>C</u>	<u>H</u>	<u>O</u>	<u>Total</u>	<u>C</u>	<u>H</u>	<u>O</u>	<u>Total</u>	<u>C</u>	<u>H</u>	<u>O</u>
CO <sub>2</sub>	2.5	0.68	-	1.8	5.5	1.5	-	4.0	8.6	2.3	-	6.3	8.7	2.4	-	6.3
CO	0.46	0.20	-	0.26	1.8	0.77	-	1.0	8.0	3.4	-	4.6	7.5	3.2	-	4.3
HC*	0.02	0.02	0.0	-	0.95	0.79	0.17	-	2.6	2.1	0.49	-	3.0	2.4	0.58	-
Tar	1.5	1.3	0.15	-	2.3	2.1	0.23	-	4.9	4.4	0.49	-	4.7	4.3	0.47	-
H <sub>2</sub> O	6.6	-	0.73	5.9	16	-	1.8	14	15	-	1.7	13	19	-	2.1	17
H <sub>2</sub>	0.0	-	0.0	-	0.01	-	0.01	-	0.50	-	0.50	-	0.50	-	0.50	-
Char	89.0	64.0	2.8	11.0	73.0	53.6	1.5	3.1	60.9	47.5	1.2	2.6	55.8	44.2	0.55	1.1
Total	100	66.2	3.68	19.0	99.9	58.8	3.71	22.1	101	59.7	4.38	26.5	99.2	56.5	4.20	28.7
Closure	100%	112%	81%	79%	100%	99%	82%	91%	101%	101%	97%	110%	99%	95%	93%	119%

\* Hydrocarbons other than tar

<sup>†</sup>Lignite (as-received) is 59.3%C, 4.53% H and 24.2%O, including H and O in lignite moisture.

### Effect of Temperature-Time History

Data points inside squares in Fig. 5.1-1 were obtained with the base conditions given above but modified as follows. The lignite was first heated to an intermediate temperature and then cooled to room temperatures as before. The resulting char was then heated to a higher temperature and cooled again. The figure shows cumulative product yields for both cycles. The intermediate temperatures for the points at 855°C and 1070°C are 480°C and 670°C, respectively. The yields of all products in both cases are not significantly different from those obtained when the lignite is heated directly to the final peak temperature. This observation is consistent with the previous conclusion from weight loss data (Anthony et al., 1975, 1976) that the pyrolysis reactions occurring at higher temperatures are largely independent of those occurring at lower temperatures. Such behavior is indicative of multiple parallel independent reactions as opposed to competitive reactions.

The encircled data points in Fig. 5.1-1 were obtained at heating rates of 7,100 to 10,000°C/s which is approximately ten-times higher than that of the base data. The points in triangles represent data taken at 270 to 470°C/s. No clear effect of heating rate is observed over the range here used. It is shown below that this behavior is expected for independent parallel, rather than competitive reactions.

### Effect of Pressure

Some runs were conducted under vacuum conditions (0.05 mm Hg) and some under very high pressures of inert gas (1000 psig He). As shown in Fig. 5.1-5, up to peak temperatures of between 750°C and 800°C (at a heating rate of 1000°C/sec), the general course of vacuum pyrolysis

shows no systematic deviations from the base case. Above 750-800°C, however, significant differences are noted. This is shown clearly in Fig. 5.1-5 and Fig. 5.1-6. The high temperature asymptote for 69 atm in Fig. 5.1-6 is drawn in with a knowledge of the results from high temperature (1000°C) isothermal runs; Table 5.1-2 compares the yields at atmospheric and high pressures in detail.

Unfortunately, there is some uncertainty in The Fig. 5.1-5 and Table 5.1-2 tar values for both vacuum and high pressure conditions. Collection of all the tar formed under vacuum is difficult. Whereas at atmospheric pressures most of the tar stays suspended as an aerosol until it is purged through the filter, tar produced under vacuum deposits uniformly across all reactor surfaces upon initiation of the purge. Recovery of the thin tar film by the methylene chloride washing procedure is somewhat inefficient. Thus the total mass balance is poorer at vacuum than at 1 atm. A carbon balance conducted as described for Table 5.1-1 shows a carbon deficit of about 3% for the vacuum data in Fig. 5.1-5. Therefore the actual yield of tar under vacuum at 1000°C may be about 9% of the lignite weight. Collection of all the tar under high pressure conditions is difficult because of the larger surface areas of the high-pressure vessel, and the fact that its walls are opaque.

The main conclusion from Table 5.1-2 and Figs. 5.1-5 and 5.1-6 is that vacuum pyrolysis of lignite produces higher yields of heavy hydrocarbon products and lower yields of light gases than are obtained at higher pressures. Since also the total weight loss is higher under vacuum, it appears that secondary cracking and char forming reactions play a role in determining product yields. In view of the thin layer of coal employed, the main contribution of the secondary reactions in this experiment

PRODUCT YIELD, WEIGHT % OF LIGNITE (AS RECEIVED)

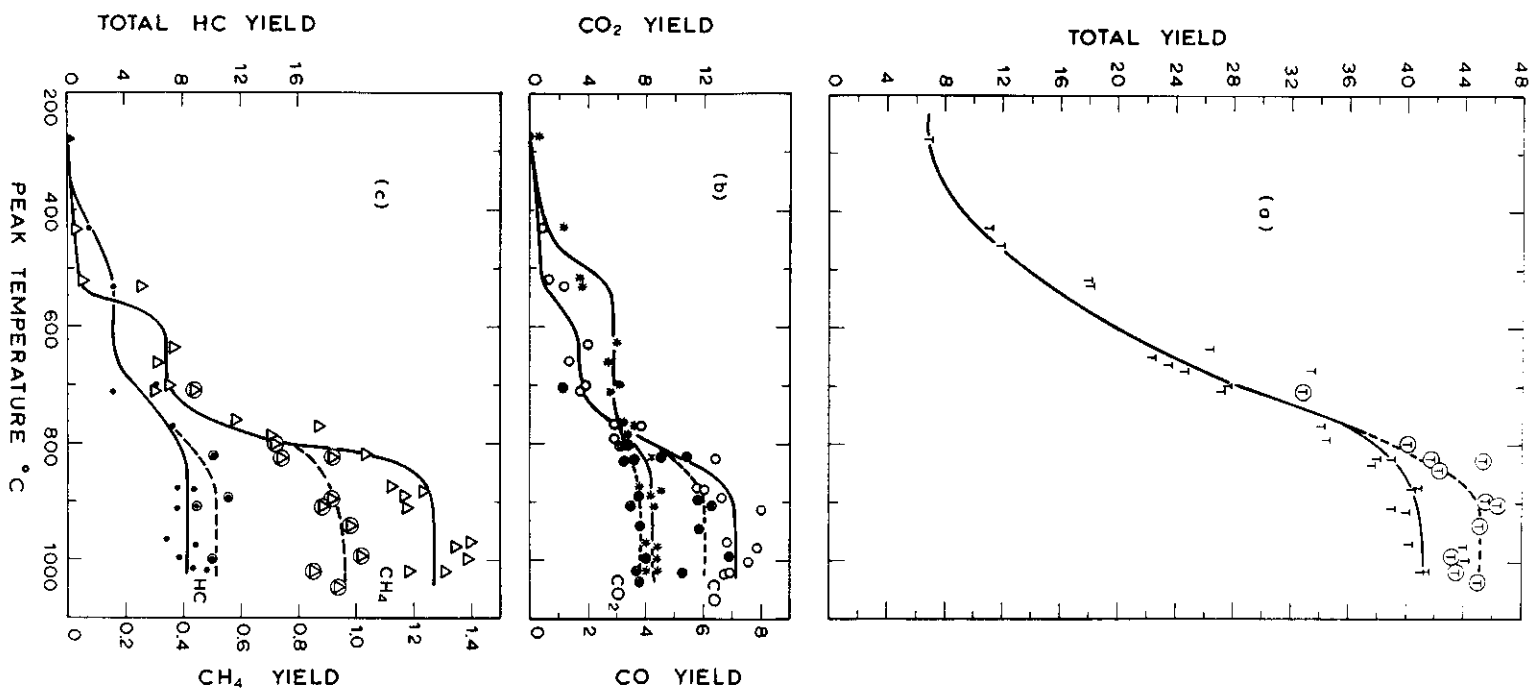


Figure 5.1-5 Effect of Pressure on Product Yields from Lignite Pyrolyzed to Different Peak Temperatures [Pressure: (single points and solid curves) 1 atm; (points inside 0 and dashed curves)  $6.6 \times 10^{-5}$  atm. Heating rate =  $1000^{\circ}\text{C/s}$ . (T) total, i.e., tar, all other hydrocarbons,  $\text{H}_2\text{O}$ ,  $\text{CO}_2$  and CO; (o) CO; (\*)  $\text{CO}_2$ ; (Δ)  $\text{CH}_4$ ; (●) total hydrocarbons including tar].

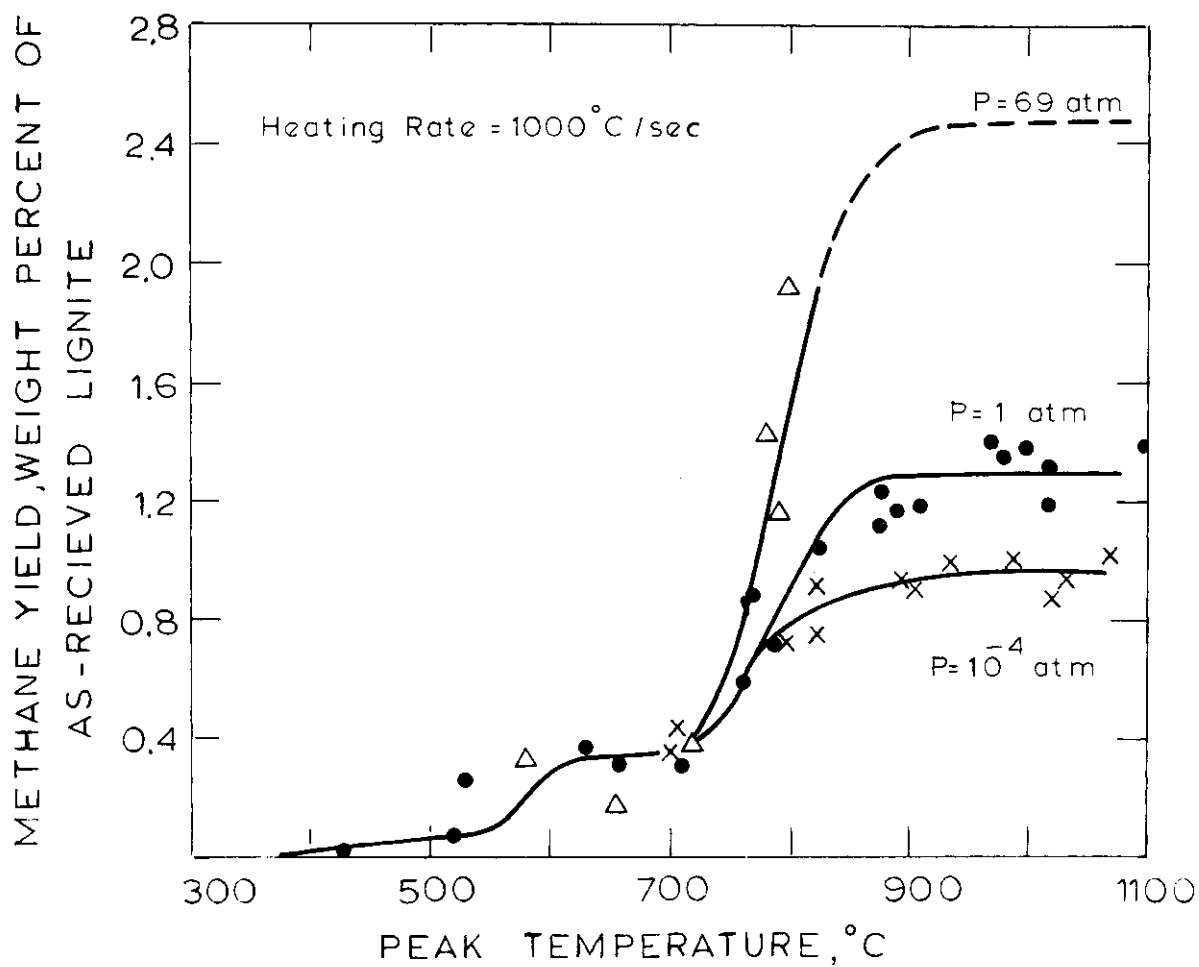


Figure 5.1-6 Effect of Pressure on the Yield of Methane from Lignite Pyrolyzed to Different Peak Temperatures (all runs in Helium).

Table 5.1-2 Comparison of Yields from Atmospheric and High Pressure Pyrolysis of Lignite ( $T \approx 1000^\circ\text{C}$ , 3-10 seconds)

	<u>1 Atm. He</u>	<u>69 Atm. He</u>	<u>Vacuum (zero holding time)</u>
CO <sub>2</sub>	9.5	10.6	7.6
CO	9.4	9.0	6.1
CH <sub>4</sub>	1.3	2.5	0.9
C <sub>2</sub> H <sub>4</sub>	0.6	0.6	0.4
C <sub>2</sub> H <sub>6</sub>	0.2	0.2	0.2
other HC	0.8	1.7	1.9
H <sub>2</sub> O	16.5	12.9	17.7
H <sub>2</sub>	0.5	not measured	NM
tar	<u>5.4</u>	<u>~3</u>	<u>~7</u>
Total	44.2	40.5	41.8
Measured total weight loss	44.0	40.2	44.8



presumably occurs within the particles. A similar but quantitatively more significant effect of secondary reactions on total weight loss from a bituminous coal was observed by Anthony et al., (1975, 1976), and verified by this study (see section on bituminous pyrolysis). Other workers, e.g., Howard (1963) and Loison and Chauvin (1964), also have observed increased yields of low-volatile species in vacuum pyrolysis of coal.

Under no conditions were the lignite particles observed to cake, swell or soften. The lignite char was always composed of particles of roughly the same size as the raw coal, and could easily be poured out of the screen holder at the conclusion of a run.

## 5.2 Pyrolysis of a Pittsburgh Seam Bituminous Coal

The results reported in this section are all for the Pittsburgh Seam (No. 8) bituminous coal described in Table 3.1. As with the lignite, the particle size range examined as the base case is 53-88 $\mu$ , with an average diameter of 74 $\mu$ . Again, all results reported in this section are reported on an as-received basis.

### Base Data

Fig. 5.2-1 describes the overall pyrolysis behavior of the bituminous coal. The method of presentation of the data is the same as in Fig. 5.1-1. The topmost curve again represents the total measured weight loss as a function of the peak temperature attained just before cooling. As before, the base case heating rate is 1000°C/sec, under 1 atmosphere of helium pressure.

The other products are plotted in a cumulative fashion, as before, with the exception of the carbon oxides, which in this presentation are grouped together.

What is immediately apparent from comparison of Figs. 5.1-1 and 5.2-1 is that whereas the oxide products dominate the volatile products of lignite pyrolysis, the tar product dominates bituminous coal pyrolysis products. This is, of course, very much in line with the results of many other studies (see Section 3.2).

This tar product appeared to be relatively homogeneous, in contrast to the lignite tar. Its color was a tawny yellow much like the lignite high temperature tar. Upon standing in air, however, the material darkened noticeably, eventually becoming a dark brown. This is a well known phenomenon attributed primarily to oxidation (Sternberg, 1977). Elemental analysis of the material could not be conducted immediately nor could the sample be handled or stored without air contact. However it is believed that

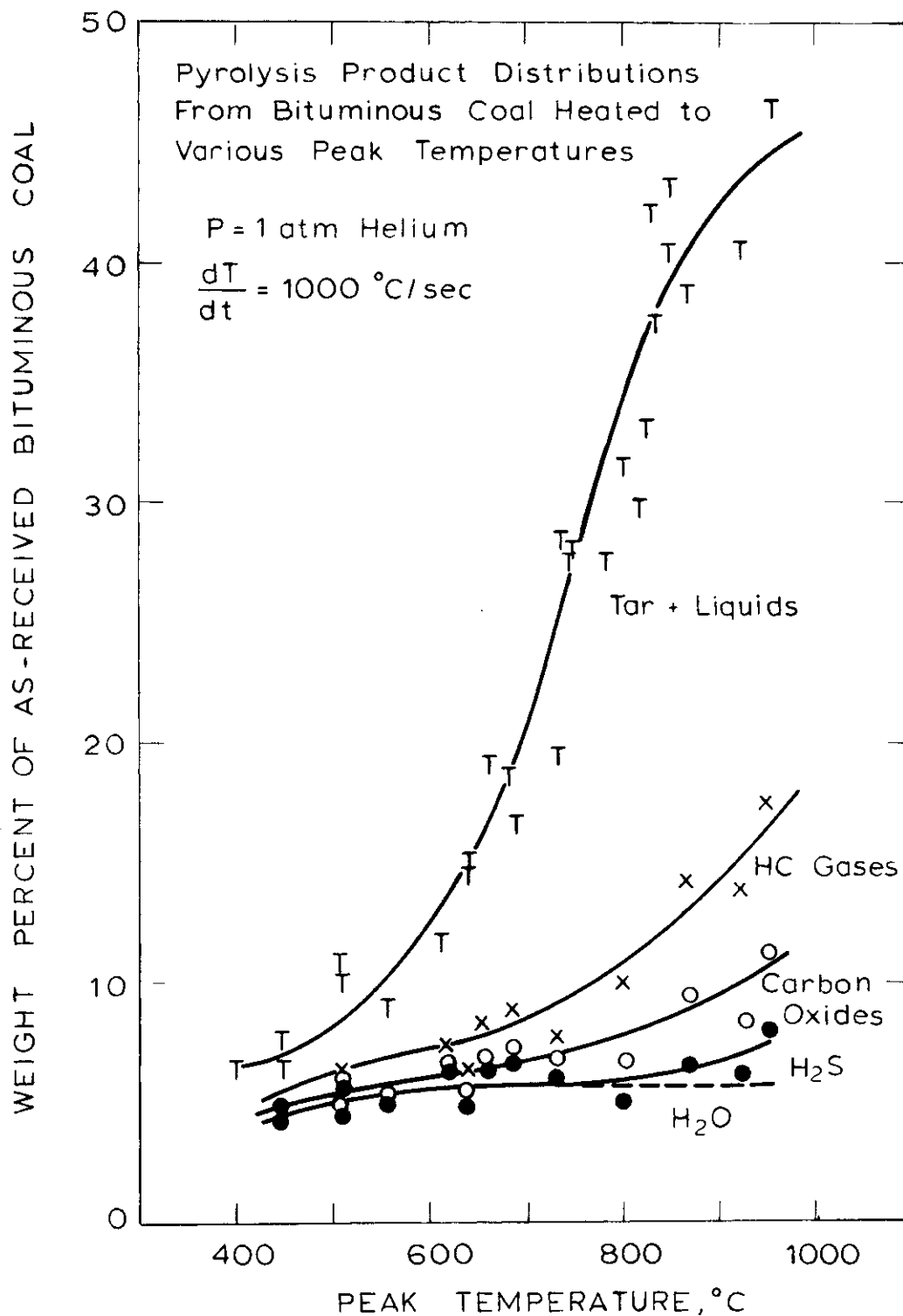


Figure 5.2-1 Pyrolysis Product Distributions from Bituminous Coal Heated to Different Peak Temperatures (•)  $\text{H}_2\text{O} + \text{H}_2\text{S}$ ; (o)  $\text{CO} + \text{CO}_2 + \text{H}_2\text{O} + \text{H}_2\text{S}$ ; (x)  $\text{CO} + \text{CO}_2 + \text{H}_2\text{O} + \text{H}_2\text{S} +$  all Hydrocarbon Gases; (T) Total Weight Loss).

the amount of oxygen responsible for the darkening is small, since weighing samples of tar before and after color change did not reveal changes that could be considered significant (<1%).

The elemental analysis of the tar was  $\text{CH}_{1.1}^{\text{O}}.08^{\text{N}}.01$ . The bituminous tar is rather strikingly lower in H/C ratio than the lignite tar (for which  $\text{H/C} \approx 1.5$ ). Nevertheless, in both cases the tars were significantly richer in hydrogen than the parent coals, but very similar to the parent coals in nitrogen to carbon ratio.

Samples of the bituminous tar were subject to gas chromatographic analysis. The eluted compound present in largest quantity (a few wt%) was pyrene,  $\text{C}_{16}\text{H}_{10}$  (MW = 202); many other compounds were present, but in quantities too small to be quantitated. Many others must have been present which had boiling points too high to elute from the OV-17 column at 350°C.

The yield vs. temperature data for the tar and water fractions alone are shown in Fig. 5.2-2. The left-hand portion of the figure shows the yield plotted in the usual manner, as a function of peak temperature. The right hand portion of the figure shows data from a set of runs whose time-temperature histories included an isothermal period; rather than cooling a sample immediately upon achieving the peak temperature, the sample is instead held at the indicated ("holding") temperature for approximately 2 to 10 seconds. As would be expected, the yield at a particular holding temperature is higher than the yield at the corresponding peak temperature, except where a particular reaction (or set of reactions) has gone to completion even without the isothermal holding period.

The data for tar do not show any two or three step behavior; the rather broad temperature dependence is suggestive of a broad distribution of reactions. The modelling of pyrolysis phenomena will be discussed in

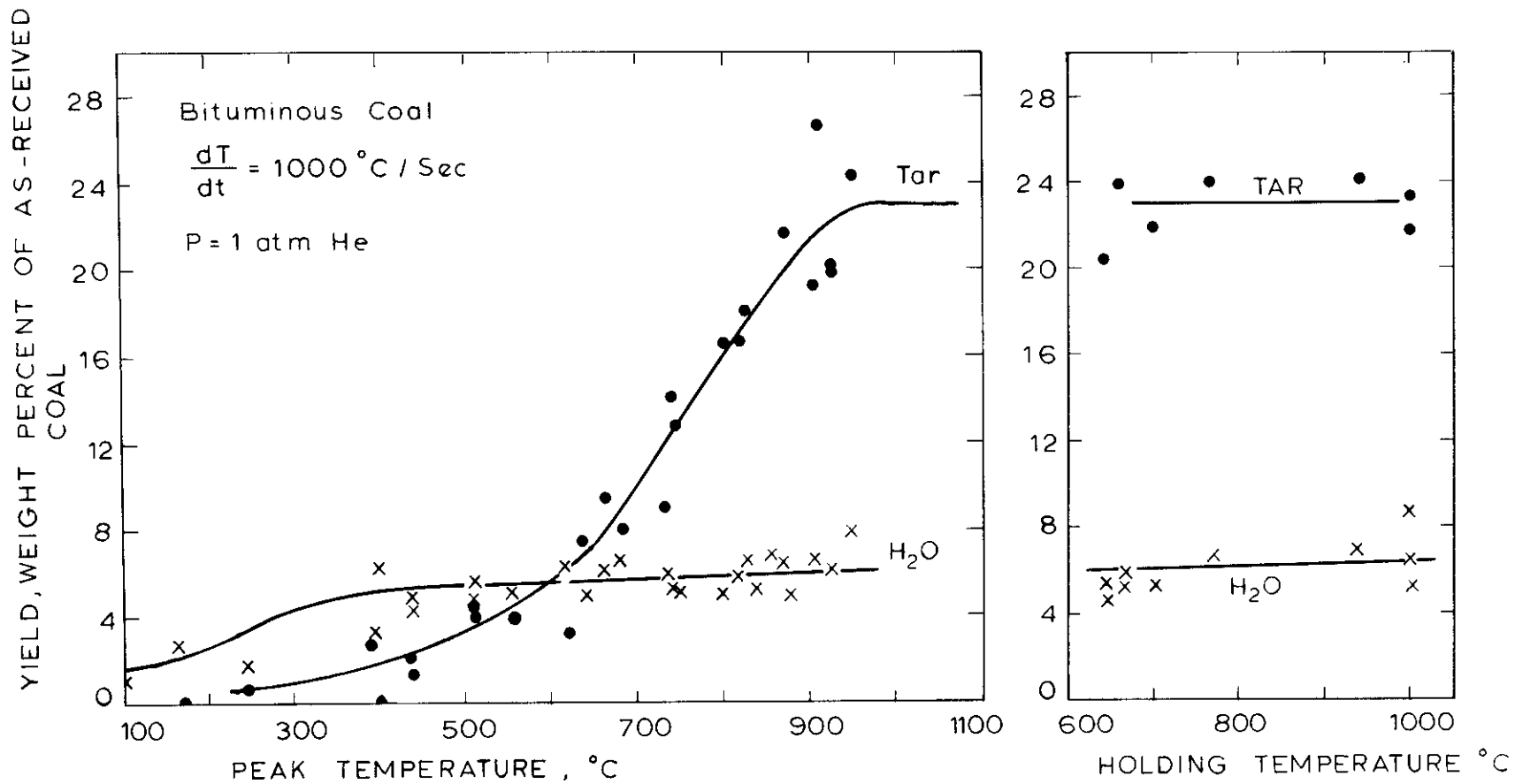


Figure 5.2-2 Yields of Tar and Water from Bituminous Coal Pyrolysis.

the next section.

Pyrolytically formed water is seen to be primarily evolved at rather low temperatures (below 400°C). This is in sharp contrast to the behavior of the lignite, in which pyrolytic water is formed at temperatures higher by 200-300°C. This suggests a substantial difference in starting materials, mechanisms, or both. This point will be discussed further in the next section.

It was necessary to correct high temperature ( $\sim 900^\circ\text{C}$ ) water measurements for a small amount of  $\text{H}_2\text{S}$  included in these measurements by the electronic integration procedure. The chromatographic technique employed did not lead to particularly good separation of  $\text{H}_2\text{O}$  and  $\text{H}_2\text{S}$ . In many high temperature runs,  $\text{H}_2\text{S}$  is present in the water peak as a rather gentle shoulder. To determine the actual amount of correction required, the dry ice cooled glass bead trap was used to remove water from the product gas stream. The chromatograph was then used to determine  $\text{H}_2\text{S}$  directly. The  $\text{H}_2\text{S}$  values so obtained were roughly 1%(wt) for runs of roughly 1000°C holding temperature. This figure represents a minimum  $\text{H}_2\text{S}$  yield, in that loss of  $\text{H}_2\text{S}$  to reactions with the stainless steel screen was possible, as has already been discussed. Also, it is possible that a small amount of  $\text{H}_2\text{S}$  may have been lost to the condensate in the dry ice trap, although this is considered insignificant because of the very small amount of condensate involved (< 1 mg) and its very low temperature (-60°C).

Figs. 5.2-3, 5.2-4, and 5.2-5 show the yields of other major products. These results generally showed no evidence of the two-step behavior seen during lignite pyrolysis.

Fig. 5.2-3 focusses upon two of the more important pyrolysis product gases, methane and hydrogen. It is clear to see that methane evolution

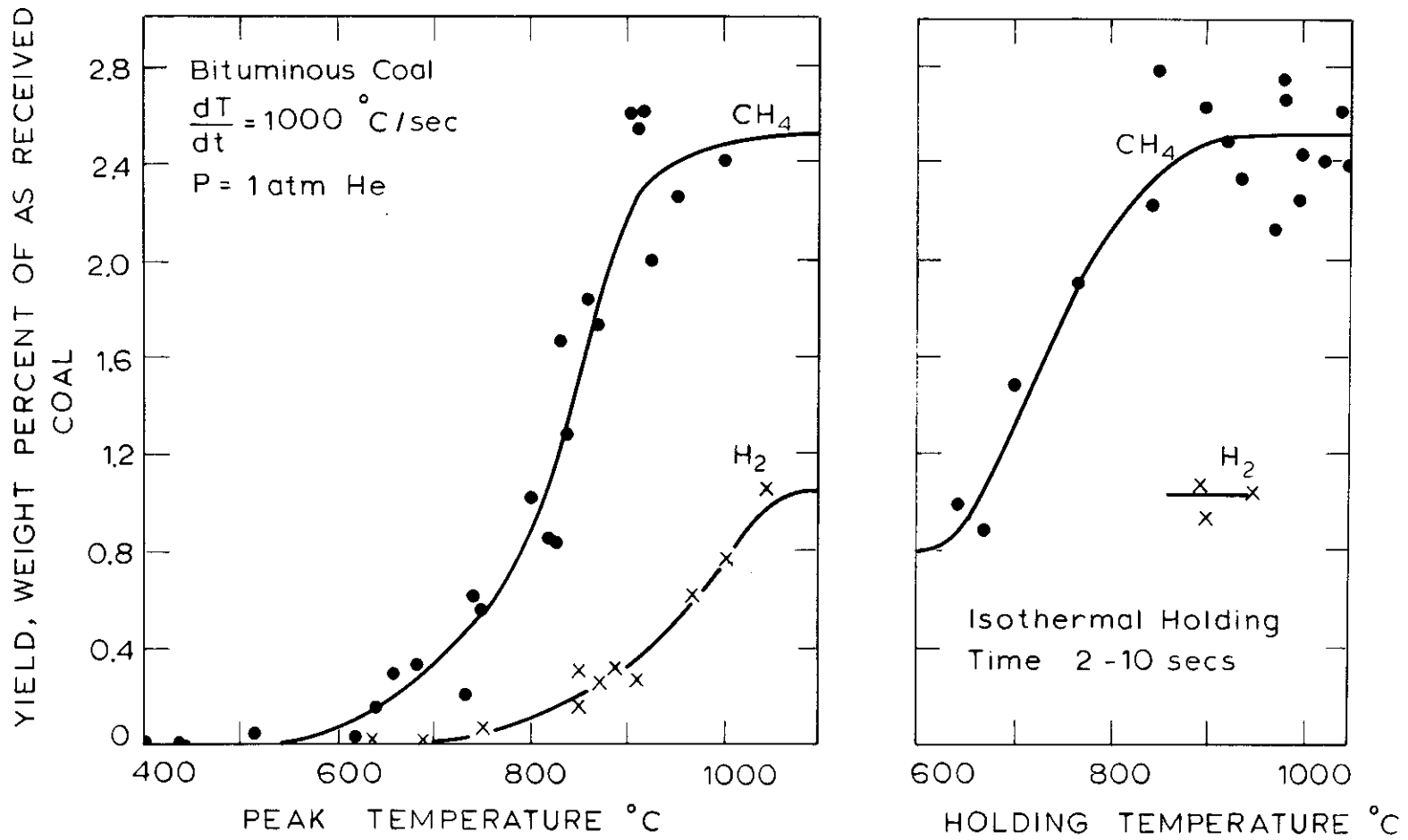


Figure 5.2-3 Yields of Methane and Hydrogen from Bituminous Coal Pyrolysis.

YIELD, WEIGHT PERCENT OF AS RECEIVED  
BITUMINOUS COAL

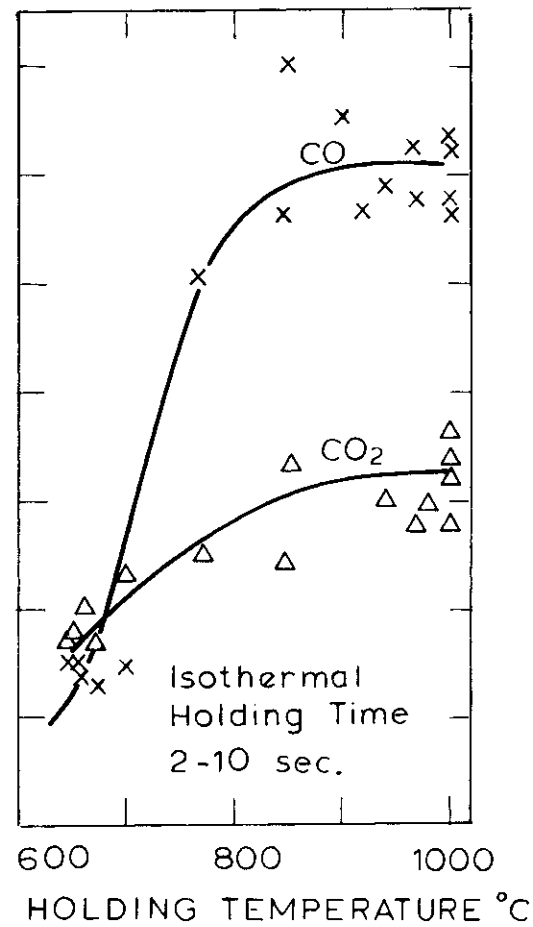
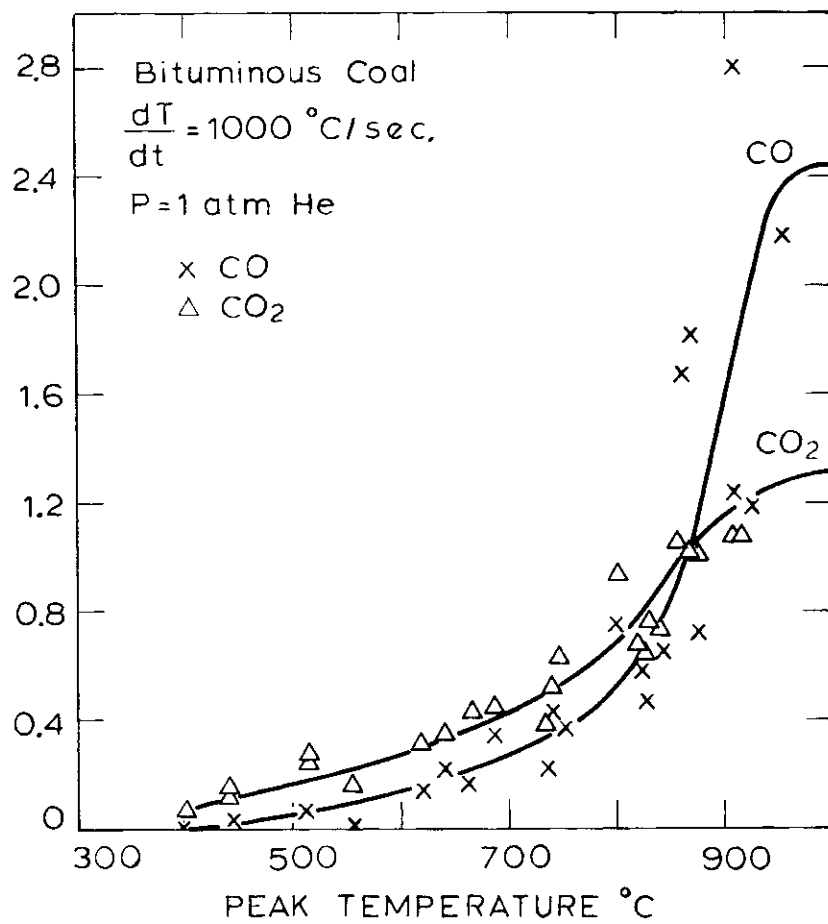


Figure 5.2-4 Yields of Carbon Monoxide and Carbon Dioxide from Bituminous Coal Pyrolysis.



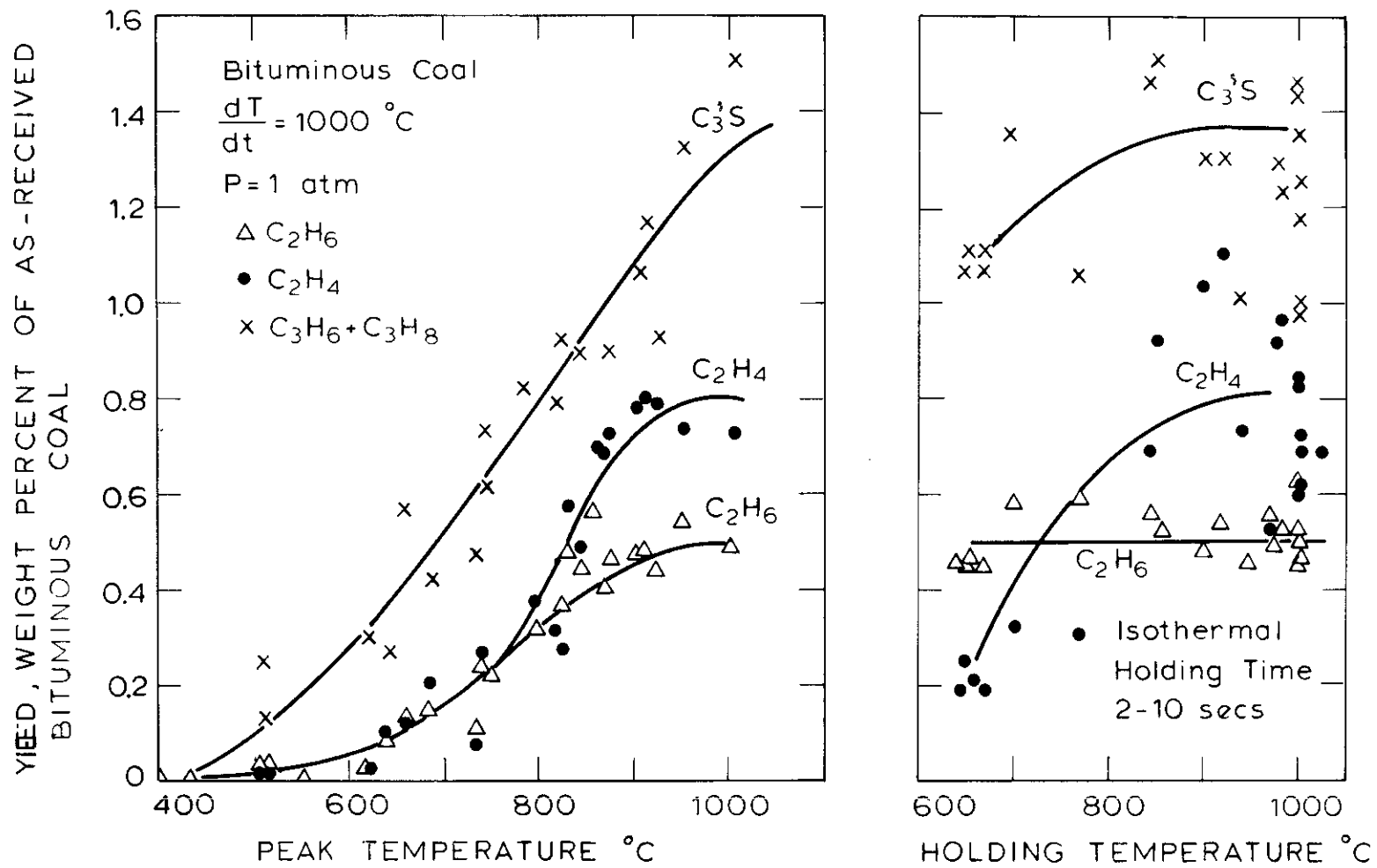


Figure 5.2-5 Yields of Various Hydrocarbon Gases from Bituminous Coal Pyrolysis.

is virtually complete before hydrogen evolution begins; this is not surprising since methane product is probably formed while there is still a fair amount of aliphatic hydrogen left in the coal, while much of the molecular hydrogen must arise from aromatization reactions. Although the temperature dependence of the whole methane curve is suggestive of a wide spectrum of activation energies, the steep rise in the peak temperature interval 800°C to 900°C is suggestive of one dominant (rate controlling) mechanism.

Fig. 5.2-4 shows the yields of carbon oxides. The rather broadly sloping CO<sub>2</sub> curve again suggests a rather broad distribution of activation energies. The CO curves are very reminiscent of CH<sub>4</sub> in shape and temperature dependence; again, the peak temperature interval of 800°C to 900°C seems to be important.

Fig. 5.2-5 shows the yields of four other principal hydrocarbon gas species (C<sub>3</sub>H<sub>6</sub> and C<sub>3</sub>H<sub>8</sub> combined). The amount of scatter in the isothermal holding period data for C<sub>2</sub>H<sub>4</sub> and C<sub>3</sub>'s is difficult to explain when compared to either the relatively modest scatter in the basic non-isothermal runs, or to the scatter for ethane in the isothermal holding period data. All three curves again show broad temperature dependence, with ethylene showing a steep rise in the 800-900°C peak temperature interval. It is curious to note that ethane and ethylene would appear to have rather similar formation rates based on a comparison of the non-isothermal curves, but exhibit markedly different behavior in isothermal runs.

Fig. 5.2-6 gives the results of analyses of the bituminous char. During pyrolysis at 1000°C, roughly half of the carbon originally present in the coal is volatilized while almost 90% of the hydrogen is volatilized. There is clearly a much more "efficient" utilization of hydrogen during

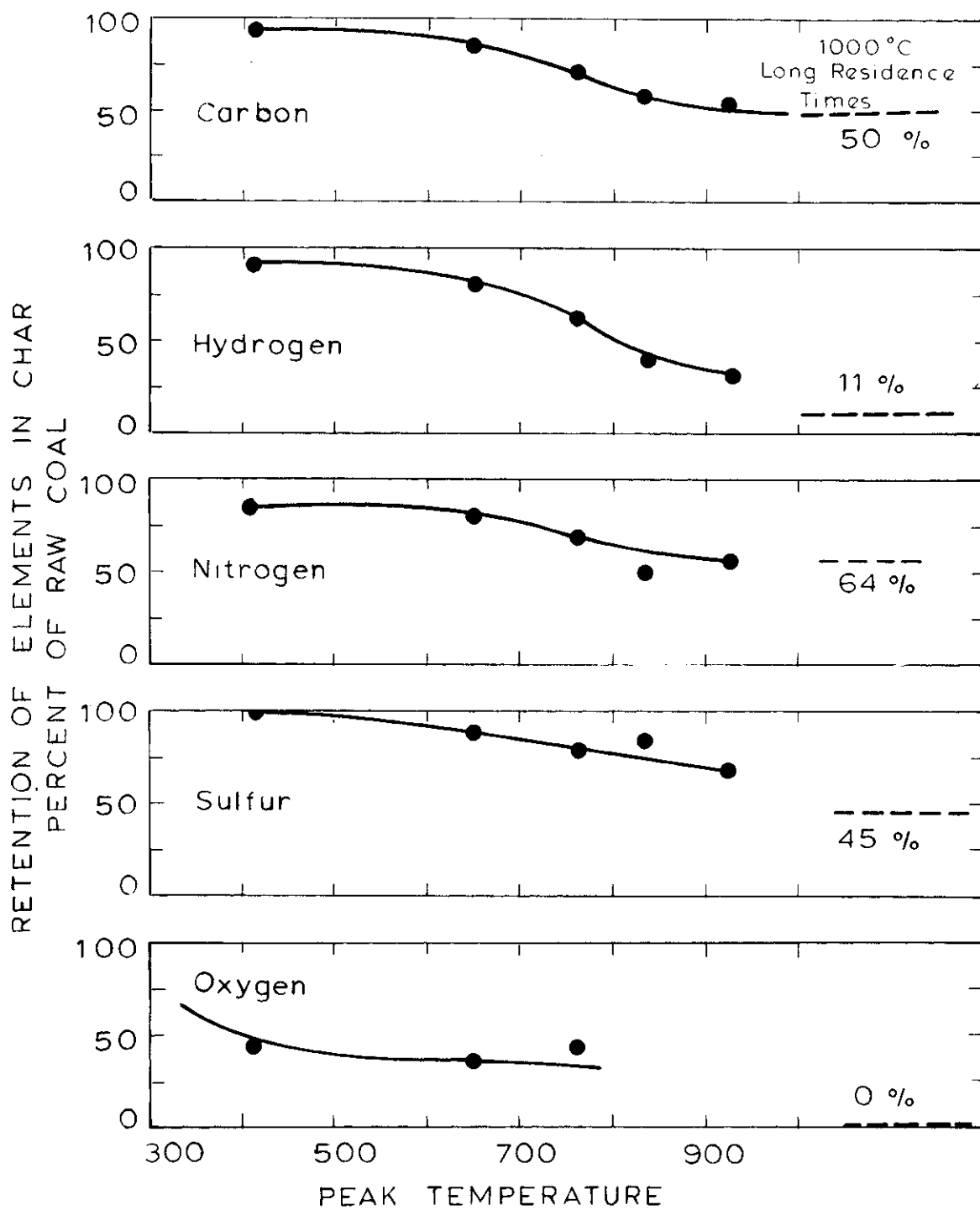


Figure 5.2-6 Elemental Compositions of Chars from Bituminous Coal Pyrolysis

bituminous pyrolysis compared with lignite pyrolysis; about twice as much carbon is volatilized during bituminous pyrolysis as is volatilized during lignite pyrolysis.

As in the case of lignite, almost 2/3 of the nitrogen remains behind in the char even at 1000°C. The sulfur is evolved rapidly between the non-isothermal point at about 925°C, and the isothermal 1000°C asymptote (for 2-10 second holding times). It is significant that this is the temperature range in which a large portion of H<sub>2</sub>S evolution is believed to occur.

The oxygen shows essentially two step behavior. There is an initial loss at temperatures below 400°C, certainly corresponding to the evolution of pyrolytic water. The next sharp drop must occur at a temperature greater than 770°C, and presumably occurs during the period of major CO evolution, 800°C to 900°C (see Fig. 5.2-4). By 1000°C, virtually no oxygen remains in the char, as indicated by the dashed lines in Fig. 5.2-6. (These lines represent analyses of char produced by isothermal pyrolysis at about 1000°C).

The total yields of all products are summarized in the first column of Table 5.2-1. It can be seen that total measured weight loss (47%) exceeds ASTM moisture plus volatiles yield (40.3%) by 17%. By far and away, the dominant gas phase species on a molar percentage basis are hydrogen (57.7%) and methane (18.0%). It is seen that total mass balance closure is fair (about 94%).

Table 5.2-2 shows sample element balances computed in a manner analagous to the element balances in Table 5.1-1 for lignite. The balances typically fall in the range 100 ± 10%. It is not surprising that the carbon balance falls off at high temperatures, since the failure to close overall mass balances at higher temperatures almost certainly reflects the difficulty

Table 5.2-1. Effect of Time-Temperature Histories on Yields from Pyrolysis of Bituminous Coal

Products	Heating Rate 1000°C/sec		350-450°C/sec	13000-15000°C/sec	2-Step <sup>a</sup>
	wt.% of coal	mole % of dry gas	wt.%	wt.%	wt.%
CO	2.4	9.9	2.4	2.3	2.1
CO <sub>2</sub>	1.2	3.1	1.6	1.1	1.6
H <sub>2</sub> O <sup>f</sup>	7.8	-	7.6	7.7	7.7
CH <sub>4</sub>	2.5	18.0	2.2	2.4	2.5
C <sub>2</sub> H <sub>4</sub>	0.8	3.3	0.4	0.7	0.3
C <sub>2</sub> H <sub>6</sub>	0.5	1.9	0.6	0.6	0.6
C <sub>3</sub> H <sub>6</sub> +C <sub>3</sub> H <sub>8</sub>	1.3	3.5	1.1	1.2	1.3
H <sub>2</sub>	1.0	57.7	NM <sup>d</sup>	NM <sup>d</sup>	NM <sup>d</sup>
other HC gas <sup>b</sup>	1.3	2.6	1.1	1.5	0.9
HC liquids <sup>c</sup>	2.4	-	2.3	2.7	2.4
Tar	<u>23.0</u>	-	<u>22.4</u>	<u>23.0</u>	<u>22.0</u>
Total	44.3 <sup>e</sup>		41.7	43.7	41.4
Measured Total	47.0		46.0	47.0	44.7
Unaccounted For	2.7		3.3	3.3	3.3
ASTM volatiles & Moisture	40.3		40.3	40.3	40.3

Table 5.2-1. Effect of Time-Temperature Histories on Yields from Pyrolysis of Bituminous Coal (continued)

All results on as-received wt. basis. Isothermal runs 850-1000°C with holding time 2-10 seconds.

P = 1 atm. He

Notes

<sup>a</sup>Sum of two step process; coal heated first at about 650°C for 3 seconds and cooled. Reheated to about 1000°C for about 3 seconds

<sup>b</sup>All other hydrocarbon gases not listed separately

<sup>c</sup>Hydrocarbon products from condensable trap

<sup>d</sup>NM = not Measured

<sup>e</sup>Columns may not add because of round off

<sup>f</sup>H<sub>2</sub>O includes H<sub>2</sub>S yield, roughly 1% by wt of coal at these temperatures

Table 5.2-2 Carbon, Hydrogen, Oxygen and Total Mass Balances for Bituminous Coal Pyrolysis

Product	Yield, average weight % of Bituminous Coal (as received) <sup>+</sup> , pyrolyzed at indicated temperature															
	Peak Temperatures 400-440°C				Peak Temperatures 620-690°C				Peak Temperatures 740-780°C				Holding Temperature 1000°C			
	Total	C	H	O	Total	C	H	O	Total	C	H	O	Total	C	H	O
CO <sub>2</sub>	0.11	0.03	-	0.08	0.39	0.11	-	0.28	0.49	0.16	-	0.43	1.23	0.34	-	0.89
CO	0.0	0.	-	0.	0.21	0.09	-	0.12	0.40	0.17	-	0.23	2.42	1.04	-	1.38
H <sub>2</sub> O	5.16	-	0.57	4.59	6.02	-	0.67	5.35	5.26	-	0.61	4.68	6.84	-	0.76	6.08
H <sub>2</sub>	0.0	-	0.	-	0.0	-	0.0	-	0.06	-	0.06	-	1.01	-	1.01	-
CH <sub>4</sub>	0.0	0.	0.	-	0.22	0.16	0.06	-	0.59	0.44	0.15	-	2.49	1.87	0.62	-
HC <sub>gas</sub> *	0.0	0.	0.	-	0.90	0.69	0.21	0.0	1.56	1.32	0.24	-	3.95	3.39	0.56	-
Tar + HC liquids	1.18	0.94	0.09	0.10	9.45	7.50	0.69	0.78	15.0	11.9	1.09	1.23	25.4	20.2	1.85	2.09
Char	93.1	63.91	4.48	3.69	83.8	57.4	3.91	2.85	71.9	46.6	2.93	3.46	53.0	34.2	0.52	0.0
Total	99.6	64.9	5.14	8.46	101.0	66.0	5.54	9.38	95.4	60.6	5.08	10.0	97.3**	61.0	5.32	10.4
Closure	100%	95%	105%	90%	101%	97%	112%	99%	95%	89%	103%	106%	97%	90%	108%	110%

\* Hydrocarbons other than CH<sub>4</sub>, Tar, and Hydrocarbon liquids

<sup>+</sup> Bituminous coal (as received) is 67.8% C, 4.91% H, 9.45% O including H and O in moisture (and calculating O by difference based on ash - see text).

\*\* includes 95% H<sub>2</sub> not shown

of tar collection; the higher the fraction of products as tar, the poorer the mass balance, and since tar is primarily carbon (80% by weight), the poorer the carbon balance. It is striking, but not surprising, that at most only about 10% of the carbon in the coal is found in the vapor phase products.

#### Effect of Temperature-Time History

The results shown in Table 5.2-1 imply that there is a slight effect of heating rate on product yields from pyrolysis of bituminous coal. Data from runs done at a heating rate of 350-450°C/sec (as opposed to the 1000°C/sec base case) gave a weight loss which is only 1% lower than the base case. Runs done at 13,000 to 15,000°C/sec gave a total weight loss identical to that of the base case. The only consistent trends with increasing heating rate are a decrease in CO<sub>2</sub> and increases in C<sub>2</sub>H<sub>4</sub> heavy hydrocarbon gases, and light hydrocarbon liquids.

The data in the last column of Table 5.2-1 were obtained from a set of 2-step heating experiments in which the coal was heated isothermally at about 650°C, cooled, and reheated isothermally between 850 and 1000°C. The indicated yields are summations over both steps. In this case, the total weight loss is again only about 2% lower than that for the base case. Since 2-step heating may be viewed as a very slow heating to a high temperature, it is not surprising that some of the trends observed at lower heating rates are also observed during 2-step heating - higher CO<sub>2</sub>, lower C<sub>2</sub>H<sub>4</sub> and heavy hydrocarbon gas yields. Although it is tempting to say that a lower yield of tar is also observed, the 1% difference from the base case is within the experimental uncertainty of the tar measurement.

Thus while the pyrolysis of bituminous coal may show a slightly greater sensitivity toward heating rate than the lignite, the effect



over the range of heating rates examined here is still rather minor, except for  $\text{CO}_2$ ,  $\text{C}_2\text{H}_4$ , and "heavy" hydrocarbon gases. The implication is that the reactions occurring at high temperatures occur independently of those which occur at low temperatures.

#### Effect of Pressure

As with the lignite, some runs were conducted under vacuum conditions (0.05 mm Hg) and some under high pressures of inert gas (1000 psig He). Anthony et al. (1975) found a substantial effect of pressure on the total weight loss obtained from pyrolysis of the same bituminous coal as examined in this study (see Fig. 3.2-17). The results from the present investigation substantiate these earlier findings and shed light on the nature of the effect.

Fig. 5.2-7 shows the dramatic effect of pressure on total yield and on the yields of various products. Compared to the atmospheric pressure base case, the total yield at .05 mm is almost 5% higher, and at 1000 psig (69 atm) is almost 10% lower. As was observed during lignite pyrolysis, the yield of tar and heavy hydrocarbons decreases with increasing pressure, while the yield of light hydrocarbons and carbon oxides increases with increasing pressure. The same interpretation of the data is therefore also suggested. As external pressure increases, the rate at which products can escape the coal particles decrease. Since the products spend a longer time in the reactive environment of a coal particle, they have more opportunity to "crack". The observed effect of pressure on yields from bituminous coal are much larger than those from lignite simply because bituminous coal is characterized by a higher concentration of "crackable" material (i.e. tar).

As in the case of lignite, the effect of pressure does not manifest itself until fairly high peak temperatures are attained. Fig. 5.2-8 shows

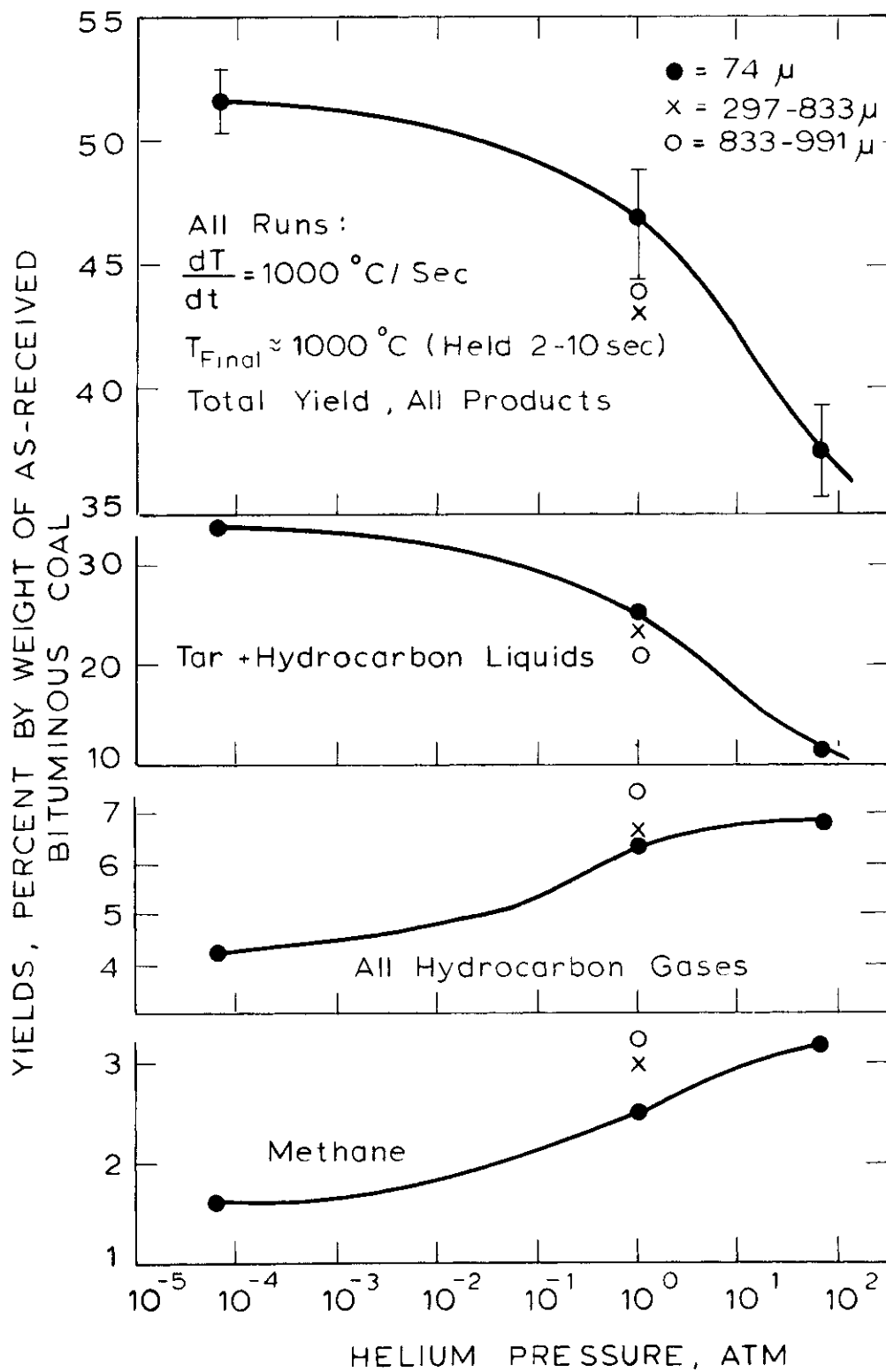


Figure 5.2-7 Effect of Pressure and Particle Diameter on Product Yields from Bituminous Coal Pyrolyzed at  $1000^\circ\text{C}$ .

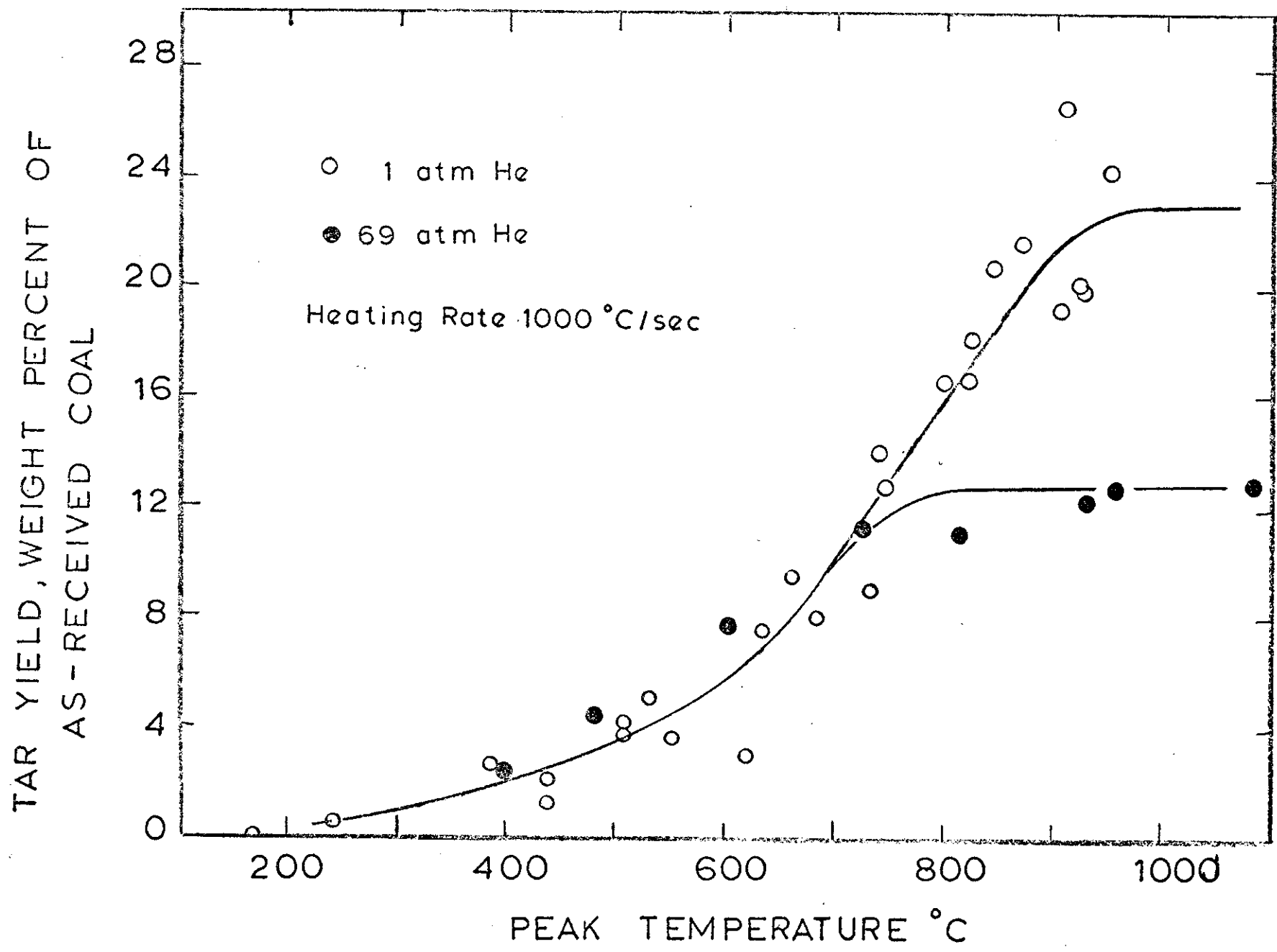


Figure 5.2-8. Effect of Pressure on Yield of Tar from Bituminous Coal Pyrolyzed to Different Peak Temperatures.

that as in the case of lignite, the curves diverge at temperatures above 700 to 750°C.

#### Effect of Particle Diameter

As has been discussed earlier, variation of particle diameter affords another method by which mass transfer limitations can be measured. Consistent with the results for increased pressure, increasing the particle diameter decreases total yield and the yield of tar while increasing the yield of light cracking products. To test for the maceral enrichment effect, a sample of the 833-991 $\mu$  coal was ground to <300  $\mu$  and run as before. Some of the results of these experiments are shown below:

<u>Diameter</u>	53.88 $\mu$	833-991 $\mu$	833-991 $\mu$
<u>Yields (wt%)</u>	(base case)	(reground to <300 $\mu$ )	
Tar	23	24	18
CH <sub>4</sub>	2.5	2.9	3.3
C <sub>2</sub> H <sub>4</sub>	0.8	1.0	1.3
CO	2.4	2.7	3.1
CO <sub>2</sub>	1.2	1.1	1.3
H <sub>2</sub> O	7.8	5.4	7.2
Total	47	43	44

In most respects, the reground material is clearly moving closer to the base case. The fact that the total weight loss of the reground material is lower than either the base case or that of the larger particles is curious, but may be due to drying out of the coal during grinding (note the lower moisture content of the reground material).

### 5.3 Hydropyrolysis of a Montana Lignite

Again, unless otherwise specified, all results in this section have been obtained on particles in the size range 53-88 $\mu$ . All mass yields are reported on the usual "weight percent of as-received lignite" basis. Of course a simple summation of weights of products can no longer serve as an indication of whether mass balance closure is attained, since part of the hydrogen in the products is supplied from the gas. Unless otherwise specified, the pressure of hydrogen is 69 atm.

The results of Anthony et al. (1976, see Fig. 3.2-22) suggested that there was a temperature (which depends on heating rate) below which hydrogen has no effect on total weight yield of products. The data in Fig. 5.3-1 support the earlier findings. The data in Fig. 5.3-1 were all taken at a heating rate of approximately 1000°C/sec, and the points represent runs in which the coal was heated to the indicated peak temperature and then immediately quenched (at a rate of 200°C/sec). The temperature at which the two sets of data begin to diverge appears to be in the range 700-800°C although the scatter in the data makes it somewhat difficult to pinpoint this temperature. Interestingly, this is the same range of temperatures over which increased inert gas pressure begins to show an effect on pyrolysis yield (see Fig. 5.1-5). Of course, increasing the pressure of inert gas always serves to reduce total yields, while increasing the pressure of hydrogen gas (above 1 to 10 atmospheres) serves to increase total yields. Table 5.3-1 compares the total yields of various products obtained at "long" residence times from ordinary 1 atm He pyrolysis, high pressure (69 atm He) pyrolysis, and high pressure (69 atm H<sub>2</sub>) hydro-pyrolysis. It is immediately apparent that the incremental yield due to hydro-pyrolysis is due largely to an increase in methane and other hydro-carbon species. The reduced yields of carbon oxides are not surprising

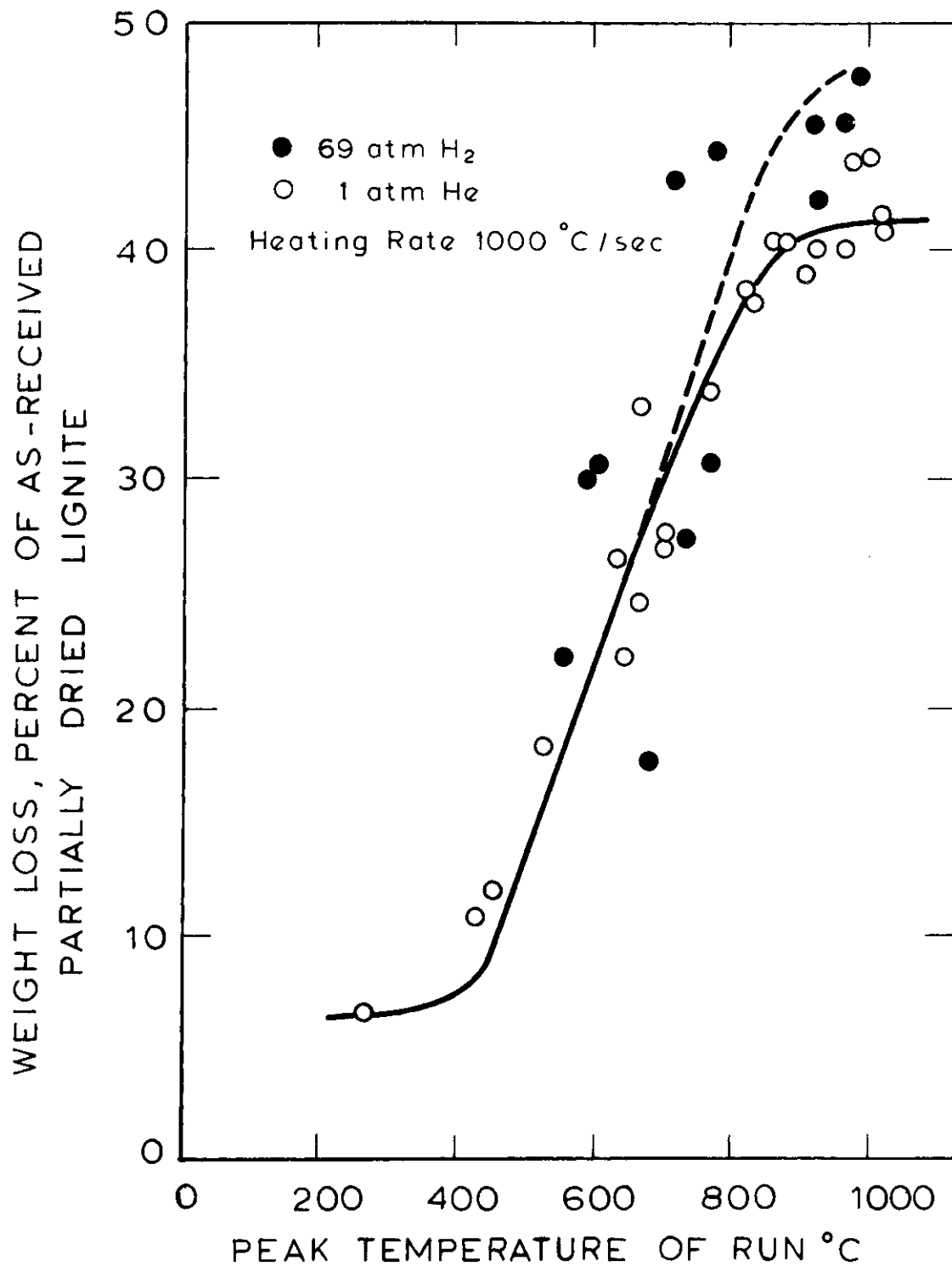


Figure 5.3-1 Comparison of Total Weight Loss from Pyrolysis and Hydropyrolysis of Lignite to Different Peak Temperatures.

Table 5.3-1 Comparison of Total Yields from Lignite Pyrolysis and Hydrolysis

	<u>Pyrolysis</u> <u>1 atm. He</u>	<u>Hydrolysis</u> <u>69 atm. H<sub>2</sub></u>	<u>Pyrolysis</u> <u>69 atm He</u>
CO <sub>2</sub>	9.5	8.5	10.6
CO	9.4	7.1	9.0
CH <sub>4</sub>	1.3	9.5	2.5
C <sub>2</sub> H <sub>4</sub>	0.6	0.2	0.6
C <sub>2</sub> H <sub>6</sub>	0.2	1.4	0.2
OTHER HC	0.8	4.1	1.7
H <sub>2</sub> O	16.5	16.0	12.9
H <sub>2</sub>	0.5	N.M.	N.M.
tar	5.4	~ 8	~ 3
Measured Total Weight Loss	44.0	51.5	40.2

Samples held approximately 10 seconds at 850-1000°C

since reverse water gas shift and other water forming reactions are thermodynamically favored. Unfortunately, the large uncertainty in the water measurement does not permit closure of the oxygen balance to test this hypothesis. It is also interesting to note that the yield of ethylene from hydrolysis is rather low.

Since methane is obviously the key component in the enhanced yield observed during hydrolysis, Fig. 5.3-2 tracks its behavior alone. Contrary to the picture presented by the total weight loss behavior in Fig. 5.3-1, methane yields show an effect of hydrogen at temperatures as low as 600°C. The pyrolysis data at the bottom of the figure are the same data as those plotted in Fig. 5.1-6. Comparison of the three sets of data shows that the enhanced methane yield which is observed during 600°C hydrolysis is due to interaction of the coal and external hydrogen, rather than being a manifestation of the "autohydrogenation" effect induced by the high external pressure alone. Note that the 69 atm He curve does not diverge from the 1 atm He curve until temperatures over 700°C are reached.

Although the curve is not well established because of the scatter in the data, it is possible that hydrolysis exhibits the same two-step behavior as pyrolysis. Such behavior would seem reasonable, since it would suggest that hydrogen participates mainly during the two principal hydrocarbon forming steps.

It is also interesting to note the behavior of ethylene during hydrolysis, compared to pyrolysis. Fig. 5.3-3 shows these data. Variation in inert gas external pressure has rather little effect on ethylene yield during ordinary pyrolysis, as the curves for pressures of 1 atm helium and 69 atm helium virtually coincide. The well established



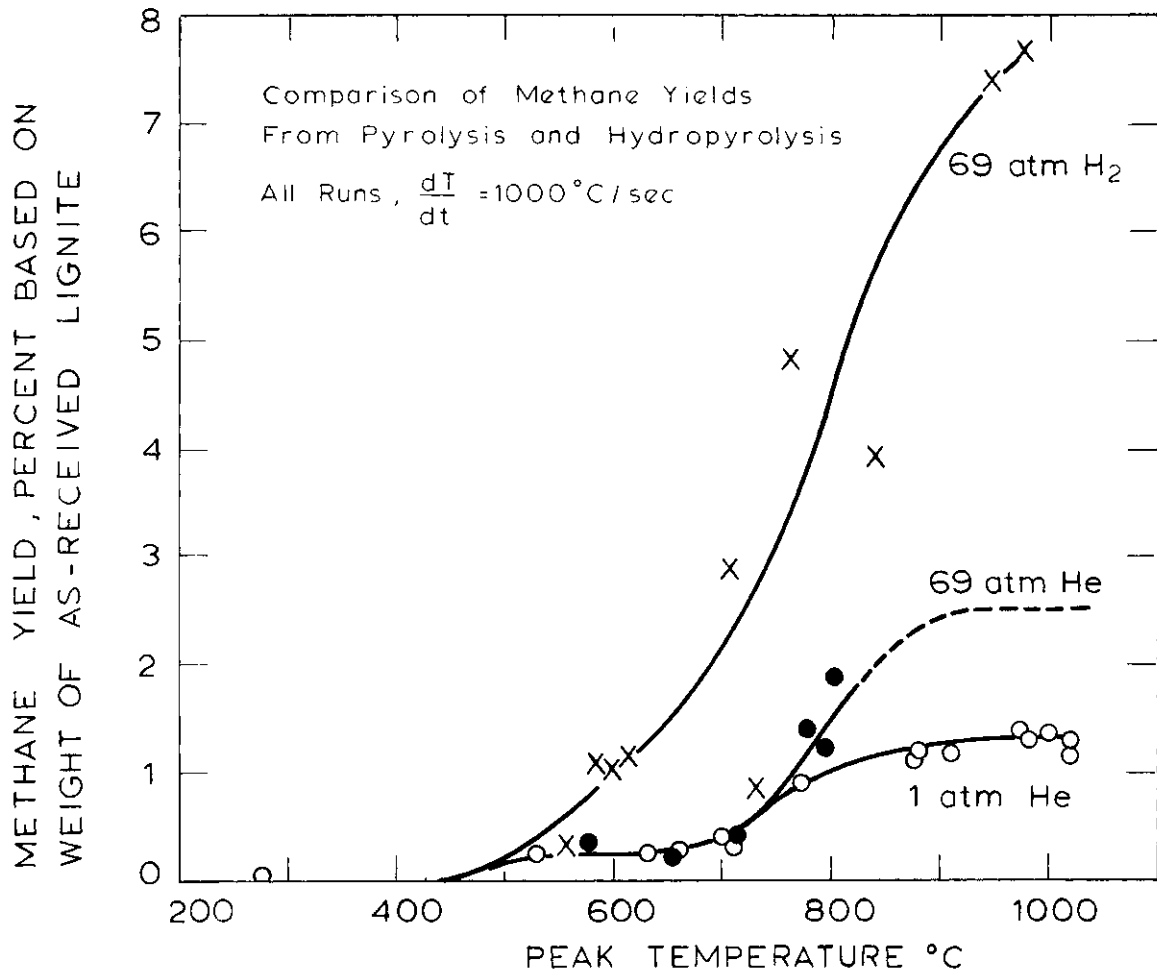


Figure 5.3-2 Yields of Methane from Pyrolysis and Hydropyrolysis of Lignite to Different Peak Temperatures.

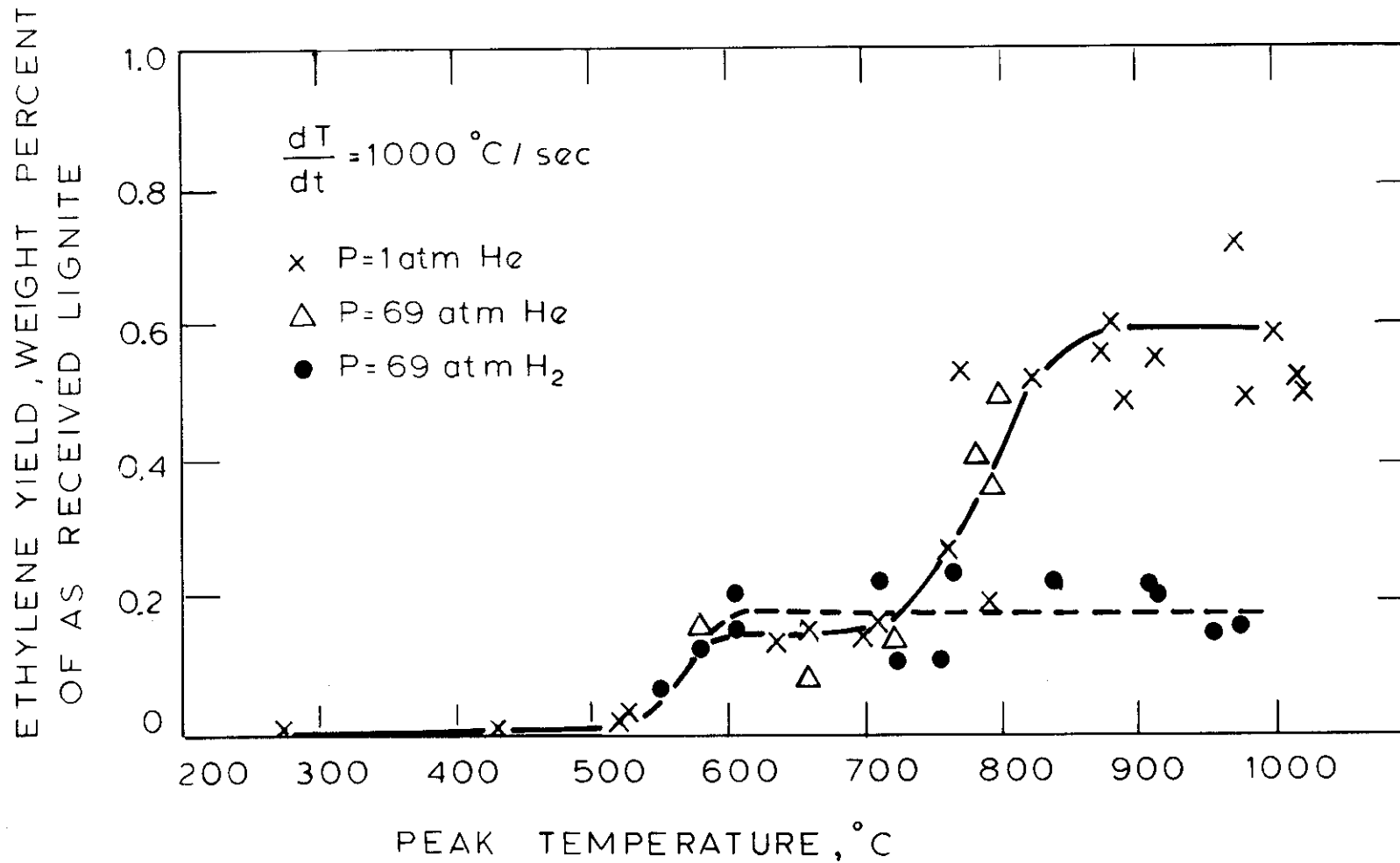


Figure 5.3-3. Yields of Ethylene from Pyrolysis and Hydropyrolysis of Lignite to Different Peak Temperatures.

2-step behavior is displayed by both sets of data. During hydropyrolysis, it appears as though ethylene is evolved during only the first step, in a quantity comparable to that evolved during the first step of ordinary pyrolysis. No further evolution is observed during the higher temperature hydrocarbon-formation stage (above 700 or 750°C). Based on the behavior of methane and ethylene, it appears as though the hydrogen begins to manifest its greatest effect above 700°C. The data on evolution of hydrocarbon gases other than methane and ethylene are shown in Fig. 5.3-4. Their behavior is analogous to that of methane, in that a low temperature (<600°C) effect of hydrogen is apparent.

As the data in Table 5.3-1 suggest, hydropyrolysis may slightly enhance the yield of tar. Unfortunately, the quantities are still small and the results a bit too scattered to permit detailed analysis of this component. Also, the yield of light hydrocarbon liquids appears to be enhanced during hydropyrolysis, but the total yield of benzene almost never exceeds one weight percent. The maximum total yield of tar plus hydrocarbon liquids obtained during 69 atm hydropyrolysis is approximately 10%.

The behavior of the oxygenated species is shown in Fig. 5.3-5. Plotted are the curves drawn through the base case lignite pyrolysis data already presented in Figure 5.1-3 (points omitted), and the data for lignite 69 atm hydropyrolysis. The agreement between the carbon oxide data for pyrolysis and hydropyrolysis is fair. The difference in the yields of carbon oxides from pyrolysis and hydropyrolysis (as recorded in Table 5.3-1) appears to manifest itself principally during the previously described third, high temperature evolution step. Again, since this high temperature stage of evolution could only be studied by runs involving an isothermal holding period, its results cannot be shown in Fig. 5.3-5.

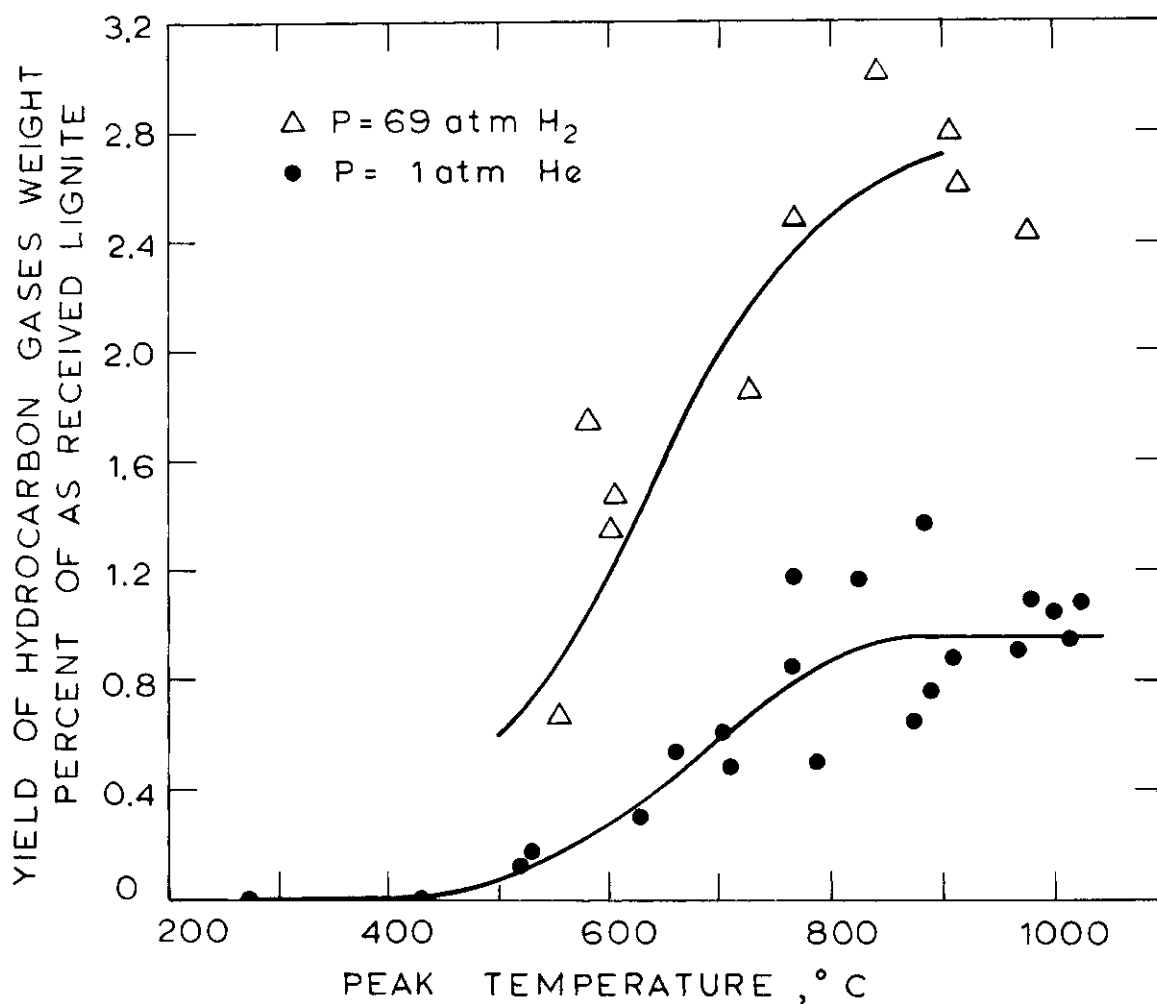


Figure 5.3-4 Yields of Hydrocarbon Gases (other than Methane and Ethylene) from Pyrolysis and Hydropyrolysis of Lignite to Different Peak Temperatures.

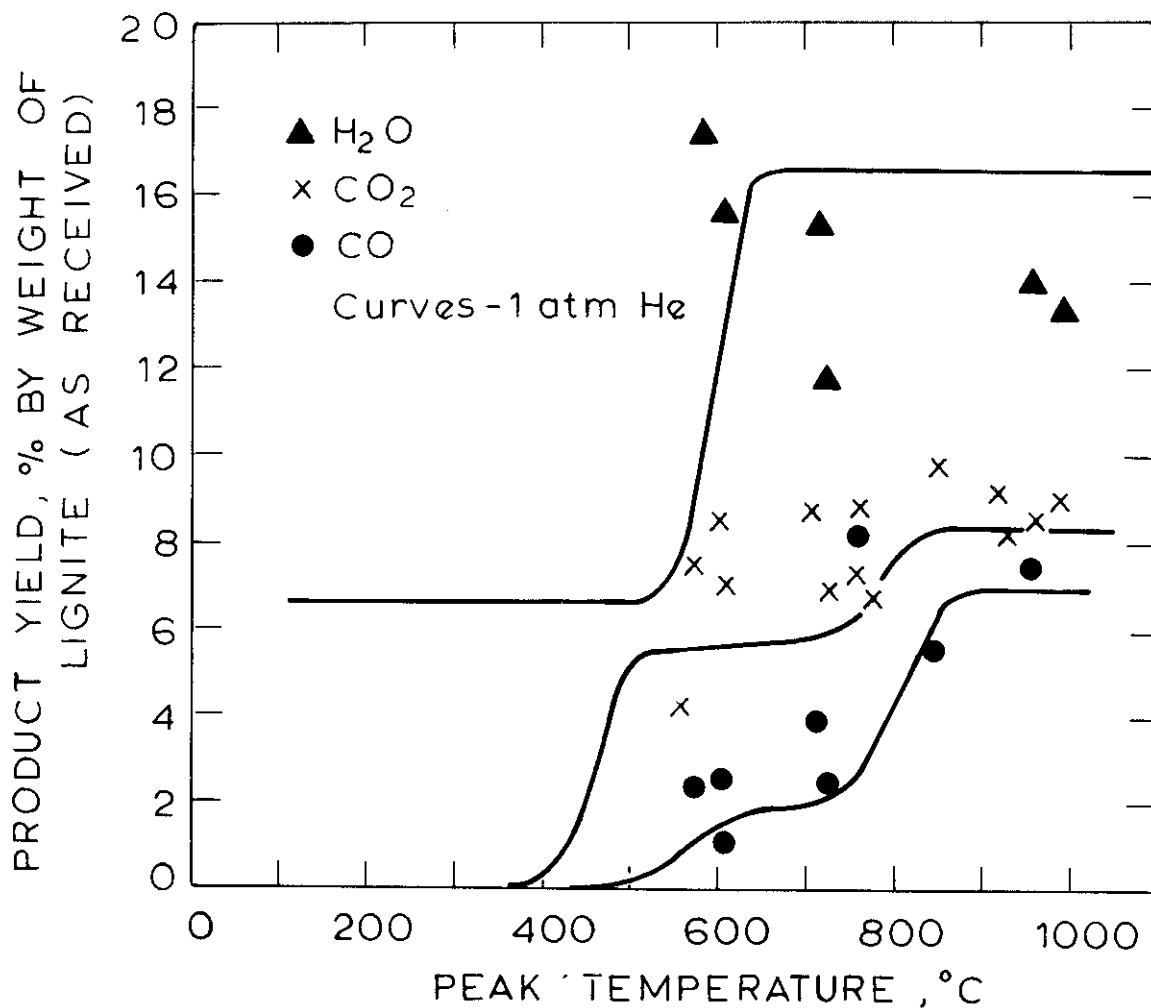


Figure 5.3-5 Yields of Water, Carbon Monoxide, and Carbon Dioxide from Pyrolysis and Hydrolysis of Lignite (data pts. for 69 atm H<sub>2</sub>; curves for 1 atm He; heating rate = 1000°C/sec for all runs).

Unfortunately the water results from hydrolysis runs tend to display more scatter than usual.

The results of ultimate analyses of lignite chars produced by pyrolysis and hydrolysis are compared in Fig. 5.3-6. The fact that the carbon conversion is higher during hydrolysis than during pyrolysis is to be expected. The retentions of hydrogen and oxygen (within the scatter of the latter) appear to be unaffected by the presence of hydrogen gas. This implies that the mechanism of removal of these species is the same during hydrolysis as during pyrolysis. Of the two species of environmental interest, the volatilization of nitrogen is greatly enhanced by the presence of hydrogen, while sulfur is curiously unaffected.

Thus far, all of the hydrolysis results presented have been for the 1000 psig (69 atm absolute)  $H_2$  base case. But as was discussed in some detail in section 3.2 and shown in Fig. 3.2-19, through 3.2-24, the total yields which can be obtained during hydrolysis are strongly a function of hydrogen pressure. Nor is the pressure dependence of yield particularly straightforward, as the data of Anthony et al. (1976, Fig. 3.2-24) and Johnson (1977, Fig. 3.2-23) clearly show.

The data in Fig. 5.3-7 address the question of the pressure dependence of hydrolysis. As has already been shown, a large portion of the yield observed during hydrolysis is a result of ordinary pyrolytic processes. To plot total yield against hydrogen pressure would therefore be misleading. The results in Fig. 5.3-7 are plotted as yield increments over that which could be obtained from ordinary pyrolysis at temperatures greater than about  $850^\circ C$ , held for between 5 and 10 seconds. Thus a value of zero on the ordinate implies a total weight loss of 44 wt.%, or a methane yield of about 1.3 wt.%. It is clear that a simple functionality of

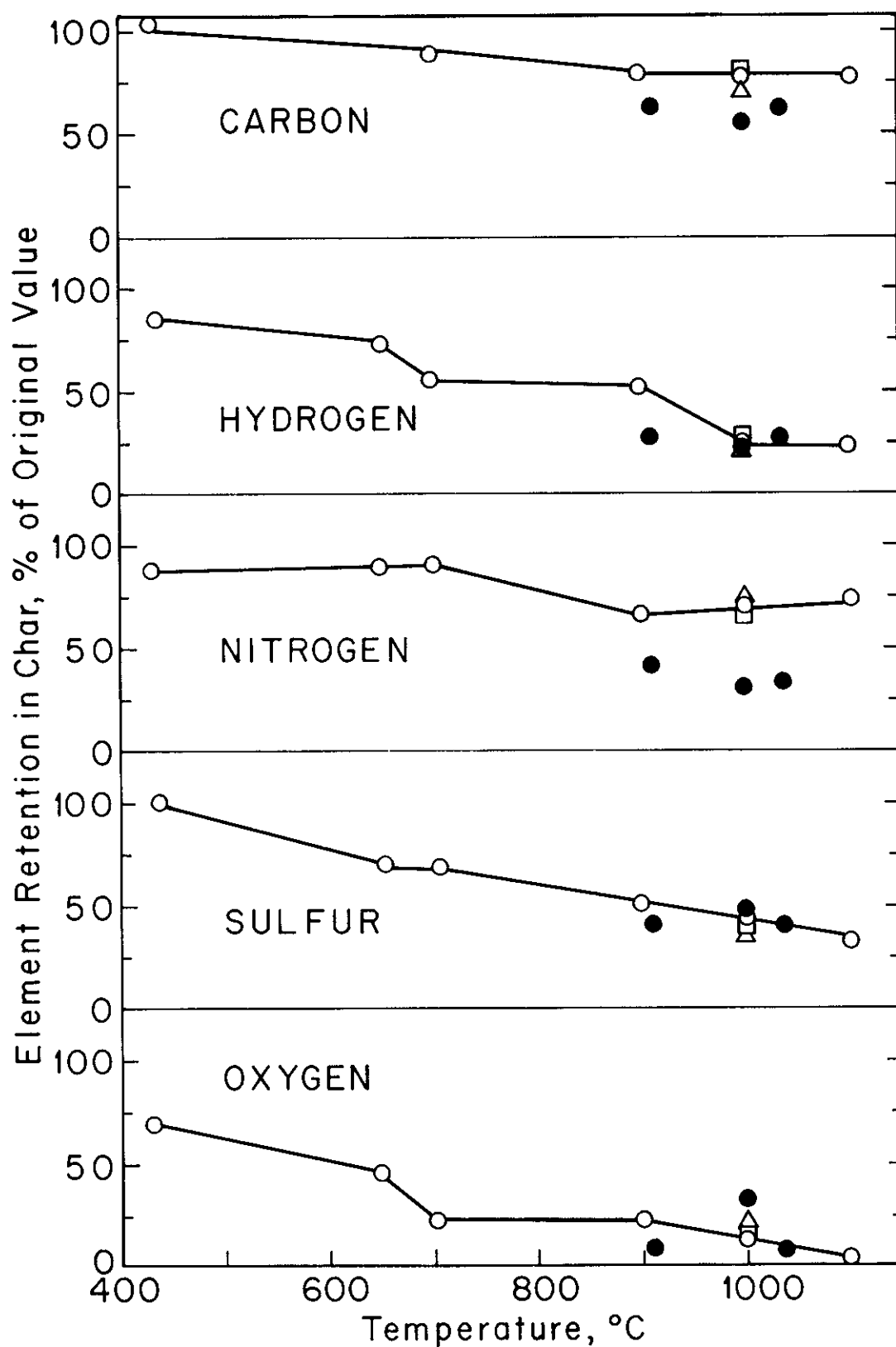


Figure 5.3-6 Comparison of Char Compositions from Pyrolysis and Hydro-pyrolysis of Lignite (o), 1 atm He, zero residence time at peak temperature; ( $\Delta$ ) 1 atm He, 5-20 sec. residence time; ( $\square$ ) 69 atm He, 5-10 sec. residence time; ( $\bullet$ ) 69 atm H<sub>2</sub>, residence time 2-30 sec.

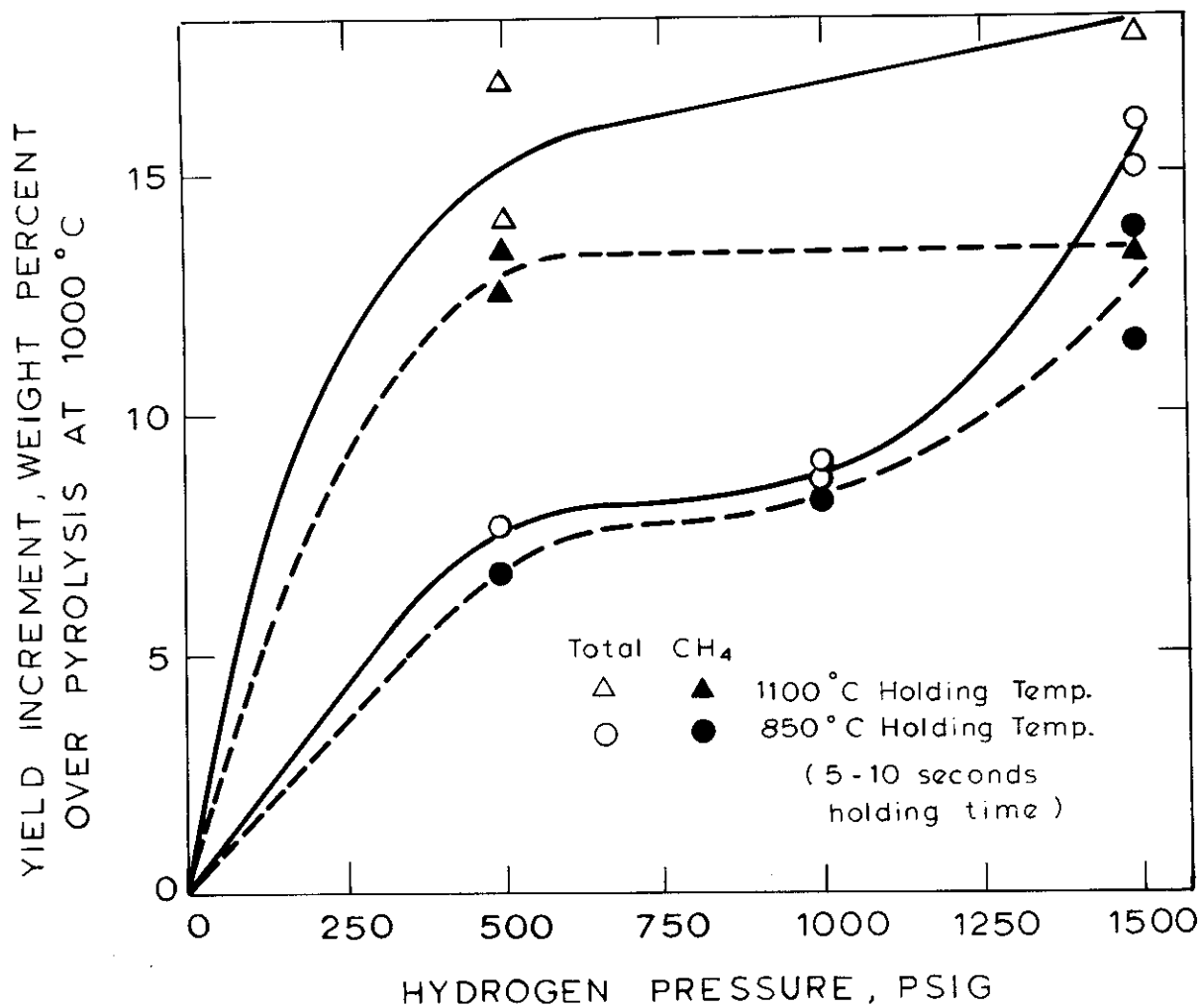


Figure 5.3-7 Effect of Temperature and Hydrogen Pressure on Increasing Yields Relative to Pyrolysis (Basis 44% weight loss, 1.3% CH<sub>4</sub> during 1 atm He pyrolysis at either 850° or 1100°C).



of pressure is not implied, either for total weight loss or for methane yield.

The results of Fig. 5.3-7 point up how large a fraction of incremental yield methane represents (though the actual fraction is not directly calculable since there is no indication as to what fraction of the hydrogen contained in the methane came from the coal itself).

A result of some practical significance is that higher temperatures serve to increase total yields as effectively as higher hydrogen pressures. The total yield at 500 psig  $H_2$  and  $1100^\circ C$  is virtually identical to that obtained at 1500 psig  $H_2$  and  $850^\circ C$  and not much lower than that at 1500 psig  $H_2$  and  $1100^\circ C$ . Unfortunately because of time limitations, this subject could not be investigated more fully; the control of sample temperature at high pressures is somewhat difficult, especially at around  $1100^\circ C$ , and the success rate of experimental runs is low.

The effect of particle diameter on total weight loss was quickly examined by working with particles in the  $295-990\mu$  range. The total yield did not change significantly relative to the  $53-88\mu$  base case (at 1000 psig  $H_2$  and a temperature of about  $1000^\circ C$  held for approximately 10 seconds). Apparently, just as the results for lignite pyrolysis under increased external (inert gas) pressure implied for volatiles outflow, these results imply perhaps only a modest mass transfer resistance to hydrogen inflow. If a resistance does exist, then it is probably not on the macroscale of particle diameters. The picture for bituminous coal, presented in the next section, is quite different.

Again, just as during ordinary pyrolysis, the lignite particles never appeared to swell, soften, or agglomerate during any hydrolysis run.

#### 5.4 Hydropyrolysis of a Pittsburgh Seam No. 8 Bituminous Coal

Like the lignite data, the base case for bituminous hydropyrolysis involves particles in the size range 53-88 $\mu$  and a hydrogen pressure of 1000 psig (69 atm absolute).

Fig. 5.4-1 shows a comparison of total yields obtained during pyrolysis at 1 atm and at 69 atm of helium pressure, and from hydropyrolysis at 69 atm of hydrogen pressure. Again, these results were obtained by heating the coal at a rate of about 1000°C/sec to the indicated peak temperature and then immediately quenching at a rate of 200°C/sec. Comparison of the pyrolysis results obtained at 1 atm and 69 atm of helium pressure illustrates again the previously discussed effect of pressure on pyrolysis. Since the helium is of course chemically inert, its effect is purely physical. The fact that the total yields from 69 atm hydropyrolysis are comparable to the yields from 1 atm pyrolysis implies that the hydrogen must interact chemically with the coal in a manner which boosts yields. This interaction, according to these data, begins at temperatures in the range 700 to 800°C. Anthony et al. (1976) advanced a theory which postulates that the hydrogen serves to "stabilize" volatiles which may otherwise be lost to cracking reactions (section 3.2). The data in Fig. 5.4-1 may be supportive of this picture, but the data in Fig. 5.4-2 shed further light upon the nature of the process.

In Fig. 5.4-2, the yield of tar, the principal product of bituminous pyrolysis at 1 atm, is plotted for the cases of 1 and 69 atm He pyrolysis and 69 atm H<sub>2</sub> hydropyrolysis. The results are striking in that they show that hydrogen does not act to stabilize the tar as such; the yields of tar from 69 atm pyrolysis and 69 atm hydropyrolysis are comparable. The indicated asymptote for tar yield from hydropyrolysis (at 12.5%) is obtained from runs in which the coal is held at temperatures between 850

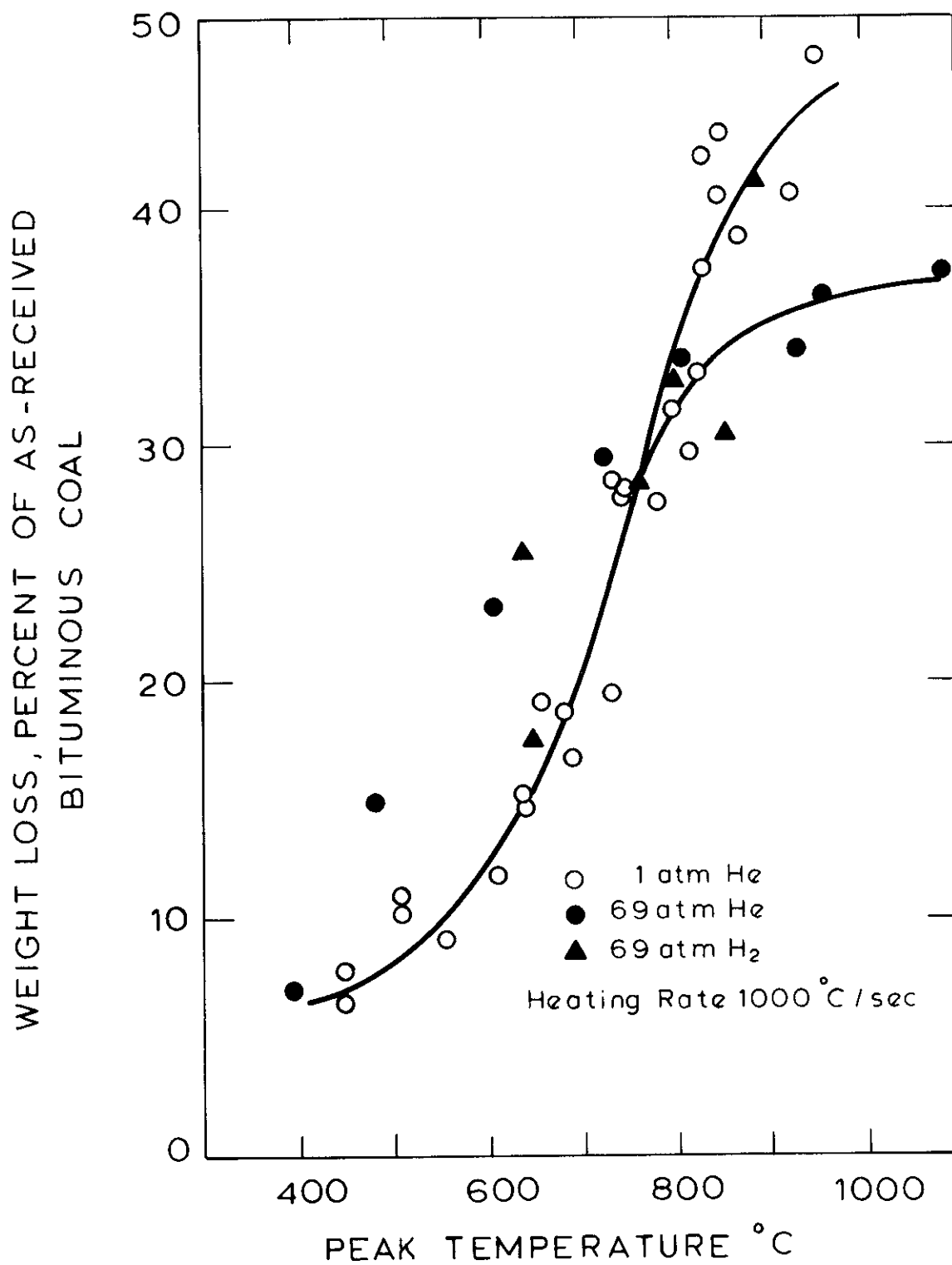


Figure 5.4-1 Comparison of Total Weight Loss from Pyrolysis and Hydrolysis of Bituminous Coal.

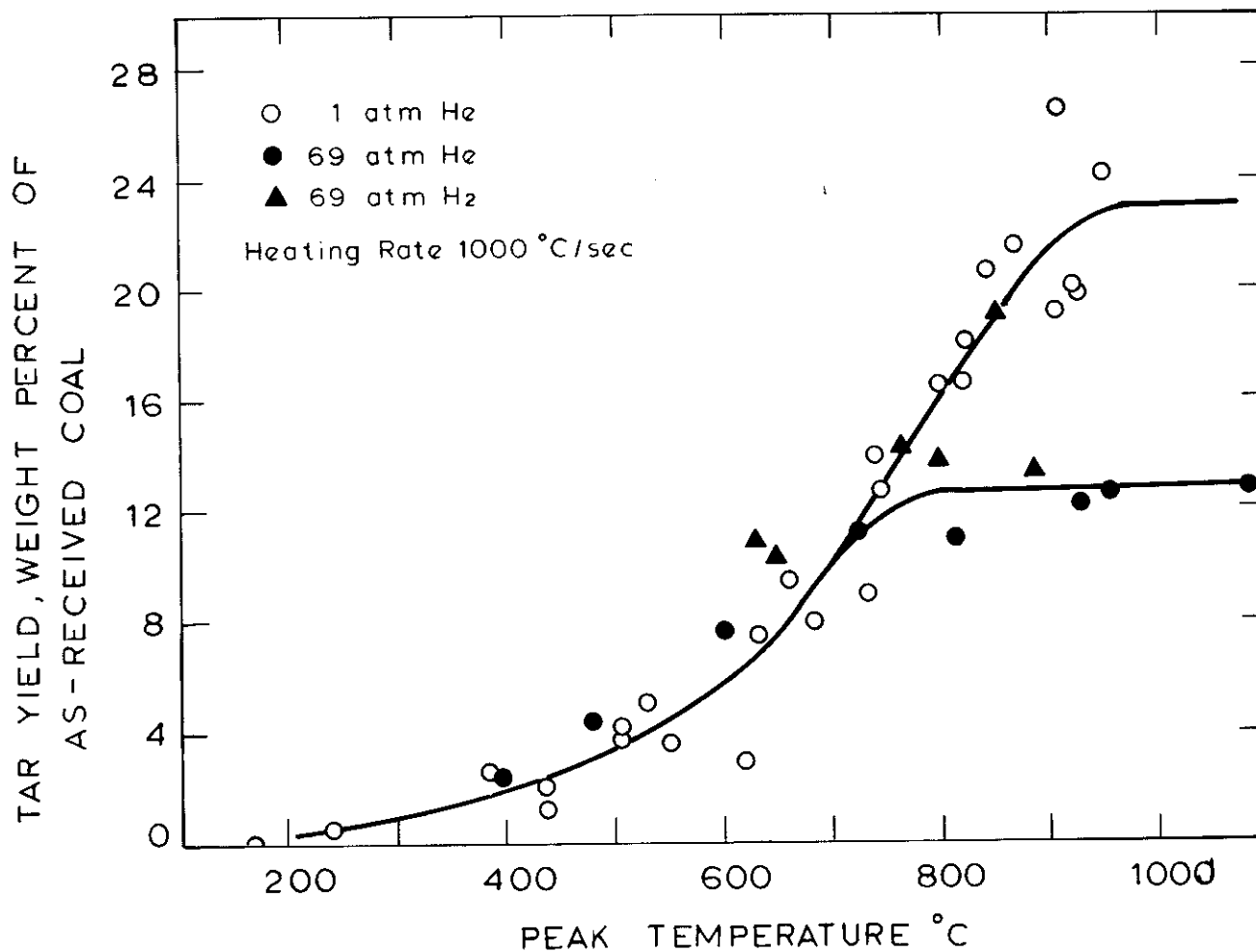


Figure 5.4-2 Comparison of Tar Yields from Pyrolysis and Hydropyrolysis of Bituminous Coal (note asymptotes drawn coincident with asymptotes based on results of non-zero holding time runs not shown here).

and 1050°C for up to 20 seconds.

The fact that the tar itself is not being stabilized suggests several possibilities for the yield enhancing effect of hydrogen. The first is that the hydrogen interferes with the tar forming reactions and stabilizes tar "precursors" which in the presence of 69 atm of helium would lead to carbon deposition. Another possibility is that the hydrogen serves to stabilize tar cracking (or hydrocracking) products. A third possibility is that the hydrogen physically interferes with the escape of tar and promotes its cracking in a manner precisely analogous to that of the helium; the yield enhancement is the result of an unrelated (or indirectly related) chemical process.

Fig. 5.4-3 compares the yields of methane from pyrolysis and hydro-pyrolysis. These data suggest that the chemical interaction of hydrogen with the coal actually begins at rather low temperatures (<600°C). This behavior is precisely analogous to that observed for the lignite (Fig. 5.3-3). It should again be emphasized that in speaking of a temperature at which an effect is observed, a particular time-temperature history is implied. In this case, a heating rate of 1000°C/sec followed by a quench at 200°C/sec is involved. At significantly slower heating rates or in case where the coal is held isothermally for any length of time, the temperature at which a particular phenomenon is observed can be lower. This point will be further explored in the section on modelling of results.

Table 5.4-1 summarizes the results for 69 atm hydro-pyrolysis and compares them with atmospheric pressure pyrolysis results. The hydro-pyrolysis results were all obtained at temperatures above 900°C, held for between 12 and 20 seconds. It can be deduced from comparison of the results in Figs. 5.4-1, 5.4-3 and Table 5.4-1 that methane is the principal product

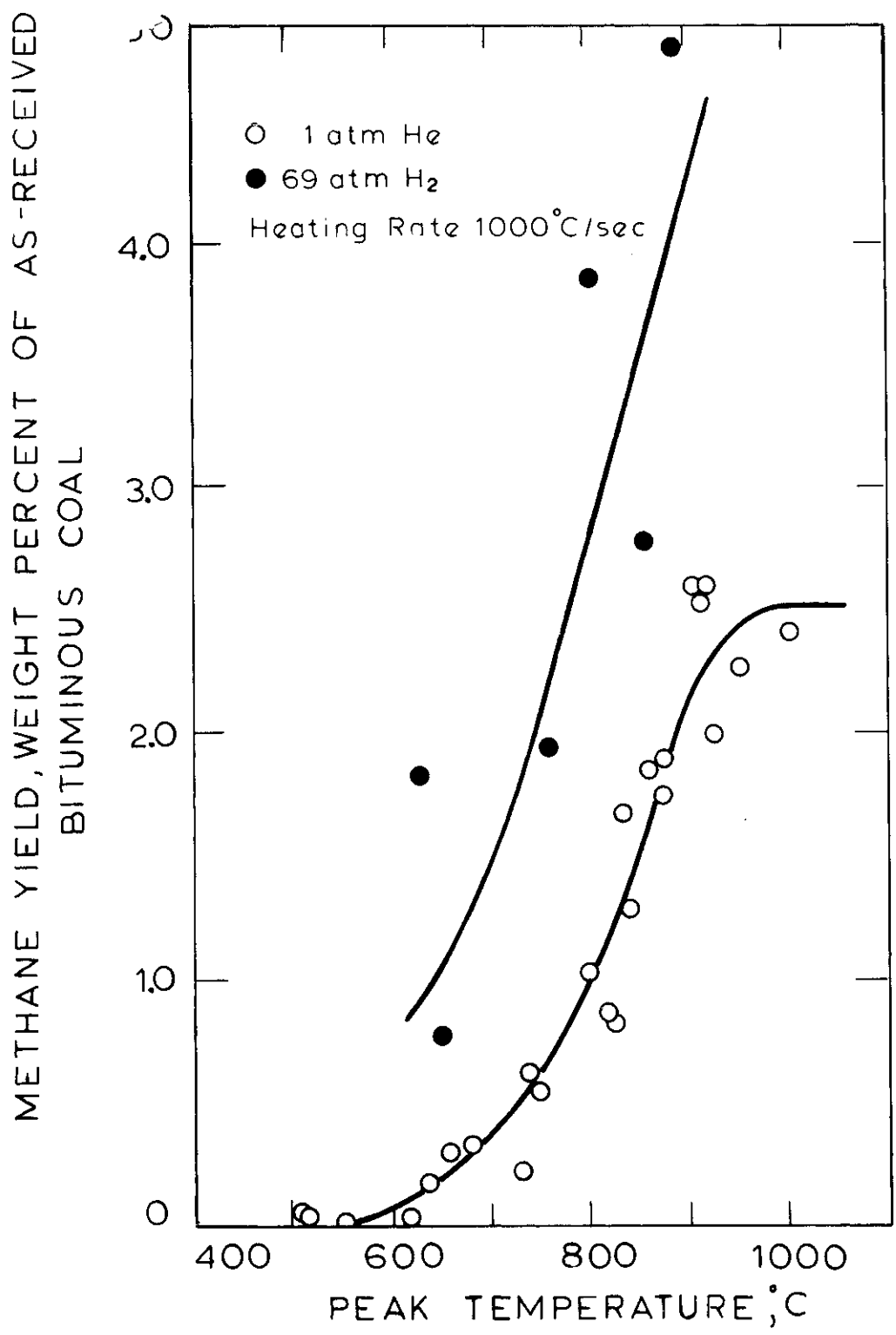


Figure 5.4-3 Comparison of Methane Yields from Pyrolysis and Hydrolysis of Bituminous Coal.

Table 5.4-1. Comparison of Yields from Atmospheric Pressure Pyrolysis and 69 atm. Hydrolysis of Bituminous Coal.

	<u>1 atm. He</u>	<u>69 atm. H<sub>2</sub></u>
Total weight loss (as.rcvd.)	47.0%	61.8%
Tar	23.	12.
CO	2.4	- <sup>†</sup>
CO <sub>2</sub>	1.2	1.3
H <sub>2</sub> O	6.8	- <sup>†</sup>
H <sub>2</sub>	1.0	-
CH <sub>4</sub>	2.5	23.2
C <sub>2</sub> H <sub>4</sub>	0.8	0.4
C <sub>2</sub> H <sub>6</sub>	0.5	2.3
C <sub>3</sub> H <sub>6</sub> + C <sub>3</sub> H <sub>8</sub>	1.3	0.7
C <sub>6</sub> H <sub>6</sub>	trace*	2.2
other HC gases	1.3	2.0
light HC liquids	2.4	3.1

All hydrolysis runs involve heating the coal to temperature 900°C and holding isothermally for 12 to 20 seconds.

\*The trace amount of benzene found during pyrolysis is usually included in the "other HC gases" or "light HC liquids".

<sup>†</sup>Measurements unreliable, not reported.

formed during the isothermal period. During the non-isothermal heating period up to about 900°C, Fig. 5.4-1 shows a total weight loss of about 41% and Fig. 5.4-3 shows a methane yield of about 5%. During the isothermal period, Table 5.4-1 indicates an additional weight loss of roughly 20% while the yield of methane has increased by roughly 15%.

There are several parallels between lignite hydrolysis and bituminous coal hydrolysis. The role of methane as the predominant product is the most obvious. Others include the decreased yield of ethylene and increased yield of ethane relative to the pyrolysis base case. Unfortunately the data on oxide species is not considered reliable, and hence not reported. In the case of carbon monoxide, a chromatographic difficulty resulted in the frequent "masking" of the CO peak by the large preceding H<sub>2</sub> peak. In an unrelated problem, the water measurements were considered unreliable because of an unidentified source of H<sub>2</sub>O contamination in the system.

The figures in Table 5.4-1 are averages over several runs. Not included in the average was a run done at roughly 1080°C (14 seconds) in which the total yield was over 70% (representing a d.a.f. conversion of about 80%) and the yield of methane was nearly 40% (representing a carbon conversion to methane of about 44%).

As observed by Anthony et al. (1976, Fig. 3.2-25), increasing particle diameter has a rather deleterious effect on total yields obtained from hydrolysis. Fig. 5.4-4 presents data from this investigation. The trends are similar to those observed by Anthony et al., although there are some small quantitative differences. The data for hydrolysis are somewhat more sensitive to the temperature of the isothermal holding period than are the data for pyrolysis (demonstrated in Fig. 5.3-7). Therefore, while the pyrolysis data in Fig. 5.4-4 include results for



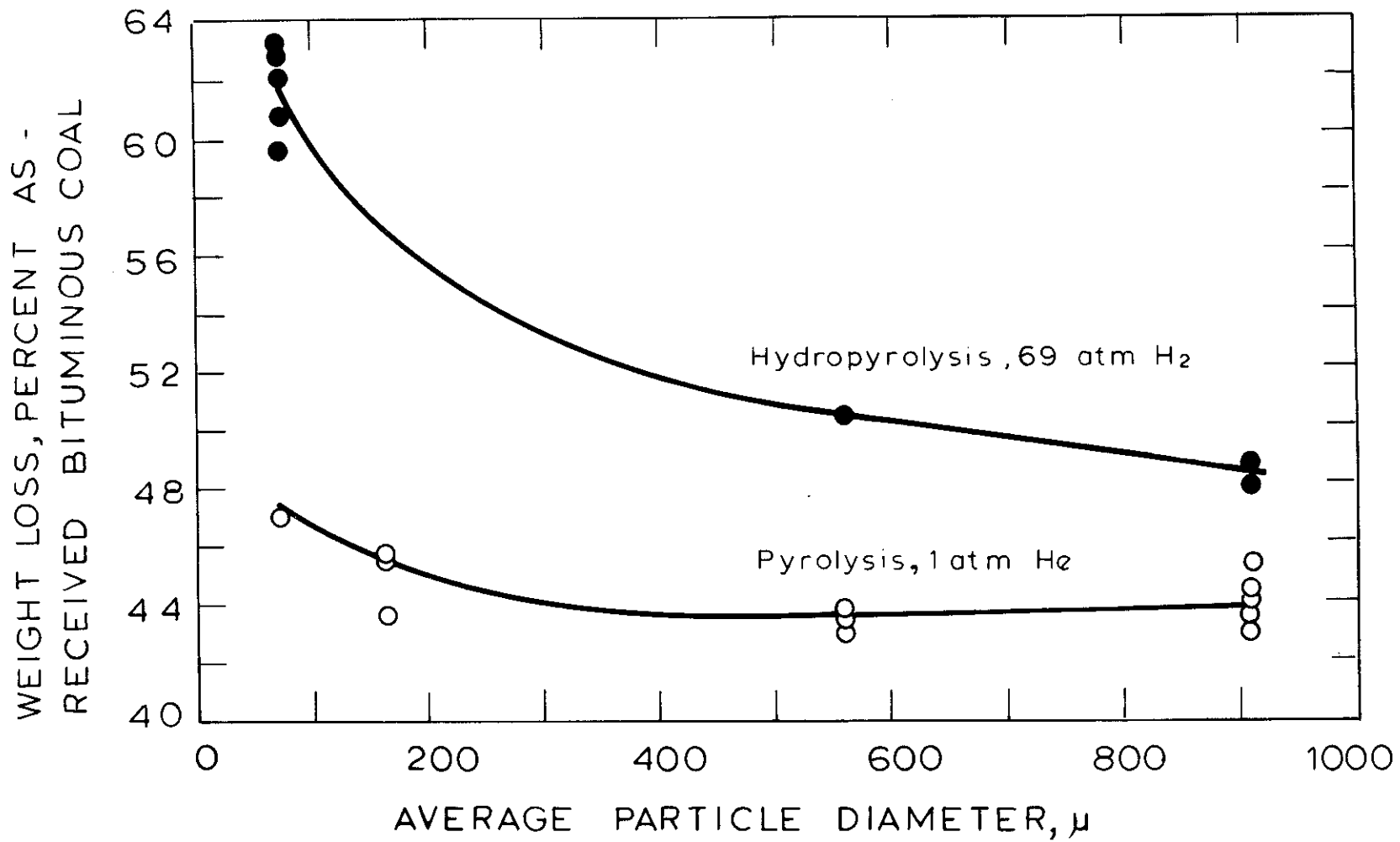


Figure 5.4-4 Effect of Particle Diameter on Total Yields from Pyrolysis and Hydropyrolysis of Bituminous Coal.

experiments run for any more than 2 seconds at temperatures over 850°C, the hydrolysis data chosen for presentation were only those from temperatures between 900 and 1050°C and with isothermal holding times greater than 10 (but all less than 20) seconds.

The following table shows the principal differences in product compositions:

<u>Product</u>	Avg. Particle Diameter( $\mu$ )		
	<u>74</u>	<u>570</u>	<u>910</u>
Tar	12	13	12
CH <sub>4</sub>	23	19	20
C <sub>2</sub> H <sub>6</sub>	2.3	1.7	1.6
other HC gases	3.1	1.4	1.2
light HC liquids	5.3	3.6	5.2
CO <sub>2</sub>	1.3	1.0	1.4

Again since carbon monoxide, water, and sulfur compound measurements are not available for all cases, total mass balances are not possible.

### 5.5 Discussion and Modelling of Pyrolysis Results

Table 5.5-1 presents a brief summary of the principal results and conclusions presented in sections 5.1 and 5.2.

The simple, stepwise behavior of the products of lignite pyrolysis, combined with the fact that the products seem to arise from reactions that are parallel and independent, suggested a rather straightforward model.

The modelling of coal pyrolysis as a set of independent parallel reactions having a statistical distribution of activation energies has been shown to provide valuable insight into the overall or global kinetics of the process. (Anthony and Howard, 1976; Anthony et al., 1976, 1975;

Table 5.5-1 A Summary of Pyrolysis Results

Montana Lignite

- Pyrolysis occurs in several distinct stages (Figs. 5.1-1 through 5.1-3).
- Volatile products dominated by oxygenated species (Fig. 5.1-1 and 5.1-3).
- The yield of hydrocarbon products and the extent of volatilization of carbon are low. (Fig. 5.1-1, 5.1-2, and 5.1-4).
- The composition of products seems to be independent of heating rate used to attain the final temperature (in the range 270-10,000°C/sec, Fig. 5.1-1).
- The composition of products is the same for coal heated to final temperature in two steps or one (Fig. 5.1-1). The conclusion is that the reactions can be considered independent and parallel.
- Although there is a measurable effect of variation of external pressure during pyrolysis (Figs. 5.1-5, 5.1-6, Table 5.1-2), the effect, overall, is rather small.
- Total weight loss agrees well with the results of the standard A.S.T.M. volatile matter test.

Pittsburgh Seam Bituminous Coal

- Bituminous coal pyrolysis also appears to occur in stages, but the well defined stages which characterize lignite pyrolysis are absent (Figs. 5.2-1 through 5.2-5).

(con't)

Table 5.5-1 A Summary of Pyrolysis Results (continued)

Pittsburgh Seam Bituminous Coal

- The volatile products are dominated by hydrocarbons (heavy tars in particular, Figs. 5.2-1 and 5.2-2).
- Softening of the coal is evident at peak temperatures as low as 450°C, and involves almost the entire sample by 700°C.
- The extent of volatilization of carbon is substantially higher than that observed in lignite (Fig. 5.2-6).
- The composition and yield of products shows only a slight dependence on rate of heating (Table 5.2-1). Similarly, coal heated to final temperatures in two steps gives only a slightly lower yield of volatiles than coal heated directly to the final temperature.
- There is a small effect of variation of particle diameter by an order of magnitude (Figs. 5.2-7 and 5.2-9).
- There is a large effect of variation of external pressure, implying an important role of mass transfer resistance (Figs. 5.2-7, 5.2-8). This effect begins to manifest itself between 700 and 800°C.
- The total yields of volatiles from atmospheric pressure or vacuum pyrolysis exceeds the standard A.S.T.M. volatile matter; the total yield from 69 atm He pyrolysis is less than A.S.T.M. volatile matter.

Anthony, 1974). With the products in the present study dominated by a few individual species and classes of species, e.g., tar, there is interest in determining whether pyrolysis can be effectively modelled as only a few reactions representing the production of these key products.

As a first test of this approach, the appearance of product  $i$  is modelled as a reaction first-order in the amount of  $i$  yet to be produced. Thus for the reaction



the assumed first-order rate is

$$dV_i/dt = k_i(V_i^* - V_i) \quad (5.5-2)$$

and the rate constant is assumed to be

$$k_i = k_{i0} \exp(-E_i/RT) \quad (5.5-3)$$

where  $k_{i0}$  is the pre-exponential factor,  $E_i$  is the activation energy of reaction  $i$ ,  $V_i$  is the amount of product  $i$  produced up to time  $t$ ,  $V_i^*$  is the amount of product  $i$  which could potentially be produced, (i.e., at  $t = \infty$ ),  $T$  is the absolute temperature, and  $R$  is the gas constant. Assuming that temperature increases linearly with time, as it does in our experiments, with the constant rate  $dT/dt = m$ , solution of the above equations gives

$$\int_0^{V_i} dV_i / (V_i^* - V_i) = \int_0^T (k_{i0}/m) \exp(-E_i/RT) dT \quad (5.5-4)$$

Since  $E_i/RT \gg 1$  is a good approximation for coal decomposition reactions, the solution becomes

$$(V_i^* - V_i)/V_i^* = \exp[-(k_{i0} RT^2/mE_i) \exp(-E_i/RT)] \quad (5.5-5)$$

This equation is plotted in Fig. 5.5-1 for activation energies typical

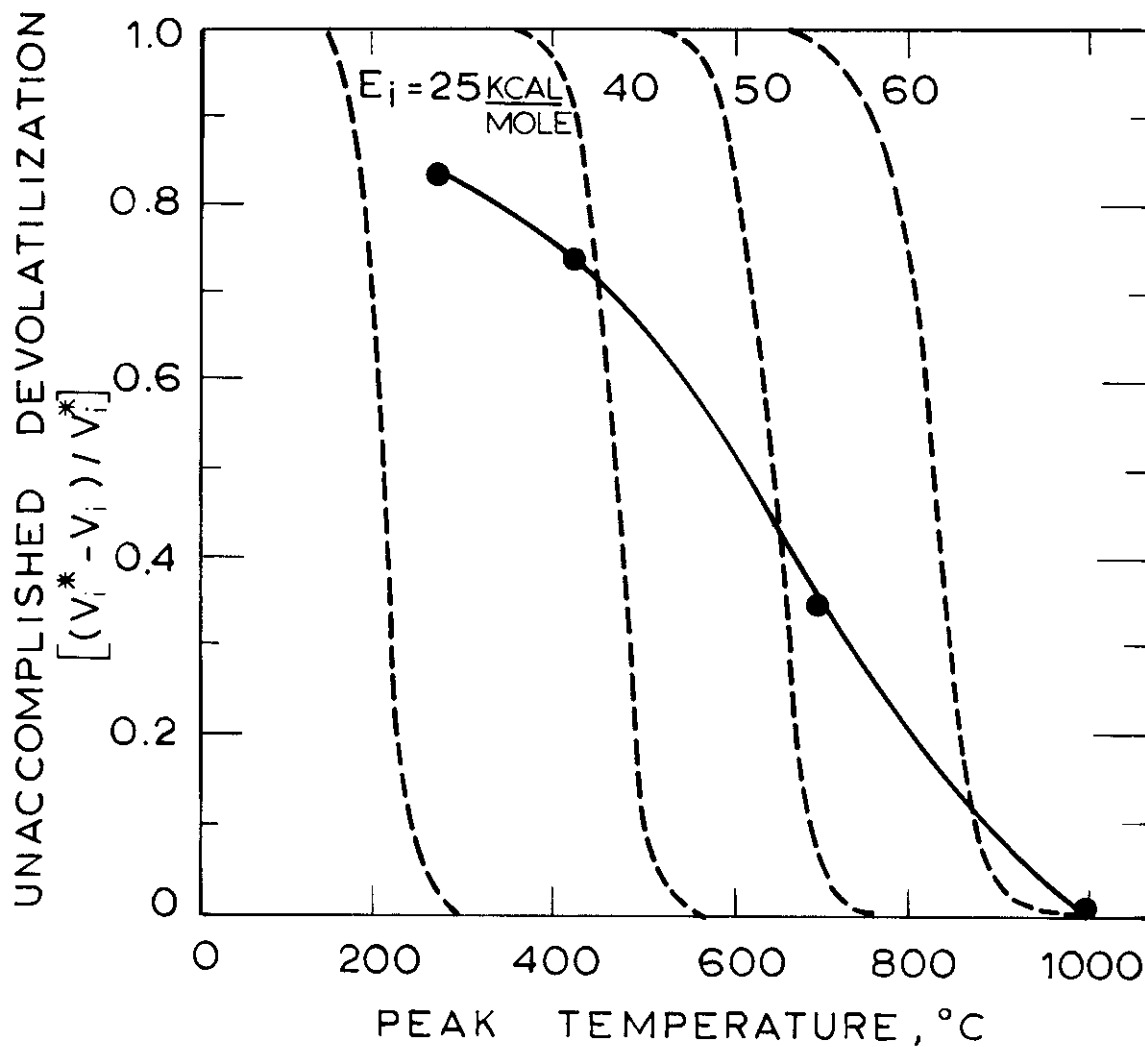


Figure 5.5-1 Comparison of Data on Overall Conversion of Lignite to Volatiles with Predictions from Single-Step First-Order Pyrolysis Model [(●) data; (dashed curves) predictions from model].

of organic decomposition reactions (see Table 3.2-3) and a typical pre-exponential factor of  $k_{10} = 1.67 \times 10^{13} \text{ s}^{-1}$ . The inadequacy of the single-reaction model in fitting the data on total yield of volatiles is evident from this figure; nevertheless, as has been discussed, this approach has been taken by many workers for correlating pyrolysis data.

It can be seen from the wide range of materials listed in Table 3.2-3 that organic decomposition reactions encompass a wide range of activation energies and pre-exponentials. It is not surprising that coal, the chemical structure of which is far more complex than that of the materials in Table 3.2-3, decomposes thermally to produce numerous products and that these products exhibit different activation energies. When a single first-order reaction is used to model coal pyrolysis, the activation energy and pre-exponential factor are forced to be very low in order to fit the overall temperature dependence that actually results from the occurrence of different reactions in different temperature intervals. The results are sometimes interpreted as reflecting transport limitations because the parameters are too low for organic decompositions. This point is discussed further by Anthony and Howard (1976).

Considerably more success is attained when the first-order is applied to the appearance of single products. As is implied in Figs. 5.1-1 to 5.1-3, many products are not adequately described by one first-order process. Rather than utilizing a large number of parallel reactions with a distribution of activation energies for individual products (Hanbaba et al., 1968), a simplifying assumption is made that one, two or three parallel reactions, depending on the observed behavior, describes the formation of certain key products. The mechanistic implication is that a given product may arise from more than one type of reactant, or from more than

one reaction pathway.

The first-order model was used with the measured time-temperature history of each experimental run to construct best fit curves for the yield data. The computer program used for the fitting is listed in the Appendix. The resulting kinetic parameters are summarized in Table 5.5-2. The curves shown in Figs. 5.1-1, 5.1-2, and 5.1-3 were calculated using these parameters and the model, for a standardized experiment in which coal is heated at 1000°C/s to the peak temperature, and then cooled at 200°C/s back to room temperature. The curves fit the data well for most species, and modelling with only one or two reactions appears sufficient in all cases except the carbon oxides which require a third reaction for data above about 1000°C. Figure 5.1-1 shows how the various individual reactions cooperate to give a smooth total weight loss curve.

In order to compare the present kinetic parameters with those obtained before using a distributed activation energy model (Anthony, 1974; Anthony et al., 1975, 1976; Anthony and Howard, 1976), the frequency distribution of the present activation energies is derived from Table 5.5-2 as follows. Data points in Fig. 5.5-2 represent the cumulative ultimate yields of all volatile components having activation energies less than or equal to those of the indicated points. Each point is labelled with the component whose ultimate yield is added to those of all other components shown on points to the left to give the indicated cumulative yield; e.g., the vertical distance between two adjacent points represents the ultimate yield of the component specified on the higher point. The slope of the smooth curve drawn through the data gives the frequency distribution curve  $dV_{cum}^*/V_{tot}^* dE$ , which is here normalized so that the area under a segment of the curve between two values of activation energy is the percentage of the total



Table 5.5-2 Kinetic Parameters for Lignite Pyrolysis

Product	Stage	$E_i$ , kcal/mole	$\log (k_{i0}/s^{-1})$	$V_i^*$ , Wt.% of lignite (as-received)
CO <sub>2</sub>	1	36.2	11.33	5.70
	2	64.3	13.71	2.70
	3	42.0	6.74	1.09
CO	1	44.4	12.26	1.77
	2	59.5	12.42	5.35
	3	58.4	9.77	2.26
CH <sub>4</sub>	1	51.6	14.21	0.34
	2	69.4	14.67	0.92
C <sub>2</sub> H <sub>4</sub>	1	74.8	20.25	0.15
	2	60.4	12.85	0.41
HC <sup>a</sup>		70.1	16.23	0.95
Tar	1	37.4	11.88	2.45
	2	75.3	17.30	2.93
H <sub>2</sub> O		51.4	13.90	16.5
H <sub>2</sub>		88.8	18.20	0.50
Total				44.0

<sup>a</sup>Hydrocarbons other than CH<sub>4</sub>, C<sub>2</sub>H<sub>4</sub> and Tar

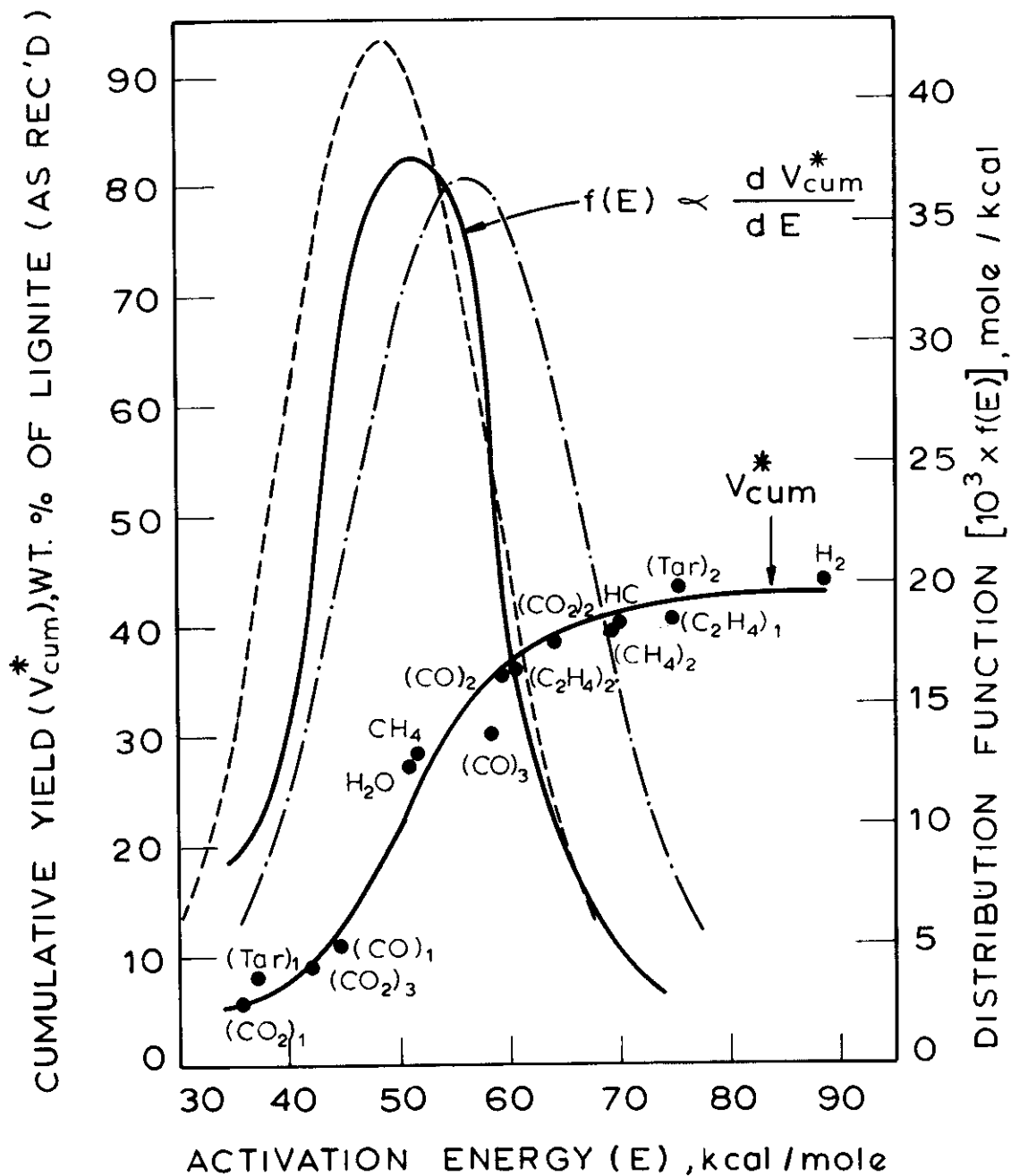


Figure 5.5-2 Distributions of Activation Energies of Pyrolysis Reactions [(●) cumulative yields, from present base data, of components indicated to left of and including a given point; (solid curves) present results based on volatiles yields; (broken curves) previous results (Anthony and Howard, 1976; Anthony, 1974) based on weight loss data and two different sets of kinetic parameters].

ultimate volatile yield that is associated with activation energies in the specific interval.

Figure 5.5-2 also presents two distributions (broken curves) obtained previously for the same lignite as was used here (Anthony, 1974; Anthony and Howard, 1976), but from a kinetic analysis of weight loss data assuming a statistically large number of reactions having a Gaussian distribution of activation energies and all having the same pre-exponential factor.<sup>†</sup> The left-hand curve was obtained when the pre-exponential factor ( $k_0 = 1.07 \times 10^{10} \text{ s}^{-1}$ ) was evaluated as one of the adjustable parameters, while the right-hand curve was obtained using a preferred fixed value of  $k_0$  ( $1.67 \times 10^{13} \text{ s}^{-1}$ ). The mean activation energies ( $E_0$ ) and standard deviations ( $\sigma$ ) of the previous distributions are, in kcal/mole, (left)  $E_0 = 48.7$  and  $\sigma = 9.38$  and (right)  $E_0 = 56.3$  and  $\sigma = 10.9$ . Statistical analysis shows that the present data are not significantly different from a Gaussian distribution with  $E_0$  and  $\sigma$  being 53.3 and 11.5 kcal/mole, respectively. The similarity of the present distribution derived from product compositions to the previous results based on weight loss is especially encouraging since  $k_0$ , which does influence  $E_0$ , was here allowed to assume a different value for each reaction whereas previously a single  $k_0$  was used for all reactions.

The bituminous coal data in Figs. 5.2-1 through 5.2-5 do not show the well defined stepwise behavior of the lignite data. As a result, application of a well defined one, two, or three step model is not as straightforward as in the case of the lignite.

Application of a two step model to the carbon monoxide and methane data yielded the following results:

<sup>†</sup>This complete model is presented in Section 3.2.

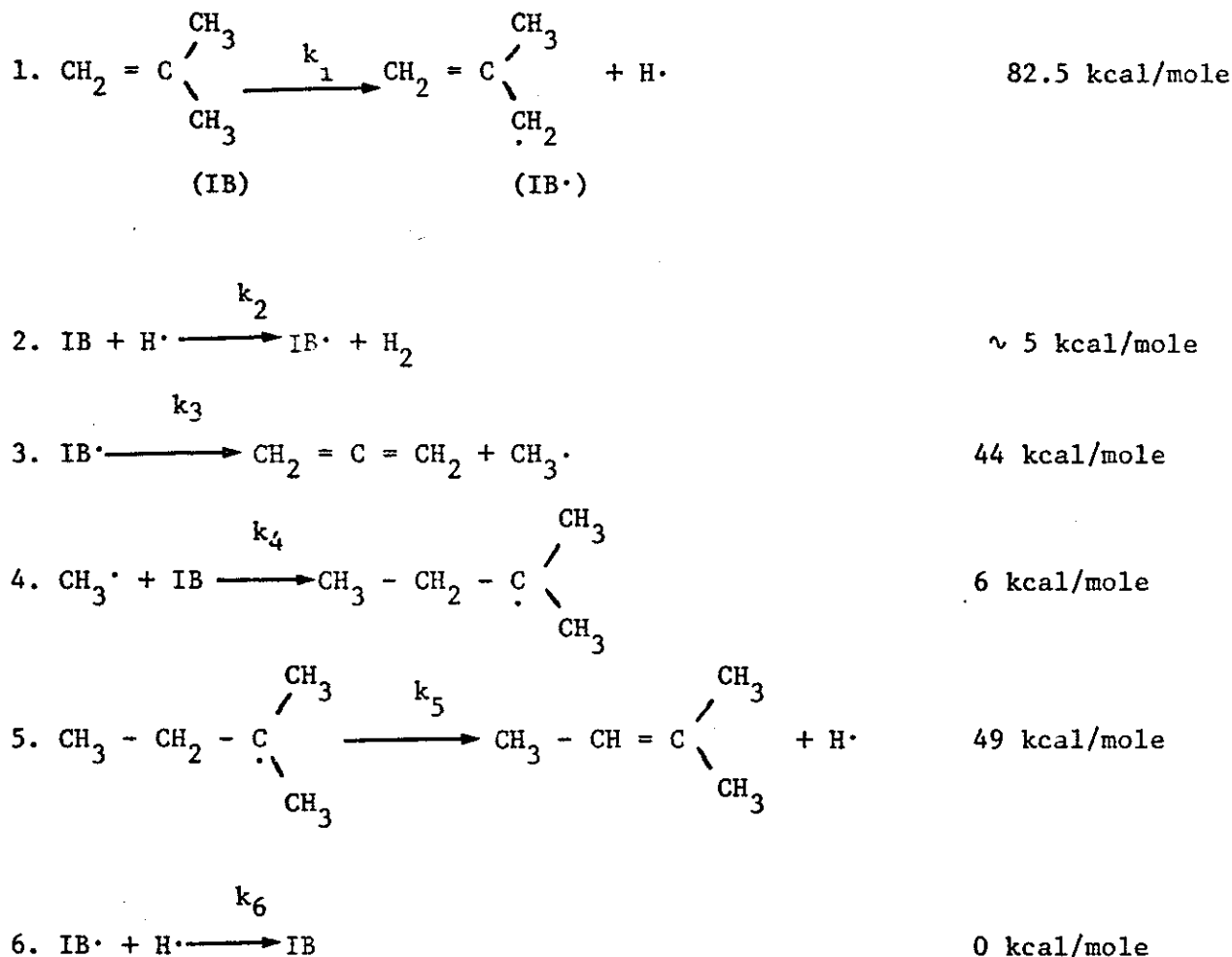
		<u>E(kcal/mol)</u>	<u>log (k/sec)</u>	<u>V*</u>
CO	1	63.4	12.5	1.84
	2	46.8	11.3	.57
CH <sub>4</sub>	1	65.4	13.3	1.78
	2	80.9	19.8	0.69

In both cases the fit is fair. Application of a single, first order model yields activation energies of about 30 kcal/mole and Arrhenius pre-exponentials of  $10^6 \text{ sec}^{-1}$  for both compounds. The fit is as good as the two step model gives, however. Application of a Gaussian distribution of activation energies to each product has thus far yielded ambiguous results; the suggestion is that a Gaussian distribution may be inappropriate and a skewed distribution of activation energies is indicated in some cases (e.g. CO, CH<sub>4</sub>, C<sub>2</sub>H<sub>4</sub>). The approach employed by Hanbaba et al. (1968), in which a Gaussian distribution was assumed for both activation energy and the log of the Arrhenius pre-exponential, was also successful in modelling (with "reasonable" values of the mean activation energy and pre-exponential) data with a similarly broad temperature dependence. Further work is required to determine the most appropriate model for these data.

While this rather simple, empirical model fits the lignite data rather well, caution must be exercised in its use, especially for elucidation of pyrolysis mechanisms. Most of the values of the activation energy and pre-exponential are "reasonable" for organic decomposition-type reactions. The fitted values of the Arrhenius pre-exponentials are as mentioned, closely correlated with the values of the activation energies. As a result, an uncertainty of but a few kilocalories per mole in the activation energy of a particular step can lead to an uncertainty of orders of magnitude in the pre-exponential factor.

The choice of a form first order in product yet to be evolved in a given step does not necessarily imply that the true mechanism leading to any product is a simple, first order bond scission. In fact, the activation energies observed are too low to be representative of a set of independent C-C bond cleavages (the bond strength of an average C-C single bond is approximately 80 kcal/mole, and that of the average C-O bond is of the same order). It is more likely that a set of concerted and/or radical initiated reactions are largely responsible for the observed behavior. In the latter case, it is possible that the cleavage of weak linkages within the coal structure (such as methylene bridges, ether linkages, or heteroatom linkages) initiates the radical process. H.C. Howard (1963) cites evidence obtained by paramagnetic resonance absorption measurements of carbonizing coal which indicates the formation of radicals may occur at temperatures as low as 300°C; "marked" increases in radical concentrations occur at about 400°C. Howard also cites the results of pyrolysis work conducted in nitric oxide, a known radical scavenger. The presence of nitric oxide at the initiation of pyrolysis retards the thermal decomposition of the coal and, only at sufficiently high partial pressures of NO, inhibits the secondary polymerization of the tar phase. It is assumed that if the higher molecular weight fractions of coal tar are the result of radical combinations of smaller tar fragments, then these reactions must occur within the coal particles themselves.

Thus substantial evidence exists to support the existence of free radical mechanisms in coal pyrolysis. This is certainly not surprising, since pyrolysis of simpler hydrocarbons often proceeds by a radical chain mechanism. As an example, the pyrolysis of isobutene is believed to proceed by the following mechanism (Leftin and Cortes, 1972):

Activation Energy

A quasi steady-state analysis gives as the rate of disappearance of isobutene:

$$-\frac{d}{dt} (\text{IB}) = 2 \left[ \frac{k_1 k_2 k_3}{k_6} \right]^{1/2} (\text{IB}) \quad (5.5-6)$$

It is straight forward to show that the overall activation energy for the process is given by  $1/2(E_1 + E_2 + E_3 - E_6) = 66 \text{ kcal/mole}$ . This value is in good agreement with experiment (63 kcal/mole).

Penninger and Slotboom (1973) have studied the cracking and hydro-cracking ( $\sim 500^\circ\text{C}$ ) of various substances which are perhaps more reminiscent of coal structure than is isobutene. In work with tetralin, they concluded

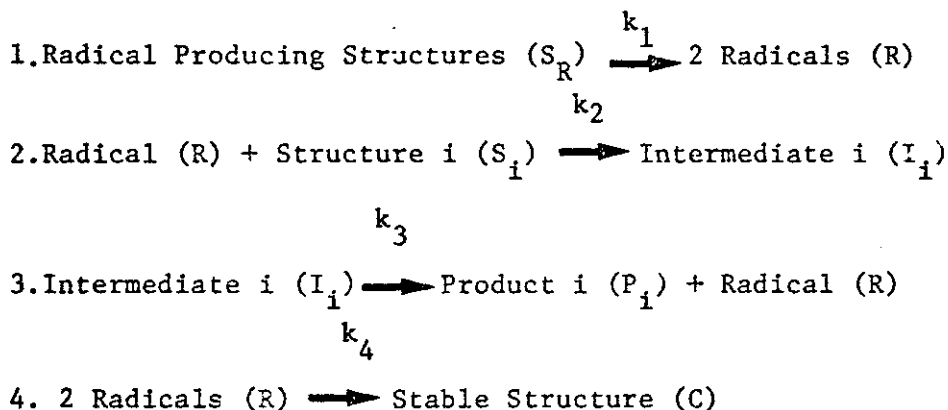


In accordance with the results for tetralin, the rate of the radical pathways again appeared to be considerably faster than ring opening via bond scissions. From these data, it was concluded that the overall sequence in cracking of condensed polyaromatic systems is:

1. Hydrogen (radical) attack on outer aromatic rings.
2. Successive naphthenic ring openings
3. Side Chain cracking

A concept of coal pyrolysis (and hydropyrolysis) which is supported by the data on pure hydrocarbons is that of a primarily radical process, initiated by scission of weak bonds within the structure. The possible roles of inter-aromatic "methylene bridges" or ether linkages have already been mentioned in this regard.

The parameter values presented in Table 5.5-2 can be shown "reasonable" by a very rough analysis of the same type as the much more refined analysis presented for isobutene pyrolysis. Assume coal pyrolysis is modelled as:



The chemical nature of the radicals (R), Structure i ( $S_i$ ), Structure R ( $S_R$ ), Intermediate ( $I_i$ ), Stable structure (C) are deliberately left vague in this analysis, so as not to reduce its generality. The major feature of  $S_R$  is that it produce radicals which can directly (or via a chain which is not rate limiting) interact with a particular structure i in the coal to yield a particular product i (e.g.  $CH_4$ ).



Then the rate of production of Product i is given by:

$$\frac{d(P_i)}{dt} = k_3(I_i) \quad (5.5-7)$$

If a quasi steady state assumption is applied to the radical species,

$$\frac{d(R)}{dt} = 0 \quad \text{and} \quad \frac{d(I_i)}{dt} = 0$$

then the concentrations of radicals (R) and ( $I_i$ ) are easily shown to be:

$$(R) = \sqrt{\frac{2k_1}{k_4}} (S_R)^{1/2} \quad (5.5-8)$$

$$(I_i) = \frac{k_2(R)(S_i)}{k_3} = \frac{k_2}{k_3} \sqrt{\frac{2k_1}{k_4}} (S_R)^{1/2} (S_i) \quad (5.5-9)$$

Hence:

$$\frac{d(P_i)}{dt} = k_2 \sqrt{\frac{2k_1}{k_4}} (S_R)^{1/2} (S_i) \quad (5.5-10)$$

The temperature dependence of the overall rate constant

$$k_{0A} = k_2 \sqrt{\frac{2k_1}{k_4}} \quad (5.5-11)$$

is given by the overall activation energy

$$E_{0A} = (E_2 + E_1/2 - E_4/2) \quad (5.5-12)$$

The bond energies for cleavage of CH bonds are of the order 100 kcal/mole, but the activation energy for formation of radicals from such a cleavage may be lower, depending upon the nature of a particular compound (as to whether it can stabilize a radical or not via resonance). Data compiled by Benson and O'Neal (1970, derived from pyrolysis experiments), indicate that the

actual range may be from over 80 to over 100 kcal/mole. Similarly, cleavages of C-C bonds and C-O bonds are in the range 50-80 kcal/mole. Thus  $E_1$  is roughly in the range 50-100 kcal/mole. Radical recombinations are extremely fast reactions and may be considered to have zero activation energy ( $=E_4$ ). Typically reactions of the type 2 have activation energies ranging from 10 to 20 kcal/mole (Benson, 1968). If  $E_2$  is set equal to 15 kcal/mole and  $E_1$  to 80 kcal/mole, then

$$E_{0A} = (15 + 80/2 - 0/2) = 55 \text{ kcal/mole}$$

This analysis is admittedly very rough, primarily because it considers only concentrations of radicals rather than their chemical nature. But the result is encouraging in that a model first order in product yet to be evolved (as per eq. 5.5-2) gives a theoretical activation energy comparable to those in Table 5.5-2.

A much more sophisticated approach involving detailed modelling with the aid of a computer is that being done by Gavalas and co-workers (Cheong, 1977). Because of the large variety of structures present in coal, use of a computing system with a statistical model of coal and a large library of possible reactions offers the only hope of developing a truly detailed model of coal pyrolysis. Simulation results thus far have suggested that the nature of the product mix may be rather sensitive to the nature of the radical formation reactions. For example, the predicted total weight loss during 500°C pyrolysis (for 30 seconds) drops by about 10% (from ~33% to ~23%) if the activation energy for the cleavage of ethylene bridges ( $\phi\text{-CH}_2\text{-CH}_2\text{-}\phi \rightarrow 2\phi\text{-CH}_2\cdot$ ) is raised by only 2 kcal/mole (from 48 to 50 kcal/mole). The hypersensitivity of predicted pyrolysis behavior to this parameter is surprising and awaits further elucidation.

### The Behavior of Functional Groups During Pyrolysis

As examination of Figs. 5.1-1 through 5.1-3 reveals, there are apparently five distinct phases during lignite pyrolysis. The first occurs at very low temperatures ( $\sim 100^\circ\text{C}$ ) and is associated with moisture evolution. The second phase at  $1000^\circ\text{C/s}$  heating rate begins at about  $450^\circ\text{C}$  and is associated with a large initial evolution of carbon dioxide, probably from low-activation energy decarboxylations. The loss of carboxyl groups as carbon dioxide at relatively low temperatures has been reported for lignites (Howard, 1963). A small amount of hydrocarbon products is also evolved at this stage. This material may contain both tar (e.g., asphaltenes and heavy oils) and also some hydrocarbon gases. The third phase involves evolution of water chemically formed in the range  $600\text{--}700^\circ\text{C}$ . It can be seen from Fig. 5.1-4 that carbon, nitrogen and sulfur during this phase remain largely in the char while the oxygen and hydrogen contents of the char sharply decrease. The fourth phase involves a final rapid evolution of carbon containing species. Carbon oxides, tar, hydrogen, and hydrocarbon gases are all rapidly evolved in the temperature range  $700\text{--}900^\circ\text{C}$ , where little water is produced. The fifth phase is the previously discussed high temperature formation of carbon oxides. To be compared with the foregoing, the pyrolysis of bituminous coal occurs in four somewhat less distinct phases. Again, surface moisture is driven off at low temperatures ( $<100^\circ\text{C}$ ) followed by the liberation of pyrolytically formed water at peak temperatures below  $400^\circ\text{C}$ . Between  $400$  and  $900^\circ\text{C}$ , the coal softens and the bulk of the hydrocarbons are evolved. Above  $900^\circ\text{C}$   $\text{CO}$  and  $\text{H}_2$  are the principal products evolved.

It has already been shown (Fig. 3.2-9) that the experimental results obtained during this investigation agree fairly well with the results of other studies in drawing a correlation between carboxyl groups in raw coal and the amount of  $\text{CO}_2$  evolved during pyrolysis (at low temperatures) and

between hydroxyl groups in raw coal and the amount of pyrolytically formed water.

The rather large difference in the temperature of water evolution for the two coals studied here however reflects either a substantial chemical difference between bituminous coal and lignite hydroxyls, or a major difference in the basic pyrolytic process. The lignite model structure of Wender (Fig. 3.1-20) suggests that some of the hydroxyl groups in lignites may be present as alcoholic rather than phenolic structures (which are the only source of hydroxyls in higher ranks of coal). It is not clear whether such a difference is responsible for the observed behavior; however the narrow temperature interval for evolution of pyrolytically formed water from lignite may speak against a structure such as that in Fig. 3.1-20, which contains two very different types of hydroxyl groups.

It appears, as Wolfs et al. (1960) hypothesized, that hydroxyl groups may play a key role in determining pyrolysis behavior. In the case of lignite pyrolysis, hydrocarbon formation is observed at temperatures, between 500 and 600°C, and between 700 and 900°C, but not between 600 and 700°C (evident in Fig. 5.1-2). This "plateau" coincides with the principal water formation step. During pyrolysis of bituminous coal, water formation occurs prior to the onset of the hydrocarbon formation phase, and no plateaus are observed. As has been suggested, it is possible that the hydroxyl groups consume hydrogen which could otherwise serve to stabilize hydrocarbon radicals; in the absence of hydrogen, these radicals repolymerize to form a solid cross-linked residue. Although the lignite initially has a slightly lower hydrogen to carbon ratio than the bituminous coal (0.77 to 0.85), adjusting for the hydrogen removed during water formation increases the gap (0.55 to 0.73). Such a difference in H/C ratio may help to explain the large

differences between these coals during pyrolysis. However, some bituminous coals with adjusted H/C ratios similar to that of the lignite show considerably more hydrocarbon formation. Thus, the explanation for the observed difference in behavior is not explained in terms of a simple elemental ratio.

Recently, other studies at M.I.T. have focussed upon the same two types of coals as examined in this investigation (Kobayashi, 1976; Kobayashi et al., 1977). The results of this investigation confirm the trend in elemental composition observed during pyrolysis of a bituminous coal (Fig. 5.5-3). As has already been discussed, the lack of significant change in the elemental trajectory implies that no major change in pyrolysis mechanism occurs with increased heating rate.

The rather striking difference shown by the two sets of lignite data is rather puzzling. Again, the data of Kobayashi, when viewed by themselves, suggest that there is no effect of heating rate on elemental trajectory, unless one occurs at an O/C ratio so low as to mask the difference near the H/C axis (i.e. at high conversions and high temperatures). The only apparent explanation for the apparently different elemental trajectories of the two studies is that there was a major chemical difference in the two samples used. The behavior of the lignite studied by Kobayashi suggests a rapid initial loss of hydrocarbon (H/C decreases and O/C increases initially). This may imply that the first phase of hydrocarbon formation, prior to water formation, is much more pronounced in the sample studied by Kobayashi. Since the two samples came from the same mine and were presumably handled in the same manner, this difference in behavior emphasizes the difficulty (and danger) involved in intercomparisons of literature data on pyrolysis.

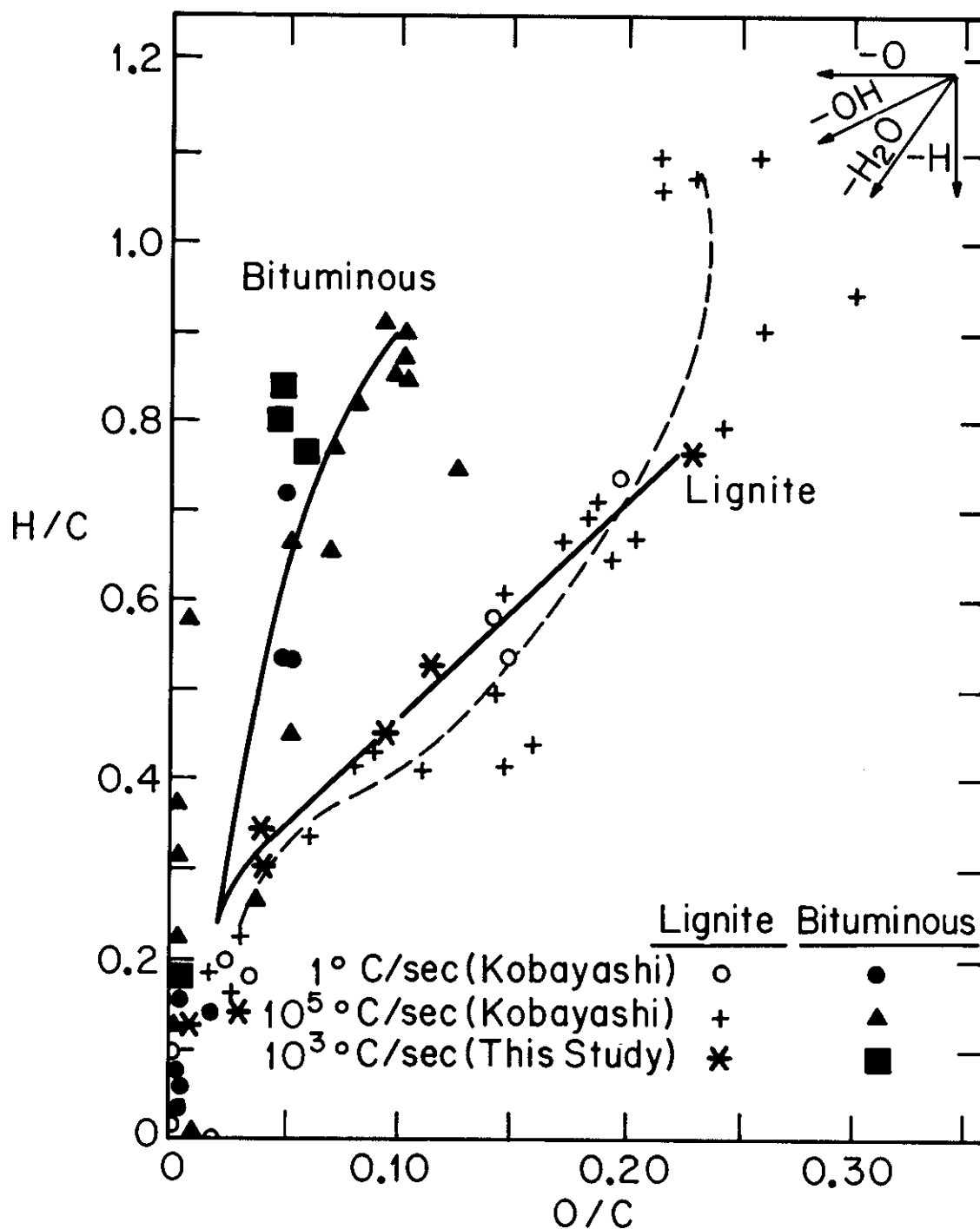


Figure 5.5-3 Comparison of H/C vs O/C Trajectories for Pyrolysis of Different Samples of Bituminous Coal and Lignite (Comparison of data from this study with data from Kobayashi, 1976 on coals from the same mines, but sampled at different times).

### Thermodynamic Aspects of Pyrolysis

In coal conversion applications, the distribution of heating value among the different products of pyrolysis is of considerable interest. So, too, is the total heat of reaction. The analysis presented below addresses both of these questions, first focusing on the lignite pyrolysis results.

Product heating value contents -- i.e., mass yield x net (lower) heating value on a mass basis -- shown in Fig. 5.5-4 were estimated from the product yields in Table 5.1-1 and some additional tar and gas measurements. Heating values of the lignite and char were calculated from the elemental analyses (Table 3.1-1 and Fig. 5.1-4) using the correlation of Mott and Spooner (1940), here adjusted to a net heating value, as-received basis:

$$\text{Btu/lb} = 144.5 (\text{C}) + 515.3 (\text{H}) - 62.5 (\text{O}) + 40.5 (\text{S}), \text{ if } (\text{O}) < 15 \text{ wt } \%$$

$$= 144.5 (\text{C}) + 515.3 (\text{H}) - [65.9 - 0.31 (\text{O})] (\text{O}) + 40.5 (\text{S}), \text{ if } (\text{O}) > 15 \text{ wt } \%$$

The net heating value of the tar and that of hydrocarbons other than  $\text{CH}_4$ ,  $\text{C}_2\text{H}_4$  and tar were assumed to be 16,000 and 19,700 Btu/lb (8.9 and 10.9 kcal/g) respectively. The heating values of  $\text{CH}_4$ ,  $\text{C}_2\text{H}_4$ ,  $\text{H}_2$ , and  $\text{CO}$  were, of course, known.

The heating value contents of the gas and tar follow the two-step behavior associated with the appearance of many of the individual components. At the higher temperatures, the gas accounts for a maximum of almost 15% of the heating value content initially in the lignite, and the tar for about 8%. At a temperature of about  $1000^\circ\text{C}$ , the char retains almost 70% of the heating value on the same basis. The volumetric net heating value of the gas produced at peak temperatures above about  $900^\circ\text{C}$  is about 380 Btu/std. cu. ft. ( $3,380 \text{ kcal/m}^3$ ) on a dry basis.

The total heating value content of all products appears first to increase and then to decrease as the peak temperature increases. Pyrolysis appears to be endothermic over a range of lower to intermediate temperatures where the total heating value content of all the products is greater than

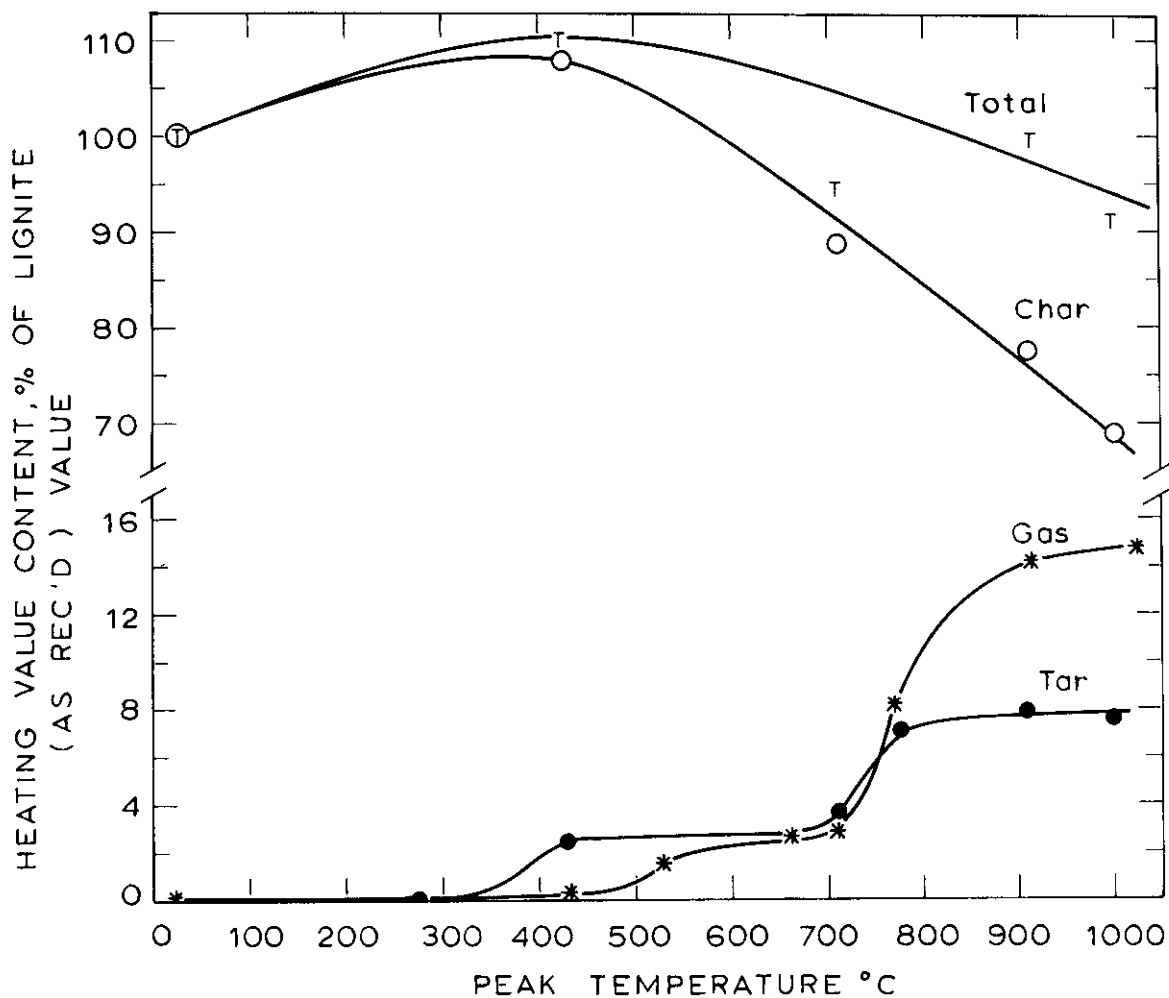


Figure 5.5-4 Variation of Product and Total Heating Values for Lignite Pyrolyzed to Different Peak Temperatures ((T) total, all products; (o) char; (\*) gas; (•) tar. Pressure = 1 atm He; Heating Rate = 1000°C/sec; 100% or ordinate corresponds to 9,500 BTU/lb lignite, as-received initial net (lower) heating value).

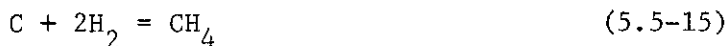
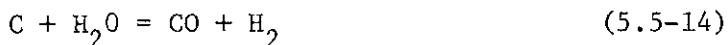


that of the starting material. At higher temperatures, however, the total becomes less than the initial value and therefore pyrolysis to those temperatures may be thermally neutral or exothermic.

Calculated on the same basis, the bituminous coal (initial net heating value 12,000 Btu/lb) shows little endo or exothermicity at any temperature. At 1000°C, roughly 45% of the original heating value is retained in the char, 35% is in the tar and liquid hydrocarbon products, and 15% is in the gaseous products (the net heating value of which is approximately 430 Btu/scf). Thus the pyrolysis of both coals at high temperatures is essentially thermoneutral.

It is also of interest to compare observed product distributions with what would be predicted from thermodynamic equilibrium (the models presented thus far have all suggested that the observed phenomena are subject to rate control rather than equilibrium control). Again, for illustrative purposes, the lignite case is examined.

It is assumed that the products are all in equilibrium in the presence of char at the peak temperature of the run. For approximation purposes the char is assumed to be graphite and the mole fraction of the ambient helium adjacent to and within the particles is assumed to be negligible. Equilibrium relations for the reactions



in the presence of excess solid carbon and with an assumed total pressure of 1000 atm are shown as curves in Fig. 5.5-5 where the points are the base data, obtained with a total pressure of 1 atm outside the particles.

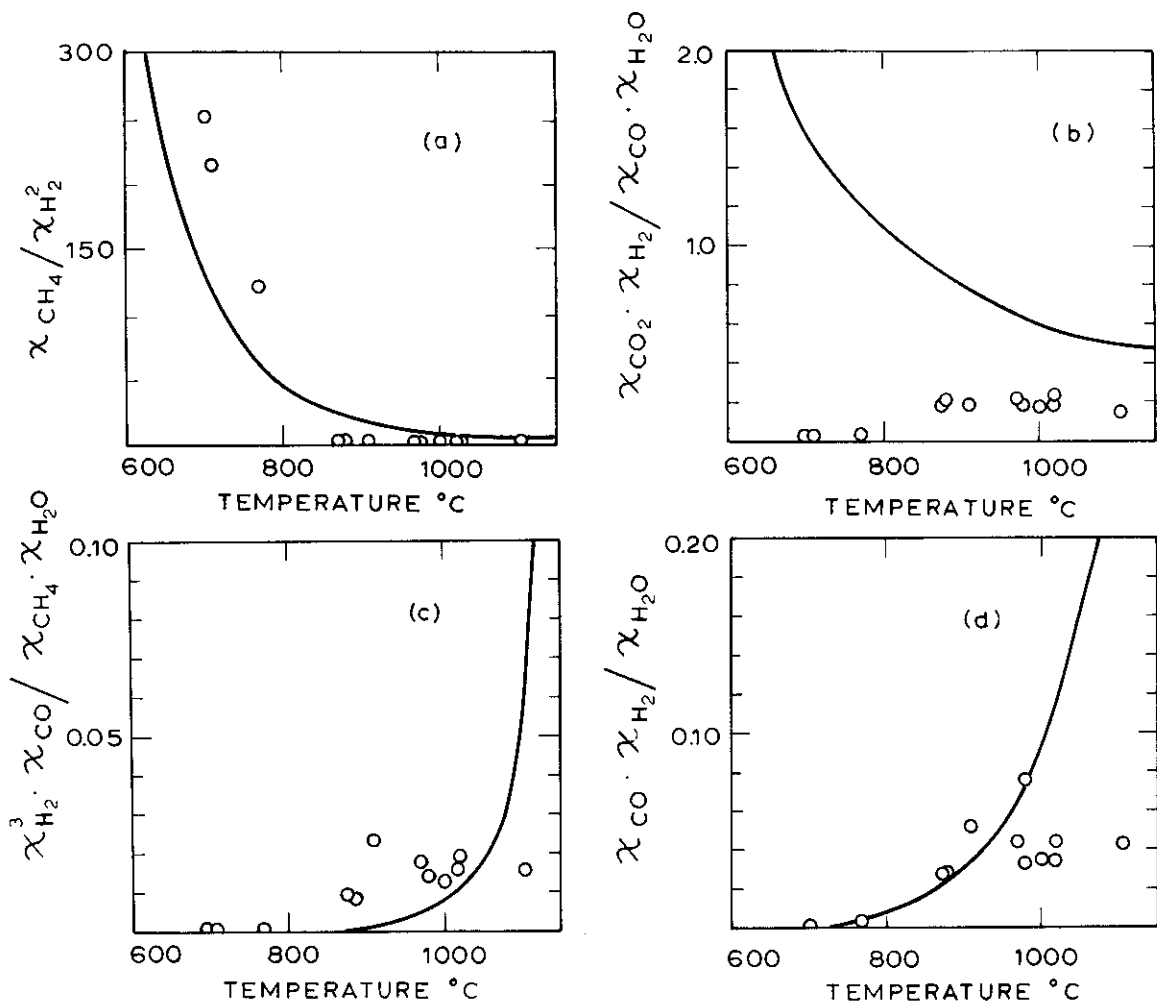


Figure 5.5-5 Comparison of Gas Composition Data for Different Peak Temperatures with Calculated Equilibrium Values under Simplified Conditions  $X_1 =$  mole fraction of  $i$ . (o) base data; (curves) equilibrium values calculated for an assumed total pressure of volatiles of 1000 atm].

Two cases are considered, one including water from the lignite moisture in the volatiles (points) and the other including only the chemically formed water (not shown). The latter case covers the possibility that moisture is lost early enough so as to be absent from the reacting mixture. The complete or partial loss of other products could also be considered but this was not done since moisture loss, which appears to offer the largest potential for an effect, is found to be of little significance in this rough analysis.

Fig. 5.5-5 shows that the data tend toward less disagreement with the equilibrium values as temperature increases. When the total pressure of volatiles is assumed to be 1 atm, all the reactions are far from equilibrium with the exception of Reaction 5.5-13 at the higher temperatures, where a rather close approach to equilibrium cannot be excluded within the large uncertainty of this calculation. Reaction 5.5-13 is the only one of the four that is independent of pressure. Improved agreement of the equilibrium values with the data is observed for the other reactions as the assumed total pressure of the volatiles is increased substantially, the values for Reactions 5.5-14, 5.5-15 and 5.5-16 depending on pressure to the powers -1, -1, and -2, respectively.

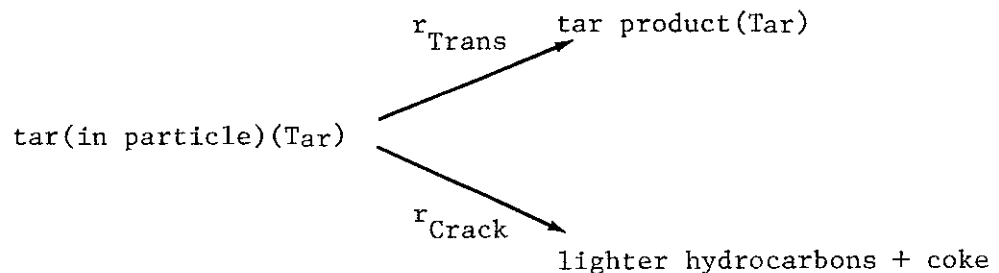
Volatiles pressures much larger than 1 atm within the pores of the particles are not inconsistent with calculated pressure drops associated with volatiles expulsion under the present conditions of rapid pyrolysis. The agreement in Fig. 5.5-5 between the equilibrium values and the data for an assumed pressure of 1000 atm is intriguing. Such a high pressure could be achieved if it is assumed that the formation of volatiles within the pores largely precedes escape therefrom. Existence of such a high internal pressure gains some support from the observed fracturing ("sparking") of lignite particles during pyrolysis.

On the other hand, the measurable effect which an external pressure change as small as 1 atm (from 1 atm to full vacuum) has on lignite pyrolysis behavior would hardly be expected if the internal pressure of a particle is 1000 atm. This, combined with the good correlation between structures in raw coal and pyrolysis products speaks for a primarily rate controlled process rather than equilibrium controlled. It is likely that the effect of mass transport limitations within the particle is to move the products closer to equilibrium, since the equilibration reactions have more opportunity to occur, the longer the residence time of volatiles in the particle.

#### Secondary Reactions and Mass Transport Limitations

This section will focus principally on the behavior of the bituminous coal; the lignite showed only small effects of external pressure variation. Fig. 5.2-7 and 5.2-8 show that the principal effects of increases pressure during pyrolysis are observed only above peak temperatures of 700 to 750°C. At these temperatures, the coal has already completely softened and forms a layer of viscous fluid on the screens. The thickness of this layer shows some dependence on the diameter of the original coal particles.

From an analysis of compositional changes occurring with increased mass transport resistance, it is apparent that the principal reactions involved are of the tar cracking variety (Fig. 5.2-7). Thus transport of the tar appears to be in competition with secondary cracking reactions:



where  $r_{\text{Trans}}$  and  $r_{\text{Crack}}$  represent the rates of transport and cracking,

respectively. Under pseudo steady conditions, the ratio of actually observed tar to the maximum possible yield is given by

$$\frac{\text{Tar}}{\text{Tar}^*} = \frac{r_{\text{Trans}}}{r_{\text{Trans}} + r_{\text{Crack}}} = \frac{1}{1 + \frac{r_{\text{Crack}}}{r_{\text{Trans}}}} \quad (5.5-17)$$

Anthony et al. (1975) proposed ( $r_{\text{Trans}} \propto 1/P_{\text{EXT}}$ ) ( $P_{\text{EXT}}$  = external pressure) by analogy with a diffusion coefficient and were successful in modelling weight loss data of the type shown in Fig. 5.2-7. A more rigorous derivation of this model is presented in section 3.2. Anthony et al. suggest that the analogy with diffusion implies that

$$r_{\text{Trans}} = \frac{k_T}{P_{\text{EXT}}} [\text{Tar}] \quad (5.5-18)$$

where  $k_T$  is a constant and  $[\text{Tar}]$  stands for the concentration of tar in the coal molecule (assumed equivalent to Anthony's reactive volatiles). It was further assumed that tar cracking is a first order process:

$$r_{\text{Crack}} = k_c [\text{Tar}] \quad (5.5-19)$$

so that:

$$\frac{r_{\text{Crack}}}{r_{\text{Trans}}} = \frac{k_c P_{\text{EXT}}}{k_T} \quad (5.5-20)$$

The fraction of tar escaping the particle is then given by:

$$\frac{\text{Tar}}{\text{Tar}^*} = \frac{1}{1 + \frac{k_c P_{\text{EXT}}}{k_T}} \quad (5.5-21)$$

As is evident from Fig. 5.2-8, there is a certain fraction of tar evolved at temperatures below which cracking can occur. A rigorous model would require that the effect of a non-isothermal temperature history be factored into (5.5-21). For the purposes of this rough analysis, it is assumed that a certain fraction of tar is evolved below a temperature  $T^*$

at which cracking reactions are very slow. This tar would be considered part of Anthony's "non-reactive" volatiles fraction. Above  $T^*$ , it is assumed that the cracking reactions occur with a rate governed by a constant  $k_c$ . Fig. 5.2-8 suggests that roughly a 12% yield of tar occurs up to the peak temperature at which cracking reactions begin to manifest themselves. If it is assumed that at vacuum conditions all tar can escape without cracking ( $\sim 32\%$  by wt.), then  $[\text{Tar}^*] = 32 - 12 = 20\%$  by weight = "reactive" volatiles. This value is identical to that derived by Anthony et al., based on weight loss data alone. The value of  $k_c/k_T$  derived by assuming this value is  $0.85 \text{ atm}^{-1}$ , also in fair agreement with the value obtained by Anthony et al. It may therefore be concluded that Anthony et al. were quite justified in their assumption that their cracking model was focussing on the behavior of the tar.

In spite of its success at fitting total weight loss and tar yield data, this model requires clarification on two points.

1. While weight loss data are adequately fit, the effects on gaseous products are not included.
2. The suggested form of the pressure dependence and its analogy with a diffusion coefficient does not appear to be consistent with the observations that volatiles emerge as "jets" from the particle surface - clearly hydrodynamic flow rather than a diffusional process.

Regarding the first point, a cursory examination of the data used to construct Fig. 5.2-8 revealed that for every weight percent of tar lost to cracking, a gain of 0.1 to 0.2 weight percent of, all other hydrocarbons resulted; most notably and consistently affected is the yield of methane, showing an average of 0.05 to 0.1 for every weight percent of tar cracked. On a molar basis, this implies that for an "average" tar molecule of molecular weight 400, one to three moles of additional methane can be produced

by cracking the tar molecule. It is not clear whether the methane comes from the cracked molecule of tar itself or whether the latter merely surrenders hydrogen which promotes further reactions in the coal matrix itself.

Griffiths and Mainhood (1967) studied the cracking of freshly produced coal tar externally to the bed of coal and observed that, as expected, the yields of light hydrocarbon liquids and gases increase as the extent of cracking increases. Another important finding was that activated carbon is an effective catalyst for the cracking reaction (better than silica or alumina). This raises the possibility that coal char itself acts as a cracking catalyst.

Since cracking reactions do not begin to manifest themselves until peak temperatures between 700 to 800°C are attained, it is possible to calculate the implied activation energy, based on a few assumptions. Equation 5.5-5 gives the fractional unaccomplished conversion of a coal heated to a peak temperature at a rate of  $m^\circ\text{C}/\text{sec}$ . It is straightforward to show that if cooling occurs at a rate  $m_1^\circ\text{C}/\text{sec}$ , the total unaccomplished fractional conversion for the entire cycle is:

$$\frac{V_i^* - V_i}{V_i^*} = \exp \left[ \frac{-k_{i0} RT^2}{E_i} \exp(-E_i/RT) \left( \frac{1}{m} + \frac{1}{m_1} \right) \right] \quad (5.5-22)$$

Assuming in this case that the conversion refers to a cracking reaction, and that 50% conversion of some crackable species is attained during a run with a peak temperature of 750°C ( $m = 1000^\circ\text{C}/\text{sec}$ ,  $m_1 = 200^\circ\text{C}/\text{sec}$ ) then for a typical pre-exponential of  $10^{13}$  to  $10^{14} \text{sec}^{-1}$ ,  $E_i \approx 60$  kcal/mole. Thus tar cracking reactions appear to have a minimum activation energy of 60 kcal/mole.

The precise nature of the transport process remains slightly hazy; a model implying diffusional transport appears to offer a good fit. Alternatively, if it is proposed that  $r_{\text{Trans}}$  is proportional to the pressure difference between the outside and inside of the particle, there is difficulty in

explaining the observed large effect of decreasing external pressure by only one atmosphere (from 1 atm to vacuum). If the internal pressure of a fluid coal particle is indeed 100 atm as the bubble model proposed by Lewellen (1975, see section 3.2) sometimes implies, it is difficult to rationalize the difference in product yields observed with a total pressure driving force of 100 atm (vacuum pyrolysis) to those obtained with a driving force of 99 atm (atmospheric pressure pyrolysis).

This dichotomy (in which volatiles transport according to fluid mechanics should be hydrodynamic and according to product behavior is diffusional) may imply that the transport is governed by both mechanisms. As was presented in section 3.2, the vapor pressure of coal tar can be assumed to follow:

$$\log P_{\text{TORR}} = -102.5 \frac{(\text{MW})^{.654}}{(T^{\circ}\text{K})} + 7.97 \pm 0.35$$

for which selected results are shown below:

<u>Temperature °K(°C)</u>	<u>Molecular weight</u>	
	<u>400</u>	<u>1000</u>
800 (527)	0.04 atm	$2 \times 10^{-7}$ atm
1000 (727)	0.9	$5 \times 10^{-5}$
1300 (1027)	13	$7 \times 10^{-3}$

It is apparent that at the temperatures at which cracking becomes important (700-800°C) a large fraction of the tar may have a vapor pressure of but a few torr. While the internal pressure of the coal particle (or "melt") may be high because of the rapid production of gases (which certainly escape via pressure driven flow), the escape of tar may be controlled by a relatively slow evaporative process at the surfaces of the melt. Except where localized turbulence results in enhanced transport, the evaporative process may be controlled by diffusion away from the surface. The weak



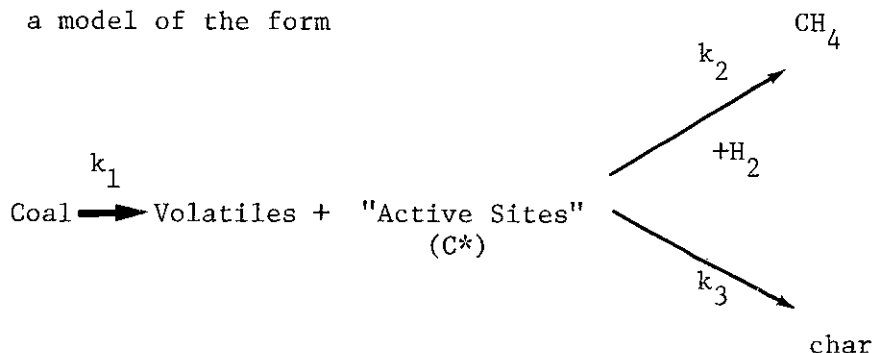
effect of particle diameter (D) on total pyrolysis yield (and on the yield of tar) could be explained in terms of a reduced surface area. The fact that the  $r_{\text{Trans}}$  shows only very roughly a  $\sqrt{1/D}$  dependence, rather than the  $1/D$  dictated by the geometry of a sphere is not surprising. Since the coal is a viscous fluid the temperatures at which secondary reactions begin to manifest themselves, geometrical factors are necessarily vague. The fluid spreads across the screen and forms a layer which depends only roughly on particle diameter. A calculation based on original particle diameter therefore can only be approximate. This feature of the model is expected to be somewhat different in a flow system, where the particle is not physically constrained by rigid boundaries and can therefore exhibit the classical cenosphere formation behavior.

It is apparent that efforts to model the coupled mass transport-secondary reaction effects may not have been detailed enough in the treatment of volatiles. There would appear to be promise in using a fluid mechanics model such as that developed by Lewellen (1975) combined with a more detailed accounting of the behavior of individual chemical species (separating tar from fixed gases) to offer a more realistic picture of the process.

#### 5.6 Discussion and Modelling of Hydropyrolysis Results

The principal product of hydropyrolysis under the conditions of this study is methane. It appears that the interaction of coal and hydrogen begins at temperatures in the same range as that characterizing onset of hydrocarbon formation during ordinary pyrolysis. It is likely that the hydrogen serves to stabilize radicals formed during cleavage of inter-aromatic cluster bridges.

In the case of lignite hydrolysis, in which variation of particle diameter indicated a regime of primarily chemical control, the pressure dependence of product yields is apparently complicated. However a model of the form



is suggested for pressures less than 69 atm  $\text{H}_2$  (=1000 psig  $\text{H}_2$ , see Fig. 5.3-7).

It is easily shown that the ultimate yield of methane predicted by such a competitive model is

$$(\text{CH}_4) = \frac{\frac{k_2 \text{Co}^*}{k_3} P_{\text{H}_2}}{1 + \frac{k_2}{k_3} P_{\text{H}_2}} \quad (5.6-1)$$

(assuming that the methane forming reaction is first order in hydrogen pressure and that the initial concentration of active sites is  $\text{Co}^*$ ).

Zahradnik and Glenn (1971) and Johnson (1977) have used such an empirical form with some success.

Physically, such a model implies that the addition of hydrogen continues to have a beneficial effect that decreases with each additional increment of pressure because eventually all active sites are consumed by hydrogenation rather than crosslinking (char-forming reactions). The large effect of temperature displayed in Fig. 5.3-7 can be construed as a manifestation of the distribution of activation energies for reactions which form active sites (symbolized by rate constant  $k_1$ ). Such a modelling

approach has been successfully employed by Johnson (1977, see section 3.2 and Fig. 3.2-27 for distribution function).

The model suggested by Anthony et al. (1976) for bituminous coal hydrolysis suggests a different mechanism in that it proposes that the effect of hydrogen is felt through stabilization of otherwise crackable volatiles (plus some solid phase hydrogenation). The model derived in section 3.2 was

$$V = V_{NR} + V_R^{**} [1 + k_1 / (k_T/P + k_2 P_{H_2})]^{-1} + k_3 P_{H_2} \quad (5.6-2)$$

where  $V$  = Total observed weight loss

$V_{NR}$  = Weight loss due to "uncrackable" (or non repolymerizable) species.

$V_R^{**}$  = potential ultimate yield of crackable species

$P, P_{H_2}$  = Total pressure and  $H_2$  partial pressure, respectively.

$k_1, k_2, k_3$  = rate constants for the volatiles formation (pyrolysis) reaction, the gas phase (homogeneous) hydrogenation - stabilization reaction, and heterogeneous hydrogenation reactions

$k_T$  = defined by rate of volatiles transport =  $\frac{k_T}{P}$  (conc. of volatiles)

The data shown in Fig. 5.4-2 clearly imply that primary volatiles are not actually stabilized by the presence of hydrogen, however additional product analysis data suggest that some hydrocracking products (i.e. light hydrocarbon liquids) of the primary volatiles are indeed stabilized (note the higher yield of light hydrocarbon liquids obtained during hydrolysis - Table 5.4-1).

Thus a basic difference between the models represented by Equations 5.6-1 and 5.6-2 is the locus of the so called "active sites", the former assuming them to be trapped in a solid phase while the latter assuming a fraction of them to be "transportable" with other volatile matter. The yield increment ascribed to "transportable active intermediates" in 5.6-2 is given by:

$$\frac{1}{1 + \frac{k_1}{(k_T/P + k_2 P_{H_2})}} = \frac{k_T/P + k_2 P_{H_2}}{k_T/P + k_2 P_{H_2} + k_1} \quad (5.6-3)$$

If it is assumed that  $k_T = 0$ , that the active intermediates are indeed not transportable, 5.6-3 reduced to

$$\frac{k_2 P_{H_2}}{k_2 P_{H_2} + k_1} = \frac{(k_2/k_1) P_{H_2}}{(k_2/k_1) P_{H_2} + k_1} \quad (5.6-4)$$

a form which has precisely the same empirical pressure dependence as 5.6-1. In the real case, it is likely that some of the potentially hydrogenable structures are transportable (e.g. tar), and some are fixed to the char matrix. This implies a model with a form:

$$V + V_{NR} + V_R^{**} \left[ 1 + k_1 / (k_T/P + k_2 P_{H_2}) \right]^{-1} + Co^* \left[ 1 + k_3' / k_2' P_{H_2} \right]^{-1} + k_3 P_{H_2} \quad (5.6-5)$$

which is essentially a combination of (5.6-1) and (5.6-2) with all nomenclature as in (5.6-1) and (5.2-6) except  $k_2$  and  $k_3$  from (5.6-1) are changed to  $k_2'$  and  $k_3'$  in (5.6-5). The interpretation of the last term in (5.6-5) is also changed to represent only the slow hydrogasification reaction and may be left out of analyses of short residence time hydrolysis results.

Also, both  $k_1$  and  $Co^*$  may be subject to a range of activation energies which may not be the same in both cases.

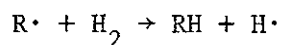
The emphasis on transportable volatiles is primarily of concern in the case of bituminous coal. It has been demonstrated that a low pressure of hydrogen ( $\sim 1$  atm) actually depresses total weight loss relative to vacuum pyrolysis (Fig. 3.2-24). Clearly a model such as (5.6-1) cannot address such an issue. Nor can the yield depressing effect of increased particle diameter (Fig. 5.4-4) be accounted for by (5.6-1); this effect can be included as part of the transport constant  $k_T$  in a model of the form 5.6-5.

The data for bituminous hydrolypyrolysis are unfortunately too sparse to permit evaluation of all constants in (5.6-5). The ratio  $k_1/k_T$  has been shown in the previous section to have a value of 0.85 atm.

It has been inferred from the data on lignite hydrolypyrolysis that the value of  $V_R^{**}$  is low (the yield of tar is low and as a result the effect of external inert gas pressure is small). Therefore it can be seen that (5.6-5) reduced back to (5.6-1) in this case, and as already mentioned, the fit is good for pressures less than 1000 psig  $H_2$  (Fig. 5.3-7). Unfortunately, the rise in yield (at 850°C) at pressures above 1000 psig is not to be expected, based on the model represented by (5.6-1). Such a complicated pressure dependence could be explained by a model in which transportable and non-transportable active intermediates were involved (5.6-5), but in the case of lignite hydrolypyrolysis, this presents a contradiction in terms of the observed low yield of crackable volatiles. This area awaits further clarification, which will require the gathering of more experimental data at a wider range of temperature and hydrogen pressures.

Regardless of the effect of these various parameters, the evidence from this study and that by Anthony et al. (1976) suggests that the

hydropyrolysis process proceeds at a rate comparable to that of ordinary pyrolysis. This implies, as did the hydrocracking work of Penninger and Slotboom (1973) that the process is indeed a radical process, the rate of which is determined by the rate of initiation steps within the hydrocarbon itself. The chemistry of the overall process is changed by the fact that the probability of reactions of the type:



is rather high compared with their probability during pyrolysis. Hence, a far greater proportion of the chain carriers during hydropyrolysis will be molecular hydrogen rather than hydrocarbon radicals. This of course leads to a greater probability of volatiles forming reactions and decreased probability of cross linking reactions. Since a high yield of char can be formed at even high pressures of hydrogen (about 50% at 69 atm  $H_2$ , in the case of lignite), apparently the hydrogen cannot stabilize all hydrocarbon radicals. This can reflect either a rate limitation or a mass transport limitation. The fact that particle diameter variation did not affect the lignite results substantially implies that if such a mass transport rate limitation exists, then it is on a micro (molecular) scale rather than on a macro (particle diameter) scale.

## 6.0 CONCLUSIONS AND RECOMMENDATIONS

The following are the major conclusions of this investigation:

1. Coal rank and pyrolysis temperature are the most significant determinants of product composition and overall pyrolysis behavior.
2. There is very little effect of heating rate on the composition of volatiles or the kinetics of their formation (conclusion drawn for high rates of heating primarily).
3. Variation of particle diameter and external pressure can substantially affect the character of products produced during pyrolysis. This effect is most pronounced in a coal normally characterized by high yields of tar and is minimal in a lignite which produces little tar. It is felt that secondary tar cracking reactions may be the reason for the frequent discrepancy between the results of the standard proximate volatile matter test and rapid pyrolysis yields.
4. There is good correlation between certain products of pyrolysis (e.g.,  $\text{CO}_2$ ,  $\text{H}_2\text{O}$ ) and structural features of the raw coal (e.g. carboxyl groups, hydroxyl groups). The rather important role ascribed to hydroxyl groups by Wolfs et al. (1960) is supported by these data.
5. The pyrolysis process occurs in several distinct stages, each characterized by a particular set of products. A pyrolysis model describing weight loss behavior with a distribution of activation energies has received support from individual product kinetic data.
6. The mechanism of decomposition is primarily radical chain (until a high degree of conversion is achieved, at which point aromatization probably proceeds by a simple scission type process and leads to hydrogen as the primary product).
7. Hydropyrolysis is intimately related to the pyrolysis process and can be

effectively understood in these terms.

A small effect of hydrogen can be seen rather 'early' in the pyrolysis process, but the full effects of hydrolysis are not observed until a substantial portion of the ordinary pyrolysis process has run its course. In the case of bituminous coal hydrolysis, hydrogen has no apparent effect on a portion of the tar which is formed at low temperatures. Hydrogen does not stabilize high temperature tar, but may stabilize small tar cracking products. The principal increment to yield from hydrolysis is in the form of methane gas.

8. It is felt that the rate of hydrolysis is closely tied to the rate of ordinary pyrolysis because the radical initiation steps are the same for both processes.

Of a practical nature, it has been shown that lignite pyrolysis produces a high heating value char (close to bituminous coal in net heating value). This char contains roughly 1/3 of the sulfur present in the original coal, and thus is a cleaner product than the raw lignite. On the other hand, only 25% of the nitrogen is removed during pyrolysis, and consequently the char is richer in nitrogen (on a percentage by weight basis) than the raw lignite. The volatile products consist of a heavy tar ( $\text{CH}_{1.5}^{\text{O}}\text{N}_{0.1}\text{O}_{0.01}$ ) which contains at most 8% of the heating value of the raw coal. The gases contain a maximum of 15% of the heating value of the raw coal and have a heating value of roughly 380 BTU/SCF (on a dry basis).

The fact that low heating value products are preferentially driven off at low pyrolysis temperatures and short contact times offers an interesting processing possibility. Rather than (or in addition to) a simple drying of the lignite at mine-mouth, a considerably higher quality solid fuel can be produced by a low temperature rapid pyrolysis of ground lignite. The



penalty in heating value of products lost is less than 8%, and the resulting material is like a non-agglomerating bituminous coal. If need as a feed for a synthetic fuels process, further high temperature pyrolysis will yield most of the hydrocarbon products without the need to separate them from a large volume of inerts ( $\text{CO}_2, \text{H}_2\text{O}$ ).

Hydropyrolysis of the lignite substantially increases the carbon and nitrogen conversions. The bulk of the extra carbon conversion is in the form of methane. If hydropyrolysis were to be applied commercially as a two stage process with the first stage being ordinary low temperature pyrolysis, some savings in hydrogen (and separations costs) should result.

In some respects, the results for bituminous coal mirror the results for the lignite. Over 50% of the sulfur but only about 1/3 of the nitrogen are removed by high temperature pyrolysis. It should also be possible to flash pyrolyze the bituminous coal at low temperatures to drive off small amounts of pyrolytically formed water and  $\text{CO}_2$ . The tar formed during bituminous pyrolysis is rather sensitive to cracking at high pyrolysis temperatures. It may be best, if high yields of liquid products are desired, to pyrolyze the coal at low pressures to produce tar and then to hydrocrack the tar separately, rather than combining the two steps.

#### Recommendations for Future Work

Experimentally, the captive sample apparatus has provided a great deal of data relatively inexpensively. There are many areas to which it can still very effectively be applied. At present, a flow reactor is under development at M.I.T., which should provide data from a system which, in processing environment, resembles more closely the entrained flow or fluid bed reactors commercially applied to coal processing. In addition to this advantage, the flow system can be run continuously for long periods of time, affording the

opportunity to produce larger samples of products, making their analysis easier and perhaps more reliable, especially in terms of sulfur and nitrogen.

Areas which warrant further study include:

- Conducting systematic studies of pyrolysis on a wider range of ranks. This would perhaps permit more correlations to be drawn between coal structure and pyrolysis behavior.
- A closer tracking of the changes in the solid phase (e.g. behavior of aliphatic H and C coupled to product analysis) would provide valuable new insight to the mechanisms of pyrolysis. This task requires drawing heavily upon the various newly developed solid phase spectroscopic techniques described in section 3.1. Of course anything new which can be learned concerning the structure of the parent coals would also be valuable.
- A better characterization of the liquid products is necessary. This study has been admittedly weak in tracking the nature of the heavy tars, which is of both mechanistic and commercial interest.
- Again with respect to the liquid products, a separate study on the cracking of coal tars on coal char could provide valuable information on the nature of secondary reactions.
- Establish more firmly the role of hydroxyl groups in determining pyrolysis behavior and determine whether the coal can be "chemically engineered" prior to pyrolysis to produce a different spectrum of products. To this end, some runs with lignite treated in

concentrated caustic solution of sufficiently low pH to remove phenolic protons yielded a solid which gave roughly the same total weight loss (no product analysis attempted) as the raw lignite. It is probable that such attempts to modify pyrolysis behavior will have to be more sophisticated. Hydrogen pretreatment is also of interest.

- Investigate the catalytic effect of mineral matter on both rapid pyrolysis and hydrolypyrolysis. In developing the power to predict pyrolysis (hydrolypyrolysis) behavior based on the characteristics of a coal, the potentially important role which the inorganic fraction may play cannot be overlooked. Also of considerable commercial interest would be the effect of any added catalysts.
- With regard to hydrolypyrolysis, the important interplay of hydrogen pressure and temperature can have a major impact on the design of commercial synthetic fuels plants. This is an area which was only lightly touched upon in this thesis and warrants considerably more examination.
- There is clearly a need to continue work on the various models presented in this thesis. In some cases, the need is principally in the area of model testing, while in other areas further experimental evidence is also called for (i.e. effect of pressure on hydrolypyrolysis at various temperatures). In other areas (modelling of transport in bituminous coals) entirely new models are called for.

## 7.0 REFERENCES

- Aczel, T., M.L. Gorbaty, P.S. Maa, and R.H. Schlosberg, "Studies on the Organic Structure of Coals", Stanford Res. Inst. Workshop on Coal Chem., Paper No. 12 (1976), and Fuel, 54, 295 (1975).
- Antal, M.J., E.G. Plett, T.P. Chung, and M. Summerfield, "Recent Progress in Kinetic Models for Coal Pyrolysis", Am. Chem. Soc. Div. of Fuel Chem. Preprints 22, No. 1, 137 (1977).
- Anthony, D.B., "Rapid Devolatilization and Hydrogasification of Pulverized Coal," Sc.D. thesis, Massachusetts Institute of Technology, Cambridge, Mass., 1974.
- Anthony, D.B., J.B. Howard, H.P. Meissner, and H.C. Hottel, "Apparatus for Determining High Pressure Coal-Hydrogen Reaction Kinetics under Rapid Heating Conditions," Rev. Sci. Instrum. 45, 992 (1974).
- Anthony, D.B., J.B. Howard, H.C. Hottel, and H.P. Meissner, "Rapid Devolatilization of Pulverized Coal," Fifteenth Symposium (International) on Combustion, p. 1303, The Combustion Institute, Pittsburgh, Pa. (1975).
- Anthony, D.B., J.B. Howard, H.C. Hottel, and H.P. Meissner, "Rapid Devolatilization and Hydrogasification of Bituminous Coal," Fuel 55, 121 (1976).
- Anthony, D.B. and J.B. Howard, "Coal Devolatilization and Hydrogasification," A.I.Ch.E. J. 22, 625 (1976).
- ASTM, "Standards on Coal and Coke", 1974 Annual Book of ASTM Standards, American Society for Testing and Materials, Philadelphia, Pa. (1974).
- Attar, A., and W.H. Corcoran, "Sulfur Compounds in Coal", I & EC Product R & D, 16 (2), 168 (1977).
- Badzioch, S., "Rapid and Controlled Decomposition of Coal," Brit. Coal Util. Res. Assn. Monthly Bulletin, 25, (8) 285 (1961).
- Badzioch, S., "Thermal Decomposition", BCURA Monthly Bulletin, 31, (4), 193 (1967).
- Badzioch, S., and P.G.W. Hawksley, "Kinetics of Thermal Decomposition of Pulverized Coal Particles," Ind. Eng. Chem. Process Design Develop. 9, 521 (1970).
- Banerjee, N.N., G.S. Murty, H.S. Rao, and A. Lahiri, "Flash Pyrolysis of Coal", Fuel, 52, 168 (1973).
- Bartuska, V.J., G.E. Maciel, J. Schaefer and E.O. Stejskal, "<sup>13</sup>C NMR Studies of Solid Coal Samples", Stanford Res. Inst. Workshop on Coal, Paper No. 17 (1976).

References (continued)

- Beimann, W. and H.S. Auvil, D.C. Coleman, "High Temperature Carbonization", in Chemistry of Coal Utilization, Supp. vol., H.H. Lowry, Ed., J. Wiley and Sons, New York, (1963).
- Belt, R.J., and M.M. Roder, "Low-Sulfur Fuel by Pressurized Entrainment Carbonization of Coal," Am. Chem. Soc., Div. of Fuel Chem. Preprints 17, No. 2, 82, August 1972.
- Belt, R.J., J.S. Wilson and J.J.S. Sebastian, "Continuous Rapid Carbonization of Powdered Coal by Entrainment, and Response Surface Analysis of Data," Fuel, 50 381 (1971).
- Benson, S.W., Thermochemical Kinetics, John Wiley and Sons, New York (1968).
- Benson, S.W., and H.E. O'Neal, Kinetic Data on Gas Phase Unimolecular Reactions, Natl. Bureau of Stds., NSRDS-NBS 21, Washington (1970).
- Bent, R., W.K. Joy, and W.R. Ladner, "An Estimate of the Methyl Groups in Coals and Coal Derivatives", Fuel, 43,5 (1964).
- Berkowitz, N., "Mechanism of Coal Pyrolysis, I," Fuel, 39, 47 (1960).
- Berkowitz, N., and W. Den Hertog, "Mechanisms of Coal Pyrolysis, V", Fuel, 41, 507 (1962).
- Bevington, P.R., Data Reduction and Error Analysis for the Physical Sciences," McGraw-Hill, New York (1969).
- Bhaumik, J.N., A.K. Mukherjee, P.N. Mukherjee, and A. Lahiri, "Ether Oxygen in Coal", Fuel, 41, 443 (1962).
- Birch, R.J., "Hydrogasification of Brown Coal, Parts 1 and 2," Div. of Chemical Engineering, C.S.R.I.O., Australia, Report No. CE/R25 (1969).
- Birch, T.J., K.R. Hall and R.W. Urie, "Gasification of Brown Coal with Hydrogen in a Continuous Fluidized-bed Reactor," J. Inst. Fuel, 33, 422 (1960).
- Bishop, M., and D.L. Ward, "The Direct Determination of Mineral Matter in Coal", Fuel 37, 191 (1958).
- Blackwood, J.D., "The Kinetics of the System Carbon-Hydrogen-Methane," Australian J. Chem., 15, 397, (1962).
- Blair, D.W., J.L. Wendt, and W. Bartok, "Evolution of Nitrogen and Other Species during Controlled Pyrolysis of Coal", Sixteenth Symposium (International) on Combustion, The Combustion Institute, Pittsburgh, Pa. (1977).
- Blayden, H.E., J. Gibson, and H.L. Riley, "An X-ray Study of the Structures of Coals, Cokes, and Chars", Proceedings of the Conf. on the Ultrafine Structures of Coals and Cokes, BCURA, London, 176, (1943).

References (continued)

- Bond, R.L., W.R. Ladner, and G.I.T. McConnell, "Reaction of Coals under Conditions of High Energy Input and High Temperatures", in Coal Science, p. 650, Advances in Chem. Series No. 55, Am. Chem. Soc., Washington, D.C. (1966).
- Bond, R.L., W.R. Ladner and R. Wheatley, "ESR of Rapidly Heated Coals," Fuel, 47, 213 (1968).
- Boyer, A.F., R. Ferrand, A. Ladam, and P. Payen, Chimie et Industrie, 86, 523 (1961).
- Brooks, J.D. and J.F. Stephens, "A Test of Diamond's Method for Estimating Size Distributions of Aromatic Ring Systems", Carbon, 2, 379 (1965).
- Brown, H.R. and P.L. Waters, "The Function of Solvent Extraction Products in the Coking Process - I", Fuel, 45, 17 (1966).
- Brown, J.K., "The Infrared Spectra of Coals", J. Chem. Soc. London, 744 (1955).
- Brown, J.K., "Infrared Studies of Carbonized Coals", J. Chem. Soc. London, 752 (1955a).
- Brown, J.K. and P.B. Hirsch, "Recent Infrared and X-ray Studies of Coal", Nature, 175, 229 (1955).
- Brown, J.K., W.R. Ladner, and N. Sheppard, "Hydrogen Distribution in Coal-Like Materials by High Resolution NMR Spectroscopy", Fuel, 39, 79 (1960).
- Brown, J.K., and W.R. Ladner, "Hydrogen Distribution in Coal-Like Materials by High Resolution NMR Spectroscopy", Fuel, 39, 87 (1960).
- Campbell, J.H. and D.R. Stephens, "Kinetic Studies of Gas Evolution during Pyrolysis of Subbituminous Coal", Am. Chem. Soc. Div. Fuel Preprints, 21, No. 7, 94 (1976).
- Cartz, L., and P.B. Hirsch, "The Structure of Coals from X-ray Diffraction Studies", Phil. Trans. Roy. Soc. London, 252A, No. 1019, 557 (1960).
- Chakrabartty, S.K. and N. Berkowitz, "Studies on the Structure of Coals", Fuel, 53, 240 (1974).
- Chakrabartty, S.K. and H.O. Kretschmer, "Studies on the Structure of Coals", Fuel, 51, 160 (1972), and Fuel, 53, 132 (1974).
- Chakrabartty, S.K., B.R. Mazumdar, S.N. Roy, and A. Lahiri, "Strukturparameter von Kohle auf Grund von Oxydationsversuchen", Brennstoff-Chemie, 41, 138 (1960).
- Chauhan, S.P., H.F. Feldmann, E.P. Stambaugh, and J.H. Oxley, "A Novel Approach to Gasification of Coal Using Chemically Incorporated Catalysts", Am. Chem. Soc. Div. Fuel Chem. Preprints, 22, No. 1, 38 (1977).

References (continued)

- Cheong, P.H., "A Modelling Study of Coal Pyrolysis", Ph.D. thesis, Dept. of Chemical Engineering, California Institute of Technology, Pasadena (1977).
- Cheong, P.H., M. Oka, and G.R. Gavalas, "Modelling and Experimental Studies of Coal Pyrolysis", NSF Workshop on Fundamental Organic Chemistry of Coal, Knoxville, TN (July, 1975).
- Chermin, H.A.G. and D.W. Van Krevelen, "A Mathematical Model of Coal Pyrolysis", Fuel, 36, 85 (1957).
- Chukhanov, Z.F., Izvest. Akad. Nauk S.S.S.R., Otdel. Tekh. Nauk, No. 8, pp. 7-22 (1954); Chem. Abs. 49, 5808 (1955).
- Coates, R.L., C.L. Chen, and B.J. Pope "Coal Devolatilization in a Low Pressure, Low Residence Time Entrained Flow Reactor", in Coal Gasification, Advances in Chem. Series No. 131, Am. Chem. Soc., Washington, D.C. (1974).
- Corrales, J.A., and D.W. Van Krevelen, "Thermogravimetric Studies of Coal and Model Substances", J. Inst. Fuel, 33, 10 (1960).
- Czuchajowski, L., "Infrared Spectra of Carbonized Coals and Coal-Like Materials", Fuel, 40, 361 (1961).
- Dainton, F.S. and K.J. Ivin, "The Phenomenon of a Ceiling Temperature", Nature, 162, 705 (1948).
- Davis, A., "The Petrographic Composition of Coals: Its Importance in Liquefaction Processes", Stanford Res. Inst. Workshop on Coal Chem., Paper No. 2 (Aug., 1976).
- Davis, J.D. and P.B. Place, "Thermal Reactions of Coal During Carbonization", Ind. Eng. Chem., 16, (6), 589 (1924).
- Dent, F.J. "The Production of Gaseous Hydrocarbons by the Hydrogenation of Coal," Gas J., 244, 502 (1944).
- Depp, E.A., C.M. Stevens, M.B. Neuworth, "Pyrolysis of Bituminous Coal Models", Fuel, 35, 437 (1957).
- Diamond, R., "X-ray Studies of Some Carbonized Coals", Phil. Trans. Roy. Soc. London, 252A, No. 1008, 193 (1960).
- Dobner, S., and R.A. Graff, and A.M. Squires, "Flash Hydrogenation of Coal-2", Fuel, 55, 113 (1976).
- Dryden, I.G.C., "Chemical Constitution and Reactions of Coal," in Chemistry of Coal Utilization Supplementary Volume, H.H. Lowry, Editor, J. Wiley and Sons, New York (1963).
- Dryden, I.G.C., "Chemistry of Coal and its Relation to Coal Carbonization," J. Inst. Fuel, 30, 193, (1957).
- Dryden, I.G.C., and K.S. Pankhurst, "Plastic Softening of Coking Coals on Heating", Fuel, 34, 363 (1955).

References (continued)

- Eddinger, R.T., L.D. Friedman and E. Rau, "Devolatilization of Coal in a Transport Reactor," Fuel, 45, 245 (1966).
- Essenhigh, R.H., "The Influence of Coal Rank on the Burning Times of Single Captive Particles," J. Eng. Power, 85, 183 (1963).
- Essenhigh, R.H., and J.B. Howard, Combustion Phenomena in Coal Dusts and the Two Component Hypothesis of Coal Constitution, Penn State Studies No. 31, The Pennsylvania State University, University Park (1971).
- Fallon, P. and M. Steinberg, "Flash Hydrolysis of Coal", paper presented at the 173rd National Meeting, Am. Chem. Soc., New Orleans, La. (March, 1977).
- Farcasiu, M., J.O. Mitchell, and D.D. Whitehurst, "On the Kinetics and Mechanisms of Solvent Refining Coals", Stanford Res. Inst., Workshop on Coal Chem., Paper No. 8 (Aug., 1976).
- Feldkirchner, H.L., and J.L. Johnson, "High-Pressure Thermobalance," Rev. Sci. Instr., 39, 1227 (1968).
- Feldkirchner, H.L., and H.R. Linden, "Reactivity of Coals in High-Pressure Gasification," Ind. Eng. Chem. Process Design Develop., 2, 153 (1963).
- Feldkirchner, H.L., and J. Huebler, "Reaction of Coal with Steam-Hydrogen Mixtures at High Temperatures and Pressures," Ind. Eng. Chem. Process Design Develop., 4, 134 (1965).
- Feldmann, H.F., W.H. Simons, J.A. Mimm and R.W. Hiteshue, "Reaction Model for Bituminous Coal Hydrogasification in a Dilute Phase," Am. Chem. Soc., Div. of Fuel Chem. Preprints 14, No. 4, 1, Sept. (1970).
- Fitzgerald, D., "The Kinetics of Coal Carbonization in the Plastic State", Trans. Faraday Soc., 52, 362 (1956) and Fuel, 35, 178 (1956a).
- Fitzgerald, D. and D.W. Van Krevelen, "The Kinetics of Coal Carbonization," Fuel, 38, 17 (1959).
- Francis, W., Coal, 2nd edition, Arnold, London (1961).
- Franz, J.A., J.R. Morrey, J.A. Campbell, G.L. Tingey, R.J. Pugmire, D.M. Grant, "Inferences on the Structure of Coal", Am. Chem. Soc. Div. Fuel Chem. Preprints, 20, No. 3, 12 (1975).
- Friedman, L.D., E. Rau and R.T. Eddinger, "Maximizing Tar Yields in Transport Reactors", Fuel, 47, 149 (1968).
- Friedman, L.D., "Development of a Fluidized Bench-Scale Reactor for Kinetic Studies", Am. Chem. Soc. Div. Fuel Chem. Preprints, 20(3), 34 (1975).
- Fuchs, W., and A.G. Sandhoff, "Theory of Coal Pyrolysis," Ind. Eng. Chem., 34, 567 (1942).



References (continued)

- Fuoss, R.M., I.O. Salyer and H.S. Wilson, "Evaluation of Rate Constants from Thermogravimetric Data", J. Polymer Sci., A-2, 3147 (1964).
- Gan, H., S.P. Nandi, and P.L. Walker, Jr., "Nature of the Porosity in American Coals", Fuel 51, 272 (1972).
- Gardner, N., E. Samuels, and K. Wilks, "Catalyzed Hydrogasification of Coal Chars", in Coal Gasification, p. 217, Advances in Chem. Series, No. 131, Am. Chem. Society, Washington, D.C. (1974).
- Gavalas, G., Personal Communication, 1977.
- Ghosh, F., A. Banerjee, and B.K. Mazumdar, "Skeletal Structure of Coal", Fuel, 54, 297 (1975).
- Given, P.H., "The Distribution of Hydrogen in Coals and its Relation to Coal Structure," Fuel, 39, 147 (1960).
- Given, P.H., "Dehydrogenation of Coals and its Relation to Coal Structure," Fuel, 40, 427 (1961).
- Given, P.H., "The Organic Chemistry of Coal Macerals," Penn State Short Course on Coal, The Pennsylvania State University, June (1976).
- Given, P.H., D.C. Cronauer, W. Spackman, A.L. Lovell, A. Davis, and B. Biswas, "Dependence of Coal Liquefaction Behavior on Coal Characteristics", Fuel 54, 34 (1975).
- Given, P.H., J.R. Jones and T.S. Polansky, "Some Aspects of the Chemistry of Sulfur in Relation to its Presence in Coal", Report submitted to the Coal Research Board, Commonwealth of Pennsylvania (August 1963).
- Given, P.H., M.E. Peover, and W.F. Wyss, "Chemical Properties of Coal Macerals - I", Fuel, 39 323 (1960).
- Glenn, R.A., E.E. Donath and R.J. Grace, "Gasification of Coal under Conditions Simulating Stage 2 of the BCR two-stage Super Pressure Gasifier," Advan. Chem. Ser., 69, 253 (1967).
- Grassie, N., Chemistry of High Polymer Degradation Processes, Butterworths, London (1956).
- Gray, D., J.G. Cogoli and R.H. Essenhigh, "Problems in Pulverized Coal and Char Combustion," Am. Chem. Soc., Div. of Fuel Chem. Preprints 18, No. 1, 135, April 1973.
- Gregory, D.R. and R.F. Littlejohn, "A Survey of Numerical Data on the Thermal Decomposition of Coal," BCURA Monthly Bulletin, 29 (6), 173 (1965).
- Griffiths, D.M.L. and J.S.R. Mainhood, "The Cracking of Tar Vapor and Aromatic Compounds on Activated Carbon", Fuel, 46, 167 (1967).
- Hamrin, C.E., Jr., P.S. Maa, and C.R. Lewis, "Measurement of Inhibition Isotherms of Kentucky Coal", Institute for Mining and Minerals Research, College of Engineering, U. of Ky., Project No. 4, Annual Report (Oct, 1973).

References (continued)

- Hanbaba, P., H. Juntgen, and W. Peters, "Nicht-isotherme Reaktionskinetik der Kohlenpyrolyse, Teil II: Erweiterung der Theorie der Gasabspaltung und experimentelle Bestätigung an Steinkohlen," Brennstoff-Chem., 49, 368 (1968).
- Heredy, L.W. and M.B. Neuwirth, "Low-Temperature Depolymerization of Bituminous Coal", Fuel, 41, 221 (1962).
- Heredy, L.A., A.E. Kostyo, and M.B. Neuwirth, "Identification of Isopropyl Groups on Aromatic Structures in Bituminous Coal", Fuel, 42, 182 (1963) and "Chemical Identification of Methylene Bridges in Bituminous Coal", Fuel, 43, 414 (1964) and "Studies on the Structures of Coals of Different Rank", Fuel, 44, 125 (1965).
- Heredy, L.A., A.E. Kostyo, and M.B. Neuwirth, "Studies on the Structure of Coals of Different Rank", in Coal Science, p. 493, Advances in Chem. Series, Am. Chem. Society, Washington, D.C. (1966).
- Hill, G.R. and L.B. Lyon, "A New Chemical Structure for Coal", Ind. Eng. Chem., 54, 36 (1962).
- Hirsch, P.B., "X-ray Scattering from Coals", Proc. Roy. Soc. London, A226, 143 (1954).
- Hiteshue, R.W., S. Friedman and R. Madden, "Hydrogenation of Coal to Gaseous Hydrocarbons," RI 6027, Bureau of Mines, Dept. of Interior (1962a).
- Hiteshue, R.W., S. Friedman and R. Madden, "Hydrogasification of Bituminous Coals, Lignite, Anthracite, and Char," RI 6125, Bureau of Mines, Dept. of Interior (1962b).
- Hiteshue, R.W., S. Friedman and R. Madden, "Hydrogasification of High-Volatile A Bituminous Coal," RI 6376, Bureau of Mines, Dept. of Interior (1964).
- Homann, K.H., Discussion Comment to presentation of H. Jinno et al., Sixteenth Symposium (International) on Combustion, Cambridge, Mass. (Aug. 1976).
- Howard, H.C., "Pyrolytic Reactions of Coal", in Chemistry of Coal Utilization, Suppl. vol., H.H. Lowry, Editor J. Wiley and Sons, New York (1963).
- Howard, J.B., "Fundamentals of Coal Pyrolysis", in preparation (1977).
- Howard, J.B. and R.H. Essenhigh, "Pyrolysis of Coal Particles in Pulverized Fuel Flames," Ind. Eng. Chem. Process Design Develop., 6, 74 (1967).
- Huston, J.L., R.G. Scott, and M.H. Studier, "Reaction of Fluorine Gas with Coal and the Aromaticity of Coal", Fuel, 55, 281 (1976).
- James, R.R. and A.F. Mills, "Analysis of Coal Particle Pyrolysis", unpublished manuscript, University of California at Los Angeles, Dept. of Chemical Engineering (1976).

- Johnson, J.L., "Means of Relating Coal Characteristics to Chemical Engineering Data," Seminar on Characterization and Characteristics of U.S. Coals for Practical Use, Penn. State Univ., Univ. Park, Penn., October 25-28, 1971.
- Johnson, J.L., "Kinetics of Bituminous Coal Char Gasification with Gases Containing Steam and Hydrogen," Am. Chem. Soc., Div. of Fuel Chem. Preprints 18, No. 1, 228, April 1973.
- Johnson, J.L., "Gasification of Montana Lignite in Hydrogen and Helium During Initial Reaction Stages", Am. Chem. Soc. Div. of Fuel Chem. Preprints, 20 (3) 61 (1975).
- Johnson, J.L., "Relationship Between the Gasification Reactivities of Coal Char and the Physical and Chemical Properties of Coal and Char", Am. Chem. Soc. Div. of Fuel Chem. Preprints 20 (4), 85 (1975).
- Johnson, J.L., "Kinetics of Initial Coal Hydrogasification Stages", Am. Chem. Soc. Div. of Fuel Chem. Preprints, 22 (1), 17 (1977).
- Jones, J.F., M.R. Schmid and R.T. Eddinger, "Fluidized Bed Pyrolysis of Coal," Chem. Eng. Progr., 60 (6), 69 (1964).
- Jones, W.I., "The Thermal Decomposition of Coal," J. Inst. Fuel, 37 (3) (1964).
- Jüntgen, H., and K.H. Van Heek, "Gas Release from Coal as a Function of the Rate of Heating," Fuel, 47, 103 (1968).
- Jüntgen, H. and K.H. Van Heek, "Reaktionabläufe unter nicht-isothermen Bedingungen," "Fortshritte der chemischen Forshung," Vol. 13, 601-699, Springer-Verlag, Berlin, 1970, translated by Belov and Assoc., Denver, Colorado, APTIC-TR-0776.
- Jüntgen, H. and K.H. Van Heek, "Fortschritte der Forshung auf dem Gebiet der Steinkohlenpyrolyse," Brennstoff-Chemie, 50, 172 (1969).
- Jüntgen, H. and K.H. Van Heek, "Research in the Field of Pyrolysis at Bergbau Forschung during the last Fifteen Years,: Paper presented at the Meeting on Coal Fundamentals, Stoke Orchard, England (Jan., 1977).
- Kawa, W.R., W. Hiteshue, W.A. Budd, S. Friedman, and R.B. Anderson, "Agglomerating Studies in the Low-Pressure Hydrogenation of Coal in a Fluidized Bed," U.S. Bureau of Mines, Bulletin 579 (1959).
- Kessler, M.F., "Interpretation of the Chemical Composition of Bituminous Coal Macerals," Fuel, 52, 191 (1973).
- Khemchandani, G.V., R.B. Ray, and S. Sarkar, "Studies on Artificial Coal," Fuel, 53, 163 (1974).
- Khemchandani, G.V. and S. Sarkar, "Studies on Artificial Coal," Fuel, 55, 303 (1976).

- Kimber, G.M. and M.D. Gray, "Rapid Devolatilization of Small Coal Particles," Combust. Flame, 11, 360 (1967a).
- Kimber, G.M. and M.D. Gray, "Measurements of Thermal Decomposition of Low and High Rank Non-Swelling Coals at MHD Temperatures," BCURA Document No. MHD 32, (January 1967b).
- Kobayashi, H., "Devolatilization of Pulverized Coal at High Temperatures," Sc.D. Thesis, Department of Mechanical Engineering, Massachusetts Institute of Technology, Cambridge, Mass., 1976.
- Kobayashi, H., J.B. Howard, and A.F. Sarofim, Sixteenth Symposium (International) on Combustion, The Combustion Institute, Pittsburgh, Pa. (1977).
- Koch, V., H. Jüntgen, and W. Peters, "Nicht-Isotherme Reaktionskinetik der Kohlenpyrolyse, Teil III: Zum Reaktionsablauf bei hohen Aufheizgeschwindigkeiten," Brennstoff - Chem., 50, 369 (1969).
- Krausz, A.S. and H. Eyring, Deformation Kinetics, Wiley and Sons, Inc., New York (1975).
- Kröger, C. and A. Pohl, Brennstoff-Chem., 38, 102-7 (1957).
- Krukonis, V.J., R.E. Gannon, and M. Modell, "Deuterium and Carbon-13 Tagging Studies of the Plasma Pyrolysis of Coal," Am. Chem. Soc. Div. of Fuel Chem. Preprints, 18 (1), 1973.
- Ladner, W.R. and A.E. Stacey, "A Proton Magnetic Resonance Study of Coals and Some Soluble Fractions of Coals," Fuel, 40, 295 (1961).
- Ladner, W.R. and A.E. Stacey, "The Hydrogen Distribution in Macerals," Fuel, 42, 75 (1963).
- Ladner, W.R. and A.E. Stacey, "An Analysis of Line Shapes of the Hydrogen Magnetic Resonance Spectra of Coals," Fuel, 43, 13 (1964).
- Ladner, W.R. and A.E. Stacey, "Broad-line NMR Measurements of Carbonized Coals," Fuel, 44, 71 (1965).
- Landolt, R.G., Fuel, 54, 299 (1975).
- Lau, E.K.L., "The Effect of Water Quenching on the Composition of Coal Volatiles," S.M. Thesis, M.I.T., Cambridge, Mass. (June, 1977).
- Leftin, H.P. and A. Cortes, "High Severity Pyrolysis of Olefins - 1. Isobutene," Ind. Eng. Chem. Process Des. Dev., 11, 4, 613 (1972).
- Lewellen, P.C., "Product Decomposition Effects in Coal Pyrolysis," S.M. Thesis, Dept. of Chemical Engineering, M.I.T., Cambridge, Mass. (1975).
- Lewellen, P.C., W.A. Peters, and J.B. Howard, "Kinetics of Cellulose Pyrolysis and Char Formation Mechanism," Sixteenth Symposium (International) on Combustion, The Combustion Institute, Pittsburgh, Pa. (1977).

- Loison, R. and F. Chauvin, "Pyrolyse Rapide Du Charbon," Chem. Ind. (Paris) 91, 269 (1964).
- Lowry, H.H. (Ed.) The Chemistry of Coal Utilization, (Vols. 1 & 2), John Wiley and Sons, Inc., New York (1945).
- Lowry, H.H. (Ed.) The Chemistry of Coal Utilization (Supplementary Volume), John Wiley and Sons, Inc., New York (1963).
- Maa, P.S., C.R. Lewis, and C.E. Hamrin, Jr., "Sulphur Transformations and Removal for Western Kentucky Coals," Fuel, 54, 62 (1975).
- Madorsky, S.L., "Rates of Thermal Degradation of Polystyrene and Polyethylene in a Vacuum," J. Polymer Science 9 (2), 133 (1952).
- Madorsky, S.L., "Rates and Activation Energies of Thermal Degradation of Styrene and Acrylate Polymers in a Vacuum," J. Polymer Science 11(5), 491 (1953).
- Madorsky, S.L., Thermal Degradation of Organic Polymers, Interscience, New York (1964).
- Maher, T.P. and H.N.S. Schafer, "Determination of Acidic Functional Groups in Low-Rank Coals," Fuel, 55, 138 (1976).
- Marsh, H. and H.P. Stadler, "A Review of Structural Studies of the Carbonization of Coals," Fuel, 46, 351 (1967).
- Martin, S., Tenth Symposium (International) on Combustion, The Combustion Institute, p. 877, Pittsburgh (1965).
- Mayo, F.R., "Application of Sodium Hypochlorite Oxidations to the Structure of Coal," Fuel, 54, 273 (1975).
- Mayo, F.R., J. Huntington, and N. Kirshen, "Oxidations of Coal, Coal Fractions and Coal Models," Stanford Res. Inst. Workshop on Coal Chem., Paper No. 14 (Aug., 1976).
- Mazumdar, B.K., Fuel, 43, 78 (1964).
- Mazumdar, B.K., S.K. Chakrabartty and A. Lahiri, "Some Aspects of the Constitution of Coal," Fuel, 41, 129 (1962).
- Mazumdar, B.K., S.K. Ganguly, P.K. Sanyal, and A. Lahiri, "Aliphatic Structures in Coal," in Coal Science, p. 475, Advances in Chemistry Series, 55, Am. Chem. Soc., Washington, D.C. (1966).
- Mazumdar, B.K., "Hydrogen in Coal," Fuel, 51, 284 (1972).
- Mazumdar, B.K. and N.N. Chatterjee, "Mechanism of Coal Pyrolysis in Relation to Industrial Practice," Fuel, 52, 11 (1973).

- Mentser, M., H.J. O'Donnell, S. Ergun, and R.A. Friedel, "Devolatilization of Coal by Rapid Heating," Am. Chem. Soc., Div. of Fuel Chem. Preprints 18, No. 1, 26, April 1973.
- Mentser, M., J.J. O'Donnell and S. Ergun, "Rapid Thermal Decomposition of Bituminous Coals," Am. Chem. Soc., Div. of Fuel Chem. Preprints 14, No. 5, 94, Sept. 1970.
- Mills, A.F., R.K. James, and D. Antoniuk, "Analysis of Coal Particles Undergoing Rapid Pyrolysis," International Centre for Heat and Mass Transfer, 1975 International Seminar, Dubrovnik (Aug., 1975).
- Moseley, F. and D. Paterson, "Rapid High-Temperature Hydrogenation of Coal Chars, Part 1," J. Inst. Fuel, 38, 13 (1965a).
- Moseley, F. and D. Paterson, "Rapid High-Temperature Hydrogenation of Coal Chars, Part 2," J. Inst. Fuel, 38, 378 (1965b).
- Moseley, F. and D. Paterson, "Rapid High-Temperature High-Pressure Hydrogenation of Bituminous Coal," J. Inst. Fuel, 40, 523 (1967).
- Neavel, R.C., "Coal Plasticity Mechanism: Inferences from Liquefaction Studies," Paper presented at Symposium on Plasticity and Agglomeration of Coal, Morgantown, W. Va. (May, 1975).
- Nsakala, N., R.H. Essenhig, and P.L. Walker, Jr., "Characteristics of Chars Produced by Pyrolysis Following Rapid Heating of Pulverized Coal," Am. Chem. Soc. Div. Fuel Chem. Preprints, 22, No. 1, 102 (1977).
- Oblad, A., personal communication (July, 1977).
- Ode, W.H., "Coal Analysis and Mineral Matter," in The Chemistry of Coal Utilization (Supplementary Volume), Lowry, Ed., Wiley and Sons, Inc., New York (1963).
- Oelert, H.H., "Chemical Characteristics of the Thermal Decomposition of Bituminous Coals," Fuel, 47, 433 (1968).
- Oka, M., H.C. Chang, and G.R. Gavalas, "Computer-Assisted Molecular Structure Construction for Coal-Derived Compounds," Fuel, 56, 3 (1976).
- Padia, A.S., "The Behavior of Ash in Pulverized Coal Under Simulated Combustion Conditions," Sc.D. Thesis, M.I.T., Cambridge, Mass. (Jan., 1976).
- Parks, B.C., "Origin, Petrography, and Classification of Coal," in Chemistry of Coal Utilization (Supplementary Volume), Lowry, Ed., Wiley and Sons, Inc., New York (1963).
- Pauling, L., The Nature of the Chemical Bond, Cornell U. Press, Ithaca, New York (1960).
- Penninger, J.M.L. and H.W. Slotloom, "Kinetics and Mechanism of Primary Cracking Reactions in High Pressure Hydrogenolysis of Tetralin and Indin," Rec. Tran. Chim. Pays-Bas., 92, 513 (1973).

- Penninger, J.M.L. and H.W. Slotloom, "Consecutive Reactions in the Thermal High Pressure Hydrogenalysis of Tetralin and Indan," Rec. Trav. Chim. Pays-Bas., 92, 1089 (1973).
- Penninger, J.M.L. and H.W. Slotloom, "Reactions of Phenanthrene and Anthracene in Thermal High Pressure Hydrogenalysis," Erdöl und Kohle, 26, 444 (1973).
- Peters, W. "Stoff-und Wärmeübergang bei der Schenllentgasung feinkorniger Brennstoffe," Chem. Ing. Tech., 32, 178 (1960).
- Peters, W. and H. Bertling, "Kinetics of the Rapid Degasification of Coals," Fuel, 44, 317 (1965).
- Pines, A., M.G. Gibby, and J.S. Waugh, J. Chem. Phys., 59, 569 (1973).
- Pitt, G.J., "The Kinetics of the Evolution of Volatile Products from Coal," Fuel, 41, 267 (1962).
- Pohl, J.H., "Fate of Coal Nitrogen," Sc.D. Thesis, Dept. of Chemical Engineering, M.I.T., Cambridge, Mass. (1976).
- Portal, C. and H. Tan, "The Effect of Heating Rate on the Devolatilization of Coal," unpublished joint 10.90 report and S.B. Thesis, Dept. of Chemical Engineering, M.I.T., Cambridge, Mass. (1974).
- Pyrcioch, E.J., H.L. Feldkirchner, C.L. Tsaros, J.L. Johnson, W.G. Blair, B.S. Lee, F.C. Schora, Jr., J. Huebler, and H.R. Linden, "Production of Pipeline Gas by Hydrogasification of Coal," Research Bulletin No. 39, Vol. 1, Institute of Gas Technology, Chicago (Dec., 1972).
- Rau, E. and J.A. Robertson, "The Use of the Microsample Strip Furnace in Coal Research," Fuel, 45, 73 (1966).
- Reggel, L, I. Wender, and R. Raymond, "Catalytic Dehydrogenation of Coal II," Fuel, 47, 373 (1968).
- Reidelbach, H. and M. Summerfield, "Kinetic Model for Coal Pyrolysis Optimization," Am. Chem. Soc., Div. Fuel Chem. Preprints, 20 (1), 161 (1975).
- Rennhack, R., "Zur Kinetik der Entgasung von Schwelkoks," Brennstoff-Chemie 45, 300 (1964).
- Sass, A., "The Garrett Research and Development Process for the Conversion of Coal into Liquid Fuels," Paper presented at the 65th Annual AIChE Meeting, New York (Nov. 30, 1972).
- Shapatina, E.A., V.V. Kalyuzhnyi, and Z.F. Chukhanov, "Technological Utilization of Fuel for Energy, 1-Thermal Treatment of Fuels," (1960), [Reviewed by Badzioch, S., British Coal Utilization Research Association Monthly Bulletin, 25, 285 (1961)].
- Skyilar, M.G., V.I. Shustikov, and I.V. Virozub, "Investigation of the Kinetics of Thermal Decomposition of Coals," Intern. Chem. Eng., 9, 595 (1969).

- Smith, I.W. and P.C. Wailes, "Oil from Coal by Flash Pyrolysis," paper No. 3 in Energy and Liquid Fuels, joint organizers Institute of Fuel, Royal Australian Chemical Institute, and Institution of Chemical Engineers, Adelaide, Australia (1975).
- Solomon, P.R., personal communication (1976).
- Solomon, P.R., "The Evolution of Pollutants during the Rapid Devolatilization of Coal," Report No. R77-952588-2 (N.S.F. Grant No. AER 75-17247, monitored by Fossil Energy Div., ERDA), United Technologies Research Center, East Hartford, Conn. (Apr., 1977).
- Speight, J.G., "The Application of Spectroscopic Techniques to the Structural Analysis of Coal and Petroleum," Applied Spectroscopy Reviews, 5 (2), 211 (1971).
- Squires, A.M., "Reaction Paths in Donor Solvent Coal Liquefaction," Paper presented at Conference on Coal Gasification/Liquefaction sponsored by U.S.-U.S.S.R. Trade and Economic Council, Inc., Moscow (Oct., 1976).
- Squires, A.M., R.A. Graff, and S. Dobner, "Flash Hydrogenation of a Bituminous Coal," Science, 189, 793 (1975).
- Steinberg, M. and P. Fallon, "Coal Liquefaction by Rapid Gas Phase Hydrogenation," Paper presented at the 68th Annual Meeting, AIChE, Los Angeles (Nov. 16-20, 1975).
- Sternberg, H.W., personal communication (1977).
- Stone, H.N., J.D. Batchelor, and H.F. Johnstone, "Low Temperature Carbonization Rates in a Fluidized Bed," Ind. Eng. Chem., 46, 274 (1954).
- Suuberg, E.M., W.A. Peters, and J.B. Howard, "Product Composition and Kinetics of Lignite Pyrolysis," Am. Chem. Soc., Div. of Fuel Chem. Preprints, 22, No. 1, 112 (1977).
- Sweeting, J.W. and J.F.K. Wilshire, "The Pyrolysis of  $\omega$ - $\omega'$ -Diphenylkanes," Aus. J. Chem., 15, 89 (1962).
- Tingey, G.L. and Morrey, J.R., "Coal Structure and Reactivity," Battelle Energy Report, Battelle Pacific Northwest Lab., Richland, Washington (1973).
- Tomita, A., O.P. Mahajan, and P.L. Walker, Jr., "Catalysis of Char Gasification by Minerals," Am. Chem. Soc., Div. Fuel Chem. Preprints, 22, No. 1, 4 (1977).
- Tschamler, H. and E. deRuiter, Brennstoff-Chemie, 44, 280 (1963) and 43, 16 (1962).
- Tschamler, H. and E. deRuiter, "A Comparative Study of Exinite, Vitrinite, and Micrinite," in Coal Science, p. 332, Advances in Chem. Series, 55, Am. Chem. Soc., Washington, D.C. (1966).



- Tschamler, H. and E. deRuiter, "Physical Properties of Coals," in Chemistry of Coal Utilization (Supplementary Volume), Lowry, Ed., Wiley and Sons, Inc., New York (1963).
- Ubhayaker, S.K., D.B. Stickler, C.W. von Rosenberg, Jr., and R.E. Gannon, "Rapid Devolatilization of Pulverized Coal in Hot Combustion Gases," Sixteenth Symposium (International) on Combustion, The Combustion Institute, Pittsburgh, Pa. (1977).
- Van Heek, K.H., H. Jüntgen, and W. Peters, "Kinetik nicht-isotherm ablaufender Reaktionen am Beispiel," Ber. Bunsenges. Physik Chemie 71, 113 (1967).
- Van der Hart, D.L. and H.L. Retrosky, "Analysis of the Aromatic Content of Whole Coals by High-Power Proton Decoupled C-13 NMR," Stanford Res. Inst. Workshop on Coal Chem., Paper No. 15 (Aug., 1976).
- Van Krevelen, D.W., Coal, Elsevier Publishing Co., Amsterdam (1961).
- Van Krevelen, D.W., C. Van Heerden, and F.J. Huntjens, "Physiochemical Aspects of the Pyrolysis of Coal and Related Organic Compounds," Fuel, 30, 253 (1951). [Numerical results modified by Jüntgen and Van Heek (1970)]
- Van Krevelen, D.W., F.J. Huntjens and H.N.M. Dormans, "Chemical Structure and Properties of Coal XVI--Plastic Behavior on Heating," Fuel, 35, 462 (1956).
- Van Krevelen, D.W., "Hydrogen Distribution in Coal," Fuel, 42, 427 (1963).
- Van Krevelen, D.W., The Properties of Polymers, 2nd Ed., Elsevier, New York (1976).
- Vestal, M.L., A.G. Day, J.S. Snyderman, G.J. Fergusson, F.W. Lampe, R.H. Essenhigh, and W.H. Johnston, "Kinetic Studies on the Pyrolysis, Desulfurization, and Gasification of Coals with Emphasis on the Non-Isothermal Kinetic Method," Revised Final Report, National Air Pollution Control Adm., Phase I, Contract No. PH 86-68-65 (N.T.I.S. No. PB-185-882) Scientific Research Instruments Corporation, Baltimore, Md. (1969).
- Virk, P.S., L.E. Chambers, and H.N. Woebcke, "Thermal Hydrogasification of Aromatic Compounds," in Coal Gasification, p. 237, Advances in Chemistry Series, No. 131, Am. Chem. Soc., Washington, D.C. (1974).
- Von Fredersdorff, C.G. and M.S. Elliott, "Coal Gasification" in Chemistry of Coal Utilization, (Supplementary Volume), H.H. Lowry Ed., Wiley and Sons, Inc., New York (1963).
- Weiler, J.F., "High Temperature Tars" in Chemistry of Coal Utilization, (Supplementary Volume), H.H. Lowry, Ed., Wiley and Sons, Inc., New York (1963).
- Wender, I., "Catalytic Synthesis of Chemicals from Coal," Am. Chem. Soc., Div. Fuel Chem. Preprints, 20, No. 4, 16 (1975).

- Winans, R.E., R. Hayatsu, R.G. Scott, L.P. Moore, M.H. Studier, "Examination and Comparison of Structure: Lignite, Bituminous, and Anthracite Coal," Stanford Res. Inst. Workshop on Coal Chem., paper No. 13, (August, 1976).
- Wiser, W.H., G.R. Hill, and N.S. Kertamus, "Kinetic Study of the Pyrolysis of a High-Volatile Bituminous Coal," I&EC Process Des. and Dev., 6 (1), 133 (1967).
- Wiser, W.H., "A Kinetic Comparison of Coal Pyrolysis and Dissolution," Fuel, 47, 475 (1968).
- Wiser, W.H., personal communication (July, 1977).
- Wolfs, P.M.J., D.W. Van Krevelen, and H.I. Waterman, "The Carbonization of Coal Models," Fuel, 39, 25 (1960) and Brennstoff-Chemie, 40 (1959).
- Wolk, R.H., N.C. Stewart, and H.F. Silver, "Review of Desulfurization and Denitrogenation in Coal Liquefaction," Am. Chem. Soc., Div. Fuel Chem. Preprints, 20 (2), 116 (1975).
- Worrall, J. and P.L. Walker, Special Report 16, Coal Research Board of Pennsylvania (1959).
- Yellow, P.C., "Kinetics of the Thermal Decomposition of Coal," British Coal Utilization Research Association Monthly Bulletin, 29 (9), 285 (1965).
- Yergey, A.L., F.W. Lampe, M.L. Vestal, A.G. Day, G.J. Fergusson, W.H. Johnston, J.S. Synderman, R.H. Essenhigh, and J.E. Hudson, "Nonisothermal Kinetic Studies of the Hydrodesulfurization of Coal," Ind. Eng. Chem., Process Des. Develop., 13, 233 (1974).
- Zahradnik, R.L. and R.A. Glenn, "Direct Methanation of Coal," Fuel, 50, 77 (1971).

## APPENDIX A -1

Location of Original Data

The original data for this thesis are in the possession of Professor Jack B. Howard of the Chemical Engineering Department, M.I.T.

A copy is in the possession of the author, at the Department of Chemical Engineering, Carnegie-Mellon University, Pittsburgh, Pennsylvania.

ACCEPTED LIGNITE RUNS  
"SHORT" RESIDENCE TIMEP = 20 psi He  
 $\frac{dT}{dt} = 1000^\circ\text{C}/\text{sec}$ 

Temp.	Run	Total	CO	CH <sub>4</sub>	CO <sub>2</sub>	C <sub>2</sub> H <sub>4</sub>	C <sub>2</sub> H <sub>6</sub>	C <sub>3</sub> H <sub>6</sub>	C <sub>3</sub> H <sub>8</sub>	HC	Tar	H <sub>2</sub> O
1106	11MVL	43.4	9.05	1.38	8.70	.76	.25	.34	.17	.51	4.53	17.7
1020	10MVL	41.1	6.95	1.31	8.63	.50	.18	.24	.12	.54	6.83	15.3
1018	15MVL	41.5	6.70	1.19	7.85	.52	.19	.25	.13	.38	5.87	17.9
1001	9MVL	44.2	7.53	1.38	8.71	.58	.19	.25	.13	.47	4.72	18.5
980	17MVL	44.0	7.93	1.35	8.66	.49	.18	.24	.14	.54	5.91	18.1
970	13MVL	40.2	6.86	1.40	8.12	.72	.16	.21	.11	.43	3.54	15.1
910	2MVL	39.1	8.01	1.18	8.55	.55	.13	.17	.05	.53	4.87	14.6
892	17ANL	40.5	6.63	1.17	8.26	.49	.15	.19	.06	.36	-	-
880	8MVL	40.5	5.98	1.23	8.95	.61	.23	.35	.12	.67	5.35	16.7
875	16MVL	40.6	5.77	1.12	7.68	.56	.12	.19	.10	.24	5.22	16.3
825	1MVL	39.0	6.42	1.04	8.42	.52	.20	.27	.09	.61	-	-
790	15ANL	34.6	2.94	.71	6.97	.20	.11	.11	.05	.24	-	-
770	12MVL	34.0	3.83	.88	7.43	.53	.17	.23	.11	.67	4.52	15.6
764	13ANL	(39.9)	2.94	.59	6.36	.27	.16	.19	.07	.43	-	-
710	15MVL	27.0	1.75	.30	5.46	.16	.08	.11	.05	.25	2.29	16.4
702	7MVL	27.6	1.88	.36	6.11	.14	.13	.13	.09	.26	5.05	13.5
662	5MVL	23.6	1.42	.31	5.26	.17	.15	.12	.10	.17	-	-
633	8ANL	(27.6)	2.01	.37	5.78	.13	.08	.11	.08	.03	-	-
532	3MVL	18.1	1.23	.26	3.50	.05	.06	.06	.06	0	2.55	10.3
520	10ANL	18.0	.57	.05	3.40	.02	.02	.02	.02	.07	-	-
430	6MVL	11.0	.46	.02	2.49	0	0	0	0	0	1.46	6.6
275	14ANL	6.8	0	0	.3	0	0	0	0	0	0	6.5
1153	LT6	43.2									5.48	-
924	LT2	40.1									7.14	-
840	LT9	37.7									4.82	-
825	LT3	38.1									5.70	-
675	LT5	33.5									3.97	-
175	23MVL	6.4									0	-
675	LT-8	24.7									4.38	-
652	LT-1	22.3									2.13	-
642	LT-4	26.5									2.67	-
463	LT-7	12.0									2.13	-

HYDROGEN DETERMINATIONS H<sub>2</sub> (P = 1 atm He)

T <sup>o</sup> C	Run	Total	H <sub>2</sub>
975	LHY-1	42.1	.51 %
991	LHY-3	39.4	.50
832	LHY-4	37.0	.20
553	LHY-5	17.8	<.04
630	LHY-6	22.0	<.04
820	LHY-9	34.9	.23
738	LHY-10	30.8	.06
810	LHY-11	33.4	.23
905	LHY-13	41.0	.48

LIGNITE LOW HEATING RATE  
( $< 500^{\circ}\text{C/s}$ ) P = 1 atm He

Temp.	Run	Total	CO <sub>2</sub>	CO	CH <sub>4</sub>	C <sub>2</sub> H <sub>4</sub>	C <sub>2</sub> H <sub>6</sub>	C <sub>3</sub> H <sub>6</sub>	C <sub>3</sub> H <sub>8</sub>	HC	H <sub>2</sub> O	Tar
837	LHR-5	42.3	9.19	5.15	1.11	.30	.17	.15	.10	.63	-	5.03
1014	LHR-6	45.2	8.52	6.54	1.47	.37	.22	.25	.10	.81	-	4.93
1034	LHR-7	46.4	8.82	7.30	1.16	.38	.17	.20	.08	.67	-	5.73
995	LHR-8	45.1	10.54	8.35	1.48	.59	.18	.33	.08	.91	-	5.13
975	LHR-9	45.1	9.00	5.75	1.14	.29	.15	.15	.08	.69	-	5.96
1020	LHR-10	43.2	9.82	5.09	1.33	.46	.17	.31	.21	.65	-	4.47
867	LHR-12	40.8	7.77	-	.94	.20	.16	.14	.07	.65	-	4.50
965	LHR-11	42.9	8.67	6.37	1.23	.37	.16	.24	.17	.73	-	3.20
733	LHR-13	32.9	7.05	-	.61	.23	.14	.14	.11	.52	-	5.43

HIGH HEATING RATE (7100-10,000<sup>o</sup>C/s) P = 1 atm He

Temp.	Run	Total	CO <sub>2</sub>	CO	CH <sub>4</sub>	C <sub>2</sub> H <sub>4</sub>	C <sub>2</sub> H <sub>6</sub>	C <sub>3</sub> H <sub>6</sub>	C <sub>3</sub> H <sub>8</sub>	HC	H <sub>2</sub> O	Tar
603	LHR-1	23.0	4.50	1.53	.26	.16	.06	.11	.05	.20	-	2.51
837	LHR-2	40.6	7.57	5.33	1.05	.60	.13	.38	.07	.90	-	5.75
895	LHR-3	41.7	8.13	4.71	1.16	.80	.17	.42	.08	.63	-	4.85
1105	LHR-4	44.7	8.57	8.88	1.38	.83	.25	.50	.13	.73	-	6.00

2-STEP HEATING (1000<sup>o</sup>C/s) P = 1 atm He

Temp.	Run	Total	CO <sub>2</sub>	CO	CH <sub>4</sub>	C <sub>2</sub> H <sub>4</sub>	C <sub>2</sub> H <sub>6</sub>	C <sub>3</sub> H <sub>6</sub>	C <sub>3</sub> H <sub>8</sub>	HC	H <sub>2</sub> O	Tar
478	L2S-1	12.1	1.32	.50	.02	.01	.01	-	-	.01	8.4	1.21
855	"	41.4	7.86	6.16	1.10	.48	.14	.18	.05	.65	15.7	5.55
671	L2S-2	25.6	5.12	1.71	.22	.15	.10	.09	.06	.42	14.9	3.81
1071	"	44.0	8.02	6.27	.93	.30	.17	.14	.09	.57	20.8	6.76

LIGNITE LONG RESIDENCE TIME P = 1 atm He

Temp.	t(s)	Run	Total	CO <sub>2</sub>	CO	CH <sub>4</sub>	C <sub>2</sub> H <sub>4</sub>	C <sub>2</sub> H <sub>6</sub>	C <sub>3</sub> H <sub>6</sub>	C <sub>3</sub> H <sub>8</sub>	HC	H <sub>2</sub> O	Tar	
925	6	19MVL	42.9	8.32	7.32	1.49	.52	.16	.27	.13	1.20	15.7	4.07	
975	3	6ANL	44.4	9.25	8.84	1.23	.42	.20	.38	.16	1.61	-	-	
1006	4	7ANL	45.6	9.79	9.79	1.34	.55	.24	.36	.18	1.88	-	-	
1000	9	20MVL	44.4	9.23	5.93	1.19	.56	.37	.44	.30	2.43	23.1	4.12	
945	10	21MVL	46.9	9.68	9.51	1.19	.54	.28	.40	.13	2.35	17.4	4.64	
1000	4	27MVL	44.4	9.08	8.92	1.45	.72	.14	← .55 →		1.67	14.9	(2.08)	
497	20	28MVL	24.0	4.88	0.78	0.10	0.03				0.24	→	10.5	2.74
485	24	29MVL	17.7	3.96	0.70	0.05	0.02				0.12	→	11.3	1.53
600	8	24MVL	25.1	5.80	1.97	0.24	0.10	0.06	0.12	0.12	0.29	13.7	2.93	
661	22	25MVL	37.1	7.88	2.65	0.82	0.22	0.16	0.23	0.19	0.47	18.2	4.39	
600	19	26MVL	31.3	7.00	2.28	0.51	0.16	0.12	0.20	0.13	0.42	8.1	2.40	

## LIGNITE VACUUM RUNS 1000°C/sec P=.05 mm Hg(He)

Temp.	Run	Total	CO <sub>2</sub>	CO	CH <sub>4</sub>	C <sub>2</sub> H <sub>4</sub>	C <sub>2</sub> H <sub>6</sub>	C <sub>3</sub> H <sub>6</sub>	C <sub>3</sub> H <sub>8</sub>	HC	HC Liq	Tar	H <sub>2</sub> O
707	LP-1	32.9	5.15	1.16	.44	-	.09	.13	.08	.15	-	3.37	18.1
800	LP-2	40.2	6.65	3.10	.72	.24	.16	.19	.09	.40	-	3.77	17.3
1020	LP-3	43.8	7.67	5.25	.86	.32	.18	.35	.18	.50	-	3.42	15.8
943	LP-4	45.2	7.60	5.82	.98	.53	.24	.39	.29	.85	-	5.67	18.2
825	LP-5	45.5	7.19	5.45	.92	.47	.29	.28	.06	1.75	-	4.71	16.4
1035	LP-6	45.0	7.68	-	.93	.62	.18	.18	.09	(.20)	-	3.88	(22.9)
1068	LP-7	47.1	7.73	7.99	1.03	.57	.22	.22	.10	.45	.94	-	19.8
895	LP-8	45.7	7.39	5.87	.92	.39	.19	.30	.20	.66	1.50	3.41	17.3
994	LP-9	43.5	7.92	6.88	1.02	.30	.26	.28	.19	.63	.63	3.65	18.9
905	LP-10	46.3	7.04	6.34	.90	.40	.20	.22	.11	.40	.98	5.78	17.9
825	LP-11	41.9	6.83	4.56	.74	.28	.15	.15	.05	.30	.75	7.74	16.2
845	LP-12	42.2										7.04	

The tar values for runs prior to LP-10 are felt to be too low due to incomplete collection.

## 1000 psig He Runs

Temp.	Run	Total	CO <sub>2</sub>	CO	CH <sub>4</sub>	C <sub>2</sub> H <sub>4</sub>	C <sub>2</sub> H <sub>6</sub>	C <sub>3</sub> H <sub>6</sub>	C <sub>3</sub> H <sub>8</sub>	HC	HC Liq	Tar	H <sub>2</sub> O
1045	LP-13	40.9	10.09	8.77	2.42	.50	.13		-.36-	.17	1.03	(2.15)	11.82
1071	LP-14	42.0	9.88	8.52	2.25	.51	.18		-.68-	.30	1.01	(3.03)	14.9
895	LP-15	39.3	11.11	9.32	2.59	.57	.17		-.21-	.14	1.19	(2.92)	11.1
986	LP-16	41.8	11.15	9.23	2.54	.60	.20		-.26-	.22	1.10	(2.94)	13.6
937	LP-17	37.1										(2.96)	

## LIGNITE 1000 psig He PYROLYSIS

Temp.	Hold Time	Run	Total	CO <sub>2</sub>	CO	CH <sub>4</sub>	C <sub>2</sub> H <sub>4</sub>	C <sub>2</sub> H <sub>6</sub>	C <sub>3</sub>	HC	HC Liq.	Tar	H <sub>2</sub> O
628°C	0	LP-17A	18.9	-	-	-	-	-	-	-	-	-	-
650	0	LP-17B	22.7	-	-	-	-	-	-	-	-	-	-
580	0	LP-18	19.9	6.58	-	0.33	0.16	0.06	0.03	0.50	0.79	(8.3)	13.5
782	0	LP-19	35.5	11.3	-	1.41	0.40	0.26	0.89	0.50	1.5	(6.1)	12.7
800	0	LP-20	38.9	11.8	6.48	1.92	0.50	0.21	0.37	0.74	1.4	(7.1)	11.9
722	0	LP-21	24.2	6.6	-	0.39	0.14	0.08	0.25	0.32	0.64	(5.0)	9.9
655	0	LP-22	21.9	4.80	-	0.18	0.08	0.07	0.16	0.24	0.77	(4.9)	5.5
793	0	LP-23	33.1	10.47	7.38	1.17	0.37	0.20	0.35	0.87	1.09	5.8	10.0



LIGNITE HYDROLYSIS - 1500 psig H<sub>2</sub>

<u>Temp.</u>	<u>Hold Time</u>	<u>Run</u>	<u>Total</u>	<u>CO<sub>2</sub></u>	<u>CO</u>	<u>CH<sub>4</sub></u>	<u>C<sub>2</sub>H<sub>4</sub></u>	<u>C<sub>2</sub>H<sub>6</sub></u>	<u>C<sub>3</sub>'s</u>	<u>HC gas</u>	<u>HC liq</u>	<u>H<sub>2</sub>O</u>	<u>Tar</u>
1100	0	LH-26	53.8	7.66	6.63	13.98	.11	.96	.22	.98	1.73	-	4.07
1140	2	LH-27	62.2	9.58	9.08	15.1	.17	1.17	.41	.95	1.93	-	3.70
844	22	LH-41	59.1	9.24	-	15.2	.27	2.81	.58	2.67	2.81	-	7.47
800	5	LH-28	55.1	7.64	5.69	7.39	.22	1.87	.42	1.96	2.67	-	5.64
840	18	LH-40	60.1	8.05	-	12.64	.19	2.31	.49	2.39	2.01	-	5.21
745	8	LH-29	49.0	8.29	7.33	6.21	.25	1.84	.56	1.27	2.33	-	7.22
750	3	LH-30	49.6	10.87	7.07	6.86	.27	1.45	.50	.91	3.13	-	5.35

LIGNITE HYDROLYSIS - 500 psig H<sub>2</sub>

1071	5	LH-43	58.0	9.98	-	13.71	.40	1.73	.55	1.75	3.20	-	6.27
1019	15	LH-44	52.3	10.61	-	10.95	.47	2.10	.63	1.89	(4.93)	-	7.65
1124	4	LH-45	60.9	9.84	-	14.96	.32	.97	.30	.57	1.93	17.6	6.26
830	11	LH-47	51.8	8.93	6.20	8.03	.37	1.50	.44	.75	2.25	-	-



ACCEPTED BITUMINOUS RUNS  
SHORT RESIDENCE TIMES ( $\frac{dT}{dt} = 1000^{\circ}\text{C}/\text{sec}$ )

Run	Peak Temperature	Total Yield	CO	CO <sub>2</sub>	H <sub>2</sub> O	CH <sub>4</sub>	C <sub>2</sub> H <sub>4</sub>	C <sub>2</sub> H <sub>6</sub>	C <sub>3</sub> 's	HC gas	HC liq.	TAR	H <sub>2</sub>
BA-4	398	6.43	0.	.07	6.36	0.	0.	0.	0.	0.	0.	0.	0.
BA-6	440	7.78	0.	.16	4.19	0.	0.	0.	0.	0.	0.	2.22	0.
BA-5	441	6.46	0.	.11	4.92	0.	0.	0.	0.	0.	0.	1.31	0.
BA-35	510	11.0	.05	.27	5.70	.05	.02	.03	.13	.06	.49	4.11	-
BA-38	510	10.2	.05	.25	4.48	.05	.02	.03	.25	.04	.67	4.03	-
BA-7	556	9.14	0.	.17	5.06	0.	0.	0.	0.	0.	-	3.91	-
BA-8	621	11.9	.13	.31	6.37	.05	.03	.03	.30	.04	-	3.06	-
BA-39	638	14.8	.21	.35	4.88	.18	.10	.09	.27	.17	.81	7.46	-
BHY-10	638	15.1	-	-	-	-	-	-	-	-	-	-	0.
BA-37	661	19.2	.17	.44	6.15	.30	.12	.13	.57	.35	1.12	9.50	-
BA-9	685	18.8	.34	.45	6.68	.33	.21	.14	.42	.27	-	8.06	-
BHY-9	690	16.8	-	-	-	-	-	-	-	-	-	-	0.
BA-36	733	19.6	.20	.39	5.99	.22	.08	.11	.47	.17	.99	9.06	-
BA-40	742	28.6	.42	.53	5.28	.62	.27	.26	.73	.33	1.38	14.1	-
BA-32	747	27.8	.37	.64	5.24	.56	.26	.26	.61	.39	1.58	12.9	-
BHY-7	752	28.2	-	-	-	-	-	-	-	-	-	-	.06
BA-24	781	27.7	-	-	-	-	-	-	-	-	-	-	-
BA-41	800	31.7	.76	.94	4.99	1.03	.38	.32	.82	.53	1.74	16.6	-
BA-33	818	29.9	.58	.68	5.76	.86	.32	.30	.78	.35	1.39	16.6	-
BA-34	825	33.2	.47	.67	6.64	.84	.28	.37	.93	1.07	1.52	18.1	-
BA-30	843	37.7	.66	.74	5.16	1.29	.49	.45	.90	.75	3.00	20.9	-
BHY-1	850	43.3	-	-	-	-	-	-	-	-	-	-	.31
BHY-8	850	40.6	-	-	-	-	-	-	-	-	-	-	.15
BA-1	830	42.1	(1.92)	.77	-	1.67	.58	.49	(1.64)	1.13	-	-	-
BA-10	862	39.2	1.67	1.06	6.88	1.85	.70	.57	1.84	.54	(.90)	(16.4)	-
BA-44	870	38.9	1.81	1.02	6.55	1.74	.69	.41	.90	.74	2.31	21.8	-
BHY-2	873	37.1	-	-	-	-	-	-	-	-	-	-	.25
BA-43	875	42.1	.73	1.01	4.93	1.89	.73	.46	.89	1.26	2.23	(18.4)	-
BHY-6	890	42.4	-	-	-	-	-	-	-	-	-	-	.30
BA-45	912	47.0	1.22	1.18	(8.38)	2.53	.80	.48	1.16	.93	2.24	26.6	-
BA-3	915	44.3	(3.10)	1.07	-	2.61	1.08	.48	1.81	.87	-	-	-
BHY-3	917	43.2	-	-	-	-	-	-	-	-	-	-	.26
BA-46	925	40.7	1.18	1.07	6.11	1.98	.79	.44	.93	.86	2.50	20.0	-
BA-47	905	47.0	(2.81)	(1.63)	6.56	2.61	.79	.48	1.06	.98	-	19.3	-
BA-31	953	46.6	2.17	1.01	7.97	2.25	.74	.54	1.27	1.07	1.95	24.2	-
BHY-13	965	46.1	-	-	-	-	-	-	-	-	-	-	.64
BHY-11	1002	46.3	-	-	-	-	-	-	-	-	-	-	.76
BA-2	1006	46.2	(3.70)	1.25	-	2.41	.73	.49	1.51	1.01	-	-	-
BHY-12	1047	47.2	-	-	-	-	-	-	-	-	-	-	1.07
BV-1	907	50.6	2.41	0.96	4.49	1.55	.69	.45	1.14	.82	1.55	(35.3)	-
BV-2	830	47.4	-	0.81	4.31	1.13	.43	.37	1.03	.56	1.67	26.8	-
BV-3	764	51.3	1.42	.97	6.15	1.47	.60	.45	1.02	.97	1.63	31.9	-
BV-4	692	-	-	.49	4.79	.22	.11	.11	.51	.37	.68	-	-
BV-5	737	48.0	.38	.64	5.77	.91	.29	.36	1.23	.62	1.49	23.6	-
BP-1	980	32.6	1.63	1.61	9.15	3.54	.56	.65	.70	.97	2.50	-	-
BA-54	390	6.02	-	-	3.22	-	-	-	-	-	-	2.8	-
BA-55	170	2.9	-	-	2.90	-	-	-	-	-	-	0.0	-
BA-56	245	2.3	-	-	1.70	-	-	-	-	-	-	0.6	-
BA-57	530	15.6	-	-	-	-	-	-	-	-	-	5.26	-

## ACCEPTED BITUMINOUS RUNS

LONG RESIDENCE TIME RUNS ( $\frac{dT}{dt} \approx 1000^\circ\text{C}/\text{sec}$  to holding temp.)

Run No.	Approximate Holding Temp. (°C)	Holding Time (sec)	Total % Yield	CO	CO <sub>2</sub>	H <sub>2</sub> O	CH <sub>4</sub>	C <sub>2</sub> H <sub>4</sub>	C <sub>2</sub> H <sub>6</sub>	C <sub>3</sub> 's	HC gas	HC liq.	TAR	H <sub>2</sub>	H <sub>2</sub> S	
BA 49	645	2	38.5	0.60	0.69	5.46	1.00	0.19	0.46	1.07	.71	1.97	20.5	-	-	
BA 53A	650	3	-	0.58	0.72	4.72	0.98	0.25	0.45	1.11	.55	-	-	-	-	
BA 52A	661	3	-	0.55	0.78	5.18	1.03	0.21	0.47	1.11	.61	-	-	-	-	
BA 50	668	2	36.8	0.52	0.66	6.05	0.90	0.19	0.44	1.07	.44	2.06	23.9	-	-	
BA 51	700	4	41.1	0.60	0.93	5.36	1.49	0.33	0.58	1.36	.68	2.47	21.9	-	-	
BA 48	770	3	44.2	2.03	1.00	6.61	1.90	0.31	0.59	1.06	.73	2.21	24.0	-	-	
BA 26	845	3	46.3	2.24	0.97	-	2.26	0.69	0.56	1.46	-	-	-	-	-	
BA 14	850	6	46.9	2.79	1.32	-	2.81	0.92	0.53	1.52	1.31	-	-	-	-	
BA 15	900	4	45.5	2.56	-	-	2.65	1.04	0.48	1.31	1.49	-	-	-	-	
BA 18	922	4	44.4	2.26	-	-	2.49	1.11	0.54	1.31	1.46	-	-	-	-	
BA 23	941	7	48.2	2.35	1.20	7.91	2.34	0.73	0.45	1.03	1.10	2.27	24.1	-	-	
BA 16	943	5	47.2	-	-	-	-	-	-	-	-	-	-	-	-	
BA 17	943	7	46.9	-	-	-	-	-	-	-	-	-	-	-	-	
BA 29	970	5	45.1	2.30	1.10	-	2.13	-	0.56	1.71	1.56	-	-	-	.94	
BA 13	976	5	48.8	2.50	-	-	2.68	0.92	0.48	1.29	1.31	-	-	-	-	
BA 27	980	9	48.2	(4.17)	1.18	-	2.76	0.96	0.53	1.23	-	-	-	-	-	
BA 28	1000	5	47.2	2.53	1.12	-	2.26	0.60	0.63	1.35	1.76	-	-	-	.95	
BA 19	1000	9	46.7	-	(2.00)	(13.3)	2.45	0.73	0.50	.99	1.26	-	-	-	-	
BA 20	1000	7	48.8	2.30	(1.91)	(13.3)	(1.55)	0.62	0.45	1.46	1.49	-	-	-	-	
BA 42	1000	4	45.9	(1.58)	1.45	7.79	2.43	0.69	0.53	0.98	1.03	2.47	23.2	-	-	
BA 25	1000	6	47.4	2.27	1.37	9.62	2.62	0.85	0.45	1.45	.96	2.45	21.7	-	-	
BA 21	1000	6	49.0	2.49	1.34	6.21	2.42	0.72	0.48	1.17	1.25	-	-	-	-	
BA 22	1000	5	47.3	(1.80)	1.28	7.42	2.54	0.83	0.47	1.25	1.07	-	-	-	-	
BHY 4	895	5	46.2	-	-	-	-	-	-	-	-	-	-	-	.94	
BHY 14	950	4	47.2	-	-	-	-	-	-	-	-	-	-	-	1.03	
BHY 5	895	5	47.0	-	-	-	-	-	-	-	-	-	-	-	1.05	
BP 2	1000	> 2	39.7	2.46	1.85	9.35	2.97	0.52	0.76	0.68	-	1.94	(11.0)	-	-	1000 psig He
BP 3	800	~10	34.2	0.99	1.40	9.23	2.75	0.45	0.82	0.99	1.12	2.05	(8.65)	-	-	" " "
BP 4	950	3	35.8	2.64	1.63	-	3.30	0.54	1.09	-	-	2.09	(9.08)	-	-	" " "
BP 5	950	5	37.3	2.40	1.61	9.67	3.31	0.33	0.82	0.74	1.58	2.07	(7.96)	-	-	" " "
BV 6	950	4	53.0	1.82	1.78	-	1.62	0.45	0.41	0.75	1.07	1.81	34.2	-	-	
BV 7	900	4	51.8	1.75	1.13	6.19	1.66	0.43	0.44	0.69	.86	1.38	29.6	-	-	
BV 8	900	4	52.0	2.36	1.24	7.39	1.68	0.46	0.46	0.69	1.02	1.47	(42.1)	-	-	
BHY 17	900	3	50.3	-	-	-	-	-	-	-	-	-	-	-	.62	
BHY 18	920	5	50.8	-	-	-	-	-	-	-	-	-	-	-	.55	
BHY 19	970	7	51.1	-	-	-	-	-	-	-	-	-	-	-	.89	
BHY 20	975	5	51.6	-	-	-	-	-	-	-	-	-	-	-	.92	

- Note:
- Holding times and temperatures are only approximate
  - For BA series P(He) = 1 atm, for BP P(He) = 1000 psi, for BV P(He) = .05 mm Hg
  - "H<sub>2</sub>O" might include some H<sub>2</sub>S; Runs BA 28 and BA 29 determined that this might amount to about .95% at ~1000°C
  - "TAR" in BP series includes only the tar trapped on the exit filter, no attempt is made to wash the reactor.

404

## ACCEPTED BITUMINOUS RUNS

Run	Approx. Peak or Holding Temp. (sec)	Holding Time (sec)	Total Yield	CO	CO <sub>2</sub>	H <sub>2</sub> O	CH <sub>4</sub>	C <sub>2</sub> H <sub>4</sub>	C <sub>2</sub> H <sub>6</sub>	C <sub>3</sub> 's	HC gas	HC liq	TAR	H <sub>2</sub>	Particle Diameter
BDP-1	945	10	43.4	2.82	1.35	7.06	3.29	1.45	.63	1.18	1.26	2.90	16.7	-	833-991 $\mu$
BDP-2	920	20	45.3	3.24	(3.53)	8.41	3.25	1.35	.65	1.17	(2.43)	(5.77)	-	-	833-991
BDP-3	945	9	44.0	3.09	1.20	6.01	3.21	1.10	.62	.99	1.24	2.50	20.1	-	833-991
BDP-4	920	7	43.5	(1.56)	1.20	5.22	2.74	.94	.56	.82	1.01	2.53	21.3	-	297-833
BDP-5	930	9	43.5	(4.92)	1.12	5.46	3.19	1.24	.53	.85	1.16	2.56	21.2	-	297-833
BDP-6	945	8	45.5	1.69	1.17	5.44	2.64	.77	.56	.97	1.12	2.48	21.8	-	149-177
BDP-7	920	8	42.9	2.69	1.14	5.35	2.86	1.04	.50	.92	1.41	2.47	24.2	-	833-991 reground to < 300 $\mu$
<u>2-Step Heating</u>															
BA-52A	661	3	-	.55	.78	5.18	1.03	.21	.47	1.11	.61	-	-	-	-
BA-52B	1000	3	44.6	2.22	1.69	8.21	2.27	.29	.57	1.27	.87	2.36	19.9	-	(Total)
BA-53A	650	3	-	.58	.72	4.72	.98	.25	.45	1.11	.55	-	-	-	-
BA-53B	970	2	44.7	1.91	1.49	7.21	2.81	.38	.55	1.28	.84	2.50	24.1	-	(Total)
<u>Heating Rate</u>															
BHR-1	955	6	46.6	2.68	1.28	5.33	2.18	.35	.58	1.05	.98	2.34	24.1	-	LHR 351 <sup>o</sup> C/sec
BHR-2	~955	~6	47.0	(3.16)	(1.95)	(9.53)	2.29	.46	.59	1.27	1.07	2.22	20.8	-	LHR
BHR-3	867	5	44.5	1.27	1.41	8.06	2.19	.38	.60	1.04	1.24	2.24	22.4	-	LHR 445 <sup>o</sup> C/sec
BHR-4	955	5	46.7	3.04	1.31	6.06	2.45	.61	.60	1.25	1.37	2.51	22.7	-	HHR 15,000 <sup>o</sup> C/sec
BHR-5	895	4	47.2	(1.57)	(2.08)	(9.36)	2.37	.71	.57	1.05	1.53	2.87	23.3	-	HHR 13,000 <sup>o</sup> C/sec
<u>Particle Diameter</u>															
BHY-15	930	11	43.6	-	-	-	-	-	-	-	-	-	-	.89	833-991
BHY-16	940	20	41.6	-	-	-	-	-	-	-	-	-	-	1.09	833-991
<u>Short Residence Time High Pressures</u>															
BP-6	813	0	33.6	-	-	-	-	-	-	-	-	-	11.0	-	1000 psi He
BP-7	484	0	15.0	-	-	-	-	-	-	-	-	-	4.6	-	1000 psi He
BP-8	1084	0	37.2	-	-	-	-	-	-	-	-	-	12.9	-	1000 psi He
BP-9	397	0	7.1	-	-	-	-	-	-	-	-	-	2.5	-	1000 psi He
BP-10	604	0	23.2	-	-	-	-	-	-	-	-	-	9.8	-	1000 psi He
BP-11	724	0	29.5	-	-	-	-	-	-	-	-	-	11.2	-	1000 psi He
BP-12	960	0	36.4	-	-	-	-	-	-	-	-	-	12.8	-	1000 psi He
BP-13	930	0	34.0	-	-	-	-	-	-	-	-	-	12.3	-	1000 psi He



Analysis of Lignite Chars Produced by Short Residence Time Pyrolysis

Raw Lignite (Mean)	Peak Temperature												
	430°C		650°C		700°C		900°C		1000°C		1100°C		
	Anal- ysis	% Reten- tion	Anal- ysis	% Reten- tion	Anal- ysis	% Reten- tion	Anal- ysis	% Reten- tion	Anal- ysis	% Reten- tion	Anal- ysis	% Reten- tion	
Carbon	59.27	71.96	107	72.81	92	73.41	90	77.96	79	79.13	77	80.18	78
Hydrogen	3.79	3.16	84	2.73	72	2.06	54	1.97	52	0.98	26	0.82	22
Nitrogen	0.91	0.86	85	1.08	89	1.18	94	0.99	65	1.15	73	1.20	76
Sulfur	1.12	1.24	98	1.05	70	1.08	70	0.96	52	0.84	43	0.66	34
Moisture	6.75	-	-	-	-	-	-	-	-	-	-	-	-
Ash	9.93	10.36	-	14.01	-	17.49	-	13.91	-	15.12	-	16.27	-
Oxygen (by difference)	18.2	12.4	68	8.32	46	4.30	24	4.21	23	2.78	15	0.87	5
% weight loss	-	11.5		25.0		27.3		39.9		42.2		42.2	

Long Residence Time Pyrolysis and Hydropyrolysis Chars

Raw Lignite (Mean)	Temperature, Pressure										
	900 <sup>+</sup> °C Pyrolysis 1 atm He		900 <sup>+</sup> °C Pyroly- 69 atm He		910 <sup>+</sup> °C Hydropy- rolysis 69 atm H <sub>2</sub>		~1050°C Hydropy- 69 atm H <sub>2</sub>		~1000°C Hydropyroly- 69 atm H <sub>2</sub>		
	Anal- ysis	% Reten- tion	Anal- ysis	% Reten- tion	Anal- ysis	% Reten- tion	Anal- ysis	% Reten- tion	Anal- ysis	% Reten- tion	
Carbon	59.27	74.21	70	76.24	77	77.09	63	77.65	62	(69.72)	56
Hydrogen	3.79	1.84	27	2.04	32	2.27	29	2.13	27	1.78	22
Nitrogen	0.91	1.21	75	1.13	74	0.80	42	0.65	34	0.60	32
Sulfur	1.12	0.80	40	0.95	45	0.98	42	0.92	39	0.91	48
Moisture	6.75	-	-	-	-	-	-	-	-	-	-
Ash	9.93	15.95	-	15.92	-	16.35	-	15.67	-	15.3	-
Oxygen (by difference)	18.2	(5.99)	(18)	3.72	12	2.51	7	2.98	8	(11.7)	(31)
% weight loss	-	44.0		40.2		51.9		52.3		52.3	

Analysis of Bituminous Coal Chars Produced by Short Residence Time Pyrolysis

	Raw Bituminous Coal (Mean)	Peak Temperature									
		390-440°C		620-690°C		730-780°C		800-860°C		900-950°C	
		Anal-ysis	% Reten-tion	Anal-ysis	% Reten-tion	Anal-ysis	% Reten-tion	Anal-ysis	% Reten-tion	Anal-ysis	% Reten-tion
Carbon	67.8	68.65	94	68.51	85	64.83	71	61.45	57	66.72	55
Hydrogen	4.75	4.77	94	4.66	82	4.08	64	3.18	42	2.94	34
Nitrogen	1.26	1.16	86	1.19	79	1.20	71	1.01	50	1.28	57
Sulfur	5.26	5.84	103	5.48	88	5.63	79	7.12	85	6.58	70
Moisture	1.38	-	-	-	-	-	-	-	-	-	-
Ash	11.33	15.57	-	16.75	-	19.44	-	-	-	-	-
Oxygen (by difference)	8.22	4.01	45	3.41	35	4.81	43	-	-	-	-
% weight loss	-	6.9		16.0		26.4		37.2		44.4	

Long Residence Time Pyrolysis Chars

	Raw Bituminous Coal (Mean)	Temperature and Pressure			
		1000°C, 1 atm He (Mean)		1000°C, vacuum (Mean)	
		Analysis	% Retention	Analysis	% Retention
Carbon	67.8	64.6	50	67.5	48
Hydrogen	4.75	0.98	11	1.17	12
Nitrogen	1.26	1.52	64	1.53	59
Sulfur	5.26	4.42	45	3.82	35
Moisture	1.38	-	-	-	-
Ash	11.33	28.8	-	24.73	-
Oxygen (by difference)	8.22	0.	0	1.21	7
% weight loss	-	47.0		51.5	

## APPENDIX

Thermal Conductivity Response Factors

(Detector Temperature 250°C)

The following response factors were determined by direct calibration on the Model 3920B chromatograph:

CO <sub>2</sub>	1.000	(chosen as reference component)
CO	0.727	
CH <sub>4</sub>	0.546	
C <sub>2</sub> H <sub>4</sub>	0.686	
C <sub>2</sub> H <sub>6</sub>	0.667	
C <sub>3</sub> H <sub>6</sub>	0.789	
C <sub>3</sub> H <sub>8</sub>	0.769	
C <sub>6</sub> H <sub>6</sub>	1.21	
C <sub>7</sub> H <sub>8</sub>	1.24	
H <sub>2</sub> O	0.8	(< 1/2 mg) to 0.66 (> 1 mg)

The above values are generally constant in the range 0 to 1 mg (except water).

The use of the response factor to calculate the number of milligrams of a component x in a sample is given by the formula:

$$\text{mg}_x = \left( \frac{A_x \text{ RF}_x}{A_{\text{CO}_2}} \right) \left( \text{mg}_{\text{CO}_2} \right)$$

where  $A_x$  is the area of the chromatographic peak produced by x,  $A_{\text{CO}_2}$  is the area of a CO<sub>2</sub> calibration peak,  $\text{RF}_x$  is the response factor for x, and  $\text{mg}_{\text{CO}_2}$  is the number of milligrams of CO<sub>2</sub> in the calibration sample.





```

TMAX=0.0
READ (9,300) FRAC(I),RCODE(I)
300 FORMAT (F10.0,8X,A4)
READ (9,400) (TIME(I,J),TEMP(I,J)),J=1,15)
400 FORMAT (8(F4.0,F5.0))
200 CONTINUE
C
C   CONVERT TEMPERATURES TO DEGREES ABSOLUTE
C
DO 502 I=1,NRUNZ
DO 502 J=1,15
502 TEMP(I,J)=TEMP(I,J) + 273.15
C
C   READ IN INITIAL ESTIMATES FOR PARAMETERS
C   (EITHER SINGLE VALUE OR RANGE)
C
DO 700 NPAM = 1,3
700 READ (9,701) BOTI(NPAM),TOP(NPAM)
701 FORMAT (2F10.0)
NPAM = 3
IFOO = NPAM + 1
C
C   IF RANGE GIVEN DO COARSE GRID SEARCH FOR 20 RANDOM POINTS
C
DO 764 JA=1,10
WRITE (12,730) JA
730 FORMAT (/ / 'PARAMETER RANGES FOR E-CONTRACTION NUMBER ',I2)
DO 731 K = 1,3
731 WRITE (12,732) BOTI(K),TOP(K)
732 FORMAT (E13.5, / - ',E13.5)
DO 733 KNT=1,30
DO 733 I = 1,NPAM
CALL RANDU (XIX,XIX,PARA)
738 TRY(I)=BOTI(I)+PARA*(TOP(I)-BOTI(I))
CALL INCRS(TRY,ERR2,0)
PRINT OUT BEST PARAMETER VALUES FROM GRID SEARCH AS STARTING
POINT FOR GRADIENT SEARCH
C
WRITE (12,4001) (TRY(I,EW),LEW=1,NPAM),ERR2
4001 FORMAT (7E15.5)
IF (ERROR-ERR2) 739,740,740
740 DO 741 K=1,NPAM
741 SAVE(K)=TRY(K)
ERROR=ERR2
739 CONTINUE
DO 744 K=1,NPAM
744 PARAM(K)=SAVE(K)
WRITE (12,750)
750 FORMAT (// / 'INITIAL PARAMETER VALUES=' )
WRITE (12,711) (I,PARAM(I),I=1,NPAM)
711 FORMAT (/ / ('12,')',E13.5)
TOP(1)=PARAM(1)+(TOP(1)-BOTI(1))/2.67
BOTI(1) = PARAM(1) - (TOP(1) - PARAM(1))
IF (JA 6) 762,761,762
761 TOP(2)=PARAM(2)+3.
BOTI(2)=PARAM(2)-3.
762 IF (JA 8) 764,763,764
763 TOP(2)=PARAM(2)+2.
BOTI(2)=PARAM(2)-2.
764 CONTINUE
CALL ENAL5
CALL EXIT

```

SUBROUTINE COAL5

\*\*\*\*\*

COAL 5 IS A MODIFIED VERSION OF CURFIT (BEVINGTON, 1969) AND  
UTILIZES A GRADIENT SEARCH TECHNIQUE

NOMENCLATURE

ALPHA(K,L) CURVATURE MATRIX  
 ARRAY(K,L) MODIFIED CURVATURE MATRIX  
 BETA(K) ROW MATRIX  
 BPAM(K) NO. OF PARAMETERS  
 DELTA INCREMENTS FOR PARAMETERS  
 DERIV(K) DERIVATIVE OF FUNCTION WITH RESPECT TO PARAMETER  
 K  
 LAMBDA PROPORTION OF GRADIENT SEARCH INCLUDED  
 LDUMMY(K) DUMMY VARIABLE FOR MATRIX INVERSION SUBROUTINE  
 MDUMMY(K) DUMMY VARIABLE FOR MATRIX INVERSION SUBROUTINE  
 VECTO(M) VECTOR EQUIVALENT TO THE ARRAY MATRIX

\*\*\*\*\*

REAL LAMBDA  
 DIMENSION FRAC(60), TIME(60, 15), TEMP(60, 15), VCALC(60), RCODE(60),  
 + PARAM(3), BPAM(3), DERIV(3), BETA(3), ALPHA(3, 3),  
 + ARRAY(3, 3), LDUMMY(3), MDUMMY(3), VECTO(9)  
 COMMON NPAM, NRUNZ, FRAC, TIME, TEMP, VCALC, VSTAR, WATER, RCODE, PARAM,  
 IIFOO, ERROR, VECTO  
 EQUIVALENCE (ARRAY(1, 1), VECTO(1))  
 LAMBDA=0.01  
 99 LAMBDA=0.1\*LAMBDA

EVALUATE ALPHA AND BETA MATRICES

DO 34 J=1, NPAM  
 BETA(J)=0.0  
 DO 34 K=1, J  
 34 ALPHA (J,K)=0.0

EVALUATE DERIVATIVES OF THE FITTING FUNCTION FOR THE ITH TERM  
WITH RESPECT TO EACH PARAMETER

DO 50 I=1, NRUNZ  
 DO 98 JFOO=1, 3  
 PARA=PARAM(JFOO)  
 DELTA=0.01\*PARA  
 PARAM(JFOO)=PARA+DELTA  
 CALL INGRS (PARAM, VAL, I)  
 VAL2=VCALC(I)  
 PARAM(JFOO)=PARA  
 CALL INGRS (PARAM, VAL, I)  
 98 DERIV(JFOO)=(VAL2-VCALC(I))/DELTA  
 DO 46 J=1, NPAM  
 BETA(J)=BETA(J)+(FRAC(I)-VCALC(I))\*DERIV(J)  
 DO 46 K=1, J  
 46 ALPHA(J,K)=ALPHA(J,K)+DERIV(J)\*DERIV(K)  
 50 CONTINUE  
 DO 53 J=1, NPAM  
 DO 53 K=1, J  
 53 ALPHA(K,J)=ALPHA(J,K)

INVERT MODIFIED CURVATURE MATRIX TO FIND NEW PARAMETERS

```

C
71 DO 74 J=1,NPAM
   DO 73 K=1,NPAM
73  ARRAY(J,K)=ALPHA(J,K)/SQRT(ALPHA(J,J)*ALPHA(K,K))
74  ARRAY(J,J)=ARRAY(J,J)*(1.+LAMDA)
   KNT=0
   DO 110 M=1,NPAM
   DO 110 N=1,NPAM
   KNT=KNT+1
110  VECTO(KNT)=ARRAY(N,M)
   CALL MINV (VECTO,NPAM,PARA,LDUMY,MDUMY)
   KNT=NPAM*NPAM
   DO 120 M=1,NPAM
   MODL=1F00-M
   DO 120 N=1,NPAM
   NROW=1F00-N
   ARRAY(NROW,MODL)=VECTO(KNT)
120  KNT=KNT-1
   DO 84 J=1,NPAM
   BPAM(J)=PARAM(J)
   DO 84 K=1,NPAM
84  BPAM(J)=BPAM(J)+BETA(K)*ARRAY(J,K)/SQRT(ALPHA(J,J)*ALPHA(K,K))
   CALL INGR5 (BPAM,ERR2,0)
   WRITE (12,4001) (BPAM(LEW),LEW=1,NPAM) , ERR2
4001  FORMAT (7E15.5)
C
C   IF ERROR INCREASES, INCREASE LAMDA AND TRY AGAIN
C
   IF (ERROR-ERR2) 95,101,101
95  LAMDA=10.*LAMDA
   GO TO 71
101  DO 105 J=1,NPAM
   IF (ABS(BPAM(J)-PARAM(J))-0.005*ABS(PARAM(J))) 105,105,106
105  CONTINUE
   GO TO 700
C
C   EVALUATE PARAMETERS
C
106  DO 107 J=1,3
107  PARAM(J)=BPAM(J)
   ERROR=ERR2
   GO TO 99
700  ERROR=ERR2
   DO 707 J=1,3
707  PARAM(J)=BPAM(J)
   CALL CDAL6
   RETURN
   END

```

SUBROUTINE COAL6

C  
C  
C  
C  
C  
C  
C  
C  
C

\*\*\*\*\*

COAL 6 IS USED AS A PRINTING PROGRAM FOR RESULTS

\*\*\*\*\*

```
REAL NCALC(60),NFRAC(60)
DIMENSION FRAC(60),TIME(60,15),TEMP(60,15),V CALC(60),RCODE(60),
+ EPAM(3)
COMMON NPARAM,NRUNZ,FRAC,TIME,TEMP,V CALC,VSTAR,WATER,RCODE,EPAM,
+ IIFOR,ERR2
EQUIVALENCE (TIME(1,1),NCALC(1)),(TEMP(1,1),NFRAC(1))
DO 59 I=1,NRUNZ
  NCALC(I)=V CALC(I)/VSTAR
59 NFRAC(I)=FRAC(I)/VSTAR
  ERN1=ERR2/(VSTAR*VSTAR)
  WRITE (12,501) (FRAC(I),V CALC(I),NFRAC(I),NCALC(I),RCODE(I),
+ I=1, NRUNZ)
501 FORMAT (// EXP. FRAC.=',F6.4,' AND CALC. FRAC.=',F6.4,6X,
+ 'NORMALIZED EXP. FRAC.=',F6.4,' AND NORMALIZED CALC. FRAC.=',
+ F6.4,2X,04)
  WRITE (12,710)
710 FORMAT (/// FINAL PARAMETER VALUES=')
  WRITE (12,711) (I,EPAM(I),I=1,NPARAM)
711 FORMAT (// ('',12,''),E13.5)
  WRITE (12,722) ERR2,ERN1
722 FORMAT (/// SUM OF SQUARED ERRORS=',E13.5,20X,'NORMALIZED ERROR SU
+ M=',E13.5)
RETURN
END
```

```

SUBROUTINE INGR5 (PAM, ERROR, ICODE)
REAL KO
DIMENSION PAM(4)
COMMON NPAM, NRUNZ, FRAC(60), TIME(60, 15), TEMP(60, 15), VCALC(60),
1VSTAR, WATER
R=1.9872
EA=PAM(1)
KO=10.**PAM(2)
SGMA=PAM(3)
ERROR=0.0
EMIN=EA-2.*SGMA
EMAX=EA+2.*SGMA
H=0.5*SGMA
SGMA2=0.5/(SGMA*SGMA)
IF(ICODE)51, 50, 51
50  ILOW=1
    IHIGH=NRUNZ
    GO TO 52
51  ILOW=ICODE
    IHIGH=ICODE
52  DO 1 I=ILOW, IHIGH
    A=TRAPS(I, EMIN)
    IF ((-KO*A-(EMIN-EA)*(EMIN-EA)*SGMA2)+35.0) 53, 54, 54
53  VAL=0.0
    GO TO 55
54  VAL=EXP(-KO*A-(EMIN-EA)*(EMIN-EA)*SGMA2)
55  A=TRAPS(I, EMAX)
    IF ((-KO*A-(EMAX-EA)*(EMAX-EA)*SGMA2)+35.0) 56, 57, 57
56  VAL=VAL+0.0
    GO TO 58
57  VAL=VAL+EXP(-KO*A-(EMAX-EA)*(EMAX-EA)*SGMA2)
58  ICODE=2
    E=EMIN
    DO 10 J=1, 7
    E=E+H
    A=TRAPS(I, E)
    IF ((-KO*A-(E-EA)*(E-EA)*SGMA2)+35.0) 59, 60, 60
59  ARGU=0.0
    GO TO 61
60  ARGU=EXP(-KO*A-(E-EA)*(E-EA)*SGMA2)
61  GO TO (2, 4), ICODE
2  VAL=VAL+2.*ARGU
   ICODE=2
   GO TO 10
4  VAL=VAL+4.*ARGU
   ICODE=1
10  CONTINUE
   VAL=0.3333333*H*VAL
   VCALC(I)=VSTAR+(WATER-VSTAR)*(VAL/(SGMA*2.50663))
1  ERROR=ERROR+(VCALC(I)-FRAC(I))*2
   RETURN
   END

```

```

SUB ROUTINE MINV(A,N,D,L,M)
DIMENSION A(I),L(J),M(K)
D=1.0
NK=N
DO 30 K=1,N
NK=NK+N
I(K)=K
M(K)=K
L(N)=K
BIGA=A(KK)
DO 20 J=K,N
LZ=N*(J-1)
DO 20 I=K,N
L=LZ+I
IF (ABS(BIGA)-ABS(A(IJ))) 15,20,20
15 BIGA=A(IJ)
I(K)=I
M(K)=J
20 CONTINUE
J=I(K)
IF(J=K) 35,35,25
25 KI=K-N
DO 30 I=1,N
KI=KI+N
HOLD=-A(KI)
JI=I-K+J
A(KI)=A(JI)
30 A(JI)=HOLD
35 I=M(K)
IF(I=K) 45,45,38
38 JF=N*(I-1)
DO 40 J=1,N
JF=JF+J
JI=JF+I
HOLD=-A(KK)
A(KK)=A(JI)
40 A(JI)=HOLD
45 IF(BIGA) 48,46,48
46 D=0.0
RETURN
48 DO 55 I=1,N
IF(I=K) 50,55,50
50 IK=NK+I
A(IK)=A(IK)/(-BIGA)
CONTINUE
DO 65 I=1,N
IK=NK+I
HOLD=A(IK)
L=I-N
DO 65 J=1,N
L=L+J
IF(I=K) 60,65,60
60 IF(J=K) 62,65,62
62 K=I-I+K
A(IJ)=HOLD+A(KJ)+A(IJ)
65 CONTINUE
K=K-N
DO 75 J=1,N
K=LK+N
IF(J=K) 70,75,70
70 A(KJ)=A(KJ)/BIGA
CONTINUE
D=D*BIGA
A(KK)=1.0/BIGA

```

```
80  CONTINUE
    K=N
100  K=(K-1)
    IF(K) 150,150,105
105  I=I(K)
    IF(I-K) 120,120,108
108  JR=N*(K-1)
    JR=N*(I-1)
    DO 110 J=1,N
        JR=JR+J
        HOLD=A(KR)
        JI=JR+I
110  A(JI)=-A(JI)
        A(JI)=HOLD
120  J=J(K)
    IF(J-K) 100,100,125
125  KI=K-N
    DO 130 I=1,N
        KI=KI+N
        HOLD=A(KI)
        JI=KI-K+J
130  A(KI)=-A(JI)
        A(KI)=HOLD
150  RETURN
    END
```

```

FUNCTION TRAPS(I,E)
COMMON NPAM, NRUNZ, FRAC(60), TIME(60, 15), TEMP(60, 15), VCALC(60),
+VSTAR, WATER
R= 1.9872
EB=E/R
TRAPS=0.0
IF ((EB/TEMP(I,1))+35.0) 10,11,11
10 ALLOW=0.0
GO TO 12
11 ALLOW=EXP(EB/TEMP(I,1))
12 DO 1 J=2,15
DELT=TIME(I,J)-TIME(I,J-1)
IF ((EB/TEMP(I,J))+35.0) 13,14,14
13 AHIGH=0.0
GO TO 15
14 AHIGH=EXP(EB/TEMP(I,J))
15 TRAPS=TRAPS+0.5*(ALLOW+AHIGH)*DELT
1 ALLOW=AHIGH
RETURN
END

```



```
UE      SUBROUTINE RANDU(XIX,YIY,YFL)
        DOUBLE PRECISION ZIZ
        ZIZ=XIX
        ZIZ=DMOD(16807.D0*ZIZ,((2D0**31)-1D0))
        YFL=ZIZ*1.D0/(2.D0**31)
        YIY=ZIZ
        RETURN
        END
```

```

// FOR
*LIST SOURCE PROGRAM
SUBROUTINE INGR3 (PAM,ERROR,ICODE)
C
C *****
C
C INGR 3 USES THE TRAPEZOIDAL RULE TO NUMERICALLY INTEGRATE THE
C RATE CONSTANT OVER TIME FOR NON-ISOTHERMAL CONDITIONS
C
C NOMENCLATURE
C EA ACTIVATION ENERGY
C ICODE USED IN DERIVATIVE DETERMINATIONS
C KO PRE-EXPONENTIAL FACTOR
C PAM(K) PARAMETERS
C
C *****
C
REAL KO
DIMENSION PAM(4)
COMMON NRUNZ,FRAC(40),NUM(40),TIME(40,15),TEMP(40,15),VCALC(40),
+ VSTAR,WATER
DATA R/1.9872/
EA=PAM(1)
KO=10.**(PAM(2))
VSTAR=PAM(3)
ERROR=0.0
EB=-(EA/R)
IF (ICODE) 51,50,51
50 ILOW=1
IHIGH=NRUNZ
GO TO 52
51 ILOW=ICODE
IHIGH=ICODE
52 DO 1 I=ILOW,IHIGH
L=NUM(I)
VCALC(I)=0.0
ALOW=EXP(EB/TEMP(I,1))
DO 2 J=2,L
DELT=TIME(I,J)-TIME(I,J-1)
AHIGH=EXP(EB/TEMP(I,J))
ARGU=0.5*(ALOW+AHIGH)
ALOW=AHIGH
2 VCALC(I)=VCALC(I) + ARGU*DELT
VCALC(I)=VSTAR+(WATER-VSTAR)*EXP(-KO*VCALC(I))
1 ERROR=ERROR+(VCALC(I)-FRAC(I))**2
RETURN
END

```

## APPENDIX

## INDUSTRIAL AND ENGINEERING CHEMISTRY

## Foresight

WHEN there began to be offered to us for publication an occasional paper on some phase of coal hydrogenation in America, the contributions were looked upon by our reviewers and ourselves as interesting in adding to the information on American coals but with no possibility of commercial utilization or industrial importance. We had all experienced times in which some prophets foresaw the early exhaustion of petroleum supplies. While we felt fairly certain that much that had been done abroad in the production of liquid from solid fuels could be repeated here, it seemed a long way in the future before this could be of any real practical interest.

But changes develop rapidly in a modern world. It has been interesting to learn that substantial appropriations have been made for further experiments in coal hydrogenation in the U. S. Bureau of Mines and to read the appeals of experienced engineers. They urge that we begin now to acquire technical information on how best to handle American coals for the production of motor fuels, if for no other reason than to conserve petroleum for high octane fuels and the superior lubricating oils demanded by the modern Diesel and other types of engines.

Nothing quite equals the completion of such work well in advance of the time when it may be needed. The likelihood of early exhaustion of petroleum resources is no greater than it seemed to be a decade ago, but so far as we know petroleum is not being replaced by Nature and it is being used at an enormously increased rate by all the nations that can lay their hands upon it. It is none too early to undertake very seriously the type of research and development that would lead to the proper use of coals for the manufacture of synthetic liquid fuels and particularly to provide the lubricating oils not duplicated elsewhere, not to mention the types of fuels which modern motive power utilizes to the best advantage. This does not necessarily mean beginning preparations for the third world war. It simply means taking precautions while we can to get the most out of our raw materials and to guard against the repetition of any of those wasteful procedures that have been so costly in the past. Let us learn all we can while we may. We should learn from present experiences the importance of time, particularly when there are differences in technique, opinion, and policy.

Dated: August 1, 1942